Doctoral Thesis

Trophic cascade modelling in bathyal ecosystems

Author:
Valeria Mamouridis

Supervisor:
Dr. Francesc Maynou

A thesis submitted in fulfilment of the requirements for the degree of Doctor of Philosophy

in the

Bio-Economic Modelling Research Group
Dept. de Recursos Marins Renovables (ICM-CSIC)

and the

Dept. de Ingeniería Hidráulica, Marítima y Ambiental (EHMA-UPC)

February 2015

Declaration of Authorship

I, Valeria MAMOURIDIS, declare that this thesis titled, 'Trophic cascade modelling in bathyal ecosystems' and the work presented in it are my own. I confirm that:

- This work was done wholly or mainly while in candidature for a research degree at this University.
- Where any part of this thesis has previously been submitted for a degree or any other qualification at this University or any other institution, this has been clearly stated.
- Where I have consulted the published work of others, this is always clearly attributed.
- Where I have quoted from the work of others, the source is always given. With the exception of such quotations, this thesis is entirely my own work.
- I have acknowledged all main sources of help.
- Where the thesis is based on work done by myself jointly with others, I have made clear exactly what was done by others and what I have contributed myself.

Signed: _____

Date: _____

INSTITUT DE CIÈNCIES DEL MAR (CSIC)
UNIVERSITAT POLITÈCNICA DE CATALUNYA

Abstract

Dept. de Ingeniería Hidráulica, Marítima y Ambiental (EHMA-UPC)
Dept. de Recursos Marins Renovables (ICM-CSIC)

Doctor of Philosophy

Trophic Cascade Modelling in Bathyal Ecosystems

by Valeria Mamouridis

~~In this Ph.D.~~ different aspects of the bathyal ecosystem have been treated with the final aim to investigate trophic cascade mechanisms driven by fishery (top-down control), a phenomenon that in bathyal systems has never been studied. This was exemplified by the in-depth study of the exploited soft-bottom continental slope off Catalonia (NW Mediterranean), where the important fishery of the highly priced red shrimp, *Aristeus antennatus*, is carried out and the structure of mayor pathways of the trophic web is known. However ~~for~~ the (almost complete) lack of information about the fauna in the sediment, this thesis presents a first quantitative seasonal study on the macrobenthos (infauna) in the studied habitat. Also an analysis on the landings per unit effort (LPUE) of the red shrimp has been developed to define the principal influential variables ~~on this stock~~. All these studies have in common the investigation of the dynamics of the bathyal system at different levels of organization (population, assemblage and ecosystem) in relation to environmental and fisheries drivers.

In Part I (Chapter 2) the infaunal assemblage in two main habitats, inside the canyon and on the adjacent slope, has been described and has been related to environmental and trophic variables. Important seasonal changes have been detected mainly inside the canyon along over the year. This seasonal variability is associated to the primary production, to river efflux (the Besós river near the study area) and to the seasonal occurrence of the Levantine Intermediate Waters (LIW) that affect to the chemical and nutritional value of sediment and near bottom waters. All variables, used as proxy for these three environmental causes, explain the seasonal variability in biomass/abundance and changes in taxonomic composition,

that reflects, when occurs, the seasonal turnover of trophic types. With respect to the environmental analysis, the canyon was found to be more influenced by seasonal variations and the terrigenous provision than the open slope, that conversely was found to be more related to primary production and in general showed less evidence of seasonality. The taxonomic/trophic composition of the infauna we observed can be explained with these environmental conditions. In fact the canyon showed high variability in trophic types for the most abundant taxa, whereas the adjacent slope was dominated by sub-surface deposit feeders. Moreover, inside the canyon a temporal turnover of major taxa and trophic habits was observed, whereas the adjacent slope showed one evident difference only in February ~~for~~ the dominance of the genus *Prochaetoderma* spp. that eats ~~on~~ foraminifera. The advection processes also explain the higher biomass and abundance in our area than in nearby areas (e.g. the Toulon canyon, that is not an extension of any river. This study was mandatory in order to reconstruct the food web, because made possible the flow estimation between this component and other components of the network.

Part II (Chapter 3 and 4) concerns a long term study of *A. antennatus* landings per unit effort (LPUE) performed through regression analysis using both frequentist and Bayesian additive models. With the frequentist approach the variability explained by the final model (using a total of six predictors) captured ~~the~~ 43% of the total LPUE variability. The set of fishery-related variables (the daily trips performed by vessels, the gross registered tonnage and the factor vessel) was the most important source, with an ~~ED~~ of 20.58%, followed by temporal (inter and intra-annual variability, ED = 13.12%) and finally economic variables (the ex-vessel shrimp price, ED = 9.30%). We found that data derived from fishery, as well as independent data provided by scientific surveys, provide similar indices of the exploited species. The study also showed that the number of trips per month is the most influential variable and that after a certain value it does not correspond to an effective increment in landings per unit effort while high LPUE corresponds to low values of shrimp price, probably the price drops due to the high availability of the product. Thus it may be appropriate reduce the limit of the number of trips per month for a reasonable management. Finally if boats hold a random effect their average effect on the response is null, so there is no need to use them for standardization purposes. For a methodological point of view, in Chapter 4 where the bayesian approach has been used, has been shown that a mixed effect model permits to account for correlated data.

Part III covers the ecosystem approach of this thesis and is divided into Chapter 5 where we built a steady-state model of the bathyal food web (soft bottom community at the continental slope at 600–800 m depth) and Chapter 6 where the occurrence of trophic cascade was investigated. A total of 40 carbon flows among 7 internal and 6 external compartments, were reconstructed using linear inverse modelling (LIM) by merging site-specific biomass data, on-board oxygen consumption rates and published parameters to create population and physiological constraints. The total carbon flux to the community was 2.62 mmol C m^{-2} d^{-1}, entering as vertical (5.2E-03 mmol C m^{-2} d^{-1}) and advecive organic matter (2.6E-00 mmol C m^{-2} d^{-1}). The influx was then partitioned between the total organic matter in sediment, 87.05%) and suspension and filter feeding (12.95%), among zooplankton (1.08%), suprabenthos (3.07%) and macrobenthos (95.74%). The fate of carbon deposited in sediments was its burial, its degradation by prokaryotes or the ingestion by metazoan deposit feeders. The total ingestion of C in sediments by the metazoan community (excluding the meiofauna) was 0.83 mmol C m^{-2} d^{-1}, corresponding to 31.68% of the total C entering the food web and to 36.34% of the C in sediments, so we deduced that the rest was used by the prokaryotes and nematods (1.58 mmol C m^{-2} d^{-1}, 69.28%) or trapped in the sediment (0.73 mmol C m^{-2} d^{-1}, 32.19%). The respiration of the whole community (including the total organic matter, TOM) was 1.89 mmol C m^{-2} d^{-1}: 83.75% for sediments, including prokaryotes and meiofauna, 13.34% for macrofauna, 2.86% for megafauna, including the red shrimp *Aristeus antennatus*. The dynamic simulation was based on a system of ordinary differential equations to predict biomass trends during 5 years after perturbations induced by red shrimp fishery (top-down driver) and by food supply limitations (bottom-up driver). Our simulation demonstrated that trophic cascades induced by fishery cannot occur through major components of the bathyal food web. We search for the incidence of trophic cascade through two and three interactions also including the organic matter in sediment for most complicate trophic cascade hypotheses, but we only found very ephemeral indirect effects persisting less than 10 days, that we considered not enough to demonstrate the occurrence of this mechanism in the system. On the contrary we found indirect effects persisting more than one month driven by the source limitation. Our results are in agreement with previous studies in which trophic cascades have not been detected in benthic/detritic food webs, that have some similarities with the bathyal food web, that depends on allochthonous detritus. We explain this lack of trophic cascade with the important role of detritus in the bathyal ecosystems. The dead organic matter or detritus, whereas it is frequently overlooked, is a

common feature of most ecosystems mainly in benthic ecosystems sustained by allochthonous sources. So, we hypothesised that it is the component controlling the food web dynamics a mechanism known as donor-control.

Resumen en español: ~~En este Ph.D.~~ diferentes aspectos del ecosistema batial han sido tratados con el objetivo final de investigar mecanismos de cascada trófica impulsados por la pesca (tipo de control top-down), un fenómeno que en los sistemas batial nunca ha sido estudiado. Esto fue ejemplificado ~~por~~ el estudio del talud continental de fondo suave ~~adelante de~~ Cataluña (Mediterráneo noroccidental), donde se lleva a cabo la pesquería de la gamba roja *Aristeus antennatus* y la estructura de la red trófica es relativamente conocida. Sin embargo, para poder conseguir ese objetivo y por la (casi total) falta de información sobre la fauna en el sedimento, esta tesis presenta un primer estudio cuantitativo del macrobentos (infauna) en el hábitat estudiado. También un análisis sobre los desembarques por unidad de esfuerzo (LPUE) de ~~la~~ gamba ha sido desarrollado para definir las principales variables ~~influyentes~~ en las variaciones de ~~biomasa~~ de la especies. Todos estos estudios tienen en común la investigación de las dinamicas del sistema batial en diferentes niveles de organización (población, ~~assemblage~~ y ecosistemas) en relación con variables ambientales y pesqueros.

En la Parte I (Capítulo 2) se ha desarrollado el estudio de la composición de la infauna en dos hábitats principales, dentro del cañón y en el talud adyacente, y se ha relacionado con variables ambientales y tróficas. Cambios estacionales importantes de biomasa, composición taxonómica y tipos de alimentación se han detectado principalmente en el interior del cañón a lo largo de todo el año. Esta variabilidad estacional se asocia con la producción primaria, el flujo desde ríos (e.g. el Besós cerca de la zona de estudio) y a la aparición estacional de las Aguas Intermedias de Levante (LIW) que afectan a la química y al valor nutritivo de los sedimentos y de las aguas cercanas al fondo. Las diferentes variables que se utilizaron se pueden reconducir a estas tres causas ambientales, explicando la variabilidad estacional en la biomasa/abundancia y en la composición taxonómica, que reflejan en parte la variabilidad en los tipos de alimentación de las especies estudiadas. Con respecto al análisis del medio ambiente, el cañón está más influenciado por las variaciones estacionales y la provisión terrígena que el talud abierto, que contrariamente resultó ser más relacionado con la producción primaria y en general mostró menos evidencia de estacionalidad. La composición taxonómica/trófico de la infauna puede explicarse con estas condiciones ambientales.

De hecho el cañón mostró una alta variabilidad en los tipos tróficos para los taxones más abundantes, mientras que el talud adyacente estaba dominado por los sub-deposit feeders. Por otra parte, en el interior del cañón se observó una rotación temporal de las principales taxones y hábitos tróficos, mientras que el talud adyacente mostró una diferencia evidente sólo en febrero por la dominancia del genero *Prochaetoderma* spp. que se alimenta de foraminiferos. Los procesos de advección también explican la mayor biomasa y abundancia en nuestra área que en las zonas cercanas (por ejemplo, el cañón de Toulon, que no es extensión de ningun río. Este estudio fue obligatorio con el fin de reconstruir la red ~~alimenticia~~, gracias a ese estudio se pudieron estimar los flujos relacionados a este componente.

Parte II (capítulos 3 y 4) se refiere a un estudio a largo plazo los desembarques por unidad de esfuerzo (LPUE) de *A. antennatus* realizado a través de un análisis de regresión utilizando modelos aditivos con ambos enfoques frecuentista y bayesiano. Con el enfoque frecuentista la variabilidad explicada por el modelo final (con un total de seis predictores) capturó el 43 % de la variabilidad total del LPUE. El conjunto de variables relacionadas con la pesca (los viajes diarios realizados por los barquos el tonelaje de registro bruto y los barcos mismos como factor) fue la fuente más importante, con ~~un ED~~ de 20.58 %, seguido de variables temporales (inter e intra-anual, ED = 13.12%) y finalmente las variables económicas (el precio de la gamba, ED = 9.30%). Encontramos que los datos derivados de la pesca, así como lo datos independientes de ella proporcionadas por estudios científicos, devuelven índices similares para la especie explotada. El estudio también mostró que el número de viajes por mes es la variable más influyente. Esa variable después de un cierto valor no se corresponde con un incremento efectivo de los desembarques por unidad de esfuerzo, mientras que al crecer de ese mismo los precios de la gamba bajan, probablemente por la alta disponibilidad del producto. Por lo tanto, puede ser apropiado reducir el límite de la cantidad de viajes al mes a ese umbral encontrado para una gestión razonable del recurso. Por último, si los barcos tienen un efecto aleatorio su efecto sobre la respuesta promedio es nulo, lo que no hay necesidad de utilizar para fines de normalización. Desde la prospectiva metodológica en el capítulo 4 se dimostró (~~atravéz del~~ enfoque bayesiano) que los modelos de efectos mixtos permiten evitar dificultades en la estimación cuando los datos temporales estan correlados.

La parte III cubre el enfoque ecosistémico de esta tesis y se divide en el capítulo 5, donde se construyó un modelo estacionario de la red ~~alimenticia~~ batial (comunidad fondo blando en el talud continental entre 600 y 800 m de profundidad) y el

Capítulo 6, donde se investigó la ocurrencia de cascada trófica. Un total de 40 flujos de carbono entre 7 compartimentos internos y 6 externos, fueron reconstruidos utilizando modelación lineal inversa (LIM) mediante la fusión de datos de biomasa específicos del lugar, las tasas de consumo de oxígeno a bordo y parámetros publicados para crear limitaciones poblacionales y fisiológicas. El flujo total de carbono a la comunidad fue 2.62 mmol C m^{-2} d^{-1}, entrando como materia orgánica vertical (5.2E-03 mmol C m $^{-2}$ d^{-1}) o advecive (2.6E-00 mmol C m $^{-2}$ d^{-1}). Después, ese flujo se repartió entre la matéria orgánica en el sedimento, 87.05 %), y suspension and filter feeding (12.95 %), entre zooplancton (1.08 %), suprabentos (3.07 %) y macrobentos (95.74 %). El destino del carbono depositado en los sedimentos es ~~el burial~~, su degradación por parte de lo~~s~~ procariotas o la ingestión por los metazoos ~~deposit feeders~~. La entrada de C total en la comunidad de metazoos (excluyendo la meiofauna) fue de 0.83 mmol C m $^{-2}$ d^{-1}, correspondiente al 31.68 % del carbono total que entra en la red ~~alimenticia~~ y al 36.34 % del C en los sedimentos, por lo que se dedujo que el resto fue utilizado por los procariotas y nemátodos (1.58 mmol C m $^{-2}$ d^{-1}, 69.28 %) o atrapado en el sedimento (0,73 mmol C m $^{-2}$ d^{-1}, 32.19 %). La respiración de toda la comunidad (incluyendo la materia orgánica total, TOM) fue de 1.89 mmol C m $^{-2}$ d^{-1}: 83.75 % de los sedimentos, incluyendo procariotas y meiofauna, 13.34 % de macrofauna, 2.86 % para megafauna, incluyendo la gamba *Aristeus antennatus*. ~~Cosa~~ La simulación dinámica se basa en un sistema de ecuaciones diferenciales ordinarias para predecir las tendencias de biomasa durante 5 años después de las perturbaciones inducidas por la pesca de la gamba (proceso top-down) y por las limitaciones de alimento primario, el detrito de origen a~~lloctono~~ (proceso bottom-up). La simulación demostró que las cascadas tróficas inducidas por la pesca no pueden ocurrir a través de los principales componentes de la red ~~alimentaria~~ batial. Se buscó su incidencia a través de dos y tres interacciones incluyendo también la materia orgánica en los sedimentos en la hipótesis más complicada, pero sólo encontramos efectos indirectos muy efímeros que persiste menos de 10 días, y que no se consideraron suficientes para demostrar la ocurrencia de este mecanismo en el sistema. Por el contrario hemos encontrado efectos indirectos que persisten más de un mes impulsado por la limitación de fuente de energía en la red. Nuestros resultados están de acuerdo con estudios previos en los que no se han detectado las cascadas tróficas en las redes ~~alimentarias~~ bentónicas/detríticas, que tienen algunas similitudes con la red ~~alimentaria~~ batial, en cuanto dependen de detritos alóctonos. Explicamos esta falta de cascada trófica con la importante función del detrito en los ecosistemas batiales. La materia orgánica muerta o detrito es una característica común de la mayoría de

los ecosistemas, principalmente en los ecosistemas bentónicos que reciben energía de orígen alótona. Valoramos la hipis de que es el detrito ~~es la~~ componente que controla la dinámica de la red ~~alimentaria~~, un mecanismo conocido como control de los donantes.

Acknowledgements

The development of this Ph.D. was financed by the Spanish National Research Council (CSIC) through the JAE-predoc grant programme that is gratefully acknowledged as well as the projects of which this thesis was a part: BIOMARE (ref. CTM2006-13508-CO2-02/MAR) and ANTROMARE.

Many professors, experts and students have taught and or collaborated and made possible its fulfillment. I thank all gratefully.

First I would like to express my deepest gratitude to my supervisor Dr. Francesc Maynou, for guiding me along this long path; a scientist with ample knowledge in both statistics and marine sciences and also his inner calm.

To Dr. Joan Cartes for the years before the Ph.D. when I worked under his supervision. His support was decisive to continue in research. Thanks also for teaching me deep-sea peracarids during preparation of samples for SIA.

To Dr. Germán Aneiros, a real teacher and to Pr. Carmen Cadarso and Pr. Thomas Kneib, to share with me their ample knowledge on statistics.

To Pr. Karline Soetaert and Dr. Dick van Oevelen, to help me in food web modelling and share their vision of doing science. Thank you very much for allowing me to start the theoretical study of food webs, that I loved so much and I hope to continue this theme after finishing with the thesis.

I am also deeply grateful to Dr. Santiago Parra for transmitting its knowledge in polychetes' taxonomy.

Then, I would like to thank all participants of the projects and other not directly involved, but whom I worked with: Pr. L. Salvini-Plawen, Dr. Ignacio Salinas, Dr. C. Salas and Dr. S. Gofas for their help in taxonomic identifications, Nadja Klein for her help in Bayesian regression, Dorina Seitaj for her help in SOC experiments, Leda Zucca (I will remember all hours we spent in the lab between the freezer and the microscope) and also Dr. E. Fanelli that helped me in the preparation of the published version of the first chapter, Dr. C. Lo Iacono, Pr. M. Carrassón, Cristina Lopez, Dr. V. Papiol and Laurine Burdorf.

I also want to show a deep gratitude to all researchers of the ICM. Especially I would like to thank Dr. Antoni Lombarte, Dr. Domingo Lloris, Dr. Eva Galimany, Dr. Teresa Madurell and Dr. Erica Vidal for their words and support.

During these years (mainly during the master) I also appreciated the passion in teaching of many professors, especially I would remember Pr. Alberto Rodriguez-Casal, Pr. Juan Carlos Pardo Fernández, José Antonio Vilar Fernández, Juan Vilar Fernández.

The professional but also very funny crew of "Garcia del Cid". Thanks for the kitchen apron "Ada carbonara", that I use so often! and also to the crew of the "Sarmiento del Gamboa".

A special thanks to all the administrative staff of the ICM for all the work they have done and do and their availability and courtesy.

Many thanks to Pablo Sáez for his drawings that have helped to illustrate this thesis. I wish you to continue your project in scientific illustration.

Then, can not miss many many many thanks to all the mates of "el pasillo de recursos", many along the entire stay at the ICM. Gracias Ainhoa mi favorida compañera de despacho aunque un poco anti-aire acondicionado (;P), el gatofilo (como yo) nemertinofilo (yo paso lo siento!!!) Fernando, Marta la mascota del pasillo, Dafni y Raquel de muy buen corazón (bailarinas), Giuliano el mejor fotógrafo del despacho, Lucie y su "que dura es la vida" (te echo de menos darling), Albert, Silvia y Andres los trotamundos, Ángel de principios sólidos, la sonriente Daniela, Ulla el clown, Sam siempre muy tranquilo, Federico que no quiere ganar (a quien lo cuentas?) y Claudio que no sabe perder partidos de volley (prrr ☺), Anabel, Marc el único andorrano biólogo marino, Sonia el vulcano de fiesta, John el pragmático, Noelia que se fue en un plis, Valerio il pescatore sportivo, Teresa, Alba otra que se ensució las manos de barro buscando poliquetos, Costantinos, Giulia, Ariadna que le gustan los gatos también, Vanesa, Laura, Rigoberto, Dani, Carol que siempre encuentro en patines, Samuele, David ... and I do not forget Anamari and el niño de Isabela (jeje) y Amalia, Natalia, Sara and toooooodos los demás compañeros del ICM. Aaaaaaaaaand, let me say: "GRANDES CHANCLAS!!!" and also: GRANDES son los de EL GRUPO ANTI-VOLLEY (q realmente no existe pero me entraron muchas risas cuando lo escuché decir) and LOS DEL INSTITUTO DE AL LADO ...;P. Si no podrá ser con todos, espero, por lo menos con algunos, seguir manteniendo el contacto. 🐟

AAAAll the folks of the de keete (the big brother), especially Silvia, Michele, Vanessa, Misha, Dorina, Tadao, Diana, Francesc and little ☾. Thanks to you I

lived a special and intense experience of life in that big house where all cultures meet. But it was very difficult to keep the kitchen clean ...

Thanks of course to the powerful network of all my friends, however you are far, you are always present: Camilla and Cecilia, Annalisa, Monica e Sandra le mie superchicche adesso tutto mamme e avete dovuto necessariamente cambiare i vostri poteri ..., Pierpaolo (aó quando ci ributtiamo in mare?),Federica my favorite classmate (anche altri lo erano ma ... tu sei rimasta!!!). Per quanto vi riguarda, cari miei, non saprei proprio sintetizzare le troppe cose che mi uniscono a voi e per cui vi adoro ... Non pensavo mi sareste mancati tanto ma per fortuna c'é Skype per i momenti critici! (:)) All you are important to me, as well as Alessandra, Alma que expresa todos sentimientos y Mike que tiene la razón lógica, Germana mio mito femminile in apnea (dopo William Trubridge però ;D), Simone che non dorme mai, Donatella il mio sopraaaaaaaano preferiiiiiiito (♪) e Alberto ovviamente che a ragione é il mio pianista preferito (♫), Emma e Giovanna (vivono, fanno e sono cultura e non solo), Renza che ha sempre un pensiero per tutti ed io per lei, Mitzi la scultura greca, Fina y Vicente que me aiudaron tanto durante mi estancia en Coruña. Y luego Chiara (✌) ovviamente, presente da prima di arrivare a Barcellona (carrer Fonollar 20), y todas sus amigas super divertidas Cecilia la loca, Nick uno sprint di energia, la romántica Carol, la pequeña Sushianti, Angela the surfer, cherie Virginie, Rosa aunque no te gusta el swing. Sois una diferente de la otra y tal vez bastante de mí, pero cada una con sus caracteristicas y calidades que aprecio mucho, sois excepcionales! E poi Rospa e Rospi alias Federica e Fabrizio, ottima famiglia di cesta di 🍃e la positiva Enrica. Y también quiero agradecer a Javier el poeta estadístico que vive por su "mar atlántico", Diana and Juan Carlos compañeros de piso exelentes, Héctor el mejor escritor contemporáneo, Natalia and Venere du' caratteri forti molto forti, Patri la campeona del cubiletras (niña te echo de menos, bueno tu también compites por el puesto de excelencia como flatmate), Elena bio-energetic-bailarina, Pina che non auguro a nessuno di conoscere in aereo ... (ahahah), Alí e la ricciuta Amal, la justa Coté and Montse gran pintora. E poi non posso dimenticare Livia, non conosco persona più risolutiva!! (Cami, per il momento lasciamo a tua madre il podio, ok?) e neanche Lello, voi siete parte della mia famiglia. E non posso dimenticare la dolce Mahbubeh che lotta per le cause giuste. Thanks to those who listened to me, understanding what it means to be there hours and weeks and I do not say how much more, to find at least one answer to thousand questions. All of you have won a big part in my big heart (:D) and I simply cannot imagine my life without you.

Thanks also to Santi and all the nice people of the Absenta and to the new cute folks I met thanks to the Lindy hop, especially Serena, Gunter and Martina. I've danced and smiled a lot with you! Thanks thanks thanks. Thanks to all "las kukas", fantastic people of the association Tota Cuca Viu , please, excuse me for leaving you during these last months. ⚘

Finally thanks to all my family, especially Michela, my "super-sister" e migliore cuoca del mondo, Luciano and my uncles Soulis, Nikos (I8ela na eimai kontá sas perisótero chróno, zitẃ signẃmi) and Takis (sýntoma 8a paízoyme mazí chartiá ;D), my aunts Daniela (e pure con te giocherò a ...burraco!! che non ci giochiamo da tanto :D), Evi and Giorgia, and my cousins Alberto il sognatore ed il suo ❀ Genziana, Despo and Ioannis (♪♪♪) and Solidea e Giovanni and all all all other components of the family.

To my parents, doubtless; and to Vittorio and Lola. Thank you a lot for what you have done for me.

Of course unquestionable thanks to my laptop ♀ and to Perro my fantastic 🖒.

Let's go discover new worlds and enjoy the life!

Contributions to chapters

- **Chapter 2: A temporal analysis on the dynamics of deep-sea macrofauna: influence of environmental variability in the Catalan Sea (western Mediterranean)**

  Published in modified form in Deep Sea Research I, 58: 323–337 (2011) doi:10.1016/j.dsr.2011.01.005

  Valeria Mamouridis[1], Joan E Cartes[1], Santiago Parra[2], Emanuela Fanelli[3], José Ignacio Saiz Salinas[4]

  VM SP and JISS made the taxonomic identification, VM and JEC made the statistical analysis, JEC and EF made the sampling design, VM JEC EF the field work, VM JEC wrote the paper

- **Chapter 3: Analysis and standardization of landings per unit effort of red shrimp from the trawl fleet of Barcelona (NW Mediterranean)**

  Published in modified form in: Scientia Marina, 78(1) (2014) doi: http://dx.doi.org/10.3989/scimar.03926.14A

  Valeria Mamouridis[1], Francesc Maynou[1], Germán Aneiros Pérez[5]

  VM FM and GAP designed the analysis, VM made the statistical analysis, VM and FM wrote the paper

- **Chapter 4: Extended Additive Regression for Analysing LPUE Indices in Fishery Research**

  Published in modified form in Reports in Statistics and Operations Research. Universidade de Santiago de Compostela. Departamento de Estadística e Investigación Operativa. Vol. 29/10/2013 (2013-01). http://eio.usc.es/index.php/es/reports-.

  Valeria Mamouridis[1], Nadja Klein[6], Thomas Kneib[6], Carmen Cadarso Suárez[7], Francesc Maynou[1]

  VM, TK and NK designed the study, VM made the statistical analysis, VM NK TK CCS FM wrote the paper.

- **Chapter 5: Food web modelling in a soft-bottom continental slope ecosystem (NW Mediterranean)** Valeria Mamouridis[1], Karline Soetaert[8], Dick van Oevelen[8], Francesc Maynou[1], Emanuela Fanelli[3], Joan E Cartes[1]

VM, DVO, KS and FM designed the study, VM and DVO made the model, VM the analysis, VM, FM, EF, JEC collected data, VM and FM wrote the chapter

- **Chapter 6: Simulation of trophic cascade in a bathyal ecosystem**

  Valeria Mamouridis[1], Francesc Maynou[1], Karline Soetaert[8], Dick van Oevelen[8]

  VM, KS, DVO and FM designed the study, VM made the model and the statistical analysis, VM wrote the chapter

Affiliations:

1. Institut de Ciències del Mar (ICM-CSIC), Passeig Marítim de la Barceloneta 37–49, 08003 Barcelona, Spain.
2. Instituto Español de Oceanografía, P.O. BOX 130, 15080 A Coruña, Spain.
3. Marine Environmental Research Centre - ENEA Santa Teresa, Pozzuolo di Lerici, 19032 (SP), Italy.
4. Dpt de Biología Animal y Genética, Fac. de Ciencias, Universidad del País Vasco, E–48080 Bilbao, Vizcaya, Spain.
5. Facultade de Informática, Campus de Elviña s/n, Universidade da Coruña, 15071 A Coruña, Spain.
6. Georg-August-University, Centre for Statistics , Platz der Göttinger Sieben, 37073 Göttingen, Germany.
7. Unidade de Bioestad´stica, Facultad de Medicina e Odontolox´a, Rúa San Francisco s/n, 15782 Santiago de Compostela, Spain.
8. NIOZ (Royal Netherlands Institute for Sea Research) Yerseke, Korringaweg 7, P.O. Box 140, 4400 AC Yerseke, The Netherlands.

Contents

Declaration of Authorship iii

Abstract v

Acknowledgements xii

Contributions to chapters xvi

Contents xviii

List of Figures xxv

List of Tables xxxi

1 General introduction 1

1.1 Justification of the study . . . 2
1.2 Food webs and trophic cascades . . . 5
1.2.1 Food webs: concepts and models . . . 5
1.2.2 Trophic cascades and other mechanisms . . . 12
1.3 The bathyal domain in the NW Mediterranean sea: energy transfer and faunal composition . . . 19
1.4 Deep-sea fisheries, management and models . . . 26
1.4.1 Deep-sea fishery in the Balearic Basin . . . 26
1.4.2 Monospecific and ecosystem approaches to fisheries and existing models . . . 28
1.4.3 The bias-variance problem of a model . . . 30
1.5 The study area . . . 33
1.6 Purposes of the study . . . 36

PART I **41**

2 A temporal analysis on the dynamics of deep-sea macrofauna: influence of environmental variability in the Catalan Sea (western Mediterranean) **43**
2.1 Introduction . . . 45
2.2 Materials and Methods . . . 47
2.2.1 The Study area and sampling design . . . 47
2.2.2 Environmental data collection . . . 48
2.2.2.1 Diversity and biomass trends by season . . . 49
2.2.3 Statistical analysis . . . 50
2.3 Results . . . 51
2.3.1 Taxonomic composition . . . 51
2.3.2 Diversity and biomass trends by habitat and season . . . 52
2.3.3 Assemblage structure: composition by habitat (canyon and adjacent slope) . . . 55
2.3.4 Environmental variables . . . 56
2.3.5 Influence of environmental variables . . . 59
2.3.6 Regression models . . . 63
2.4 Discussion . . . 63
2.4.1 Comparison with other quantitative studies . . . 65
2.4.2 Dynamics of infauna assemblages . . . 66

PART II **75**

3 Analysis and standardization of landings per unit effort of red shrimp from the trawl fleet of Barcelona (NW Mediterranean) **77**
3.1 Introduction . . . 79
3.2 Materials and Methods . . . 81
3.2.1 Data source . . . 81
3.2.2 Model construction . . . 82
3.2.3 Theoretical response probability function . . . 84
3.2.4 Selection criteria and explained deviance . . . 85
3.2.5 LPUE standardization . . . 85
3.3 Results . . . 86
3.3.1 Overview of data and response distribution . . . 86
3.3.2 Model building and comparison . . . 87
3.3.3 The descriptive model . . . 88
3.3.4 LPUE standardization . . . 92
3.4 Discussion . . . 93
3.4.1 The role of explanatory variables . . . 93
3.4.2 Implications for management . . . 94

4 Extended Additive Regression for Analysing LPUE Indices in Fishery Research **97**
4.1 Introduction . . . 99

4.2 Materials and Methods . . . 104
4.2.1 Data description . . . 104
4.2.2 Methodology . . . 105
4.3 Results . . . 109
4.3.1 Model selection, diagnostics and comparison . . . 109
4.3.2 Description of partial effects . . . 114
4.4 Discussion . . . 118

PART III **123**

5 Food web modelling in a soft-bottom continental slope ecosystem (NW Mediterranean) **125**
5.1 Introduction . . . 127
5.2 Materials and Methods . . . 130
5.2.1 The study area . . . 130
5.2.2 Biomass data . . . 131
5.2.3 Other data . . . 133
5.2.4 Literature data . . . 135
5.2.5 Linear inverse modelling . . . 137
5.2.6 Food web structure . . . 139
5.2.7 Network indices . . . 141
5.2.8 Software . . . 146
5.3 Results . . . 146
5.3.1 Oxigen consumption results . . . 146
5.3.2 The food web in steady state . . . 146
5.3.3 The network indices . . . 151
5.4 Discussion . . . 152
5.4.1 Inputs and resource partitioning . . . 153
5.4.2 Community respiration . . . 156
5.4.3 Network analysis . . . 157

6 Simulation of trophic cascade in a bathyal ecosystem **159**
6.1 Introduction . . . 161
6.2 Materials and Methods . . . 163
6.2.1 The dynamic model . . . 164
6.2.2 Local stability of the food web . . . 165
6.2.3 The simulation . . . 166
6.2.3.1 Couples of species . . . 168
6.2.4 Software . . . 168
6.3 Results . . . 169
6.3.1 The stability analysis . . . 169
6.3.2 The total biomass . . . 169
6.3.3 Relative biomasses . . . 171
6.3.4 Interactions effected . . . 172
6.4 Discussion . . . 173

PART IV **179**

7 General discussion **181**
7.1 General discussion . . . 182
7.2 PART I The infauna in the continental slope . . . 182
7.3 PART II Landings per unit effort LPUE . . . 184
7.4 PART III The bathyal food web . . . 187
7.5 PART III Trophic cascades and drivers in the bathyal ecosystem. . . . 192

8 Conclusions **195**
8.1 Conclusions . . . 196

APPENDICES **199**

A Bathyal species **201**

B Field and Laboratory material **207**

C Complementary material – Chapter 3 **215**
C.1 Exploratory study on the response variable LPUE . . . 216
C.2 Diagnostic plots of the final model . . . 217

D Complementary material – Chapter 4 **219**
D.1 Model selection . . . 220
D.2 Comparison of partial effects among models . . . 221

E Complementary material – Chapter 5 **229**
E.1 Sediment Oxygen Consumption . . . 230
E.2 LIM equations . . . 230
E.3 Results of the food web model . . . 231
E.4 Network indices equations and results . . . 236

F Complementary material – Chapter 6 **241**
F.1 Dynamic simulation for 20 years . . . 242

G Offprint **249**
G.1 Publications . . . 250
G.2 Congress presentations . . . 333
G.2.1 A temporal analysis on the dynamics of deep-sea macrofauna: influence of environmental variability off Catalonia coasts (Western Mediterranean) . . . 333
G.2.2 Additive Mixed Models applied to the study of red shrimp CPUE: comparison between frequentist and Bayesian perspectives . . . 334

G.2.3 ANALYZING CPUE INDICES IN FISHERY RESEARCH THROUGH STRUCTURED ADDITIVE REGRESSION MODELS . . . 336
G.2.4 Frequentist or Bayesian Mixed Models? A comparison to provide better estimates of CPUE . . . 337
G.2.5 Dynamic simulations of food webs with R . . . 342
G.2.6 Structured Additive Distributional Regression in Fishery Research . . . 346
G.2.7 Multivariate techniques in ecology: The infauna associated to a CWC habitat (facies of *Isidella elongata*), influences of fishing activity and natural variability. Oral presentation. . . . 347
G.2.8 EFFECTS OF DEEP-SEA FISHERIES ON THE DYNAMICS OF BATHYAL FOOD WEBS (NW MEDITERRANEAN). Oral presentation. . . . 348
G.2.9 Poster . . . 349
G.2.10 Poster . . . 350

References **351**

List of Figures

1.1 The red shrimp *Aristeus antennatus* (Risso, 1816). 2
1.2 Three examples of theoretical food webs. In columns: (A) binary and (B) quantified food webs. In rows: (1) Random model, (2) Cascade model and (3) Niche model with $N = 9$ compartments S and $L = 30$ number of links. 8
1.3 The fate of consumed energy for a given component (or an individual). Symbols represent: C = energy consumed, A = energy assimilated, E = the egested energy, P = the produced energy, M = the energy used for maintenance. 9
1.4 Output of the dynamic simulation for the niche food web in Figure **??**, C. The time span is 20 years and plot, headed by a number from 1 to 9, corresponds to each species of the food web. On the y axis are shown the biomasses. Dark: unperturbed biomass; red: biomasses perturbed by 1/2 of the original value; green: biomass perturbed by 2 of the original value. 12
1.5 Example of the trophic cascade between otter, sea urchin and kelp (then also extended to killer whale) in the ecosystem of the Aleutian Islands (Alaska, USA) (Estes et al., 1998). 13
1.6 Description of the hypothesis of two alternative states in the ecosystem nearby the Medes Reserve (western Mediterranean) explainable by mechanisms of trophic cascade. From Pinnegar et al. (2000). . . 15
1.7 Principal domains of benthic and pelagic regions. Depths are not to scale. 20
1.8 Principal pathways in the bathyal domain. BBL = Benthic Boundary Layer. Modified from WWF/IUCN (2004), pg. 28. 21
1.9 Global distribution of cold-water corals. From Roberts et al. (2006). 23
1.10 A) The Blackmouth catshark *Galeus melastomus*, Rafinesque, 1810; B) The half-naked hatchetfish *Argyropelecus hemigymnus*, Cocco, 1829. 2015. 25

1.11 The bias-variance trade-off in model fitting with increasing complexity (the more parametrization, the higher complexity). Increasing the model complexity also the variance increases, while the bias decreases. The best fit occurs when both are minimized (vertical arrow). Here error define whatever measure used to summarise the error of the model, being the integrated or the average mean square error or the predictive risk. See the text for more details. 31
1.12 The Balearic basin and study area inside the red polygon. 34

2.1 Map of the study area off the Catalan coast, showing the positions of samples inside canyons Besòs and Berenguera (C1, C2) and on the adjacent slopes (S1, S2) stations. 47
2.2 Diversity parameters: S represents the total number of species, H' is the Shannon index in S1 (white dots) and C1 (black dots). 52
2.3 (a) Annual mean biomass (WWmg/m^2) profiles of total infauna and major taxa, (b) Annual mean density (ind/m^2) of total infuna, polychaetes and crustaceans, (c) individual mean weight (WWmg/ind) of polychaetes, crustaceans and molluscs. Dark gray bars indicate C1 samples and light gray bars indicate S1 samples. 53
2.4 nMDS ordination of samples from a full year (B1, B2, B3 and B4). Labels indicated: HOM = water column homogenization and STR = water column stratification for the factor WATER CONDITIONS. Symbols indicate: full cycles = canyon; empty cycles = adjacent slope for the factor HABITAT. 55
2.5 Environmental variables as a function of season. Temperature above the bottom (T_{5mab}); salinity (S_{5mab}); fluorescence (f_{0-500m}); water turbidity close to the bottom ($turb_{5mab}$); potential redox of sediments (at a depth of 1 cm: Eh); TOM in sediments. (dark dots): canyon; (white dots): adjacent slope. 58
2.6 Environmental variables. a) Chla in surface by satellite imagery (dark dots: canyon; white dots: adjacent slope); b) river flow (m^3 s^{-1}) of the two most important rivers in central Catalan coasts. 59
2.7 PCAs of environmental variables collected in (a) canyon stations and (b) adjacent slope. 59
2.8 CCA of broad taxa, considering both canyon and adjacent slope samples, with selected environmental variables. 60
2.9 CCA of dominant species (a) inside the canyon and (b) on the adjacent slope and the environmental variables. For the full name of species' acronyms see Table 2.2. 62

3.1 Time series from 1994 to 2008 of LPUE data and spline estimation (upper panel) and mean annual North Atlantic Oscillation (NAO) (lower panel). 87
3.2 From top to bottom: spline estimation of the fuel price, monthly total number of trips performed by the fleet from year 1996 to 2008, and relationship between the fuel price and the total monthly number of trips. 88

3.3 Partial effects of model 7. Bayesian credible intervals (95%). 91
3.4 Comparison between the fishery-derived index (standardized LPUE) and the SGMED index. Variables have been normalized for comparison. 92

4.1 Boxplots for MSEP calculated for all models. See Table 4.2 and Equations in the text for model specifications. 112
4.2 QQplots of the normalized residuals calculated as described in the methodology section for the 8 models. 113
4.3 QQplots for normality of catching units parameters as random effects in the mixed model M8. α_μ refer to random effects in the predictor for location, while α_σ refers to the predictor for the shape. 114
4.4 Interval plots of estimated random effects in the predictor for location (α_μ) and shape (α_σ) on the upper and lower plots respectively. Bars indicates 95% CI. 116
4.5 Nonparametric effects for the GA mixed effect of the selected gamma model (M8). Effects on predictor for μ (left side) and for σ (right side). Grey shapes represent 95% credible intervals. 117

5.1 The food web study area comprises the soft-bottom slope in front of the Catalonia at 600-800 m. 131
5.2 Binary food web. 142
5.3 Sediment Community Oxygen Consumption (mmol O_2 m^{-2} d^{-1}) as a function of depth (m). The grey points are observations, the continuous line represents the mean fitted value, the dashed lines corresponds to the average SCOC value (also in the Figure) at comparable depths (here we set 700 m the interpolations between 600-800 m depths, the range of our food web) and the estimation by our food web model is represented in red, the average is the red dot (with the corresponding number) and the segment represents the range. The function is the model in Equation E.2, Appendix E. Also the r^2 is reported. 147
5.4 Food web carbon flows (mmol C m^{-2} d^{-1}). See Table 5.2 for abbreviations of food web compartments and Tables E.4 and E.4 for the values of the flows. The legend shows maximum and minimum flow values estimated through the parsimonium solution. 148
5.5 Barplot of the food web flows (mean ± sd, mmol C m^{-2} d^{-1}) estimated using the MCMC method in descending order from the left to the right. 149
5.6 Food web carbon flows (mmol C m^{-2} d^{-1}) as in Figure 5.4 but divided in A) input (green), B) output (red) and C) internal (black) flows. See Table 5.2 for abbreviations of food web compartments and Tables E.4 and E.4 for flows' estimations. The legend shows maximum and minimum flows estimated through the parsimonium solution. 153

6.1 (A) Food web net flows and (B) trophic position of components. Colours correspond to compartments: orange = zooplankton (ZPL); red = suprabenthos (SBN); green = macrobenthos (MABN); blue = invertebrates from megafauna (MEBN); light blue = fish from megafauna (ICT); violet = red shrimp *Aristeus antennatus* (AANT). 164
6.2 A) Changes of total biomass during the 5 years using p=(0,5,-5). . . 171
6.3 B) Changes of total biomass during the 5 years using p=(0,5,-5). . . 172
6.4 C) Changes of total biomass during the 5 years using p=(0,50,-50). 173
6.5 A) Changes of relative biomasses during the 5 years using p=(0,5,-5). 174
6.6 B) Changes of relative biomasses during the 5 years using p=(0,20,-20). 175
6.7 C) Changes of relative biomasses during the 5 years using p=(0,50,-50). 176

A.1 Deep-sea fish. A) The Shortfin spiny eel *Notacanthus bonaparte* Risso, 1840. Latium, MEDITS-IT, 2004; B) The macrurid Roughtip grenadier *Nezumia sclerorhynchus* (Valenciennes, 1838). Latium, MEDITS-IT, 2004; C) The Jewel lanternfish *Lampanyctus crocodilus* (Risso, 1810). Latium, MEDITS-IT, 2004; D) *Cyclothone braueri*, Jespersen & Tåning, 1926. Antromare survey, 2010. 202
A.2 1) The Rabbit fish *Chimaera monstrosa*, Linnaeus, 1758. Latium, MEDITS-IT, 2003; 2) *Alepocephalus rostratus* Risso, 1820. Catalan Sea, Biomare 2007; 3) The deep-water coral *Isidella elongata*. Catalan Sea, Antromare July 2011. 203
A.3 A) The bivalve *Kelliella miliaris* (Philippi, 1844) B) The cumacean *Leucon* (*Epileucon*) *longirostris* Sars, 1871, ♂; C) A caudofoveat belonging to the genus *Falcidens* Salvini-Plawen, 1968; D) The bivalve *Ennucula aegeensis* (Forbes, 1844); E) The amphipod *Carangoliopsis spinulosa* Ledoyer, 1970; F) The ophiurid *Amphiura chiajei* Forbes, 1843 (oral view); G) *Campilaspis glabra* G. O. Sars, 1879; H) The ophiurid *Amphipholis squamata* (Delle Chiaje, 1828) (dorsal view). Specimens from boxcorer and suprabenthic sledge. Biomare 2007, Antromare 2010-2011. 204
A.4 A) *Leucon* (*Macrauloleucon*) *siphonatus* Calman, 1905; B) *Campylaspis squamifera* Fage, 1929; C) The amphipod *Stegocephaloides christianiensis* (Boeck, 1871); D) *Leucon* (*Crymoleucon*) *macrorhinus* Fage, 1951; E) The amphipod *Idunella nana* (Schiecke, 1973); F) *Diastyloides serrata* (Sars G.O., 1865); G) *Eudorella truncatula* (Bate, 1856); H) Postnauplius of a cumacean (probably *L. longirostris*). Specimens from boxcorer and suprabenthic sledge. Biomare 2007, Antromare 2010-2011. 205

B.1 Boxcorer. B/O García del Cid, Catalan Sea, BIOMARE October, 2007. 208
B.2 Multicorer. B/O García del Cid, Catalan Sea, BIOMARE October, 2007. 209

B.3 (A) WP2 used to sample zoplankton and micronekton. (B) Suprabenthic sledge used to sample suprabenthos. B/O García del Cid, Catalan Sea, BIOMARE October, 2007. 210
B.4 A) A lid with different holes used to introduce the stirrer, sensors for digital records or pipettes for the Winkler titration; B) The perspex chambers (d = 30 cm). All material provided by the Ecosystem studies department of the NIOZ-Yerseke. 211
B.5 A lip containing a Teflon-coated magnetic stirrer. All material provided by the Ecosystem studies department of the NIOZ-Yerseke. . 212
B.6 An incubation with water. Prepearing experiments at the NIOZ-Yerseke, 2011. 213

C.1 From left to right, upper panels, histogram and kernel density estimations of lpue; middle panels, box-plot and cumulative distribution function of data and of the gamma distribution; lower panels, QQ-plots of sample quantiles versus gamma and normal distribution quantiles. 216
C.2 Residual diagnostics for model 7. (A) Histogram of deviance residuals; (B) QQ-plot of deviance residuals; (C) deviance residuals against linear predictor; (D) response against fitted values. 217

D.1 Nonparametric effects on the predictor for μ for the LN fixed effect model M1 and the mixed effects model M2 with best DIC score. Grey shapes represent 95% credible intervals. 223
D.2 Nonparametric effects for the LN fixed effect model M3 with best DIC score. Effects on predictor for μ (left side) and for σ^2 (right side). Grey shapes represent 95% credible intervals. 224
D.3 Nonparametric effects for the LN mixed effect model M4 with best DIC score. Effects on predictor for μ (left side) and for σ^2 (right side). Grey shapes represent 95% credible intervals. 225
D.4 Nonparametric effects on the predictor for μ for the GA fixed effect model M5 and the mixed effects model M6 with best DIC score. Grey shapes represent 95% credible intervals. 226
D.5 Nonparametric effects for the GA fixed effect model M7 with best DIC score. Effects on predictor for μ (left side) and for σ (right side). Grey shapes represent 95% credible intervals. 227
D.6 Nonparametric effects for the GA mixed effect model M8 with best DIC score. Effects on predictor for μ (left side) and for σ (right side). Grey shapes represent 95% credible intervals. 228

E.1 Range estimation of food web flows. The dark point represents the parsimonious solution, the segments minimum to maximum ranges. 233

F.1 Dynamic output when perturbing red shrimp biomass with increasing fishing effort. Blue line = 2 times the actual fishing flow; yellow line = 5 times the actual fishing flow; and red line = 20 times the actual fishing flow. 243

F.2 Dynamic output when perturbing red shrimp biomass with decreasing fishing effort. Blue line = 2 times less the actual fishing flow; yellow line = 5 times less the actual fishing flow; and red line = 20 times less the actual fishing flow. 244
F.3 Dynamic output when perturbing all megafauna biomasses with increasing fishing effort. Blue line = 2 times the actual fishing flow; yellow line = 5 times the actual fishing flow; and red line = 20 times the actual fishing flow. 245
F.4 Dynamic output when perturbing all megafauna biomasses with decreasing fishing effort. Blue line = 2 times less the actual fishing flow; yellow line = 5 times less the actual fishing flow; and red line = 20 times less the actual fishing flow. 246
F.5 247
F.6 248

List of Tables

1.1 Size-based classication of benthos with size range and main groups (examples) in each size class. 6
1.2 Soft-bottom trophic cascades recompiled from literature. Cascades in parenthesis are based on circumstantial evidence. Ref: (1) Pipitone et al. (2000) ; (2) Pauly (1985); (3) Christensen (1998); (4) Caddy (1983); (5) Aronson (1990); (6) Virnstein (1977). 16
1.3 Alphabetical list of models used in the ecosystem approach of fisheries (PART 1/2). Revised from (Plagányi, 2007). References are: 1. Fulton, Smith and Johnson, 2004, 2. Fulton et al., 2005, 3. Yodzis and Innes, 1992, 4. Yodzis, 1998, 5. Koen-Alonso and Yodzis, 2005, 6. Bogstad et al., 1997, 7. **?**, 8. Butterworth and Thomson, 1995, 9. Mori and Butterworth, 2004, 10. Mori and Butterworth, 2005, 11. Mori and Butterworth, 2006, 12. Thomson et al., 2000, 13. Constable, 2006, 14. Baretta-Bekker et al., 1997, 15. Livingston and Methot, 1998, 16. Hollowed et al., 2000, 17. Tjelmeland and Lindstrøm, 2005, 18. Christensen and Pauly, 1992, 19. Christensen and Walters, 2004, 20. Polovina, 1984, 21. Walters et al., 1997, 22. (Walters et al., 2000), 23. Begley and Howell, 2004, 24. Trenkel et al., 2004, 25. Taylor and Stefánsson, 2004, 26. Taylor and Taeknigardur, 2011, 27. Finnoff and Tschirhart, 2003, 28. Finnoff and Tschirhart, 2008, 29. Alonzo et al., 2003, 30. DeAngelis and Gross, 1992, 31. Purcell and Kirby, 2006, 32. Shin and Cury, 2004, 33. Fulton, Smith and Johnson, 2004, 34. Fulton, Parslow, Smith and Johnson, 2004, 35. McDonald et al., 2006, 36. Watters et al., 2005, 37. Watters et al., 2006, 38. Punt and Butterworth, 1995, 39. Jurado-Molina et al., 2005, 40. Garrison et al., 2010, 41. Sparholt, 1995, 42. Sparre, 1991, 43. Tjelmeland and Bogstad, 1998, 44. Colomb et al., 2004, 45. Shin and Cury, 2001, 46. Bertignac et al., 1998, 47. Lehodey et al., 2003, 48. Lehodey et al., 2008, 49. Tjelmeland and Lindstrøm, 2005, 50. Bax, 1985, 51. Plagányi and Butterworth, 2006, 52. Sekine et al., 1991, 53. Hamre and Hatlebakk, 1998. 38

1.4 Alphabetical list of models used in the ecosystem approach of fisheries (PART 2/2). Revised from (Plagányi, 2007). References are: 1. Fulton, Smith and Johnson, 2004, 2. Fulton et al., 2005, 3. Yodzis and Innes, 1992, 4. Yodzis, 1998, 5. Koen-Alonso and Yodzis, 2005, 6. Bogstad et al., 1997, 7. **?**, 8. Butterworth and Thomson, 1995, 9. Mori and Butterworth, 2004, 10. Mori and Butterworth, 2005, 11. Mori and Butterworth, 2006, 12. Thomson et al., 2000, 13. Constable, 2006, 14. Baretta-Bekker et al., 1997, 15. Livingston and Methot, 1998, 16. Hollowed et al., 2000, 17. Tjelmeland and Lindstrøm, 2005, 18. Christensen and Pauly, 1992, 19. Christensen and Walters, 2004, 20. Polovina, 1984, 21. Walters et al., 1997, 22. (Walters et al., 2000), 23. Begley and Howell, 2004, 24. Trenkel et al., 2004, 25. Taylor and Stefánsson, 2004, 26. Taylor and Taeknigardur, 2011, 27. Finnoff and Tschirhart, 2003, 28. Finnoff and Tschirhart, 2008, 29. Alonzo et al., 2003, 30. DeAngelis and Gross, 1992, 31. Purcell and Kirby, 2006, 32. Shin and Cury, 2004, 33. Fulton, Smith and Johnson, 2004, 34. Fulton, Parslow, Smith and Johnson, 2004, 35. McDonald et al., 2006, 36. Watters et al., 2005, 37. Watters et al., 2006, 38. Punt and Butterworth, 1995, 39. Jurado-Molina et al., 2005, 40. Garrison et al., 2010, 41. Sparholt, 1995, 42. Sparre, 1991, 43. Tjelmeland and Bogstad, 1998, 44. Colomb et al., 2004, 45. Shin and Cury, 2001, 46. Bertignac et al., 1998, 47. Lehodey et al., 2003, 48. Lehodey et al., 2008, 49. Tjelmeland and Lindstrøm, 2005, 50. Bax, 1985, 51. Plagányi and Butterworth, 2006, 52. Sekine et al., 1991, 53. Hamre and Hatlebakk, 1998. 39

2.1 A) Permanova based on Sperman rank correlation distance matrix of whole dataset and B) pairwise tests (Only significant tests are reported; Monte Carlo significance within brackets if differs from permanova's). (ns: not significant; *: < 0.05,**: < 0.01, ***: < 0.001). Factors: habitat (levels: CAN, SLO) and water column condition (levels: homogenized, HOM, and stratified, STR) 56

2.2 One way SIMPER analysis (factor used: habitat) based on Bray-Curtis similarity (cut-off: 80%). Percentage contribution and cumulative percentage of taxa are reported for each level of the factor, as well as the acronyms of taxa used as labels in CCAs. AM: amphipoda, PO: polychaeta,IS: isopoda, SI: sipuncala, EC: echinodermata, BI: bivalvia, CA: caudofoveata, CU: cumacea. 57

2.3 GAMs for A) the total biomass of the macrofauna, B) Polychaetes' biomass C) Crustaceans' biomass and D) Molluscs' biomass. For each response, the right side of the model, the significance of the effect, the GCV, the AIC, the adjusted r-squared (R2) and the deviance explained (DE) are given. 63

2.4 List of species (PART 1/3). Mean number of specimens (ind/m^2) collected from canyon adjacent slope. 71

2.5 List of species (PART 2/3). Mean number of specimens (ind/m^2) collected from canyon adjacent slope. 72

2.6 List of species (PART 3/3). Mean number of specimens (ind/m^2) collected from canyon adjacent slope. 73

3.1 List of variables. Differences between pairs of categories of the variable *month* were checked through Tukey HSD test. Non-significantly different categories were grouped to create the new variable *period*, to which the same test was applied. The same procedure was applied for the variable *code*, to create the variable *group* (all significant tests with $p \leq 0.001$). 83

3.2 Model construction. N, number associated with each model; model, models right part of the formula; df, models degree of freedom; RD, residual deviance, DE, percentage of deviance explained by each model; AIC, Akaike Information Criterion; term(ns), insignificant terms in a model; term (+), terms not incorporated in next steps (i.e. models with the incorporation of *hp* or *fprice* gave a lower DE than the incorporation of *grt* and *time*, respectively). Model 12 is the model used for standardization. 89

3.3 Results of the final model (Equation 3.4). Results associated with (a) linear terms, (b) smooth terms and (c) global estimations. μ: estimation of the mean; σ: standard deviation; t: value of t-statistic; F: the F-statistic value; p: p-value associated to the t or the F statistic; DE: deviance explained by each term in percentage; *edf*: effective degrees of freedom; λ: estimated smoothing parameter; *df*: total degree of freedom; *scale*: estimation of the scale parameter; R^2(adj): adjusted R-squared; AIC: Akaike Information Criterion; GCV, generalized cross validation; DE_{tot} (%): percentage of total deviance explained by the model. 90

4.1 List of variables. 105

4.2 Global scores of selected models. M: model coding; A: the assumed distribution is log-normal (LG) or gamma (GA); B: (LO) the location varies w.r.t. explanatory variables while the second parameter is constant or (LS) both vary; C: if the unit-specific effect is considered as fixed, thus the model has only fixed effects (FI) or random and the model is a mixed effects model (MI); DEV, the residual deviance; EP: Effective total number of Parameters, DIC: Deviance Information Criterion, MSEP, mean and sd of the mean square error of predictions calculated through 10-fold validation. 111

4.3 Estimations of linear fixed effects for the model M8, Eq. (4.3) associated to A) μ and B) σ respectively. 115

5.1 Main information about sampling statios: 1) the code of each stetion, 2) the position, 3) the depth and 4) the syear. 130

5.2 Standing stocks of the food web compartments for the soft bottom slope food web. The binary structure is defined in Section 5.2.6 and quantified by data available in Section 5.2.2. A) Compartments' name, B) Abbreviation used through the text, C) Stock values (mean, mmol C m^{-2}), D) Origin of data: A=ANTROMARE B=BIOMARE, E) Number of samples. (*) Excluding megaichthyofauna and *A. antennatus*. (**) % C_{org} in sediment (gDW). 136
5.3 Derived global estimations, $[min, max]$, (mmol C m^{-2} d^{-1}) of important processes in the food web. 150
5.4 Derived estimations of flows related to the red shrimp fishery, $[min, max]$. (A) expressend in mmol C m^{-2} d^{-1}; (B) expressed in Kg km^{-2} y^{-1}; (C) expressed in Kg $boat^{-1}$ d^{-1}, here d is "working day" and has the same units of LPUE in Chapters 3 and 4. F_t is the total fishing rate; F_a is the portion of fishing pressure on red shrimp; F_i is the portion of fishing pressure on the fish stock; F_b is the portion of fishing pressure on invertebrates. 151
5.5 The trophic level and omnivory index (mean ± sd) for all living components. 152

6.1 Relationship investigated. 169
6.2 List of indicators (response variables) and their description. 170
6.3 Couples of components between which the $shift$ occurs. 177
6.4 Possible pathways of trophic cascade.MLT = mid trophic levels, AANT, ICT and MEBN, LTL = lower trophic levels, MABN, SBN and ZPL. * Jointly. ** Jointly or all subsets.*** Jointly or MEBN (Does not make sense consider other subsets because the biomasses are very close to the following trophic level). 177

D.1 Global scores for LN models. 1a) fixed effects models with predictor η_μ, 1b) fixed effects models with predictors η_μ and η_{σ^2}, 2a) mixed effects models with predictor η_μ, 2b) mixed effects models with predictors η_μ and η_{σ^2}. PRED: specifies the predictor, and VAR: defines the variables in the corresponding predictor. DEV: residual deviance; EP: Effective total number of Parameters, DIC: Deviance Information Criterion. Models without global scores could not be estimated (see the corresponding Chapter). 220
D.2 Global scores for GA models. 1a) fixed effects models with predictor η_μ, 1b) fixed effects models with predictors η_μ and η_σ, 2a) mixed effects models with predictor η_μ, 2b) mixed effects models with predictors η_μ and η_σ. PRED: specifies the predictor, and VAR: defines the variables in the corresponding predictor. DEV: residual deviance; EP: Effective total number of Parameters, DIC: Deviance Information Criterion. Models without global scores could not be estimated (see text). 221

E.1 Constraints imposed to the model. (A) TOM compartment, (B) Faunal compartments, (C) Diet constraint (only for the red shrimp). A: assimilation, R: respiration, U: Uptake. SOC = sediment oxygen consumption; BE = burial efficiency; RR = respiration rate; NGE = net growth efficiency; AE = assimilation efficiency; MR = maintenance respiration; PR = production rate; DP = proportion of source j in the diet of predator j. 230

E.2 Equations of the binary food web and steady-state assumption incorporated in the food web model. 231

E.3 Parameters and constrains for the food web model. In brackets minimum and maximum values of parameters are reported, while single values correspond to the mean of parameters. $Tlim$ = temperature limitation; SOC = sediment oxygen consumption; BE = burial efficiency; RR = respiration rate; NGE = net growth efficiency; AE = assimilation efficiency; MR = maintenance respiration; PR = production rate; DP = proportion of source j in the diet of predator j; FR = fishing rate; CR = catch rate. References: (1) Epping et al., 2002, (2) Own data from ANTROMARE survey, (3) Burdige et al., 1999, (4) van Oevelen et al., 2006 and references therein, (5) Mahaut et al., 1995, (6) Company and Sardà, 1998, (7) van Oevelen, Soetaert, García, de Stigter, Cunha, Pusceddu and Danovaro, 2011, (8) Cartes, Brey, Sorbe and Maynou, 2002, (9) Own data from BIOMARE survey, (10) Fauchald and Jumars, 1979, (11) Cartes, Papiol and Guijarro, 2008, (12) From longitudinal data of the Catalan government. 232

E.4 Food web flows' estimations: range (minimum and maximum), least distance and least square (mean) solutions. Flows in mmol C m^{-2} d^{-1}. 234

E.5 MCMC (mean and standard deviation) solution and Coefficient of Variation (CoV) for the food web flows. 235

E.6 Nomenclature of symbols used in calculation of network index equations (Table E.7). Revised from Kones et al. (2009). 236

E.7 Network Index formulas (PART 1/2). See Table E.6 for the definition of terms. References: (1) Hirata and Ulanowicz, 1984, (2) Latham II, 2006, (3) Kones et al., 2009, (4) Pimm and Lawton, 1980, (5) Finn, 1976, (6) Finn, 1980, (7) Patten and Higashi, 1984, (8) Allesina and Ulanowicz, 2004, (9) Ulanowicz, 1986, (10) Ulanowicz and Norden, 1990, (11) Ulanowicz, 2004, (12) Ulanowicz, 2000, (13) Christensen and Pauly, 1992, (14) Lindeman, 1942. Revisited from ref. 3. 237

E.8 Network Index formulas (PART 2/2). See Table E.6 for the definition of terms. References: (1) Hirata and Ulanowicz, 1984, (2) Latham II, 2006, (3) Kones et al., 2009, (4) Pimm and Lawton, 1980, (5) Finn, 1976, (6) Finn, 1980, (7) Patten and Higashi, 1984, (8) Allesina and Ulanowicz, 2004, (9) Ulanowicz, 1986, (10) Ulanowicz and Norden, 1990, (11) Ulanowicz, 2004, (12) Ulanowicz, 2000, (13) Christensen and Pauly, 1992, (14) Lindeman, 1942. Revisited from ref. 3. 238
E.9 Estimations of network indices. A) Basic properties and Pathway analysis; B) Network uncertainty and constraint efficiencies; C) Environmental analysis. 239
E.10 Indices of system growth and development. 240

To Virginia, Dimitri, Eleonora and Vittorio
and all children of my cousins and dear friends.

Look forward bringing the awareness of the past.

1

General introduction

1.1 Justification of the study

Deep sea occupies more than two-thirds of the Earths surface of which a very small fraction has been investigated. Deep sea remains still largely unexplored in terms of biota and their spatial and temporal dynamics. Studies have been directed toward interesting habitats such as the canyons crossing the slope (Vetter and Dayton, 1998), the seamounts (de Forges et al., 2000), the mid-ocean ridges and the hydrothermal vents (Van Dover, 1995; Van Dover et al., 2002).

In recent decades the interest towards deep-sea ecosystems increased due to warnings about fisheries impacts. Researchers realised that fishing in the deep sea might affect or already has affected these widely considered fragile ecosystems (in the North Atlantic: Gordon, 2001; Koslow et al., 2000; in the Mediterranean: Moranta et al., 2000; Politou et al., 2003). Many deep-sea species show k-selection (and so fragile) characteristics: longevity, late age at maturity, slow growth and low fecundity, leading to an exceptionally low productivity (Devine et al., 2006). The consequences are high vulnerability to overfishing and potentially little resilience to overexploitation (Koslow et al., 2000). Examples of fragile species are the Blue ling (*Molva dypterygia*) and the roundnose grenadier (*Coryphaenoides*

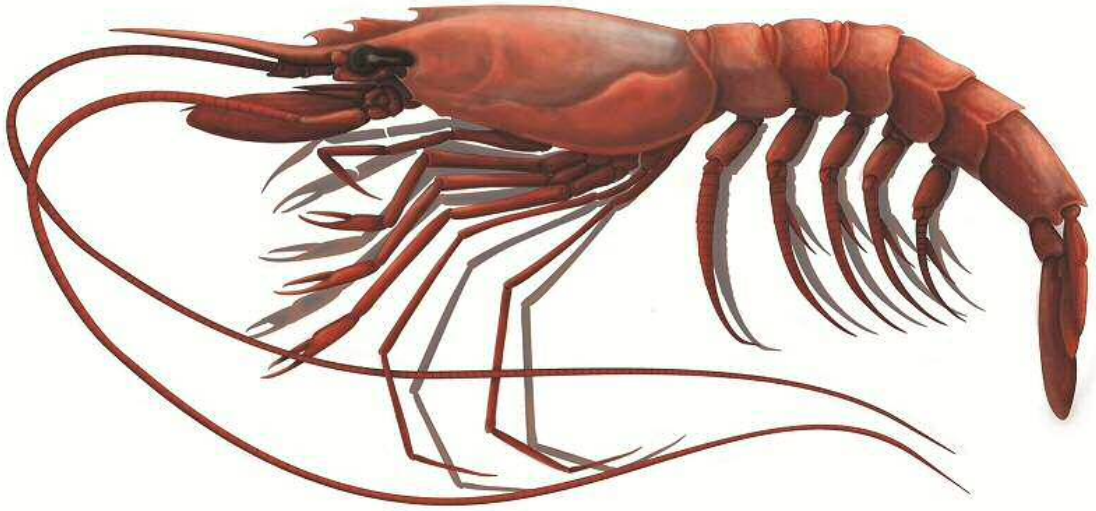

FIGURE 1.1: The red shrimp *Aristeus antennatus* (Risso, 1816).

rupestris) harvested in the Atlantic and Norwegian Sea. Another example is the orange roughy (*Hoplostethus atlanticus*) usually fished in Australian waters (Gordon, 2001; Koslow et al., 2000), whose vulnerability depends on its practice to concentrate in restricted areas, i.e. the high aggregation on seamounts (Gordon, 2001).

In the Mediterranean, harvested deep-sea species are mainly represented by crustaceans decapoda, such as the deep-water shrimps *Aristeus antennatus* (Figure 1.1) and *Aristeomorpha foliacea*, while among fishes and cephalopods there are *Lophius* spp., *Phycis* spp., *Merluccius merluccius* and *Illex coindettii* (Politou et al., 2003). They represent a moderate part of the deep-sea landings. By-catch examples without any economic interest are macrourids, e.g. *Nezumia* spp. (Figure **??**) and *Hymenocephalus italicus*, and sharks, such as the lantern shark *Etmopterus spinax* and *Galeus melastomus* (Figure **??**). Sharks are top predators and more likely present k-selectivity behaviour and their decline in abundance has been demonstrated in the Mediterranean by Cartes, Fanelli, Lloris and Matallanas (2013); Ferretti et al. (2008); Maynou et al. (2011). The causes probably rely on a combination of direct human impacts that have grown in intensity in the 20th century and the intrinsic characteristics of this fauna, as mentioned above, such as slow growth rates, high longevity (e.g. 20 years in *E. spinax*: Coelho and Erzini, 2008), low fecundity and high trophic position (Dulvy et al., 2003; Ferretti et al., 2008; Myers and Worm, 2005). Recently the same k-characteristics have been proved in the production of macrourid fishes (Fernandez-Arcaya et al., 2013). On the contrary we should be aware that not all declines are due to overfishing. For example has been argued that the local extinction of the deep-water shrimp *A. foliacea* is probably due to the warming and salinization of Mediterranean deep waters as a consequence of the decreased freshwater flow from the Nile since the completion of the High Aswan Dam in 1964 (Cartes, Maynou and Fanelli, 2011).

In any case, threats of fishing in deep-sea environments engrave on the target and by-catch species and probably on other components of the system and its dynamics through indirect mechanisms. One of the clearest impacts of deep water fisheries has been demonstrated on benthic habitats, because these fisheries are almost represented by large trawling boats, notoriously destructive of the seabed, influencing the biomass and the structure of communities (see e.g. Cartes et al., 2009).

An holistic approach to investigate possible damages on ecosystem functioning is to analyse the energy flows and their changes after external perturbations. Changes in flows are strictly related to changes in biomasses. For example, the impact of excessive fishing effort on predators jointly with unfavourable state of the environment, can cascade down to lower trophic levels of the food web, affecting such populations and/or the whole ecosystem, with the selective reduction or expansion of some trophic guilds (e.g. Casini et al., 2008; Reid and Croxall, 2001). This top-down control has been documented in many near-shore ecosystems as well as other types of control.

In bathyal systems these phenomena have not been documented yet for the paucity of data. The identification and quantification of functional interactions between biological components are the basis to eventually predict the response of the system to fisheries. This goal is strongly hampered by the lack of high-quality empirical data in deep-sea ecosystems (e.g. Brown and Gillooly, 2003), being direct measurements or experimentations notoriously difficult even for comparatively well studies shallow water ecosystems (van Oevelen et al., 2006). Nevertheless, an ecosystemic approach is urgently needed because human pressures are increasing more rapidly than our understanding of the systems being exploited (Glover and Smith, 2003), in line with the ecosystem approach to fisheries (**EAF**) framework (see paragraph on EAF for more details on existing models). Traditional marine research investigates isolated parts of the ecosystem, while mathematical models can merge this fragmentary information into an integrative framework. Food web modelling (i.e. ECOPATH and LIM) developed in last decades (e.g. Angelini and Agostinho, 2005; Coll, Lotze and Romanuk, 2008; van Oevelen et al., 2009; Vézina and Savenkoff, 1999; Woodward et al., 2005) can identify the missing information to improve research in this direction.

The final objective of this Ph.D. thesis is to quantify the effects of fishing activity (usually referred to as a top-down control) in the food web of a bathyal ecosystem (NW Mediterranean) accounting also to bottom-up processes such as the entry of energy to the system. The top-down control usually might evolve into trophic cascade i.e. alteration of the relative abundances between predator and prey. So, what does happen in bathyal ecosystems when the abundance of the main harvested species (the red shrimp) decreases? Which is its role?

This is exemplified by the in-depth study of the exploited continental slope ecosystem in the Catalan sea, where the important fishery of the highly priced red shrimp

(*Aristeus antennatus*) is carried out and the trophic web structure is relatively well documented (e.g., Carrassón and Cartes, 2002; Cartes et al., 2009; Fanelli, Cartes and Papiol, 2011).

Concrete objectives are:

1. Identify and fill important lacks to built up the food web. No quantitative data of deep-sea infauna (macrobenthos) were collected in the study area before this thesis, however the infauna is a key component of benthic pathways. Similarly any knowledge about oxygen consumption of sediment (SOC) was available.

2. Describe the red shrimp fishery, in terms of landings, at least to understand which are the influential factors affecting landings and so the abundance variability of the species.

3. Describe the bathyal food web and dynamically simulate top-down and bottom-up effects, considering the red shrimp as the key species of the model. The simulation study is mandatory being time series unavailable.

1.2 Food webs and trophic cascades

1.2.1 Food webs: concepts and models

Since 70s when networks were imported from physic and social sciences into ecology biologists have become increasingly interested in describing and analysing the trophic dynamics of ecosystems (Lindeman, 1942; Odum, 1957). In 2010 the 5% of scientific production in ecology included the word "network" in title, abstract or keywords (Heleno et al., 2014). These studies have shown a promising approach for deepening our understanding of ecological processes in ecosystems (O'Neill, 1969). Now significant progresses are making in e.g. moving from static to temporal dynamic networks and using network analysis as a practical conservation tool (Heleno et al., 2014).

Food webs (who eats whom) describe the exchange of matter among different compartments within a community or more generally within an ecosystem when also abiotic components are included. The exchange (or transfer) is represented

by a flow from a component to another and it can be measured as organic matter (wet or dry weight), energy (joule) or as an element, C, N, P (mole) transferred in a given unit of time. For instance, the latter is used to draw the elements' cycles.

A common categorization of food webs is through the origin of energy they belong to. Usually they are divided into two categories: 1) based on primary production or 2) based on detritus. Another possibility is the combination of both. This is a convention used in understanding pathways and define different modes of organisation as well as different dynamics. Primary producer based webs start with one or more primary producers that take energy incorporated in inorganic compounds and make it available for all other consumers as organic matter. Detritus based webs start with one or more forms of nonliving organic matter that originates outside the system (allochthonous source) or produced by system's components e.g. faeces (autochthonous source).

In theoretical ecology food webs can be described qualitatively, quantitatively and through the function of its components. The basic (qualitative) description is through the "binary" food web, that defines the structure of the interacting components, i.e., if a flow exists or not between each component of the web. In practise applied researchers have been classified the components (single species or functional groups) through the size (e.g. for the benthos in Table 1.1), because in general the bigger eats the smaller. It is also a good practical method because abundance data are typically collected in distinct size classes (especially for macrofauna and below) and weight-specic physiological processes scale with body size.

The literature is full of theoretical studies on binary food web models. For a given number N of species S_i, $i = 1, \ldots, N$ and links L, a binary food web can be represented as a $N \times N$ matrix $\mathbf{S}$, where if the species i (in rows) is a prey of species j (in columns), then element $s_{i,j} = 1$ otherwise $s_{i,j} = 0$. Theoretical

Size class	Size ranges	typifying groups
Bacteria	0.5 - 4 μm	aerobic, anaerobic, chemo-autotrophs, fermenters
Microbenthos	< 63 μm	agellates, ciliates
Meiobenthos	63 - 500 μm	nematodes, foraminifera, ostracods
Macrobenthos	0.5 - 20 mm	polychaetes, bivalves, peracarids, echinoderms
Megabenthos	> 2 cm	crustacean decapods, fish, cephalopods

TABLE 1.1: Size-based classication of benthos with size range and main groups (examples) in each size class.

ecologists have suggested simple rules to generate binary food webs, based on theoretical distributions for L or some other parameter in more complex models, e.g. the assumption that $L \in U(0,1)$ (the uniform distribution) in the simplest case. Currently existing models are: the random, the cascade, the niche and the nested-hierarchy models (Cattin et al., 2004; Cohen and Newman, 1985; Williams and Martinez, 2000). The two latter models describe more realistic food webs. Examples of binary food webs are shown in column (A), Figure 1.2. But, species interactions are only feasible (can exist) if enough energy is transferred to the predator. To assess the "energetic feasibility", a food web needs to be quantified. Also the qualitative feasibility of a food web can be assessed, however it needs and gives less information (Moore and de Ruiter, 2012). The quantification generates a $N \times N$ flow matrix $\mathbf{X}$, whose elements $x_{i,j}$ are estimates of the magnitudes of the feeding flows. The corresponding quantified food webs of the examples given in column (A) are shown in column (B) of the same Figure 1.2. It can be observed that not all binary models return quantitative solutions, so they are not feasible, such as the case of the random model in (1).

These "quantified food webs" represent a gateway to achieve a quantitative understanding of the functional interactions between biological (and when possible abiotic) components, in order to eventually predict the response of the system to anthropogenic and environmental forces. It can be argued that quantification of flows should need a good knowledge of the structure of the food web under study, however in most cases it is impossible. In fact, the quantification of biological interactions is strongly hampered by the lack of sufficient high-quality empirical data, because the elucidation of food web flows from direct measurement or experimentation is notoriously difficult (e.g., Brown and Gillooly, 2003; van Oevelen et al., 2006). For example, deep-water data sets are emblematic of under-sampled food webs. To overcome these data limitations and extract as much information as possible from them, modelling of real food webs have been developed, e.g. through linear inverse techniques (e.g., Angelini and Agostinho, 2005; van Oevelen et al., 2009; Woodward et al., 2005).

Mathematical models used for quantification are based on the first and second lows of thermodynamics, possible through the so called mass balance equations (O'Neill, 1969). The main concept is that all energy must be taken onto account and all the energy loss from a component must flows to other components. The assumption of steady state is essential for the basic design of the model. However the equilibrium in real systems is seldom fulfil, it is reasonable considering the

average compartment size as constant when the interval of time is properly chosen (O'Neill, 1969).

Each mass balance describes the rate of change of a compartment in terms of difference between inputs and outputs. Dropping the i, a mass balance example of a living compartment S (same function of species in the above described binary food webs) could look like

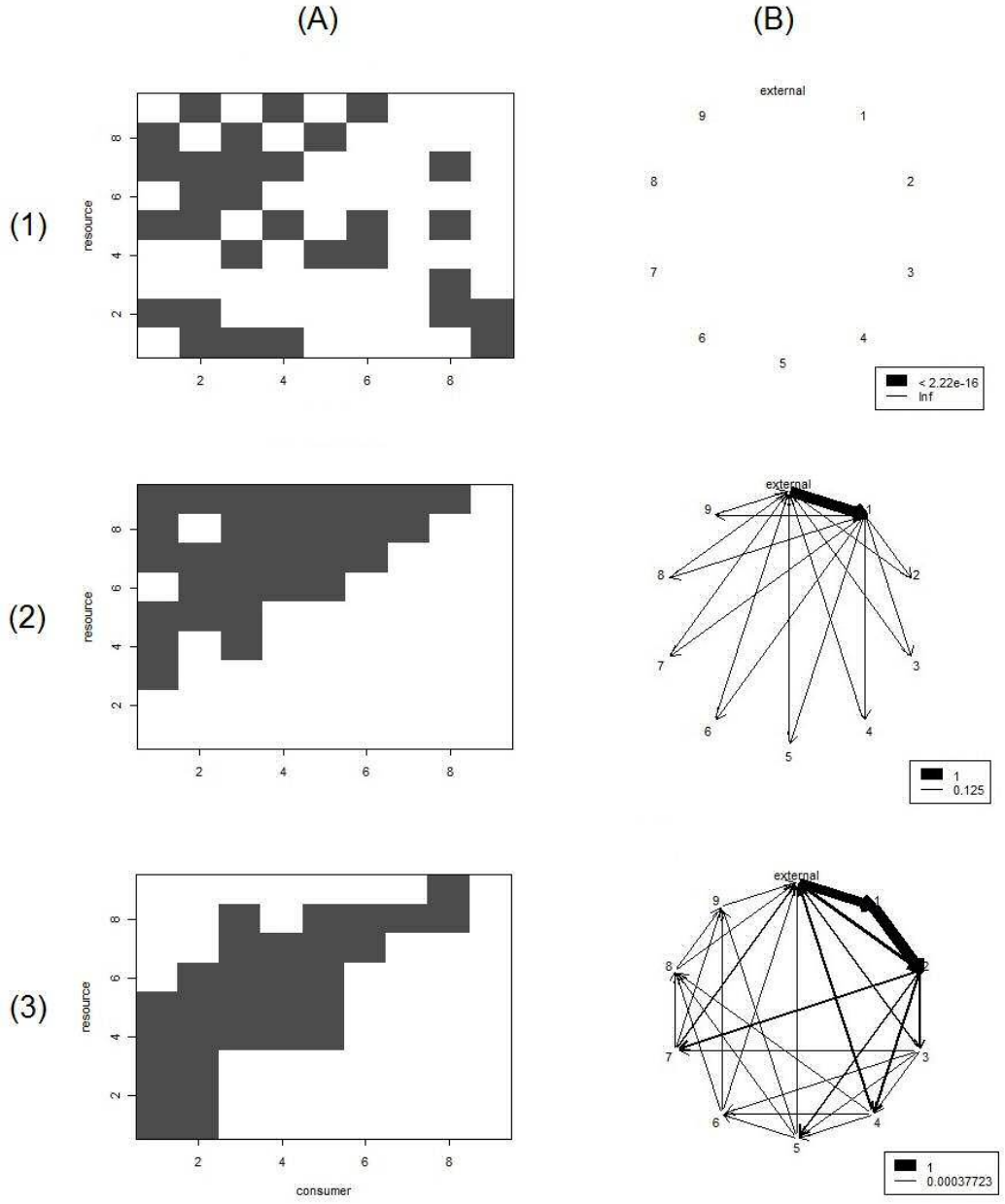

FIGURE 1.2: Three examples of theoretical food webs. In columns: (A) binary and (B) quantified food webs. In rows: (1) Random model, (2) Cascade model and (3) Niche model with $N = 9$ compartments S and $L = 30$ number of links.

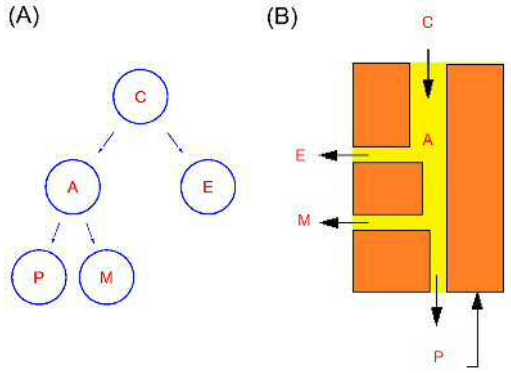

FIGURE 1.3: The fate of consumed energy for a given component (or an individual). Symbols represent: C = energy consumed, A = energy assimilated, E = the egested energy, P = the produced energy, M = the energy used for maintenance.

$$\frac{dS}{dt} = G_c - (L_e + L_m + L_p) \tag{1.1}$$

where G_c is the gain of mass by consumed (ingested) energy, L_e is the loss through egestion (or unassimilated energy), L_m is the loss due to metabolic activity and L_p is the loss due to predation by other compartments. In a steady-state model the derivative of S with respect to the time t is $dS/dt = 0$ (S does not change in time). Usually models consider the energetic efficiency, e, of trophic interactions as the product of the assimilation efficiency, a, and the production efficiency, p or also expressed by the ratio of the new energy produced, P (in form of individual growth or reproduction) to the energy consumed, C,

$$e = a \times p = \frac{P}{C}. \tag{1.2}$$

Equation 1.2 implies that $0 \leq e \leq 1$, otherwise the population dies. The portion of energy of a prey consumed by a predator that is not assimilated (e.g. faeces) and the assimilated portion that is mineralized (i.e. maintenance respiration) is

$$1 - e = \frac{E + M}{C} \tag{1.3}$$

where E represents the egested (unassimilated) energy and M is the energy used for maintenance (maintenance respiration).

Figure 1.3 shows the fate of consumed energy for a given component and can be divided into three main processes: assimilation, production and mineralization that occur in two steps. The first considers that the consumed biomass (C) is divided into assimilated (A) and unassimilated (E) biomass. So, the assimilation efficiency is

$$a = \frac{A}{C}. \tag{1.4}$$

The proportion of the unassimilated portion, $1 - a$, is

$$1 - a = \frac{E}{C}. \tag{1.5}$$

The portion E returns to the surrounding through different processes, and refers only to organic material, it is not lost to the environment and serves to other livings as energy source. This different forms of unassimilated organic compounds are autochthonous inputs to detritus and return to the labile or refractory detritus depending on their respective C:N ratios. They also can leave the system if they are allochthonous source for other systems. So, the assimilation efficiency can vary depending on the quality of the source.

The second step refers to the assimilated portion, that is transformed into new energy, i.e. production, or it is mineralized in e.g. CO_2. Thus,

$$p = G + \frac{R}{A} \tag{1.6}$$

and

$$1 - p = \frac{M}{A}. \tag{1.7}$$

For example, the organic carbon is mineralized in different forms of dissolved CO_2. e.g. carbonate or bicarbonate, and the organic nitrogen in ammonium which represent the corresponding "waste". Taking into account both a and p the energy efficiency in Equation 1.2 can be then fully defined. The energy budget scheme described in Figure 1.3 and Equations from 1.2 to 1.7 can be further partitioned, for example P into production for growth and production for reproduction, that are

respectively associated to the respiration for maintenance and respiration during reproductive period. Thus, the scheme is a simplification, but to date the assessment through sensitivity analyses leads to believe that the impact is relatively small (Moore and de Ruiter, 2012). All modelling approaches consider these basic assumptions or some reasonable modification. Very common is the use of matrix calculation, such as in the linear inverse modelling (LIM), used in the present thesis. For each component S_j the main equation in a LIM is

$$\frac{dS_j}{dt} = \sum flow_{i \to j} - \sum flow_{j \to k} \tag{1.8}$$

where the arrows define connections between each component S_j and his sources or prey with incoming ($flow_{i \to j}$) and outgoing flows ($flow_{j \to k}$) and such relationships are fixed. When the model describes the variation of the biomasses in time,

$$\frac{dS}{dt} \neq 0,$$

the system shifts to a dynamic problem. In this case, the relationships are not fixed and are functions of e.g. the state variables (s = biomass), parameters (p^1 and p^n) and the time (t), such that

$$\frac{ds}{dt} = \sum f(s, p^1, t) - \sum f(y, p^n, t). \tag{1.9}$$

Figure 1.4 represents the dynamic output of the simulation made for all species of the niche food web in row (3), Figure 1.2. The black line represents the stable unperturbated biomasses, while red and green lines show respectively negatively and positively perturbed biomasses (the half or the double of the original biomasses).

As introduced at the beginning of the Chapter different types of perturbation can influence the system, such as fishery and environmental factors among others. The impact can engrave the component directly involved in the perturbation (i.e. the harvested species) but also other components positioned more or less away from the origin of the disturbance in the network (e.g. distant one or more trophic levels from the affected species). The change in relative biomass can be used as a measure of the effect of the perturbation and associated mechanisms are e.g. trophic cascades and phase shifts.

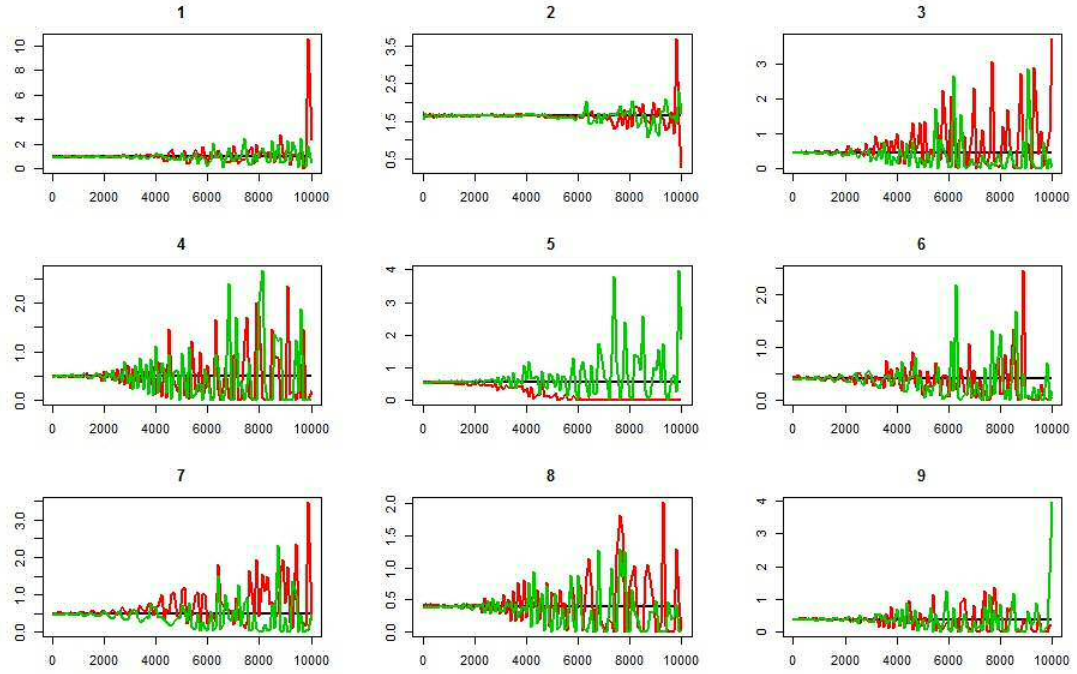

FIGURE 1.4: Output of the dynamic simulation for the niche food web in Figure **??**, C. The time span is 20 years and plot, headed by a number from 1 to 9, corresponds to each species of the food web. On the y axis are shown the biomasses. Dark: unperturbed biomass; red: biomasses perturbed by 1/2 of the original value; green: biomass perturbed by 2 of the original value.

1.2.2 Trophic cascades and other mechanisms

The term was coined by Paine (1980) to describe the alteration in abundances of lower rungs after the loss of apex predators. It has been then applied to the three-trophic levels, (the Green World Hypothesis, GWH, proposed by Hairston et al., 1960 in terrestrial ecosystems) and then generalized to systems of one to five trophic levels, as in the Exploitative Ecosystem Hypothesis (EEH) of (Fretwell, 1987). Strictly defined (Menge, 1995; Strauss, 1991), trophic cascades are predatory interactions involving three trophic levels, e.g. primary carnivores, by suppressing herbivores, increase plant abundance. Although cascade-type effects have been reported to extend through four or more trophic levels (e.g. Carpenter and Kitchell, 1988). Over the past 50 years the debate on the existence and importance of trophic cascades has produced numerous analyses. Experimental studies have addressed this subject in a variety of habitats, in terrestrial (e.g. Spiller and Schoener, 1994) and aquatic ecosystems, such as lakes and streams (Carpenter et al., 1985, 2001; Scheffer et al., 1993), near-shore systems (Estes et al., 1998)

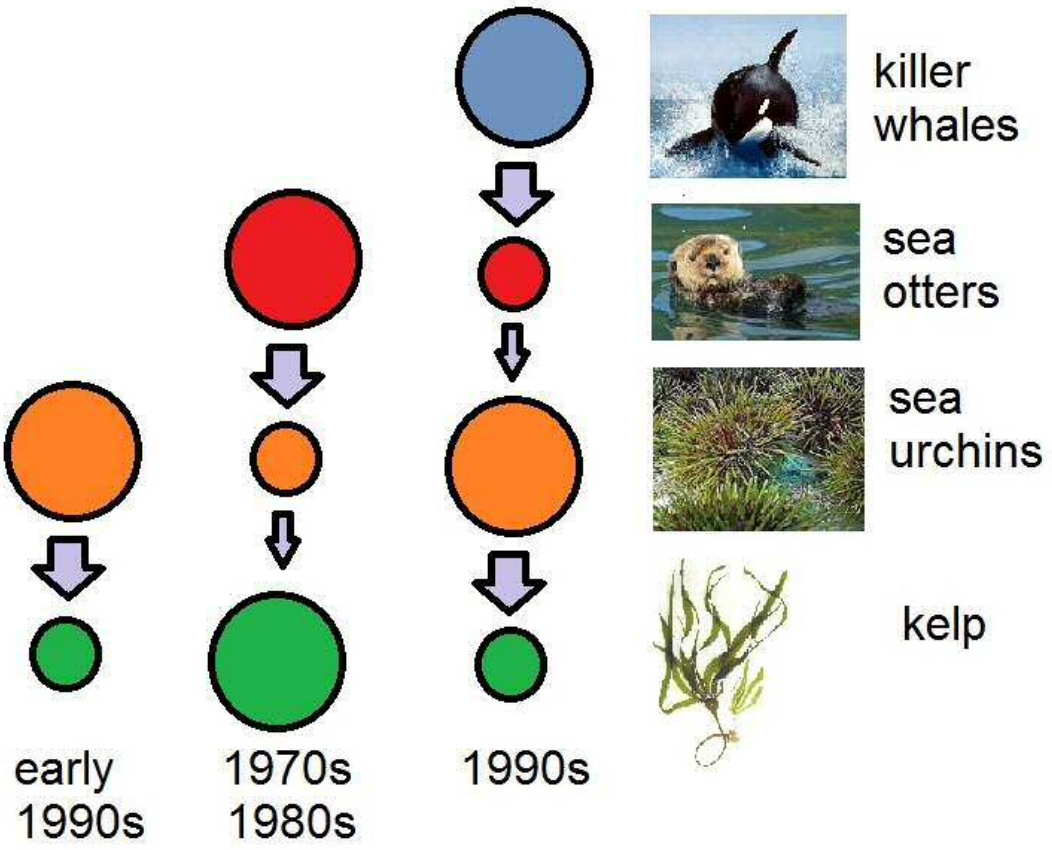

FIGURE 1.5: Example of the trophic cascade between otter, sea urchin and kelp (then also extended to killer whale) in the ecosystem of the Aleutian Islands (Alaska, USA) (Estes et al., 1998).

and open ocean (Casini et al., 2008; Jackson et al., 2001; Scheffer et al., 2001; Shiomoto et al., 1997).

In the literature there is a predominance of aquatic cases of trophic cascades, something that led Strong (1992) to assert "trophic cascades are all wet" and the mechanism is prominent in simple food chains. In more diverse ecosystems with spatial heterogeneity and trophic specialisation, trophic cascades were hypothesised to be less evident because buffered by complex interactions (Strong, 1992). Nowadays, conscious of the complexity held by ecosystems, we do not even refer to simplified trophic chains (although in some cases it is still a good approximation, e.g. in some pelagic ecosystems) but to trophic networks, hence trophic cascading refers to the effects of one component on another component n-trophic levels far, that may trickle across the entire web till its basis.

A famous example of trophic cascade is the interactions between otter, sea urchin and kelp (then also extended to killer whale) in the ecosystem of the Aleutian

Islands (Alaska, USA) described by Estes et al. (1998) (Figure 1.5). The sea otter (*Enhydra lutris*) was abundant before the unregulated exploitation performed across the North Pacific (Kenyon, 1969). Then, after protection in early 1990s, was able to recover reaching in 1970s maxima abundances in few areas but was completely absent in others (Rotterman and Jackson, 1988). In the areas without *E. lutris* (also in early 1900s), the populations of sea urchin *Strongylocentrotus polyacanthus* grew and kelp forest declined. Conversely, zones with sea otter populations, showed low sea urchin populations and high production of kelps (Estes and Palmisano, 1974). Has been hypothesised that suppressing the carnivorous, herbivorous expands its population till algae decline and vice versa. So, the predator acts in a top-down control. Then, during 1990s, another unexpected synchronous decline was observed in otter populations. That synchronism avoids the hypothesis of populations redistribution, on the contrary lines of evidence pointed to increased predation by killer whale (*Orcinus orca*). The most likely explanation is the shift of prey source base for killer whale, that feeds on marine mammals (Felleman et al., 1991), such as Steller sea lions and harbor seals. Both populations collapsed few years before sea otter decline, inducing the feeding shift of the killer whale to sea otter populations, reducing its abundance and in turn restoring sea urchin populations with the consequent depletion of kelp (Figure 1.5).

In the Mediterranean, works concerning possible trophic cascades have a limited history, however they comprise some of the most comprehensive data of any littoral system (Pinnegar et al., 2000). One example is the system sparid, sea urchin and fleshy algae (Sala et al., 1998). The sparid fish eats on sea urchin, that in turn grazes on fleshy algae. In the rocky littoral of the Medes protected areas invertebrate-feeding fish are more abundant compared to sites outside (e.g. Bell, 1983). The sparids (*Diplodus sargus* and *D. vulgaris*) and the wrasse *Coris julis* are the major predators of adults and juveniles respectively of sea urchins, mainly *Paracentrotus lividus* (Sala, 1997*a*). At adjacent non-protected sites with a low density of predatory fish, *P. lividus* populations were shown to be 3-4 times higher (Sala and Zabala, 1996). At these sites, the sea urchins remove large erect algae and induce the formation of coralline barrens. Sala et al. (1998) suggested that the increment of coralline algae may be one symptom of intensive human exploitation. Transition from coralline barrens back to erect algal assemblages is possible when sea urchins are eliminated as has been observed by experimental removal (Nédélec, 1982). Parallel studies found that also epifaunal groups (e.g. amphipods, gastropods, decapods and ophiuroids) became more abundant when

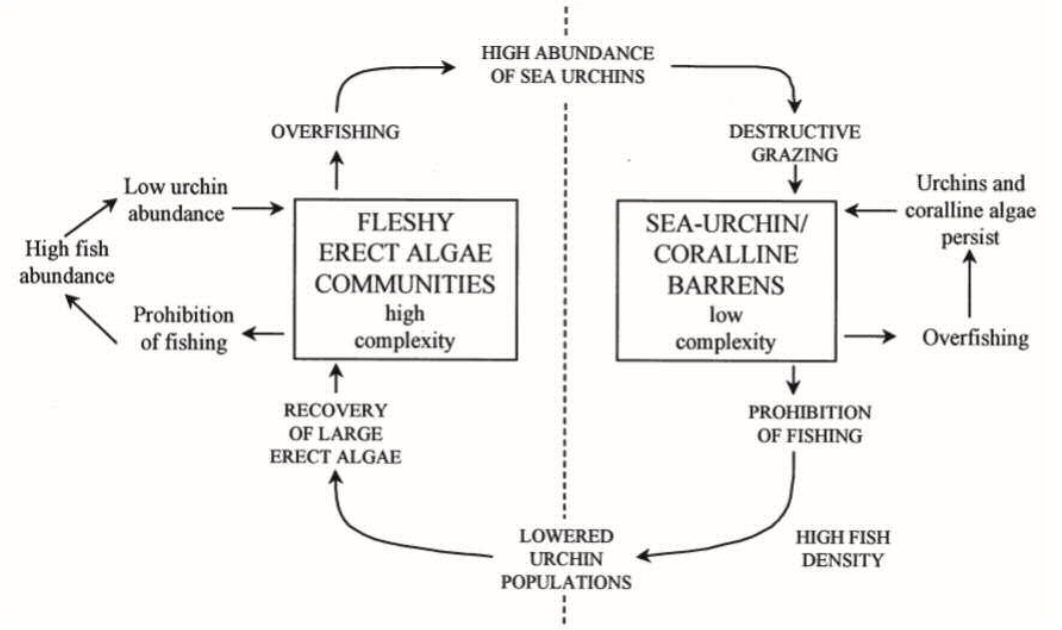

FIGURE 1.6: Description of the hypothesis of two alternative states in the ecosystem nearby the Medes Reserve (western Mediterranean) explainable by mechanisms of trophic cascade. From Pinnegar et al. (2000).

fish were excluded, probably as a consequence of reduced predation and of the increment of fleshy erect algae that provide a structural habitat and food for many of the invertebrates (Sala, 1997*b*).

An energy-based simulation of the Mediterranean rocky-sublittoral system predicted how depletion of invertebrate-consuming fish such as *Diplodus* spp. might result in the dominance of sea urchins, that would dramatically reduce algae, epifauna and gross and net primary production (McClanahan and Sala, 1997). The indication is that once a high population of sea urchins has developed, recovery of those fish that eat algae and epifauna might be slowed or even made impossible because their food resources drop below the minimum threshold necessary for in situ population development (McClanahan and Sala, 1997). In conclusion, two alternative states were described for this ecosystem (Figure 1.6): (1) an overgrazed community with high abundance of sea urchins and low algal biomass with coralline barrens and (2) a "developed" community with an abundance of fish and dominance of fleshy algae (McClanahan and Sala, 1997).

A more recent study (Cardona et al., 2007), performed off northern Minorca (Balearic Islands), found no evidence of trophic cascade for the same ecosystem explained by the limited recruitment of both fish and sea urchins due to the extreme oligotrophy of the area.

Among benthic marine systems, there is comparatively little evidence for trophic cascade in soft bottom communities in shallow waters and are summarised in Table 1.2.

Fishery-target populations may recover after a cessation of fishing activities (Pipitone et al., 2000), but there has been little regard for potential indirect effects on prey species. Caging experiments in shallow soft bottom communities have showed that the exclusion of predators generally results in large increases in density and diversity of infaunal species (Virnstein, 1977). However, because trawls and dredges may inflict considerable physical damage on infauna populations (Kaiser and Spencer, 1996; Prena et al., 1999), the effects of predation and thus observation of any potential trophic cascades may be obscured (see review by Jennings and Kaiser, 1998); populations may even show increases after cessation of trawling, despite increases in their predators. Pipitone et al. (2000) reported an eight-fold increase in fish biomass over the four years following a trawling ban in the Gulf of Castellammare (Sicily, Italy). Biomasses of certain target species such as *Mullus barbatus* increased 33-fold with respect to data collected prior to the closure, however the biomass of cephalopods (excluding *Octopus vulgaris*) declined. This was in agreement with the findings by Pauly (1985) for the Gulf of Thailand. Where predators of squid pre-recruits were common, squid was less common, but as fishing intensified and indeed rays and sawfish virtually disappeared, cephalopods became more important. Similar trends were predicted by Christensen (1998) using a simulation model, where increased fishing pressure resulted in declines of most demersal groups like rays, crabs, lobsters and large piscivorous fish, and, indirectly, increases in some of their potential prey such as cephalopods, scads and shrimp. These "prey-release" predictions also agreed with an observed increase in shrimp recruitment in the Gulf of Thailand by Pauly (1982) following the increase

	Components	Location	ref
1	Humans-fish-cephalopod	Gulf of Castellammare (Italy)	1
2	Humans-large fish-scad/shrimp/cephalopod	Gulf of Thailand	2, 3
3	(Humans-fish-cephalopod)	NW Africa	4
4	(Humans-fish-ophiuroid)	Irish Sea & English Channel	5
5	(Humans-fish-infauna)	Chesapeake Bay (USA)	6

TABLE 1.2: Soft-bottom trophic cascades recompiled from literature. Cascades in parenthesis are based on circumstantial evidence. Ref: (1) Pipitone et al. (2000) ; (2) Pauly (1985); (3) Christensen (1998); (4) Caddy (1983); (5) Aronson (1990); (6) Virnstein (1977).

in fishing pressure and an observed decrease in total shrimp production following a trawl ban in Indonesia (Garcia, 1986).

Another example comes from the coasts of west Africa, where Caddy (1983) argued that the occasional domination by cephalopods (particularly squid) may be a general feature of intensively fished soft-bottom demersal systems. Between 1960-1970 has been observed a relevant increment of cephalopods in catches, simultaneously with a dramatic decline in sparid fishery. Indirect effects through trophic relationships have been hypothesised without suggesting any clear mechanism such as trophic cascade (Caddy, 1983).

On the south-west coast of Great Britain an example involves ophiuroids, that have experienced considerable changes in abundance over the past century (Holme, 1984). Also Aronson (1989) demonstrated that predation pressure on ophiuroids was signicantly lower where fishes and portunid crabs were rare amongst soft bottoms, in comparison with adjacent sites on rocky reefs where potential predators (e.g. fish, crabs and starfish) were relatively abundant. Overfishing along UK and Irish coasts has severely depleted teleost predators, and it has been suggested that this has resulted in a system dominated by echinoderms and crustaceans (Aronson, 1989, 1990, 1992).

Trophic cascades have been found also in a temperate seagrass (*Zostera marina*) community in Sweden through cage experiment coupled with nutrient enrichment (Moksnes et al., 2008). In this work cascades results in high diversified system in contrast with the suggestion that community-wide trophic cascades are unusual and restricted to low-diversity systems with simple trophic interactions (Strong, 1992). They suggest that the interaction strength in the community was strongly skewed towards two functionally dominant components, the algae *Ulva* sp. and amphipod *Gammarus locusta*, consistent. So, it is the number and complexity of only strong interactions that determines whether trophic cascades can develop (Duffy, 2003).

Trophic cascade is a consequence of top-down controls, but more hypotheses of control exist in food web dynamics, such that by the lower reaches of the web and by intermediate species. The first consists of changes in basal species mediated by resource limitations at the basis of the food web, such as plants and phytoplankton (their abundances are driven by physical and chemical forces, e.g. nutrient limitations) and are subjected to a bottom-up control. The trophic cascades sensu stricto are top-down controlled, however Strong (1992) states that in real trophic

cascades top-down influence combines with the always strong bottom-up influence through a food chain (Carpenter and Kitchell, 1988; Oksanen, 1990; Power, 1992). So, it seems that top-down dominance is not the norm and not necessarily all trophic interactions cascade. Strong (1992) argued that among all ecological communities, cascades are restricted to fairly low-diversity areas as mentioned above. Contrariwise, where consumption is highly differentiated the overall effect of trophic cascades is buffered.

DeAngelis (1980) discussed the presence of a particular type of bottom-up control, existing in detritus based food webs, called donor-control. Moore and de Ruiter (2012) explained that when a system is controlled by a donor-control process, the population density and rate of input of the donor has an effect on the consumer population density, whereas the population density and dynamics of the consumer has no direct effect on the dynamics of the donor population or resource.

Finally the last control type consists of population changes in intermediate trophic levels and has been called wasp-waist control (Cury et al., 2000). This kind of control has been found in upwelling ecosystems, where the intermediate trophic level is occupied by small planktivorous fish, usually represented by one or few schooling species, such as sardine and anchovy, that influence the dynamics of predators, such as piscivorous fish, seabirds and mammals, in order of importance (Cury et al., 2000).

It has been suggested that large-scale oceanographic factors may influence the susceptibility of the system to show a trophic cascade. Studies suggest a high spatial variation in trophic forces, as documented comparing different regions of the North Atlantic. At the northern areas top-down control dominates, where species diversity and ocean temperatures are lower, whereas bottom-up control dominates southern areas in warmer waters and biological diversity (Frank et al., 2007, 2006). Southern ecosystems may be more resilient to overfishing because high species diversity facilitates replacement of the overfished species and warmer temperatures support higher demographic rates.

Other examples of all types of mediation have been described and are supported by literature. For example the control of the nutrient P inputs was shown to be effective in mitigating cultural eutrophication working as a bottom-up control (Schindler, 2006). Contrariwise the meta-analysis by Worm and Myers (2003) in the North Atlantic sea tested the consistency of either the "top-down" or the "bottom-up" hypothesis for a well-documented predator-prey couple represented

by the atlantic cod, *Gadus morhua* (an overfished stock) and northern shrimp (*Pandalus borealis*). Their result strongly supported the "top-down" hypothesis. Notwithstanding these results proceeding from a relatively simplified system, in real systems it is difficult to separate the two forces that probably act synergistically or antagonistically. Möllmann et al. (2008) found a species-level trophic cascade involving three trophic levels (copepods-sprat-cod). The decreasing biomass of *G. morhua* is significantly and negatively correlated with the sprat (*Sprattus sprattus*) biomass, indicating top-down control. Trophic cascading proceeded down to the copepod *Pseudocalanus acuspes*, whose biomass time-series is negatively related to the increased sprat stock. The cascading effect over two trophic levels is further demonstrated by the significantly positive relationship between cod and *P. acuspes*. The same authors investigated climate-induced changes at all trophic levels, discovering that the most pronounced changes occurred at the zooplankton and fish trophic levels. In the zooplankton, dominance changed between the copepods *P. acuspes* and *Acartia* spp. as a result of reduced salinities and increased temperatures. The change in hydrography also affected the reproductive success of the major fish species, resulting in a change in dominance from the piscivorous cod to the planktivorous sprat. Thus, both causes probably act together and also induce a "regime shift" of the ecosystem.

1.3 The bathyal domain in the NW Mediterranean sea: energy transfer and faunal composition

Conventionally, the bathyal domain corresponds to the continental slope and the corresponding water masses (Figure 1.7) at the same depths. Some authors refer to the deep sea for waters below the 1000 m, but for others it begins at 200 m depth. Once deep sea (and the bathyal domain) was considered lifeless and without alterations, albeit this viewpoint has been changing throughout last decades. In the Mediterranean sea the bathyal domain matches depths between 200 m where the continental shelf ends, and 3000 m where the abyssal domain starts. The water masses corresponding to the (benthic) bathyal domain are subdivided into meso- and bathypelagic (Figure 1.7).

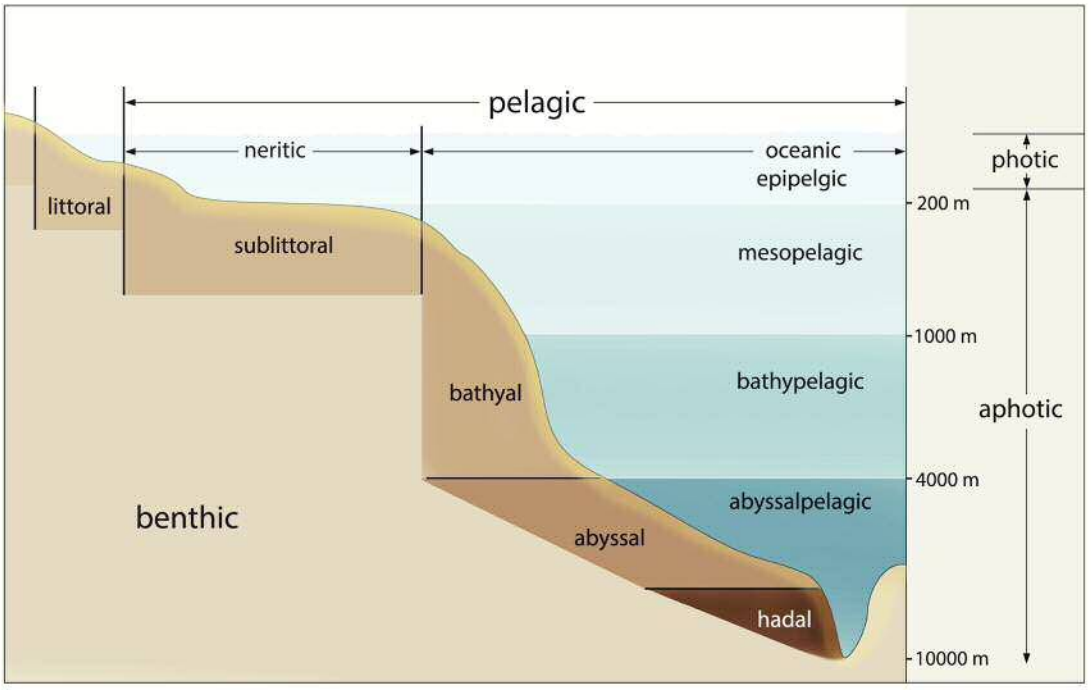

FIGURE 1.7: Principal domains of benthic and pelagic regions. Depths are not to scale.

The deep sea mostly belongs to allochthonous energy sources deriving from the photic zone, where the sun's rays and nutrients allow the primary production (Broecker, 1991). The main pathways are the vertical flux of organic matter from the photic zone, which origin is usually called pelagic, and the advective flux through the slopes (and even more through canyons), of which the origin is partially or mainly terrigenous, and also a vertical active migration of zooplankton, micronekton and bigger meso- and bathypelagic fish (Figure 1.8).

Early investigations pointed to a high stability of deep sea ecosystems, regarding both their structure and dynamics (Grassle and Sanders, 1973), also assumed at seasonal and inter-annual time scales (Sanders, 1968). This point of view, however, has progressively changed in recent decades with the increasing evidence of aspects such as the seasonal influx of the phytodetritus to deep sea environments (Billett et al., 1983; Deuser et al., 1981; Hecker, 1990) and the non-continuous reproduction or peaks in the recruitment reported for deep sea species. In the north Pacific the primary production, the particulate organic matter produced in the surface and reaching bathyal depths (around 500 m) has been estimated to range from 20% to 50%, while does not reach the 5% at abyssal depths (Buesseler et al., 2007). In the Mediterranean the percentage at same depth could be less due to the constant high temperature of water column, that should permits a rapid degradation of

particles by bacteria (Goutx et al., 2007).

Population densities are lower in the Mediterranean then in the Atlantic, a feature related to the much lower availability of organic matter on the Mediterranean seabed, due to the oligotrophic characteristics of the Mediterranean sea. Globally, the Mediterranean sea is an oligotrophic sea. The flux of particles along the water column (total particle flux has been estimated 32.9 and 8.1 g m^{-2} y^{-1} at 80 and 1000 m respectively: Miquel et al., 1994 in the Ligurian Sea) and the concentration of (total or labile) organic matter on deep-sea bottoms follow a seasonal pattern with peaks coupled with the spring peak of primary production (Cartes, Grémare, Maynou, Villora-Moreno and Dinet, 2002).

Continental margins are important areas in terms of energy input, biogeochemical cycles and biological production (Levin and Sibuet, 2012; Valiela, 1995; Walsh, 1991). The physical processes, that transfer water and particulate matter from the continental shelf to the deep sea (Nittrouer and Wright, 1994) mainly through submarine canyons (northern California: Puig et al., 2003; north-western Mediterranean: Puig et al., 2008), provide favourable environments to sustain highly diversified communities, such as the cold water communities (CWC habitats: Huvenne et al., 2011).

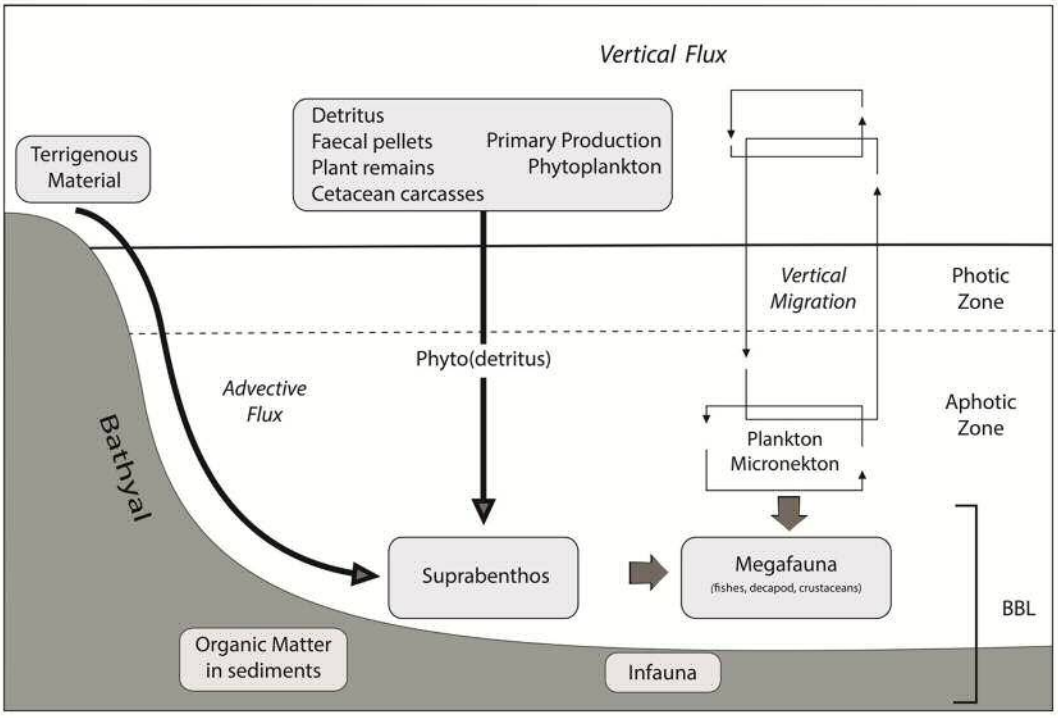

FIGURE 1.8: Principal pathways in the bathyal domain. BBL = Benthic Boundary Layer. Modified from WWF/IUCN (2004), pg. 28.

Time-series studies have shown that deep sea can experience rapid inputs of food supplies from overlying surface waters (Billett et al., 1983), as well as rapid responses by micro-, meio- and macrofaunal taxa (e.g. foraminifera Gooday, 1988). In the Pacific Ocean a coupling between the particulate organic carbon (POC) production at the surface and the seafloor (~ 4000 m) communities has been observed with a time lag of 40 to 60 days (Baldwin et al., 1998; Ruhl and Smith, 2004). Also in the Mediterranean coupling between phytoplankton production and deep-sea organisms responses as been proved (Fanelli et al., 2009). However here, the high temperatures of water column make that organic matter undergoes a rapid degradation while falling to the deep, and mitigate the response of benthic fauna to the phytoplankton blooms. Energy in the deep sea is only produced by chemosynthesis e.g. in hydrothermal vents (Corliss, 1979), but its quantification is still scant; in fact, it is likely that the majority of these structures have been not yet discovered. In the oceanic abyssal floor, such structures and seamounts are not dominant, occupying less than 1% (Smith et al., 2009). Conversely soft-sediments constitute the most characteristic biotope of deep sea bottoms and energy flow and carbon cycling in these environments more realistically could describe the "usual" dynamics of a deep sea ecosystem. Soft bottom are also much more accessible and thus influenced by anthropogenic processes such as mineral extraction and fishing activity (Smith et al., 2009).

The deep Mediterranean fauna displays a high degree of eurybathic species along the slope and the abyssal domains. Certain areas of the Mediterranean deep sea are benthic diversity hotspots, harbouring high densities of endemic taxa, e.g. submarine canyons (Gili et al., 1999), cold seeps associated to mud volcanoes (hosting the chemosynthetic communities), cold water coral reefs (CWC) (Roberts et al., 2006), seamounts and brine pools. Among bathyal amphipods, a high percentage (49.2%) is endemic (Bellan-Santini, 1990), even higher than in coastal zones, probably due to the absence of pelagic free larvae (Cartes et al., 2004). Canyons present unique characteristics with large differences in the sediment uxes and hydrodynamic features (Canals et al., 2009; Palanques et al., 2006), affecting the abundance and species composition of the fauna (Gili et al., 2000). Cold water corals are cnidarians encompassing stony corals (Scleractinia), soft corals (Octocorallia, including "precious" corals and bamboo corals, i.e. *Isidella elongata*, Figure A.2), black corals (Antipatharia), and hydrocorals (Stylasteridae). They are azooxanthellate (i.e., lacking symbiotic dinoflagellates) and often form colonies

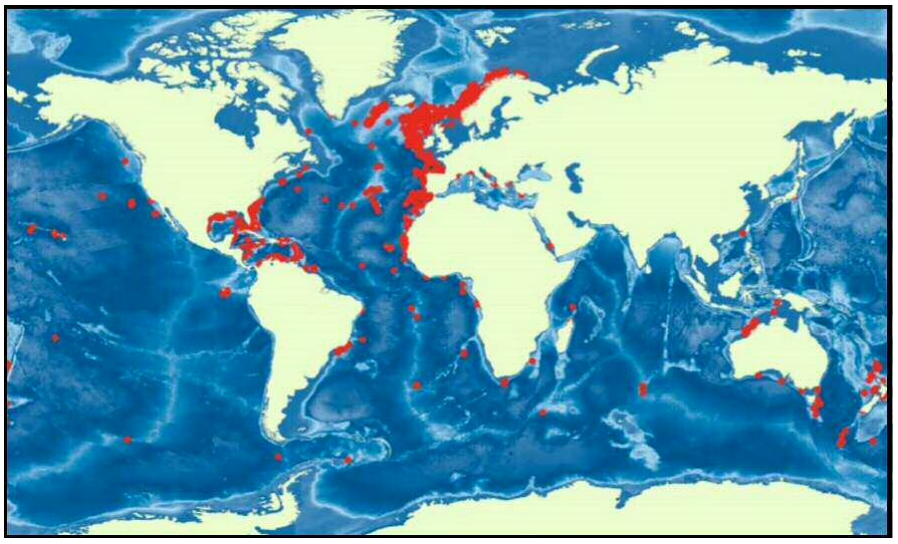

FIGURE 1.9: Global distribution of cold-water corals. From Roberts et al. (2006).

supported by a common skeleton, providing structural habitat for other species. They have been observed mainly in oceanic waters at high latitudes (Figure 1.9).

Although this distribution is skewed due to the intensive research activity performed almost by the developed world (Roberts et al., 2006). CWC communities in the Mediterranean, dominated by *Madrepora oculata* and with less abundance by *Lophelia pertusa*, have been observed at the heads of some canyons within the Gulf of Lions, one of the areas of the world's oceans with the highest canyon density (Harris and Whiteway, 2011). CWC promotes the presence of a highly diverse associated fauna (Buhl-Mortensen et al., 2010) acting as potential areas of refuge, breeding and feeding for many deep-sea species, including commercially important fish (D'Onghia et al., 2010; Gori et al., 2013; Ross and Quattrini, 2007). Higher biomass and diversity of mega and macrofauna has been found also in habitats with the soft-bottom *Isidella elongata* (Cartes, LoIacono, Mamouridis, López-Pérez and Rodríguez, 2013; Mamouridis, Cartes and Fanelli, 2014*a*,*b*) (Figure A.2, Appendix A).

In the continental slope the fish assemblage from 200 to 2250 m (Moranta et al., 1998; Stefanescu et al., 1994) comprises ca. 90 species in the western Mediterranean. The biomass strongly decreases from 200 m to 800 m (the odd is around 10:1). About decapod crustaceans, the number of species reported from 200 to 4000 m is ca. 60. From these, 20 are of commercial interest (including some species that are predominant in shallow waters). Regarding to the macrofauna, Fredj and Laubier (1985) reported ca. 2100 benthic species deeper than 200 m in

the Mediterranean. However the densities in the Mediterranean are about 1/10 of the Atlantic at comparable depths (Flach and Heip, 1996). In contrast the swimming macrofauna (suprabenthos or hyperbenthos) showed diversity peaks at mid-bathyal depths in the Balearic and in the Algerian Basin, with some variation depending on the taxon considered (around 600 m for amphipods; around 1200 m for cumaceans) (Cartes et al., 2003; Cartes and Sorbe, 1996, 1999; Cartes, Mamouridis and Fanelli, 2011).

Pérès and Picard (1964) established the transition between the circalittoral and bathyal domains in the Mediterranean at around 180-200 m depth. Two main broad biocenoses ("facies") in the bathyal Mediterranean have been defined (Pérès, 1985; Pérès and Picard, 1964): (1) soft-bottom communities and (2) hard-bottom communities. Depending on the nature of the sediment, the hydrodynamism and mainland influence, the broad soft-bottom biocenosis has been further divided into three horizons: the (1) upper, (2) middle and (3) lower slope horizons (Pérès, 1985). This community zonation related to the depth has been adopted also for bentho-pelagic megafaunal species, belonging to invertebrates and icthyofauna and another division has been then proposed in the middle slope, between upper and lower mid-slops (e.g. Cartes, 1998; Cartes and Sardà, 1993; Colloca et al., 2003).

The upper slope horizon holds characters of a transitional zone between the continental shelf and the bathyal domain, comprising a large share of eurybathic forms and extending to 400-500 m deep. Within megafauna, the crustaceans *Parapenaeus longirostris* and *Nephrops norvegicus* are characteristic species of this horizon. The middle slope horizon, characterized by firmer and more compact muds, is the zone where most taxonomic groups achieve maximum diversity, mainly Peracarida. Within megabenthos, the *Aristeus antennatus* is a characteristic species of this zone. The lower horizon of the slope is characterised by the decapods *Stereomastis sculpta*, *Acanthephyra eximia* and *Nematocarcinus exilis* (Abelló and Valladares, 1988), and the fishes *Bathypterois mediterraneus*, *Alepochephalus rostratus* (Figure A.2), *Lepidion lepidion* and *Coryphaenoides guentheri*. Then, bentho-pelagic communities incorporate also bathy-pelagis species, although they live mostly in open waters (e.g. the *Argyropelecus hemigymnus*, Figure 1.10, B, and the *Lampanyctus crocodilus* Figure A.1, C).

Common chondrichthyans are *Galeus melastomus* (Figure 1.10, A) and *Etmopterus spinax*. New research suggested a direct relationship between environmental changes (increases in temperature and salinity in intermediate waters) and the decline of

this deep-water sharks (Cartes, Fanelli, Lloris and Matallanas, 2013), confirming a trend that has been seen in many regions of the world. These authors also suggest that the increased fishery effort is another factor explaining the drop in shark abundance in the Catalan slope while in other regions of the western Mediterranean, also subjected to fishery pressure, *E. spinax* is still dominant (e.g. in the Sicily Channel: Fiorentino, 2009) and in the Eastern Mediterranean, where deep-sea sharks (*Centrophorus* spp., *Hexanchus griseus* and *E. spinax*) are among the most abundant fish species in Levantine bathyal communities.

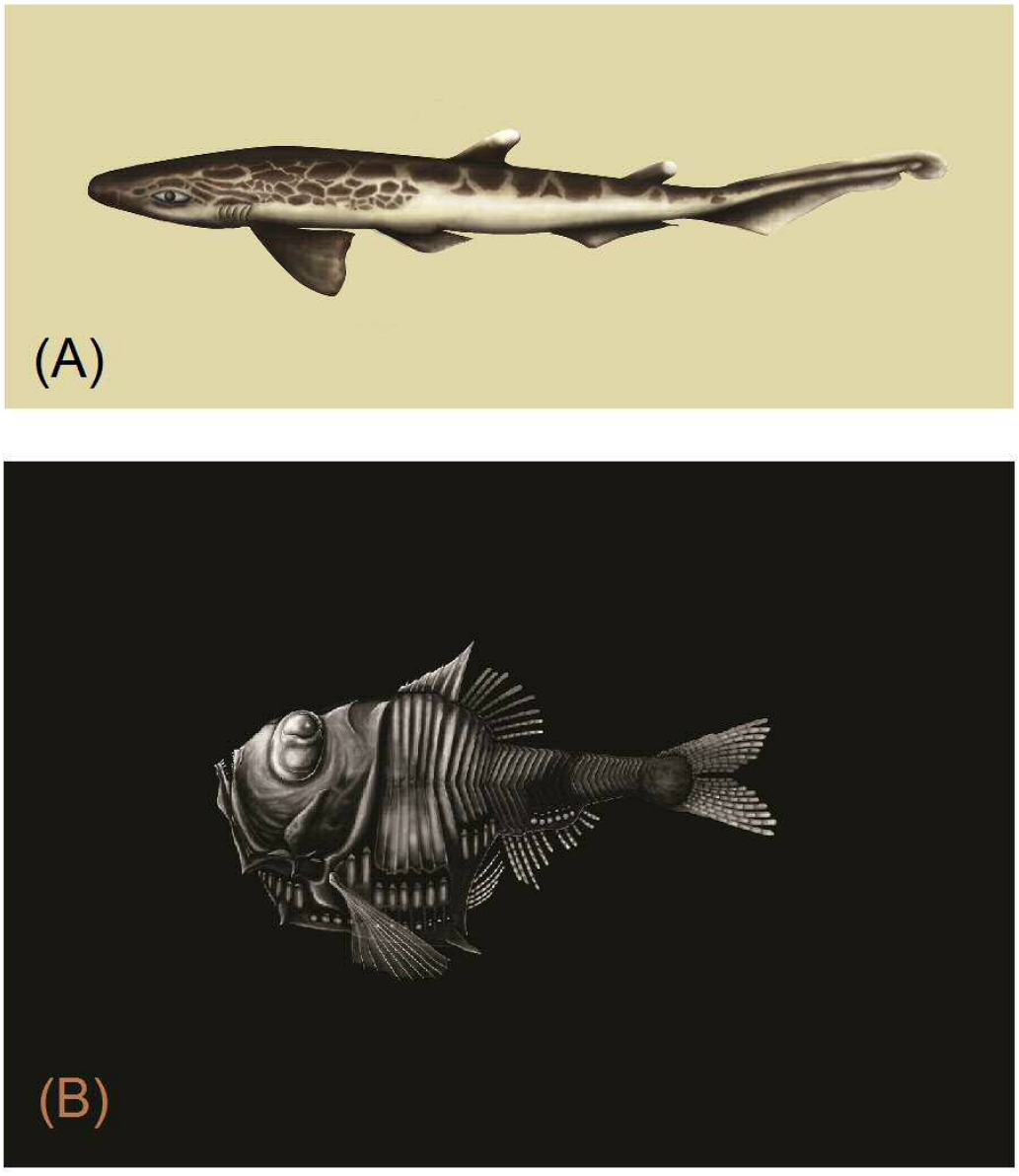

FIGURE 1.10: A) The Blackmouth catshark *Galeus melastomus*, Rafinesque, 1810; B) The half-naked hatchetfish *Argyropelecus hemigymnus*, Cocco, 1829. 2015.

With respect to bacteria and meiofauna, there is high variability in their contribution to the community. E.g. below 500 m depth in the western Mediterranean the contribution of bacteria to organic matter degradation is low (2.5 times of the total). Contrariwise in the eastern Mediterranean bacteria represent 35.8% of the living biomass and the bacteria-meiofauna biomass ratio is very high (20 times) (Western Mediterranean: Danovaro et al., 1999; Eastern Mediterranean: Danovaro and Serresi, 2000; Danovaro et al., 1995).

The food web is likely a "coupled bentho-pelagic trophic system", mainly composed by the "pelagic" zooplankton feeding on particulate organic matter in the water column (e.g. the gasteropod *Cymbulia peroni*, with δ^{15}N=2.6% corresponding to TL=2 in pelagic food webs) and "benthic" deposit feeders *Leucon longirostris* and *Amphipholis squamata* (Figure A.3, B and H) with mean δ^{15}N of 4.6% and 4.6% respectively also corresponding to TL=2 in benthic food webs (Fanelli, Cartes and Papiol, 2011; Fanelli, Papiol, Cartes, Rumolo, Brunet and Sprovieri, 2011). Has been found that predators with higher trophic levels in the bathyal network are *Alepocephalus rostratus* and *Nezumia aequalis*, that tend to be more planktivorous and benthivorous respectively. Suspension feeders have relatively little importance in the Mediterranean, due to its ologotrophic waters, so they are important only locally. "Intermediate" species between TL=1 and 2 are common and bentho-pelagic megafauna show overlapped trophic position, however fish TLs are higher in average than decapod crustaceans (δ^{15}N ranges for fishes: 7.27-11.31%; δ^{15}N ranges for decapods: 6.36-9.72%) (Papiol et al., 2013).

1.4 Deep-sea fisheries, management and models

1.4.1 Deep-sea fishery in the Balearic Basin

Recently, there has been an increase in public awareness, leading to a demand for better management of marine resources in the Mediterranean area (e.g. WWF/IUCN, 2004, UNEP, 2009). Have been suggested that during the past decade in EU waters, the 88% of monitored marine fish stocks have been overfished (Thurstan et al., 2010). In this context, other authors have predicted a global collapse of fisheries within the next few decades (Worm et al., 2006, 2009). International treaties have been already signed by Mediterranean countries, such as the Convention on

Biological Diversity (CBD) or the UN Framework Convention on Climate Change (UNFCCC) (Coll and Libralato, 2012).

During the last 50 years the ultimate target of industrial fisheries worldwide is the deep sea (Glover and Smith, 2003), following the relentless depletion of fish communities on the continental shelves (Christensen et al., 2003, e.g.), in a sort of "(over)fishing down the bathymetric range effect" (Haedrich et al., 2001; Morato et al., 2006, e.g.). This trend can have dangerous effects when considering that deep-sea species are highly vulnerable (k-selection characteristics) and with little resilience to over exploitation (Haedrich et al., 2001).

Deep-water fisheries are documented since the early 1930s targeting especially the highly prized decapod crustaceans Norway lobster and red shrimps (Oliver, 1993). Fisheries production of deep-living decapods are actually increasing in the last years (Politou et al., 2003) and do not show symptoms of decline yet. In the western Mediterranean deep water fisheries are limited to the continental slope shallower than 900 m, corresponding to the upper and middle zones (Carbonell et al., 1999; Righini and Abella, 1994; Sardà et al., 1994), while the eastern deep sea began to be exploited in 2000s (Politou et al., 2003). The fishery of the highly priced red shrimp *Aristeus antennatus* is the main fishing activity performed in the NW deep sea. Also by-catch species, such as *Merluccius merluccius*, *Micromesistius poutassou*, *Phycis blennoides* and deep-sea sharks are fished and some of them sold. The red shrimp is predator of a wide range of sources and present a relatively high trophic level, however it is not the highest found in this community. It presented δ^{15}N values of 9.50±0.64‰ in the mainland slope and eats preferentially on benthic dwellers (Papiol et al., 2013). The documentation on trophic relationships based on experimental studies in soft sediment communities of the upper and middle slope has been increasing during last decade as discussed in the previous paragraph (e.g., Carrassón and Cartes, 2002; Fanelli, Papiol, Cartes, Rumolo, Brunet and Sprovieri, 2011; Papiol et al., 2013).

On the other hand, finding useful tools in understanding and managing exploited ecosystems is important in this environment where relevant data for fisheries management is still scarce. Additionally, and especially in deep sea environments, it is difficult to predict the impact of human activities due to observational difficulties, but such predictions are greatly needed because human pressures on these ecosystems are increasing rapidly.

1.4.2 Monospecific and ecosystem approaches to fisheries and existing models

Since ancient times fishing has been a major source of food and has provided employment and economic benefits for humanity. Besides, with increasing knowledge and development of fishing technologies and effort, it was realised (middle of the 20th century) that aquatic resources are not unlimited. Proper management systems must be set up to sustain fisheries because they largely contribute to feeding the human population and at the same time the best way to respect the environment and ecosystems be found. Fisheries usually target from one to several species, depending on the fishing method. Until early the 1990s fisheries management focused on regulating the fishing activity of only target species ("Target Resource Oriented Management" or TROM paradigm). However fisheries often affect other components of the ecosystem: the fishing of by-catch non-target species is very common and such species can be either commercialised or discarded at sea. Moreover the removal of some species and the destruction of the environment due to invasive gears may affect other species or the habitat.

In addition is reasonable to consider that human activities interact with natural changes, so, when analysing and managing marine resources, is straightforward the need to adopt an integrated view of such complex systems (Botsford et al., 1997; Cury et al., 2003; Duda and Sherman, 2002). This implies a progress towards the so-called ecosystem approach to fisheries (EAF) (e.g. Botsford et al., 1997; Coll and Libralato, 2012; FAO, 2003).

Fisheries management in Europe is still largely based on single-species assessments and does not fully incorporate the wider ecosystem context and impacts in fisheries policy. The reason is yet the lack of a coherent strategy (Möllmann et al., 2013), although policy principles are in place (e.g. the Marine Strategy Framework Directive; the Good Environmental Status indicators). The scientific community has shown a growing interest on ecosystem-based studies, with an increasing application of ecological and bio-economic models such as ECOPATH with ECOSIM (Coll, Lotze and Romanuk, 2008; Coll and Libralato, 2012) or the MEFISTO (Merino et al., 2007) and several other models. All such mathematical models deal with the ecosystem approach: as "simple" as studying predator-prey interactions or more complex models studying the impact on the whole ecosystem. Some examples will be given later.

The different types of models can be summarized into three categories:

1. Extensions of single-species assessment models.
2. Multi-species models, that allows few interactions (see Punt and Butterworth, 1995).
3. Ecosystem models (Christensen and Pauly, 1992; Pauly et al., 2000; Polovina, 1984; Walters et al., 1997).

All models are listed in tables 1.3 and 1.4 (from Plagányi, 2007). Give a description of all existing models is not the purpose of this thesis, for which, if the reader has the interest may consult the extensive review for multi-species and ecosystem approaches applied to fisheries by Hollowed et al. (2000) and its revision by Plagányi (2007). Plagányi highlighted the different characteristics and data requirements for each of these models inasmuch as the importance to select the best model that fits with the real situation. The issue is complex, also due to the high number of processes involved and difficulties in the selection of parameters. It is therefore a very difficult selection, as well as the proper use of this wide range of models.

The ECOPATH software, the most widely used in the scientific community, offers a systematic approach to ecosystem modelling dealing with the massbalancing problem (Christensen and Walters, 2004; Christensen and Pauly, 1992). A clear benefit is that data input and massbalancing are performed in a standardized and user-friendly way (van Oevelen et al., 2010). The model was originally formulated by Polovina (1984) as an ensemble of linear equtions and has been development during 90's (Christensen and Pauly, 1992), with Ecosim (Walters et al., 2000, 1997), allowing for dynamic modelling, and Ecospace (Walters et al., 1999) for spatial modelling. The linear system is solved using standard matrix algebra. To solve the system a generalized inverse is used if the determinant is zero or the matrix is not square (that works in most cases, Mackay, 1981). If the set of equations (see Christensen and Pauly, 1992) is over-determined (more equations than unknowns), and the equations are not mutually consistent the generalized inverse method provides least squares estimates, which minimize discrepancies (Christensen and Pauly, 1992). Thus, the ECOPATH is able to solve even- or over-determined problems, but it is also able to estimate a posteriori "missing" stocks (an under-determined situation). An algorithms tries to estimate iteratively as many "missing" stocks as possible before setting up the set of linear equations becoming then an even-

or over-determined system, that can be solved by the generalized inverse method. Thus, ECOPATH circumvents the problem of mathematical indeterminacy artificially upgrading the number of equations until the matrix equation is completely determined by imposing fixed values for, e.g., physiological parameters.

When the algebraic system become even- or over-determined, then the energy balance is ensured within each group using an equation pretty similar to the following:

$$C = P + R + U$$

where C is consumption, P production, R respiration and U unassimilated food, in line with energy conservation assumptions for biological units Winberg (1956) and pretty similar to the set of equations discussed in Section 1.2.1. However the energy equation in ECOPATH does not account for gonadal production and is defined a priori such that it is impossible to change its energetic assumptions, an opportunity that would be very useful when dealing with real data. Moreover the ECOPATH remains restricted to singlecurrency data (t km^{-2}), as it does not allow the simultaneous solution of mass balances for multiple elements.

In conclusion, the major problems arise from the under-determined solution method and rigidity of model settings in ECOPATH. These problems are differently approached in the so-called Linear Inverse Modelling (LIM) developed by Soetaert and Petzoldt (2010); van Oevelen et al. (2006, 2010) and originally proposed by Vézina and Platt (1988). In this thesis there is no intention to criticise the ECOPATH approach, that is to date the most used by the scientific community and the most productive, although we are interested in using other promising methods in ecological modelling that could support and improved ecosystem approach to fisheries management.

1.4.3 The bias-variance problem of a model

There is another important problem we are interested to be introduced: the trade-off between variance and bias of a model, that is statistically speaking an estimator. An estimator is any quantity calculated from the sample data which is used to give information about an unknown variable in the population. For example, the linear regression of variable Y with respect to some covariates X is an estimator. When modelling we try to reduce the error of the estimator (or model) to augment

its "quality". Solving the variance-bias trade-off is meant to choose a model that accurately captures the regularities in the sample (reducing the bias), but also generalizes well to unseen data (reducing the variance). So, there are two sources of error, the bias and the variance, that the bias-variance trade-off problem tries to minimize. Figure 1.11 is a graphical explanation of such a problem.

The bias refers to the portion of error from erroneous assumptions and is the difference between the estimator's expected value and the true value of the unknown variable being estimated. An estimator with zero bias is called unbiased, otherwise the estimator is said to be biased.

the variance refers to the portion of error from sensitivity to fluctuations in the sample. It measures how far a sample is spread out. A variance of zero indicates that all the values are identical and it is always non-negative.

Formally, if we want to estimate the real function $f(x)$ using a sample of the random variable, X with observations, $x_1, \ldots, x_n$, through $\hat{f}(x)_n$, as estimator of

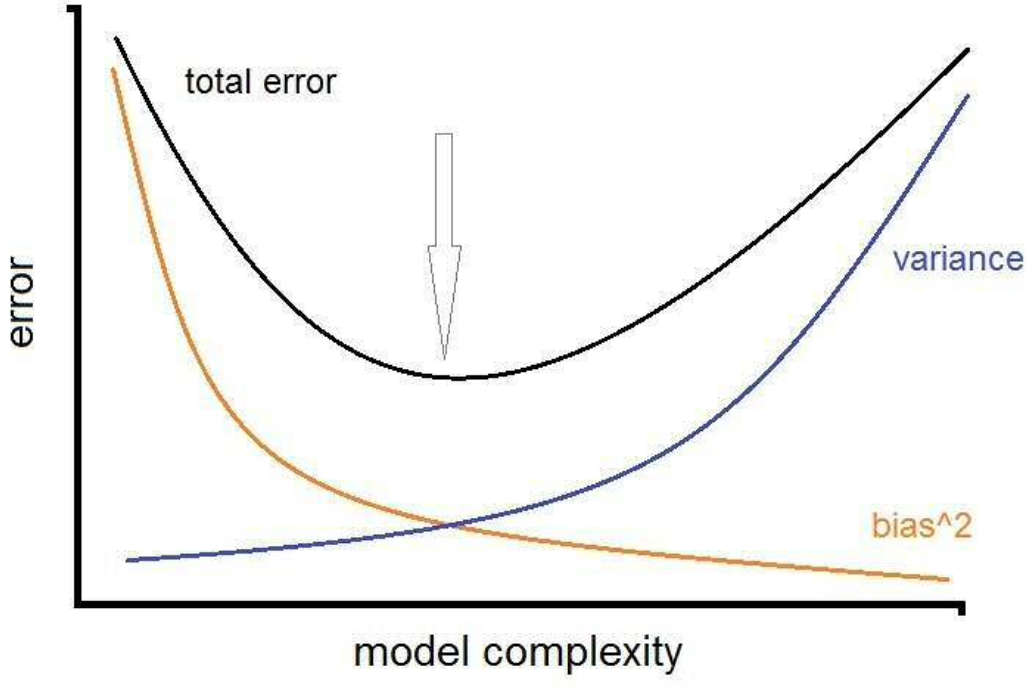

FIGURE 1.11: The bias-variance trade-off in model fitting with increasing complexity (the more parametrization, the higher complexity). Increasing the model complexity also the variance increases, while the bias decreases. The best fit occurs when both are minimized (vertical arrow). Here error define whatever measure used to summarise the error of the model, being the integrated or the average mean square error or the predictive risk. See the text for more details.

the function, then the squared error loss function is

$$L(f(x), \hat{f}(x)_n) = (f(x) - \hat{f}(x)_n)^2. \tag{1.10}$$

The average of this loss is called risk or mean squared error (MSE)

$$\text{MSE} = R(f(x), \hat{f}(x)) = E(L(f(x), \hat{f}(x))). \tag{1.11}$$

The mean squared error can be discomposed into bias and variance of the estimator

$$\text{MSE} = Bias(\hat{f}_n(x))^2 + Var(\hat{f}_n(x)) \tag{1.12}$$

where

$$Bias(\hat{f}_n(x)) = E(\hat{f}_n(x)) - f(x)$$

and

$$Var(\hat{f}_n(x)) = E((\hat{f}_n(x) - E(\hat{f}_n(x)))^2).$$

The above definition refers to the risk at a point x. To summarise the risk over different values of x we use the integrated mean squared error

$$R(f, \hat{f}_n) = \int R(f(x), \hat{f}_n(x))dx \tag{1.13}$$

for density estimations while for regression problems where the response random variable Y with observations $y_1, \ldots, y_n$ and covariate X with observations $x_1, \ldots, x_n$, and regression function, $r(x)$, such that

$$y_i = r(x_i) + \epsilon,$$

can also be used the average mean squared error

$$R(r, \hat{r}_n) = \frac{1}{n} \sum_{x=1}^{n} R(r(x_i), \hat{r}_n(x_i)). \tag{1.14}$$

In the practise we do note calculate the average mean squared error using the true function, because we do not know it. In theoretical statistics they perform simulations and in applications is common practice estimate it through sub sets or equally simulations and it is of common use for quantifying the goodness of a model fit without the necessity to distinguish between bias and variance. In conclusion, a model could not be nether too simple nor to complex to perform well.

In ecosystem modelling, the increment of model complexity should imply a more realistic description. The complexity can be summarised with the number of parameters in the model: the higher number, the more complex model. But along with the increment of realism, the model becomes too specific, losing any kind of generalization. Moreover a very complex parametrization does not imply realism if the ecosystem is under-sampled and still poorly known. If limited and noisy data, then the drawback is that also results are uncertain even in complex models (Plagányi, 2007). In such cases a reliable alternative is to consider data-poor or even data-less approaches (Johannes, 1998) and th LIM is one of such solutions.

1.5 The study area

This study were carried out on mainland slope of the Balearic basin located in the NW Mediterranean (Figure 1.12). The sampling was performed along the mid-slope off the Catalonian coast (between 40°48′9″ N and 41°09′3″ N - 2°04′0″ E and 2°35′4″ E) near Barcelona within projects BIOMARE (ref. CTM2006-13508-C02-02/MAR) and ANTROMARE (ref. CTM2009-12214-C02-01-MAR).

The Balearic Basin is located in the western Mediterranean and represents a transitional region between the Liguro-Provençal and Algerian basins 1.12. It includes the Catalan Sea, located between the Balearic Islands and the Iberian peninsula, and the wide Gulf of Valencia in the south of this sea. With the exception of the Gulf of Lions, the continental shelves of the NW Mediterranean are narrow.

The hydrology in the western basin is defined by three main water masses: the surface Modified Atlantic Water (MAW), the Levantine Intermediate Water (LIW)

and the West Mediterranean Deep Water (WMDW). The MAW inflows through the Strait of Gibraltar subject to evaporation and mixing with the underlying waters. That increases salinity towards the east from 36.3 in the Strait of Gibraltar to 37.3 ppt in the Strait of Sicily (Zavatarelli and Mellor, 1995), while the mean value of deep Mediterranean salinity is 38.2 ppt associated to a mean temperature of about 12.8°C. LIW takes place in the Eastern sub-basin in winter and flows between 200 to 400 m in the Western basin. Deeper waters remain separate between East and West. The source of the deep western current, the WMDW,

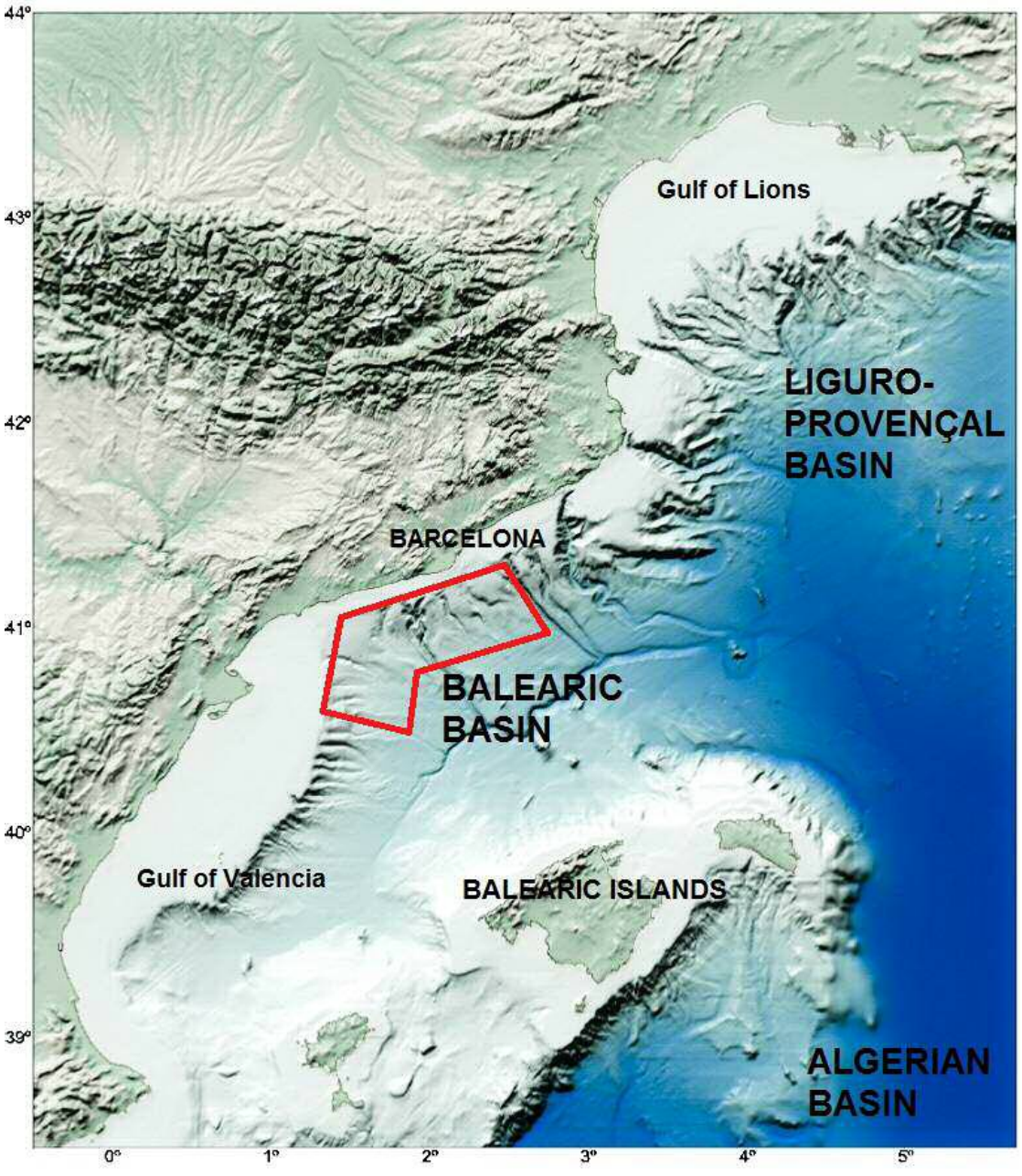

FIGURE 1.12: The Balearic basin and study area inside the red polygon.

is located in the Gulf of Lions, where in winter the convective movements occur influenced by cold and dry winds, causing the sinking and mixing of cold and salty surface waters to a depth of about 1200 to 1500 m (Zavatarelli and Mellor, 1995). This water mass can outflow at Gibraltar without mixing with the LIW (Kinder and Parrilla, 1987). These currents can affect and alter the presumed homogeneity of the deep sea environment Garcia-Ladona et al. (1996).

At surface, in Liguro-Provençal Basin, dense waters originated in the north are associated with a permanent circulation along the continental slope: the Northern Current (NC). The Algerian Basin, in the south, is dominated by intense mesoscale eddies and the unstable Algerian Current (AC). The NC flows southward along the Iberian peninsula slope and during summer is covered by a warm surface layer spreading over the whole Catalan Sea. This warming creates the intense thermal Pyrenees Front. Near the Balearic Islands, another Front, the Balearic Front, is created by the recent Atlantic water and anticyclonic eddies from the Algerian Current and contributes to mesoscale variability (Garcia-Ladona et al., 1996).

The NW Mediterranean is classified as oligotrophic (however less than the eastern basin), as the whole Mediterranean, where chlorophyll concentration in the open areas rarely exeeds 2-3 mg m^{-3} (Margalef and Castellví, 1967). The primary production shows a seasonal dynamic, with higher biomass in winter and lower during summer, a pattern that has been regularly observed for more than 20 years (Marty et al., 2002). Plankton blooms occur in autumn, at the beginning of the mixing period and in winter-spring: wind driven winter up-wellings are important in the Gulf of Lions, where the coastal profile is favourable (Minas, 1968). There the winter deep convection after breakdown of the thermocline enhances productivity, bringing nutrients from deep waters to the surface layers. Thus, large bloom have been observed in the Liguro-Provencal Region (D'ortenzio and Ribera d'Alcalà, 2009). With a minor scale and intensity up-wellings occur also in the Catalano-Levantine coast of Spain (Margalef and Castellví, 1967).

Phytoplankton estimates show a Deep Chlorophyll Maximum (DCM) during a large part of the year, when there is a certain degree of stratification of the water column. The DCM occurs within the pycnocline (see Fig. 2 in Estrada, 1996), at a depth in which nutrients become available and light, although generally of the order of 1% that at surface, is still sufficient for growth. The presence of the DCM accentuates the strong vertical differentiation of the pelagic ecosystem into a light-sufficient but nutrient-limited upper layer, based mainly on recycled

production, and a nutrient sufficient but light-limited lower layer, where new production takes place (Herbland and Voituriez, 1979). These vertical patterns affect the structure of the trophic links among the diverse plankton components and are accompanied by changes in the relative importance of the microbial versus the classical, zooplankton-based, food web.

The responsible hydrographic features include: 1) turbulent mixing in the Straits, which drags nutrient from deep Mediterranean waters into the euphotic zone (Minas et al., 1984); 2) up-welling in the Alboran Sea and frontal zones associated with the anticyclonic gyres caused by the inflow of Atlantic water (Lohrenz et al., 1988; Minas et al., 1984); and 3) the effects of the Atlantic current, which has a higher nutrient content than surface Mediterranean waters and presents strong dynamic activity along the Algerian coast, where meanders and eddies can produce points of enhanced phytoplankton growth (Millot et al., 1990).

The NW basin also presents a cyclonic circulation which extends from the Gulf of Genoa to the Gulf of Valencia, across the Liguro-Provençal and Balearic basins. This feature is bound by shelf/slope fronts associated with the SW-flowing northern current on the continental side, and NE currents on the Corsican, Sardinian and Balearic Islands side (Estrada and Margalef, 1988; Prieur and Tiberti, 1984). The central zone, marked by a doming of isotherms and isopycnals, has lower vertical stability than the margins and can be interpreted as a divergence. Both the shelf/slope fronts and the central dome or ridge-like structure play a key role in the primary production of this part of the Mediterranean.

Land run-off is also important in the northern zone, where rivers like the Rhône, flowing into the Ligurian Sea and to a lesser extent the Ebro in the Catalonian Sae, are important sources of phosphorus, nitrogen and other nutrients. Temporary discharges due to storms may produce intense local enrichment (Estrada, 1996).

1.6 Purposes of the study

The final objective of this thesis is to quantify the effects driven by the fishing activity on the soft-sediment communities in the continental mid-slope of the Balearic basin (bathyal domain). Such effects can be characterised by high alternation of biomass in consecutive components of the community and defined in literature as

trophic cascade and top-down process, driven by by the fishery of the red shrimp *Aristeus antennatus*.

This main objective involved several other problems: (1) the complete lack of quantitative data on the macrobenthos in the area; (2) lack of an updated study of the red shrimp landings.

The first reason led to the study of the macrofauna in soft-bottom sediments, developed in the PART I, Chapter 2, the second reason to the PART II, Chapters 3 and 4 and the main objective to Chapters 5 and 6.

Concrete aims of PART I, Chapter 2 are

- Study the structure and seasonal dynamics of soft-bottom infauna (macrobenthos) in the NW Mediterranean slope and define relationships between the community and environmental variability. The main purposes of this study are: i) analyze the seasonal dynamics of the macrobenthos, and ii) relate environmental and trophic variables with the faunistic composition.

Concrete aims of PART II, Chapters 3 and 4 are

- Study factors and variables affecting *A. antennatus* LPUE off Barcelonas port, that offers an exhaustive data set of high quality compared to other Mediterranean areas. In particular study which variables (within environmental, temporal, effort and economic variables) affect the LPUE fluctuation through time by means of regression analysis (GAM, GAMM and GAMLSS models), in order to obtain an updated overview of the development of this fishery and the status of the stock.

Concrete aims of PART III, Chapters 5 and 6 are

- Reconstruction of the soft-bottom food web of the continental slope in NW Mediterranean(bathyal domain) defining its principal characteristics through the network analysis and study the current fishing impact.
- Explore the existence of the trophic cascade mechanism in the modelled food web considering both top-down (fishery) and bottom-up (source availability) processes as possible drivers of ecosystem changes.

Acronym	Name/description	Ref.
ATLANTIS	ATLANTIS	1, 2
Bioenergetic/ allometric model	Multi-species trophodynamic model usingbioenergetic and allometric approach	3, 4, 5
BORMICON	BOReal MIgration and CONsumption model	6, 7
CCAMLR	models Commission for the Conservation of Antarctic Marine Living Resources	8, 9, 10, 11, 12
EPOC	Ecosystem Productivity Ocean Climate Model	13
ERSEM II	European Regional Seas Ecosystem Model	14
ESAM	Extended Single-species Assessment Model	15, 16, 17
EwE	ECOPATH with ECOSIM	18, 19, 20, 21, 22
GADGET	Globally applivable Area Disaggregated General Ecosystem Toolbox	23, 24, 25, 26
GEEM	General Equilibrium Ecosystem Model	27, 28
IBM	Individual-Based Models	29, 30, 31, 32
IGBEM	Integrated Generic Bay Ecosystem Model	33, 34
INVITRO	INVITRO	35

TABLE 1.3: Alphabetical list of models used in the ecosystem approach of fisheries (PART 1/2). Revised from (Plagányi, 2007). References are: 1. Fulton, Smith and Johnson, 2004, 2. Fulton et al., 2005, 3. Yodzis and Innes, 1992, 4. Yodzis, 1998, 5. Koen-Alonso and Yodzis, 2005, 6. Bogstad et al., 1997, 7. **?**, 8. Butterworth and Thomson, 1995, 9. Mori and Butterworth, 2004, 10. Mori and Butterworth, 2005, 11. Mori and Butterworth, 2006, 12. Thomson et al., 2000, 13. Constable, 2006, 14. Baretta-Bekker et al., 1997, 15. Livingston and Methot, 1998, 16. Hollowed et al., 2000, 17. Tjelmeland and Lindstrøm, 2005, 18. Christensen and Pauly, 1992, 19. Christensen and Walters, 2004, 20. Polovina, 1984, 21. Walters et al., 1997, 22. (Walters et al., 2000), 23. Begley and Howell, 2004, 24. Trenkel et al., 2004, 25. Taylor and Stefánsson, 2004, 26. Taylor and Taeknigardur, 2011, 27. Finnoff and Tschirhart, 2003, 28. Finnoff and Tschirhart, 2008, 29. Alonzo et al., 2003, 30. DeAngelis and Gross, 1992, 31. Purcell and Kirby, 2006, 32. Shin and Cury, 2004, 33. Fulton, Smith and Johnson, 2004, 34. Fulton, Parslow, Smith and Johnson, 2004, 35. McDonald et al., 2006, 36. Watters et al., 2005, 37. Watters et al., 2006, 38. Punt and Butterworth, 1995, 39. Jurado-Molina et al., 2005, 40. Garrison et al., 2010, 41. Sparholt, 1995, 42. Sparre, 1991, 43. Tjelmeland and Bogstad, 1998, 44. Colomb et al., 2004, 45. Shin and Cury, 2001, 46. Bertignac et al., 1998, 47. Lehodey et al., 2003, 48. Lehodey et al., 2008, 49. Tjelmeland and Lindstrøm, 2005, 50. Bax, 1985, 51. Plagányi and Butterworth, 2006, 52. Sekine et al., 1991, 53. Hamre and Hatlebakk, 1998.

Acronym	Name/description	Ref.
KPFM	Krill-Predator-Fishery Model (KPFM, KPFM2)	36, 37
MRM	Minimally Realistic Model	38
MSM	Multi-species Statistical Model	39
MSVPA/ MSFOR	Multi-species Virtual Population Analysis and Multi-species Forecasting Model	40, 41, 42
MULTSPEC	Multi-species model for the Barents Sea	6
AGGMULT	simplified version connected to an ECONMULT model describing the economies of the fishing fleet	43
MOOVES	Marine Object-Oriented Virtual Ecosystem Simulator	44
OSMOSE	Object-oriented Simulator of Marine ecOSystem Exploitation	45
SEAPODYM	Spatial Ecosystem and Population Dynamics Model (previously SEPODYM)	46, 47, 48
SEASTAR	Stock Estimation with Adjustable Survey observation model and Tag-Return data	49
SKEBUB	SKEleton Bulk Biomass ecosystem model	50
SMOM	Spatial Multi-species Operating Model	51
SSEM	Shallow Sea Ecological Model	52
SYSTMOD	System Model for the Norwegian and Barent Sea	53

TABLE 1.4: Alphabetical list of models used in the ecosystem approach of fisheries (PART 2/2). Revised from (Plagányi, 2007). References are: 1. Fulton, Smith and Johnson, 2004, 2. Fulton et al., 2005, 3. Yodzis and Innes, 1992, 4. Yodzis, 1998, 5. Koen-Alonso and Yodzis, 2005, 6. Bogstad et al., 1997, 7. **?**, 8. Butterworth and Thomson, 1995, 9. Mori and Butterworth, 2004, 10. Mori and Butterworth, 2005, 11. Mori and Butterworth, 2006, 12. Thomson et al., 2000, 13. Constable, 2006, 14. Baretta-Bekker et al., 1997, 15. Livingston and Methot, 1998, 16. Hollowed et al., 2000, 17. Tjelmeland and Lindstrøm, 2005, 18. Christensen and Pauly, 1992, 19. Christensen and Walters, 2004, 20. Polovina, 1984, 21. Walters et al., 1997, 22. (Walters et al., 2000), 23. Begley and Howell, 2004, 24. Trenkel et al., 2004, 25. Taylor and Stefánsson, 2004, 26. Taylor and Taeknigardur, 2011, 27. Finnoff and Tschirhart, 2003, 28. Finnoff and Tschirhart, 2008, 29. Alonzo et al., 2003, 30. DeAngelis and Gross, 1992, 31. Purcell and Kirby, 2006, 32. Shin and Cury, 2004, 33. Fulton, Smith and Johnson, 2004, 34. Fulton, Parslow, Smith and Johnson, 2004, 35. McDonald et al., 2006, 36. Watters et al., 2005, 37. Watters et al., 2006, 38. Punt and Butterworth, 1995, 39. Jurado-Molina et al., 2005, 40. Garrison et al., 2010, 41. Sparholt, 1995, 42. Sparre, 1991, 43. Tjelmeland and Bogstad, 1998, 44. Colomb et al., 2004, 45. Shin and Cury, 2001, 46. Bertignac et al., 1998, 47. Lehodey et al., 2003, 48. Lehodey et al., 2008, 49. Tjelmeland and Lindstrøm, 2005, 50. Bax, 1985, 51. Plagányi and Butterworth, 2006, 52. Sekine et al., 1991, 53. Hamre and Hatlebakk, 1998.

PART I

2

A temporal analysis on the dynamics of deep-sea macrofauna: influence of environmental variability in the Catalan Sea (western Mediterranean)

Abstract

A seasonal analysis of deep-sea infauna (macrobenthos) based on quantitative sampling was conducted in two stations on the continental slope: 1) within the Besós canyon (at ~ 550 – 600 m) and 2) on the adjacent open slope (at 800 m). Both sites were sampled in February, April, June-July and October 2007, covering all seasons. Environmental variables were also recorded in the sediment and sediment/water interface. Dynamics of macrobenthos at the two stations showed differences in biomass/abundance patterns and trophic structures. Biomass was higher inside the Besòs canyon than on the adjacent slope. The community was mostly dominated by surface-deposit feeding polychaetes (Ampharetidae, Paraonidae, Flabelligeridae) and crustaceans (amphipods such as *Carangoliopsis spinulosa* and *Harpinia* spp.) inside the canyon. On the contrary subsurface deposit feeders (mainly the sipunculan *Onchnesoma steenstrupii*) were dominant on the adjacent slope. Inside the canyon we found a clear temporal succession of species that we related to both food availability and quality and the proliferation of opportunistic species was consistent with higher variability in food sources (TOC, C/N, δ^{13}C) in comparison to adjacent slope. This was likely caused by a greater influence of terrigenous inputs from river discharges. Inside the canyon, Capitellidae, Spionidae and Flabelligeridae, in general considered as deposit-feeders, were more abundant in June-July (when the water column is stratified) coinciding with a clear signal of terrigenous carbon (depleted δ^{13}C, high C/N) in the sediments. By contrast, during October and under conditions of high water turbidity and TOM increment, (mainly) carnivorous polychaetes (Glyceridae, Onuphidae) increased. Total macrobenthos biomass found on the Catalan canyon, were higher than in the neighbouring Toulon canyon, probably because the two canyons are influenced by different river inputs, connected with distinct terrigenous sources.

Keywords: macrofauna, canyon, seasonal dynamics, food availability

2.1 Introduction

The deep sea, is composed of a variety of ecosystems distributed on hard and soft bottoms and is not as homogeneous as once believed. Continental slopes are mainly covered by soft sediments (Pérès, 1985; Thistle, 2003). However, they also constitute a variety of habitats and the canyons crossing them comprise a mosaic of patches and faunal assemblages (Curdia et al., 2004; Macquart-Moulin and Patriti, 1996; Reyss, 1971). Continental slopes and especially canyons represent zones of matter and energy transfer between the continental shelf and the abyssal domain (Gardner, 1989; Griggs et al., 1969) often providing focused sources of high quality food (Epping et al., 2002; Josselyn et al., 1983; Rowe et al., 1982).

The main energy flow probably depends on advective fluxes (Féral et al., 1990) and in submarine canyons terrestrial inputs may be the most important for their ecodynamics. Organic matter is often channelled through canyons, enhancing food supply and creating depocenters where hotspots of benthos production can be observed (Vetter and Dayton, 1999). This channelling can change seasonally, establishing varying seasonal environmental dynamics at the sea floor in and close to canyons, mostly driven by changes in food availability (Vetter, 1998). This may influence assemblage composition, life cycles of benthos and trophic relationships, including the role of benthic taxa, the main prey for deep-sea shrimps (Cartes, 1994) and fishes (Fanelli and Cartes, 2010; Madurell and Cartes, 2005) in this environments.

The distribution and diversity of deep macrobenthos have mainly been related with depth gradients at several spatial scales, and with sediment size (Stora et al., 1999; Tselepides and Eleftheriou, 1992; Tselepides et al., 2000). Small-scale changes in the sediment structure and in the distribution of food on sedimentary bottoms are associated with adaptation of fauna and with its high diversification in the deep sea (Gage and Tyler, 1991; Sanders et al., 1965). In the western Mediterranean many canyons traverse the continental slope close to mainland areas. The Balearic Basin resembles a large submarine canyon, represented by the Valencia Trough, that separates the mainland and insular slopes (the latter belonging to the Balearic Islands. The mainland slope is crossed by a system of tributary canyons (from N to S: Palamós, Blanes, Arenys/Besòs, Berenguera and Foix).

Quantitative data on benthic deep-sea macrofauna are still too scarce to describe the dynamics of margin systems. Studies on infaunal macrobenthic assemblages in

the Mediterranean Deep Sea have been performed mainly by dredging, which permits only qualitative descriptions (Carpine, 1970; Pérès and Picard, 1964; Reyss, 1971; Vamvakas, 1970), and rarely by sediment cores (Gerino et al., 1994; Stora et al., 1999; Tchukhtchin, 1964) that allow quantitative analyses. Quantitative studies, both in the deep Mediterranean and elsewhere, have lacked until now a temporal-seasonal approach, that surprisingly reveals the crucial role of infauna in food webs around submarine canyons (Cartes, 1994; Cartes, Grémare, Maynou, Villora-Moreno and Dinet, 2002; Cartes et al., 2009). Studies of ecosystem functioning on the Catalan slope have focused on megafauna, fishes and decapods crustaceans, collected by different kind of trawls (e.g. Cartes, 1994; Cartes et al., 2009) and on suprabenthic macrofauna collected with sledges (Cartes, 1998). There has also been a study of the distribution of megafaunal invertebrates, both epifauna and infauna (Cartes et al., 2009). The multidisciplinary project BIOMARE, focused on the natural variability of, and human impact on, marginal ecosystems off the Catalan coasts, included studies of the temporal dynamics of all macrofaunal compartments (the infauna for the first time) in deep environments and of the possible environmental factors influencing their distributions and biomass. The difficulty in collecting environmental and biological samples simultaneously is the most evident reason for the lack of information of environment-biota coupling in deep sea (as noted by Stora et al., 1999).

In this chapter a temporal study of deep-sea infauna (macrobenthos) is presented based on a quantitative approach. The study has been conducted simultaneously in two characteristic slope environments. The main aim was to analyse the seasonal dynamics of deep-sea macrobenthos (between 600 and 800 m) in the Mediterranean sea.

The study has been focused on:

- describing the seasonal composition of the infaunal macrobenthos in two characteristic environments of the Catalan Slope, inside the Besòs canyon and on its adjacent slope at 800 m depth;
- identifying the main variables both in the sediment and close to the sediment-water interface (the Benthic Boundary Layer), that explain trends observed in the taxonomic composition and biomass of the infaunal macrobenthos.

2.2 Materials and Methods

2.2.1 The Study area and sampling design

The sampling was performed along the mid-slope (Figure 2.1) on the mainland part of the Balearic Basin: between 40°48′9″ N and 41°09′30″ N - 2°04′00″ E and 2°35′4″ E, within the project BIOMARE (ref. CTM2006-13508-CO2-02/MAR).

Samples were collected at four stations situated within two canyons and on their adjacent slopes. At two of these stations (the Buscarró canyon, C1, a tributary of the larger Besòs canyon and on its adjacent slope, S1), four cruises were performed seasonally (B1 cruise February 2007, B2 April 2007, B3 June-July 2007, B4 October 2007). In the Berenguera canyon station (C2), and the adjacent slope station (S2), sampling was carried out only in June-July 2007. The Besòs (C1) and Berenguera (C2) canyons stations were located at depths of 550 – 600 m approx. near the southern walls of the canyons, close to the canyon heads. The adjacent slope stations were located at approximately 800 m depth in two fishing grounds known by local fishermen as Serola (S1) and Abissinia (S2), close to Besòs and Berenguera canyons respectively. Both canyons are also fishing grounds, though there was hardly any fishing activity at C1 in the last 5 years. The seasonal analyses were based only on C1 and S1 samples.

A total of 34 box-cores were collected. The replicates (cores taken very close to the same positions, i.e. ¡ 200 m between replicates) were distributed as follows:

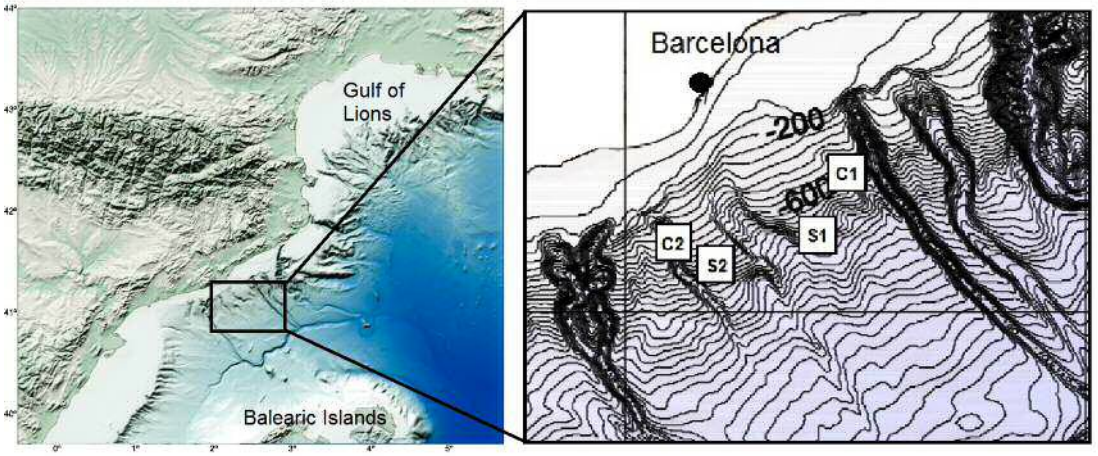

FIGURE 2.1: Map of the study area off the Catalan coast, showing the positions of samples inside canyons Besòs and Berenguera (C1, C2) and on the adjacent slopes (S1, S2) stations.

cruise B1 (3 at C1 and 3 at S1), cruise B2 (4 at C1 and 4 at S1), cruise B3 (4 at C1 and 3 at C2; 4 at S1 and 1 at S2) and cruise B4 (4 at C1 and 4 at S1). The box-corer used was a Reineck model, with 21x31 cm box sides, sampling a surface area of 0.065 m2. The uppermost 20 cm of sediments were sieved through a 0.5 mm mesh size to retain macrofauna, as in other similar studies performed in the deep Mediterranean (see Stora et al., 1999). Infauna was sorted, classified to the lowest possible taxonomic level, counted and weighed (wet weight, WW). Some keys used for the identification are available in Day (1967); Parapar et al. (2012); San Martín Peral (2004); Viéitez Martín et al. (2004).

2.2.2 Environmental data collection

Biological data were analysed together with a number of environmental variables defining both the characteristics of the sediments and the near-bottom water column. During each cruise, one CTD per station was performed in parallel to the biological sampling using Seabird-25 profilers furnished with pressure, temperature, salinity, fluorescence and turbidity sensors (obtaining 24 data sets s^{-1}). The CTD recorded data from the surface to 5 m above the bottom. Sediments were collected with a multi-corer at the same stations where box-cores were taken (three samples per multi-corer) and the first 5 cm were used for environmental analyses.

The CTD measured the following variables:

- Temperature and salinity 5 m above the sea bottom (T_{5mab}, S_{5mab}).
- Fluorescence (f_{0-200m}, mean value in the range 0 – 200 m) as the sum of fluorometer readings each 1 m in vertical bins from surface to 200 m depth; values were proportional to Chl a and indicative of surface phytoplankton standing stock.
- Turbidity at 5 m above the sea bottom ($Turb_{5mab}$).

Multi-corer samples were used to measure the following parameters:

- Percentage of total sedimentary organic matter (TOM), calculated as the difference between dry weight (DW: 60°C for 24 h until constant weight reached) and ash weight (500°C in a furnace for 2 h).

- Percentage of total organic carbon (TOC), carbon-nitrogen ratios (C/N) and the stable isotope ratio (δ^{13}C) in sediments (for details of sample treatment and isotope analysis see Fanelli and Cartes, 2008; Fanelli et al., 2009). δ^{13}C indicates the origin of food sources (terrigenous or pelagic) arriving on the seafloor. Detailed sediment C/N and δ13C are published in Papiol et al. (2012).

REDOX (*Eh*) was measured directly in box-corer sediments using a ThermoOrion 250A sensor. Voltage was read at the sediment surface and at 5 cm depth in the sediment.

Mean monthly flow estimates (m^3 s^{-1}) for the main rivers discharging off the central Catalan coasts (Llobregat, see Figure 2.1) were obtained from the website `http://aca-web.gencat.cat/aca/appmanager/aca/aca/`. Phytoplankton pigment concentration (ppc, mg Chla m^{-3}) were obtained from `http://reason.gsfc.nasa.gov/Giovanni`. Values of ppc were used as indicators of the surface primary production in the area. A monthly average reading of ppc of the positions of stations was used.

2.2.2.1 Diversity and biomass trends by season

All infaunal taxa were classified to the lowest possible taxonomic level. Within BIOMARE, we attempted to analyse the stable isotopic composition of macrofauna. We therefore undertook an initial sorting of fauna on board the ship, and then froze specimens, remaining bulk samples and sediment at −20°C for later analysis. In the laboratory, the macrofaunal sorting was completed and the animals classified into groups in order to obtain the required minimum masses for isotope analysis. This treatment partially damaged polychaetes. As a result, some specimens could only be determined to genus or family level. Taxa were counted and weighted individually in order to obtain the wet weight (WW, grams, after eliminating water by blotting). Taxa abundance and biomass were standardized to individuals and weight per m^2, both per station (600 m and 800 m) and cruise. For comparisons with data from other benthic studies, we transformed WW to dry weight (DW) using the factor 0.2 (source: EMPRELAT data base, Alfred Wegener Institute).

2.2.3 Statistical analysis

An analysis of all the box-core data was first conducted using nMDS, PERMANOVA and SIMPER. A seasonal analysis (PCA, CCA, biomass and diversity trends etc) was then carried out based on data from stations C1 and S1, where 3 – 4 replicate samples were available from all cruises.

All multivariate analyses were performed on individual box-core replicates. The non-parametric Multidimensional Scaling procedure (Clarke and Warwick, 1994, nMDS) was performed using Spearman's Rank Correlation as a distance measure. The matrix of all taxa identified was used (removing taxa appearing less than twice). Principal factors in the hauls ordination were: "habitat" (2 levels: canyon, CAN, vs adjacent slope, SLO), and "water condition" (= water column temperature conditions, with 2 levels: homogeneous, HOM, during February and April, and stratified, STR, during June-July and October).

Distance-based permutational multivariate analysis of variance (PERMANOVA, Anderson, 2001) was used in a 2 factors complete model design, testing the null hypothesis H_0 of no significant main effects and interaction. The factors included in the model, considered as fixed and crossed, were "habitat" and "water condition". The same matrix and distance measure were used as in the nMDSs and we applied a permutation of residuals under a reduced model (maximum number of permutations = 9999) (Anderson and Ter Braak, 2003; Anderson and Legendre, 1999). For each Pseudo-F test, Monte Carlo and post-hoc tests were also obtained.

One-way SIMPER analysis (Clarke, 1993) was performed on the taxon matrix using Bray-Curtis distances in order to identify contributions of taxa to assemblages at the two habitats: inside the canyon and on the adjacent slope.

Principal components analysis (PCA) was performed on a correlation matrix of the environmental data, and a bi-plot was used to describe the resulting ordination patterns of samples. Canonical correspondence analysis (CCA) (Ter Braak, 1986) was applied to study the association of environmental variables with taxon/species abundances. Three CCAs were constructed. The first used the broad matrix of taxa, the other two used separate species data matrices for the canyon and the adjacent slope sites. A permutation test with 500 random permutations was used to test the null hypothesis of no linear relationship between abundances and environmental variables, with p-level = 0.05.

Generalized additive models (GAMs) (Hastie and Tibshirani, 1990) using penalized cubic regression splines (Wood, 2006) were implemented to point out relationships between taxon biomasses and environmental/trophic variables. Independent models were initially constructed to identify variables with best explanatory values. Also interactions between variables were tested. The final models, selected according to both the Akaike information criterion (AIC: Akaike, 1973) and the percentage of explained deviance (ED), had the following structure

$$G(\mu) = \beta_0 + f(x, z) \tag{2.1}$$

where $\mu = E(y)$ is the expectation of the response random variable Y; $G(\cdot)$ is the link function, while β_0 is the intercept. The function $f(x, z)$ is an arbitrary smooth function representing the effect of the interaction between two covariates, x and z, on the response. The variable selected as response for models was biomass of: (1) total fauna, (2) polychaetes, (3) crustaceans and (4) molluscs separately. It was assumed that the underlying probability distribution of the response belonged to the Gamma family and the appropriate link function was the natural logarithm. All predictors were continuous. Generalized Cross Validation criterion (GCV: Craven and Wahba, 1979; Golub et al., 1979) was used to select automatically smoothing parameters. Also taxon abundances were examined. Since models for abundances yielded fairly similar patterns in regression analysis, only biomass results are reported. Also the cumulative number of species (S) and the Shannon's index (H') were calculated considering all replicate by season.

All statistical analyses were performed using PRIMER6 and PERMANOVA+ (Clarke and Gorley, 2006), XLSTAT (Addinsoft TM) for CCAs and R2.9.0 (www.r-project.org) for general analyses, GAMs (mgcv-package) and PCA analyses.

2.3 Results

2.3.1 Taxonomic composition

A total of 106 taxa (ranging from species to families) was identified, belonging to 19 higher groups from Order to Class (Tables 2.4, 2.5, 2.6). Although not identified to the lowest taxonomic level, polychaetes included the largest number

of taxa (34). Among the groups identified to species, gammaridean amphipods were the most specious (at least 15 species), followed by cumaceans and bivalves (both with 9 species).

2.3.2 Diversity and biomass trends by habitat and season

The cumulative number of species showed some stabilization after the analysis of 3-4 cores at 800 m. However, at the shallowest station in Besòs canyon (Station C1, 600 m) we did not find any asymptotic stabilization of the cumulative number of species after analysis of 6 cores.

The number of species (S) increased from February to October both inside the canyon and at the adjacent slope (from 39 to 44 inside the canyon; from 32 to 48 at the adjacent slope: Figure 2). S was higher inside the canyon, except in October 2007. Diversity measured as Shannon's index, H', increased from February to April both inside the canyon and on the adjacent slope, decreasing in June-July (mainly inside the canyon) and increasing later (Figure 2.2). Maximum H' was found in April inside the canyon, H' = 3.53, and in October on the adjacent slope, H' = 3.56.

Total biomass of infauna increased within Besòs canyon (C1) from February-April to June/July 2007 (Figure 2.3), while at the adjacent slope (S1) peaks of biomass were also found in February and again in June/July. Among individual taxa, polychaetes showed maximum biomass in June/July and October inside the canyon and in June/July at the adjacent slope. Crustaceans (mainly peracarids) showed maximum biomass in April inside the canyon and in February on the adjacent

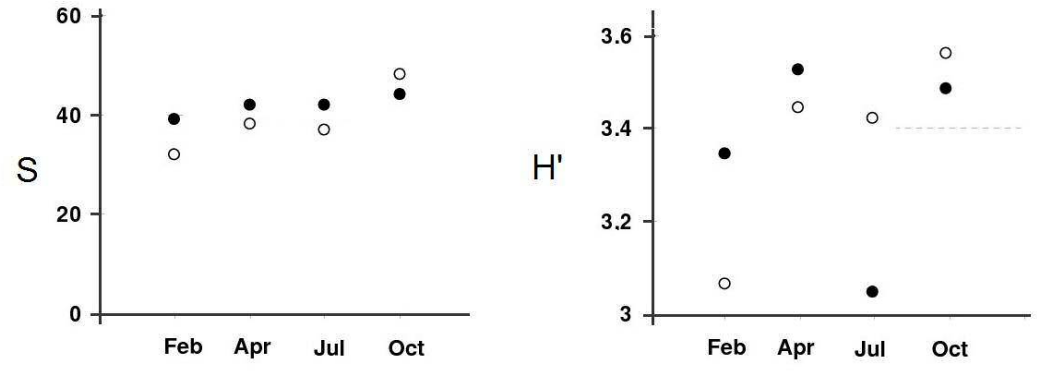

FIGURE 2.2: Diversity parameters: S represents the total number of species, H' is the Shannon index in S1 (white dots) and C1 (black dots).

slope (1-Way ANOVA at the adjacent slope: $F_{1,13}$ = 16.000, p = 0.002; significant paired Tukey's comparisons: February > April, p = 0.004; June/July > October, p = 0.005). The remaining, rather secondary, taxa showed some irregular variations, perhaps influenced by the limited number of replicates. However, peaks of

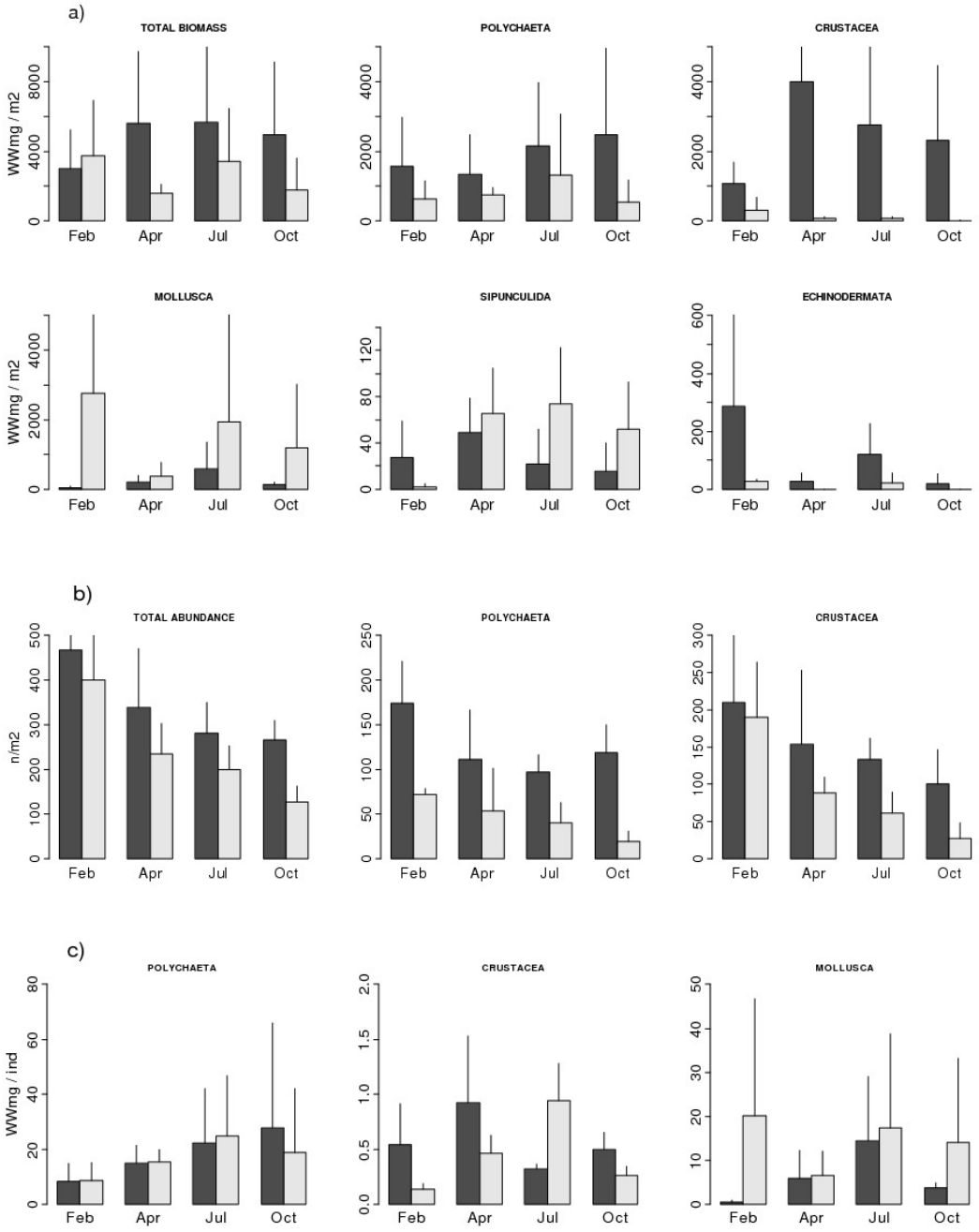

FIGURE 2.3: (a) Annual mean biomass (WWmg/m^2) profiles of total infauna and major taxa, (b) Annual mean density (ind/m^2) of total infuna, polychaetes and crustaceans, (c) individual mean weight (WWmg/ind) of polychaetes, crustaceans and molluscs. Dark gray bars indicate C1 samples and light gray bars indicate S1 samples.

biomass were found regularly in February (for echinoderms inside the canyon and for bivalves at the adjacent slope) and in June/July (molluscs inside the canyon and sipunculans at the adjacent slope). Variance of data was high, and most temporal trends were not significant, except that of echinoderms in February (1-Way ANOVA at adjacent slope: $F_{1,13}$ = 9.152, p = 0.011, paired Tukey's significant comparisons: February > April, p = 0.001; June-July > October, p = 0.003). Total biomass and biomasses of crustaceans and echinoderms were higher inside the canyon than at the adjacent slope (t test: total biomass, p = 0.074; crustaceans, p = 0.006; echinoderms, p = 0.002).

All taxa (total infauna, polychaetes, peracarids - see Figure 2.3,b - sipunculans and echinoderms) showed the highest N (ind/m^2) in February 2007 inside the canyon. Bivalves represented an exception with peaks in April and June/July. Echinoderms also showed maximum N in June/July. These differences, however, were not significant. Only on the adjacent slope did we find significant seasonal changes in infauna abundance. This was true for total infauna N ($F_{1,13}$ = 14.22, p = 0.001, higher in February than in October: Tukey's test, p = 0.021, Figure 2.3,b), for crustaceans ($F_{1,13}$ = 20.08, $p = 6 \times 10^{-4}$, higher N in February than in October: Tukey's test, p = 0.009, Figure 3b) and for echinoderms ($F_{1,13}$ = 17.16; p = 0.001, higher N in February than in the other seasons: Tukey's tests, p = 0.001). Total N and was significantly higher inside the canyon (338.2 ± 107.1) than at the adjacent slope (240.2 ± 71.4; t tests; p = 0.004).

Mean weight (Figure 2.3,c) showed the lowest values in February 2007 for polychaetes both inside the canyon and on the adjacent slope sites (1-Way ANOVA at the adjacent slope: $F_{1,13}$ = 5.16, p = 0.016; inside the canyon: $F_{1,13}$ = 2.11, p = 0.075). Crustacean mean weight was low in October inside the canyon and on the adjacent slope (1-Way ANOVA at adjacent slope: $F_{1,13}$ = 4.24, p = 0.057). Inside the canyon, the mean weight for all dominant taxa (polychaetes, crustaceans and molluscs) increased in April, a tendency that was still evident in June/July for polychaetes and molluscs. This same tendency was observed at the adjacent slope, excluding molluscs which had higher mean weight in February.

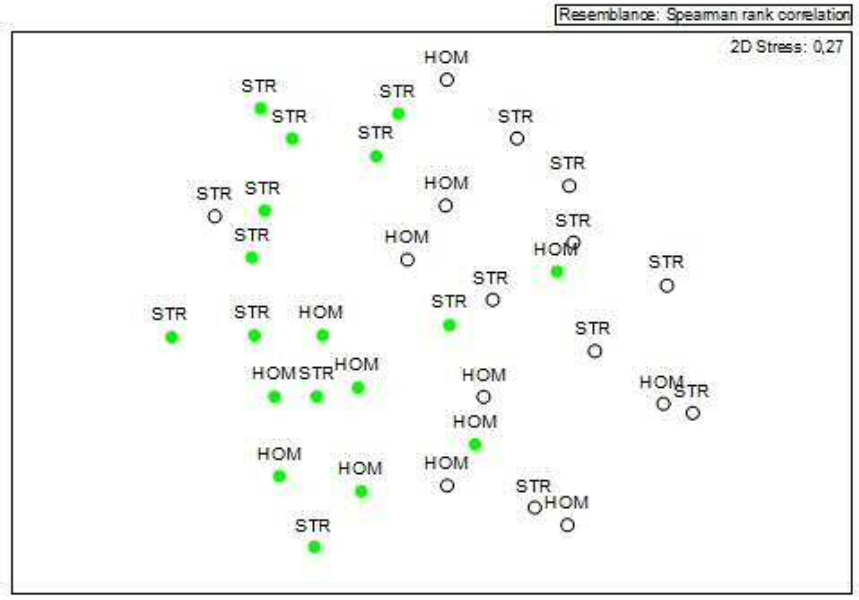

FIGURE 2.4: nMDS ordination of samples from a full year (B1, B2, B3 and B4). Labels indicated: HOM = water column homogenization and STR = water column stratification for the factor WATER CONDITIONS. Symbols indicate: full cycles = canyon; empty cycles = adjacent slope for the factor HABITAT.

2.3.3 Assemblage structure: composition by habitat (canyon and adjacent slope)

The nMDS plot shows the hauls grouped according to both habitat (canyon or adjacent slope) and water column condition (stratified or homogenised) (Figure 2.4).Samples from the canyon are grouped in the left part of the graphic, while samples from the adjacent slope are grouped in the right part. In contrast samples collected during stratified water column condition occupy mainly the top, while samples collected during homogenized conditions occupy the bottom of the graphic.

The two-way PERMANOVA (Table 2.1) showed statistically significant main effects, i.e. effect of both habitat ($p = 3 \times 10^{-4}$) and water column condition ($p = 0.031$). The test did not showed a significant effect of the interaction between the two factors. Pairwise tests indicated higher abundance inside the canyon than at the adjacent slope, especially under stratified water column conditions.

SIMPER analyses of abundances (Table 2.2) showed that the amphipod *Carangoliopsis spinulosa*, ampharetid polychaetes and amphipods of the genus *Harpinia* spp. were the most abundant taxa at the canyon site, representing less than 50%

of total abundance. At the adjacent slope site the sipunculan *Onchnesoma steenstrupii* dominated in the assemblage, followed by the bivalve *Ennucula aegeensis* and *C. spinulosa*. These three species together represented the 54.6% of the total abundance.

2.3.4 Environmental variables

Temperature (T_{5mab}) varied within a narrow range through the year both inside the canyon and especially at the adjacent slope (Figure 2.5). Anyhow T_{5mab} was always lower at the adjacent slope rather than at the canyon station. Inside the canyon site, T_{5mab} increased between June/July and October. At the adjacent slope site T_{5mab} was quite constant all year round except for a slight rise in April. There was a period of water column homogeneity in February and April and of stratification in June-October. Salinity 5 m above the bottom (S_{5mab}) ranged between 38.43 and 38.56 (Figure 2.5). S_{5mab} showed higher values at the canyon station, where it increased from April to October. This pattern was not observed at the adjacent slope where S_{5mab} showed the same pattern found for T_{5mab}. Fluorescence (f_{0-200m}) followed the same temporal pattern at both the canyon and the slope stations. As regularly happens in the study area with surface *Chl* a (satellite imagery, see below), maximum f_{0-200m} was found in January-February (winter) and minimum f_{0-200m} was observed in July-August (summer) (Figure 2.5). Water turbidity at

A) Main test				
Source	df	MS	Pseudo-F	P-value
habitat	1	1.578	4654	3×10^{-4}
water condition	1	0.766	2258	0.031
habitat × water condition	1	0.335	0.988	0.448
Res	30	0.339		
Total	33			

B) Pairwise tests
CAN > SLO
HOM>STR
CAN > SLO (within STR)

TABLE 2.1: A) Permanova based on Sperman rank correlation distance matrix of whole dataset and B) pairwise tests (Only significant tests are reported; Monte Carlo significance within brackets if differs from permanova's). (ns: not significant; *: < 0.05,**: < 0.01, ***: < 0.001). Factors: habitat (levels: CAN, SLO) and water column condition (levels: homogenized, HOM, and stratified, STR)

A) Canyon		Av. sim.: 28.29		
Code	**Acr.**	**Taxon**	**Con. (%)**	**Cum. (%)**
AM	Cspi	*Carangoliopsis spinulosa*	20.14	20.14
PO	Amph	Ampharetidae	15.99	36.12
AM	Harp	*Harpinia* spp.	14.97	51.09
PO	Para	Paraonidae	5.06	56.15
AM	Pocu	*Paraphoxus oculatus*	3.65	59.8
PO	Flab	Flabelligeridae	3.31	63.12
IS	Pfre	*Pilosanthura fresii*	2.99	66.11
PO	Glyc	Glyceridae	2.98	69.09
SI	Oste	*Onchnesoma steenstrupii*	2.87	71.96
EC	Achi	*Amphiura chiajei*	2.76	74.71
PO	Spio	Spionidae	2.18	76.9
PO	Onup	Onuphidae	1.88	78.77
PO	Capi	Capitellidae	1.74	80.52
B) Adj. slope		Av. sim.: 22.09		
Code	**Acr.**	**Taxon**	**Con. (%)**	**Cum. (%)**
SI	Oste	*Onchnesoma steenstrupii*	33.93	33.93
BI	Eaeg	*Ennucula aegeensis*	13.15	47.07
AM	Cspi	*Carangoliopsis spinulosa*	7.52	54.6
CA	Proc	*Prochaetoderma* spp.	6.53	61.13
BI	Alon	*Abra longicallus*	5.55	66.68
PO	Para	Paraonidae	5.26	71.94
CA	Falc	*Falcidens* spp.	4.63	76.57
CU	Llon	*Leucon longirostris*	2.52	79.1
IS	Pfre	*Pilosanthura fresii*	2.38	81.47

TABLE 2.2: One way SIMPER analysis (factor used: habitat) based on Bray-Curtis similarity (cut-off: 80%). Percentage contribution and cumulative percentage of taxa are reported for each level of the factor, as well as the acronyms of taxa used as labels in CCAs. AM: amphipoda, PO: polychaeta,IS: isopoda, SI: sipuncala, EC: echinodermata, BI: bivalvia, CA: caudofoveata, CU: cumacea.

5 m above the seafloor ($Turb_{5mab}$) reached maximum values in February at the adjacent slope and in April inside the canyon (Figure 2.5). At both stations $Turb_{5mab}$ decreased in June/July, when minimum values were observed, increasing again in October. REDOX Potential (Eh: Figure 2.5) showed different trends at the canyon and the slope stations. Inside the canyon sediments were least reduced in February (-24.4 mV) with an abrupt drop in Eh in April-June/July-October (between −40.4 and −37.7 mV). At the adjacent slope Eh was on average a little more reduced than at the canyon station, with lower Eh in June/July than October. Inside the canyon the total organic matter (TOM) in sediments increased from February to June/July then decreased (Figure 2.5). At the adjacent slope TOM increased from February to April and decreased in June/July and October. TOM was, on average, higher in samples taken at slope than inside the canyon,

the difference being significant in April. Flow volume of the most important rivers in the area was maximal in April-May (15.5-4.5 m^3 s^{-1}) and minimal in June-July (2.5 m^3 s^{-1}), followed by some increase in August-October (Figure 2.6). *Chl* a at the surface, obtained by satellite imagery, decreased sharply from a maximum value in April to an annual minimum in July-August (Figure 2.6).

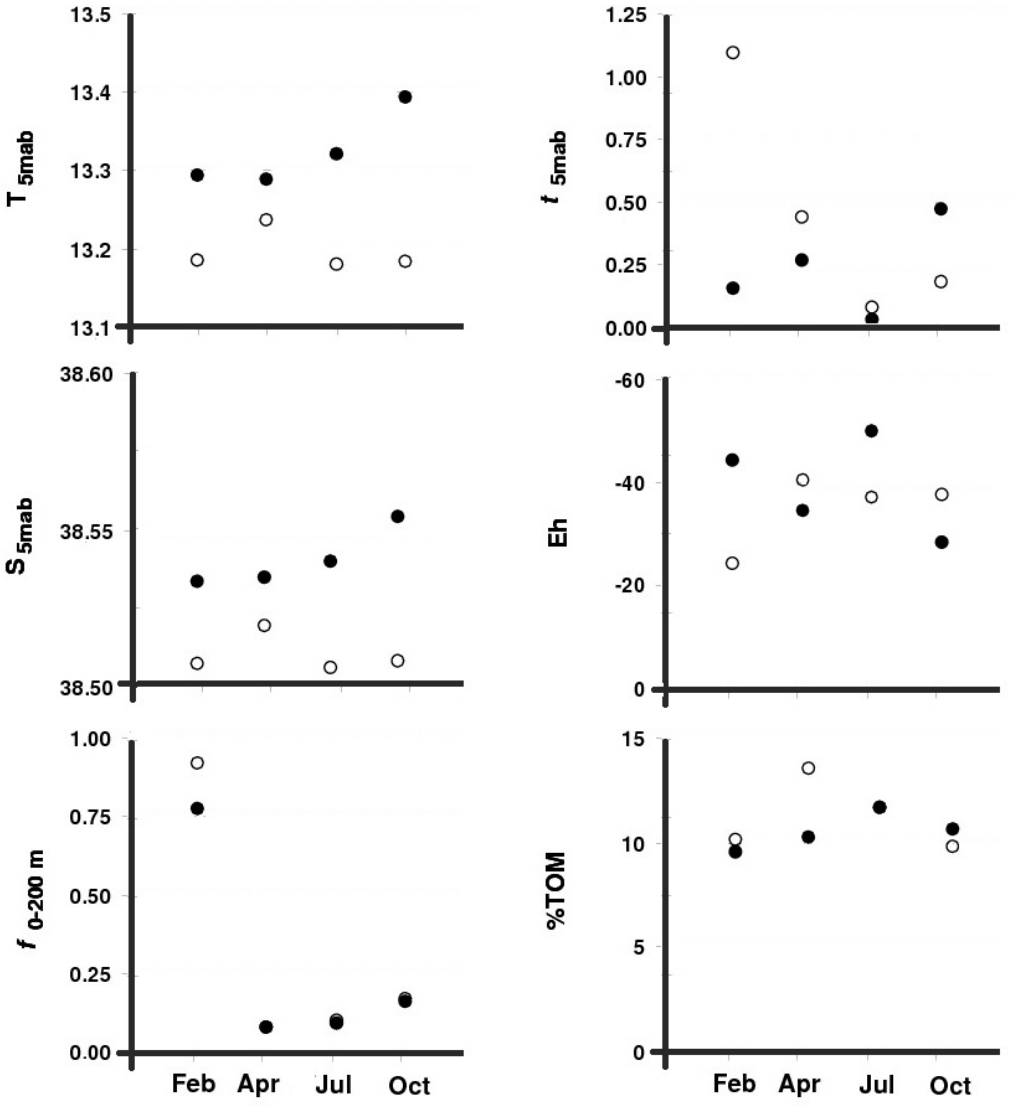

FIGURE 2.5: Environmental variables as a function of season. Temperature above the bottom (T_{5mab}); salinity (S_{5mab}); fluorescence (f_{0-500m}); water turbidity close to the bottom ($turb_{5mab}$); potential redox of sediments (at a depth of 1 cm: Eh); TOM in sediments. (dark dots): canyon; (white dots): adjacent slope.

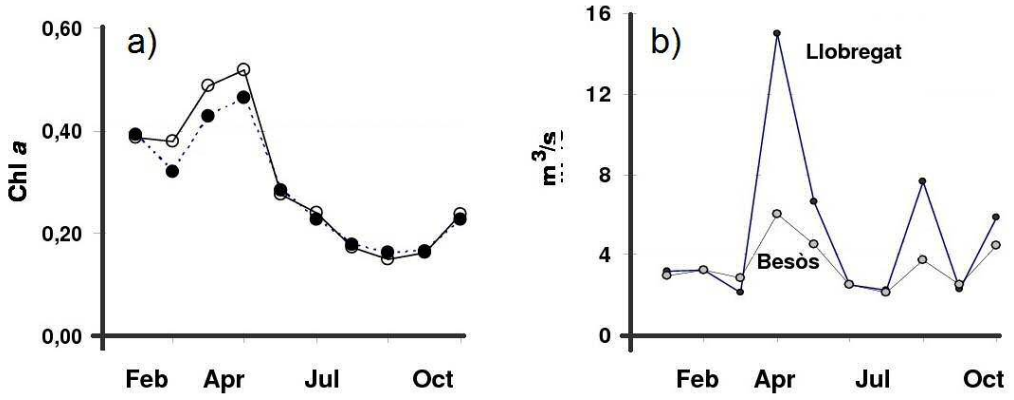

FIGURE 2.6: Environmental variables. a) *Chl*a in surface by satellite imagery (dark dots: canyon; white dots: adjacent slope); b) river flow (m^3 s^{-1}) of the two most important rivers in central Catalan coasts.

2.3.5 Influence of environmental variables

The first two principal components in the PCA of C1 stations (Figure 2.7, a) explained 46% and 32% of the total variance, respectively. A strong seasonality was evident in the ordination of samples, with habitat variables often associated with specific sample stations. Thus, fluorescence was associated with February (B1), river discharge, TOC and δ^{13}C with April (B2), C/N with July (B3) while T_{5mab} , S_{5mab}, $Turb_{5mab}$ and less reduced sediments (Eh) were associated with October (B4).

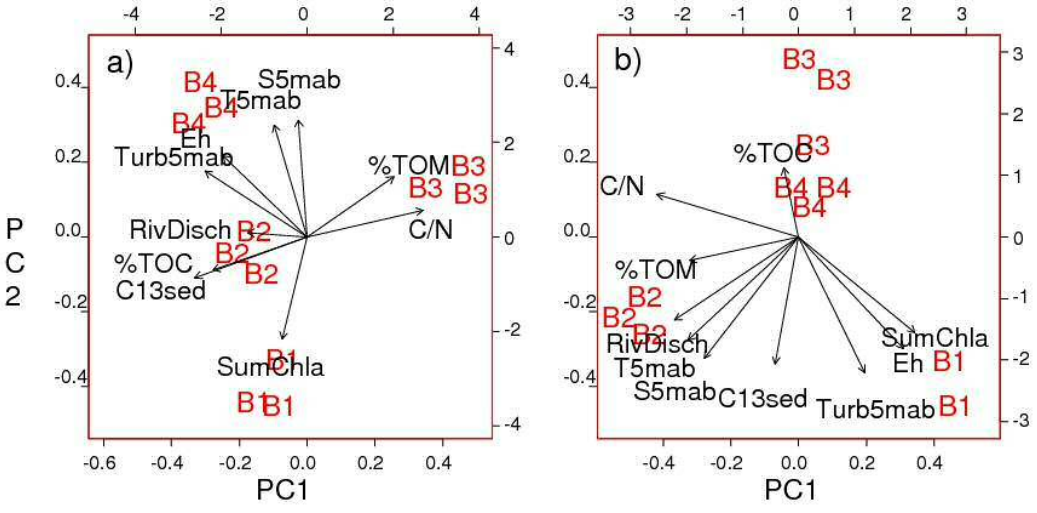

FIGURE 2.7: PCAs of environmental variables collected in (a) canyon stations and (b) adjacent slope.

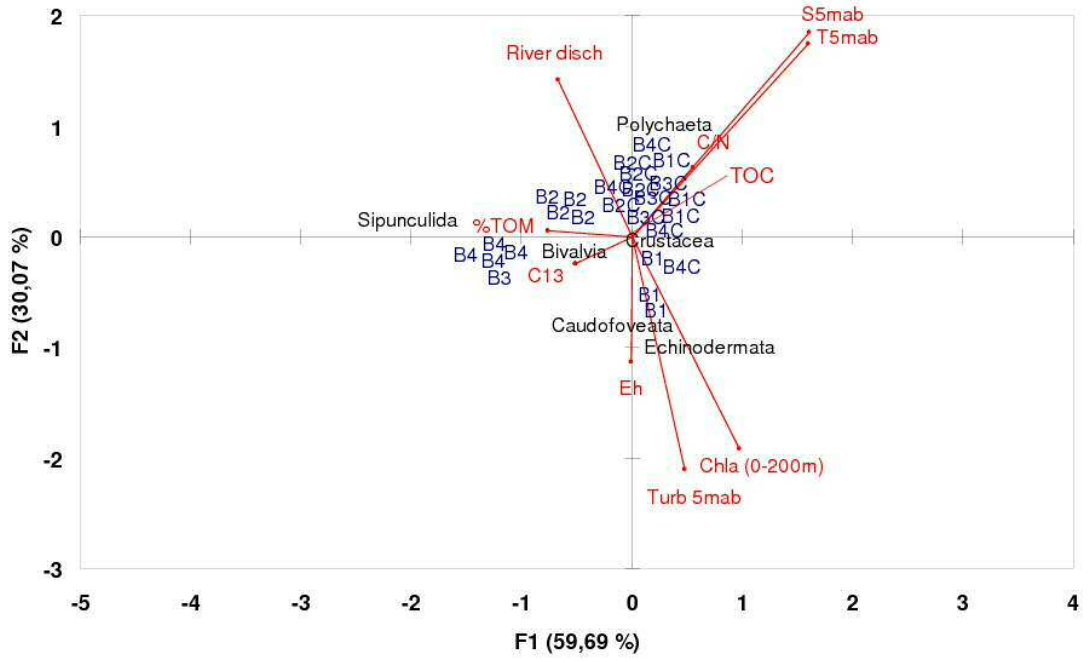

FIGURE 2.8: CCA of broad taxa, considering both canyon and adjacent slope samples, with selected environmental variables.

The first two principal components in the PCA for S1 (adjacent slope: Figure 2.5, b) explained 44% and 36% of the total variance, respectively. Those samples also showed a seasonal relationship in the ordination, but it was less evident than that inside canyon. Moreover, the strength of the association with habitat variables varied across the canyon samples: February (B1) was coupled with fluorescence, but also with less reduced sediment (Eh) and Turbidity; April (B2) was associated with river discharge, but also with T_{5mab}, S_{5mab}, and TOM; July-Octuber (B3 and B4) were related to gradients of TOC (positively) and to δ^{13}C in the sediment (negatively).

Canonical correspondence analyses (CCAs; Figure 2.8) produced an ordination of the most abundant taxa and their relationship with environmental variables, as a function of both habitat and season. CCA of the joint data set from C1 and S1 (Figure 2.8) explained 89.8% of the total variance. The permutational test revealed a significant linear relationship between taxa abundances and environmental variables (pseudo$-F$ = 0.580; p = 0.009). Clear segregation between canyon station and adjacent slope samples was observed, with an evident association between canyon samples and the abundance of polychaetes and also of crustaceans. This segregation was mainly linked to higher salinity (S_{5mab}) and temperature (T_{5mab}) inside the canyon. Canyon samples were also linked to higher TOC, indicating

a response to the amount of available food, and with C/N, i.e. organic matter quality. To a lesser extent canyon station samples were associated with higher river discharge, more reduced sediments and more depleted δ^{13}C. Canyon samples were grouped in one subset. Seasonality is masked by stronger difference between habitats (Canyon versus adjacent slope), although to some extent that was related to the seasonal condition (e.g. homogeneity in B2, B1) of the water column. Adjacent slope samples showed some seasonal segregation, with different dominant taxa in each season. Caudofoveata and Echinoderms were related to *Chl* a and $Turb_{5mab}$ in February (B1) and to greater reduction of the sediments. Sipuncula and to a lesser extent Bivalvia were related to TOM and to enriched δ^{13}C values in July-October (B3-B4).

The two CCAs performed on dominant species (except polychaetes distinguished only to Family level) showed some ordination of species both at canyon station and on the adjacent slope (Figures 2.9 a and 2.5 b, respectively). The CCA for station C1 explained 75.1% of the total variance (Permutational test: pseudo$-F$ = 0.301, p = 0.058). Sample ordination showed some seasonal pattern. B1 and B2 from February-April (obtained under homogenized water mass conditions) were located together in the left-upper part of the biplot, while samples collected under stratified conditions (B3, B4 from July and October) were in the opposite corner. B1 and B2 were mainly associated with Paraonidae, *Harpinia* spp. and *O. steenstrupii*, which were positively related to *Chl*a, TOC, enriched δ^{13}C and high river discharge. B4 (July) cores were associated with Onuphidae and Glyceridae, both opportunistic carnivorous polychaetes, and with reduced Eh in sediments. Ampharetidae and the ophiuroid *Amphiura chiajei* were related more to high T_{5mab} and S_{5mab}. A number of surface and sub-surface deposit-feeding polychaetes (Capitellidae, Spionidae, Flabelligeridae) were more abundant in B3 (July) cores and associated with high C/N. C/N is indicative of fresh OM, probably lipids, in sediments.

On the adjacent slope (S1) CCA explained 70.9% of the total variance and the permutational test was significant (pseudo$-F$ = 0.507, p = 0.021). Samples showed some seasonal grouping (less clear than in the Besòs canyon CCA): B1 was associated with Caudofoveata (*Falcidens* spp., *Prochaetoderma* spp.), Paraonidae and with the amphipod *C spinulosa*. These were positively correlated in turn with $Turb_{5mab}$, fluorescence and reduced Eh in sediments. Caudofoveats are surface deposit feeders preying on foraminiferans (meiofauna) and Paraonidae, and they can also feed selectively on small diatoms. The bivalve *Abra longicallus* and the isopod *Paranthura fresii* seemed mainly associated with B2 in April and with a

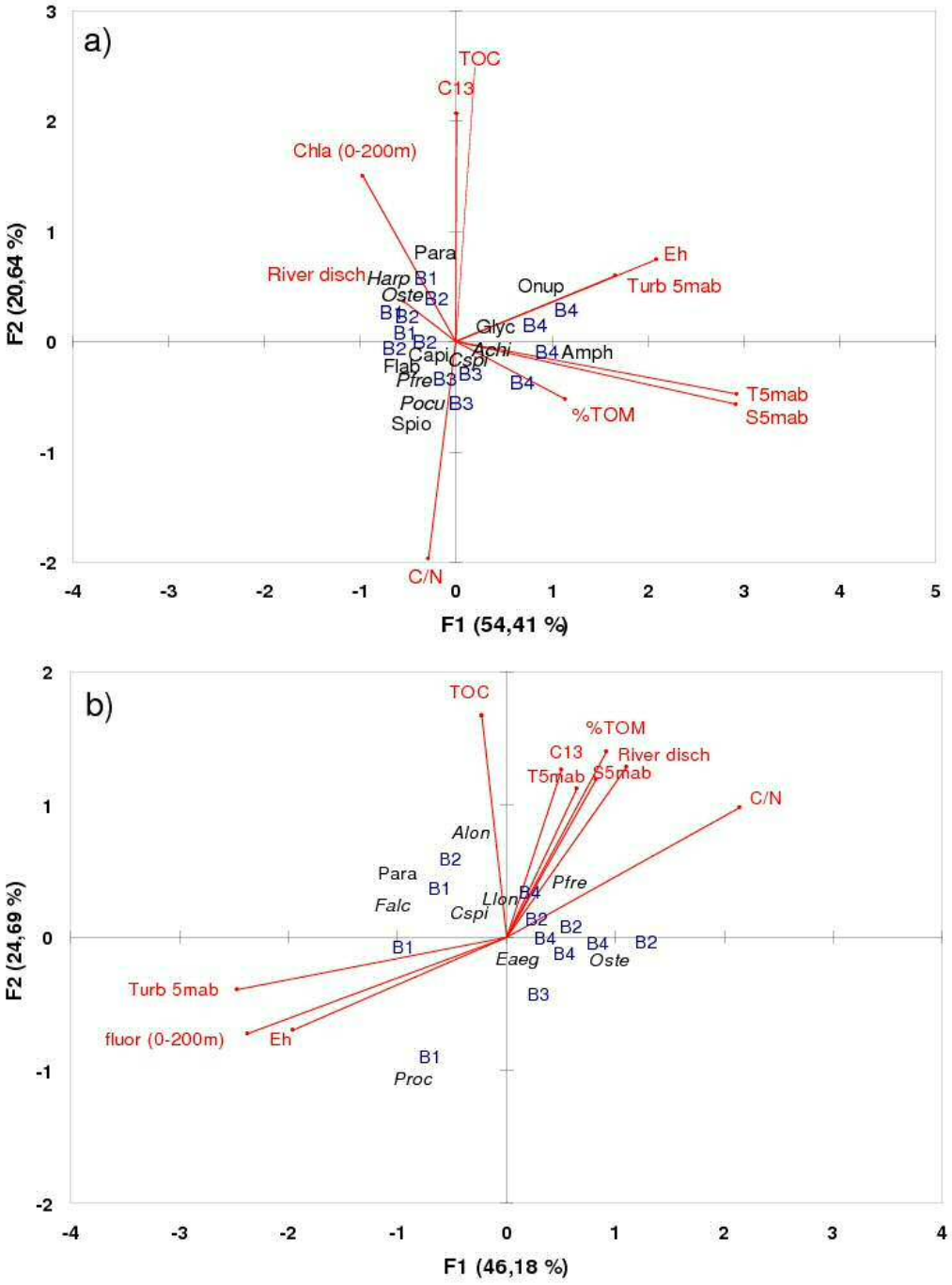

FIGURE 2.9: CCA of dominant species (a) inside the canyon and (b) on the adjacent slope and the environmental variables. For the full name of species' acronyms see Table 2.2.

high number of variables; among the most important were TOC, TOM, enriched δ^{13}C in sediments and river discharge. *O. steenstrupii* and the bivalve *E aegensis* were more abundant in July (B3) and October (B4) under conditions of low $Turb_{5mab}$, and high C/N in sediments.

Response	Model's right side	$p-$value	GCV	AIC	R^2(adj)	DE (%)
Total						
	$= f(T_{5mab}, TOC)$	0.006	1071	281	0.236	75.3
	$= f(T_{5mab}, C/N)$	0.013	1251	335	0.196	29.0
Polychaetes						
	$= f(S_{5mab}, TOC)$	0.014	1194	235	0.430	72.8
Crustaceans						
	$= f(T_{5mab}, TOC)$	0.006	5680	183	0.434	76.5
	$= f(T_{5mab}, RivDisch)$	0.013	4956	230	0.228	46.8
Molluscs						
	$= f(T_{5mab}, RivDisch)$	0.031	4989	190	0.089	39.1
	$= f(T_{5mab}, f_{0-200m})$	0.039	5502	192	0.046	38.8

TABLE 2.3: GAMs for A) the total biomass of the macrofauna, B) Polychaetes' biomass C) Crustaceans' biomass and D) Molluscs' biomass. For each response, the right side of the model, the significance of the effect, the GCV, the AIC, the adjusted r-squared (R2) and the deviance explained (DE) are given.

2.3.6 Regression models

Models with higher explanatory deviance are reported in Table . Total biomass, and the biomass of principal taxa, are functions of interactions among several environmental variables, including T (or S, strongly correlated with T) and trophic variables, especially TOC in the sediment, and to a lesser extent with river discharge, Chla, C/N, δ^{13}C and turbidity. Total biomass, as well as polychaete and crustacean biomasses, showed higher values when high TOC and low T were combined (figures not reported), while total biomass was positively related to C/N (fresh organic matter) and to T. Crustaceans and molluscs showed a strong positive relationship with changes in river discharges, as did molluscs with Chla at medium values of T.

2.4 Discussion

Benthos is the dominant trophic resource for fish and large crustaceans inside the Catalan canyons (e.g. Carrassón and Cartes, 2002; Cartes, 1994; Cartes and Maynou, 1998; Macpherson, 1981; Maynou and Cartes, 1998), quantitative studies on macrofauna are required to establish, for instance, mass-balance models.

This is the first seasonal quantitative study performed on deep-sea macrobenthos in the NW Mediterranean Sea. Previous studies analysed patterns of biomass and assemblage distribution as e.g. a function of depth (e.g. Stora et al., 1999; Tselepides and Eleftheriou, 1992). In addition, most previous studies have been performed on large epifauna-infauna (i.e. the megafauna) (Cartes et al., 2009; Pérès, 1985; Pérès and Picard, 1964) and non-quantitative (e.g. Reyss, 1971).

The analysis of deep-sea macrofauna distribution with environmental variables returned significant effects of depth (Pérès, 1985) and of a group of factors related with sediment characteristics (Reyss, 1971), such as the grain size (Stora et al., 1999) and the organic matter content (Tselepides and Eleftheriou, 1992; Tselepides et al., 2000). These explanatory variables for macrobenthos variability have been evaluated in these previous works along a wide depth range on the continental slope (200 – 1000/2000 m).

As supported by a variety of statistical analyses, changes in macrofauna assemblages and trends in biomass are related with variables associated to sediment characteristics, particularly nutritional value (TOC, C/N, δ^{13}C), but also with characteristics of near-bottom water masses (T, S), typifying the overall status of the benthic boundary layer, BBL (Gage and Tyler, 1991).

The macrofauna is related mainly to the total organic carbon (TOC) in sediments, i.e. the quantity of food available to the mactofauna. This relation has also been found deeper in both the Atlantic Ocean (Sibuet et al., 1989) and the Angola Basin (Kröncke and Türkay, 2003).

Fresh organic matter inside the Besòs canyon in June-July has a terrigenous origin, as shown by the increase of C/N and depletion of δ^{13}C. Apart from the highly depleted δ^{13}C, the C/N ratio was very high in June-July, as expected from terrestrial POM (Thornton and McManus, 1994) and the main food input is from advective fluxes. On the adjacent slope (800 m), C/N has lower values, and the food input is more indipendent from advective flux. Regarding to water-mass dynamics, higher infaunal abundance was found inside Besòs when T and S were higher. This coincided with the arrival of the Levantine intermediate water (LIW) in the Balearic Basin, once the flow of winter intermediate water is interrupted in the area (López-Jurado et al., 2008). Changes in deep-water masses can influence the re-suspension of particles and inputs of POM from other areas, in our case from the most productive region of the Ligurian Sea, situated to the east of the

Balearic Basin. Thus, this current produces more favourable conditions, especially a large supply of nutrients, that favours the proliferation of macroifauna.

We assumed in our study design that our sample replication would be enough to characterize infaunal communities, although species accumulation curves did not reach an asymptotic shape after analysing 3 or 4 replicates per station at the Besòs canyon site, although considering both stations was sufficient. Stora et al. (1999) tested sample replicability in muddy bottoms of the neighbouring Toulon canyon using the same 0.06 m^2-box corer used here. Except for the shallowest stations (at 250 m), they concluded that "3 replicates would have been enough to assess assemblage variation at depths between 500 – 2000 m". The station C1 was inside the canyon, close to its head, where the temporal pattern of food supply was similar to that on the continental shelf at 60 m (e.g. $\delta^{13}C$: Authors' unpubl. data). This higher variability probably requires more replicates to fully capture the diversity of fauna in the canyon. However, our replicates, by contrast, showed higher within cruise affinity than between cruise affinity, as demonstrated in PCAs-CCAs where replicates belonging to the same cruise were grouped together and linked to the same environmental conditions.

2.4.1 Comparison with other quantitative studies

There are only a few quantitative studies on benthos in the deep Mediterranean (Stora et al., 1999; Tselepides and Eleftheriou, 1992). Off the deep Catalan slope mean annual biomass ranges between 3.1 g WW/m^2 at 800 m and 4.8 g WW/m^2 inside canyon (ca. 0.62 – 0.96 g DW/m^2 respectively). Biomass was ca. two-times higher than levels recorded in or close to Toulon canyon at comparable depths (500 m: 0.32 – 0.54 g DW/m^2: Stora et al., 1999). This could be related, among other things (e.g. seasonal variation), to the existence of a small river (mean annual flow 3.4 m^3/sec in 2007) debouching to the north of Barcelona, of which the Besòs canyon is the natural extension, while the Toulon canyon is not an extension of any existing river on the continent (Stora et al., 1999) The higher diversity (S) (despite not including foraminiferans or classifying polychaetes to species level) and total abundance (338.2 ind/m^2) found within Besòs in comparison to the Toulon canyon (S = 36; N = 176 ind/m^2: Stora et al., 1999) confirms that food availability is higher in our small canyon. As expected, our biomass data were clearly higher than values in the South Cretan Sea (Tselepides et al., 2000), where biomass (0.05 – 0.09 g DW/ m^2) was an order of magnitude lower than at comparable

depths on Catalan slopes. This is explained by the increasing oligotrophy from West to East in the Mediterranean (Azov, 1991; Salihoğlu et al., 1990) and by the particularly low food sources in the southern Aegean Sea (Tchukhtchin, 1964; Tselepides et al., 2000). On the Catalan slope, sediment redox potential (Eh) was clearly lower (on average −40.7 mV) than in the South Aegean Sea (Tselepides et al., 2000), indicating higher organic matter availability for benthos.

The taxonomic composition of infauna varied between stations at different depths on the Catalonian slope. Inside the Besòs canyon polychaetes (Ampharetidae, Paraonidae, Flabelligeridae), amphipods (*C. spinulosa*, *Harpinia* spp., *Paraphoxus oculatus*) and the echinoderm *A. chiajei* dominated. On the adjacent slope the sipunculan *O. steenstrupii* and bivalves (*E. aegeensis*, *A. longicallus*) were more important, together with several caudofoveats (*Falcidens* spp., *Prochaetoderma* spp.). From a trophic perspective, surface deposit feeders (e.g. Ampharetidae among polychates and the echinoderm *A. chiajei*) dominated in Besòs canyon, replaced by subsurface deposit feeders (e.g. sipunculans) on the adjacent slope. This is consistent with existing literature on deep-sea macrobenthos food webs (Flach and Heip, 1996; Kröncke et al., 2003): species feeding mainly at the sediment surface are linked to fresh organic matter, whereas subsurface deposit-feeders and predators are found in sediments with more refractory material. The same replacement of trophic guilds with depth was observed in the abyssal Indian Sea (Pavithran et al., 2009). Stora et al. (1999) found a similar increase of subsurface deposit feeders at 1000-1500 m in Toulon canyon. At our slope station, adjacent to Besòs canyon, we attributed the shift to higher habitat stability on deeper bottoms: temporal fluctuations of food sources (TOC, C/N, δ^{13}C) are less evident on the adjacent slope than inside Besòs (Authors' unpubl. data). That reasonably explains why the Besòs canyon assemblage was dominated by surface deposit feeders thoughout the year and seasonally by opportunistic trophic groups (Capitellidae, Flabelligeridae, Glyceridae), better able to adapt to rapid temporal changes in food inputs.

2.4.2 Dynamics of infauna assemblages

Continental shelf infaunal assemblages often show intra-annual variability, with shifting peaks of biomass and diversity during short lag times after triggering events (e.g. the change from a spring assemblage to a summer one: de Juan and Cartes, 2011). This is probably a consequence of both spatial heterogeneity and

coupling with a diversified food source. Off Banyuls (western Mediterranean) both the highest growth rates of the deposit-feeding bivalve *Abra ovata* and peaks of meiofauna were found in spring, coupled with maximal pigment concentrations at the surface of the sediment (Gremare et al., 1997). Close to river mouths, the distribution of species is also related to fluctuations in hydrodynamic regime that influence substrate characteristics and particle re-suspension. Sediment discharges of rivers can change species composition close to delta fronts (Akoumianaki and Nicolaidou, 2007; Cartes et al., 2007). Such information is not generally available for deep-sea systems.

The two stations we sampled on the Catalan slope showed of course differences in the amount of biomass (higher in the Besòs canyon), but also some important differences in seasonal dynamics. Biomass in the canyon increased progressively from February to June-July, while at adjacent slope it remained low, increasing moderately in February and/or July. Also assemblage diversity inside canyon and on adjacent slope showed different patterns through the year. While station C1 showed higher diversity during the period of water column homogeneity (February and April) with a minimum in June-July, the adjacent slope site showed higher diversity during the period of water column stratification with a minimum in February. This is probably linked to higher organic matter quantity (TOC) and quality of sedimentary food (higher C/N) inside Besòs canyon (Authors' unpubl. data) supplied by river discharges. At Besòs canyon we found depleted δ^{13}C values closer to those found at 60 m at a shelf station (Authors' unpubl. data). Depleted δ^{13}C indicates terrigenous origin of organic matter by river flows.

The quality of POM deposited at the seafloor determines changes in the composition and biomass of macrofauna communities (e.g. off Banyuls: Gremare et al., 1997, in the North Sea: Dauwe et al., 1998; Wieking, 2002; Wieking and Kröncke, 2003). These changes correspond to the feeding types of the constituent taxa/species, matches being established between the available food and the feeding modes of the dominant consumers. Highly mobile predators can proliferate, consuming new production derived from abundance peaks of species belonging to lower trophic levels (Mamouridis et al., 2011).

Among infauna, we found consistent relationships between feeding types and the quantity and quality of POM arriving on Catalan slopes. At the level of broad taxa, polychaetes were more abundant under canyon environmental conditions that include: (1) high TOC and high C/N, which are indicative of low fresh food

availability because C/N is often correlated with lipid contents (Bodin et al., 2007), an important source of fresh food for benthos (Cartes, Grémare, Maynou, Villora-Moreno and Dinet, 2002; Gremare et al., 1997), (2) high river discharge, with a delay of ~ 2 months, which suggests an important food source of terrigenous origin for benthos, and (3) increase of T and S indicating changes in water masses (LIW) in the study area (Hopkins, 1978). By contrast outside the canyon, caudofoveats and echinoderms (mainly small surface feeding ophiurids) were linked to high near-bottom turbidity and pigment fluorescence in the water column, conditions found especially in February. This suggests stronger coupling with peaks of primary production at surface. Caudofoveats (e.g. *Falcidens* spp.) prey on foraminiferans (meiofauna) (Salvini-Plawen, 1981, 1988). Amphipholidae are surface deposit feeders (Buchanan, 1964), which probably benefit from turbidity increases (more suspended particles) close to the bottom. On the other hand, sipunculans are sub-surface deposit feeders (Romero-Wetzel, 1987) that were more abundant on the slope in October, when more recycled POM (enriched in δ^{13}C) and rather more TOM (~ 10%) were found in sediments. In general, such ecological relationships are subject to strong spatio-temporal variations, with seasonal shifts in the species occupying the dominant trophic guilds. Sipunculans, for instance, can save up fresh labile material below the sediment-water interface (Galeron et al., 2009), hence becoming surface deposit feeders. Such relationships were more difficult to establish at species level, due to the lack of detailed information on species diets. In general, dominant species in the canyon during February and April (Paraonidae and *Harpinia* spp.) were more clearly related with variables indicating inputs of pigments in the water column, probably derived from the peak of surface primary production. Paraonidae are partially surface feeders (Fauchald and Jumars, 1979) consuming diatoms, and foraminiferans, though only a single species has been studied (Röder, 1971). However, *Harpinia* spp. gave an isotopic signal corresponding to omnivory (Fanelli et al., 2009), and they may also prey on meiofauna. Most polychates (Capitellidae, Spionidae, Flabelligeridae) were more abundant in June-July in Besòs canyon coinciding with a decrease of TOC in sediments, but also with a clear signal of terrigenous C (depleted δ^{13}C and high C/N: Cartes et al., 2010; Authors' unpubl. data). These polychates are considered to be opportunistic and non-selective in food-particle selection (Fauchald and Jumars, 1979). Spionidae are potentially mobile and can behave as suspension-feeders (Pardo and Zacagnini Amaral, 2004), while Flabelligeridae are typically tubiculous. Inside Besòs canyon other surface deposit feeders were found in this period (e.g. the ampharetid *Melinna* sp.: Gaston, 1987, and *A. chiajei*: Buchanan,

1964). Surface deposit feeders also dominate (representing between 36% and 73% of abundance) in Toulon canyon assemblages (Stora et al., 1999) in samples mainly taken in May-July. By contrast on Catalan slopes, during October and under conditions of maximum water turbidity and increases of TOM and TOC, carnivorous polychaetes (Glyceridae, Onuphidae: Fauchald and Jumars, 1979) were dominant, together with Ampharetidae, considered as surface deposit feeders. Carnivorous polychaetes were also more abundant at the two shallowest stations at Toulon canyon (Stora et al., 1999). This trophic group is more characteristic of disturbed areas (i.e. with high hydrodynamism) exposed to strong organic inputs (Pearson and Rosenberg, 1978). These conditions were likely found at the sediment-water interface rather than deeper in the sediment. This explains why carnivorous polychaetes (*Harmothoe* sp., *Nephthys* spp.) collected with the suprabenthic sledge dominated this "suprabenthic" habitat, showing their maximum abundance under higher $Turb_{5mab}$ (Mamouridis et al., 2011).

At the slope site temporal relationships between species and environmental variables were less marked than in the Besòs canyon, as indicated by PCA and CCA results. This tendency is in agreement with higher fluctuations of food sources (TOC, C/N, δ^{13}C) at the Besòs canyon (see above); conditions were more stable at the adjacent slope stations. The only consistent relationships at the adjacent slope were caudofoveats (*Falcidens* spp., *Prochaetoderma* spp.) and Paraonidae with $Turb_{5mab}$ and fluorescence, likely because these taxa are surface deposit feeders that can eat diatoms and foraminiferans (meiofauna) (Fauchald and Jumars, 1979; Jones and Baxter, 1987). As foraminiferans respond rapidly to inputs of fresh organic matter (Gooday, 1988), it is possible that they already reach high densities in February because the maximum of primary production at the surface begins in November-December off Catalan coasts (from `http://reason.gsfc.nasa.gov/Giovanni`).

In conclusion, the dynamics of macrobenthos at the two stations sampled over Catalan slopes showed differences in biomass and abundance patterns and in their trophic structure. Biomass was higher inside the Besòs canyon than on the adjacent slope. Communities inside the canyon are mostly dominated by surface detritus polychaetes and crustaceans and on the adjacent slope by subsurface deposit feeders (mainly sipunculans). Also epibenthic-mobile assemblages of polychaetes were clearly different in composition from those of infauna, being composed of carnivorous forms associated with higher near-bottom turbidity. The proliferation of opportunistic species inside the Besòs canyon and a stronger temporal succession

there of species in relation of food availability and quality were consistent with greater variability in food sources (TOC, C/N, δ^{13}C) (Authors unpubl. data) and with greater influence of terrigenous inputs by river discharges. Total macrobenthos biomass found over Catalan slopes was higher that found in the neighbouring Toulon canyon (Stora et al., 1999), probably because the canyons are differently conditioned by their relationships with rivers and river flows.

Acknowledgements: The authors thank all the participants of the BIOMARE (ref. CTM2006-13508-CO2-02/MAR) surveys, especially the crew of the F/V García del Cid for their inestimable help. A number of taxonomists helped us in the determination of different taxa. Our acknowledgements to Drs C. Salas and S. Gofas (Univ. Málaga) for their help determining some bivalves and gastropods, and to Dr L. Salvini-Plawen (Univ. of Vienna) for caudofoveats.

TAXA	Canyon	Ad. slope
Cnidaria		
Stephanoscyphus spp. Allman, 1874	0.0	2.0
Archianellida		
Archianellida unid	0.0	1.0
Polychaeta		
Ampharete sp. Malmgren, 1866	0.9	0.0
Ampharetidae Malmgren, 1867	34.5	1.9
Arabellidae Hartman, 1944	0.5	0.5
Aricidea spp. Webster, 1879	7.6	6.4
Capitellidae Grube, 1862	6.6	1.5
Diplocirrus sp. Haase, 1915	5.5	1.9
Eunicidae Berthold, 1827	4.3	0.0
Flabelligeridae Joseph Saint, 1894	0.9	0.5
Galathowenia sp. Kirkegaard, 1959	0.5	0.0
Glycera sp. Savigny, 1818	0.9	0.5
Glyceridae Grube, 1850	3.2	2.9
Levinsenia gracilis (Tauber, 1879)	2.8	2.9
Levinsenia spp. Mesnil, 1897	3.6	1.5
Lumbrineridae Schmarda, 1861	1.4	1.0
Lumbrineris sp. Blainville, 1828	0.9	0.5
Maldanidae Malmgren, 1867	3.6	3.5
Marphysa bellii (Audouin & Milne Eduards, 1833)	4.8	0.5
Mediomastus sp. Hartman, 1944	0.0	0.5
Melinna sp. Grube, 1869	10.9	0.5
Nephtydae sp. A Grube, 1850	2.4	0.5
Nephtys sp. Grube, 1850	0.9	0.0
Notomastus sp. Sars, 1851	0.5	0.5
Ophelidae Malmgren, 1867	3.7	0.0
Orbinidae Hartman, 1942	1.4	0.5
Paradiopatra cuadricuspis(M. Sars, 1872)	6.9	7.8
Paradoneis lyra (Southern, 1914)	0.5	0.0
Paraonidae Cerruti, 1909	3.6	2.9
Pilargidae St. Joseph, 1899	0.9	0.0
Pista sp. Malmgren, 1866	0.9	0.0
Prionospio sp. Malmgren, 1867	0.0	0.5
Sabellidae Malmgren, 1867	0.5	0.0
Spionidae Grube, 1850	6.9	2.9
Syllidae Grube, 1850	0.5	0.0
Terebellidae Grube, 1851	0.0	0.5
Polychaeta unid [D]	1.4	0.5
Crustacea decapoda		
Calocaris macandreae (Bell, 1846)	2.3	1.5
Ebaliacranchii (Leach, 1817)	0.5	0.0

TABLE 2.4: List of species (PART 1/3). Mean number of specimens (ind/m^2) collected from canyon adjacent slope.

TAXA	Canyon	Ad. slope
Monodaeuscouchi (Couch, 1851)	1.4	0.5
Copepoda		
Calanoidea	0.9	9.2
Amphipoda		
Carangoliopsis spinulosa Ledoyer, 1970	82.9	12.8
Eriopisa elongata (Bruzelius, 1859)	0.9	0.5
Idunella nana (Schiecke, 1973)	0.0	0.5
Harpinia crenulata (Boeck, 1871)	12.8	0.0
Harpinia dellawallei Chevreux, 1910	5.4	3.5
Harpinia spp. Boeck, 1876	9.5	2.1
Lilljeborgia psaltrica Krapp-Schickel, 1975	0.9	0.0
Maera schmidtii Stephensen, 1915	3.2	0.5
Metaphoxus simplex (Bate, 1857)	3.7	4.0
Monoculodes sp. Stimpson, 1853	1.9	0.0
Orchomenella nana (Krøyer, 1846)	0.0	1.9
Paraphoxus oculatus (G. O. Sars, 1879)	6.4	0.5
Pardaliscidae Boeck, 1871	0.0	1.9
Phoxocephalidae [D] G.O. Sars, 1891	0.0	0.5
Psammogammarus sp. A. S. Karaman, 1955	0.0	1.9
Sophrosyne hispana Chevreux, 1887	1.4	0.5
Urothoe corsica (Bellan-Santini, 1965)	1.4	6.4
Cumacea		
Diastyloides serrata (G. O. Sars, 1865)	0.0	0.5
Epileucon ensis (Bishop, 1981)	1.9	0.0
Eudorella truncatula (Bate, 1856)	7.7	0.5
Leucon longirostris Sars, 1871	15.7	6.9
Leucon macrorhinus (Fage, 1951)	1.9	2.1
Leucon siphonatus Calman, 1905	5.8	0.0
Makrokylindrus gibraltarensis (Bacescu, 1961)	0.0	3.8
Makrokylindrus insignis (G. O. Sars, 1871)	0.0	1.0
Makrokylindrus longipes (G. O. Sars, 1871)	0.9	0.0
Isopoda		
Pilosanthura fresii (Wägele, 1980)	5.0	4.0
Chelator chelatus (Stephensen, 1915)	7.5	6.9
Desmosoma linearis (Linnaeus, 1767)	0.9	0.5
Eugerda sp. Meinert, 1890	1.9	0.0
Gnathia spp.[L] Leach, 1814	0.5	0.0
Ilyarachna longicornis (G. O. Sars, 1864)	1.9	0.0
Tanaidacea		
Apseudes spinosus (M. Sars, 1858)	0.5	0.0
Tanaidacea unid.	5.8	0.5
Ostracoda		
Cypridinidae	3.8	0.0

TABLE 2.5: List of species (PART 2/3). Mean number of specimens (ind/m^2) collected from canyon adjacent slope.

TAXA	Canyon	Ad. slope
Ostracoda unid	0.0	4.0
Pycnogonida		
Pycnogonida unid	1.9	0.0
Crustacea unid [L]	0.0	0.5
Caudofoveata		
Falcidens strigisquamatus Salvini-Plawen, 1977	4.3	9.2
Falcidens aequabilis Salvini-Plawen, 1972	1.8	1.5
Falcidens gutturosus (Kowalesky, 1901)	6.2	0.0
Prochaetoderma alleni (Scheltema & Ivanov, 2000)	0.5	0.5
Prochaetoderma boucheti Scheltema & Ivanov, 2000	8.1	0.0
Prochaetoderma spp. Thiele, 1902	5.0	11.4
Scutopus ventrolineatus Salvini-Plawen, 1968	1.9	0.0
Scaphopoda		
Scaphopoda unid	3.8	0.0
Gastropoda		
Eulimella neoattenuata (Gaglini, 1992)	0.5	0.5
Euspira fusca (Blainville, 1825)	1.9	0.0
Bivalvia		
Abra longicallus (Scacchi, 1894)	8.9	9.9
Axinulus croulinensis (Jeffreys, 1847)	1.4	0.5
Cochlodesma tenerum (Fischer, 1882)	0.5	0.0
Ennucula aegeensis (Forbes,1844)	4.5	14.9
Kelliella miliaris (Philippi, 1844)	36.0	2.1
Ledella cf. *marinostri* La Perna 2004	1.8	1.5
Limatula bisecta Allen, 2004	0.0	0.5
Mendicula ferruginosa (Forbes, 1844)	0.5	0.5
Yoldiella messanensis (Jeffreys, 187)	0.5	4.9
Sipuncula		
Aspidosiphon muelleri Diesing, 1851	1.9	1.0
Nephasoma cf. *abyssorum* (Koren & Danielssen, 1876)	0.0	1.9
Nephasoma cf. *diaphanes* (Gerould, 1913)	0.0	1.9
Onchnesoma steenstrupii Koren & Danielssen 1875	4.5	19.0
Echiurida		
Echiurus abyssalis Skorikov, 1906	0.0	0.5
Echinodermata		
Amphipholis squamata (Delle Chiaje, 1828)	1.9	3.6
Amphiura chiajei (Forbes, 1843)	18.6	0.0
Amphiura filiformis (Müller, 1776)	0.9	0.0
Amphiura cf. *grandisquama* Lyman, 1869	1.9	0.0
Ophiuroidea unid [J]	1.9	1.9
Brissopsis lyrifera (Forbes, 1841)	0.5	0.5
Nematoda		
Nematoda unid	0.9	4.4

TABLE 2.6: List of species (PART 3/3). Mean number of specimens (ind/m^2) collected from canyon adjacent slope.

PART II

3

Analysis and standardization of landings per unit effort of red shrimp from the trawl fleet of Barcelona (NW Mediterranean)

Abstract

Monthly landings and effort data from the Barcelona trawl fleet (NW Mediterranean) were selected to analyse and standardize the landings per unit effort (LPUE) of the red shrimp (*Aristeus antennatus*) using generalized additive models. The dataset covers a span of 15 years (1994 – 2008) and consists of a broad spectrum of predictors: fleet-dependent (e.g. number of trips performed by vessels and their technical characteristics, such as the gross registered tonnage), temporal (inter- and intra-annual variability), environmental (North Atlantic Oscillation [NAO] index) and economic (red shrimp and fuel prices) variables. All predictors individually have an impact on LPUE, though some of them lose their predictive power when considered jointly. That is the case of the NAO index. Our results show that six variables from the whole set can be incorporated into a global model with a total explained deviance (DE) of 43%. We found that the most important variables were effort-related predictors (trips, tonnage, and groups) with a total DE of 20.58%, followed by temporal variables, with a DE of 13.12%, and finally the red shrimp price as an economic predictor with a DE of 9.30%. Taken individually, the main contributing variable was the inter-annual variability (DE = 12.40%). This high DE value suggests that many factors correlated with inter-annual variability, such as environmental factors (the NAO in specific years) and fuel price, could in turn affect LPUE variability. The standardized LPUE index with the effort variability removed was found to be similar to the fishery-independent abundance index derived from the MEDITS programme.

Keywords: landings per unit effort, bathyal ecosystem, red shrimp fishery, NW Mediterranean, LPUE standardization

3.1 Introduction

Deep-water red shrimp is one of the main resources in Mediterranean fisheries in terms of landings and economic value (Bas et al., 2003), primarily in Spain and Algeria, where catches reach more than 1000 t y^{-1} (FAO/FISHSTAT, 2011). In the Mediterranean Sea, two red shrimp species, *Aristeus antennatus* and *Aristaeomorpha foliacea*, are caught by specialized trawl fleets operating on the upper and middle continental slope. The distribution of these two species varies geographically and in the NW Mediterranean catches are composed exclusively of *A. antennatus* (Bas et al., 2003). Cartes, Maynou and Fanelli (2011); Cartes, Maynou, Abelló, Emelianov, de Sola and Solé (2011) have suggested environmental causes to explain the extinction of *A. foliacea* in these waters.

The deep-water distribution of red shrimp stocks extends to below 2000 m depth (Cartes and Sardà, 1992) but commercial trawlers fish from 400 to 900 m depth. The red shrimp life-cycle includes seasonal, bathymetric and spatial migrations of different fractions of the population with great size and sex segregation: juveniles and small-sized males are more abundant in autumn and early winter in submarine canyons, while reproductive females concentrate on the open slope fishing grounds in late winter and spring (Sardà et al., 1997). This complex life cycle, coupled with a relatively long life span (more than 10 years according to Orsi Relini et al., 2013) differentiates this species from tropical coastal shrimp resources elsewhere (Neal and Maris, 1985).

The catches of *A. antennatus* show inter–annual fluctuations that have been related to environmental factors determining strong recruitment (Carbonell et al., 1999; Maynou, 2008). Maynou (2008) suggested that winter NAO (North Atlantic Oscillation) is positively correlated with landings of *A. antennatus* two to three years later and that enhanced trophic resources for maturing females in winter and early spring result in stronger recruitments. The NAO has been demonstrated to be a pervasive environmental driver in other marine stocks elsewhere in the Mediterranean and Atlantic (e.g. Brodziak and O'Brien, 2005; Dennard et al., 2010). However, the effect of technical and economic variables has received less attention. For instance, in the red shrimp fishery of the NW Mediterranean, Maynou et al. (2003) showed the importance of individual fisher behaviour in determining catch rates, and Sardà and Maynou (1998) discuss the effect of prices on changes of daily fishing effort targeting this species. Intra–annual variability in landings has been linked to market–driven variations in prices, which may result in changes

in the fishing effort applied to the stocks, as the trawl fleet moves to alternative resources (Sardà et al., 1997).

Despite the commercial importance of *A. antennatus* in the Mediterranean (Sardà et al., 1997), deriving standardized catches or landings per unit effort (CPUE or LPUE) is not straightforward because of the lack of reliable time series at regional or sub-regional level (Lleonart and Maynou, 2003). In fact, determining the abundance of marine stocks is notoriously a widespread problem (Hilborn and Walters, 1992). Methodologies basically rely on two different data sources: sheries–dependent or sheries-independent data. Fisheries-dependent data tend to be the preferred source to assess the status of marine stocks (Lassen and Medley, 2000) but since the applicability of these traditional assessment methods is limited when it comes to crustaceans, fisheries–independent methods are usually preferred. However, fisheries–independent experimental trawl surveys in the western Mediterranean (Mediterranean International Trawl Surveys: MEDITS, Bertrand et al., 2002) are also problematic because they only partially cover the distribution depth range of *A. antennatus*. Thus, fisheries-dependent data are indeed used but methods that require age data are avoided and instead only regression style methods are used. For instance, in the Spanish Mediterranean sub-area 6 (ca. 1000 km long) just 4 to 12 trawl hauls are carried out annually in the 500-800 m depth stratum and none any deeper (Cardinale et al., 2012). Additionally, obtaining reliable landings including age information is problematic owing to difficulties in determining age in crustaceans (Orsi Relini et al., 2013). In these cases the information collected by a fishery is the main source of abundance data available (Maunder et al., 2006) and, when appropriately standardized, can be used to produce series of population abundance that should help fishery managers to promote the sustainable production of marine stocks.

Here, we evaluate the landings per unit effort from the daily sale slips provided by the Barcelona Fishers Association from 1994 to 2008, corresponding to all the commercial transactions involving *A. antennatus* by a total of 21 trawlers operating on continental slope fishing grounds. The landings of *A. antennatus* have varied by almost an order of magnitude in this area in the last ten years, from a historical low of 13 t y^{-1} in 2006 to 96 t y^{-1} in 2012. Considering that the average ex-vessel price of the species in this period was 36 *e* kg^{-1} (among the highest seafood prices in Europe), these inter-annual fluctuations in landings have important economic consequences. Fisheries in Spanish Mediterranean waters are allowed between 50 and 1000 m depth for a maximum of 12 h during daytime,

except weekends. Hence, trawl skippers must decide which fishing grounds to visit taking into account that on the continental shelf they can be reached in a shorter time but will produce relatively cheap finfish, whereas deep-water fishing produces more valuable red shrimp but entails high economic costs and the risk of losing or damaging fishing gear.

The main objective of this study was to establish the factors influencing the LPUE (for terminology see e.g. Denis, 2002) of *A. antennatus* in order to evaluate their relative importance (fishery-related, economic and environmental), which can be considered to manage effort constraints and to obtain a standardized series of LPUE as a reliable relative abundance index to assess natural abundance. We used generalized additive models (GAMs: Hastie and Tibshirani, 1990) to capture the possible nonlinear dependence of LPUE on explanatory variables (Su et al., 2008, among others).

3.2 Materials and Methods

3.2.1 Data source

Trawlers from the Barcelona port operate on the continental shelf and slope fishing grounds (50 – 1000 m depth) located between 1°50′ and 2°50′ longitude east and 40°50′ and 41°30′ latitude north (Sardà et al., 1997). The fleet operates on a daily basis (with mandatory exit from port after 6 am and return to port before 6 pm) and a limited license system whereby total effort in the area has been frozen since 1986. New boats are only permitted if an existing boat is decommissioned. In addition to effort control, the only other measure of control is limiting mesh sizes (minimum 40 mm cod-end stretch mesh size) and neither in the study area nor in any other Mediterranean areas is there output control. Fish is auctioned daily at the premises of the port fish market and all transactions are recorded electronically for statistical purposes by the Barcelona Fishers Association.

We used the daily sale slips containing all transactions of red shrimp (*A. antennatus*) over the period 1994 – 2008 to calculate the total monthly landings (kg month^{-1}, *lands*), the effort measured as total number of trips performed monthly by each vessel (number of trips per month, *trips*), and the monthly average ex-vessel shrimp price (€kg^{-1}, *shprice*). The same data set contained information on

the engine power (horse power, *hp*) and gross registered tonnage (tons, *grt*), which we used as boat capacity indicators. As an indicator of fishing costs we used the average monthly fuel price (10^{-3} €L^{-1}, *fprice*) from the EUROSTAT website: http://ec.europa.eu/energy/observatory/oil/bulletin_en.htm. As the environmental driver we used the NAO index, taken from the website of the Climate Analysis Group of the University of Exeter (UK): http://www1.secam.ex.ac.uk/cat/NAO. We considered: *nao*1, *nao*2 and *nao*3, corresponding to one, two and three years before the year of observed landings, using the significant time lags reported in Maynou (2008).

The response variable, *lpue*, was estimated as

$$lpue = \frac{lands}{trips} \tag{3.1}$$

hence, *lpue* is the monthly average landings of one vessel in each trip, corresponding to one fishing day (kg $boat^{-1}$ d^{-1}), which will form the basis for providing a standardized abundance index.

To assess the individual effect of each vessel, a numeric variable code was assigned to each of the 21 vessels in the fleet. Each observation was attributed to a sequential time variable from January 1994 to December 2008 (180 months) and a month variable describing the month of the year. Two more variables were derived a posteriori from code and month, after checking for statistical differences among their categories in the model, and then by performing the Tukey Honest Significant Differences test (TukeyHSD). We thus derived the new variables, *group* and *period*, for *code* and *month*, respectively. The *group* variable combines the 21 trawlers into three groups of increasing *lpue* and *period* is a binary variable which classifies the months in "high effect" (*period*1: all months excluding June and November) and "low effect" (*period*2: June and November). All variables are listed in Table 3.1.

3.2.2 Model construction

We used generalized additive models, GAM, as described by Hastie and Tibshirani (1990)

$$G(y) = x\beta + \sum s_j(x_j) + \epsilon \tag{3.2}$$

where $G(\cdot)$ is the link function, y is the response variable, x is the vector of linear predictors (explanatory variables), β is the corresponding vector of parameters, x_j are scalar predictors with unknown nonlinear effects represented by the functions $s_j(\cdot)$, and ϵ is the vector of random errors. The model building process consists of the following steps: 1) selection of the underlying distribution of the response (see Section 2.2.2 for more details); 2) selection of predictors building independent models for each covariant deleting insignificant effects in the final model; 3) selection between correlated predictors through the Pearson correlation coefficient (threshold value: $\rho = |0.6|$) to avoid problems of collinearity (Brauner and

Variable	Description (unit)
lands	total monthly landings per vessel (kg month^{-1})
lpue	landings per unit effort derived from *lands* and *trips* (kg boat^{-1} day^{-1})
code	a categorical variable assigned to each boat, $c = 1, \ldots, 21$
time	time index of months, $t = 1, \ldots, 180$, from Jan 1994 to Dec 2008
trips	number of trips performed by each vessel during the time t
hp	engine power of vessels
grt	gross registered tonnage of vessels
shprice	red shrimp ex-vessel price (kg^{-1})
fprice	fuel price one month before the observed *lands* (10^{-3} €L^{-1})
nao_k	mean annual NAO index, $k = 1, \ldots, 3$ years before the year of observed lands
month	12 categories corresponding to months from January to December
code	21categories corresponding to a code assigned to each vessel
period	categorical variable with 2 categories of grouped months *period*1: all month excluding Jun and Nov and *period*2: Jun and Nov
group	3 categories corresponding to groups of vessel

TABLE 3.1: List of variables. Differences between pairs of categories of the variable *month* were checked through Tukey HSD test. Non-significantly different categories were grouped to create the new variable *period*, to which the same test was applied. The same procedure was applied for the variable *code*, to create the variable *group* (all significant tests with $p \leq 0.001$).

Shacham, 1998) using the covariant with the most explanatory potential; and 4) analysis of residuals diagnostics.

All analyses were performed in R3.0.1 (mgcv-Rpackage: Wood, 2006). The generalized cross validation (GCV: Craven and Wahba, 1979) and the outer Newton iteration procedure were used to estimate model parameters. GCV is preferable to the UBRE/AIC method in the case of unknown smoothing parameters λ (Wood, 2006). Second order P–spline as defined by Marx and Eilers (1998) was used as a smoother for nonlinear functions.

3.2.3 Theoretical response probability function

Landings per unit effort are usually modelled following Gaussian or gamma distribution functions, often without formal justifications (Stefánsson, 1996). Here, we assigned a theoretical probability function to the *lpue*, using nonparametric techniques described by Wasserman (2006). The density function, $f(y_n)$, was estimated using a histogram and the Gaussian kernel. The nrd described by Scott (2009) was the rule-of-thumb used to select the bandwidth. The empirical cumulative distribution function, $F(y_n)$, and the 95% lower, $L(y_n)$ and upper, $U(y_n)$, confidence intervals were calculated as follows:

$$F(y) = \frac{[rank(y) - 0.5]}{N}$$

$$L(y) = maxF(y) - \epsilon, 0$$

$$U(y) = minF(y) + \epsilon_n, 1,$$

where $rank(y)$ is the ranked vector of observations and ϵ is the associated error resulting from the DKW (Dvoretzky-Kiefer-Wolfowitz) inequality

$$\epsilon = \sqrt{\frac{1}{2n} log_e \left(\frac{2}{\alpha}\right)}$$

The hypothesis tested is $\mathbf{H_0}$: $F(y) = F_0(y)$ versus the alternative hypothesis $\mathbf{H_1}$: $F(y) \neq F_0(y)$, where $F_0(y)$ is a theoretical function belonging to the exponential family, especially $F_0(y) = Ga(a, b)$, the gamma distribution, whose density function is

$$p(y) \propto y^{(a^{-1})} e^{(-by)}$$

for $y > 0$. Parameters a and b are derived from the estimated expectation, $E(y) = a/b$, and variance $Var(y) = a/b^2$. Then the resulting distribution functions were graphically compared.

3.2.4 Selection criteria and explained deviance

Both AIC (Akaike, 1973) and percentage of deviance explained (DE) were used as selection criteria: the selected model presented both the lowest AIC and the highest DE and all term parameters significantly different from zero.

The DE for each variable was also calculated in order to determine their relative importance in the final model. The residual deviance of the full model and the deviances of reduced models (i.e. the model excluding variable x_i) were calculated to derive the proportion explained by variable x_i:

$$\mathrm{ED}_{x_i} = \frac{[\mathrm{D}(\mathrm{M}_r)\,\mathrm{D}(\mathrm{M}_f)]}{\mathrm{D}(\mathrm{M}_n)}$$

where M_f, M_n and M_r are the full, null and reduced models and $\mathrm{D}(\cdot)$ represents the deviance for a given model. In the reduced model variable x_i is omitted.

3.2.5 LPUE standardization

The model used for standardization was built in order to avoid dependency on fleet variables, maintaining environmental variables, which are expected to be related to the natural abundance of the species. The standardized LPUE, $lpue_s$ is then

$$lpue_s = E(lpue) + (lpue - E(lpue|\Theta = \theta, \Lambda = \lambda)) \tag{3.3}$$

where *lpue* is the "nominal" or "raw" LPUE defined in Equation 1, $E(lpue)$ is the unconditional expectation of the LPUE and $E(lpue|\Theta = \theta, \Lambda = \lambda)$ is the conditional expectation of the LPUE given the vectors of parameters θ and λ, estimated using the appropriate standardization model. Finally we compared our standardized LPUE with an alternative abundance index derived from fisheries-independent data, available in the technical report SGMED–12–11 (Cardinale et al., 2012, pp. 136–150) after normalization of both variables.

3.3 Results

3.3.1 Overview of data and response distribution

Figure 3.1 provides the raw *lpue* time series as reckoned in Equation 4.1 with its spline estimation (upper plot) and annual average of the NAO index (lower plot). The *lpue* series, initially constant, started to decline at the end of 1998 with a sharp maximum low in the period 1999 – 2000. Then the trend changed to inter-annual variation. Conversely, the NAO index shows the lowest records in the period 1995 – 1996. The *lpue* begins to decrease after three years from the first year of negative NAO. In Figure the time series of the fuel price shows an increasing trend during the observed period (upper panel). The total number of trips per month performed by the whole fleet declines during the same period (middle panel), but it declines only at the beginning of the fuel price rise, then remaining almost constant (lower panel). Low *lpue* in the period 2000 – 2001 is also related to the peak of *fprice* in the same period (compare upper plots of Figures 3.1 and 3.2).

Characteristics of *lpue* are plotted in Figure C.1, Appendix C. The probability density function (*pdf*) is positively skewed (upper panels). Data hold atypical values in the right tail (see the box-plot, left middle panel) and the distribution function of the gamma distribution lies approximately inside the 95% confidence intervals of the empirical cumulative distribution function (*ecdf*) of *lpue* (right middle panel). Finally, the QQ-plots for the gamma and the Gaussian distributions provide evidence of a better fit of data to the gamma rather than the Gaussian distribution (on the left and the right lower panels respectively).

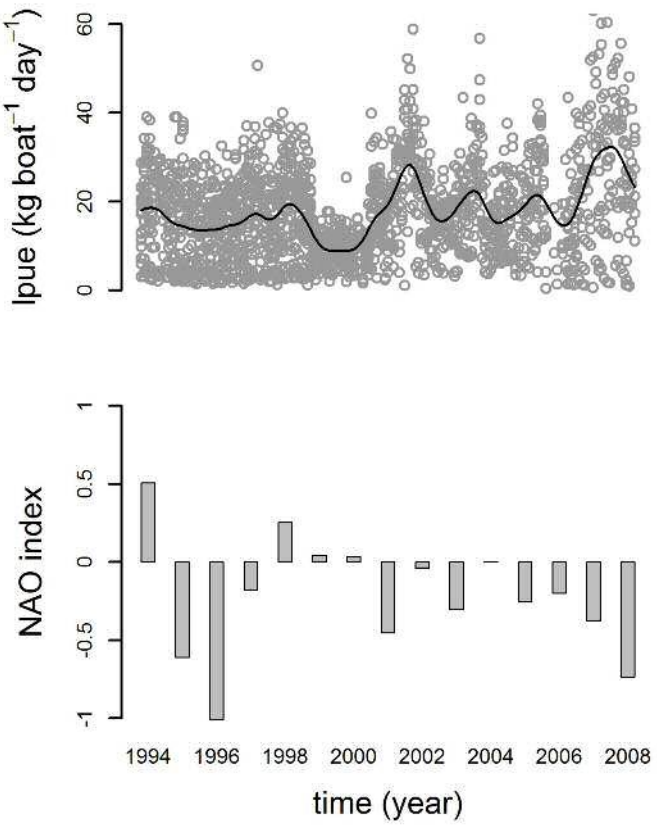

FIGURE 3.1: Time series from 1994 to 2008 of LPUE data and spline estimation (upper panel) and mean annual North Atlantic Oscillation (NAO) (lower panel).

3.3.2 Model building and comparison

The model building process is summarized in Table . All linear terms are reported before all smooth functions. Models are sorted in ascending order of total DE, with the exception of models 11 and 12, corresponding to the GLM version of the final model 7 and the standardization model respectively. In comparison with the GLM (model 11), GAMs AIC decreases and the DE increases substantially (1.56 times), though the number of degrees of freedom increases considerably (df_{GAM} = 27.7 versus df_{GLM} = 9). Variables *grt* and *time* were selected as better predictors than *hp* and *fprice*, respectively, according to the Pearson correlation coefficients ($grt-hp$ was $\rho = 0.61$; $time-fprice$ $\rho = 0.69$) and larger ED of former variables. All other correlations were $\rho < |0.6|$. Table 2 incorporates the NAO terms, though their explanatory potential in the full model is too weak to be significant. Adding NAO terms to model 7 (Table : models 8, 9, 10) did not improve model fit in terms

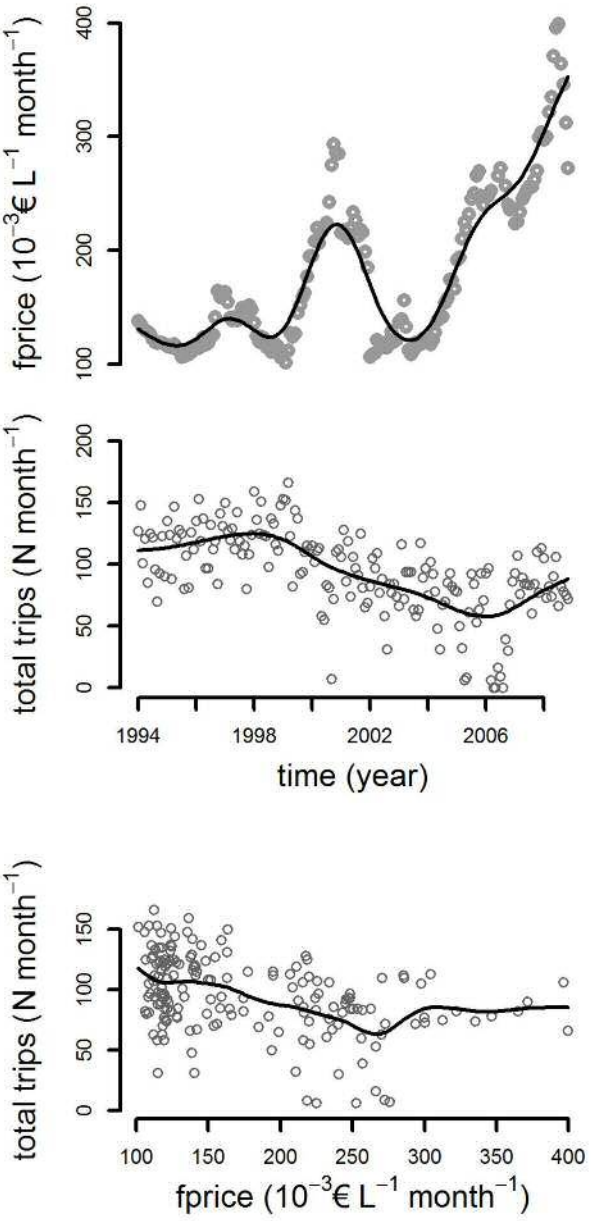

FIGURE 3.2: From top to bottom: spline estimation of the fuel price, monthly total number of trips performed by the fleet from year 1996 to 2008, and relationship between the fuel price and the total monthly number of trips.

of DE and AIC. Nevertheless, we found significant NAO effect in less complex models.

3.3.3 The descriptive model

The final model for *A. antennatus* LPUE is

$$G(y) = \theta + \alpha x_1 + \beta x_{2,2} + \sum_{k=2,3} (\gamma_k x_{3,k}) + s_1(x_4) + s_2(x_5) + s_3(x_6) + \epsilon \qquad (3.4)$$

where y is the response $lpue \in Ga(a, b)$, $G(\cdot)$ is the logarithmic link function log_e, $x_1, \ldots, x_6$ correspond the explanatory variables *grt*, *period*, *group*, *trips*, *time* and *shprice*, θ is the intercept, α is the parameter associated with the linear effect of *grt*, and β and γ_k are the effects associated with the dummy coded categorical variables *period* and *group*. The functions $s_j(\cdot)$, with $j = 1, \ldots, 3$ represent the smooth effects associated with *trips*, *time* and *shprice*, while ϵ is the random errors of the model.

Figure C.2 in Appendix C shows the diagnostic plots for the selected model (corresponding to Equation 3.4 in the text and model 7 in Table 3.2). Residual quantiles lie on the straight line of the theoretical quantiles, although slightly heavy-tailed;

n	model	df	RD	DE (%)	AIC
1	Int	2	863.8	0	13544
2	$Int + hp^{(+)}$	3	844.4	2.2	13501
2.1	$Int + grt$	3	815.3	5.6	13432
3	$Int + grt + group$	5	741.0	14.2	13250
4	$Int + grt + group + period$	6	734.7	15	13235
5	$Int + grt + group + period + s(trips)$	8.9	627.8	27.3	12936
6	$Int + grt + group + period + s(trips)$ $+s(fprice)^{(+)}$	12.4	614.0	28.9	12900
6.1	$Int + grt + group + period + s(trips)$ $+s(time)$	24.8	527.0	39	12632
7	$Int + grt + group + period + s(trips)$ $+s(time) + s(shprice)$	27.7	493.5	43.0	12512
8	$Int + grt + group + period + s(trips)$ $+s(time) + s(shprice) + s(nao1)^{(ns)}$	28.7	493.3	43.0	12513
9	$Int + grt + group + period + s(trips)$ $+s(time) + s(shprice) + s(nao2)^{(ns)}$	28.7	493.5	43.0	12514
10	$Int + grt + group + period + s(trips)$ $+s(time) + s(shprice) + s(nao3)^{(ns)}$	28.7	493.4	43.0	12513
11	$Int + grt + group + period + trips + time$ $+shprice$	9	626.4	27.5	12932
12	$Int + grt + code + s(trips)$	24.75	608.7	29.5	12910

TABLE 3.2: Model construction. N, number associated with each model; model, models right part of the formula; df, models degree of freedom; RD, residual deviance, DE, percentage of deviance explained by each model; AIC, Akaike Information Criterion; term(ns), insignificant terms in a model; term (+), terms not incorporated in next steps (i.e. models with the incorporation of *hp* or *fprice* gave a lower DE than the incorporation of *grt* and *time*, respectively). Model 12 is the model used for standardization.

in the histogram, residuals are consistent with normality and the relationship between response and fitted values is linear and positive. Residuals versus the linear predictor (that is, the sum of all partial effects) show a faint heteroscedasticity.

Table 3.3 shows results related to (a) the linear part, (b) the smooth functions and (c) the global parameters of the final model (Equation 3.4), with a total explained deviance of 43.00%. The predictor with the highest explanatory potential was time (DE = 12.40%), which captured the intra-annual fluctuations in red shrimp *lpue*. The second predictor in terms of explained deviance was *trips* (DE = 11.38%). Red shrimp price was the third most important predictor (DE = 9.30%). Other variables such as *grt*, *group* and *period* had less impact. The model returned all significant parameters ($p \ll 0.001$).

All partial effects are reported in Figure 3.3. The partial effect for time shows a substantial difference before and after the period 1999 – 2000, when a clear drop is exhibited in the shape. Before this threshold the shape is almost constant, whereas after the abrupt decay increasing variation is observed over recent years.

(a)	μ	σ	t	p	DE (%)
int	1.746	0.103	16.980	≤ 2E-16	0
*eriod*2	−0.152	0.035	−4.383	1.24E-05	0.72
*group*2	0.281	0.081	3.449	5.75E-04	3.58
*group*3	0.637	0.086	7.404	2.02E-13	
grt	0.010	0.001	16.205	≤ 2E-16	5.62
(b)	*edf*	λ	F	p	ED (%)
$s(time)$	15.239	0.011	24.82	≤ 2E-16	12.40
$s(trips)$	2.457	30.007	71.01	≤ 2E-16	11.38
$s(shprice)$	4.026	0.059	26.36	≤ 2E-16	9.30
(c)					
df	*scale*	R^2(adj)	AIC	GCV	DE_{tot} (%)
27.722	0.274	0.488	12512	0.282	43.00

TABLE 3.3: Results of the final model (Equation 3.4). Results associated with (a) linear terms, (b) smooth terms and (c) global estimations. μ: estimation of the mean; σ: standard deviation; t: value of t-statistic; F: the F-statistic value; p: p-value associated to the t or the F statistic; DE: deviance explained by each term in percentage; *edf*: effective degrees of freedom; λ: estimated smoothing parameter; *df*: total degree of freedom; *scale*: estimation of the scale parameter; R^2(adj): adjusted R-squared; AIC: Akaike Information Criterion; GCV, generalized cross validation; DE_{tot} (%): percentage of total deviance explained by the model.

Predictor trips represents a positive and monotonic relationship, reaching a plateau for *trips* > 15; *shprice* reached its maximum value around 30 €kg^{-1}; *lpue* was significantly lower for *period*2, representing June and November, than for the rest of the year (*period*1). There were significant differences between the three groups of vessels. Variable *grt* showed a positive linear effect, meaning that larger vessels had higher *lpue*.

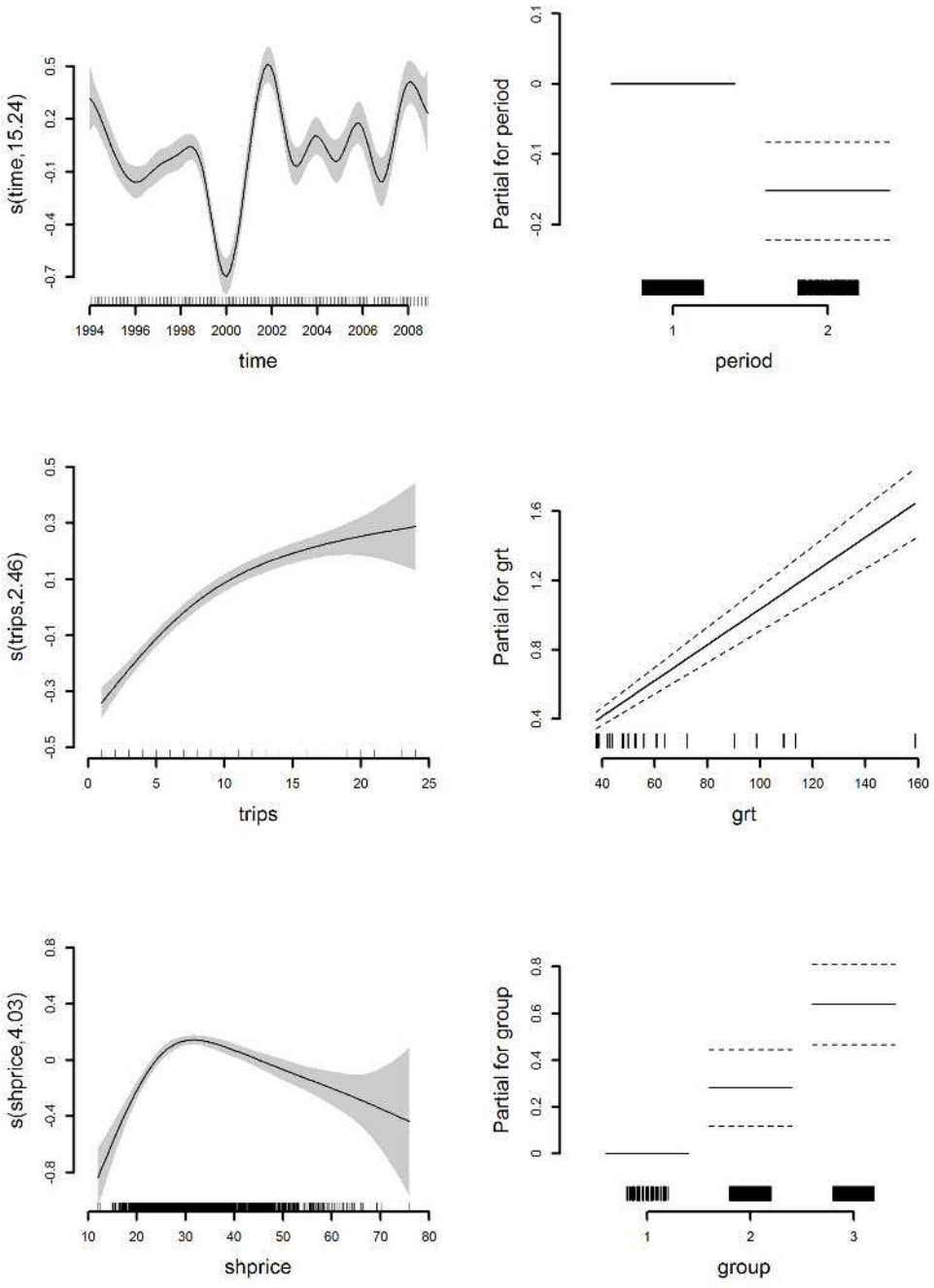

FIGURE 3.3: Partial effects of model 7. Bayesian credible intervals (95%).

3.3.4 LPUE standardization

The model used to standardize *A. antennatus* LPUE is

$$log_e(lpue) = \theta + \alpha grt + \sum_{j=2,21} (\gamma_j code_j) + s(trips) + \epsilon \tag{3.5}$$

where $lpue \in Ga(a, b)$, θ is the intercept, α the parameter for grt and γ_j the effects associated with $code$. $s(trips)$ is the smooth function for trips and the random errors. With the aim of standardizing, this model comprises all fleet-dependent variables, whose effect must be removed from the nominal value. The diagnostic plots show reasonably good outputs (not shown).

Finally, LPUE index and the SGMED in 2002 – 2008 with their confidence intervals after normalization of variables are plotted in Figure 3.4. The normalized Barcelona fisherys LPUE, calculated using Equations 3.3 and 3.5, has narrower confidence intervals than the normalized SGMED index. Only in 2004 were the two indices statistically different and in 2005 index estimates were at the limit of the other CI. Thus, five out of seven estimates can be considered equivalent.

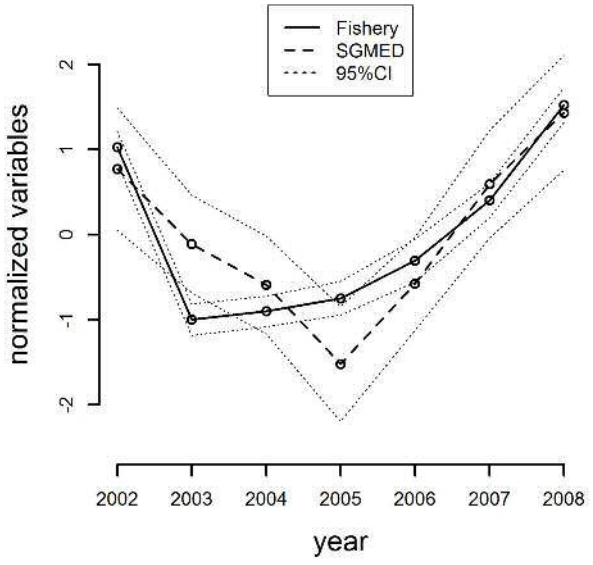

FIGURE 3.4: Comparison between the fishery-derived index (standardized LPUE) and the SGMED index. Variables have been normalized for comparison.

3.4 Discussion

This study presents models for relative abundance of *A. antennatus* harvested by one important Catalan fleet in the NW Mediterranean from 1994 to 2008. To our knowledge it is the first combined use of commercial fisheries data from Spain analysing environmental and economic variables with GAM techniques. Our objectives were: 1) to define the relative importance of predictors (model 7, Tables 3.2 and 3.3) and 2) to construct a standardized fishery-dependent index to compare with fishery-independent indices (Figure 3.4). The results contribute to the identification of simple roles in red shrimp fishery management.

3.4.1 The role of explanatory variables

We incorporated effort, temporal, economic and environmental variables into a global regression model to evaluate their relative importance. Model 7 captures LPUE variability with a total deviance of 43% explained by six predictors. In order to quantify the different sources of LPUE variability, we found that the set of fishery-related variables (*trips*, *grt* and *group*) was the most important source, with a DE of 20.58%, followed by temporal (time and period, DE = 13.12%) and finally economic variables (*shprice*, DE = 9.30%). Among the variables taken from fishery data, trips has provided the greatest impact to date. A low number of trips per month could be associated with generalist trawlers operating usually on the continental shelf and with less knowledge about red shrimp fishing grounds than trawlers specialized in this fishery (Maynou et al., 2003), suggesting that the higher activity of non-specialized trawlers in deep-water harbours yields lower LPUE values (see Figure 3.3: partial for *trips*). Conversely, boats performing a higher number of trips per month are expert in deep-water fishing grounds and their skippers are more likely to find high-concentration shoals through a process of trial and error (as hypothesized by Sardà and Maynou, 1998). Boat characteristics (*grt*) also influence LPUE, as was to be expected. The greater the gross registered tonnage, the higher the LPUE that is observed. The variable *group* captures other capabilities of fishermen and technical characteristics of vessels, such as the type of engine, net shape and skipper's expertise, which have been shown to positively bias the LPUE (Marriott et al., 2011; Maynou et al., 2003) and are expected to be important in many fisheries (Maunder and Punt, 2004). The importance of these predictors implies that their influence should be eliminated during

standardization. Inter-annual variable (*time*) is much more important than intra-annual variable (*period*) (Table 3.3). The former is more strongly determined by a range of sources, such as environmental and economic drivers, than the latter. The same order of importance was found by Maynou et al. (2003). The LPUE was almost constant before 1999 – 2000, when a sharp decline was observed. We hypothesized a relationship with low NAO in the previous three years (see Figure 3.1 and the introduction) that confirms the findings of Maynou (2008) and a possible relationship with the increase in fuel prices beginning in 2000. The following years were characterized by high inter-annual variability, when the price of fuel increased and showed greater variations. We believe that the trend could be explained by economic factors (Figure 3.2), especially since very high fuel-related costs are incurred in the fishing of red shrimp as a result of it being performed in deep-water (Sardà et al., 1997). The partial effect of ex-vessel prices, *shprice*, shows a parabolic-like shape and significant explanatory potential (DE = 9.30%). Low selling prices do not induce fishermen to practice this deep-water fishery, because they could not offset the high associated costs, and trawlers would rather switch to continental shelf fisheries, with lower costs and lower risk. When there are profits to be made, probably owing to the low availability of the product, fishermen practice this deep-water fishery more intensely and landings per unit effort also increase. At the higher sales price bracket (i.e. more than about 30 €kg^{-1}) decreasing landing rates mean higher sale prices. Here, an alternation of cause and effect between the two variables probably comes into play. As mentioned, *fprice* is also an important explanatory variable, although it was not inserted in the final model because of its correlation with time. Fuel price has a significant effect on LPUE and can reach approximately 1.6% of explained deviance (as can be deduced from the model building process in Table 3.2).

3.4.2 Implications for management

Obtaining information on deep-sea species population dynamics is notoriously difficult, but our analysis suggests that the peculiarity of red shrimp fishery makes it possible to use fishery-dependent data to accurately describe the relative abundance of this resource. There are no discards for this fishery and the by-catch fraction of commercial interest, represented for example by *Merluccius merluccius*, *Micromesistius poutassou* and *Phycis blennoides*, is small. These characteristics

enable landings to be considered equivalent to catches and interchange LPUE and CPUE as indices (Denis, 2002; Hilborn and Walters, 1992).

In turn, the definition of the relative importance of explanatory variables enables their impact on LPUE to be understood and makes intervention on the relevant variables possible from a management perspective. Fishery-related variables tend to have a significant effect on LPUE (DE = 21% in our case), and management measures aiming to reduce fishing mortality in this heavily harvested stock (Cardinale et al., 2012) could be based on limiting the size of the trawlers. Furthermore, the number of trips permitted in deep-water fishing grounds in this fishery could be limited, for example, by defining a threshold when the number of trips does not significantly increase the partial effect for LPUE (see Figure 3.3). In addition, to evaluate the impact of predictors on the LPUE, the regression analysis could be the basis to provide a standardized index for assessing species stocks. Standardization of landings data allows an index of the real species abundance to be developed, assuming that the explanatory variables available remove (or explain) most of the variation in the data that is not attributable to natural changes (Maunder and Punt, 2004). We advocate the selection of effort predictors for standardization.

Trends in CPUE (and LPUE) are usually assumed to reflect changes in the abundance of marine stocks (Maunder and Punt, 2004), but the raw index is often not proportional to abundance (Maunder et al., 2006). The raw LPUE is in fact dependent on many human factors that could be avoided. Time variables have a strong relationship with the abundance and environmental factors, which in turn are related to abundance, so they cannot be used in the model during standardization (e.g. see Maunder and Punt, 2004). The economic source of variability should be considered, but shrimp price and LPUE realistically have a cause-effect relationship, so they could be not properly used. Conversely, fishery-related variables seem to be the most reliable for this purpose. During the study period, the fleet was practically constant, making monthly trips a good indicator of fishing effort and landing ability, and remained almost constant despite potential technological creep (Marriott et al., 2011) because no significant changes in fishing technology have occurred in the area in the last 20 years. Studies of deep-water systems, where harsh conditions limit methods for evaluating sheries, often suffer from a lack of data in order to assess stock status. Although the goal of sheries managers is to promote sustainable production of sh stocks through formal stock assessment, it is often impractical to collect shery-independent data in isolated or harsh environments. In these cases the information collected by a shery is the

main (or only) source of abundance data available (Maunder et al., 2006).

Acknowledgements: The authors would like to express their sincere thanks to the Fisheries Directorate of the Government of Catalonia for giving access to the sales data of the Barcelona Fishers Association, as well as to fishers of Barcelona. The first author is also very grateful to A. Rodríguez Casal and C. Cadarso Suárez for transmitting their knowledge in nonparametric statistics, to A. Gallen for revising the English and to M. Reyes for his suggestions on the manuscript. G. Aneiros is partly supported by Grant number MTM2011-22392 from the Ministerio de Ciencia e Innovación (Spain). Finally, this study was financed by the Spanish National Research Council (CSIC) through the JAE-predoc grant programme.

4

Extended Additive Regression for Analysing LPUE Indices in Fishery Research

Abstract

We analysed the landings per unit effort (LPUE) from the Barcelona trawl fleet (NW Mediterranean) of the red shrimp (*Aristeus antennatus*) using the novel Bayesian approach of additive extended regression or distributional regression, that comprises a generic framework providing various response distributions, such as the log-normal and the gamma and allows estimations for location and scale or shape (as the frequentist counterpart GAMLSS does). The dataset covers a span of 17 years (1992-2008) in which the whole fleet has been monitored and consists of a broad spectrum of predictors: fleet-dependent (e.g. number of trips performed by vessels and their technical characteristics, such as the gross registered tonnage), temporal (inter- and intra-annual variability) and environmental (NAO index) variables. This dataset offers a unique opportunity to compare different assumptions and model specifications. So that we compared (1) log-normal versus gamma distribution assumption, (2) modelling the location parameter of the LPUE versus modelling both location and scale (or shape) of of the variable, and finally (3) fixed versus random specifications for the catching unit effects (boats). Our results favour the gamma over the log-normal and modelling of both location and shape parameters (in the case of the gamma) rather than only the location, while not noticeable differences occur in estimation when considering catching units as fixed or random, however accounting for random effects avoids problems related to time-series, such as correlations in data.

Keywords: landings per unit effort, red shrimp fishery, NW Mediterranean, generalized additive models for location, scale and shape; mixed models

4.1 Introduction

In fishery research, the LPUE (Landings Per Unit Effort or CPUE when it refers to the catch) is an index of abundance widely used in stock assessment to estimate the relative abundance of an exploited species (Marchal et al., 2002; Mendelssohn and Cury, 1989). The "landings" portion of the measure is the quantity of the stock brought to the port by each boat and is usually expressed as number of specimens or weight of the stock, while the "unit effort" portion refers to the unit of time spent by a unit of the gear used to catch (e.g. boat or meters of net soaked per unit of time). LPUE constitutes one of the most common pieces of information used in assessing the status of fish stocks and can be applied within the newer ecosystem approach to fisheries management when searching for suitable abundance parameters. When data derive from catches of the stock (e.g. from scientific surveys), the LPUE is more properly defined as CPUE.

The LPUE is reckoned in different ways depending on data availability. Its use is based on different assumptions. Usually it is taken to be proportional to the natural quantity of the target species, such that

$$\text{LPUE} = q \times \text{B}$$

where B is the biomass landed and q a constant of proportionality called catchability. This proportionality needs strong assumptions (e.g. Maunder and Punt, 2004; Paloheimo and Dickie, 1964) that make its use an open debate (e.g. Bannerot and Austin, 1983; Gulland, 1964; Maunder and Punt, 2004). Assumptions are often questionable and related answers are seldom available, thus, they must be consider with great caution. Another approach is to undertake regression modelling (e.g. Venables and Dichmont, 2004), in order to standardize the index removing the bias induced by influential factors (Maunder et al., 2006), related to the fishery, as in our case.

In fact, many factors can affect the index (e.g. time, seasonality, fishing area and fleet characteristics, among others). Many of them are related to the life-cycle of the species, other to environmental variability and other have an origin that is independent from natural factors, that if not considered can lead to biased interpretations of stock states. The idea of the standardization is to detect and avoid the influence on the LPUE of latter variables, that are, for instance, methodologies

used to catch and fishermen abilities, that can change under different conditions. Also the economy associated to the fishery can be very influential, either directly or indirectly. But we will not analyse this issue (an attempt to introduce this source of variability in regression modelling has been given in Chapter 3 or Mamouridis, Maynou and Aneiros Pérez 2014).

The most common class of regression models to determine the impact of covariates $x_1, \ldots, x_p$ on the expectation of the LPUE are generalized linear models (GLM, McCullagh and Nelder, 1989) and generalized additive models (GAM, Hastie and Tibshirani, 1990). In GLM the expectation of LPUE is related to a linear combination of the covariate effects, i.e.

$$E(\text{LPUE}_i) = h(\beta_0 + \beta_1 x_{i1} + \ldots + \beta_p x_{ip}), \qquad i = 1, \ldots, n$$

with a suitable transformation function h that ensures positivity of the expected LPUE and regression coefficients $\beta_0, \beta_1, \ldots, \beta_p$ (see see Goñi et al., 1999; Maynou et al., 2003, for GLM applications in CPUE and LPUE). Popular special cases for modelling LPUE include the gamma distribution or the normal distribution applied to log-transformed LPUE values (which is equivalent to assume a log-normal distribution).

For some of the influential variables, a simple linear impact on LPUE as often assumed in standard statistical models may not be flexible enough and alternative, semiparametric modelling approaches may be required. To overcome the limitation of GLMs to purely linear effects of covariates, generalized additive models, GAM have been introduced (see Damalas et al., 2007; Denis, 2002) where now the expectation is specified as

$$E(\text{LPUE}_i) = h(\beta_0 + f_1(x_{i1}) + \ldots + f_p(x_{ip})).$$

The nonlinear functions $f_1, \ldots, f_p$ remain unspecified and should be estimated flexibly from the data, for example using penalized spline approaches (see Ruppert et al., 2003; Wood, 2006).

Moreover, in most cases LPUE data are collected repeatedly for the same catching units over time leading to the necessity to account for unobserved characteristics of these units to avoid correlations in the repeated measurements. Thus, another direction for extending the GLM approach is the inclusion of catching unit-specific effects to acknowledge the effect that usually multiple observations are collected

and that unobserved heterogeneity remains even when accounting for some covariate effects. Regression analysis is thus able to capture the variability among fishing vessels (Thorson and Ward, 2014; Thorson and Berkson, 2010), the importance of which has been recognized for more than a century when interpreting fishery data (Beverton and Holt, 1957; Garstang, 1900; Wilberg et al., 2009). If the individual catching units are indexed as $i = 1, \ldots, n$ and the repeated measurement for one catching unit are indexed as $j = 1, \ldots, n_i$, the resulting model can be written as

$$E(\text{LPUE}_{ij}) = h(\beta_0 + \beta_1 x_{ij1} + \ldots + \beta_p x_{ijp} + \alpha_i), \qquad i = 1, \ldots, n,\ j = 1, \ldots, n_i.$$

The additional parameter α_i is introduced to stand for any effect specific to the catching unit that is not represented in the effects of covariates $x_1, \ldots, x_p$. Of course, similar extensions can be defined for generalized additive models. In the statistical community, the most common assumption for α_i would be the specification as a random effect, i.e. α_i i.i.d. $N(0, \tau^2)$, to acknowledge the fact that the catching units represent a sample from the population of catching units. This leads to the class of generalized linear mixed models (GLMMs, Pinheiro and Bates, 2000) or generalized additive mixed models (GAMMs, Wood, 2006). An alternative specification is to treat the α_i as usual, fixed parameters that result from dummy coding of the catching units. This may be considered more appropriated if, for example, the complete fleet of catching units for a specific area has been observed. We will return to this debate later when discussing the methods in more detail, see also Bishop et al. (2004), Cooper et al. (2004) or Helser et al. (2004) for the use of mixed models in this field.

Another important aspect when modelling LPUE is the choice of the response distribution. In most cases, skewed distributions have been considered, including in particular the gamma distribution (Maynou et al., 2003; Stefánsson, 1996), the log-normal distribution (Brynjarsdóttir and Stefánsson, 2004; Myers and Pepin, 1990) and the delta distribution (Gavaris, 1980; Pennington, 1983). The latter provides a form of zero-adjustment where zero catches are modelled separately from the nonnegative catches via a Bernoulli distribution. As a possibility to differentiate between gamma and log-normal distribution, the Kolmogorov-Smirnov test has been applied to fitted values from corresponding GLMs. Then, the distribution leading to a lower value for the test statistic can be considered to be closer

to the distribution of the data (Brynjarsdóttir and Stefánsson, 2004; Stefánsson and Palsson, 1998).

In this paper, structured additive distributional regression models (Klein et al., 2013) has been considered as a comprehensive, flexible class of models that encompasses all special cases discussed so far and a number of further extensions. More specifically, this class of models allows to deal with the following problems:

- Selection of the response distribution: Additive distributional regression comprises a generic framework providing various response distributions and in particular the log-normal and the gamma distributions. Extensions including zero-adjustment to account for an inflation of observations with zero catch are also be possible but not required in the data set considered here. Tools for effectively deciding between competing modelling alternatives will also be considered.

- Linear versus nonlinear effects: Effects of continuous covariates can be estimated nonparametrically based on penalized splines approximations that allow for a data-driven amount of smoothness and therefore deviation from the linearity assumption.

- Models for location, scale and shape: instead of restricting attention to only modelling the expected LPUE, distributional regression allow to specify a further parameter of the distribution that correspond to scale or shape. This both enables for additional flexibility and a better understanding of how different covariates affect the distribution of LPUE.

- Fixed versus random effects: both fixed and random specifications for the catching unit-specific effects are supported and can be compared in terms of their ability to fit the data.

- Mode of inference: Distributional regression can be formulated both from a frequentist and a Bayesian perspective and corresponding estimation schemes either rely on penalized maximum likelihood or Markov chain Monte Carlo simulations. This paper is focused on the Bayesian inference.

Structured additive distributional regression is in fact an extension of structured additive regression (STAR, Brezger and Lang, 2006; Fahrmeir et al., 2004) in the framework of generalized additive models for location, scale and shape (GAMLSS,

Rigby and Stasinopoulos, 2005). The parameter specifications rely very much on STAR, a comprehensive class of regression models for the expectation of the response that comprises geoadditive models (Kammann and Wand, 2003), generalized additive models (Hastie and Tibshirani, 1990) and generalized additive mixed models (Lin and Zhang, 1999) as special cases.

Our analysis deals with the red shrimp (*Aristeus antennatus*) LPUE. The red shrimp is the target species for the deep-water trawl fishery in the western Mediterranean (Bas et al., 2003), where catches have reached more than 1000 t/yr (FAO/-FISHSTAT, 2011). This species occurs between 300 and 2000 m (Sardà and Cartes, 1993; Tudela et al., 1998) and its biological and ecological characteristics have been deeply studied (Bianchini and Ragonese, 1994; Carbonell et al., 2008; Demestre, 1995; Demestre and Fortuño, 2013; Ragonese and Bianchini, 1996). Its fishery is developed in deep-waters (450-900 m) on the continental slope and near submarine canyons (Sardà et al., 1997; Tudela et al., 1998). *A. antennatus* LPUE has already been studied: its fluctuations have been related to changes in oceanographic conditions, e.g. at least partially triggered by changes in the North Atlantic Oscillation (Maynou, 2008) or explained by seasonal availability of the resource, linked to the fishing activity in turn influenced by economic factors, such as fuel and red shrimp prices (Mamouridis, Maynou and Aneiros Pérez, 2014) and market demand or (with a minor importance) to its life-cycle (Carbonell et al., 1999; Sardà et al., 1997). In our case LPUE and CPUE terms are perfectly interchangeable because all the catch of commercial trawlers is landed to the port, thus there are no discarding or other losses at sea for this lucrative species (Mamouridis, Maynou and Aneiros Pérez, 2014). However, for formal congruences we will refer to the LPUE, because data derive from landings.

The main objective of this study is to demonstrate the usefulness of structured additive distributional regression in modelling and predict shrimp LPUE and to provide guidance for model choice and variable selection, questions that arise in the process of developing an appropriate model for a given data set. Therefore, we will discuss tools such as quantile residuals, information criteria and predictive mean squared errors to evaluate the ability of models to describe and predict LPUE adequately.

The rest of the chapter is structured as follows: In Section 4.2.1 a description of the data set is given to illustrate the application of structured additive distributional

regression. Section 4.2.2 provides an overview of the methods dealing with the real data set, including the choice of an appropriate response distribution and variable selection. In Section 4.3, we perform an extensive analysis of the red shrimp data, comparing different response distributions, regression specifications and random versus fixed effects for the repeated observations. The final Section 4.4 concludes and comments on main results and directions of future research.

4.2 Materials and Methods

4.2.1 Data description

Data proceed from the daily sale slips of the Barcelona trawling fleet, granted by the Barcelona Fishers' Association. This data set comprises the information for 21 trawlers, with their total monthly landings (*landings*, kg), their monthly number of trips performed (*trips*) and the Gross Registered Tonnage (*grt*, GRT). Furthermore, the monthly average value of the North Atlantic Oscillation index (NAO) was obtained from the web site of the Climatic Research Unit of the University of East Anglia (Norwich, UK): `http://www.met.rdg.ac.uk/cag/NAO/slpdata.html`. Then we computed the year average of NAO, whose relationship with landings of three years later has been detected through cross-correlation analysis in previous studies by Maynou (2008).

The total number of observations, N, amounts to $N = 2314$ using the whole data set: 21 trawlers having practised deep-fishing in the period from January 1992 to December 2008 (17 complete years). Landings of the whole fleet were monitored over time, so, they depict the entire population of the fleet in the studied area and period. Red shrimp fishery is a specific fishery, thus, all the product caught on board appears in landings, due to its high commercial value, while, when landings are not reported for a given boat is due to its inactivity, rather than to zero catches of the source.

The landings and number of trips were used to estimate the "nominal" LPUE index,

$$lpue_{ij} = \frac{landings_{ij}}{trips_{ij}}, \tag{4.1}$$

where i and j refer to the observation i of the vessel j. The adjective "nominal" refers to the variable not standardized. Table 4.1 and the introductory part of this section provides information on the variables. Trips are always performed in one day, hence, the *lpue* represents the daily biomass average caught by a boat during one day (kg d^{-1}) with a monthly resolution. As in previous regression analysis, months associated to not significant parameters of the categorical variable *months* with categories $month_k$, $k = 1, \ldots, 12$ were backward assembled into two categories of a new variable *period* (period of the year): *period*1 defines all months excluding June and November and *period*2 refers to June and November. All variables are summarised in Table 4.1.

Variable	Description
landings	the total catches landed at port by each boat in one month
lpue	the daily LPUE index for each boat calculated as in Eq. 4.1
code	a categorical variable assigned to each boat, $c = 1, \ldots, 21$
time	a total of 204 months from January 1992 to December 2008 coded with a letter and two digits, e.g. J92 is January 1992
trips	the number of trips performed by each vessel during one month
grt	Gross Registered Tonnage of each boat
nao_3	mean annual NAO index of 3 years before the year of estimated *lpue*
month	categorical variable with $m = 1, \ldots, 12$ from January to December
period	binary variable with grouped months holding the same effect *period*1 = all month excluding June and November *period*2 = June and November

TABLE 4.1: List of variables.

4.2.2 Methodology

It has become quite popular to model the expected LPUE as a function of linear covariate effects. The results obtained from linear mean regression are easy to interpret but depreciated by possible misspecification due to a more complex underlying covariate structure, violation of homoscedastic errors or correlations caused by clustered data. To deal with these problems we apply Bayesian distributional structured additive regression models (Klein et al., 2013) a model class originally proposed by Rigby and Stasinopoulos (2005) in a frequentist setting. The idea is to assume a parametric distribution for the conditional behaviour of the response and to describe each parameter of this distribution as a function of explanatory variables. In the following, we consider log-normal and gamma distribution since the response in this study is always greater than zero.

We consider the log-normal distribution with parameters μ_{ij} and σ_{ij}^2 such that

$$E\left(lpue_{ij}\right) = \exp\left(\mu_{ij} + \frac{\sigma_{ij}^2}{2}\right)$$

$$Var\left(lpue_{ij}\right) = \left(\exp\left(\sigma_{ij}^2\right) - 1\right)\exp\left(2\mu_{ij} + \sigma_{ij}^2\right).$$

Accordingly, $\log\left(lpue_{ij}\right)$ is normal distributed with $E(\log(lpue_{ij})) = \mu_{ij}$ and $Var(\log(lpue_{ij})) = \sigma_{ij}^2$. As an alternative, we assume a gamma distribution with parameters $\mu_{ij} > 0$, $\sigma_{ij} > 0$ and density

$$f(lpue_{ij}|\mu_{ij}, \sigma_{ij}) = \left(\frac{\sigma_{ij}}{\mu_{ij}}\right)^{\sigma_{ij}} \frac{lpue_{ij}^{\sigma_{ij}-1}}{\Gamma(\sigma_{ij})} \exp\left(-\frac{\sigma_{ij}}{\mu_{ij}} lpue_{ij}\right).$$

Then, the expectation and variance are given by

$$E(lpue_{ij}) = \mu_{ij} \qquad Var(lpue_{ij}) = \frac{\mu_{ij}^2}{\sigma_{ij}}$$

such that μ_{ij} is the location parameter and σ_{ij} is inverse proportional to the variance.

All parameters involved are linked to structured additive predictors, yielding

$$\eta_{ij,\mu} = \mu_{ij} \qquad \eta_{ij,\sigma^2} = \log\left(\sigma_{ij}^2\right)$$

for the log-normal distribution where the log-link is used to ensure positivity of the σ_{ij}^2. For the gamma distribution, both parameters are restricted to be positive so that we obtain

$$\eta_{ij,\mu} = \log\left(\mu_{ij}\right) \qquad \eta_{ij,\sigma} = \log\left(\sigma_{ij}\right).$$

Dropping the parameter index, a generic structured additive predictor is of the form

$$\eta_{ij} = z_{ij}'\gamma + \sum_{p=1}^{P} f_p(x_{ijp}) + \alpha_i.$$

Here, z_{ij} is a vector containing binary, categorical or continuous linearly related variables and $f_1, \ldots, f_P$ are smooth functions of continuous variables $x_{ij1}, \ldots, x_{ijP}$ modelled by Bayesian P(enalized) splines (Lang and Brezger, 2004). The basic assumption is that the unknown functions f_p can be approximated by a linear

combination of B-spline basis functions (Eilers and Marx, 1996). Hence, f_p can be written in matrix notation as $Z_p\beta_p$, where Z_p is the design matrix with B-spline basis functions evaluated at the observations and β_p is the vector of regression coefficients to be estimated. To enforce smoothness of the function estimates we use second order random walk priors for the regression coefficients such that

$$p(\beta_p|\tau_p^2) \propto \left(\tau_p^2\right)^{-0.5\text{rank}(K)} \exp\left(-\frac{1}{\tau_p^2}\beta_p' K \beta_p\right)$$

where $K = D'D$ for a second order difference matrix D and τ_p^2 are the smoothing variances with inverse gamma hyperpriors.

The additional, boat-specific effect α_i is introduced to represent any effect specific to the catching unit that is not represented in the covariate effects of $z_{ij}, x_{ij1}, \ldots, x_{ijP}$. A standard assumption for this effect would be α_i i.i.d. $N(0, \tau^2)$, to acknowledge the fact that the catching units represent a sample from the population of catching units. Alternatively, α_i can be treated as a fixed effect resulting from dummy coding of the different catching units. There has been considerable debate in the past (Bishop et al., 2004; Cooper et al., 2004; Helser et al., 2004; Venables and Dichmont, 2004) about whether it is more appropriate to specify α_i as random or fixed effects from a methodological perspective, but then random effects have been rarely considered (e.g. Marchal et al., 2007). One differentiation goes along the lines discussed above, i.e. differentiating between situations where the catching units in the data set define a (random) subsample of the population of the catching unit (which would favour the specification as random effects) and situations where (almost) the complete fleet has been observed (which would favour the specification as fixed effects). From the Bayesian perspective, this differentiation provides an incomplete picture since the differentiation between random and fixed parameters only corresponds to a difference in prior specifications. From a practical point of view the random effects assumption can also be seen as a possibility to regularise estimation in case of large numbers of catching units and/or small individual time series where estimation of fixed effects may easily become unstable. Note also that in case of a fixed effects specification, no other time-constant covariates z_i characterising the catching units can be included since they can not be separated from the fixed effects. In our data set, this applies for the gross register tonnage which may be expected to provide important information on LPUE but which can not be included in a fixed effects analysis. This problem can be avoided for example by clustering catching units but with a probable loss

of information (as the solution used in Mamouridis, Maynou and Aneiros Pérez, 2014). In the next section, we compare the performance of random and fixed effects specifications based on model fit criteria to decide which model has a better explanatory ability.

Our inferences is based on efficient Markov chain Monte Carlo (MCMC) simulation techniques (for more details see Klein et al., 2013). In principle, the approach in all models could also be performed in a frequentist setting (Stasinopoulos and Rigby, 2007) via direct optimization of the resulting penalized likelihood which is often achieved by Newton-type iterations with numerical differentiation. However, many models turned out to be numerically unstable leading to no estimation results or warnings concerning convergence. Therefore the study is restricted to the Bayesian analysis. The Bayesian approach with MCMC also reveals several additional advantages, e.g. simultaneous selection of the smoothing parameters due to the modularity of the algorithm, credibility intervals which are directly obtained as quantiles from the samples and the possibility to extend the model for instances with spatial variations. All models have been estimated in the free open source software BayesX (Belitz et al., 2012).

The performance of models is compared in terms of the Deviance Information Criterion, DIC (Spiegelhalter et al., 2002). The DIC is similar to the frequentist Akaike Information Criterion, compromising between the fit to the data and the complexity of the model. Furthermore it can easily be computed from a sample $\theta^1, \ldots, \theta^M$ of the posterior distribution $p(y|\theta)$,

$$\text{DIC} = 2\overline{D(\theta)} - D(\overline{\theta}),$$

with deviance $D(\theta) = -2\log\left(p(y|\theta)\right)$ and $\overline{D(\theta)} = \frac{1}{M}\sum_{m=1}^{M} D\left(\theta^m\right)$, $\overline{\theta} = \frac{1}{M}\sum_{m=1}^{M}\theta^m$ respectively. We also use the DIC to determine important variables and optimal predictors $\eta_{i,\mu}$ and η_{i,σ^2} or $\eta_{i,\sigma}$.

To validate the distribution assumption we used normalized quantile residuals. That allowed to decide between equivalent models under different response assumptions. Normalized quantile residuals are defined as $r_i = \Phi^{-1}(u_i)$. Here, Φ^{-1} is the inverse cumulative distribution function of a standard normal distribution and u_i is the cumulative distribution function of the estimated model and with plugged in estimated parameters. For consistent estimates, the residuals r_i, $i = 1, \ldots, n$ follow approximately a standard normal distribution if the estimated distribution is

the true distribution. Therefore, models can be compared graphically in terms of quantile-quantile-plots.

Finally, we performed a k-fold Cross Validation to assess the predictive accuracy of the models using the mean squared error of prediction (MSEP)

$$\text{MSEP}_k = \frac{\sum_{i=1}^{N} \left(lpue_{i,k} - \tilde{E}\left(lpue_{i,k}\right)\right)^2}{N}.$$

Here $lpue_{i,k}$ is the observation i of subset k, $\tilde{E}(lpue_{i,k})$ is the expectation of the prediction in the validation set, given parameters estimated on the k-th training set and N refers to the number of observations of the corresponding validation set. We performed a 10 fold random partition within each catching unit to ensure a minimum number of observations for each boat in both the training and the validation sets. Taking the 10% of the data to built the latter, we ensure at least 10 observations per unit in the validation set. If at least one catching unit is not represented in one of the partitions, the prediction for the missing catching unit in fixed effects models could not be computed. This clarifies the usefulness of mixed effects models when interested on predictions for unobserved units.

4.3 Results

4.3.1 Model selection, diagnostics and comparison

Variables were chosen using a stepwise forward procedure according to DIC scores. For each distribution we first modelled the predictor for location, adding variables till the best combination. Then, using the most appropriate predictor for location, also the predictor for the second parameter, scale or shape, depending on the distribution assumed, has been modelled using the same procedure. We imposed the same number of knots found in Chapter 3 using the effective degree of freedom (edf) returned by the frequentist approach (Wood, 2006).

According to the DIC scores, for log-normal assumption, the appropriate predictor structures for location η_μ and scale η_{σ^2}, are

$$\begin{aligned} \eta_\mu &= \beta_{0,\mu} + \beta_{1,\mu} period_2 + f_{1,\mu}(trips) + f_{2,\mu}(time) + f_{3,\mu}(nao_3) + \sum_i \alpha_{i,\mu} \\ \eta_{\sigma^2} &= \beta_{0,\sigma^2} + f_{1,\sigma^2}(trips) + f_{2,\sigma^2}(time) + \sum_i \alpha_{i,\sigma^2} \end{aligned} \tag{4.2}$$

for both fixed and mixed effects specification. Here the $\beta_{k,\cdot}$ are parameters associated to the intercept and linear fixed effects of the variable *period*. The $\alpha_{i,\cdot}$ are parameters associated to the effects of *code*, specified as fixed in fixed effects models and as random in mixed effects models. Instead, $f_{l,\cdot}$ are smooth functions associated to nonlinear effects of the variables *trips*, *time* and nao_3. The second sub-index of all parameters identifies which predictor the parameter or function belongs, η_μ or η_{σ^2} respectively.

Using fixed effects specification for *code* the inclusion of variable *grt* leads to instability, due to the reasons mentioned in Section 4.2.2, so then, the model with *grt* cannot be estimated in these cases. On the contrary, *grt* could be estimated in mixed effect models and it returned significant positive effect, however the DIC score was equal or lightly higher (although with minimum difference). Thus, for the purpose of this study it has been backward eliminated to be able to compare consistently fixed and mixed effects models with the same variables.

Under the gamma distribution assumption, the log-link function has been chosen, since the support of both parameters is the positive real domain and the final predictor structures for location and shape are

$$\begin{aligned} \eta_\mu &= \beta_{0,\mu} + \beta_{1,\mu} period_2 + f_{1,\mu}(trips) + f_{2,\mu}(time) + f_{3,\mu}(nao_3) + \sum_i \alpha_{i,\mu} \\ \eta_\sigma &= \beta_{0,\sigma} + f_{1,\mu}(trips) + f_{2,\sigma}(time) + \sum_i \alpha_{i,\sigma} \end{aligned} \tag{4.3}$$

for both fixed and mixed effects specification. The notation here is the same specified for the log-normal models however here the second parameter, the shape, is denoted with σ.

The Table 4.2 provides a selection of models that we used for comparison purposes and their corresponding global parameters: the deviance, the effective number of parameters and the DIC, estimated on the whole dataset, and the MSEP calculated by predictions on the validation subsets as described in the methodology.

These eight models present a combination between alternatives of the following parametrisations:

- (A) The log-normal (LN) or gamma (GA) as the underlying distribution assumption;
- (B) Only location (LO) or both location and scale/shape (LS) parameters explicitly modelled using one or more explanatory variables;
- (C) Effects of *code* as fixed or random leading to a fixed effects model (FI) or mixed effects model (MI) respectively;

The predictors for location in models denoted as M1, M2, M5 and M6 (with B=LO) have the same structure of η_μ in Equations 4.2 and 4.3, while the corresponding predictor for scale/shape is a constant. Both predictors in models M3, M4, M7 and M8 correspond to Equations 4.2 and 4.3.

Concerning to (A), model specifications widely favour the gamma over the log-normal distribution. In fact DIC scores are lower under the gamma assumption, with approximately 100 scores of difference between analogous models (i.e. same variables specified in the predictors). The benefit in assuming the gamma distribution is also evident comparing MSEP scores (lower scores for better predictions).

M	A	B	C	DEV	EP	DIC	MSEP
M1	LN	LO	FI	16163.9	47.1	16258.0	98.3 ± 12.3
M2	LN	LO	MI	16164.2	46.8	16257.7	96.9 ± 12.4
M3	LN	LS	FI	15138.4	91.2	15320.8	436.2 ± 434.9
M4	LN	LS	MI	15142.7	87.2	15317.2	315.0 ± 307.4
M5	GA	LO	FI	16095.7	45.6	16187.0	77.8 ± 11.5
M6	GA	LO	MI	16096.8	43.9	16184.7	77.3 ± 11.7
M7	GA	LS	FI	15027.1	90.9	15208.9	71.5 ± 9.2
M8	GA	LS	MI	15032.4	86.9	15206.1	71.7 ± 9.4

TABLE 4.2: Global scores of selected models. M: model coding; A: the assumed distribution is log-normal (LG) or gamma (GA); B: (LO) the location varies w.r.t. explanatory variables while the second parameter is constant or (LS) both vary; C: if the unit-specific effect is considered as fixed, thus the model has only fixed effects (FI) or random and the model is a mixed effects model (MI); DEV, the residual deviance; EP: Effective total number of Parameters, DIC: Deviance Information Criterion, MSEP, mean and sd of the mean square error of predictions calculated through 10-fold validation.

Nevertheless, results of log-normal models' MSEP is not entirely satisfactory, because when accounting for both predictors MSEP should behave as in the gamma models, i.e. lower scores when considering both predictors than accounting only for η_μ. Regarding to the estimation of both predictors for first and second parameters (B), models under the gamma assumption show an improvement when explicitly modelling the dependence of second parameter σ from explanatory variables in both DIC and MSEP scores (both decrease). Contrariwise, under the log-normal assumption, however the DIC decreases, the MSEP increases and presents higher variability, suggesting worse predictions, when the second parameter is explicitly modelled. But as discussed few lines above, η_{σ^2} follows a strange behaviour and further research is needed.

Finally no notable leaps have been observed between fixed and random effects models (C). Whereby the best DIC and MSEP scores and QQplots lead to the final model with predictors given in (4.3).

According to the DIC (Table 4.2) the model providing better estimations is the gamma model (M8, predictors given in Equation 4.3) specifying catching units as random effects.

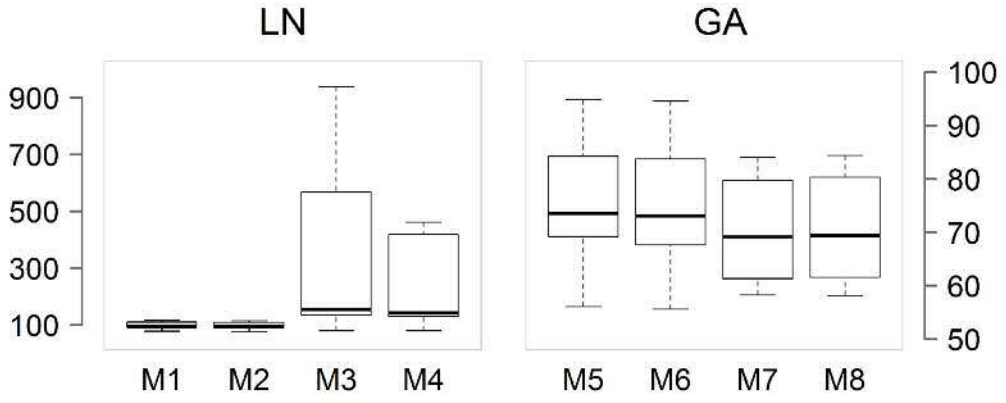

FIGURE 4.1: Boxplots for MSEP calculated for all models. See Table 4.2 and Equations in the text for model specifications.

The boxplots of MSEPs also favour the gamma assumption (see Figure 4.1 and values in Table 4.2). The minor MSEP the better prediction, MSEP results divide models into three distinguishable groups from highest to lowest mean MSEP: 1) log-normal models considering scale modelling, 2) log-normal models considering η_{σ^2} constant (compare M1-M2 with M3-M4), and 3) all gamma models (M1, M4, M5 and M8). Within this group, modelling the shape in dependence to variables,

consistently decreases MSEP estimates, e.g. in terms of median and variance of the MSEP (compare M5 and M6 with M7 and M8).

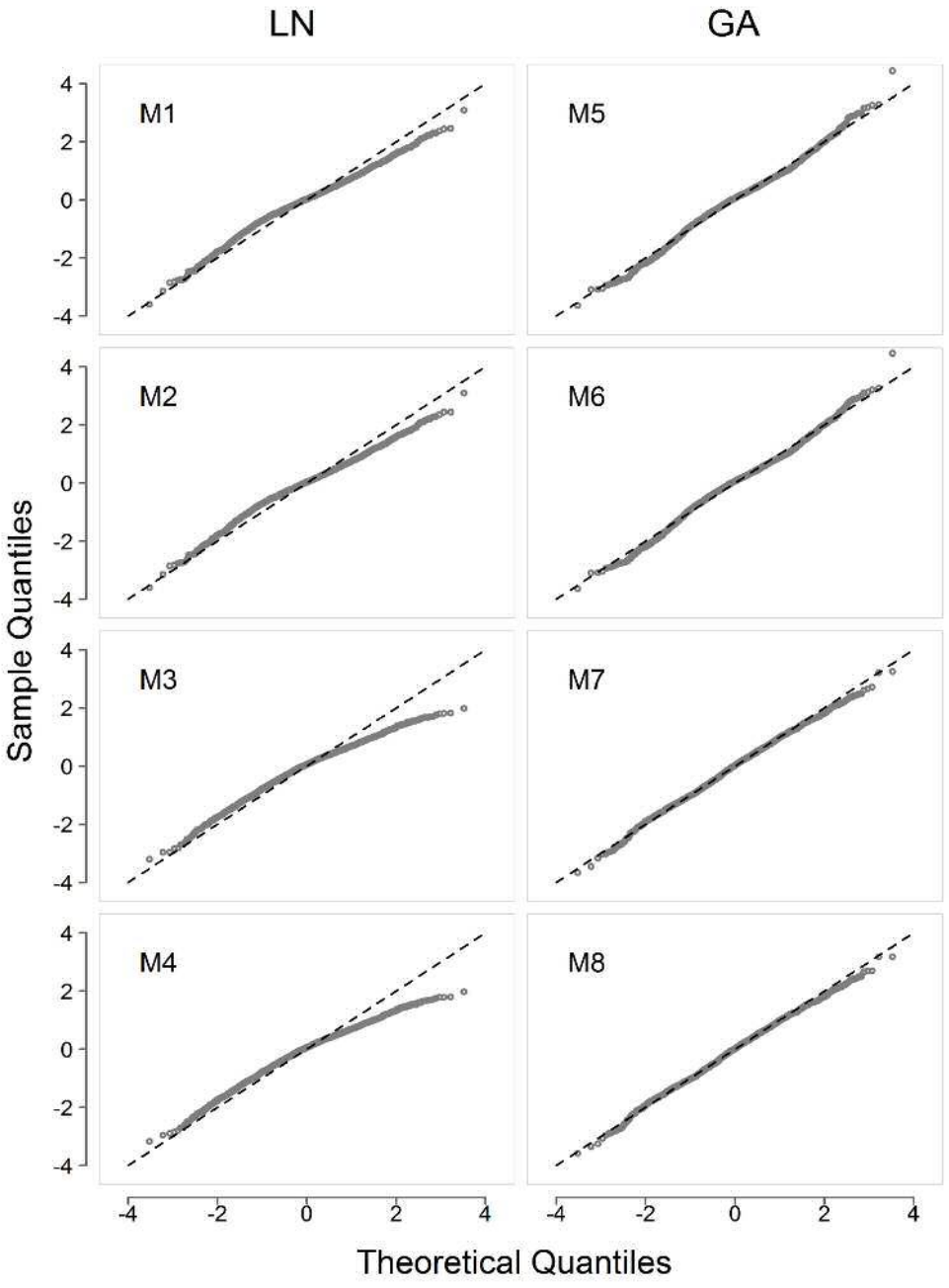

FIGURE 4.2: QQplots of the normalized residuals calculated as described in the methodology section for the 8 models.

In order to validate the distribution assumptions, QQplots for residuals are reported in Figure 4.2, from which it follows that:

- the residuals in gamma models almost follow the straight line (M5 and M8 in the Figure), while in the log-normal they show upward-humped curves

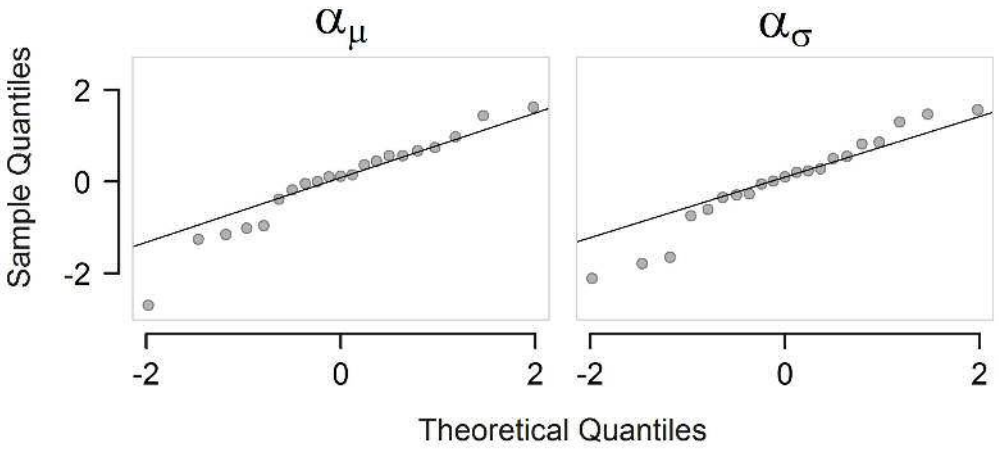

FIGURE 4.3: QQplots for normality of catching units parameters as random effects in the mixed model M8. α_μ refer to random effects in the predictor for location, while α_σ refers to the predictor for the shape.

(M1 and M4), suggesting a definitively "better approximation" of models to the gamma distribution.

- Modelling the second parameter in gamma models improves QQplot outputs, while the opposite happens for log-normal models. Focusing only in gamma models, the outlier is "absorbed" into the straight line in the right part validating the improvement in estimations (compare M5 and M6 with M7 and M8 in Figure 4.2).

We finally assessed the normality for random effects for the model M8 corresponding to Equation 4.3. Figure 4.3 provides the QQplots of the random effects for both predictors. The majority of sample quantiles approximatively follow the normal quantiles, however they depart from it at the extremes, especially evident in the lower tails and for α_μ (on the left).

4.3.2 Description of partial effects

Estimations of linear fixed effects for A) μ and B) σ predictors of final model M8, (4.3), are reported in Table 4.3 and nonparametric effects are shown in Figure 4.5.

All partial effects associated to η_μ are linked to the expectation of LPUE, E(LPUE), through the exponential of η_μ. When partial effects hire positive values, the expectation increases while decreases otherwise. Contrariwise the variance of LPUE

is affected by both predictors being directly proportional to μ and inverse proportional to σ.

A)			B)	
	mean	sd	mean	sd
const	2.891	0.058	-1.551	0.099
$period_2$	-0.153	0.024		

TABLE 4.3: Estimations of linear fixed effects for the model M8, Eq. (4.3) associated to A) μ and B) σ respectively.

The variable *period* describes the intra-annual variability and shows a negative effect in $period_2$, corresponding to June and November in comparison to the rest of the year. That should be related to a lower demand of this source during these months.

The variable *grt* (results not reported), referring to the gross registered tonnage of boats, returns a significant and positive slope parameter, causes a linear increment on the predictor for location. Its effect has been estimated in Chapter 3. However it has a minor impact in the considered dataset, it can be important when comparing with other fisheries where it could (or not) have a major impact on the response. *grt* is not the only variable characterising a fleet, nevertheless it is the only reliable available metric for boats of this fishery.

The second fishery-related variable is *code*, representing catching units' effect. The variable captures abilities of fishermen and technical characteristics of the fleet, appropriate technologies and strategies, e.g. the power and type of the engine, the net shape and the skipper's expertise and ability. Results (Figure 4.4) show that many trawlers have similar effects (around zero), but many of them hold positive or negative effects. The former are very specialised and powerful boats catching large amounts of the resource leading to higher values of LPUE while the latter are not specialised in deep-sea fisheries and capture lower amounts, leading to lower LPUE (see the partial effects on μ). At the same time catching units associated to higher effects on the predictor of μ also present higher effects on the predictor for σ, while boats associated to lower effects on μ also hold lower effects on σ. In summary, more specialised trawlers capture more quantities and also present less variability (see the relationship between shape and variance in gamma distribution). Contrariwise not specialised trawlers catch less quantities and present more variability in landings. This fraction of the fleet more likely is

represented by boats that fish on the continental shelf and occasionally displace towards deeper waters going in search of the red shrimp.

Concerning to nonparametric effects (Figure 4.5), *trips* and *time* influence both η_μ and η_σ, while nao_3 showed to slightly affect only η_μ.

Variable *trips* shows a negative effect on the predictor for μ when $trips \leq 8$, while positive otherwise. The rate of the effect rises moving through the covariate interval till a plateau beginning around $trips = 17$. For extreme high values *trips* has an uncertain effect. Low values of its effect could be associated with the trawlers operating usually on the continental shelf and with less knowledge of red shrimp fishing grounds (Maynou et al., 2003) and/or to period of bad weather and vice versa for high values. Increasing the number of trips per month, also the probability to find high-concentration shoals inside the fishing grounds increases for a given boat in a process of trial and error as suggested by Sardà and Maynou 1998.

The effect of *time* on the predictor for μ shows high inter-annual variability, certainly caused from multiple factors. Between 1992-1996, the effect decreases while increases in next three years. We could not find a reasonable explanation to this

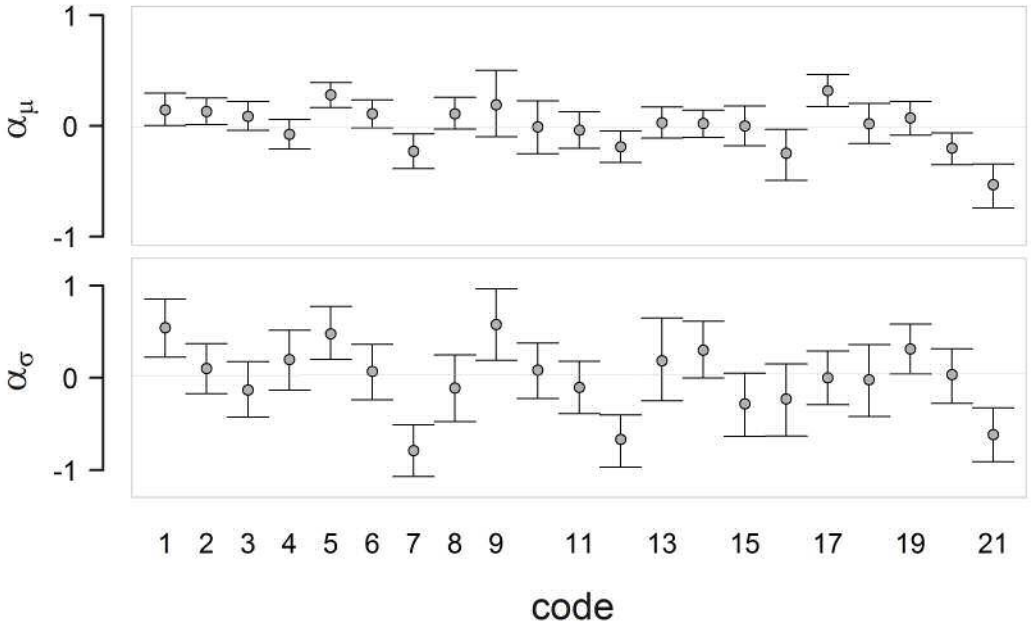

FIGURE 4.4: Interval plots of estimated random effects in the predictor for location (α_μ) and shape (α_σ) on the upper and lower plots respectively. Bars indicates 95% CI.

trend. Afterwards, between 1999-2000, it drops till a minimum low followed by a rapid increase up to a pick in 2004. We believe that the minimum is related to both negative NAO observed in previous years and to the rising of fuel price started in 2000, that in turn is related to a lower number of trips performed by trawlers (see discussion in Chapter 3. Then, for five years it presents a slightly oscillatory trend till the last year characterised by another positive pick probably related to the rise of the economic value of the resource, that offsets the increase in the fuel price.

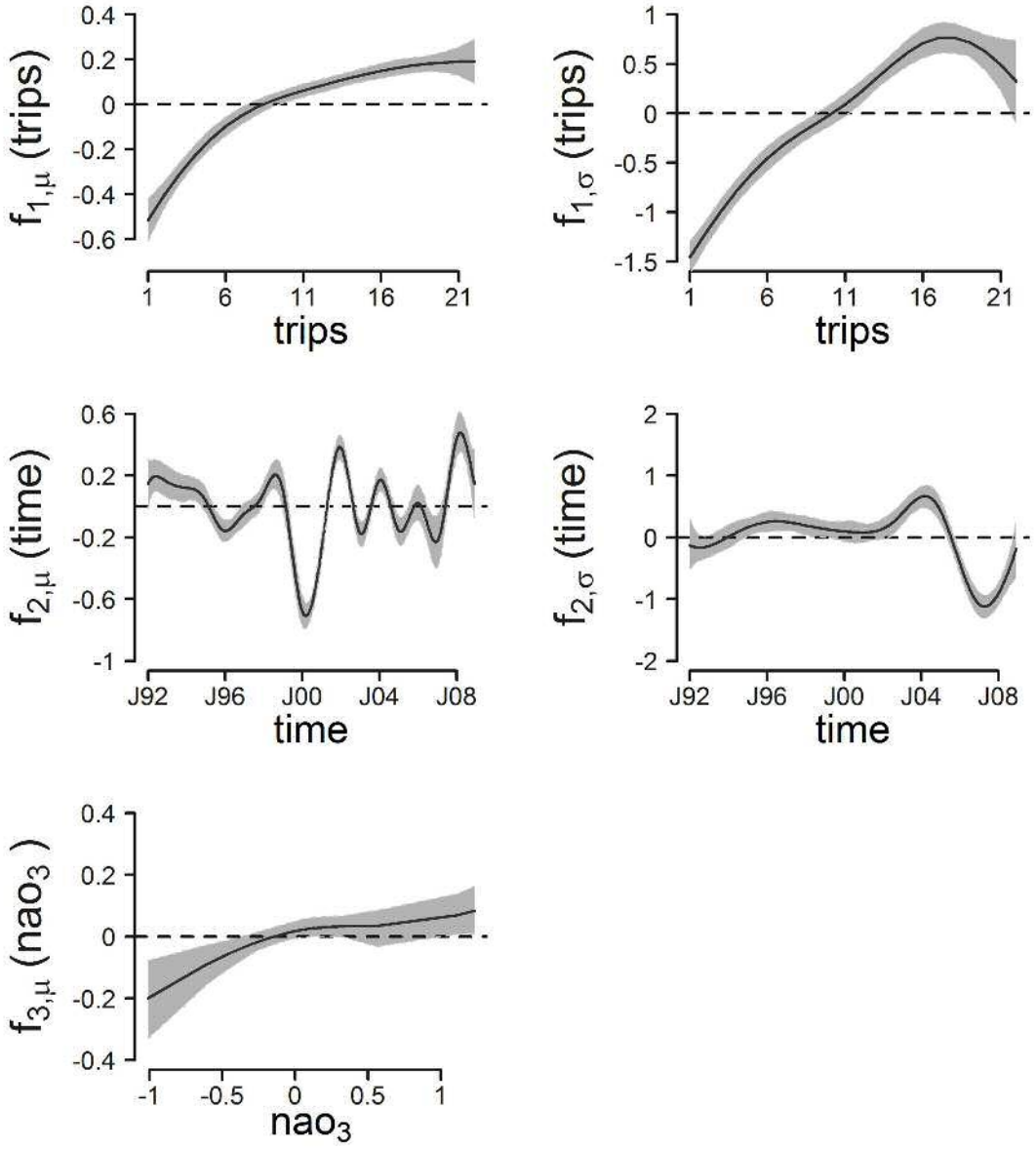

FIGURE 4.5: Nonparametric effects for the GA mixed effect of the selected gamma model (M8). Effects on predictor for μ (left side) and for σ (right side). Grey shapes represent 95% credible intervals.

Finally, results show that nao_3 has a moderate effect for this deep-sea species, however it can lead to a significant reduction of LPUE when reaches negative values shown by the partial effect lower than zero for negative NAO values. On the contrary the positive effect on LPUE for high values of the NAO is less evident.

In the predictor for σ, the effect of *trips* is negative for low values of the covariate ($trips \leq 10$) and positive for higher values. It also shows a high increment till a maximum corresponding to $trips = 17$, while decreasing again for higher values, but continuing to be positive. The effect of *time* is slightly negative before 1995 and slightly positive between 1995 and 2000. Then for two years has no effect. Then, in 2002 it switches clearly positive again till 2006, showing a high pick in 2004 and finally negative in the last years during 2006-2008, reaching an abrupt drop in late 2007. Thus, regarding to the Var(LPUE), results that values of covariates associated to positive effects in η_μ and negative effects in η_σ, in turn affect positively (increase) the variance. We can therefore deduce that *time* is the driver in causing the heteroscedasticity in LPUE, mainly in last years when its effect on η_μ is positive and its effect on η_σ is strongly negative. This high variability could be related to different factors, mainly of economic origin, such as the fuel and ex-vessel shrimp prises as discussed above.

4.4 Discussion

In this study we proposed distributional structured additive models (DSTAR) for the first time to model the LPUE index (or CPUE) widely used in fisheries research. Data deal with the LPUE of red shrimp (*A. antennatus*) from the Barcelona's fleet during years 1992 – 2008.

On a methodological view, we demonstrated that the gamma distribution more properly describes residuals providing better estimations as shown by results of the deviance information criterion (DIC) and the QQ-plots and also better predictions (MSEP).

In addition, distributional structured additive models, as the frequentist counterpart GAMLSS, allowed to model both first and second order moments of the response, returning even better estimates, when considering the second parameter. In fact the second moment (the shape for gamma distribution or scale for log-normal) can be explained by many of the explanatory variables we used (i.e.

trips and *time*). Thanks to this kind of models we rose a more detailed understanding of how and why LPUE changes and how it is affected by the covariates. For example the analysis performed on (almost) the same data set, a frequentist approach using GAM accounting only for the location, could not avoid the heteroscedasticity in the residuals (see Figure C.2). Here we demonstrated that both the number of trips and time strongly influence the second parameter, that in turn is (inverse) proportional to the variance (while the location is directly proportional). This meant, e.g., that during years 2007-2008 the variance is higher and is effected by both μ and σ, such that the predictor for location increases, while the predictor for the shape decreases. This high variability could be related to different factors, mainly of economic origin, such as the fuel and ex-vessel shrimp prises. Thus, regarding to the $Var(\text{LPUE})$, results that values of covariates associated to positive effects in η_μ and negative effects in η_σ, in turn affect positively (increase) the variance.

The LPUE also showed a seasonality probably related to the demand of this source across the months. The gross registered tonnage of boats returns a significant and positive effect the LPUE. The effects and importance of these variables have been estimated in Chapter 3. However significant they returned very low impact with respect to all other variables considered.

The NAO is a very interesting environmental variable. It has a moderate effect for this deep-sea species, however results suggest that it can lead to a significant reduction of LPUE when it reaches negative values. Numerous publications demonstrated its influence on marine populations and on different exploited stocks, including this and other fish stocks (e.g. Báez et al., 2011; Maynou, 2008). These authors show that the NAO can bear important effects when either it is extremely positive or negative. Considering both results of TIME and NAO and comparing data series of both the raw LPUE and the NAO, we believe that the LPUE low starting at the end of 1999 can be related to consecutive negative NAO during the previous four years, especially during 1996, corresponding to three years before the beginning of the decline of LPUE. Negative NAO leads to paucity of resources while it enhances productivity when it is highly positive. Between $nao_3 = 0.50$ and $nao_3 = 1$ the effect increases however without a significant evidence. In the middle region of the variable span, there is no effect, that could represent a "buffering region" related to "normal" weather conditions for the stock. In some studies the relationship NAO-stock has been explained by the modulation of the recruitment strength (in cod: Brodziak and O'Brien, 2005) and the effect is stronger when the

spawning stock biomass is low (Brander, 2005). In many cases has been found that the relationship is mediated by changes in prey composition and biomass, i.e. zooplankton (see e.g. Fromentin and Planque, 1996; Reid and Croxall, 2001; Stige et al., 2006). In our case, we found that NAO strongly influences the red shrimp biomass when it is low. That is in accordance with the founding by Brander (2005) for the cod. In fact, being landing and so the lpue as well, composed mainly by mature individuals, we can infer that NAO play a higher role when the spawning stock biomass is low. To the other hand we found a positive relationship when both NAO and stock are high. This is in agreement with (Maynou, 2008). The author suggested that positive NAO is related to low rainfall, that in turn is linked to enhanced vertical mixing of water masses in the NW Mediterranean (Gulf of Lions: Demirov and Pinardi, 2002; Jordi and Hameed, 2009, because when rainfall is low, waters are saltier (and so more dense), and superficial waters tend to fall dawn. Has been postulated that when this occurs the red shrimp switch from its generalistic diet to a high-energy content diet based on zooplankton (Cartes, Madurell, Fanelli and López-Jurado, 2008; Maynou, 2008; Vicente-Serrano and Trigo, 2011). Increasing the resource (of high quality), the predator (red shrimp in this case) assimilates more energy and the stock is expected to increase as well.

Catching-units captures all abilities of fishermen and technical characteristics. We found that many trawlers have similar effects (or no effect). However many of them hold positive effects on mean LPUE and vice versa on variance. This portion of the fleet is composed by very specialised and powerful boats that catch large amounts of the resource. The LPUE also returns lower variability. On the contrary those holding a negative effect capture less amounts and the LPUE presents high variability. They are probably specialised in other fisheries. Also low values of TRIPS effect could be associated with not specialised trawlers operating usually on the continental shelf and with less knowledge of red shrimp fishing grounds (Maynou et al., 2003) and/or to period of bad weather and vice versa for high values. The number of trips is also associated to find high-concentration shoals improving the expertise of fishermen in a process of trial and error as suggested by Sardà and Maynou 1998.

Finally we point out another methodological issue concerning to fixed versus mixed specification. In our study the fixed effects can be considered appropriate representing sampling units the whole population of the studied fleet (in accordance to the definition by Pinheiro and Bates, 2000), however mixed models are particularly suitable not only for unobserved catching units but also for correlated

observations in time series analysis. In practise we clashed with estimation instability when trying to incorporate both CODE and TRB in fixed effects models. We could avoid the problem clustering catching units when modelling LPUE with generalized additive models in Chapter 3. In the present Chapter with the incorporation of random effects into a mixed effects model, we avoided this drawback.

Acknowledgements: Authors would like to thank the Fisheries Directorate of Catalonia's Autonomous Government to facilitate access to the sales data of the Barcelona Fishers' Association, as well as fishers of Barcelona. Financial support from the Spanish National Council of Research (CSIC) through the JAE-predoc grant and the German Research Foundation (DFG) grant KN 922/4-1 are gratefully acknowledged.

PART III

5

Food web modelling in a soft-bottom continental slope ecosystem (NW Mediterranean)

Abstract

We present a quantitative food-web analysis of the soft bottom community at the continental slope of the NW Mediterranean at 600–800 m depth. A total of 40 carbon flows among 7 internal and 6 external compartments, were reconstructed using linear inverse modelling (LIM) by merging site-specific biomass data, on-board oxygen consumption rates and published parameters to create population and physiological constraints. The total carbon flux to the community was 2.62 mmol C m^{-2} d^{-1} (range estimations: 0.92 – 4.16 mmol C m^{-2} d^{-1}), entering as vertical OM (average: 5.2E-03, range: 8.9E-04 – 2.5E-02) and advecive OM (average: 2.6E-00, range: 9.2E-01 – 4.1E-00). The influx was then partitioned between the total organic matter in sediment, 87.05%) and suspension and filter feeders (12.95%), comprising zooplankton (1.08%), suprabenthos (3.07%) and macrobenthos (95.74%). The suspension feeding of some invertebrates belonging to the megafauna, e.g. the brachiopod *Gryphus vitreus*, has been neglected in the model, because rarely observed.

The fate of carbon deposited in sediments was its burial, its degradation by prokaryotes or the ingestion by metazoan deposit feeders. The total ingestion of C in sediments by the metazoan community (excluding the meiofauna, e.g. nematods) was 0.83 mmol C m^{-2} d^{-1}, corresponding to 31.68% of the total C entering the food web and to 36.34% of the C in sediments, the rest was used by the prokaryotes and nematods (1.58 mmol C m^{-2} d^{-1}, 69.28%) or trapped in the sediment (0.73 mmol C m^{-2} d^{-1}, 32.19%).

The respiration of the whole community (including the TOM) was 1.89 mmol C m^{-2} d^{-1} (ranging between 0.84 – 2.34): 83.75% for sediments, including prokaryotes and meiofauna, 13.34% for macrofauna, 2.86% for megafauna, including the red shrimp *Aristeus antennatus*.

Keywords: food web, bathyal ecosystem, NW Mediterranean, linear inverse modelling

5.1 Introduction

Food webs are descriptions of biological interactions between consumers and resources which help to determine the dynamics of populations, as well as the transfer of matter and energy in marine ecosystems (de Ruiter et al., 2005; Polis, 1999). Quantifying the dynamics of deep-sea trophic webs is an important step to increase our understanding of these ecosystems, which are increasingly subject to human exploitation through the extraction of mineral resources or harvesting of fisheries products (de Ruiter et al., 2005). Fishing has direct and indirect impacts on the dynamics of ecosystems, altering their structure and function (Pikitch et al., 2004). The quantitative analysis of networks and their sensitivity to disturbance (mainly changes in the fluxes due to fish harvesting) (de Ruiter et al., 2005) may be of use to fisheries assessment in the newest context of an Ecosystem Approach to Fisheries (EAF, de Ruiter et al., 2005). In deep-sea ecosystems, where traditional data for fisheries assessment is often inadequate as there is limited scientific sampling (van Oevelen et al., 2009), is even more important to find the appropriate techniques in data-limited contexts.

Early ecosystem ecology emphasized the nature of the trophic structure of ecosystems and patterns of energy flow in them (Lindeman, 1942). This is the topology of the network, where interactions among compartments are marked as either present or absent (Pimm, 1991). This is the fundamental basis for a quantitative approach. In last decades (more than 30 years of research), ecologists have realised the usefulness of accounting for the magnitude of the flows, also known in the literature as "interaction strength" (Berlow et al., 2004). Its analysis reveals important features of the food web functioning, i.e., its stability, that critically depends on different patterns dominating the web (De Ruiter et al., 1995). For example, the dominance of weak interactions in long trophic loops dampens the potentially destabilizing effect of such long loops (Neutel et al., 2002), while the coupling of fast and slow trophic pathways by top predators increases food web stability (Rooney et al., 2006).

Important food web properties are the level of omnivory, food chain length, connectance and the number of basal, intermediate and top species (e.g. see Williams and Martinez, 2000). These food web descriptors are typically calculated from topological food webs. However, a lot of other ecosystem attributes require flux estimation, such as the gross production, the total respiration, the energy cycling and the ascendency among others (Patten, 1995). Furthermore, Banašek-Richter

et al. (2004) show that descriptors based on quantified food webs are superior because less sensitive (or more robust) to varying levels of sampling effort, however they lead to a loss in precision, compensated by increasing the accuracy. Unfortunately, there is not a systematic and standardized method to produce quantified food webs to fully explore their structure and properties (Woodward et al., 2005) and allow a consistent comparison among food webs. Communities often contain thousands of species but food webs include only a few, being either highly aggregated or representing only a part of the system.

Another problem basically comes down to find the most likely set of flow values, assuming a certain food web topology and given an empirical data set. Anyhow, more than hundred of marine food webs have been described and a number of generalizations have emerged from these works. For example, the (general) Lindeman's rule of 10% of efficiency of energy transfer (Lindeman, 1942) has been verified by Pauly et al. (1998). Secondly, most fish production is consumed by other fish and not by exploitation (Christensen, 1996; Pauly, 1996).

Many tools are available to describe trophic interactions. The most used and popular is ECOPATH with Ecosim (EwE) (Christensen and Walters, 2004). ECOPATH is based on mass balance equations and steady state assumption for the quantitative estimations of flows. It was originally initiated by Polovina (1984) and has been development since 90's (Christensen and Pauly, 1992) into a software, allowing spatio-temporal dynamic simulations (Walters et al., 1999, 2000, 1997). The mathematics below makes use of standard matrix algebra. A generalized inverse is used if the determinant is zero or the matrix is not square (Mackay, 1981). If the set of equations is over-determined (more equations than unknowns) and the equations are not mutually consistent the generalized inverse method provides least squares estimates, which minimise discrepancies (Christensen and Pauly, 1992). ECOPATH also solves under-determined problems for missing stocks, using an iterative algorithm before setting up the set of linear equations, becoming then an even-or over-determined system, that can be solved by the generalized inverse method. It makes use of a defined energy balance within each group using an equation similar to

$$C = P + R + U$$

where C is consumption, P production, R respiration and U unassimilated food, that represents the basic energy conservation assumption for biological units (Winberg, 1956). However ECOPATH does not explicitly estimate gonadal growth and energetic assumptions cannot be changed.

Also the Linear Inverse Modelling (LIM, Soetaert and van Oevelen, 2009*b*) is based on mass balance equations but it also allows more flexible construction of physiological constraints giving a flexible tool to formulate energetic assumptions that better fit to available data. The LIM is a modified version of the original LIM proposed by Niquil et al. (1998); Vézina and Savenkoff (1999); Vézina and Platt (1988) and which are based on Least Distance Programming (LDP) or linear Programming (LP) techniques that estimate the flows within biologically reasonable bounds (Diffendorfer et al., 2001). In its original version, these methods selected one food web, the parsimonious (simplest) one, amongst the infinite number of foodwebs that satisfy the data. Later methods were developed to also return the uncertainty of the flows, e.g. by a monte carlo analysis Kones et al. (2006). For under-determined problems, the LIM also permits the estimation of the ranges of physiological parameters (not for stocks).

Thanks to this flexibility, the LIM is particularly suitable for quantifying deep-sea food webs, where data limitation is the normal situation (Soetaert and van Oevelen, 2009*b*). To date available reconstructed deep-sea food web models using LIM are given for a cold-water coral (*Lophelia pertusa*) community around 800 m depth at Rockall Bank (van Oevelen et al., 2009), in three sections (300-750 m, 2700-3500 m and 4000-5000 m) of the Nazaré canyon (van Oevelen, Soetaert, García, de Stigter, Cunha, Pusceddu and Danovaro, 2011), of a sub-arctic deep sea macrofaunal community in the Faroe-Shetland Channel at 1080 m (Gontikaki et al., 2011), at 2500 m in the deep-sea observatory HAUSGARTEN (Fram Strait, Artic Ocean) (van Oevelen, Bergmann, Soetaert, Bauerfeind, Hasemann, Klages, Schewe, Soltwedel and Budaeva, 2011) and at 4850 m in the Porcupine Abyssal Plain (northeast Atlantic) (van Oevelen et al., 2012).

Another example of food web modelling using the LIM methodology (but not in the deep-sea) is the benthic food web in the Molenplaat intertidal flat located in the saline part (salinity 2025) of the Scheldt estuary (Belgium, The Netherlands) (van Oevelen et al., 2006).

In this Chapter we aim to quantify the principal pathways through the food web of the continental slope between 600-800 m in the Catalan Sea (Balearic basin,

NW Mediterranean) subjected to red shrimp, *Aristeus antennatus*, fishery (more information on this fishery is given in Chapters 3 and 4). In particular we aimed to: 1) describe the main pathways involved in the bathyal food web and their strength with particular attention on the energy input, the loss due to fishery and the role of red shrimp; 2) characterise the food web through the analysis of network indices, that condense the information contained in the trophic networks (Fath and Patten, 1999; Ulanowicz, 2004).

5.2 Materials and Methods

5.2.1 The study area

The study area is located on the continental margin of the mainland part of the Balearic basin (NW Mediterranean, Figure 5.1). Data were derived from oceanographic surveys performed along the mid-slope at 600-800 m depth between the Ebro delta and Barcelona city within the BIOMARE (ref. CTM2006-13508-CO2-02/MAR) and ANTROMARE (ref. CTM2009-12214-C02-01-MAR) projects.

All 7 stations are fishing grounds for *A. antennatus* and are subjected to different intensities of exploitation. Detailed information of the sampled stations are reported in Table 5.1.

Code	Position	depth (m)	year
S1-a	41°15N – 02°40E	600	2008
S1-b	41°15N – 02°40E	800	2008
S2-a	41°09S – 02°24E	600	2008
S2-b	41°09S – 02°24E	800	2008
S3	40°54N – 1°35E	615–648	2011
S4	40°41N – 01°26E	615–648	2011
S5	40°34N – 01°26E	615–648	2011

TABLE 5.1: Main information about sampling statios: 1) the code of each stetion, 2) the position, 3) the depth and 4) the syear.

In the NW Mediterranean, the deep sea presents unique characteristics, e.g. warm temperatures (13°C in comparison to the deep ocean, 2 – 4°C) and high salinity (38 ppt) below 150 m. The area is characterized by soft-sediments at the bottom and by late winter blooms at the surface with a deep chlorophyll maximum (DCM) in open waters during summer (Estrada, 1996). The open slope is influenced

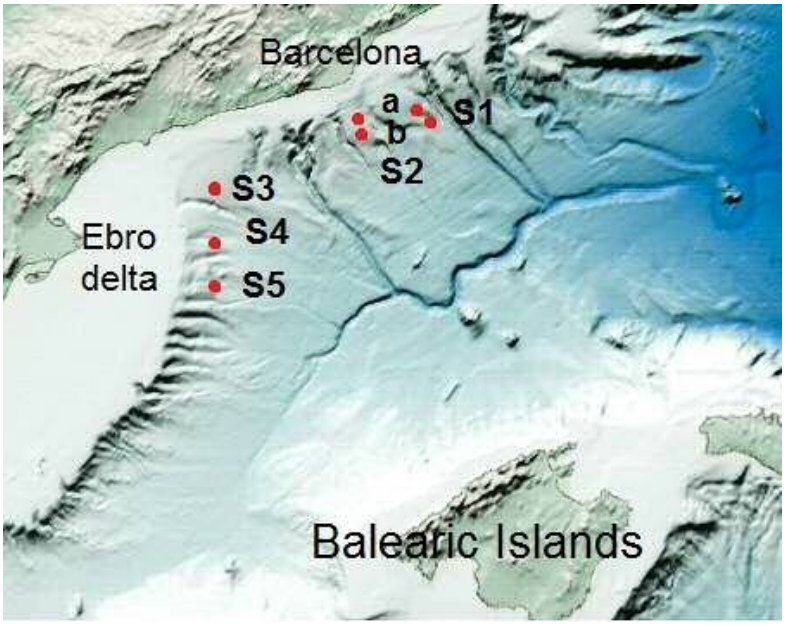

FIGURE 5.1: The food web study area comprises the soft-bottom slope in front of the Catalonia at 600-800 m.

by river discharges, lathough inside the submarine canyons that are particularly numerous in this area, this process is more evident. Although less than in the Gulf of Lions, there is a significant vertical mixing during winter in front of the Ebro river, enhancing the circulation of water masses and the coupling between surface and deep waters (Marty et al., 2002; Salat et al., 2002). The organic matter thus reaches the deep-sea regions along two main pathways: the vertical flux of settling partciles and the advective flux across the slope (Pusceddu et al., 2010; Vetter and Dayton, 1999). Advective fluxes are strongly enhanced by river discharges. In contrast, vertical settling is the result of organic matter produced in the epipelagic zone (the phytodetritus, fecal pellets and dead animals). The matter originating from advection can reach significantly higher values than that of pelagic origin (for example in the Gulf of Lions a difference of two orders of magnitudes has been calculated) (Durrieu De Madron et al., 2000).

5.2.2 Biomass data

Samples of fauna were collected using four types of gears for the different typologies of fauna (megafauna, macrobenthos, suprabenthos and zooplankton-micronekton, described below). We used:

1. A Reineck's box-corer (surface: A = 0.065 m^2) to sample the benthic macrofauna, mainly infauna (0.5–20 mm). The uppermost 20 cm of sediments were picked up and sieved through a 0.5 mm mesh size to retain specimens. This mesh size samples sometimes animals belonging to the meiofauna (size range usually inbetween 0.1–0.5 mm), such as nematodes, benthic ostracods and very small polychaetes, i.e. some paraonid species. The fraction of meiobenthic specimens did not affect the total biomass of the samples analysed. A total of 28 box-corers were collected (3–4 replicates per station depending on the supposed diversity of stations). The distance between replicates was less than 200 m in BIOMARE and less the 30 m in ANTROMARE cruises for each station. In the model the corresponding macrobenthic compartment is called MACBN.

2. A Macer-GIROQ sledge was used to sample suprabenthos, mainly crustaceans such as amphipods, cumaceans and isopods (0.5–20 mm) during daytime. The sledge was equipped with two superimposed nets with mouth openings between 10–40 cm and 50–90 cm above the bottom. Both nets where processed. The sledge nets have 0.5 mm mesh size and were trawled to a speed of 1.5 knots. The duration of sledge hauls over the bottom were 10 min. Both vessel speed with hauls duration and standard 2030 flowmeters (General Oceanics Inc.) reading (attached to sledge mouth) were used to estimate the area of samples for standardizing abundances. A total of 6 sledges were taken. In the model the corresponding compartment is called SUPBN.

3. A WP2 net was used to sample zooplankton-micronekton (meso- /macrozooplankton /micronekton). The net was equipped with 0.5 mm mesh size with mouth area of 1 m^2 and a system of closure (1000DT General Oceanics Ltd) performed as closer to the bottom as possible. We used a SCANMAR sensor to estimate the closest distance per sample (range between 4 and 43 m). During tows (total duration = 10 min) the boat speed was around 1.5 knots. A standard 2030 flowmeter was attached to the mouths of nets to measure the amount of water filtered and/or the distance covered in each haul to estimate the volume. A total of 6 samples were taken, all during daytime. This WP2 allows to collect mesoplankton (species ranging from 0.2 mm to 0.5 mm, such as copepods, ostracods and some small pteropods), macroplankton (0.5–20 mm, i.e. hyperiids, euphausiids, jellyfish) and micronekton (small but actively swimming organisms ranging in

size between 2 and 10 cm, i.e. mesopelagic fish and natantian decapods). However, considering the mesh size of the net (0.5 mm) it is more suitable for macrozooplankton-micronekton, but the mesoplanktonic fraction is not well sampled. 1 haul is considered enough to represent the faunistic composition of zooplankton in a concrete depth/period (see Cartes, Fanelli, Lloris and Matallanas, 2013). In the model this component is called ZPLMNK.

4. An OTSB-14 bottom trawl was used to catch the megafauna (larger than 2 cm). The OTSB-14 is a standard sampler for deep-sea megafauna (Merrett et al., 1991), it is a 1-warp trawl with 6 mm mesh size at the codend, an horizontal opening between wings of ca. 7 m and a vertical opening of ca. 1.2 m (recorded by a SCANMAR sensor in the mouth of the trawl). Towing speed was 2.5 knots. The position of the start and end of the hauls was recorded with a GPS (Global Positioning System). A total of 15 hauls were collected (three replicates per station). In the model the megafauna was divided into megaichthyofauna (called MEGAICT), megabenthos (MEGABN) and the red shrimp *Aristeus antennatus* (AANT).

All macrofauna samples were sieved through filters of 0.5 mm mesh size on board, fixed in buffered formaldehyde or frozen at −20°C and the individuals identified at the laboratory. Animals were classified to the lowest possible level under a stereomicroscope (at 10×–40×), counted and weighed (wet weight after eliminating blotting water, balance resolution: 1E – 05 g). Polychaetes were also analysed under a compound microscope (at 10 × –40×).

The difference between these three compartments relates to their habitat preference and their mobility. The macrobenthos lives mainly in or occasionally on the sediment and usually leads a sedentary lifestyle. The suprabenthos has high swimming ability and lives the most of its life in the benthic boundary layer (BBL), one to two meters above the bottom. Suprabenthos remains fairly close to the sediment, however it can show some vertical migration. Finally zooplankton comprises both motile and not motile taxa and can be found in the open water. This component can be highly migratory and can reach almost the bottom.

5.2.3 Other data

Other data we collected are:

1. Total sediment Organic matter (TOM) was calculated as percentage of OM in sediment samples, taken by multi-corer and preserved at −20°C. At the laboratory it was dried at 60°C for 24 h till reaching constant weight and then oxidised (ashed) at 500°C for 2 h in a muffle furnace and weighted before and after the oxidation. The first measure represents the weight of both organic and inorganic matter, called dry weight (DW), while the second is called ash weight and represents the inorganic matter. Thus, their difference is the portion of organic matter. The TOM is a heterogeneous compartment comprising both abiotic and biotic organic matter. In fact, it contains detritus, labile and refractory organic matter, as well as micro and meiofauna (biotic matter ≤ 0.5 mm). The total organic matter was included in the model as another component, called TOM. Thus the model does not distinguish the detritus pool from the micro and meiofauna.

2. Sediment oxygen consumption (SOC) estimates the "respiration of sediments" and has been measured during the ANTROMARE cruise in June 2011. Sediments and the overlying water required for the experiment derived from three box-corers (one from S3 and two from S4). Each incubator consists of a perspex chamber (d = 30 cm) with a detachable lid containing a Teflon-coated magnetic stirrer. Water samples were analysed every 6 hours in triplicate for dissolved oxygen concentration with the modified Winkler method (Carpenter, 1965). Incubations lasted between 24 and 37 hours, up to find no changes between consecutive measures. All measurements were done in the absence of light by covering the chambers with black plastic. Afterwards SOC rates, expressed in mmol O_2 m^{-2} d^{-1}, were calculated by means of linear regression of the initial decrease in oxygen concentration during time (extended methodology in Glud (2008)). Chambers are described in Figures , Appendix B.

3. We used fishery's data of red shrimp from the temporal series available from the Catalan government. We estimated maximum and minimum of fishing rates on the *A. antennatus* (AANT → LANDS in the model) combining the information about landings, number of boats and trips per boats performed in each month during years 1996 – 2008, and the extension of the fishing ground Serola (comprising three sub-areas called by local fishermen: Serola, Abissinia and Morràs) in the depth range between 600 – 800 m (covering approximately an area of 230 km^2) and considering that trawlers cover approx. 400,000 m^2 h^{1-} and haul duration is around 4 h per day. So, we

could standardize the flow to $gm^{-2}d^{-1}$ (minimum, maximum and mean values). Contrariwise for fish (MEGAICT) and invertebrates (MEGABN) catch rates, we used the proportion found for MEGAICT and MEGABN with respect to AANT in BIOMARE surveys and multiplied the fishing rate of AANT with the proportion of MEGAICT and MEGABN for BYCATCH rate parameters (MEGAICT → BYCATCH and MEGABN → BYCATCH in the model). Fisheries data do not permit to estimate bycatch species, because a considerable portion is usually thrown back to sea by the fishermen. However, considering that the catch is sorted later, during the return to the port or (when saleable) in the same port, the bycatch portion represents a loss of biomass from the network and must be considered in the model.

All biomasses were converted from wet weight (WW g) to dry weight (DW g) and/or ash fee dry weight (AFDW g), depending on the available information and then to carbon content (mmol C) using conversion factors from Brey (2001) and standardized to mmol C m^{-2} (Table 5.2).

5.2.4 Literature data

In addition to our measurements, a variety of data on process rates is available from the literature for the same area, from other deep-sea areas or, in lack of the previous, parameters from shallow waters were used, and to which a temperature correction was applied. All data were implemented as constraints by setting the minimum and maximum values found as lower and upper bounds respectively (Table E.3, Appendix E). Biomass-specific maintenance respiration of all faunal compartments was defined as 0.01 d^{-1} at 20°C (see references in van Oevelen et al., 2006; van Oevelen, Bergmann, Soetaert, Bauerfeind, Hasemann, Klages, Schewe, Soltwedel and Budaeva, 2011) and temperature-corrected with a Q10 of 2 (correction factor $Tlim$). We used the literature revised in other models (van Oevelen et al., 2006; van Oevelen, Bergmann, Soetaert, Bauerfeind, Hasemann, Klages, Schewe, Soltwedel and Budaeva, 2011) as basis for constraints of assimilation efficiencies and biomass-specific maintenance respiration.

The model did not consider some important processes in benthic food webs, such as the hydrolisation to dissolved organic carbon of detritus due to prokaryotes included in detritus pools (OM and TOM), because we did not estimate prokaryote stocks. Part of the ingested matter by the faunal compartments is not assimilated

	A	B	C	D	E
Internal	zooplankton-micronekton	ZPLMNK	0.047	B	
	Macrobenthos	MACBN	23.712	B-A	
	Suprabenthos	SUPBN	0.094	B	
	Megabenthos*	MEGABN	5.700	B	13
	A. antennatus	AANT	0.076	B	13
	megaichthyofauna	MEGAICT	0.830	B	13
	Total organic matter in sediment	TOM	76157	B	4
External	Particulate organic matter from water column	OMv			
	Particulate organic matter from upper sediment strata	OMa			
	Landings	LANDS			
	Bycatch	BYCATCH			
	Dissolved inorganic carbon	DIC			
	Burial	BUR			

TABLE 5.2: Standing stocks of the food web compartments for the soft bottom slope food web. The binary structure is defined in Section 5.2.6 and quantified by data available in Section 5.2.2. A) Compartments' name, B) Abbreviation used through the text, C) Stock values (mean, mmol C m^{-2}), D) Origin of data: A=ANTROMARE B=BIOMARE, E) Number of samples. (*) Excluding megaichthyofauna and *A. antennatus*. (**) % C_{org} in sediment (gDW).

but instead expelled as faeces and this is represented by a flow directed to the TOM. Respiration by faunal compartments is defined as the sum of maintenance respiration (biomass-specific respiration) and growth respiration (overhead on new biomass production).

We also set OM input from advection 500 times OM from vertical fall, to take into account the different magnitudes between the two flows. In fact in the bibliography the mean OM vertical flux is 0.998 mmol C m^{-2} d^{-1} in the productive area of the Gulf of Lions (converted from Durrieu De Madron et al., 2000) with minima around 0.293 mmol C m^{-2} d^{-1} in autumn and maxima around 21.667 mmol C m^{-2} d^{-1} during winter (Buscail et al., 1995, 1990). In the Pacific ocean at 4000 m the flow is much weaker (maximum around 1.67 mmol C m^{-2} d^{-1}, Ruhl et al., 2008; Ruhl and Smith, 2004). Advective fluxes on the continental slopes are instead much higher (from 50 to 4583.33 mmol C m^{-2} d^{-1}) and mean value of 291.67 mmol C m^{-2} d^{-1} in the Gulf of Lions (Durrieu De Madron et al., 2000).

5.2.5 Linear inverse modelling

The model developed for this food web was built using the linear inverse modelling (LIM) methodology according to van Oevelen et al. (2009, 2010). We used both observed and literature data to derive model parameters as described in Sections 5.2.2, 5.2.3, 5.2.4. The topology of the food web is determined by the number of compartments and their connections (see Section 5.2.6 and Figure 5.2) and is represented in the model by the mass balance of each compartment (Table E.2).

All parameters are defined by ranges provided in Table E.3. Representing (uncertain) parameters by ranges rather than single values, avoids undesirable overfitting. The result of this procedure is that the flow magnitudes are constrained within reasonable upper and lower boundaries (rather than one value).

The LIM consists of equalities and inequalities that are solved simultaneously to obtain quantitative values for each flow x:

$$\begin{aligned} \mathbf{Ax} &= \mathbf{b} + \epsilon \\ \mathbf{Ex} &= \mathbf{f} \\ \mathbf{Gx} &\geq \mathbf{h}. \end{aligned} \tag{5.1}$$

Here, the first equation defines both the topology of the food web and the mass balance conservation of involved compartments: the matrix $\mathbf{A}$ represents the topology and $\mathbf{b}$ is a vector with growth rates or rates of change for each component. For a given number of components, K, then for each component, S_k, the mass balance equation is

$$\frac{dS_k}{dt} = \sum_i f_{ki}^{in} - \sum_j f_{kj}^{out} \tag{5.2}$$

dS_k/dt is the derivative of the mass of compartment S_k w.r.t. the time t, f_{ki}^{in} and f_{kj}^{out}, with $i = 1, \ldots, I$ and $j = 1, \ldots, J$, represent the I incoming and J outgoing flows to and from the compartment S_k. In steady-state $dS_k/dt = 0$. The vector $\mathbf{x}$ represents the unknown flows, and ϵ is the error term that is minimized. The rest of the equations contains restrictions as equalities (in the case of $\mathbf{E}$) or inequalities

(**G**) and the vectors **f** and **h** contain the empirical data or data from the literature. The third set of equations leads to ranges in estimated flows consistent with parameters' ranges. The model can be solved within such ranges to minimize the error ϵ.

The solution of the model is given by the set of flows **x**, that is consistent with the set of linear equations. These models are usually under-determined, because of a general lack of data and the large number of the unknown flows (Soetaert and van Oevelen, 2009*b*; Van den Meersche et al., 2009; van Oevelen et al., 2009). In the ECOPATH modelling framework (Christensen and Pauly, 1992) the under-determinacy is avoided by adding literature data and reaching the state of even-determinacy (Soetaert and van Oevelen, 2009*b*).

In contrast, in the LIM there are three methods to solve under-determinacy models.

One type is to find the parsimonious solution (originally proposed by Vézina and Platt, 1988). This method minimizes the objective function

$$min\left(\sum_i {x_i}^2\right),$$

where x_i represents the i-th unknown flow. Another, similar, approach, the Least Squares with Equalities and Inequalities, uses

$$min\left(\parallel \mathbf{Ax} - \mathbf{b} \parallel^2\right).$$

In this method, if the equality constraints $\mathbf{Ex} = \mathbf{f}$ cannot be satisfied, a generalized inverse solution residual vector is obtained and is the minimal length for $\parallel \mathbf{Ex} - \mathbf{f} \parallel^2$.

These two methods return however biased flows, taking extreme values of the solution space (Kones et al., 2006).

Recently two more solution methods have been proposed to take into account the uncertainty of flows: the range (Klepper and Van de Kamer, 1987) and the MCMC solution methods (Van den Meersche et al., 2009), (Kones et al., 2006). Each method can be used for different reasons.

The range estimation is used as a measure of identifiability (i.e. the quality of estimated flows). The ranges are calculated by minimizing and maximizing each

flow successively using Equations 5.1. This permits to identify which additional data could be used for constraining the food web so as to reduce ranges till they attain reasonable values.

The MCMC methodology uses markov sampling to pick random food webs that comply with the equations and allows to estimate the mean and standard deviation of each unknown. It can also be used to estimate mean and standard deviation of ecosystem indices Kones et al. (2009) as we did. Technical and methodological aspects of linear inverse modelling can be found in Soetaert and van Oevelen (2009*b*) and van Oevelen et al. (2010).

In this study we used all methods (parsimonious, range and MCMC). For the MCMC simulation, 10,000 samples of flows have been generated. Running the model 10,000 times, the uncertainty in the empirical input data is propagated onto an uncertainty estimate of the carbon flows as indicated by its standard deviation. Previous studies on the convergence of the mean and standard deviation of the flows verified the adequacy in setting this number of solutions (van Oevelen, Soetaert, García, de Stigter, Cunha, Pusceddu and Danovaro, 2011).

To build the model we used the R-package LIM (Soetaert and van Oevelen, 2009*a*,*b*).

5.2.6 Food web structure

The compartments in the food web model were chosen based on three criteria:

1. size (macrofauna: 0.5–20 mm; megafauna: larger than 2 cm),
2. vertebrates versus invertebrates within megafauna (i.e. megabenthic invertebrates and megabenthic ichtyofauna) and
3. compartments spatially divided within macrofauna (i.e. the zooplankton-micronekton, which performs vertical migrations in the water column, the suprabenthos, that lives close to the bottom, and the macrobenthos, that lives in the sediment).

Hence finally six faunal compartments have been created:

1. MACBN: benthic invertebrate macrofauna, mainly represented by polychaetes, crustaceans and molluscs,
2. SUPBN: active swimming macrofauna in the benthic boundary layer (BBL), the so-called suprabenthos, mainly represented by peracarids,
3. ZPLMNK: zooplankton and micronekton close to the BBL, that occasionally occupies this transitional zone,
4. MEGAICT: megafauna (vertebrates or megaichtyofauna), which comprises species strictly related to the bottom but also migratory species,
5. MEGABN: megabenthic invertebrates, such as crustaceans, echinodermata, sipunculans and cephalopods, and that also comprises migratory and non migratory species (among crustaceans),
6. AANT: the red shrimp *Aristeus antennatus*, target species of deep-sea fishery in the area.

The structure of the food web was chosen to describe the major flows between larger groups of the whole community, while the red shrimp was left as a own compartment to be able to relate its changes with changes in all other components.

We considered that these components are very heterogeneous categories in terms of C content, whereby we separate the different (available) groups to calculate the carbon content separately.

A seventh compartment has been considered:

7. TOM: total organic matter in sediments, including detritus (POM), bacteria, viruses and meiofauna. Percentage of total sedimentary organic matter (TOM) was calculated as the difference between dry weight (DW: 60°C for 24 h until constant weight reached) and ash weight (500°C in a furnace for 2 h).

The POM in sediment derives from the POM in the water, that settles on the bottom through sedimentation. The POM near to the bottom in turn derives from upper water strata and from advective processes downward the slope. The first has pelagic origin (e.g. phyto and zooplankton) while the second is mainly of terrigenous origin (river discharges). The quantities of these entries can vary

strongly. Detritus is also produced by the living fauna in the slope community through mortality and faecal production. This detritus can be then available again and recycled by the community. We modelled two external entries, the organic matter from vertical fall (OMv) and from advection (OMa). OMv and OMa enter the continental slope food web through sedimentation to the TOM, suspension and filter feeding of macrofauna compartments.

Efflows from the food web are: respiration of all compartments to the dissolved inorganic carbon (DIC), the burial of the TOM (BUR) and the efflux to humans due to fishing activity on the target species, the red shrimp (LANDS), and on the accompanying fish and invertebrates (BYCATCH). The fraction of bycatch species usually returns to the sea as discards having no commercial interest, although it is a considerable biomass removed from the ecosystem. Few species are brought to the port, such as Gadiformes species, *Phycis blennoides* and *Merluccius merluccius* and occasionally cephalopods, that are rarely fished.

The relationships among compartments described in this section (binary food web) are shown in Figure 5.2, the quantities of stocks are in Table 5.2 and the mass balance equations included in the model and describing the relationships between components are given in Table E.2 in Appendix E.

We considered our sampling (performed during one year) to be consistent with the assumption of steady-state. With the inclusion of ANTROMARE samples for the infauna, we corrected for the possible bias related to the depth of this component during BIOMARE surveys, where only samples at 800 m were available for the open slope. The mass-balance equations of the model are reported in Table E.2, parameters ranges in Table E.3 and more constraint equations in Table E.1.

5.2.7 Network indices

The network indices were calculated on the 10,000 MCMC samples using the R-package NetIndices (Kones et al., 2009). The notation and details on the calculation of the indices are shown in Tables E.6, E.7 and E.8 and more information can be found in e.g. Ulanowicz (2004) and Kones et al. (2009) among others. Following Kones et al. (2009), indices can be calculated if assuming n internal compartments and an undefined number of external components. Each flow is defined with T_{ij}, of which direction is from source j to destination i ($j \rightarrow i$). All flows are categorised into four groups: (1) imports (2) internal (3) export of usable

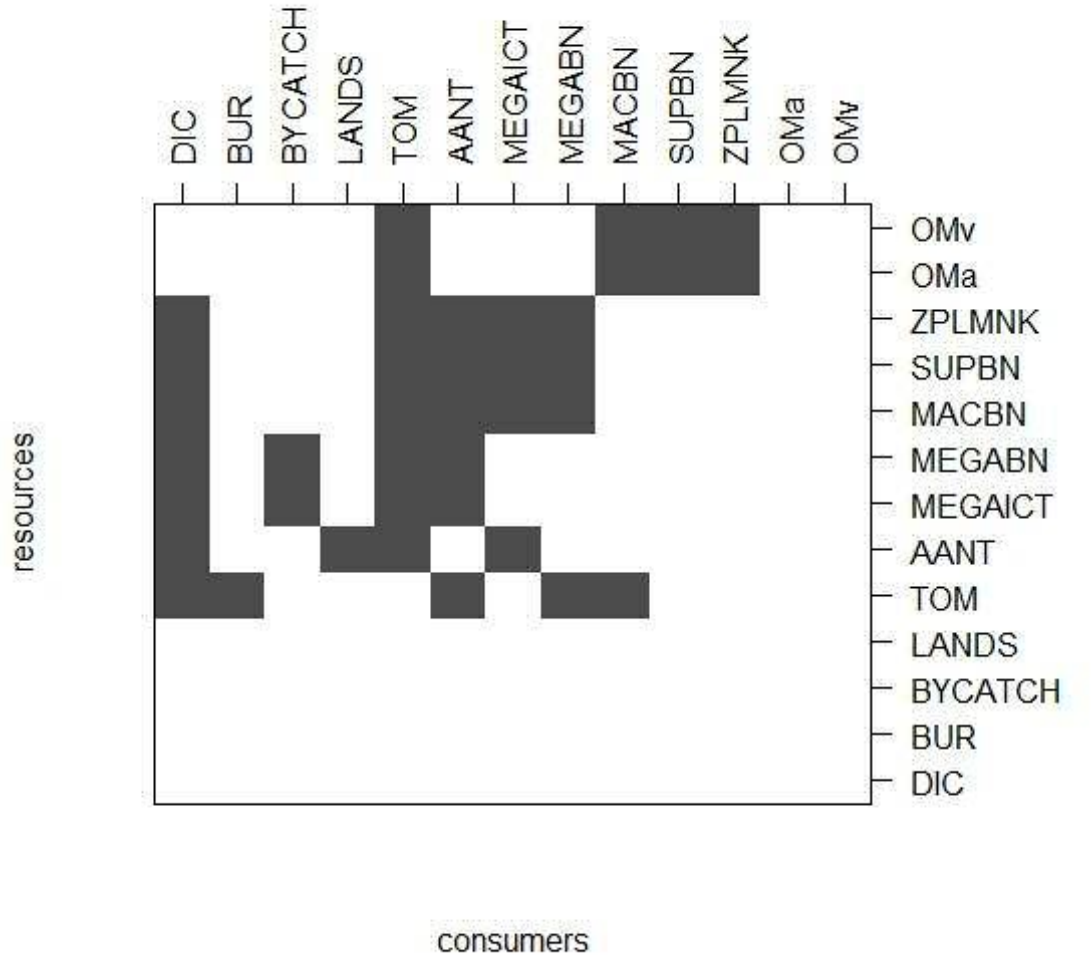

FIGURE 5.2: Binary food web.

energy and (4) dissipation of unusable energy (see Table E.6 in Appendix E for the corresponding nomenclature).

General network indices are descriptors of general system's properties, e.g.

1. The Total System Throughput (T..., Hirata and Ulanowicz, 1984) and the Total System Throughflow (TST, Latham II and Scully, 2002) measure the total exchange transpiring in the system. But Although the former is the sum of all flows the latter is the sum of all components throughflows

2. The system size, n, refers to the number of nodes or compartments.

3. L and Lint are the number of total links and internal links respectively.

4. The LD is the link density and is the ratio between L and n (Bersier et al., 2002).

5. The Connectance (C) plays a key role in community ecology being fundamental for many theories of community stability (Pimm, 1984) and structure (Martinez, 1992). Different measures of connectance exist (see Warren, 1994 for details on definitions), all based on internal number of links and number of components. A widely used measure of connectance is the Directed Connectance (L/n^2), that corresponds to the number of actual links over the number of possible links, including cannibalistic loops (Martinez, 1992). The measure used here is slightly different (see the Table).

6. Average link weight ($\overline{T}_{ij}$) is the average of all components' links.

7. Average compartment throughow ($\overline{TST}$) is the average of all components' throughows.

8. The Compartmentalization $\overline{C}$ assesses the degree of well-connected subsystems within a network. It can only be used to compare systems with the same number of compartments and connectance. Higher values represent higher levels of compartmentalization (i.e. more or stronger subsystems).

9. Average path length $\overline{PL}$ is the average path length of the average inflow weighted by the sizes of the inflows.

Some indices refer to the cycling behaviour of the system. They rely on how much energy is is used by recycling processes and available again for the system itself (Allesina and Ulanowicz, 2004). Such indices also measure system's independence from energy inputs. They are:

1. The Total System cycled Throughow (TSTc) represents the recycled energy by the system and the Total system non-cycled throughow (TSTs) also called Total system straight throughow represents the non-cyclic pathways or the portion of total system throughflow that passes straight through the system. It gives information about the net loss of energy.

2. The Finn's cycling Index (FCI), cast as the ratio between TSTc and TST, and the revised FCIb, conceptually the same of TST, are useful for among network comparisons, because they vary between 0 and 1: 0 meaning that there is no cycling at all and 1 meaning that all flow is recycled.

There are also weighted measures for networks:

1. The Effective connectivity (Cz) is the analogous of the link density in unweighted network weighted for the size of links. It might fall between 1 and 3.25.
2. The Effective flows (Fz) is analogous to the number of links.
3. The Effective nodes (Nz) is the weighted mean of the normalized throughflow of each node.
4. The Effective roles (Rz) is a measure of weighted, differentiated, distinct functions in a network (components that take input energy and pass it to other components). It might fall between 2 and 5.

Among these measures, particularly important are Cz and Rz, because the bidimensional range of Cz and Rz has been called "window of vitality" by Zorach and Ulanowicz (2003).

Measure of network constraint and uncertainty are:

1. The Average Mutual Information (AMI) is the measure of the average amount of constraint placed upon an arbitrary unit of flow anywhere in the network. If highly constrained a flow in the network, the system is unable to persist when perturbed.
2. The Statistical uncertainty (H_R) is the upper bound of the AMI.
3. The Conditional uncertainty (D_R) is the difference between HR and AMI. In a developing system, when the AMI falls the DR rises. The Uncertainty is a measurable quantity expressing the degree of uncertainty about what flow will be produced by a source. The more that is known about a source, the less the uncertainty there is in what flow will be produced. In communication theory the uncertainty was termed "entropy" by Shannon, but its meaning is different from the entropy in physics. In physics, entropy is disorder, while here is synonymous of uncertainty.
4. The Realized uncertainty (RU_R) is the fraction of the total uncertainty accounted by the network. It is useful to compare the degree of constraint across systems.

5. Given a network of n compartments, any compartment may transfer material/energy to itself or to any other compartment. The total uncertainty of a system is expressed as Hmax and specifies the uncertainty with regard to a network where every node is interacting evenly with every other node (Latham II, 2006). It is expressed by the Shannon uncertainty equation and is the maximum possible uncertainty. Hsys is the uncertainty expressed by the system. MacArthur (1955) used Hsys as a measure of the communitys stability. The difference between the maximum uncertainty, Hmax, and the actual uncertainty, Hsys, may be taken as the amount of uncertainty reduced by the structure of the network, the Hc.

6. The Constraint efficiency (CE) is based upon a total of the constreints that govern flow out of individual compartments. It is a scale independent ratio of the constreint. This measure depends on Hmax and the Network constraint (Hc).

Measures of growth and development or maturity of the system, originally developed by Ulanowicz (1986):

1. The Ascendency (A) quantifies increasing organization and size in growth and development of the system. The organization component is measured by the AMI and the size of component is measured by the T... The Ascendency can be decomposed in four quarters: 1) internal, 2) import, 3) export, and 4) dissipation.

2. The Development capacity (DC) represents the upper bound of the Ascendency.

3. The Overhead (ϕ) is the difference between the former two indices and describes how much the Ascendency can increase. In other words it is a measure of the system's strength in reserve from which it can draw to meet unexpected perturbations.

4. The Extent of development (AC) is the fraction between A and DC and is useful for comparing ascendency across networks.

All these indices can be decomposed as the Ascendency. That was proposed by Ulanowicz and Norden (1990) to study specific aspect of the network.

The ascendency as well as other properties of an ecosystem is affected by the number of groups that are included in the system description. Noteworthy is that the ascendency diminishes notably only when the system is aggregated to less than six groups Ulanowicz (1986).

The use of A, DC, ϕ and AC in describing the maturity of a system derives from the correlation between A and most of Odum's properties (1969) of "mature" ecosystems (Ulanowicz and Norden, 1990).

All descriptions of symbols are given in the Appendix E, Table E.6, while equations are reported in Tables E.7 and E.8.

5.2.8 Software

All analysis and simulations were performed into the R environment (R3.0.2 version). The LIM (van Oevelen et al., 2010) and other required R-packages, limSolve and deSolve (Soetaert and van Oevelen, 2009*a*; Soetaert et al., 2010*a*), and its extensions (NetIndices: Kones et al., 2009) provide estimation methods that also permit a statistical analysis on the food web, network indices and dynamic simulations.

5.3 Results

5.3.1 Oxigen consumption results

Our results from SOC experiments are in agreement with published data (Figure 5.3, available in Andersson et al. (2004). Our estimation (in red average value, lower and upper boundaries) has the same order of magnitude although lies below the SCOC estimated by the model (dark line). Details on the model are described in the Appendix E.

5.3.2 The food web in steady state

The total number of unknowns (the flows involved in the food web) is 40, within 13 total compartments, 7 internal and 6 external. The three types of solutions

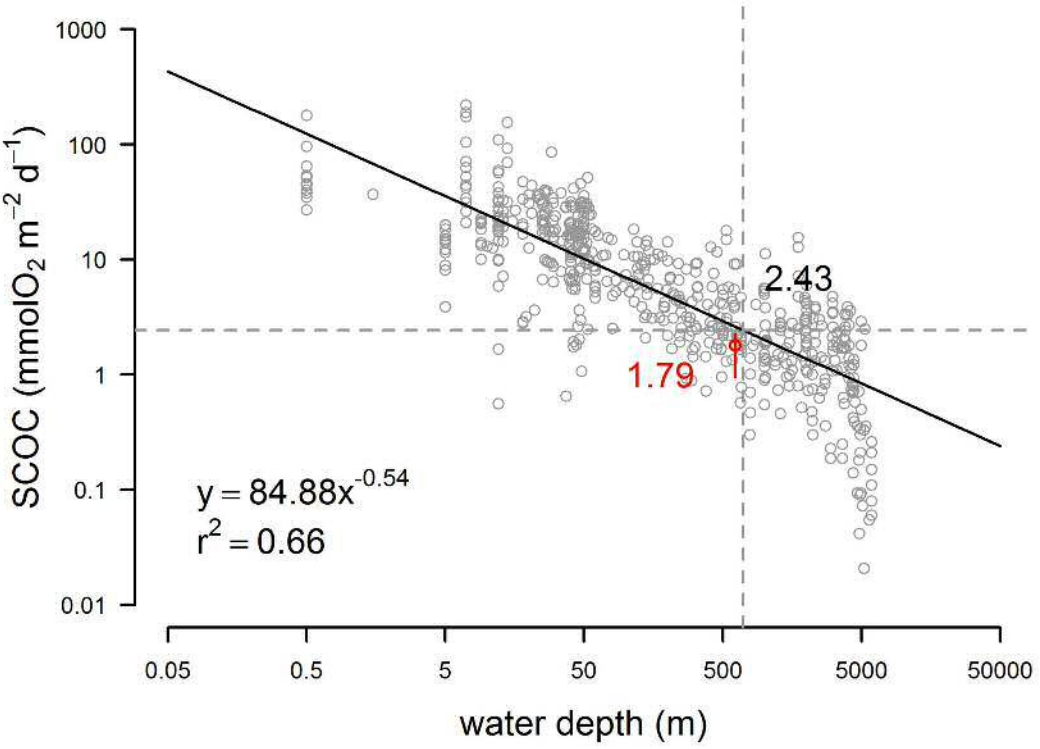

FIGURE 5.3: Sediment Community Oxygen Consumption (mmol O_2 m^{-2} d^{-1}) as a function of depth (m). The grey points are observations, the continuous line represents the mean fitted value, the dashed lines corresponds to the average SCOC value (also in the Figure) at comparable depths (here we set 700 m the interpolations between 600-800 m depths, the range of our food web) and the estimation by our food web model is represented in red, the average is the red dot (with the corresponding number) and the segment represents the range. The function is the model in Equation E.2, Appendix E. Also the r^2 is reported.

(methods: range, parsimonious - both ldei and lsei - and MCMC) are reported in Tables E.4 and E.5 (Appendix E). In what follows, we will refer to the MCMC estimates (if mean and sd are given) or to the range estimates (min and max).

The food web is visualised in Figure 5.4, representing the circular diagram of the food web, plotted with flows as net values. Flow values ranges from 0.84, estimated for TOM → DIC, to 2.5E^{-06} mmol C m^{-2} d^{-1}, estimated for MEGABN → MEGAICT (derived from the parsimonious solution ldei). The strongest flows are the incoming flow to the community from the particulate organic matter of the upper sediment strata (OMa) to the (total) organic matter in sediment (TOM) and the efflux from the TOM to the dissolved organic carbon (DIC). The second most important component, where most of the organic matter passes after the TOM, is the

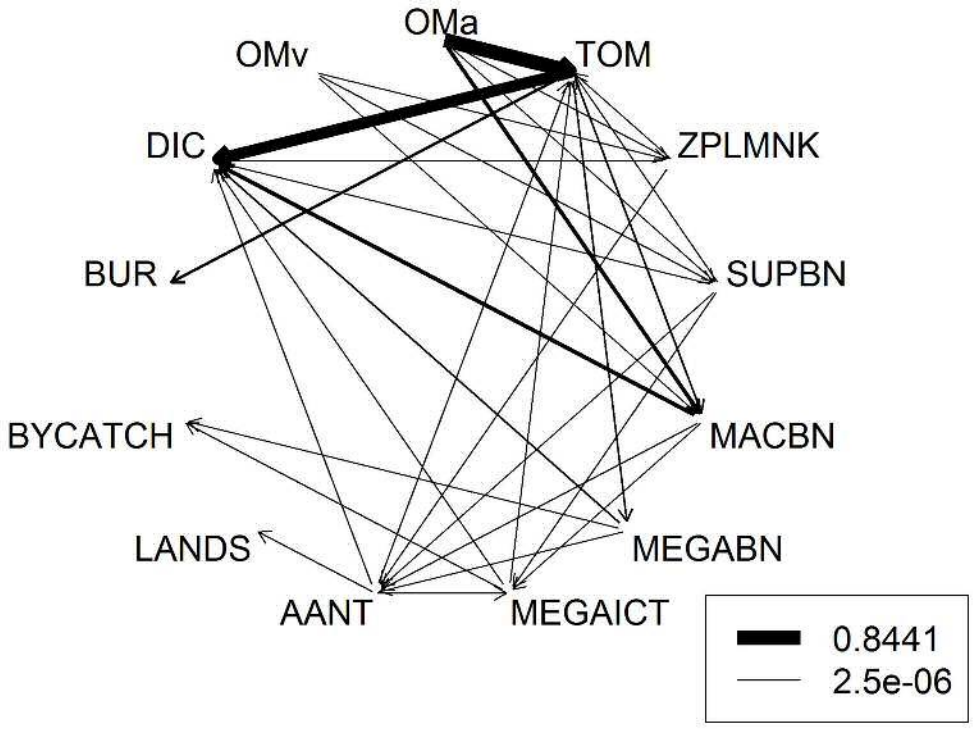

FIGURE 5.4: Food web carbon flows (mmol C m^{-2} d^{-1}). See Table 5.2 for abbreviations of food web compartments and Tables E.4 and E.4 for the values of the flows. The legend shows maximum and minimum flow values estimated through the parsimonium solution.

macrobenthos (MACBN). Within this component, excluding few filter and suspension feeders, the majority of animals are deposit-feeders eating on the detritus in sediment (a portion is also carnivorous but not estimated).

In Figure 5.5, mean and standard deviation of flows estimated through MCMC simulations are arranged in descending order from the left to the right. Nearly all flows involving TOM and macrobenthos (MACBN) are "strong" interactions (= high values), related to their high carbon content (stocks). Other important flows in terms of strength are those involving biogeochemical processes, such as sediment respiration, advection, sedimentation and the burial process. All low-biomass compartments, suprabenthos, zooplankton and the red shrimp are involved in weak interactions (close to zero) and are potentially vulnerable.

Flows' ranges are visualised in Figure E.1 (Appendix E) and are measures of both feasibility and uncertainty. The flows with highest uncertainty are these related to the total organic matter in sediment (TOM). The coefficient of variation, CoV (Table E.5, Appendix E), represents a better measure of the residual uncertainty

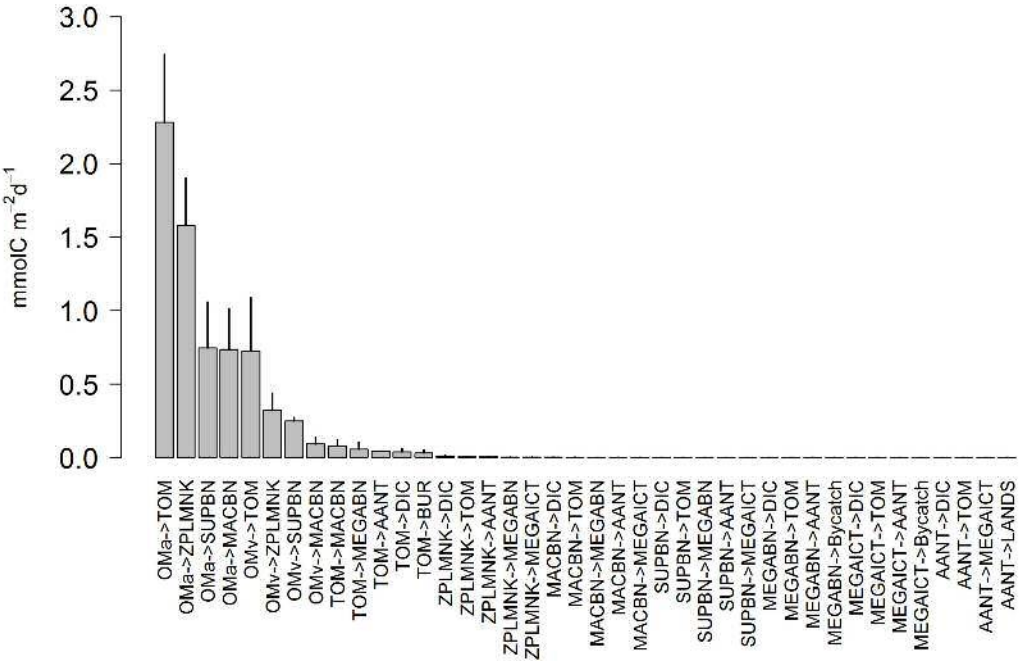

FIGURE 5.5: Barplot of the food web flows (mean ± sd, mmol C m^{-2} d^{-1}) estimated using the MCMC method in descending order from the left to the right.

than the standard deviation and better indicates the "quality" of the model solution. The CoV is a measure independent from the mean value, so the estimations of flows can be directly compared between each other: the lower CoV smaller the uncertainty and better flow estimate. All CoVs are smaller than 1 except two flows (OMv → TOM and OMv → ZPLMNK); the 80% is smaller than 0.75 and the 70% of the flows is smaller than 0.50. These results suggest a good performance considering other food web models (e.g. van Oevelen et al., 2009; van Oevelen, Soetaert, García, de Stigter, Cunha, Pusceddu and Danovaro, 2011).

Using the MCMC estimations in E.5 we derived mean values of the main processes in the food web (range estimations are shown in Table 5.3).

The total carbon input to the food web has a mean value of 2.62 mmol C m^{-2} d^{-1} and is the sum of the suspension feeding (12.95%) and the deposition of organic matter by vertical settling or through advective processes (87.05%). The suspension-feeding is partitioned among zooplankton (1.08%), suprabenthos (3.07%) and macrobenthos (95.74%). Percentages are given with respect to the total. The suspension feeding of some invertebrates belonging to the megafauna, e.g. the brachiopod *Gryphus vitreus*, has been neglected in the model, because rarely observed. The total ingestion of C in sediments by the metazoan community (excluding the meiofauna, e.g. nematods) was 0.83 mmol C m^{-2} d^{-1}, corresponding to 31.68%

of the total C entering the food web. Deposit-feeders feed on the detritus incorporated in the sediments. Our model does not distinguish flows from the TOM to detritivores and to carnivores eating on prokaryotes and meiobenthos in sediments. We necessarily assumed that almost all compartments in the sediment are both detritivores or carnivores (however detritivores are definitely more abundant), comprising each of them a broad number of species. The rest of the OC deposited was used by the prokaryotes and nematods (1.58 mmol C m^{-2} d^{-1}, 69.28%) or trapped in the sediment (0.73 mmol C m^{-2} d^{-1}, 32.19%).

The total respiration of the community (including the TOM) was 1.89 mmol C m^{-2} d^{-1} ranging between 0.84 – 2.34 and each component contributed in a descending order as follows: 83.75% for prokaryotes and meiofauna (TOM), 13.34% for macrofauna, 2.86% for megafauna, including the red shrimp *Aristeus antennatus*.

Process		value
Vertical OM input	=	[0.002,0.007]
Advective OM input	=	[1.051,3.508]
Total OM input	=	[1.047,3.515]
OMv Deposition	=	[0 0.006]
OMa Deposition	=	[0.843,3.419]
Total OM Deposition	=	[0.843,3.419]
faunal detritus production	=	[0.168,2.271]
C Burial Rate	=	[0.110,1.265]
Suspension feeding (pelagic orig)	=	[0.001,0.007]
Suspension feeding (terr orig)	=	[0.083,0.692]
Total Suspension feeding	=	[0.090,0.699]
Deposit-feeding	=	[0.316,1.913]
Total secondary production (except TOM)	=	[0.021,0.249]
Sediment Respiration	=	[0.603,2.002]
Total respiration	=	[0.941,2.247]
Total Fishery	=	[0.002,0.002]

TABLE 5.3: Derived global estimations, $[min, max]$, (mmol C m^{-2} d^{-1}) of important processes in the food web.

We also derived estimations of the loss of secondary production due to fishing activity (shown in Table 5.4) representing minimum and maximum flows estimated by area during one day (A) or one year (B). In the case of the red shrimp, if the value is multiplied for the total fishing area, it could reflect the estimation of landings per year. The estimations in (C) have the same units of the LPUE in Chapters 3 and 4. Any comparison between estimations is very difficult because

a monitoring systems (e.g. satellite systems) should be used and bathymetric differences should be also considered. To estimate column C we made the following assumptions: 1) the OTSB covers approximately 65000 m^2 h^{-1}, while the commercial trawlers cover more than two times the OTSB area (×2.5); 2) moreover the fishing boats trawls for 4–6 hours, so we considered a mean value of 5 h per each working day; 3) we considered also one month stop. Obviously this is a very rough estimate.

Process		A	B	C
F_t	=	[2.00E-03, 2.21E-03]	[63.34, 69.99]	[0.17, 0.19]
F_a	=	[5.00E-04, 5.53E-04]	[15.83, 17.51]	[0.04, 0.05]
F_i	=	[1.50E-03, 1.66E-03]	[47.50, 52,57]	[0.13, 0.14]
F_b	=	[2.50E-06, 2.76E-06]	[0.08, 0.09]	[2.17E-04, 2.39E-04]

TABLE 5.4: Derived estimations of flows related to the red shrimp fishery, $[min, max]$. (A) expressend in mmol C m^{-2} d^{-1}; (B) expressed in Kg km^{-2} y^{-1}; (C) expressed in Kg $boat^{-1}$ d^{-1}, here d is "working day" and has the same units of LPUE in Chapters 3 and 4. F_t is the total fishing rate; F_a is the portion of fishing pressure on red shrimp; F_i is the portion of fishing pressure on the fish stock; F_b is the portion of fishing pressure on invertebrates.

5.3.3 The network indices

All estimations of the network indices are shown in Tables E.9, E.10, **??**, **??** and 5.5 in the Appendix E. Also formulae and symbols are reported in the same Appendix (Tables E.6 and E.7).

The estimations of general indices are reported in Table E.9. Among them, the total exchange transpiring the food web (T..) is 7.04 ± 1.38, the total throughflow (TST) is 4.42 ± 0.97 and average throughflow is 0.63 ± 0.14. The no-cycled throughflow is very close to the TST, such that the recycled energy is very low (TSTc = 0.83 ± 0.44). Also other cycling indices (FCI and FCIb) return very low values (see Table E.9, B).

The estimates of trophic indices, (formula in Table E.8), are shown in Table 5.5. The mean trophic level for each component is affected by the resolution of the food web. It should reflect the "mean" value among all species incorporated in the component. The trophic level ranges approximately between 2 and 3.08, while the omnivory index is less than 0.1.

COMPONENT	LT	OI
ZPLMNK	2.000 ± 0.000	0.000 ± 0.000
SUPBN	2.000 ± 0.000	0.000 ± 0.000
MACBN	2.000 ± 0.000	0.000 ± 0.000
MEGABN	2.391 ± 0.263	0.168 ± 0.073
AANT	3.082 ± 0.060	0.051 ± 0.043
MEGAICT	3.041 ± 0.021	0.043 ± 0.021
AVERAGE	2.419 ± 0.531	0.043 ± 0.069

TABLE 5.5: The trophic level and omnivory index (mean ± sd) for all living components.

5.4 Discussion

The Catalan slope is one of the most studied bathyal ecosystems in the Mediterranean. However, as is the case for food webs in general (Moore et al., 2004), the identification of pathways within communities is difficult and even more so is its quantification.

The main trophic relationships in this environment were recently studied, unravelling very diversified and unexpected components, within the lower section of the food web structure, showing specialised to omnivory behaviour (Fanelli et al., 2009; Fanelli, Cartes and Papiol, 2011; Fanelli, Papiol, Cartes, Rumolo, Brunet and Sprovieri, 2011). However the estimation of the proportion among different types of feeding behaviours is still unavailable due to the high number of species living this ecosystem and the relatively low number of species of which diet has been examined. Moreover these studies suggest a modular structure of the food web (see, e.g. Fanelli, Cartes and Papiol, 2011), such that higher modules can be considered to semplify the model and make it manageable. This fact and the necessity to build a food web model for immediate use in fishery management (FAO, 2003) requires a compromise between complexity and simplicity, so as to study the main pathways of this complicated system and could make the model useful for a rapid management of the fishery in deep sea habitats within the ecosystem approach of fisheries (EAF).

With respect to other ecosystem modelling approaches, the great advantage of the LIM method is the ability to quantitatively reconstruct the food web even when the problem is under-determined (data-limited). We restricted the number of compartments, differentiating among large groups and distinguishing between

two fundamental pathways in the bathyal environment that depend on external resources (vertical settling and advective processes) and recycled material.

In our area, the total biomass (only macro- and megafauna) was 30.46 mmol C m^{-2}, very close to the bioass in the deep Faroe-Shetland Channel (30.22 mmol C m^{-2}) (Gontikaki et al., 2011), and approximately 2/3 of that found at higher depths in the same region (45.93 mmol C m^{-2}, converted from Tecchio et al., 2013) and also lower than at the Nazaré canyon (van Oevelen, Soetaert, García, de Stigter, Cunha, Pusceddu and Danovaro, 2011) and Rockall Bank (van Oevelen et al., 2009); the latter two are more diversified habitats and show higher secondary production. On the contrary, in our area the biomass is higher than in the Fram Strait (van Oevelen, Bergmann, Soetaert, Bauerfeind, Hasemann, Klages, Schewe, Soltwedel and Budaeva, 2011), as expected for being a food web in the Arctic Ocean and at deeper waters (2500 m). Also at the Porcupine Abyssal Plain the biomass was lower, summing the biomasses with the same size classes returned a value of 9.77 mmol C m^{-2} (van Oevelen et al., 2012), that is 1/3 of that we found in the continental slope.

5.4.1 Inputs and resource partitioning

Organic matter inputs to the community from advective processes are more important than those from vertical fall (see for the magnitudes e.g. Buscail et al., 1995, 1990; Durrieu De Madron et al., 2000). This implies a higher structural role of this input. Infauna receives more OM from advective than vertical origin

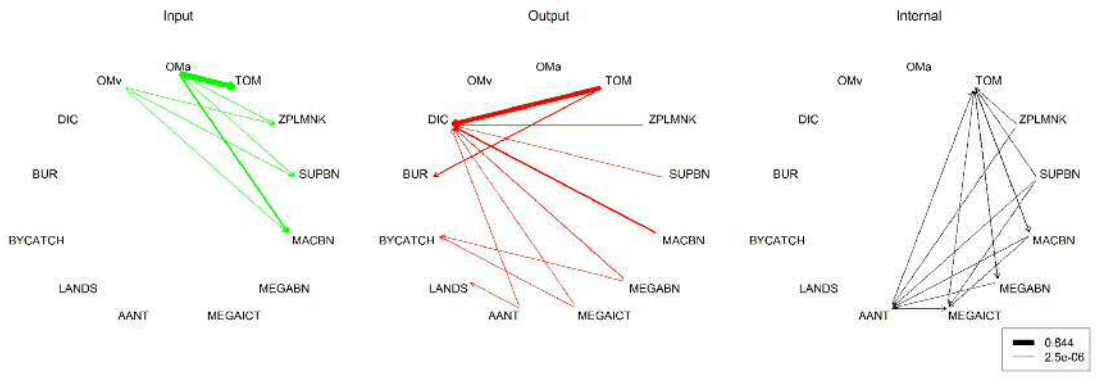

FIGURE 5.6: Food web carbon flows (mmol C m^{-2} d^{-1}) as in Figure 5.4 but divided in A) input (green), B) output (red) and C) internal (black) flows. See Table 5.2 for abbreviations of food web compartments and Tables E.4 and E.4 for flows' estimations. The legend shows maximum and minimum flows estimated through the parsimonium solution.

and then from the particulate organic matter in sediment. Between internal flows, those related to the TOM and the infauna showed higher and more uncertainty values. That is also related to their structural role in this ecosystem.

The secondary production in deep sea mainly depends on inputs of detrital matter deriving from the upper levels of the water mass and dropping down as phytodetritus, dead animals, faecal pellets, empty shells, skeletons and small organic particles of different nature. These particles falling down to the seabed have been usually called "marine snow" (Alldredge and Silver, 1988). Pelagic animals eat and also bacteria living in the water column mass degrade this source of energy during its way down, especially in the Mediterranean, where the temperature is relatively high with respect to the open oceans (Fanelli, Cartes and Papiol, 2011). The remaining detritus is deposited on the sea floor where more bacteria deteriorate it enter in competition with metazoans which benefit of the remaining source. Deep ocean communities' carbon demand can exceed the vertical supply, being potentially supplied by lateral advection (Burd et al., 2010). That is the reason of the more structural role of advective processes in bathyal ecosystems. We found that a very low portion of this energy is recycled by the system (low Finn's index: FCI = 0.179 ± 0.066).

The total input of C estimated by the model ranges between 0.92 and 4.16 mmol C m^{-2} d^{-1} (mean value: 2.62 mmol C m^{-2} d^{-1}), while the total secondary production (excluding prokaryotes and meiofauna) ranges between 0.02 and 0.25 mmol C m^{-2} d^{-1} that represents only the 2.17 – 6.01% of the organic matter that enters the community. The reason lies on biogeochemical processes and dissipation of the energy, i.e. the burial estimated to be 0.11 – 1.27 mmol C m^{-2} d^{-1}, equivalent to the 11.96 – 54.09% of the total organic input and the respiration, including the TOM (0.84 – 2.34 equivalent to 56.31 – 91.70% of the input).

The total input is approximately 7 times less than the input at comparable depths in the canyon of Nazaré but almost similar to the value in the lower section of the same canyon (at 4000–5000 m) (van Oevelen, Soetaert, García, de Stigter, Cunha, Pusceddu and Danovaro, 2011), this can be explained by the oligotrophic character of the Mediterranean sea, with respect to the Atlantic ocean and the habitat of canyons. Also the burial of organic carbon was lower in the Mediterranean continental slope, 0.73 ± 0.28 mmol C m^{-2} d^{-1}, in comparison with same depths in the Nazaré canyon (van Oevelen, Soetaert, García, de Stigter, Cunha, Pusceddu and Danovaro, 2011), however the same parameters have been applied for this

process. In contrast it was much higher than the values estimated estimated by (0.19 mmol C m^{-2} d^{-1}) in the Rockall Bank's cold-water community and by van Oevelen et al. (2012) (0.03 mmol C m^{-2} d^{-1}) in the Porcupine Abyssal Plain, where the burial efficiency has been considered much lower than in the continental margins (van Oevelen et al., 2012).

Regarding to the feeding types, deposit and suspension feeding represent the 93.30% of the total consumption in the food web and the remaining percentage belongs to carnivores. Of this 93.30% the deposit feeding represents the 73-78%. Deposit feeders are mostly represented by the infauna (90.14% of the total deposit feeding), while the rest is consumed by megafaunal components. On the contrary suspension feeders belongs to the zooplankton and suprabenthos. Carnivorous feeding among megafauna represents the 56.37%, such that suspension and deposit feeding are still important in these groups. Also the macrofauna comprises carnivorous species (feeding on micro- and meiofauna and on the "smaller" macrofauna). Thus carnivores are under-estimated by this model.

Has been argued that deep-sea macrobenthos (mostly detritus feeders) exhibit an expansion of trophic niches and species tend to be omnivorous to avoid competition for food (Gage and Tyler, 1991). This suggests that grouping many detritivorous in a single compartment, as in the present model, is a good compromise. Nonetheless more recent studies with isotopic methodologies found high variability in the relationship between δ^{13}C and δ^{15}N particularly among deposit feeders, suggesting exploitation of particulate organic matter at different stages of degradation: from fresh phytodetritus to highly refractory or recycled material (e.g. Fanelli, Papiol, Cartes, Rumolo, Brunet and Sprovieri, 2011). Also the seasonal turnover of opportunistic species is reasonable as evidenced in (Mamouridis et al., 2011). This scenario suggests a continuum in species trophic niches and the consequent difficult to compartmentalise the food web. Many examples of this repartition in food web modelling are available (van Oevelen et al., 2009; van Oevelen, Soetaert, García, de Stigter, Cunha, Pusceddu and Danovaro, 2011). When such information is not available, the compromise is to enlarge constrains in the model.

Our model gives necessarily a simplified picture of the trophic structure of the bathyal ecosystem and results represent an average within all species belonging to each modelled compartment. The TOM is considered as dead component however it comprises also living matter, but necessarily we set its TL = 1. However,

micro- and meiofauna that could not be modelled present higher TL. For instance in the Nazaré canyon for nematodes the TL of deposit-feeders was estimated around 2 and omnivores and predators around 2.75 (van Oevelen, Soetaert, García, de Stigter, Cunha, Pusceddu and Danovaro, 2011).However considering that they usually have very low biomass with respect to the particulate organic matter in the sediment, is reasonable to consider that their TL do not affect to the average TL of the TOM as whole compartment. Zooplankton-micronekton (ZPLMNK), suprabenthos (SUPBN) and infauna (MACBN) have the same level (TL=2) occupying the "basis" of the bathyal food web almost eating on detritus (however of different source and quality) and as mentioned there are some carnovorous species eating on microplankton, microbenthos or meiobenthos (see also Fanelli, Cartes and Papiol, 2011). Fish (MEGAICT) and the red shrimp (AANT) show very similar positions (close to 3), while big invertebrates (MEGABN) are in the middle between lower and upper (modelled) levels. The difficult to capture the highest trophic levels of the food web must also be considered, when discussing results, that is the case of pelagic cephalopods and bigger sharks, that could show trophic levels higher then 4. These species with pelagic behaviour can also be sustained by other sources in the water column far from the bottom.

With respect to the index of omnivory, lower trophic levels showed specialized diets, a result that in this case is an artefact of the model. Setting higher deegree of compartmentalization will give higher values of omnivory, in fact many species are omnivores but can also present seasonally specialised diets. For example that happens in some polychaets, that turn their behaviour in relation to the environmental conditions from deposit to suspension feeding (e.g. species belonging to the family paraonidae) or are both deposit feeders and carnivores (e.g. caudofoveats) (Mamouridis et al., 2011).On the contrary higher trophic levels showed some degree of omnivory.

5.4.2 Community respiration

The total respiration with a mean value of 1.89 mmol C m^{-2} d^{-1}, ranges between 0.84 – 2.34 mmol C m^{-2} d^{-1} and is very low with respect to the cold-water coral community (e.g. van Oevelen et al., 2009). In our model only the sediments (without macrofauna) account for the 83.75% of the total respiration with the value of 1.58±0.32 mmol C m^{-2} d^{-1}, while the percentages for macrofauna

and megafauna are respectively 13.39% and 2.86% (sum of respirations of components of each size: 0.25 and 0.04 mmol C m^{-2} d^{-1}). Thus carbon processing is mainly due the living portion of the TOM (to prokaryotes and meiofauna) and only partially to metazoa (macro- and megafauna). In fact bacteria have the highest contribution within TOM compartment and for the whole community, as has been proven in other deep-sea benthic ecosystems (in the Nazaré canyon: van Oevelen, Soetaert, García, de Stigter, Cunha, Pusceddu and Danovaro, 2011 and in the Faroe-Shetland Channel: Gontikaki et al., 2011). In comparison with the CWC community at Rockall bank (van Oevelen et al., 2009), the respiration of our food web is more than 50 times lower. Despite, it is not surprising because the CWC community has characteristics of a hot spot habitat and thus respiration is higher than all literature data available (van Oevelen et al., 2009). Respiration is instead higher than that found at higher depths in our region (Tecchio et al., 2013), where only metazoan community was modelled and respiration was estimated around 0.64 mmol C m^{-2} d^{-1} after conversion. However we cannot say that it is statistically lower, having no estimates of the variability. Finally, however lower than the conditional mean calculated by the model E.1 (see Appendix E), our estimation falls into the range of other deep-sea soft bottoms data at comparable depths (Andersson et al., 2004) (see also Figure 5.3 in Appendix E to compare oxygen consumption data).

5.4.3 Network analysis

The total system throughput (T..), measuring the total food web activity has a very low value, was 7.04 ±1.38, does not significantly differ to that found in the lower section of the Nazaré canyon at 4000–5000 m depth while is more than four times lower than at comparable and higher depths of the canyon (van Oevelen, Soetaert, García, de Stigter, Cunha, Pusceddu and Danovaro, 2011). The total system throughput (conventionally defined in Ecopath as TST, however for the definition given in Libralato et al., 2010 seems to refers to the T..) was 18.62 at higher depths (Tecchio et al., 2013). Our estimation of the TST was 12.657±3.572. The network analysis suggests that almost all the energy passing through the food web is not recycled (see TST and low values of TSTc and Finn's indices). Our value of FCI was 0.18±0.07, thus statistically there were no significant differences with the upper and lower sections of the Nazaré canyon in contrast with the middle section at comparable depths (van Oevelen, Soetaert, García, de Stigter, Cunha,

Pusceddu and Danovaro, 2011). The Finn's index for deep sea food webs is low in comparison to other food web models in the Mediterranean considering more extended systems (Coll et al., 2007, 2006; Piroddi et al., 2010; Tsagarakis et al., 2010).

Among system development measures, the Ascendency is relatively low if compared with the development capacity of the system (5.75 ± 1.12 versus 19.54 ± 3.99). In fact total AC is only 0.30 ± 0.03. Such indices define the maturity of the system, so, results show that the system may undergo significant changes if disturbed.

The average mutual information of the system is 0.82 ± 0.04, a very low value indicating a low trophic specialisation (Ulanowicz, 2004). However, such value must be taken with caution, because it strongly depends on the resolution of the binary food web.

Acknowledgements: The authors thank all the participants of the BIOMARE (ref. CTM2006-13508-CO2-02/MAR) and ANTROMARE (ref. CTM2009-12214-C02-01-MAR) surveys. The first author would also like to thank Dorina Seitaj, PhD student at NIOZ, Yerseke (NL) for her help in SOC experiments.

6

Simulation of trophic cascade in a bathyal ecosystem

Abstract

We present a dynamic simulation of the continental slope food web in the Catalan Sea (NW Mediterranean). After reconstruction of carbon flows among major compartments using linear inverse modelling (LIM) we performed a dynamic simulation based on a system of ordinary differential equations to predict biomasses behaviour during 5 years after perturbations induced by red shrimp fishery (top-down driver) and by the quantity of food supply entering the web (bottom-up driver). The main purpose was the detection of indirect trophic interactions encompassing three or more trophic levels.

Our simulation demonstrates that trophic cascades induced by fishery cannot occur through major interactions of the bathyal food web. We only found very ephemeral indirect effects persisting less than 10 days, that we considered not enough to demonstrate the occurrence of this mechanism in the system. There are empirical studies in which trophic cascades have not been detected. Nevertheless, we investigated also interactions in couples of components and we found alternating phases that we considered as effects of the disturbances we imposed. In such cases we demonstrated which, among the perturbations, is the most relevant in altering relative biomasses. We found that organic matter inputs are stronger drivers than fishery activity in the bathyal food web, result in agreement with the findings by other authors in different ecosystems.

The dead organic matter or detritus, a common feature of most ecosystems, is frequently overlooked. However our results emphasize the importance of detritus in benthic ecosystems sustained by allocthonous sources, helping to understand its role in structuring and bathyal food webs.

Keywords: dynamic food web, trophic cascades, bathyal ecosystem, red shrimp fishery, species interactions

6.1 Introduction

The trophic cascade consists in the removal of a predator that may result in a "release" of its prey or competitors. This signal may proliferate throughout the food web and descend till more than four trophic levels in some cases (Pinnegar et al., 2000). Such forces are called top-down drivers and usually are considered human induced. This mechanism was described first by Hairston et al. (1960) and Estes and Palmisano (1974) and coined by Paine (1980) and one of the most famous trophic cascade examples is the interactions between killer whale, otter, sea urchin and kelp widely described by Estes et al. (1998). The exploitation (intensive fishing) on top predators is thus considered as the main factor inducing trophic cascades (Pinnegar et al., 2000) and leading to imbalances in ecosystem function (Jennings and Kaiser, 1998; Pinnegar et al., 2000). Many examples of profound changes in distinct ecosystem configurations triggered by fishing have been documented: shifts in community assemblages have been reported reported from New Zealand and Mediterranean subtidal reefs (Guidetti and Sala, 2007; Shears and Babcock, 2002), Caribbean and African coral reefs (Hughes, 1994; McClanahan and Shafir, 1990) or the Gulf of Maine (Steneck et al., 2004). More examples can be found and are widespread evidence of trophic cascade (e.g. Estes et al., 2011; Frank et al., 2005, 2006). Trophic cascades have been detected in systems containing sea urchins and fish, while other potentially important organisms introphic cascades, such as the macrofauna (polychaetes and small crustaceans or molluscs), have not been usually taken into account.

Studies on trophic cascades in the Mediterranean are almost nonexistent (see also Chapter 1). The mechanism has been argued in shallow hard or soft bottom communities (e.g. Pinnegar et al., 2000; Sala et al., 1998). Results are usually inferential or based on small-scale experiments, while large-scale and long-term implications remain untested (Elner and Vadas Sr, 1990; Pinnegar et al., 2000; Sala et al., 1998).

Equally, (but few) cases exist in which intense fishing has not triggered cascading effects (e.g. Cardona et al., 2007; Reid et al., 2000)..For example Cardona et al. (2007) discuss as possible explanation of this results the oligotrphy of the studied area (close to Mallorca) with respect to previous studies performed on the mainland continental shelf (in front of Catalonia, Spain). A completely lack of information there is about trophic cascades in food-limited ecosystems, such as in the deep sea

In the continental slope of the NW Mediterannean the red shrimp (*Aristeus antennatus*) fishery is the main human activity, as we described in different chapters. Early stock assessments of this species showed that the exploitation status was close to the optimum in the 1980s and 1990s (Demestre and Lleonart, 1993; García Rodríguez and Esteban, 1999), but recent stock assessments warn of excessive fishing mortality coupled to low stock abundance (Anderson et al., 2012; García Rodríguez et al., 2007). As has been demonstrated in other cases the extensive fishing can lead to trophic cascade events.

Fishing remains the most studied key driving force in ecosystem changes at the scale of decades (Coll, Libralato, Tudela, Palomera and Pranovi, 2008; Daskalov et al., 2007; Jackson et al., 2001; Jennings and Kaiser, 1998; Palkovacs et al., 2012; Pauly et al., 1998; Shackell et al., 2010; Zhou et al., 2010), recently enhanced by the general awareness that water ecosystems are undergoing high pressures by modern fisheries. There are still disputes about which analytical tool should be used to study trophic interactions in ecosystems (Walters and Martell, 2004) and how can be applied in a management perspective. But what is actually suggested by current analyses is the full exploitation of most demersal and pelagic stocks (Aldebert and Recasens, 1996; Bas et al., 2003; FAO, 2009; Papaconstantinou and Farrugio, 2000; Sardà, 1998) that can lead to ecosystem unbalances .

Trophic cascades and any other event that results from changes in predator abundance are top-down mechanisms that are set off by exogenous drivers like fishery but also climatic changes leading for example invasive predators. To the other extreme of the food web there are potential drivers of bottom-up processes. An example of bottom-up stressor is the nutrient enrichment that can lead to significant changes in the ecosystem and can be driven by human (in most cases of eutrofication) or environmental forces (seasonal changes or occasional events) usually related with climate changes (Verity et al., 2002). All trophic levels are potentially limited by available food resources (e.g. Hunter and Price, 1992). Thus any factor influencing the source availability can "cascades up" the system and affect population dynamics of upper trophic levels.

The main source sustaining deep sea life is the allochthonous (and dead) organic matter, except for (few) chemosynthetic spots. It has been demonstrated that its input shows a seasonal pattern (Billett et al., 1983) or depend on interannual production changes (El Niño in the Pacific) (Arntz et al., 2006) and also that deep sea fauna can respond rapidly to its variations (Gooday et al., 1990). In the

NW Mediterranean the vertical mixing of water masses is particularly important, mainly in winter (and specially strong in the Gulf of Lions: Marty and Chiavérini, 2010). The organic matter belongs to two main pathways: the vertical settling and the advective flux across the slope (Pusceddu et al., 2010; Vetter and Dayton, 1999). The latter is enhanced by river discharges, e.g. the Rhône in the Gulf of Lions and the Ebro in the Balearic basin. In contrast, vertical fluxes are the result of organic matter produced in the waters of the epipelagic zone (phytodetritus, faecal pellets and dead animals falling down to the bottom). Due to the high temperatures in the Mediterranean, the "marine snow" and organic matter in general is rapidly consumed by bacteria. The amount that reaches the bottom is therefore very little. The matter proceeding from advection and horizontal currents can reach significantly higher values, e.g. in the Gulf of Lions advective flows establish two order of magnitude higher than the "marine snow" Durrieu De Madron et al., 2000. Also the active vertical migration of zooplankton and micronekton Vinogradov and Tseitlin (1983), or benthopelagic megafauna (Papiol et al., 2013) provide potential energy inputs for deep-sea ecosystems.

Many studies assessed the relative importance of bottom-up and top-down processes in regulating and structuring ecosystems (e.g. Cury and Shannon, 2004; Hunter and Price, 1992; Power, 1992). It has been argued that both forces act simultaneously (Hunter and Price, 1992), and their roles could vary among biological systems depending on the biotope (Pinnegar et al., 2000).

The main aim of this Chapter was to identify possible trophic cascades in the bathyal food web induced by the fishery of the red shrimp. In turn we examined 1) the relative strength between top-down and bottom-up processes, 2) between the two major inputs of source in the web (vertical and advective) and 3) between the selective fishing on the red shrimp with respect to harvesting on the whole megafauna comprising by-catch species.

6.2 Materials and Methods

We used the food web model developed in Chapter 5 and shown again in (A) Figure 6.1, and in (B) all components plotted with respect to their trophic level (Table 5.5, previous Chapter).

6.2.1 The dynamic model

The dynamic model used to describe temporal changes in component biomasses after a disturbance (see below) is mathematically represented as an initial value problem (IVP) of ordinary differential equations (ODE, Ascher and Petzold, 1998). The ODE for standing stocks is represented as

$$\mathbf{s}' = f(\mathbf{s}, \mathbf{v}, \mathbf{t}),$$

where $\mathbf{s}$ is the set of differential variables and $\mathbf{v}$ and $\mathbf{t}$ are independent variables ($\mathbf{v}$ are some parameters of the model and t is the time). Some initial conditions are required, i.e.

$$\mathbf{s}(t = t_0) = \mathbf{c}$$

where $\mathbf{c}$ are constants and are the initial standing stocks of compartments at t_0 5.2.

In addition to ordinary differential equations the differential variables could obey some constraints at each time, such as the growth efficiencies of compartments.

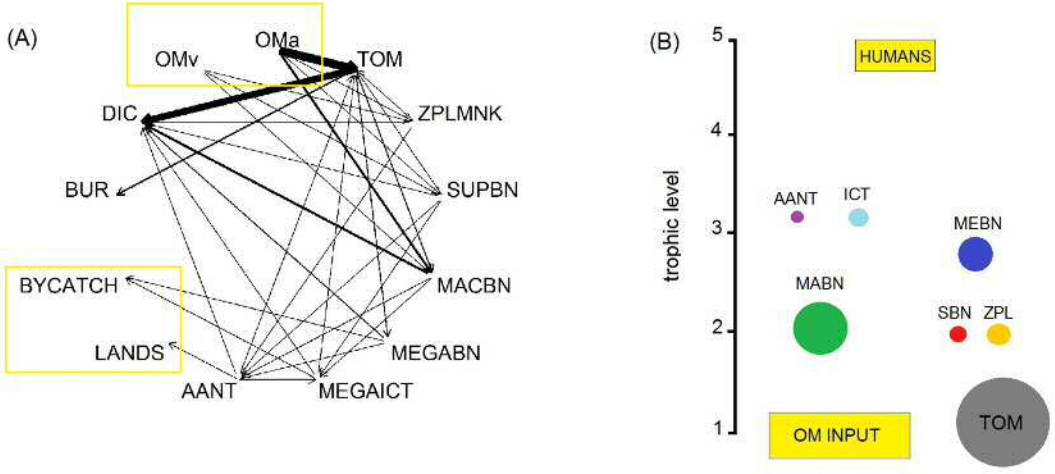

FIGURE 6.1: (A) Food web net flows and (B) trophic position of components. Colours correspond to compartments: orange = zooplankton (ZPL); red = suprabenthos (SBN); green = macrobenthos (MABN); blue = invertebrates from megafauna (MEBN); light blue = fish from megafauna (ICT); violet = red shrimp *Aristeus antennatus* (AANT).

In this case ODEs are called DAE (differential algebric equations), formally written

$$0 = F(\mathbf{s}', \mathbf{s}, \mathbf{v}, t),$$

and the initial values must obey:

$$0 = F(\mathbf{s}'(t_0), \mathbf{s}(t_0), \mathbf{v}, t_0).$$

DAEs can be solved by numerical techniques capable to solve "stiff" problems, i.e. when the eigenvalue spectrum is large (Hairer et al., 2008). The large spectrum in turn implies that the system contains both very rapidly and very slowly changing terms, and require the creation of the Jacobian matrix

$$J = \frac{\partial f}{\partial s}$$

and solving the corresponding system.

6.2.2 Local stability of the food web

Different definitions of ecological stability have been developed centring on the capability of the system to maintain or return to its original state after perturbation (and originally supposed at equilibrium, the steady state) (McCann, 2000). Other definitions refer to the species composition or to the size of populations in a community (McCann, 2000).

Here we define the stability when the system is near to equilibrium. In this case the system must show a feasible equilibrium, i.e. all components i have positive biomasses, $s_i > 0$. If the system is disturbed, causing a deviation, Δs_i, of any species from its original biomass and the system returns to its original equilibrium after a time, then the system is locally stable, otherwise it is unstable. Mathematically it is possible to describe this using the Jacobian of the system (May, 1972). Let call it $\mathbf{A}$, with elements α_{ij}

$$\alpha_{ij} = \frac{\partial \frac{dS_i}{dt}}{\partial S_j}.$$

The element α_{ij} represents the rate of change of the biomass in species s_i with respect to the biomass of species s_j. The stability of the system is then governed by the eigenvalues λ of the matrix **A**

$$\lambda ij(t) = \sum_{j=1}^{m} \alpha_{ij} s_j(t).$$

Eigenvalues can be complex numbers, such that,

$$\lambda = \chi + i\xi$$

with a real part χ and an imaginary part ξ. The real part describes the degree of the the growth or decay while the imaginary part describes the sinusoidal oscillation of the deviation. The system is stable if the real part of all the eigenvalues is less than zero. If one or more λ have positive real part, than the system is unstable and will deviate from its original values. The Jacobian of the steady-state model can be used to assess the stability of the system in the time t_0.

6.2.3 The simulation

We set the values of the state variables, i.e. the biomasses of components (Chapter 5, Table 5.2), the flow matrix estimated through the parsimonious solution (4th column in Table E.4, Chapter 5), the model parameters (see Table E.3) and the time (5 yeas = 1825 days)

We controlled the following causes of perturbation:

1. Changes in the input of pelagic organic matter from vertical fall (OMv),
2. Changes in the input of terrigenous organic matter from advective processes (OMa),
3. Changes in the fishing pressure on red shrimp population,
4. Changes in the fishing pressure on bycatch components.

The first and second are both bottom-up, while the third and fourth are top-down drivers. Different components are involved in each process. The components directly effected from perturbing events are defined by the binary web (see Table

E.2 in Chapter 5). Thus, changes in vertical or advective inputs directly perturb the following components: Zooplankton-Micronekton (ZPL), Suprabenthos (SBN), Macrobenthos (MABN) and the total organic matter in sediment (TOM), while changes in outflows due to fishery/bycatch perturb red shrimp (AANT), Ichthyofauna (ICT) and Megabenthos (MEBN) stocks.

The simulation is composed of three steps: 1) we first predicted the biomasses of all components for all levels of each type of disturbance, 2) we then calculated the proportion of components at each time (we excluding nonliving components, TOM) and finally 3) we analysed the presence of shift in abundances between couples and triplets of species and so the presence of trophic cascade during the simulated time span.

Thus, we run dynamically the food web onece with the steady-state solution, to ensure the stability of the model in its original built. It should remain constant, unless the food web is very unstable. Then we run the simulation for all other conditions as described below.

We built a four-nested loop to account for all types of perturbation, all calculations were made in the inner loop. We directly changed the biomasses involved in each of the processes at $t = 1$,

$$s_i^{t_1} = s_i^{t_0} + (f_i \times p),$$

where $s_i^{t_0}$ is the original biomass of component i at $t = 0$, f_i is the value of the flow involved in the process, and p is a factor, indicating the magnitude of the perturbation and its direction. In practice we considered $p \in 0, 5, 20, 50, -5, -20, -50$ for all processes. For example, let consider OMv → ZPL. This flow goes from OMv to ZPL. When $p = 0$, the biomass does not change ($s^{t_1} = s^{t_0}$), when $p \in 5, 20, 50$ the flow increases with a factor of 5, 20 or 50 times, while if $p \in -5, -20, -50$, likewise it decreases. We used matrix calculation to change all components together. This setting allowed for one control level (0) that is, without perturbation and six more levels: three with increasing and three with decreasing disturbance. In this way the comparisons between the same magnitudes for all processes is possible as well as quantify the main effect for each one of the process and the interaction (till three factors).

The dynamic simulation returned a list of 2401 matrices (7^4, 4 factors with 7 levels each one) containing the simulated biomasses in each time, $\mathbf{B}_{(T\times S)}$, with $T = 1825$ days (equivalent to 5 years) and the number of compartments, $S = 7$.

6.2.3.1 Couples of species

We calculated the proportion of the biomasses of each compartment in the community at each time step.

Possible interactions between couples of components in the community (combinations) are

$$C(n, r) = n!/r!(n - r)!$$

where the number of components is $n = 6$, and interacting components are $r = 2$. C in our case is $C = 15$. However we must distinguish between combinations, because some of them are between components with the same trophic level (or compeating, partially or entirely, for the same resource) or adjacent trophic levels (i.e. predator-prey interactions) as reported in Table 6.3.

We used as trade-off for the proportion the $f = 2$. If one component biomass (higher at the beginning) returned a proportion lower than 1/2 of another and of its original proportion and if such conditions continued for more then 10 days, then we considered enough to give evidence of a shift between the two biomasses. We also considered the opposite situation, i.e. when the biomass is more than 2 of the other component and of its initial proportion. That allowed to detect both negative and positive shifts in relative proportions.

We summarised such results calculating some basic statistics shown in Table 6.2.

6.2.4 Software

The simulations and all statistical analyses have been performed in the R statistical programming environment (R Development Core Team, 2013).

We used R-package deSolve (Soetaert et al., 2010*b*) to run the dynamic model. It implements a variety of solvers and permits to specify the Jacobian and to select

the solver according to the Jacobian's nature. Within the amplitude of methods we used the lsoda, because it automatically selects a stiff or nonstiff method and may switch between them during the simulation, in case the stiffness of the system changes. This is the default method used in ode and specially well suited for simple problems as our food web model is.

6.3 Results

6.3.1 The stability analysis

The system in its steady state returned eigenvalues close to zero.

6.3.2 The total biomass

The trends of total biomass (mmol C m^{-2}) are shown in Figures 6.2, 6.3 and 6.4 in three different scenarios (A, B, C) corresponding to the three different intensities (5, 20 and 50). In each scenario are represented the levels for factors (OM input

type rel	comb	components
1)	PREDATION	PREY-PREDATOR
	comb3	ZPL,MEBN
	comb4	ZPL,ICT
	comb5	ZPL,AANT
	comb7	SBN,MEBN
	comb8	SBN,ICT
	comb9	SBN,AANT
	comb10	MABN,MEBN
	comb11	MABN,ICT
	comb12	MABN,AANT
2)	COMPETITION	
	LOWER TL	
	comb1	ZPL,SBN
	comb2	ZPL,MABN
	comb6	SBN,MABN
	UPPER TL	
	comb13	MEBN,MEICT
	comb14	MEBN,AANT
	comb15	ICT,AANT

TABLE 6.1: Relationship investigated.

indicator	description
collapse	(binary) describes if one or both biomasses drop to zero during the studied period (1) or not (0)
$p.shift$	(binary) describes if component i returned higher proportion than component j during the studied period (1) or not (0)
$n.shift$	(binary) describes if component i returned lower proportion than component j during the studied period (1) or not (0)
c.times	returns how many times *collapse* occurs during the period
p.times	returns how many times $p.shift$ occurs during the period
n.times	returns how many times $n.shift$ occurs during the period
c.duration	returns the mean period (days) of *collapse* events
p.duration	returns the mean period (days) of $p.shift$ events
n.duration	returns the mean period (days) of $n.shift$ events

TABLE 6.2: List of indicators (response variables) and their description.

and fishing effort). With the aim to summarise the results we show only a selection of possible interactions (n=21 different plots within N=49 possible interactions) and where the base-base interaction is replicated in all Figures. The base case corresponds to the unperturbed run, that, if the food web in its steady state is stable, must return a strait line (as is actually shown in A11, B11, C11 for each figure). Each row (or column) corresponds to zero (base), positive (more) or negative (less) perturbation. Different Rows correspond to different levels of energy input while columns to fishing intensity.

In all figures the difference between levels of organic matter input is evident (comparing graphics vertically), while unobservable differences exist among levels of fishing intensity. Only in the first horizontal line of all figures, corresponding to unperturbed organic matter inputs, A1·, B1·, C1·).

All lower rows in all figures and the middle row in Figure 6.4 exhibit unstable dynamics that which will be analysed in depth when describing relative biomasses behaviour 6.3.3 in Section 6.3.3.

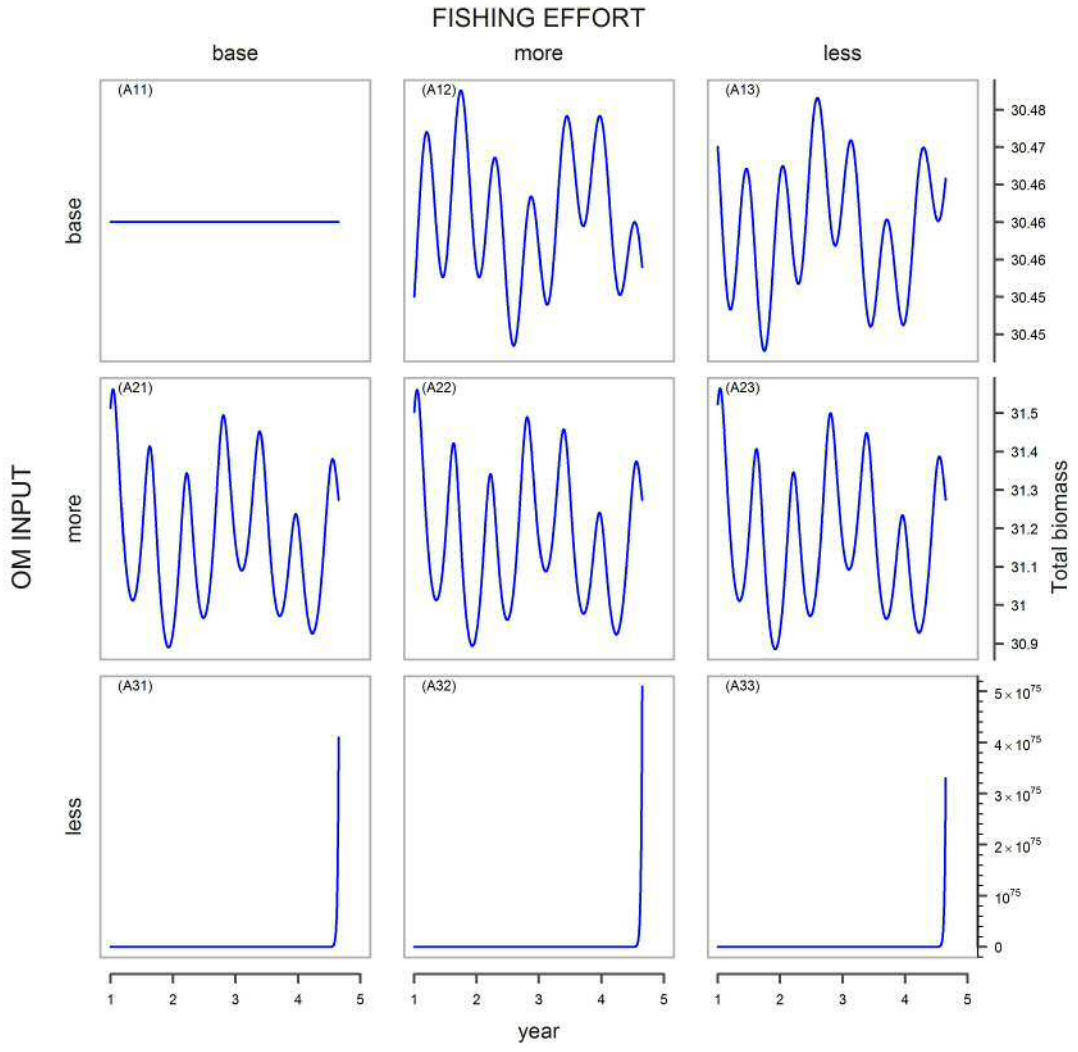

FIGURE 6.2: A) Changes of total biomass during the 5 years using p=(0,5,-5).

6.3.3 Relative biomasses

With the same logic are shown the relative biomasses of components in Figures 6.5, 6.6 and 6.7.

In this case as for previous figures differences are evident among levels of organic matter input (vertical comparison), while unobservable are differences among levels of fishing effort (horizontal comparison). Notable differences can be observed in the last row (in each figure) with respect to the above rows of the same figure and between last rows of all figures (precisely between A3· and both B3· and C3·).

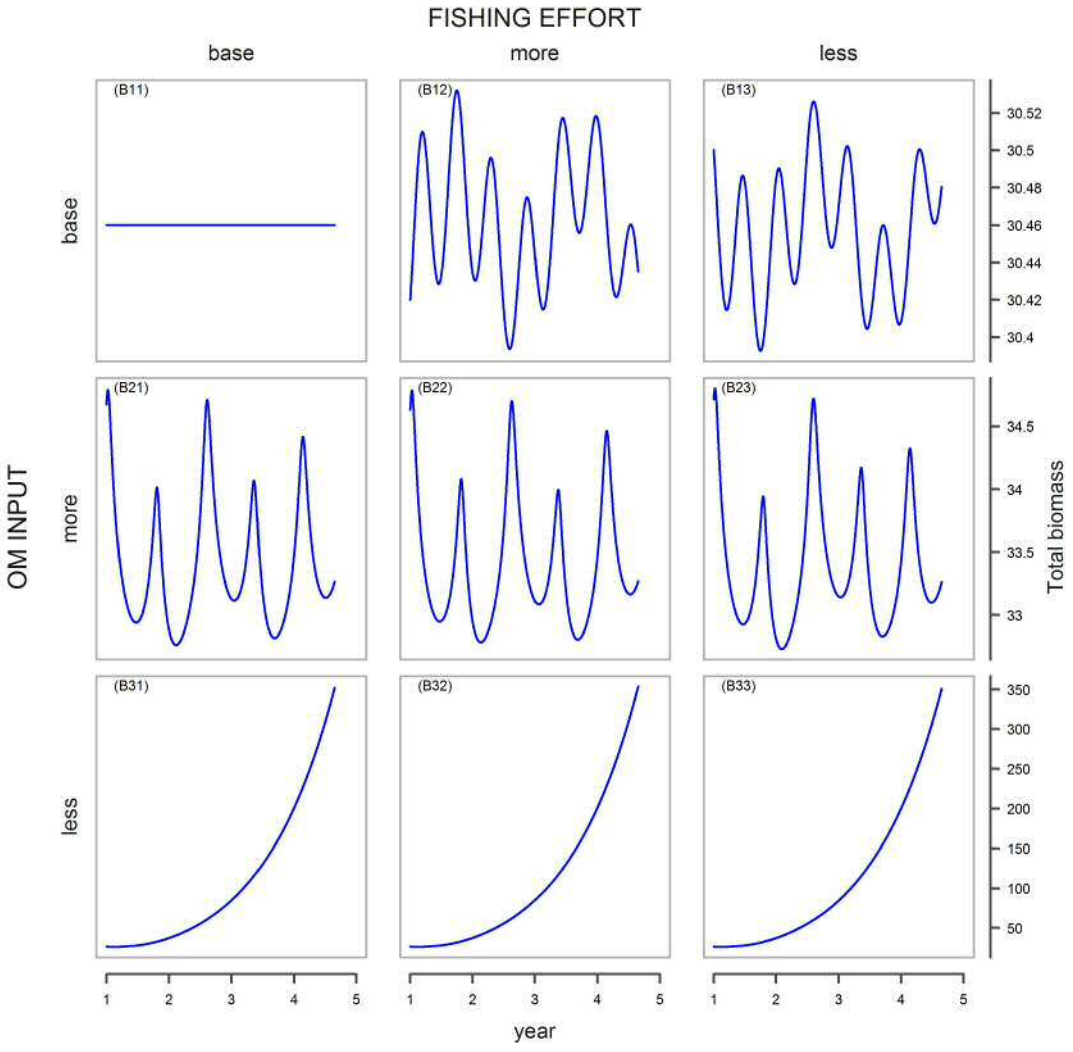

FIGURE 6.3: B) Changes of total biomass during the 5 years using p=(0,5,-5).

6.3.4 Interactions effected

In Table 6.3 results of variable $shift$ are shown for different combinations of sudied factors and each interaction between species.

In the simulation we also distinguished between selective catching of the red shrimp or of red shrimp and the accompanying fauna, i.e. all other megabenthos. But in this case as well no difference were observed.

When we checked the simultaneous existence of positive (or negative) effect on upper level and negative (or positive) on lower level, we did not find the conditions required for the existence of trophic cascades. All possible trophic cascade are shown in Table 6.4.

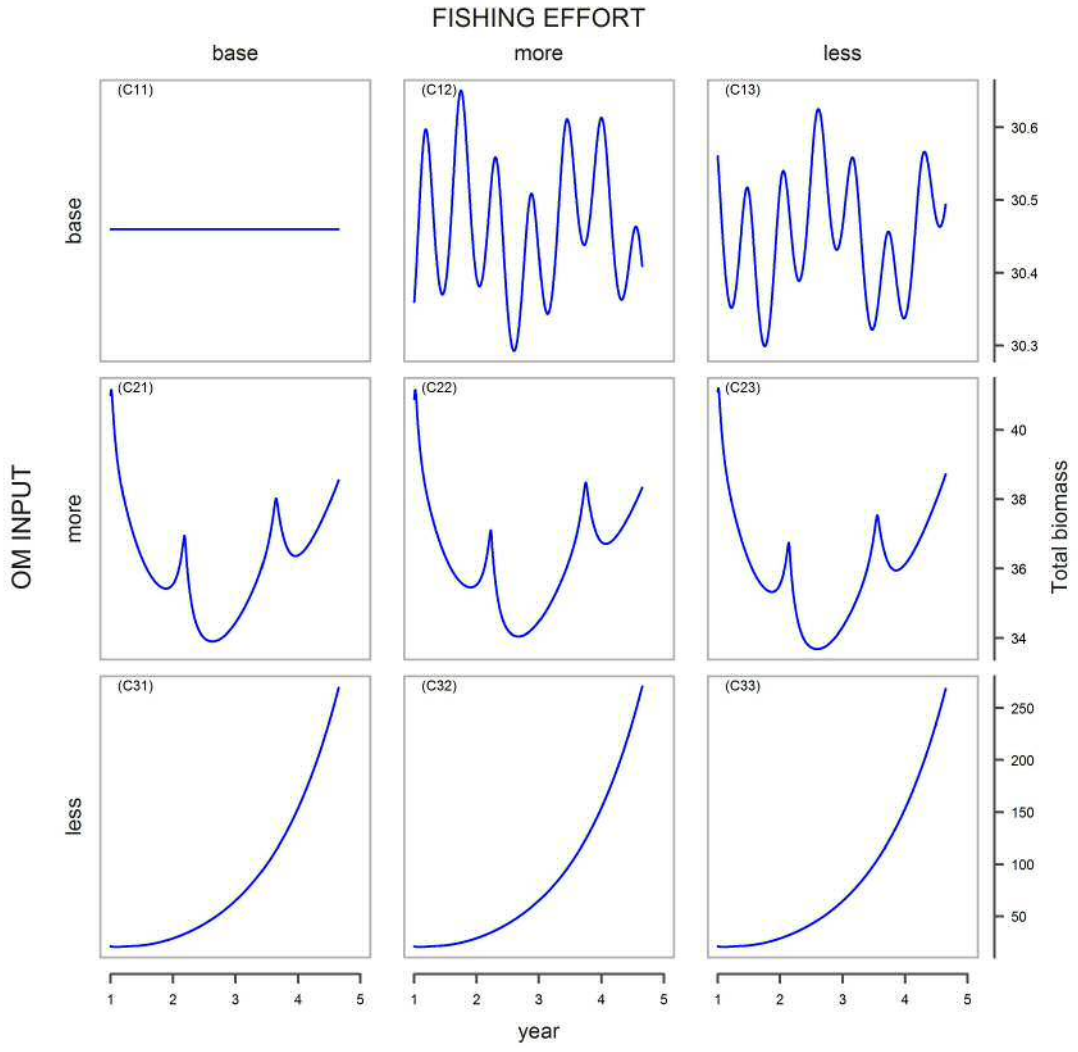

FIGURE 6.4: C) Changes of total biomass during the 5 years using p=(0,50,-50).

6.4 Discussion

In this study we applied dynamic simulations to the quantified food web model (fully described in Chapter 5) to evaluate the presence of trophic cascade in the bathyal ecosystem. To do so we studied all possible pathways in the food web that might be subjected to this mechanism.

However many studies highlights the presence of trophic cascades in different ecosystems (e.g. Estes et al., 2011; Frank et al., 2005, 2006; Guidetti and Sala, 2007; Pinnegar et al., 2000; Shears and Babcock, 2002), here we did not find any evidence of this mechanism.

Ecosystems for which trophic cascades have been shown present some common characteristics: low species diversity, simple food webs and small geographic size

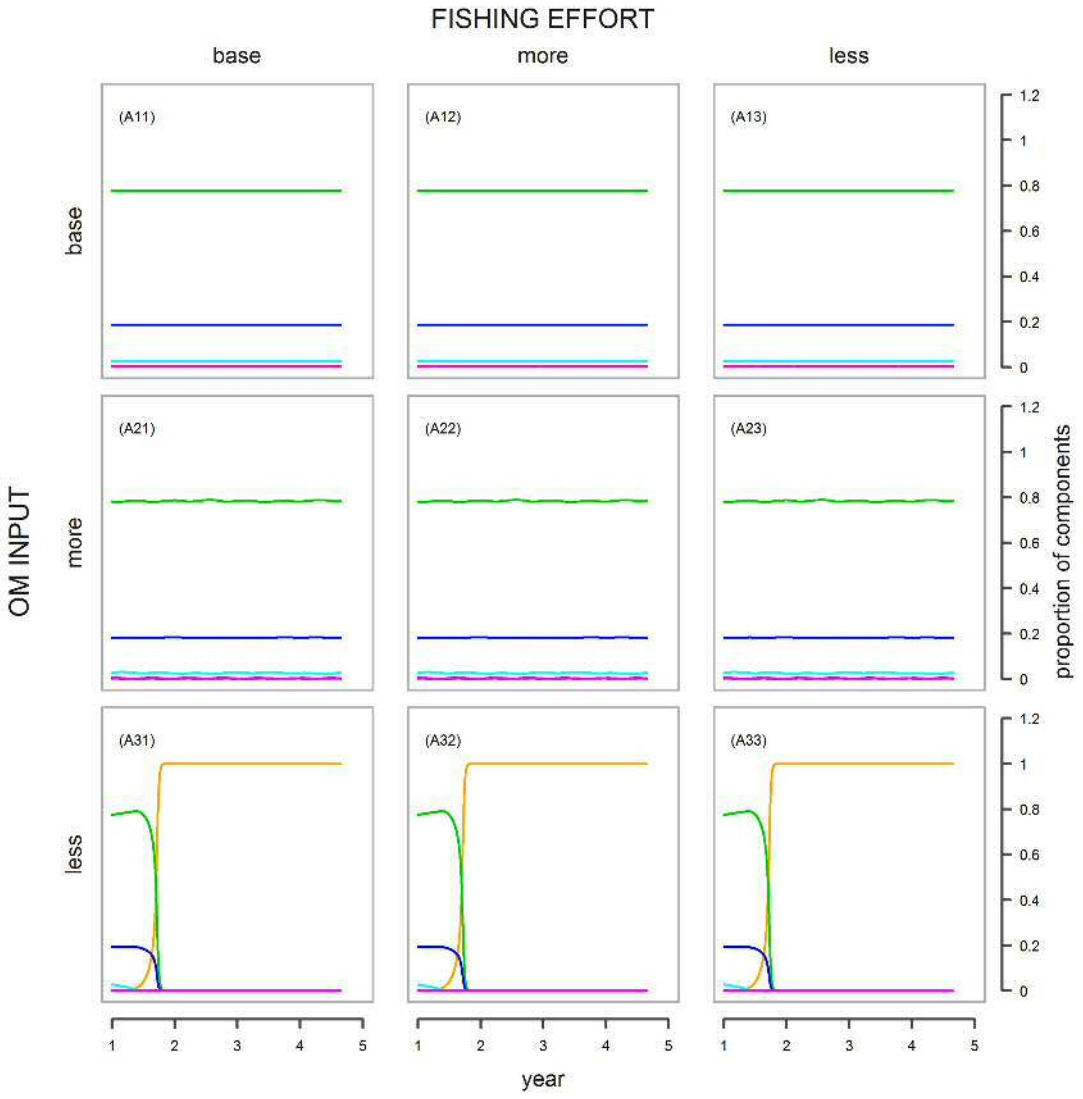

FIGURE 6.5: A) Changes of relative biomasses during the 5 years using p=(0,5,-5).

(Shurin et al., 2002; Strong, 1992). On the contrary Frank et al. (2005) asserted that marine continental shelf ecosystems, which generally have large spatial scales, high species diversity, and food web complexity, have not yet revealed unequivocal evidence of trophic cascades.

In fact considering humans as the upper level of the food web, we could consider different possible cases triggering a trophic cascade (Table 6.4), but we did not find any. However, we are not facing a unique case. In fact we found other studies demonstrating the no existence of trophic cascade (at least Cardona et al., 2007; Reid et al., 2000). Other studies showed that detritus has a considerable implication in benthic food webs in both terrestrial and water ecosystems for

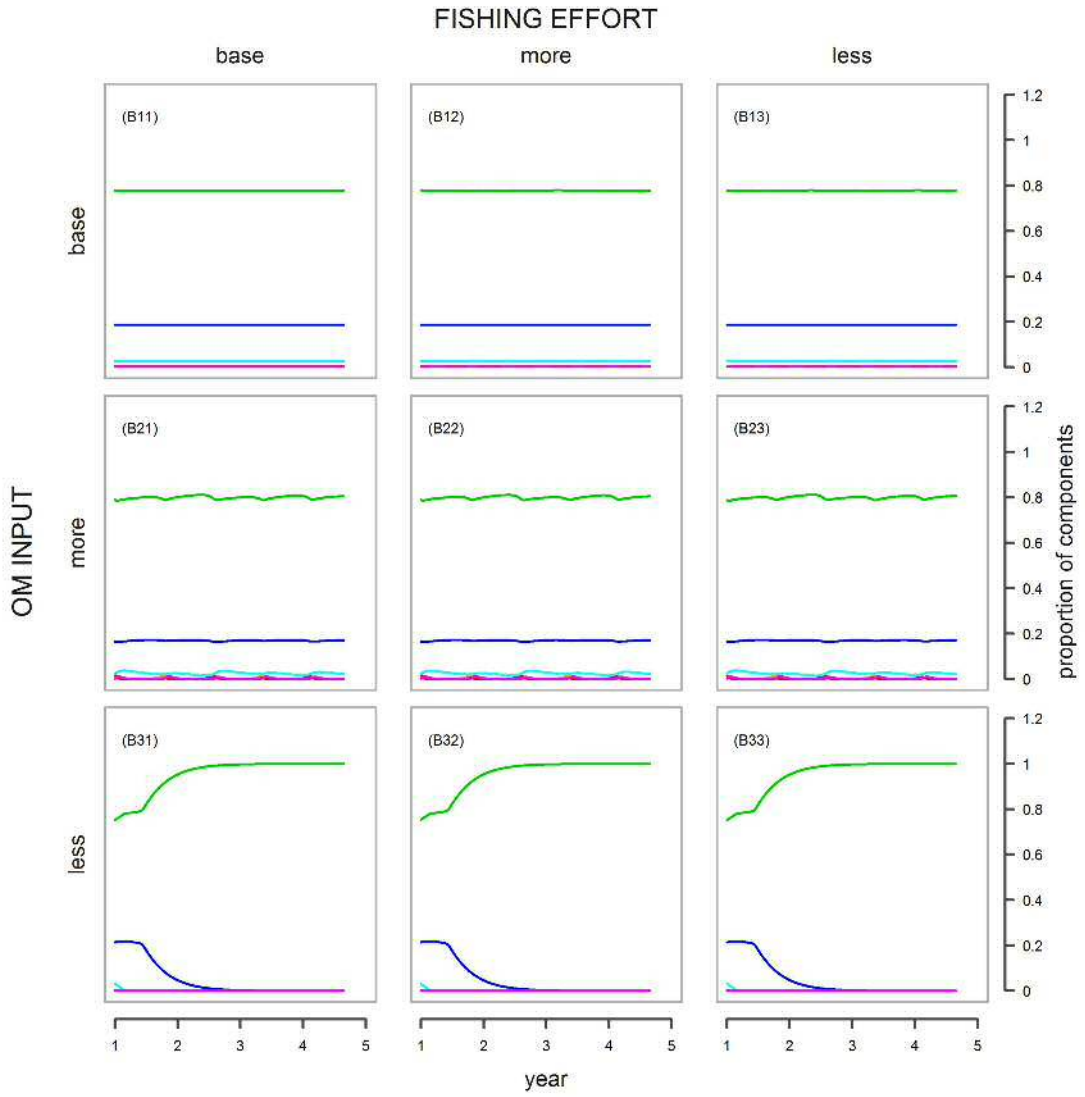

FIGURE 6.6: B) Changes of relative biomasses during the 5 years using p=(0,20,-20).

example in relation to the high importance of bacteria (Hall Jr and Meyer, 1998; van Oevelen et al., 2012).

Has been argued that detritus based food webs are not controlled by predators, whereas only by the source (mainly allochthonous detritus such as in the deep sea) and have been called "donor-controlled" food webs (DeAngelis, 1980; Moore and de Ruiter, 2012). Examples considering detritus as allochthonous source have been described e.g. by Polis and Strong (1996) and Moore et al. (2004).

This hypothesis (the donor control) induced e.g. Huxel and McCann (1998) to study allochthonous versus autochthonous sources in food webs finding that the food webs collapsed when the allochthonous source predominates. So, an allochthonous resource brings instability in the network. Also our simulation found

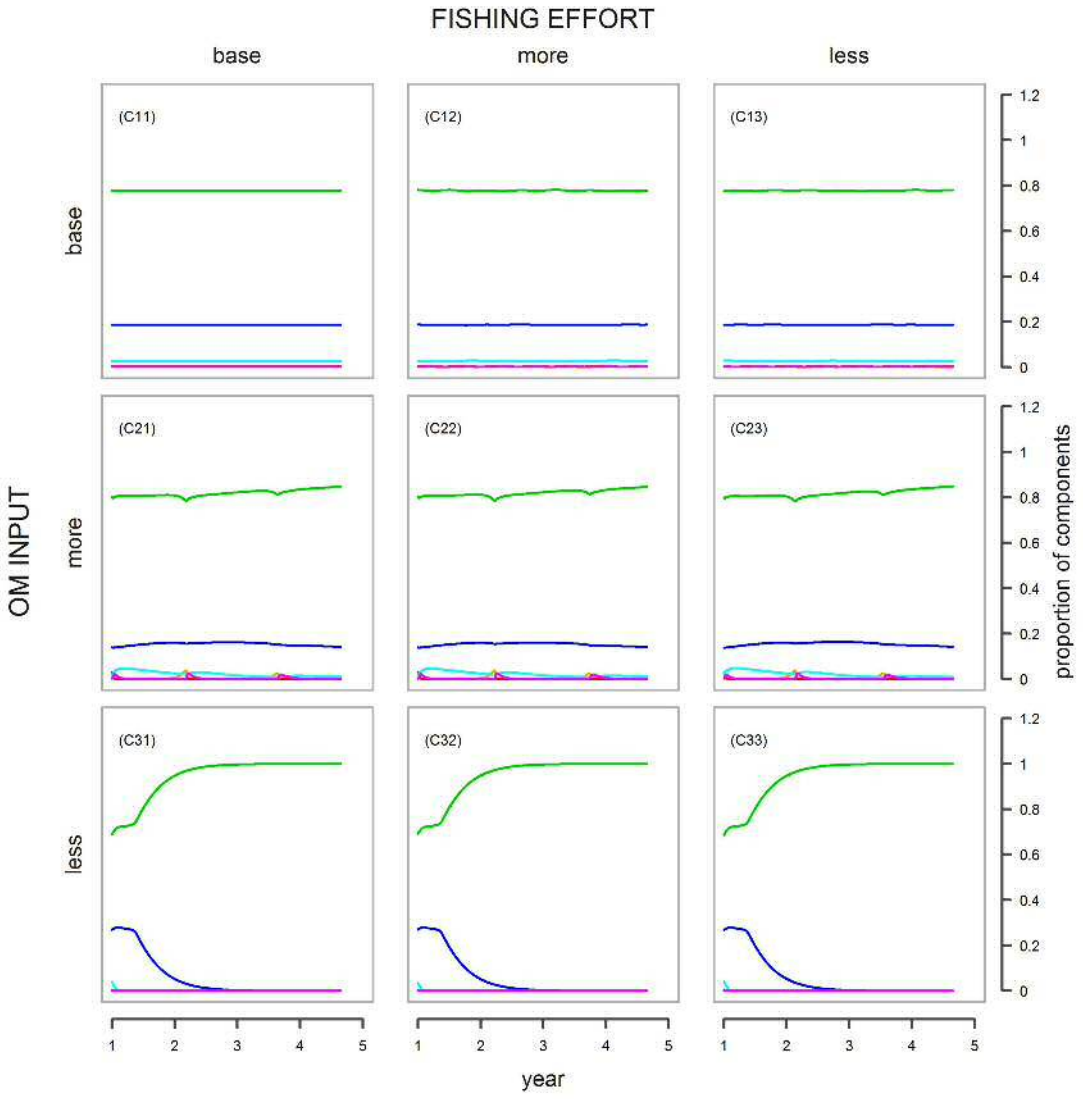

FIGURE 6.7: C) Changes of relative biomasses during the 5 years using p=(0,50,-50).

high instability related to the (allochthonous) inputs. In some cases, components tended to zero (e.g. predators near to TL=3) or even very high (e.g. the zooplankton due to the fact that no more predators existed and which can be more competitive than other components with the same TL).

Recent results (Fanelli et al., 2009) show that continental trophic webs can show complex interconnections which we could not consider in our initial trophic web model (Chapter 5), which has a relatively low resolution. However, most of these complex interactions take place within the larger compartments considered, evidenced for lower trophic leveles (e.g. Fanelli et al., 2009) (they represents substructures within larger structures or modules), while higher trophic levels (decapods

and fish) show a continuum in their trophic niches, e.g. a continuum of benthopelagic sources (Papiol et al., 2013), so when grouped eat a little of everything. For this reason, our low resolution food-web model is a compromise solution and should not be affected to a large extent by within compartment complexities, because with its simplicity our model describes the multiplicity of interactions among larger components.

The changes we found between red shrimp and the zooplankton and suprabenthis are not consistent with trophic cascade because their biomasses are both very small with respect to the total.

But apart from the observation or not of trophic cascade, the simulation was also designed in order to define the relative importance of top-down and bottom-up processes that in fact returned a very important role of resource availability in

		(A-B-C)		
		base	more	less
	base	-	-	-
(A)	more	-	-	-
	less	ZPL-Ma ZPL-Me ZPL-I ZPL-A	ZPL-Ma ZPL-Me ZPL-I ZPL-A	ZPL-Ma ZPL-Me ZPL-I ZPL-A
(B)	more	ZPL-S S-A ZPL-A	ZPL-S S-A ZPL-A	ZPL-S S-A ZPL-A
	less	-	-	-
(C)	more	ZPL-SBN Z-Me S-A Z-A	ZPL-SBN Z-Me S-A Z-A	ZPL-SBN Z-Me S-A Z-A
	less	-	-	-

TABLE 6.3: Couples of components between which the *shift* occurs.

1)	HUMANS	→	MTL*	⇒	LTL
2)	HUMANS	→	MTL**	⇒	MABN
3)	HUMANS	⇒	MTL***	→	ZPL/SBN

TABLE 6.4: Possible pathways of trophic cascade.MLT = mid trophic levels, AANT, ICT and MEBN, LTL = lower trophic levels, MABN, SBN and ZPL. * Jointly. ** Jointly or all subsets.*** Jointly or MEBN (Does not make sense consider other subsets because the biomasses are very close to the following trophic level).

organizing the bathyal food webs much more than the fishing activity. Many studies in the past claimed the always important bottom-up in comparison to the top-down drivers (e.g. Shurin et al., 2012).

Acknowledgements: The authors thank all the participants of the BIOMARE (ref. CTM2006-13508-CO2-02/MAR) and ANTROMARE surveys, especially the crew of the F/V García del Cid for their inestimable help.

PART IV

7

General discussion

7.1 General discussion

In this Ph.D. thesis all topics considered aimed to understand different aspects of the bathyal ecosystem with the final intention to discuss the possibility of trophic cascade induced by fishing activity. The following sections summarise some important aspects discussed in each chapter separately but also some new features and goals, listed below.

7.2 PART I The infauna in the continental slope

Results from Chapter 2 show that macrofauna variability is related to physic-chemical variables in the water column and in sediments. Higher temperature and salinity, corresponding to the arrival of the Levantine intermediate water (LIW) in the Balearic Basin, and changes in water masses can influence the re-suspension of particles and inputs of the particulate organic matter (POM) from other areas, e.g. the Ligurian Sea, situated to the East of the Balearic Basin, and transferred to the studied sites from the current. These events affect to the nutritional value of sediment (not only temperature and salinity): for example TOC (quantity), C/N and δ^{13}C (quality), with which we found significant relationship with macrofauna. The relationship between macrobenthos and TOC (the quantity of food) has been found also in other studies, e.g. in the Atlantic Ocean (Sibuet et al., 1989) and the Angola Basin (Kröncke and Türkay, 2003).

We found that the biomass in our area is higher than in nearby areas (Toulon canyon, Stora et al., 1999). Annual biomass ranges between 0.62 g DW/m^2 outside the canyon and 0.96 g WW/m^2 inside the canyon, two-times higher than in or close to Toulon canyon at comparable depths (500 m: 0.32−0.54 g DW/m^2: Stora et al., 1999).

Also diversity (S) and total abundance (338.2 ind/m^2) in the canyon are higher here in comparison to the Toulon canyon (S = 36; N = 176 ind/m^2). We related this difference to the existence of a river in the north of Barcelona, the Besós river, while the Toulon canyon is not an extension of any river. Such different conditions are probably related to differences in food availability.

We also found differences in comparison to the eastern Mediterranean as we could expect. In our study the biomass is clearly higher (one order of magnitude) than

values in the South Cretan Sea (Tselepides et al., 2000), where biomass ranged between 0.05 – 0.09 g DW/ m^2 (Tchukhtchin, 1964) and that is explained by the increasing oligotrophy from West to East in the Mediterranean.

Regarding to trophodynamics, surface deposit feeders (e.g. Ampharetidae among polychates and the echinoderm *A. chiajei*) dominant in the canyon, are replaced by subsurface deposit feeders (e.g. sipunculans) on the adjacent slope, in agreement with existing literature (Flach and Heip, 1996; Kröncke et al., 2003): species feeding mainly at the sediment surface are more linked to fresh organic matter (lower C/N), whereas subsurface deposit-feeders and predators are found in sediments with more refractory material (higher C/N). Other studies associated this replacement of trophic guilds with the depth (Pavithran et al., 2009; Stora et al., 1999) but we believe that it depends on trophic variables changing by depth. At the adjacent slope caudofoveats (*Falcidens* spp., *Prochaetoderma* spp.) and polychates Paraonidae biomasses were related to turbidity and fluorescence, likely because these taxa are surface deposit feeders but also carnivorous on diatoms and foraminiferans (meiofauna) (Fauchald and Jumars, 1979; Jones and Baxter, 1987). In fact as foraminiferans respond rapidly to inputs of fresh organic matter (Gooday, 1988), it is possible that they already reach high densities becoming abundant prey for the abovementioned macrofauna. That happens in February because the maximum of primary production at the surface begins in November-December, so then there is a lag of 1-2 months.

The quality of the POM deposited at the seafloor determines changes in the composition and biomass of macrofauna communities (e.g. off Banyuls: Gremare et al., 1997, and in the North Sea: Dauwe et al., 1998; Wieking, 2002; Wieking and Kröncke, 2003). These changes correspond to the feeding types of the structural taxa/species, matches being established between the available food and the feeding modes of the dominant consumers. Fresh matter inside the canyon in June-July has a terrigenous origin. Thus, the dominant energy flux was advective. On the adjacent slope, the advective flux is lower. On the contrary, temporal fluctuations of food sources (TOC, C/N, δ^{13}C) are less evident on the adjacent slope (more stability). That reasonably explains why the canyon assemblage was seasonally dominated by opportunistic trophic groups (Capitellidae, Flabelligeridae, Glyceridae), better able to adapt to rapid temporal changes in food inputs (and throughout the year by the always present surface deposit feeders). The proliferation of opportunistic species inside the canyon and a stronger temporal succession of species is related to food availability and quality (TOC, C/N, δ^{13}C) and with

greater influence of terrigenous inputs by river discharges. That should be not surprise because advection is many order higher (roughly 1:50 or more, strongly dependent on the season) than vertical fall and higher inside canyon than on the open slope.

The biomass in the canyon undergoes major changes throughout the year, while at adjacent slope it remained low. Diversity inside canyon reached higher values during the period of water column homogeneity (February and April) while is very low during heterogeneous periods. In the adjacent slope diversity was higher during the period of water column stratification and viceversa during homogeneous periods. This is probably linked to higher organic matter quantity (TOC) and quality of sedimentary food (lower C/N) inside canyon supplied by river discharges.

Another important consideration is that also in the successive study on the infauna performed in a nearby area (Mamouridis, Cartes and Fanelli, 2014*a*,*b*), we found similar trends in predominant taxa and trophic behaviour diversification found in Chapter 2. In fact habitats with taxonomic diversity, with the coral *Isidella elongata* (however had been strongly reduced in last years) or inside the canyon, the heterogeneous composition reflects the coexistence of different trophic behaviours for the diversified source availability. On the contrary, the open slope is dominated (Mamouridis, Cartes and Fanelli, 2014*a*,*b*) or seasonally dominated (Chapter 2) by the genus *Prochaetoderma* spp. a carnivorous caudofoveat feeding on foraminifera followed by different (sub)surface deposit feeders species and rare suspension feeders.

We finally highlight that during this study new records of caudofoveats have been found in the study area, e.g. *Falcidens gutturosus* and *Prochaetoderma alleni* with a total of five new records (Salvini-Plawen, 2009).

7.3 PART II Landings per unit effort LPUE

In Part II we combined commercial fisheries data, environmental and economic variables to model the landings per unit effort (LPUE) index of *A. antennatus* using more conventional (Generalized additive models, GAM, Chapter 3) and novel regression techniques (the Bayesian distributional regression models, DSTAR, Chapter 4).

In the GAM model the combination of variables (six predictors) captures the 43% of the total LPUE variability. The set of fishery-related variables (*trips*, *grt* and *group*) was the most important source, with an ED of 20.58%, followed by temporal (*time* and *period*, ED = 13.12%) and finally economic variables (*shprice*, ED = 9.30%). The importance of *trips* is associated to increasing experience of fishermen, through a process of trial and error (Maynou et al., 2003; Sardà and Maynou, 1998). Boats' *grt* also influence positively LPUE. The trawlers captures other capabilities of fishermen which can bias the LPUE (Marriott et al., 2011; Maynou et al., 2003) and are expected to be important in many fisheries (Maunder and Punt, 2004). Inter-annual variable (*time*) is much more important than intra-annual variability (*period*). The former is associated to environmental changes and probably macro-economic factors. We hypothesised a relationship with low NAO in the previous three years, that confirms the findings of Maynou (2008) and a possible relationship with the increase in fuel prices beginning in 2000. The following years were characterized by high inter-annual variability, when the price of fuel increased and showed greater variations. The variable *period* is more likely associated to local economy. The ex-vessel prices, *shprice*, shows a significant explanatory potential (ED = 9.30%). Low selling prices do not induce fishermen to practice this deep-water fishery, because they could not offset the high associated costs, and trawlers would rather switch to continental shelf fisheries, with lower costs and lower risk.

Obtaining information on deep-sea species population dynamics is notoriously difficult, but our analysis suggests that the use of fishery-dependent data to accurately describe the relative abundance of this resource is possible (at least it is not very different from the available fishery-independent data).

In turn, the definition of the relative importance of explanatory variables enables to make intervention on the relevant variables possible from a management perspective. Fishery-related variables tend to have a significant effect on LPUE (ED = 21% in our case), and management measures aiming to reduce fishing mortality could be based on limiting the trawlers or the number of trips permitted in deep-water fishing grounds, by defining a threshold when the number of trips does not significantly increase the partial effect for LPUE (the profit does not exceed the cost). Also the boat size can be reduced, however the effect of the *grt* is lower, so a measure of this type becomes less effective.

Studies of deep-water systems, where harsh conditions limit methods for evaluating fisheries, often suffer from a lack of data in order to assess stock status. Although the goal of fisheries managers is to promote sustainable production of fish stocks through formal stock assessment, it is often impractical to collect fishery-independent data in isolated or harsh environments. In these cases the information collected by a fishery is the main (or only) source of abundance data available (Maunder et al., 2006). In this context it is useful the usage of random effects when data are limited or correlated as discussed below.

Concerning to the statistical methodology, in Chapter 4 we proposed distributional structured additive models, used here for the first time to model fishery index (LPUE or CPUE). DSTAR allowing to model both first and higher order moments of the response, returns lower DIC values (that is even better estimates) and a better understanding of the variability in the response, when considering the second parameter. In fact the second moment (the shape for gamma distribution or scale for log-normal, the two distributions we considered in the study) can be explained by many of the variables we used in Chapter 4 (i.e. *trips* and *time*). For example the analysis performed on (almost) the same data set, where the GAM accounts only for the location, could not avoid the heteroscedasticity in the residuals (see Figure C.2). This heteroscedasticity can be (partially) explained by modelling also the second parameter. Here we demonstrated that both the number of trips and time strongly influence the second parameter, that in turn is (inverse) proportional to the variance (while the location is directly proportional).

Finally we point out another methodological issue concerning fixed versus mixed specification. In our study the fixed effects can be considered appropriate, representing sampling units the whole population of the studied fleet. However, mixed models are particularly suitable for both unobserved catching units and correlated observations in time series. In practise we clashed with estimation instability when trying to incorporate both catching units (called *code* in Chapter 4) and *grt* in fixed effects models. In Chapter 3 we could avoid the problem with clustering catching units into three groups, however this practise can bring to a loss of information or be wearisome. Finally, if boats hold random effects, it is not more necessary to consider them for standardization, because it is not affecting parameters estimation (the expectation or both expectation and shape/scale) of the conditional distribution of the response variable, the LPUE. Another important function of using random effects is the possibility to predict for unobserved catching units,

only if the effects of observed catching units truly represent a random sample of the entire (unobservable) population.

7.4 PART III The bathyal food web

The Catalan slope is one of the most studied bathyal ecosystems in the Mediterranean. However, as is the case for food webs in general (Moore et al., 2004), the identification of pathways within communities is difficult and even more so is its quantification.

The main trophic relationships in this environment were recently studied, unravelling very diversified and unexpected components, within the lower section of the food web structure, showing specialised to omnivory behaviour (Fanelli et al., 2009; Fanelli, Cartes and Papiol, 2011; Fanelli, Papiol, Cartes, Rumolo, Brunet and Sprovieri, 2011). However the estimation of the proportion among different types of feeding behaviours is still unavailable due to the high number of species living this ecosystem and the relatively low number of species of which diet has been examined. Moreover these studies suggest a modular structure of the food web (see, e.g. Fanelli, Cartes and Papiol, 2011), such that higher modules can be considered to semplify the model and make it manageable. This fact and the necessity to build a food web model for immediate use in fishery management (FAO, 2003) requires a compromise between complexity and simplicity, so as to study the main pathways of this complicated system and could make the model useful for a rapid management of the fishery in deep sea habitats within the ecosystem approach of fisheries (EAF).

With respect to other ecosystem modelling approaches, the great advantage of the LIM method is the ability to quantitatively reconstruct the food web even when the problem is under-determined (data-limited). We restricted the number of compartments, differentiating among large groups and distinguishing between two fundamental pathways in the bathyal environment that depend on external resources (vertical settling and advective processes) and recycled material.

In our area, the total biomass (only macro- and megafauna) was 30.46 mmol C m^{-2}, very close to the bioass in the deep Faroe-Shetland Channel (30.22 mmol C m^{-2}) (Gontikaki et al., 2011), and approximately 2/3 of that found at higher depths in the same region (45.93 mmol C m^{-2}, converted from Tecchio et al.,

2013) and also lower than at the Nazaré canyon (van Oevelen, Soetaert, García, de Stigter, Cunha, Pusceddu and Danovaro, 2011) and Rockall Bank (van Oevelen et al., 2009); the latter two are more diversified habitats and show higher secondary production. On the contrary, in our area the biomass is higher than in the Fram Strait (van Oevelen, Bergmann, Soetaert, Bauerfeind, Hasemann, Klages, Schewe, Soltwedel and Budaeva, 2011), as expected for being a food web in the Arctic Ocean and at deeper waters (2500 m). Also at the Porcupine Abyssal Plain the biomass was lower, summing the biomasses with the same size classes returned a value of 9.77 mmol C m^{-2} (van Oevelen et al., 2012), that is 1/3 of that we found in the continental slope.

Organic matter inputs to the community from advective processes are more important than those from vertical fall (see for the magnitudes e.g. Buscail et al., 1995, 1990; Durrieu De Madron et al., 2000). This implies a higher structural role of this input. Infauna receives more OM from advective than vertical origin and then from the particulate organic matter in sediment. Between internal flows, those related to the TOM and the infauna showed higher and more uncertainty values. That is also related to their structural role in this ecosystem.

The secondary production in deep sea mainly depends on inputs of detrital matter deriving from the upper levels of the water mass and dropping down as phytodetritus, dead animals, faecal pellets, empty shells, skeletons and small organic particles of different nature. These particles falling down to the seabed have been usually called "marine snow" (Alldredge and Silver, 1988). Pelagic animals eat and also bacteria living in the water column mass degrade this source of energy during its way down, especially in the Mediterranean, where the temperature is relatively high with respect to the open oceans (Fanelli, Cartes and Papiol, 2011). The remaining detritus is deposited on the sea floor where more bacteria deteriorate it enter in competition with metazoans which benefit of the remaining source. Deep ocean communities' carbon demand can exceed the vertical supply, being potentially supplied by lateral advection (Burd et al., 2010). That is the reason of the more structural role of advective processes in bathyal ecosystems. We found that a very low portion of this energy is recycled by the system (low Finn's index: FCI = 0.179 ± 0.066).

The total input of C estimated by the model ranges between 0.92 and 4.16 mmol C m^{-2} d^{-1} (mean value: 2.62 mmol C m^{-2} d^{-1}), while the total secondary production (excluding prokaryotes and meiofauna) ranges between 0.02 and 0.25 mmol C m^{-2}

d^{-1} that represents only the 2.17 – 6.01% of the organic matter that enters the community. The reason lies on biogeochemical processes and dissipation of the energy, i.e. the burial estimated to be 0.11 – 1.27 mmol C m^{-2} d^{-1}, equivalent to the 11.96 – 54.09% of the total organic input and the respiration, including the TOM (0.84 – 2.34 equivalent to 56.31 – 91.70% of the input).

The total input is approximately 7 times less than the input at comparable depths in the canyon of Nazaré but almost similar to the value in the lower section of the same canyon (at 4000–5000 m) (van Oevelen, Soetaert, García, de Stigter, Cunha, Pusceddu and Danovaro, 2011), this can be explained by the oligotrophic character of the Mediterranean sea, with respect to the Atlantic ocean and the habitat of canyons. Also the burial of organic carbon was lower in the Mediterranean continental slope, 0.73 ± 0.28 mmol C m^{-2} d^{-1}, in comparison with same depths in the Nazaré canyon (van Oevelen, Soetaert, García, de Stigter, Cunha, Pusceddu and Danovaro, 2011), however the same parameters have been applied for this process. In contrast it was much higher than the values estimated estimated by (0.19 mmol C m^{-2} d^{-1}) in the Rockall Bank's cold-water community and by van Oevelen et al. (2012) (0.03 mmol C m^{-2} d^{-1}) in the Porcupine Abyssal Plain, where the burial efficiency has been considered much lower than in the continental margins (van Oevelen et al., 2012).

Regarding to the feeding types, deposit and suspension feeding represent the 93.30% of the total consumption in the food web and the remaining percentage belongs to carnivores. Of this 93.30% the deposit feeding represents the 73-78%. Deposit feeders are mostly represented by the infauna (90.14% of the total deposit feeding), while the rest is consumed by megafaunal components. On the contrary suspension feeders belongs to the zooplankton and suprabenthos. Carnivorous feeding among megafauna represents the 56.37%, such that suspension and deposit feeding are still important in these groups. Also the macrofauna comprises carnivorous species (feeding on micro- and meiofauna and on the "smaller" macrofauna). Thus carnivores are under-estimated by this model.

Has been argued that deep-sea macrobenthos (mostly detritus feeders) exhibit an expansion of trophic niches and species tend to be omnivorous to avoid competition for food (Gage and Tyler, 1991). This suggests that grouping many detritivorous in a single compartment, as in the present model, is a good compromise. Nonetheless more recent studies with isotopic methodologies found high variability in the relationship between $\delta^{13}C$ and $\delta^{15}N$ particularly among deposit feeders, suggesting

exploitation of particulate organic matter at different stages of degradation: from fresh phytodetritus to highly refractory or recycled material (e.g. Fanelli, Papiol, Cartes, Rumolo, Brunet and Sprovieri, 2011). Also the seasonal turnover of opportunistic species is reasonable as evidenced in (Mamouridis et al., 2011). This scenario suggests a continuum in species trophic niches and the consequent difficult to compartmentalise the food web. Many examples of this repartition in food web modelling are available (van Oevelen et al., 2009; van Oevelen, Soetaert, García, de Stigter, Cunha, Pusceddu and Danovaro, 2011). When such information is not available, the compromise is to enlarge constrains in the model.

Our model gives necessarily a simplified picture of the trophic structure of the bathyal ecosystem and results represent an average within all species belonging to each modelled compartment. The TOM is considered as dead component however it comprises also living matter, but necessarily we set its TL = 1. However, micro- and meiofauna that could not be modelled present higher TL. For instance in the Nazaré canyon for nematodes the TL of deposit-feeders was estimated around 2 and omnivores and predators around 2.75 (van Oevelen, Soetaert, García, de Stigter, Cunha, Pusceddu and Danovaro, 2011).However considering that they usually have very low biomass with respect to the particulate organic matter in the sediment, is reasonable to consider that their TL do not affect to the average TL of the TOM as whole compartment. Zooplankton-micronekton (ZPLMNK), suprabenthos (SUPBN) and infauna (MACBN) have the same level (TL=2) occupying the "basis" of the bathyal food web almost eating on detritus (however of different source and quality) and as mentioned there are some carnovorous species eating on microplankton, microbenthos or meiobenthos (see also Fanelli, Cartes and Papiol, 2011). Fish (MEGAICT) and the red shrimp (AANT) show very similar positions (close to 3), while big invertebrates (MEGABN) are in the middle between lower and upper (modelled) levels. The difficult to capture the highest trophic levels of the food web must also be considered, when discussing results, that is the case of pelagic cephalopods and bigger sharks, that could show trophic levels higher then 4. These species with pelagic behaviour can also be sustained by other sources in the water column far from the bottom.

With respect to the index of omnivory, lower trophic levels showed specialized diets, a result that in this case is an artefact of the model. Setting higher deegree of compartmentalization will give higher values of omnivory, in fact many species are omnivores but can also present seasonally specialised diets. For example that

happens in some polychaets, that turn their behaviour in relation to the environmental conditions from deposit to suspension feeding (e.g. species belonging to the family paraonidae) or are both deposit feeders and carnivores (e.g. caudofoveats) (Mamouridis et al., 2011).On the contrary higher trophic levels showed some degree of omnivory.

The total respiration with a mean value of 1.89 mmol C m^{-2} d^{-1}, ranges between 0.84 – 2.34 mmol C m^{-2} d^{-1} and is very low with respect to the cold-water coral community (e.g. van Oevelen et al., 2009). In our model only the sediments (without macrofauna) account for the 83.75% of the total respiration with the value of 1.58±0.32 mmol C m^{-2} d^{-1}, while the percentages for macrofauna and megafauna are respectively 13.39% and 2.86% (sum of respirations of components of each size: 0.25 and 0.04 mmol C m^{-2} d^{-1}). Thus carbon processing is mainly due the living portion of the TOM (to prokaryotes and meiofauna) and only partially to metazoa (macro- and megafauna). In fact bacteria have the highest contribution within TOM compartment and for the whole community, as has been proven in other deep-sea benthic ecosystems (in the Nazaré canyon: van Oevelen, Soetaert, García, de Stigter, Cunha, Pusceddu and Danovaro, 2011 and in the Faroe-Shetland Channel: Gontikaki et al., 2011). In comparison with the CWC community at Rockall bank (van Oevelen et al., 2009), the respiration of our food web is more than 50 times lower. Despite, it is not surprising because the CWC community has characteristics of a hot spot habitat and thus respiration is higher than all literature data available (van Oevelen et al., 2009). Respiration is instead higher than that found at higher depths in our region (Tecchio et al., 2013), where only metazoan community was modelled and respiration was estimated around 0.64 mmol C m^{-2} d^{-1} after conversion. However we cannot say that it is statistically lower, having no estimates of the variability. Finally, however lower than the conditional mean calculated by the model E.1 (see Appendix E), our estimation falls into the range of other deep-sea soft bottoms data at comparable depths (Andersson et al., 2004) (see also Figure 5.3 in Appendix E to compare oxygen consumption data).

The total system throughput (T..), measuring the total food web activity has a very low value, was 7.04 ±1.38, does not significantly differ to that found in the lower section of the Nazaré canyon at 4000–5000 m depth while is more than four times lower than at comparable and higher depths of the canyon (van Oevelen, Soetaert, García, de Stigter, Cunha, Pusceddu and Danovaro, 2011). The total system throughput (conventionally defined in Ecopath as TST, however for the

definition given in Libralato et al., 2010 seems to refers to the T..) was 18.62 at higher depths (Tecchio et al., 2013). Our estimation of the TST was 12.657±3.572. The network analysis suggests that almost all the energy passing through the food web is not recycled (see TST and low values of TSTc and Finn's indices). Our value of FCI was 0.18±0.07, thus statistically there were no significant differences with the upper and lower sections of the Nazaré canyon in contrast with the middle section at comparable depths (van Oevelen, Soetaert, García, de Stigter, Cunha, Pusceddu and Danovaro, 2011). The Finn's index for deep sea food webs is low in comparison to other food web models in the Mediterranean considering more extended systems (Coll et al., 2007, 2006; Piroddi et al., 2010; Tsagarakis et al., 2010). Among system development measures, the Ascendency is relatively low if compared with the development capacity of the system (5.75 ± 1.12 versus 13.79 ± 3.03). In fact total AC is only 0.30 ± 0.03. Such indices define the maturity of the system, so, results show that the system may undergo significant changes if disturbed (this will be the main topic of the next Chapter 6). Moreover if we consider the repartition of the indices in internal, import, export and dissipation, A is lower for import and dissipation rather than internal and export flows, thus related flows are more unstable and are more vulnerable to changes.

7.5 PART III Trophic cascades and drivers in the bathyal ecosystem.

We found changes in relative abundances of couples of components. That suggested some indirect effects of (only bottom-up) drivers on the community. In fact we did not find indirect effect for more then two levels (indicating trophic cascades). Results showed the no existence of trophic cascade, a top-down mechanism, in bathyal ecosystems. In fact the possible trophic cascades in our food web, summarised in Table 6.4, do not exist neither for increasing nor for decreasing fishing effort. At least in the resolution we used for the dynamic simulation. Other studies in benthic ecosystems came to the same conclusion (at least Cardona et al., 2007) although they gave other explanations.

However in marine environments top-down controls have been often documented as the major force (e.g. Steele, 1998), in lack of evidences of opposite drivers on an ecosystem scale of botto-up mediation. But this mechanism is generally supported by studies on eutrofication (Reid et al., 2000). In fact both forces are likely to

operate in ecosystems supported by primary producers in varying proportions (Roff et al., 1988) in different time-scale scenarios (Reid et al., 2000).

Also where trophic cascade is well documented (pelagic systems) its indirect effects are not always striking because the difference between prey-predator abundances is not surprisingly high (except for some very popular and known examples of trophic cascade, e.g. Estes and Palmisano, 1974). For example, Rudstam et al. (1994) explained the low strength of top-down drivers with the high impact of other factors (changes in the interannual productivity or nutrient inputs) that could override any effect from predation.

Switching back to the bathial food web, other studies showed that detritus has a considerable implication on the dynamics of benthic food webs in water ecosystems for example in relation to the great importance of bacteria (van Oevelen et al., 2012) as well as in terrestrial ecosystems (Hall Jr and Meyer, 1998). This is to say that food webs based on detritus have perhaps a very different behavior from other food webs. In fact has been argued that detritus based food webs are not controlled by predators, whereas only by the source (Moore and de Ruiter, 2012) (mainly allochthonous detritus such as in the deep sea) and have been called "donor-controlled" food webs (DeAngelis, 1980; Moore and de Ruiter, 2012). Examples considering detritus as allochthonous source have been described e.g. by Polis and Strong (1996) and Moore et al. (2004).

This hypothesis (the donor control) induced e.g. Huxel and McCann (1998) to study allochthonous versus autochthonous sources in food webs finding that the food webs collapsed when the allochthonous source predominates. So, an allochthonous resource brings instability in the network. Also our simulation found high instability related to the (allochthonous) inputs. In some cases, components tended to zero (e.g. predators near to TL=3) or even very high (e.g. the zooplankton due to the fact that no more predators existed and which can be more competitive than other components with the same TL).

In addition we did not find significant effect with respect to fishing pressure (and we simulated almost to the extinction of the red shrimp). The changes we detected as discussed are not evidences of trophic cascades. Even though, their existence (that we called *shift* in Chapter 6) may have the role of indicators of direct or indirect effects of some perturbations on the ecosystem.

We then considered the occurrence of these changes as an indicator of the strength of the perturbation in order to point out the relative importance between top-down (fishery) and bottom-up drivers (resource availability). We detected an unequivocal dominance of bottom-up forces. In fact both mechanisms can affect some aspect of the fauna and their strength may be scale-dependent and vary seasonally and spatially. Thus, it is of great utility to seek evidence for where and when each mechanism is likely to have its greatest effect.

But except to the observation or not of trophic cascade the simulation was designed also in order to define the relative importance of top-down and bottom-up processes. The latter in fact returned a very important role of source availability in re-organizing the bathyal food webs much more than the fishing activity. Many studies in the past claimed the always important bottom-up in comparison to the top-down drivers (i.e. Shurin et al., 2012).

8 Conclusions

8.1 Conclusions

1. Our analysis showed that the infaunal assemblage changes in compsition in relationship to the nutritional value of sediments, TOC, C/N, δ^{13}C, that are different in and outside the canyon. In the canyon surface deposit feeders (e.g. Ampharetidae and *Amphiura chiajei*), linked to fresh organic matter, are always dominant and occasionally are accompanied by opportunistic groups (e.g. Capitellidae), able to adapt their feeding behaviour according to food availability and to respond rapidly to temporal changes in food inputs. At the adjacent slope, where sediments are refractory, subsurface deposit feeders (e.g. sipunculans) are abundant.

2. According to the generalized regression modelling, the variables explaining the Landing per Unit Effort variation in red shrimp fishery were of three types: fishery-related, temporal and finally economic variables and they captured the 43% of the total variability. In descending order of importance they are: time, number of trips, shrimp price, gross registered tonnage, boats and period of the year. Fishery-dependent data provided an index reasonably similar to fishery-independent indices from bottom-trawls surveys. Moreover, the detection of influential variables, such as the number of trips, can be used to define a threshold on the number of daily trips and is of practical use in fisheries management.

3. I conclude that regression models based on Bayesian inference, such as Distributional Structured additive models (DSTAR), compare favourably with the traditional regression models of GAM type. In our case, DSTAR allowed to 1) objectively define the response distribution function, 2) specify fixed and random effects in a Mixed Model setting, 3) Specify unobserved catching units (boats) and correlated observations as random effects. 4) Finally, if boats really hold random effects, then there is no need to consider them for standardization.

4. I conclude that the LIM Methodology has the ability to reconstruct quantitatively the food web even when the problem is under-determined in data-limited contexts, such as the deep sea. This method also provided a measure of the uncertainty in the estimations of flows.

5. In the dynamic simulation of the food web we found no evidence of top-down mechanism due to fishery, i.e. trophic cascades for all possible pathways.

On the contrary bottom-up controls occurs especially when resources are limited (scenarios of low input of organic matter). In fact, modifying the fishing effort maintaining the input constant the proportions of components do not change in time. On the contrary the proportion changes when the resource is modified. The continental slope ecosystem is based on detritus derived from the upper photic systems. We thus conclude that our detritus based food web is affected by the dynamics of the source and not by the (top)consumer, a control type called "donor control".

APPENDICES

A

Bathyal species

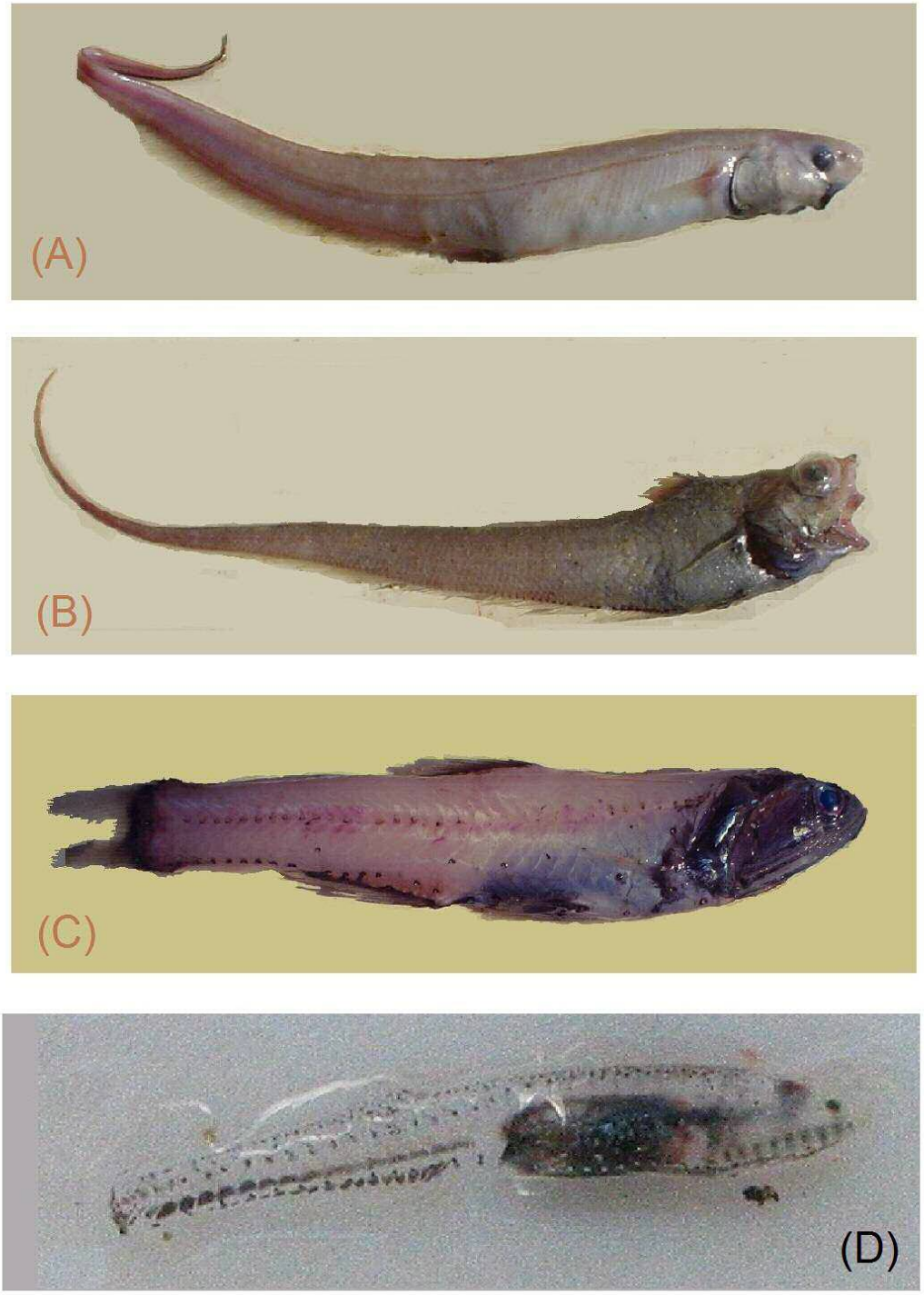

FIGURE A.1: Deep-sea fish. A) The Shortfin spiny eel *Notacanthus bonaparte* Risso, 1840. Latium, MEDITS-IT, 2004; B) The macrurid Roughtip grenadier *Nezumia sclerorhynchus* (Valenciennes, 1838). Latium, MEDITS-IT, 2004; C) The Jewel lanternfish *Lampanyctus crocodilus* (Risso, 1810). Latium, MEDITS-IT, 2004; D) *Cyclothone braueri*, Jespersen & Tåning, 1926. Antromare survey, 2010.

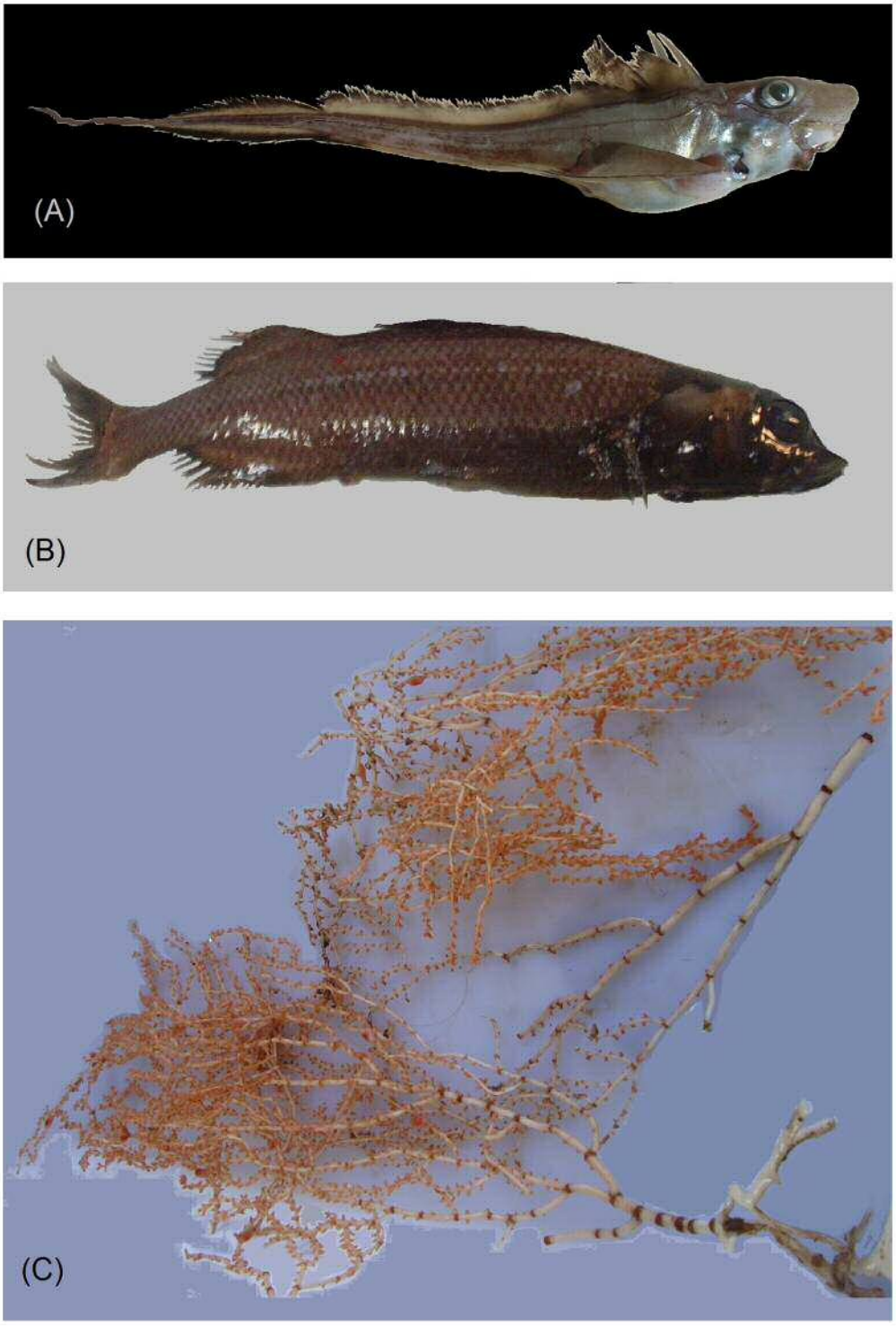

FIGURE A.2: 1) The Rabbit fish *Chimaera monstrosa*, Linnaeus, 1758. Latium, MEDITS-IT, 2003; 2) *Alepocephalus rostratus* Risso, 1820. Catalan Sea, Biomare 2007; 3) The deep-water coral *Isidella elongata*. Catalan Sea, Antromare July 2011.

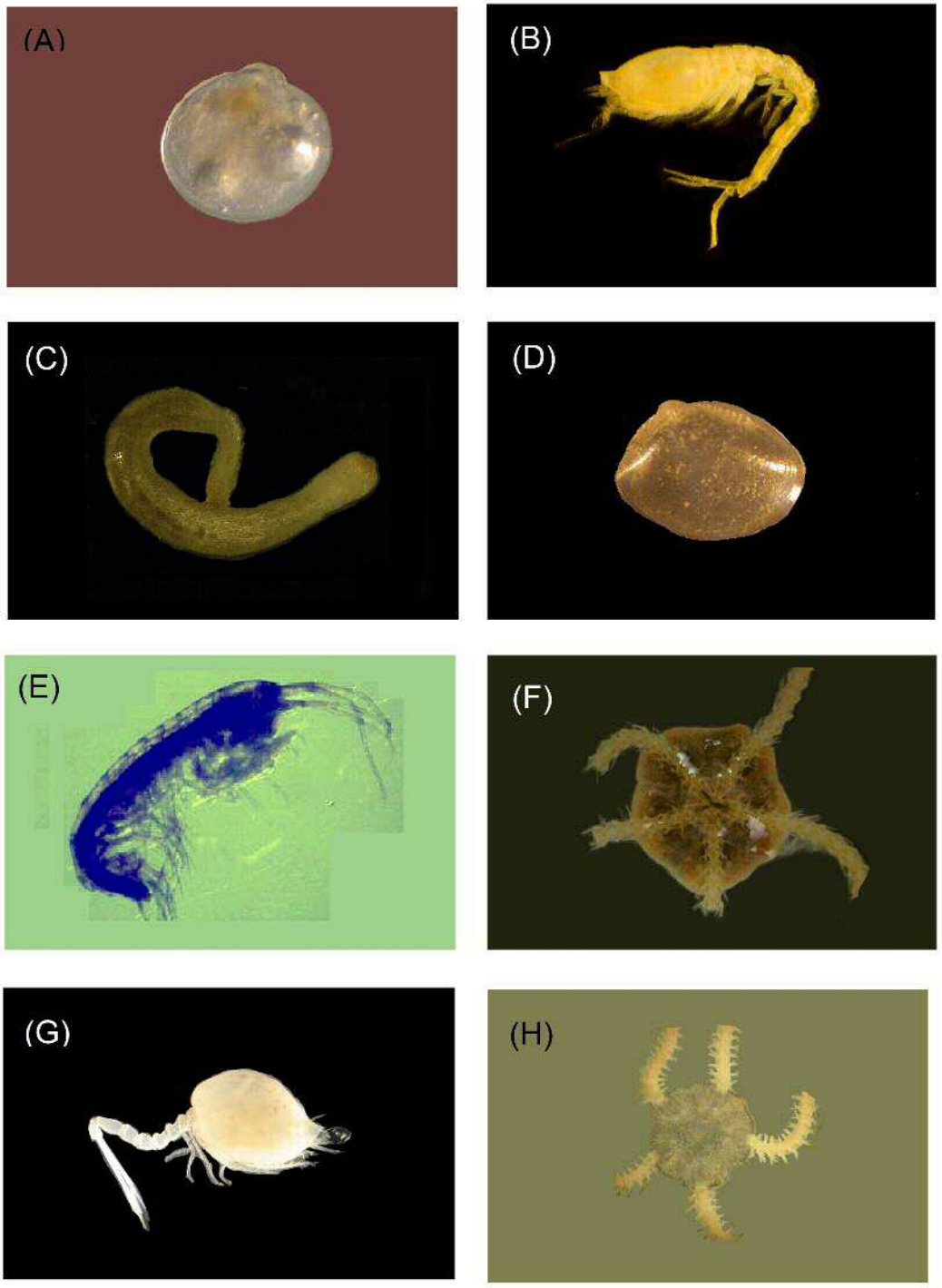

FIGURE A.3: A) The bivalve *Kelliella miliaris* (Philippi, 1844) B) The cumacean *Leucon* (*Epileucon*) *longirostris* Sars, 1871, ♂; C) A caudofoveat belonging to the genus *Falcidens* Salvini-Plawen, 1968; D) The bivalve *Ennucula aegeensis* (Forbes, 1844); E) The amphipod *Carangoliopsis spinulosa* Ledoyer, 1970; F) The ophiurid *Amphiura chiajei* Forbes, 1843 (oral view); G) *Campilaspis glabra* G. O. Sars, 1879; H) The ophiurid *Amphipholis squamata* (Delle Chiaje, 1828) (dorsal view). Specimens from boxcorer and suprabenthic sledge. Biomare 2007, Antromare 2010-2011.

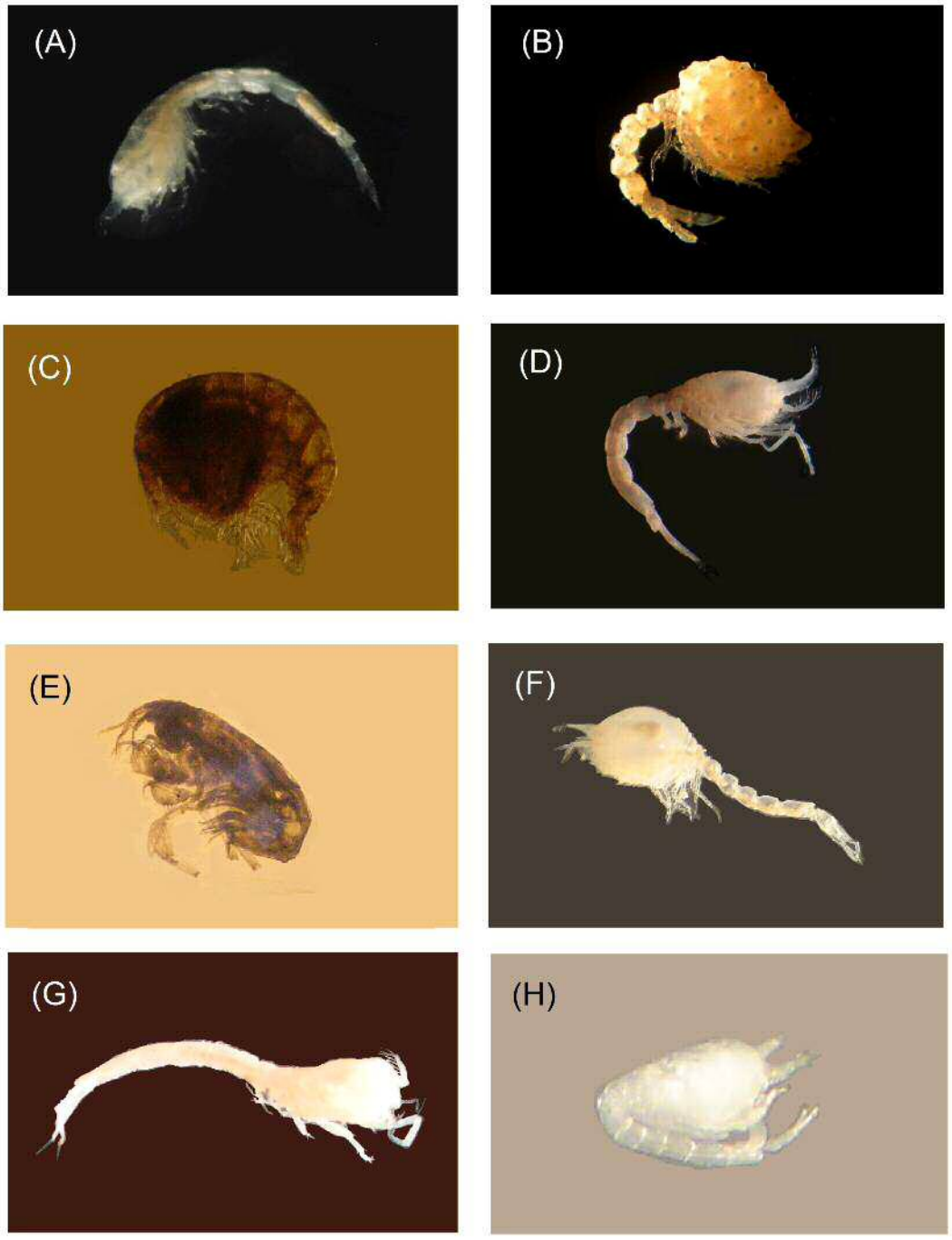

FIGURE A.4: A) *Leucon* (*Macrauloleucon*) *siphonatus* Calman, 1905; B) *Campylaspis squamifera* Fage, 1929; C) The amphipod *Stegocephaloides christianiensis* (Boeck, 1871); D) *Leucon* (*Crymoleucon) macrorhinus* Fage, 1951; E) The amphipod *Idunella nana* (Schiecke, 1973); F) *Diastyloides serrata* (Sars G.O., 1865); G) *Eudorella truncatula* (Bate, 1856); H) Postnauplius of a cumacean (probably *L. longirostris*). Specimens from boxcorer and suprabenthic sledge. Biomare 2007, Antromare 2010-2011.

B

Field and Laboratory material

FIGURE B.1: Boxcorer. B/O García del Cid, Catalan Sea, BIOMARE October, 2007.

FIGURE B.2: Multicorer. B/O García del Cid, Catalan Sea, BIOMARE October, 2007.

FIGURE B.3: (A) WP2 used to sample zoplankton and micronekton. (B) Suprabenthic sledge used to sample suprabenthos. B/O García del Cid, Catalan Sea, BIOMARE October, 2007.

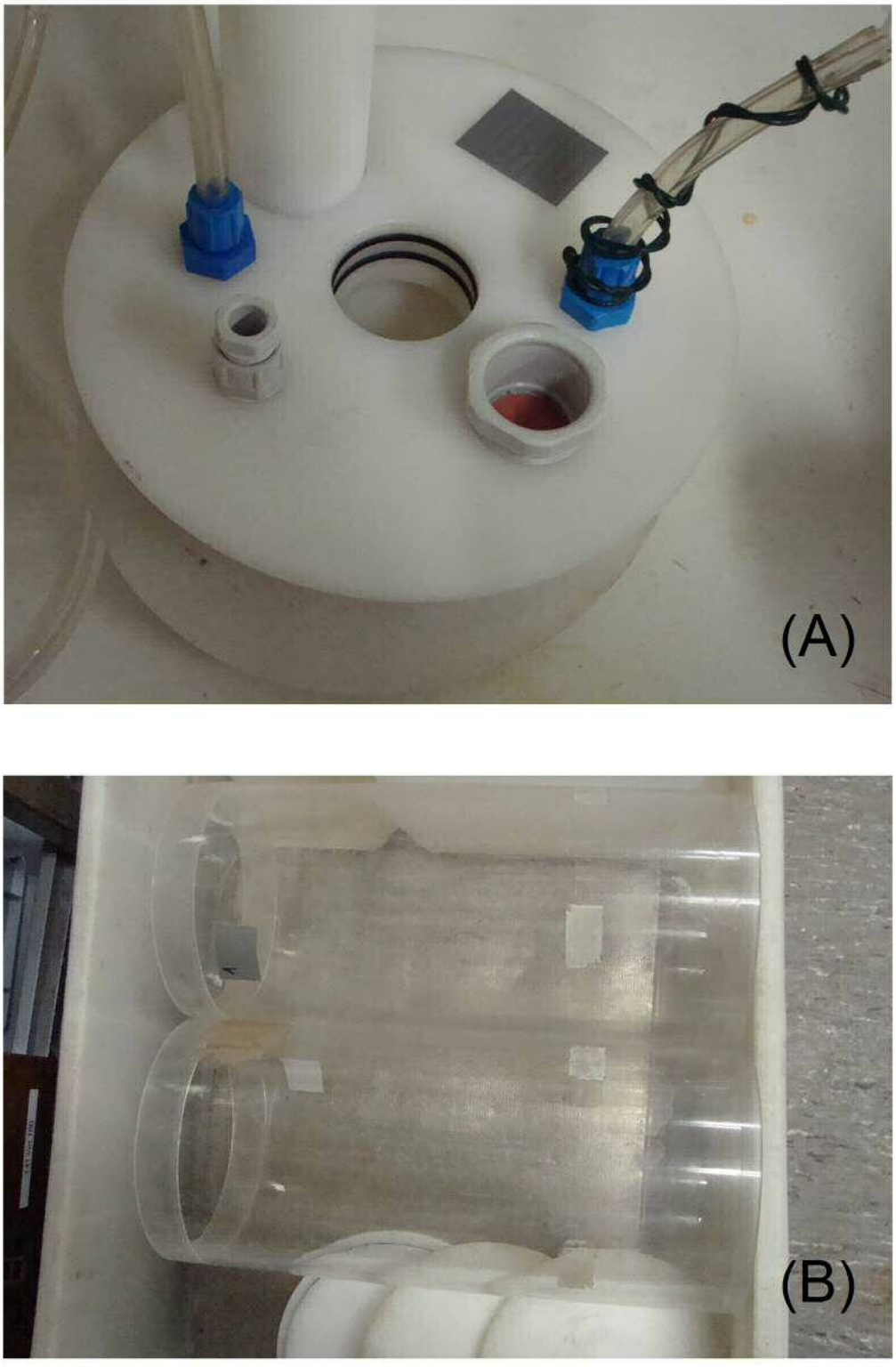

FIGURE B.4: A) A lid with different holes used to introduce the stirrer, sensors for digital records or pipettes for the Winkler titration; B) The perspex chambers (d = 30 cm). All material provided by the Ecosystem studies department of the NIOZ-Yerseke.

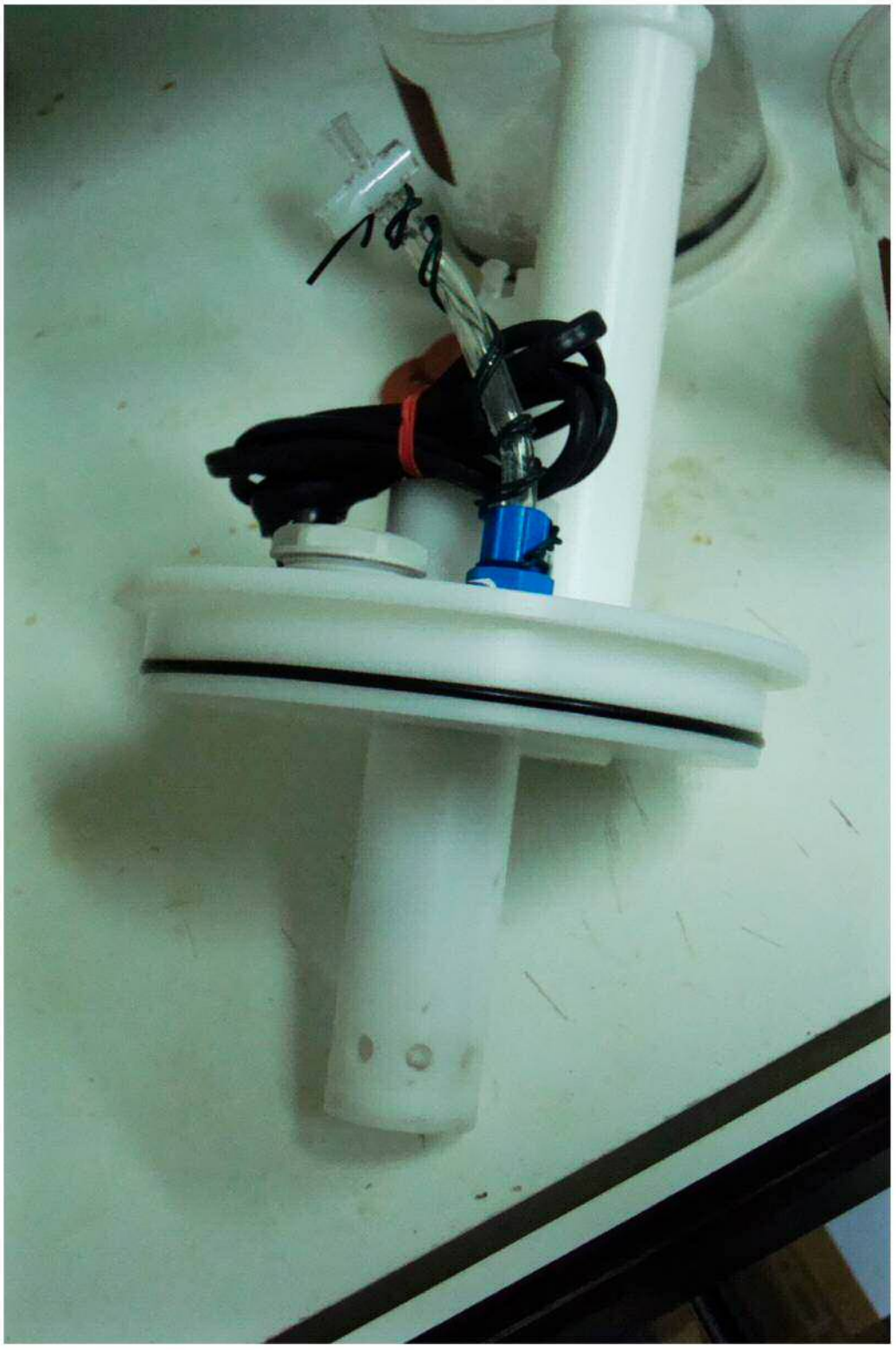

FIGURE B.5: A lip containing a Teflon-coated magnetic stirrer. All material provided by the Ecosystem studies department of the NIOZ-Yerseke.

FIGURE B.6: An incubation with water. Prepearing experiments at the NIOZ-Yerseke, 2011.

C

Complementary material – Chapter 3

C.1 Exploratory study on the response variable LPUE

In Figure C.1 are shown the characteristics of the variable *lpue*.

The probability density function (*pdf*) is positively skewed (upper panels). Data hold atypical values in the right tail (see the box-plot, left middle panel) and the distribution function of the gamma distribution lies approximately inside the 95%

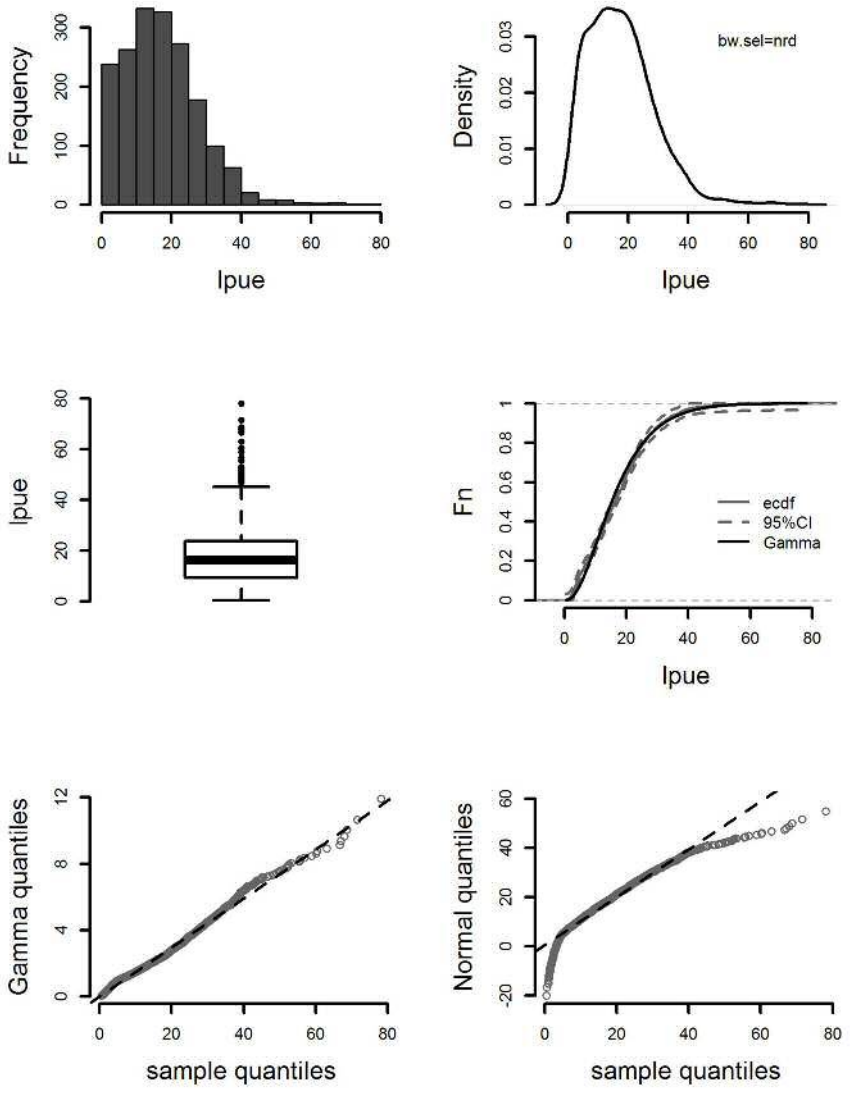

FIGURE C.1: From left to right, upper panels, histogram and kernel density estimations of lpue; middle panels, box-plot and cumulative distribution function of data and of the gamma distribution; lower panels, QQ-plots of sample quantiles versus gamma and normal distribution quantiles.

confidence intervals of the empirical cumulative distribution function (*ecdf*) of *lpue* (right middle panel). Finally, the QQ-plots for the gamma and the Gaussian distributions provide evidence of a better fit of data to the gamma rather than the Gaussian distribution (on the left and the right lower panels respectively).

C.2 Diagnostic plots of the final model

Figure C.2 shows the diagnostic plots for the selected model (corresponding to Equation 3.4 in the text and model 7 in Table 3.2, Chapter 3).

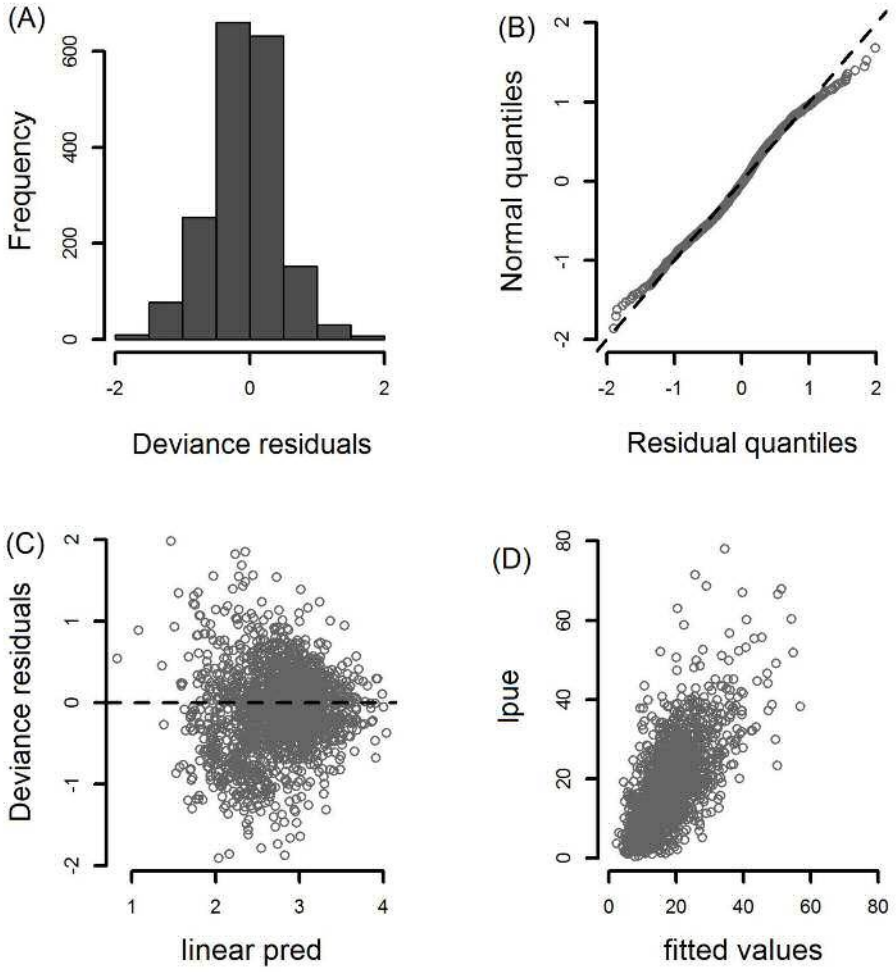

FIGURE C.2: Residual diagnostics for model 7. (A) Histogram of deviance residuals; (B) QQ-plot of deviance residuals; (C) deviance residuals against linear predictor; (D) response against fitted values.

Residual quantiles lie on the straight line of the theoretical quantiles, although slightly heavy-tailed; in the histogram, residuals are consistent with normality and the relationship between response and fitted values is linear and positive. Residuals versus the linear predictor (that is, the sum of all partial effects) show a faint heteroscedasticity.

D

Complementary material – Chapter 4

D.1 Model selection

All global results of estimated models in order to select the best final model are given in Tables D.1 (LN models) and D.2 (GA models).

	PRED	VAR	DEV	EP	DIC
		NULL	17744.4	2.06493	17748.5
1a)	η_μ	code	17016.4	21.5726	17059.5
		code trips	16552.1	26.5423	16605.1
		code trips time	16185.7	44.6647	16275.1
		code trips time grt	NA	NA	NA
		code trips time period	16170.7	45.6919	16262.1
		code-trips-time period nao	**16163.9**	**47.0787**	**16258**
1b)	η_μ	code trips-time period nao			
	η_{σ^2}	code	15805.5	68.1142	15941.7
		code trips	15427.2	73.2771	15573.7
		code trips time	**15138.4**	**91.1983**	**15320.8**
		code trips time period	15139.2	91.6031	15322.4
		code trips time nao	15139.8	92.432	15324.7
2a)	η_μ	code	17016.9	21.5708	17060
		code trips	16553	25.463	16603.9
		code trips time	16186.5	44.0283	16274.6
		code trips time grt	16186.7	43.7525	16274.2
		code trips time period	16171.1	45.1612	16261.4
		code trips time nao	16180.6	46.1108	16272.8
		code trips time period nao	**16164.2**	**46.7896**	**16257.7**
2b)		code trips time period nao grt	16164.8	47.0348	16258.9
	η_μ	code trips time period nao			
	η_{σ^2}	code	15808.2	66.493	15941.2
		code trips	15430	71.1313	15572.2
		code trips time	**15142.7**	**87.2506**	**15317.2**
		code trips time nao	15145.2	88.6634	15322.5

TABLE D.1: Global scores for LN models. 1a) fixed effects models with predictor η_μ, 1b) fixed effects models with predictors η_μ and η_{σ^2}, 2a) mixed effects models with predictor η_μ, 2b) mixed effects models with predictors η_μ and η_{σ^2}. PRED: specifies the predictor, and VAR: defines the variables in the corresponding predictor. DEV: residual deviance; EP: Effective total number of Parameters, DIC: Deviance Information Criterion. Models without global scores could not be estimated (see the corresponding Chapter).

D.2 Comparison of partial effects among models

Also smooth effects of all models M1-M8 are shown in Figures D.1, D.2, D.3, D.4, D.5, D.6. All models return reasonably similar results. Even so, some important differences can be observed in *time* effects. Let concentrate on the second part of the corresponding functions, after the important low in 2000 up to the end. In

	PRED	VAR	DEV	EP	DIC
		NULL	17302.7	2.00455	17306.7
1a)	η_μ	code	16719.5	22.1251	16763.7
		code trips	16412.4	25.9486	16464.3
		code trips time	16127.9	42.2318	16212.3
		code trips time grt	NA	NA	NA
		code trips time nao	16118.9	44.5393	16208
		code trips time nao period	**16095.7**	**45.6132**	**16187**
1a)	η_μ	code trips time nao period			
	η_σ	code	15700.2	66.5351	15833.3
		code trips	15282.2	71.7128	15425.6
		code trips time	**15027.1**	**90.8856**	**15208.9**
		code trips time nao	15033	92.5788	15218.2
		code trips time period	15026.3	91.2336	15208.8
2a)	η_μ	code	16720.1	21.4365	16763
		code trips	16413.2	24.4744	16462.2
		code trips time	16128.5	41.309	16211.1
		code trips time nao	16119.5	43.6533	16206.8
		code trips time nao period	**16096.8**	**43.9236**	**16184.7**
		code trips time nao period grt	16096.7	44.2528	16185.2
2b)	η_μ	code trips time nao period			
	η_σ	code	15703.1	64.5204	15832.1
		code trips	15285.7	69.3473	15424.4
		code trips time	**15032.4**	**86.8765**	**15206.1**
		code trips time nao	15037.5	88.4923	15214.4
		code trips time period	15031.3	88.0569	15207.4
		code trips time grt	15032.8	87.049	15206.9

TABLE D.2: Global scores for GA models. 1a) fixed effects models with predictor η_μ, 1b) fixed effects models with predictors η_μ and η_σ, 2a) mixed effects models with predictor η_μ, 2b) mixed effects models with predictors η_μ and η_σ. PRED: specifies the predictor, and VAR: defines the variables in the corresponding predictor. DEV: residual deviance; EP: Effective total number of Parameters, DIC: Deviance Information Criterion. Models without global scores could not be estimated (see text).

models accounting only for location parameter (Figures D.1 and D.4) the estimations show a second low that is not present in those models accounting for both parameters. This second low exists due to a moderate but concentrated number of low values of the response but data also hold high variability during last years, so these models tend to skip this variability, under-fitting the data and highlight the scant landing. On the contrary GA models accounting for both parameters do not model this second low in the predictor for μ, while they better capture the oscillation of data (Figures D.5 and D.6). Finally LN models accounting for both parameters capture both negative and positive picks (Figures D.2 and D.3). So then it seems they capture the "best" shape. However none of the models correctly estimate the numerous changes that LPUE showed in last years, when four positive picks can be observed in the time series of the raw LPUE (see Figure 3.1 in Chapter 3). Note also that in the raw series the low captured by the model is not easy to detect within the cloud of observations.

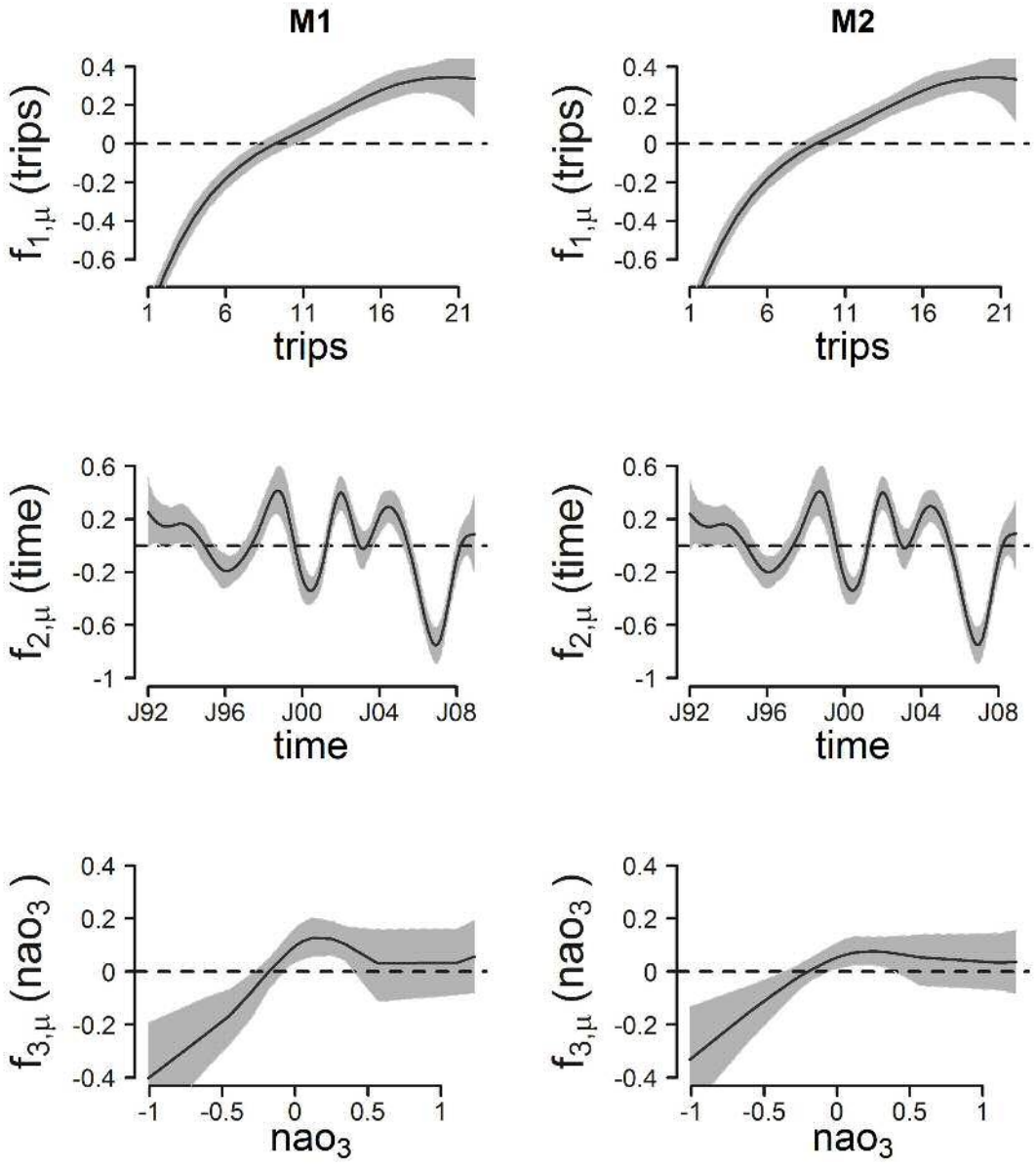

FIGURE D.1: Nonparametric effects on the predictor for μ for the LN fixed effect model M1 and the mixed effects model M2 with best DIC score. Grey shapes represent 95% credible intervals.

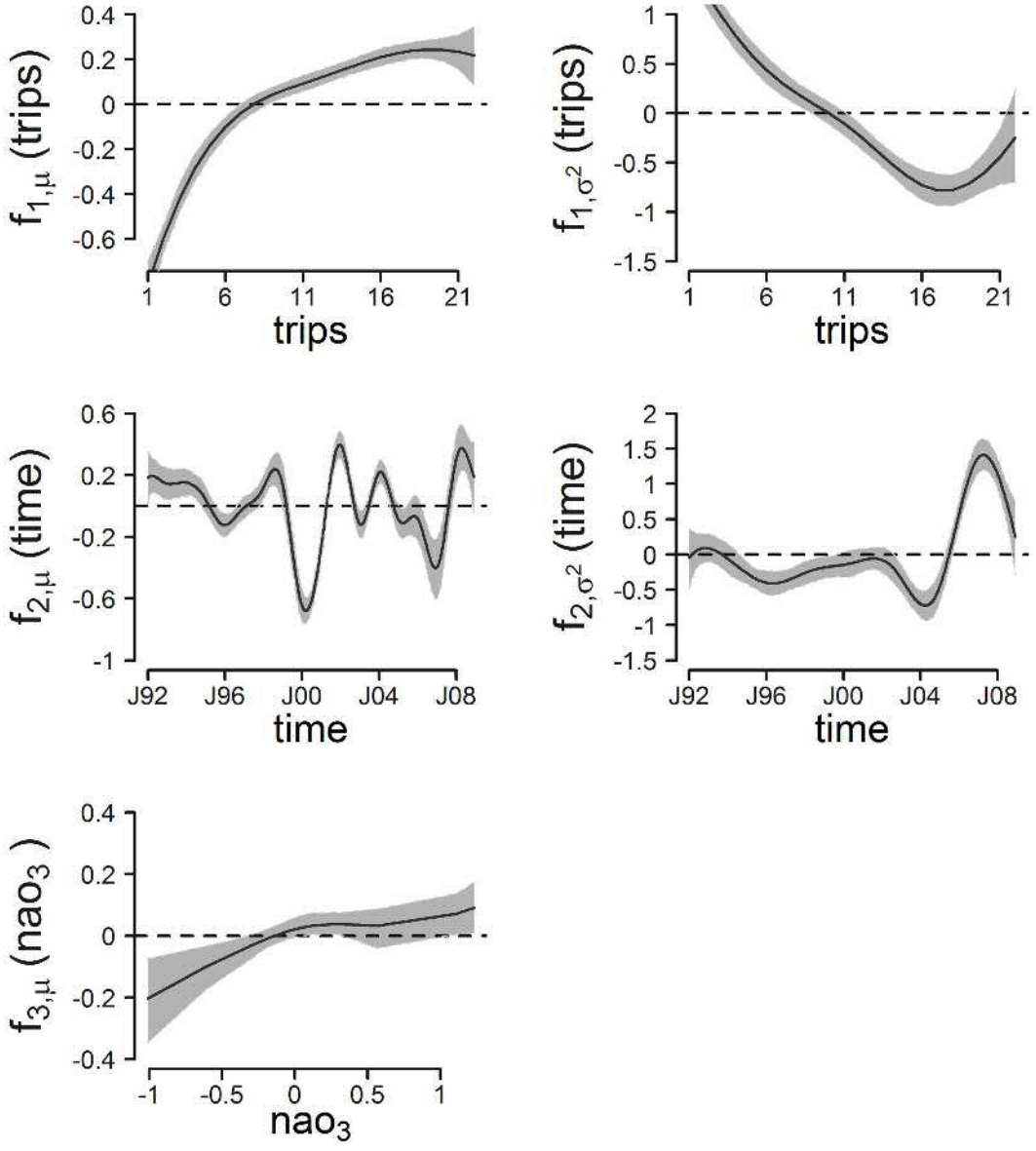

FIGURE D.2: Nonparametric effects for the LN fixed effect model M3 with best DIC score. Effects on predictor for μ (left side) and for σ^2 (right side). Grey shapes represent 95% credible intervals.

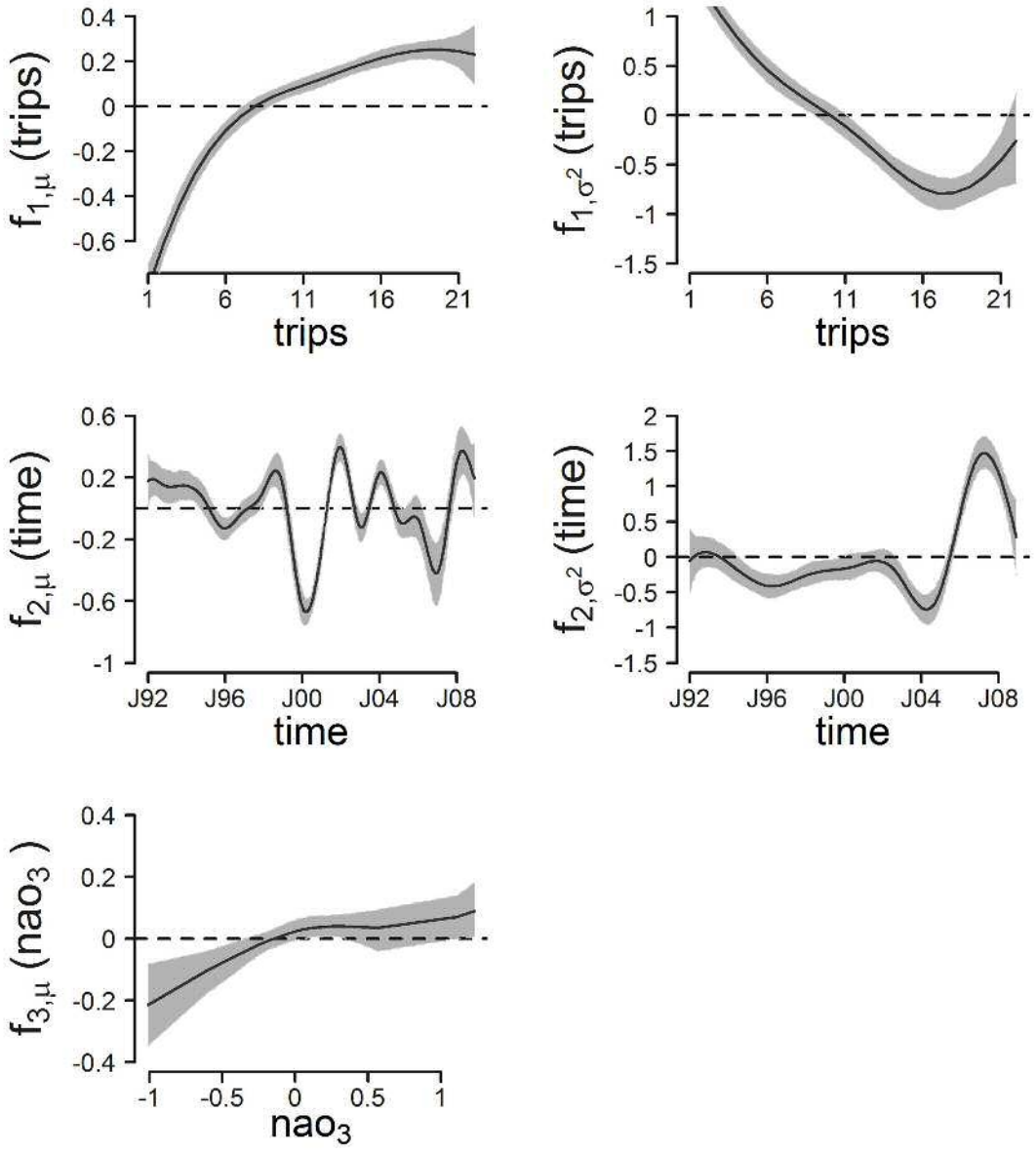

FIGURE D.3: Nonparametric effects for the LN mixed effect model M4 with best DIC score. Effects on predictor for μ (left side) and for σ^2 (right side). Grey shapes represent 95% credible intervals.

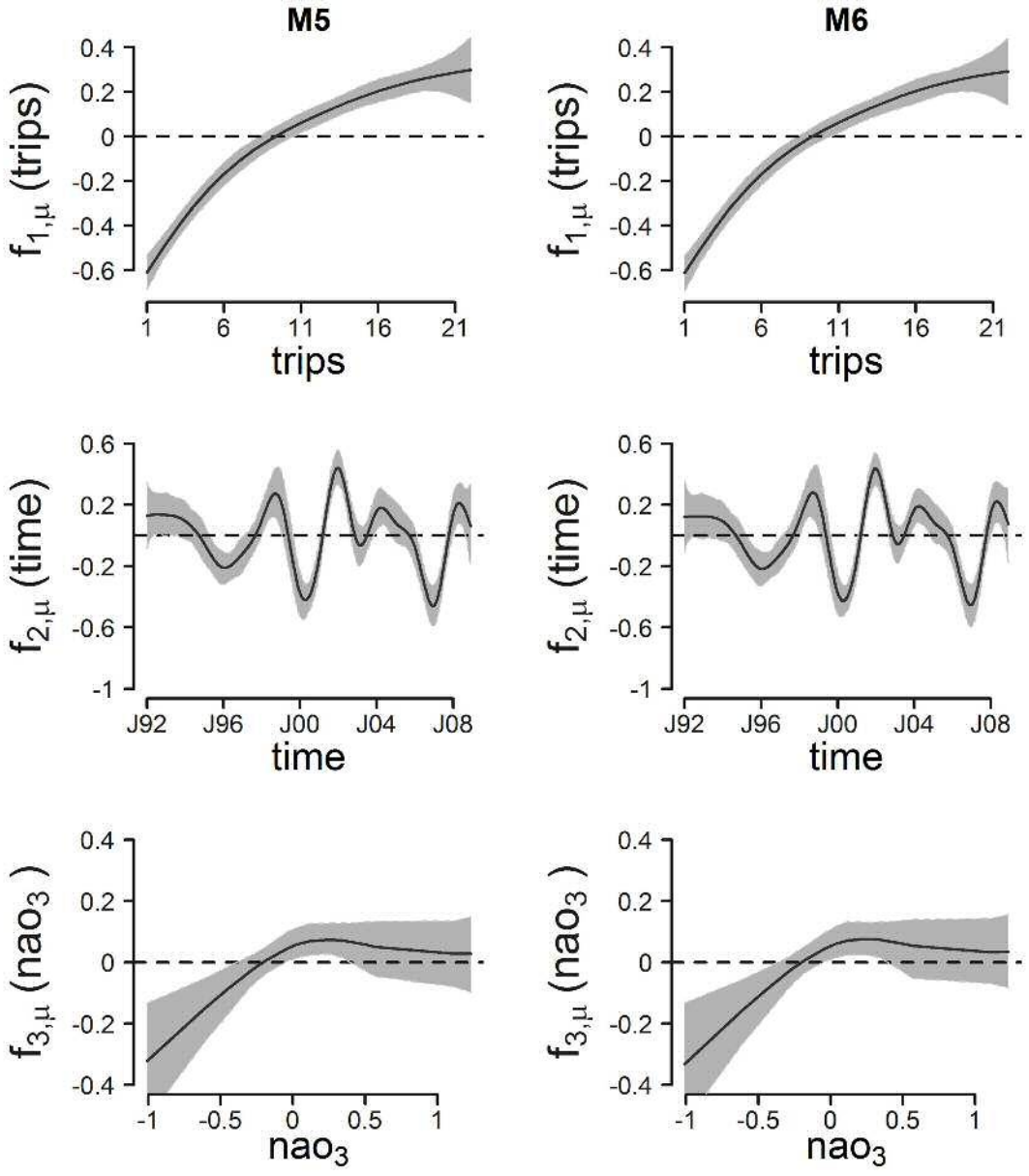

FIGURE D.4: Nonparametric effects on the predictor for μ for the GA fixed effect model M5 and the mixed effects model M6 with best DIC score. Grey shapes represent 95% credible intervals.

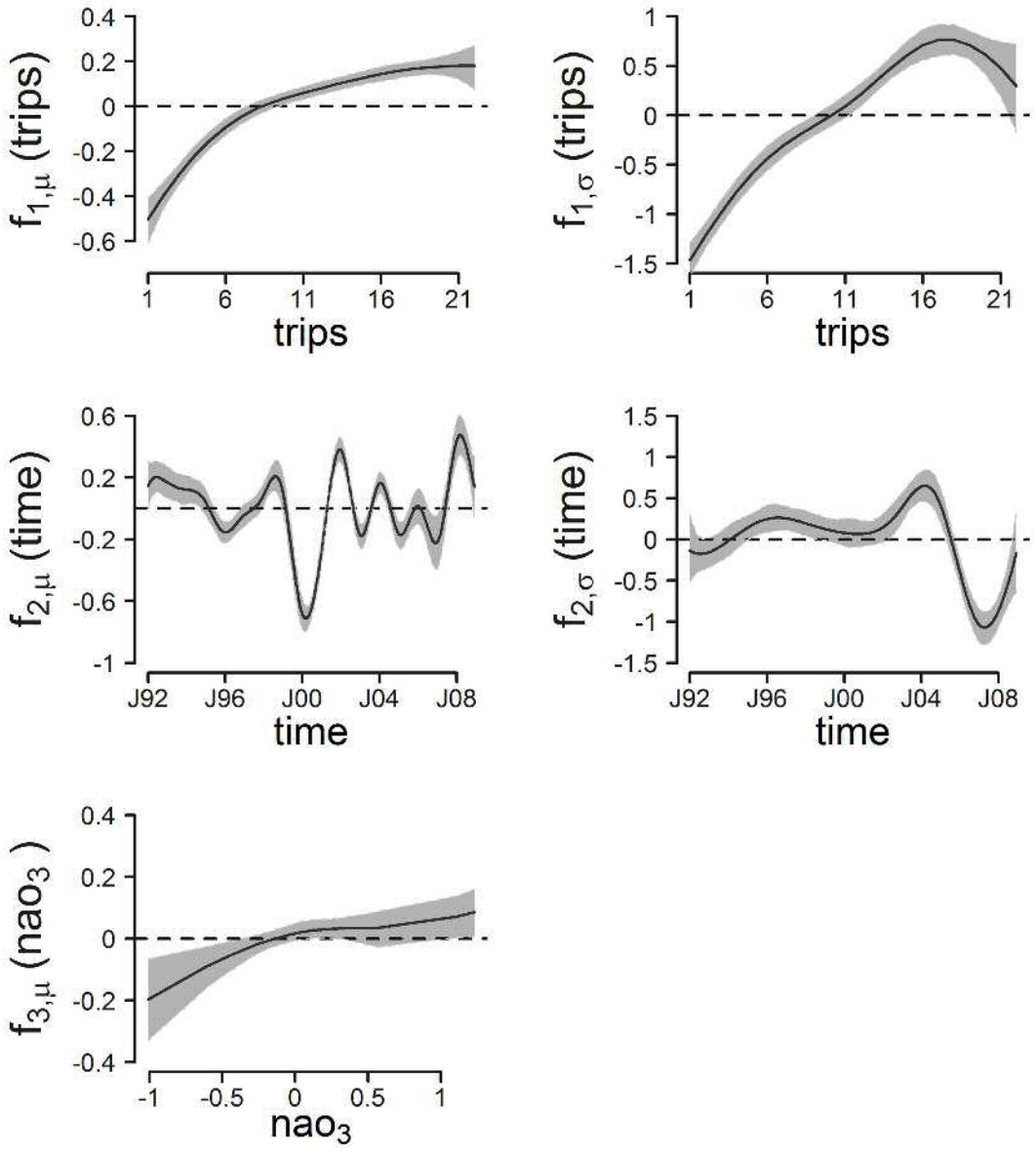

FIGURE D.5: Nonparametric effects for the GA fixed effect model M7 with best DIC score. Effects on predictor for μ (left side) and for σ (right side). Grey shapes represent 95% credible intervals.

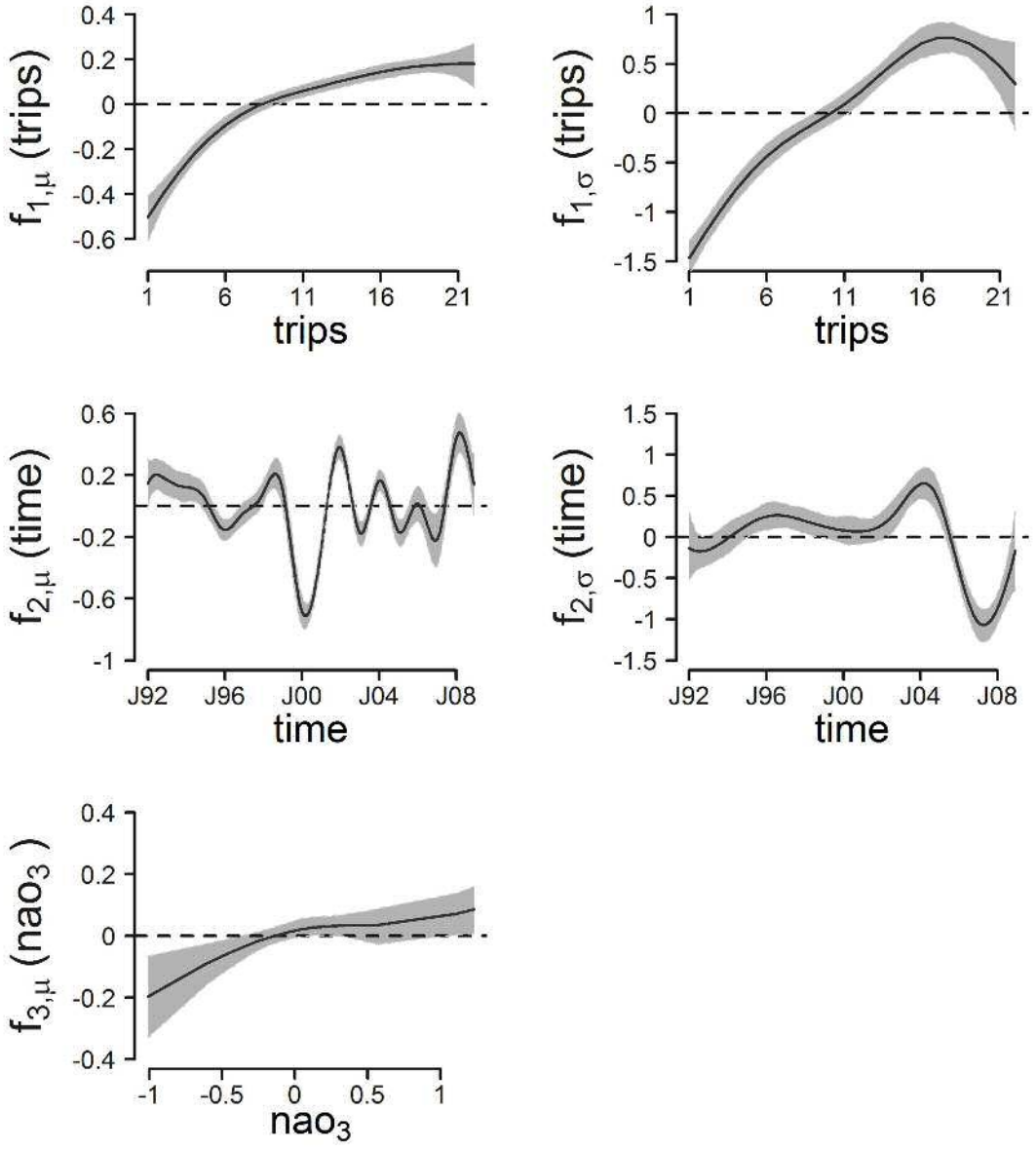

FIGURE D.6: Nonparametric effects for the GA mixed effect model M8 with best DIC score. Effects on predictor for μ (left side) and for σ (right side). Grey shapes represent 95% credible intervals.

E

Complementary material – Chapter 5

E.1 Sediment Oxygen Consumption

The sediment community oxygen consumption rates in Figure 5.3, Chapter 5 with respect to the depth derive from the R-package ecolMod (see Andersson et al. 2004. Experiments were performed in situ incubations or via modelling of oxygen microprofiles. Here the SCOC is in mmol O_2 m^{-2} d^{-1} equivalent to mmol C m^{-2} d^{-1}. The model in the Figure is derived by a log-log regression

$$log(scoc) = \beta_0 + \beta_1 log(depth) + \epsilon, \tag{E.1}$$

where *scoc* is the response variable, *depth* the explanatory variable and β_0 and β_1 are the intercept and the slope respectively, while ϵ is the error term of the regression. Thus, the model can be expressed as

$$scoc = a \times depth^b \tag{E.2}$$

where the parameters are $a = \exp(\beta_0)$ and $b = \beta_1$.

E.2 LIM equations

All equations incorporated in the food web model in Chapter 5 are shown in Table E.2 and Table E.1 and all parameters used to constrain the model are shown in

(A)	Burial of org C = BE × Total org C input
	TOM R = SOC − MACBN R
(B)	A = AE × U
	A − R + MR = NGE × A
	A − R + MR = PR × stock
	R = RR × stock
(C)	$flow_{j \to i}$ = PD × U_j

TABLE E.1: Constraints imposed to the model. (A) TOM compartment, (B) Faunal compartments, (C) Diet constraint (only for the red shrimp). A: assimilation, R: respiration, U: Uptake. SOC = sediment oxygen consumption; BE = burial efficiency; RR = respiration rate; NGE = net growth efficiency; AE = assimilation efficiency; MR = maintenance respiration; PR = production rate; DP = proportion of source j in the diet of predator j.

table E.3.

E.3 Results of the food web model

Figure E.1 shows the range estimations of the flows, a measure of both feasibility and uncertainty, however better estimator of flows' quality is represented by the

$\frac{d\ \text{TOM}}{dt} = 0 =$	OMv → TOM + OMa → TOM + ZPLMNK → TOM +MACBN → TOM + SUPBN → TOM + AANT → TOM +MEGAICT → TOM + MEGABN → TOM −TOM → MACBN − TOM → MEGABN −TOM → AANT − TOM → BUR − TOM → DIC
$\frac{d\ \text{ZPLMNK}}{dt} = 0 =$	OM_v → ZPLMNK + OM_a → ZPLMNK − ZPLMNK → MEGABN −ZPLMNK → MEGAICT − ZPLMNK → AANT −ZPLMNK → TOM − ZPLMNK → DIC
$\frac{d\ \text{MACBN}}{dt} = 0 =$	OMv → MACBN + OMa → MACBN +TOM → MACBN − MACBN → AANT −MACBN → MEGABN − MACBN → MEGAICT −MACBN → TOM − MACBN → DIC
$\frac{d\ \text{SUPBN}}{dt} = 0 =$	OMv → SUPBN + OMa → SUPBN −SUPBN → AANT − SUPBN → MEGABN −SUPBN → MEGAICT − SUPBN → TOM − SUPBN → DIC
$\frac{d\ \text{MEGABN}}{dt} = 0 =$	TOM → MEGABN ZPLMNK → MEGABN + SUPBN → MEGABN +MACBN → MEGABN −MEGABN → AANT −MEGABN → TOM − MEGABN → DIC
$\frac{d\ \text{MEGAICT}}{dt} = 0 =$	ZPLMNK → MEGAICT + SUPBN → MEGAICT +MACBN → MEGAICT + MEGABN → MEGAICT +AANT → MEGAICT − MEGAICT → BYCATCH −MEGAICT → TOM − MEGAICT → DIC
$\frac{d\ \text{AANT}}{dt} = 0 =$	TOM → AANT + ZPLMNK → AANT + SUPBN → AANT +MACBN → AANT + MEGABN → AANT +MEGAICT → AANT −AANT → MEGABN − AANT → MEGAICT −AANT → LANDINGS − AANT → TOM − AANT → DIC

TABLE E.2: Equations of the binary food web and steady-state assumption incorporated in the food web model.

Process	Value	units	Ref.
Tlim	0.54	–	1
SOC	[0.888,2.19]	mmol C m^{-2} d^{-1}	2
BE	[0.105,0.36]	–	3
Faunal MR	Tlim * 0.01 * stock	mmol C m^{-2} d^{-1}	4
RR of ZPLMNK and SUPBN	[0.0001,0.032]	d^{-1}	5
RR of MACBN	[0.0055,0.012]	d^{-1}	5
RR of MEGABN	[0.0029,0.008]	d^{-1}	6
RR of MEGAICT	[0.00023,0.0087]	d^{-1}	5
RR of AANT	[0.0051,0.039]	d^{-1}	5
NGE of ZPLMNK and SUPBN	[0.7,0.9]	–	4
NGE of other Fauna	[0.5,0.7]	–	4
ZPLMNK PR	Tlim*[0.01,0.05]	d^{-1}	7
SUPBN PR	[0.00487,0.06882]	d^{-1}	8
MACBN PR	[0.0014,0.0689]	d^{-1}	8
MEGABN PR	[0.00055,0.01373]	d^{-1}	7,9
MEGAICT PR	Tlim*[0.00274,0.0137]	d^{-1}	7
AE on OM	[0.29,0.77]	–	7
AE on fauna	[0.10,0.60]	–	4
MACBN DP on OMv	[0,0.25]	–	9,10
MACBN DP on TOM	[0.75,1]	–	9,10
AANT DP on MACBN	[0.15,0.34]	–	11
AANT DP on MEGABN	[0.1,0.25]	–	11
AANT DP on SUPBN	[0.11,0.33]	–	11
AANT DP on ZPLMNK	[0.12,0.67]	–	11
AANT FR	[0.5E-003,0.046]	mmol C m^{-2} d^{-1}	12
MEGAICT CR	AANT FR × 3	mmol C m^{-2} d^{-1}	9,12
MEGABN CR	AANT CR × 5E-003	mmol C m^{-2} d^{-1}	9,12

TABLE E.3: Parameters and constrains for the food web model. In brackets minimum and maximum values of parameters are reported, while single values correspond to the mean of parameters. *Tlim* = temperature limitation; SOC = sediment oxygen consumption; BE = burial efficiency; RR = respiration rate; NGE = net growth efficiency; AE = assimilation efficiency; MR = maintenance respiration; PR = production rate; DP = proportion of source j in the diet of predator j; FR = fishing rate; CR = catch rate. References: (1) Epping et al., 2002, (2) Own data from ANTROMARE survey, (3) Burdige et al., 1999, (4) van Oevelen et al., 2006 and references therein, (5) Mahaut et al., 1995, (6) Company and Sardà, 1998, (7) van Oevelen, Soetaert, García, de Stigter, Cunha, Pusceddu and Danovaro, 2011, (8) Cartes, Brey, Sorbe and Maynou, 2002, (9) Own data from BIOMARE survey, (10) Fauchald and Jumars, 1979, (11) Cartes, Papiol and Guijarro, 2008, (12) From longitudinal data of the Catalan government.

Coefficient of Variation shown in Table E.5.

Tables E.4 and E.5 return all estimations of flows in mmol C m^{-2} d^{-1} derived from the existing types of solution methods: (1) range (minimum and maximum), (2) least distance, (3) least square (mean) solutions, (4) Markov Chain Monte Carlo (mean and standard deviation) and the Coefficient of Variation (CoV).

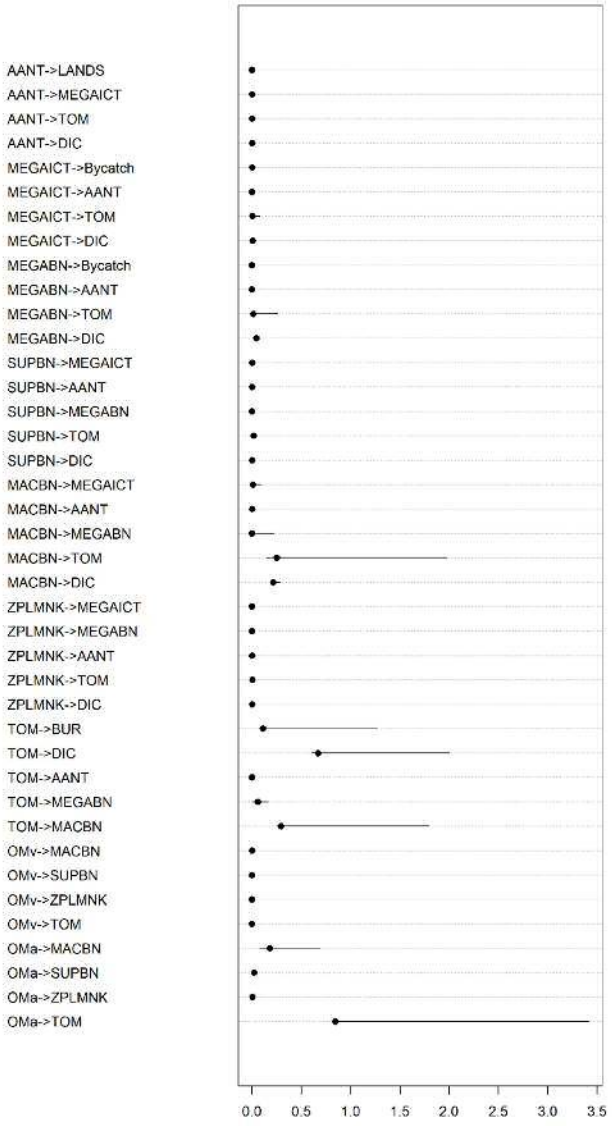

FIGURE E.1: Range estimation of food web flows. The dark point represents the parsimonious solution, the segments minimum to maximum ranges.

flow	min	max	mean$_{ldei}$	mean$_{lsei}$
OMa → TOM	8.44E-001	3.42E+000	8.44E-001	8.44E-001
OMa → ZPLMNK	1.22E-005	6.20E-003	6.20E-003	6.20E-003
OMa → SUPBN	2.07E-005	2.13E-002	2.13E-002	2.13E-002
OMa → MACBN	7.88E-002	6.90E-001	1.81E-001	1.81E-001
OMv → TOM	0.00E+000	6.08E-003	0.00E+000	0.00E+000
OMv → ZPLMNK	1.22E-005	6.10E-003	6.26E-005	6.26E-005
OMv → SUPBN	2.07E-005	6.14E-003	2.15E-004	2.15E-004
OMv → MACBN	8.58E-004	6.97E-003	1.83E-003	1.83E-003
TOM → MACBN	2.57E-001	1.80E+000	2.94E-001	2.58E-001
TOM → MEGABN	0.00E+000	1.65E-001	5.81E-002	5.81E-002
TOM → AANT	4.41E-005	7.63E-005	4.41E-005	4.41E-005
TOM → DIC	6.03E-001	2.00E+000	6.73E-001	7.00E-001
TOM → BUR	1.10E-001	1.27E+000	1.10E-001	1.10E-001
ZPLMNK → DIC	3.48E-004	7.99E-004	7.99E-004	7.99E-004
ZPLMNK → TOM	2.80E-004	4.45E-003	4.45E-003	4.45E-003
ZPLMNK → AANT	5.88E-004	1.02E-003	1.02E-003	1.02E-003
ZPLMNK → MEGABN	0.00E+000	4.29E-004	0.00E+000	0.00E+000
ZPLMNK → MEGAICT	0.00E+000	4.29E-004	0.00E+000	0.00E+000
MACBN → DIC	1.87E-001	2.85E-001	2.15E-001	1.88E-001
MACBN → TOM	1.45E-001	1.97E+000	2.50E-001	2.42E-001
MACBN → MEGABN	0.00E+000	2.27E-001	0.00E+000	0.00E+000
MACBN → AANT	9.72E-004	2.88E-003	1.67E-003	1.67E-003
MACBN → MEGAICT	8.93E-003	8.77E-002	9.62E-003	9.62E-003
SUPBN → DIC	6.70E-004	1.13E-003	1.13E-003	1.13E-003
SUPBN → TOM	4.76E-004	1.53E-002	1.53E-002	1.53E-002
SUPBN → MEGABN	0.00E+000	4.18E-003	0.00E+000	0.00E+000
SUPBN → AANT	9.23E-004	2.80E-003	1.62E-003	1.62E-003
SUPBN → MEGAICT	0.00E+000	4.18E-003	3.49E-003	3.49E-003
MEGABN → DIC	4.42E-002	4.56E-002	4.42E-002	4.42E-002
MEGABN → TOM	1.34E-002	2.64E-001	1.34E-002	1.34E-002
MEGABN → AANT	5.31E-004	2.12E-003	5.56E-004	5.56E-004
MEGABN → BYCATCH	2.50E-006	2.76E-006	2.50E-006	2.50E-006
MEGAICT → DIC	7.05E-003	7.22E-003	7.05E-003	7.05E-003
MEGAICT → TOM	5.70E-003	7.99E-002	5.70E-003	5.70E-003
MEGAICT → AANT	0.00E+000	4.24E-005	0.00E+000	0.00E+000
MEGAICT → BYCATCH	1.50E-003	1.66E-003	1.50E-003	1.50E-003
AANT → DIC	1.33E-003	2.96E-003	1.33E-003	1.33E-003
AANT → TOM	1.93E-003	5.50E-003	1.93E-003	1.93E-003
AANT → MEGAICT	1.09E-003	1.55E-003	1.14E-003	1.14E-003
AANT → LANDS	5.00E-004	5.53E-004	5.00E-004	5.00E-004

Table E.4: Food web flows' estimations: range (minimum and maximum), least distance and least square (mean) solutions. Flows in mmol C m^{-2} d^{-1}.

flow	mean ± sd	CoV
OMa → TOM	2.28E+000 ± 4.60E-001	2.01E-001
OMa → ZPLMNK	3.17E-003 ± 1.10E-003	3.47E-001
OMa → SUPBN	1.02E-002 ± 3.38E-003	3.31E-001
OMa → MACBN	3.21E-001 ± 1.16E-001	3.62E-001
OMv → TOM	4.64E-004 ± 5.15E-004	1.11E+000
OMv → ZPLMNK	4.91E-004 ± 4.92E-004	1.00E+000
OMv → SUPBN	5.70E-004 ± 5.16E-004	9.04E-001
OMv → MACBN	3.71E-003 ± 1.09E-003	2.94E-001
TOM → MACBN	7.47E-001 ± 3.09E-001	4.14E-001
TOM → MEGABN	8.16E-002 ± 3.82E-002	4.68E-001
TOM → AANT	5.67E-005 ± 5.36E-006	9.46E-002
TOM → DIC	1.58E+000 ± 3.19E-001	2.02E-001
TOM → BUR	7.34E-001 ± 2.79E-001	3.80E-001
ZPLMNK → DIC	5.91E-004 ± 1.12E-004	1.90E-001
ZPLMNK → TOM	2.10E-003 ± 9.81E-004	4.66E-001
ZPLMNK → AANT	8.39E-004 ± 7.41E-005	8.83E-002
ZPLMNK → MEGABN	6.19E-005 ± 5.35E-005	8.64E-001
ZPLMNK → MEGAICT	6.04E-005 ± 5.24E-005	8.67E-001
MACBN → DIC	2.51E-001 ± 2.35E-002	9.37E-002
MACBN → TOM	7.23E-001 ± 3.65E-001	5.05E-001
MACBN → MEGABN	5.64E-002 ± 4.62E-002	8.19E-001
MACBN → AANT	2.01E-003 ± 2.24E-004	1.11E-001
MACBN → MEGAICT	3.98E-002 ± 2.01E-002	5.06E-001
SUPBN → DIC	1.05E-003 ± 6.63E-005	6.31E-002
SUPBN → TOM	6.15E-003 ± 3.07E-003	4.99E-001
SUPBN → MEGABN	8.31E-004 ± 6.34E-004	7.63E-001
SUPBN → AANT	1.94E-003 ± 2.19E-004	1.13E-001
SUPBN → MEGAICT	8.34E-004 ± 6.41E-004	7.69E-001
MEGABN → DIC	4.51E-002 ± 2.93E-004	6.51E-003
MEGABN → TOM	9.24E-002 ± 4.46E-002	4.83E-001
MEGABN → AANT	1.44E-003 ± 1.78E-004	1.24E-001
MEGABN → BYCATCH	2.61E-006 ± 6.91E-008	2.65E-002
MEGAICT → DIC	7.15E-003 ± 4.13E-005	5.78E-003
MEGAICT → TOM	3.32E-002 ± 2.01E-002	6.05E-001
MEGAICT → AANT	1.54E-005 ± 9.25E-006	6.01E-001
MEGAICT → BYCATCH	1.57E-003 ± 4.14E-005	2.65E-002
AANT → DIC	1.71E-003 ± 2.71E-004	1.58E-001
AANT → TOM	2.79E-003 ± 4.51E-004	1.62E-001
AANT → MEGAICT	1.27E-003 ± 1.12E-004	8.82E-002
AANT → LANDS	5.22E-004 ± 1.38E-005	2.65E-002

TABLE E.5: MCMC (mean and standard deviation) solution and Coefficient of Variation (CoV) for the food web flows.

E.4 Network indices equations and results

Finally Tables E.6, E.7 and E.8 show all symbols and formulas of the indices used for the ecosystem analysis, of which the corresponding results are in Tables E.9, E.10, **??** and **??**.

The following tables show the estimations of the network indices in the following order: general indices in Table E.9, indices related to system growth and development in Table E.10 and finally indices of network uncertainty and constraint efficiencies and indices for the environmental analysis in Table **??**. Trophic indices have been shown in Table 5.5, Chapter 5.

Term	Description
n	Number of internal compartments in the network
$j = 0$	External source
$i = n + 1$	Usable export from the network
$i = n + 2$	Unusable export from the network (respiration, dissipation)
T_{ij}	Flow from compartment j to i; in the flow matrix j are columns and i the rows
$T_{i.}$	Total inflows to compartment i
$T_{.j}$	Total outflows from compartment j
T_i	Total inflows to compartment i excluding inow from external sources
T_j	Total outflows from compartment j, excluding outow to external sources
$(\dot{x}_i)_-$	A negative state derivative, considered as a gain of energy to the system
$(\dot{x}_i)_+$	A positive state derivative, considered as a loss of energy from the system
z_{i0}	Flow into compartment i from outside the network
y_{n+j}	Flow from compartment j to compartments $n + 1$ and $n + 2$
c_{ij}	The number of species with which both i and j interact divided by the number of species with which either i or j interact
$\mathbf{T}^*_{ij}$	Flow matrix, excluding flows to and from the external
$\mathbf{I}, \delta_{ij}$	Identity matrix and its elements
$\mathbf{G'}, g_{ij}$	matrix given by $\mathbf{T}^*_{ij}/max(T_i, T_j)$ and its elements
$\mathbf{Q}, q_{ij}$	matrix given by $(\mathbf{I} - \mathbf{G'})^{-1}$ and its elements

TABLE E.6: Nomenclature of symbols used in calculation of network index equations (Table E.7). Revised from Kones et al. (2009).

Index	Formula	Ref.
T..	$\sum_{i=1}^{n+2}\sum_{j=0}^{n} T_{ij}$	1
TST	$\sum_{i=1}^{n}\sum_{j=1}^{n}\left[T_{ij} + z_{i0}(\dot{X}_i)_-\right]$	2
L	$\sum_{i=1}^{n+2}\sum_{j=1}^{n}(T_{ij} \geq 1)$	2
LD	$\frac{\sum_{i=1}^{n+2}\sum_{j=1}^{n}(T_{ij}\geq 1)}{n}$	2
Lint	$\sum_{i=1}^{n}\sum_{j=1}^{n}(T_{ij} \geq 1)$	3
C	$\frac{\sum_{i=1}^{n}\sum_{j=1}^{n}(T_{ij}\geq 1)}{n(n-1)}$	2
$\overline{\text{T}}_{\text{ij}}$	$\frac{\sum_{i=1}^{n+2}\sum_{j=0}^{n} T_{ij}}{\text{L}}$	4
$\overline{\text{TST}}$	$\frac{\sum_{i=1}^{n}\sum_{j=1}^{n}\left[T_{ij}+z_{i0}(\dot{X}_i)_-\right]}{n}$	2
$\overline{\text{C}}$	$\frac{1}{n(n-1)}\sum_{i=1}^{n}\sum_{j=1}^{n} c_{ij}$ where $j \neq i$	4
TSTc	$\sum_{j=1}^{n}(1 - 1/q_{ij}T_j)$	5, 6, 7
TSTs	$\sum_{i=1}^{n}\sum_{j=1}^{n}\left[T_{ij} + z_{i0}(\dot{X}_i)_-\right] - \sum_{j=1}^{n}(1 - 1/q_{ij}T_j)$	5, 6, 7
FCI	$\frac{\sum_{j=1}^{n}(1-1/q_{ij}T_j)}{\sum_{i=1}^{n}\sum_{j=1}^{n}\left[T_{ij}+z_{i0}(\dot{X}_i)_-\right]}$	5, 6, 7
FCIb	$\frac{\sum_{j=1}^{n}(1-1/q_{ij}T_j)}{\sum_{i=1}^{n+2}\sum_{j=0}^{n} T_{ij}}$	8, 9
$\overline{\text{PL}}$	$\frac{\sum_{i=1}^{n}\sum_{j=1}^{n}\left[T_{ij}+z_{i0}(\dot{X}_i)_-\right]}{\sum z_{i0}-\sum(\dot{x}_i)_+}$	5, 6, 7
Cz	$\prod_{ij}\left[\frac{T_{ij}^2}{T_{i.}T_{.j}}\right]^{-(1/2)(T_{ij}T_{..})}$	2
Fz	$\prod_{ij}\left[\frac{T_{ij}}{T_{..}}\right]^{-(T_{ij}/T_{..})}$	2
Nz	$\prod_{ij}\left[\frac{T^2}{T_{i.}T_{.j}}\right]^{-(1/2)(T_{ij}T_{..})}$	2
Rz	$\prod_{ij}\left[\frac{T_{ij}T_{..}}{T_{i.}T_{.j}}\right]^{(T_{ij}/T_{..})}$	2

TABLE E.7: Network Index formulas (PART 1/2). See Table E.6 for the definition of terms. References: (1) Hirata and Ulanowicz, 1984, (2) Latham II, 2006, (3) Kones et al., 2009, (4) Pimm and Lawton, 1980, (5) Finn, 1976, (6) Finn, 1980, (7) Patten and Higashi, 1984, (8) Allesina and Ulanowicz, 2004, (9) Ulanowicz, 1986, (10) Ulanowicz and Norden, 1990, (11) Ulanowicz, 2004, (12) Ulanowicz, 2000, (13) Christensen and Pauly, 1992, (14) Lindeman, 1942. Revisited from ref. 3.

Index	Formula	Ref.
A	$\sum_{i=1}^{n+2}\sum_{j=0}^{n} T_{ij} log_2 \frac{T_{ij}T_{..}}{T_{i.}T_{.j}}$	10, 11
DC	$-\sum_{i=1}^{n+2}\sum_{j=0}^{n} T_{ij} log_2 \frac{T_{ij}}{T_{..}}$	10, 12
ϕ	$\left[-\sum_{i=1}^{n+2}\sum_{j=0}^{n} T_{ij} log_2 \frac{T_{ij}}{T_{..}}\right] - \left[\sum_{i=1}^{n+2}\sum_{j=0}^{n} T_{ij} log_2 \frac{T_{ij}T_{..}}{T_{i.}T_{.j}}\right]$	10, 12
AC	$-\frac{\sum_{i=1}^{n+2}\sum_{j=0}^{n} T_{ij} log_2 \frac{T_{ij}T_{..}}{T_{i.}T_{.j}}}{\sum_{i=1}^{n+2}\sum_{j=0}^{n} T_{ij} log_2 \frac{T_{ij}}{T_{..}}}$	10, 12
AMI	$\sum_{i=1}^{n+2}\sum_{j=0}^{n} \frac{T_{ij}}{T_{..}} log_2 \frac{T_{ij}T_{..}}{T_{i.}T_{.j}}$	12
H_R	$-\sum_{j=0}^{n} \frac{T_{.j}}{T_{..}} log_2 \frac{T_{.j}}{T_{..}}$	2, 10
D_R	$\left[-\sum_{j=0}^{n} \frac{T_{.j}}{T_{..}} log_2 \frac{T_{.j}}{T_{..}}\right] - \left[\sum_{i=1}^{n+2}\sum_{j=0}^{n} \frac{T_{ij}}{T_{..}} log_2 \frac{T_{ij}T_{..}}{T_{i.}T_{.j}}\right]$	2, 10
RU_R	$-\frac{\sum_{i=1}^{n+2}\sum_{j=0}^{n} \frac{T_{ij}}{T_{..}} log_2 \frac{T_{ij}T_{..}}{T_{i.}T_{.j}}}{\sum_{j=0}^{n} \frac{T_{.j}}{T_{..}} log_2 \frac{T_{.j}}{T_{..}}}$	2, 10
Hmax	$\sum_{i=1}^{n} log_2(n+2)$	2
Hc	$\sum_{i=1}^{n} log_2(n+2) - \left[-\sum_{i=1}^{n+2}\sum_{j=1}^{n} \frac{T_{ij}}{T_{..}} log_2 \frac{T_{ij}}{T_{..}}\right]$	2, 10
Hsys	$-\sum_{i=1}^{n}\sum_{j=1}^{n} \frac{T_{ij}}{T_{..}} log_2 \frac{T_{ij}}{T_{..}}$	2
CE	$\frac{\sum_{i=1}^{n} log_2(n+2) - \left[-\sum_{i=1}^{n+2}\sum_{j=1}^{n} \frac{T_{ij}}{T_{..}} log_2 \frac{T_{ij}}{T_{..}}\right]}{\sum_{i=1}^{n} log_2(n+2)}$	2
TL_j	$1 + \sum_{i=1}^{n} \frac{\mathbf{T}^*_{ij}}{T_{j.}} TL_i$	13, 14
OI_j	$\sum_{i=1}^{n} \left[TL_i - (TL_j - 1)\right]^2 \frac{\mathbf{T}^*_{ij}}{T_{j.}}$	13

TABLE E.8: Network Index formulas (PART 2/2). See Table E.6 for the definition of terms. References: (1) Hirata and Ulanowicz, 1984, (2) Latham II, 2006, (3) Kones et al., 2009, (4) Pimm and Lawton, 1980, (5) Finn, 1976, (6) Finn, 1980, (7) Patten and Higashi, 1984, (8) Allesina and Ulanowicz, 2004, (9) Ulanowicz, 1986, (10) Ulanowicz and Norden, 1990, (11) Ulanowicz, 2004, (12) Ulanowicz, 2000, (13) Christensen and Pauly, 1992, (14) Lindeman, 1942. Revisited from ref. 3.

	Index	mean ± sd
A)	Number of components (n)	7.000 ± 0.000
	Number of total links (L)	39.998 ± 0.084
	Number of internal links (Lint)	20.999 ± 0.070
	Link density (LD)	5.714 ± 0.012
	Connectance (C)	0.499 ± 0.001
	Compartmentalization $\overline{C}$	0.537 ± 0.001
	Average link weight ($\overline{T}_{ij}$)	0.175 ± 0.034
	Effective Connectivity (Cz)	1.316 ± 0.044
	Effective Flows (Fz)	1.974 ± 0.210
	Effective Nodes (Nz)	1.496 ± 0.112
	Effective Roles (Rz)	1.135 ± 0.053
	Total System Throughput ($T_{..}$)	7.036 ± 1.375
	Total System Throughflow (TST)	4.415 ± 0.973
	Total System cycled Throughflow (TSTc)	0.827 ± 0.440
	Total System non-cycled Throughflow (TSTs)	3.588 ± 0.658
	Finns Cycling Index (FCI)	0.179 ± 0.066
	Revised Finns Cycling Index (FCIb)	0.114 ± 0.048
	Average compartment throughflow ($\overline{TST}$)	0.630 ± 0.139
	Average Path Length ($\overline{PL}$)	1.696 ± 0.261
B)	Average mutual information (AMI)	0.817 ±0.038
	Statistical uncertainty (H_R)	1.644 ±0.070
	Conditional uncertainty (D_R)	0.827 ±0.104
	Realized uncertainty (RU_R)	0.498±0.043
	Hmax	24.216±0.000
	Network constraint (Hc)	14.330±0.427
	Hsys	9.885±0.427
	Constraint efficiency (CE)	0.591±0.017
C)	Network aggradation = average path length (NAG)	1.696 ± 0.261
	Homogenization (HP)	1.558 ± 0.065
	Synergism index (BC)	21.613 ± 6.499
	Dominance indirect effect (ID)	0.753 ± 0.235
	Mean of non-dimensional flow-matrix (MN)	0.313 ± 0.030
	Mean of direct flow-matrix (MG)	0.096 ± 0.005
	Coefficient of variation of non-dimensional flow-matrix (CVN)	1.347 ± 0.053
	Coefficient of variation of direct flow-matrix (CVG)	2.097 ± 0.056

TABLE E.9: Estimations of network indices. A) Basic properties and Pathway analysis; B) Network uncertainty and constraint efficiencies; C) Environmental analysis.

Index		mean ± sd
Ascendency (A)	total	5.746 ± 1.122
	internal	1.308 ± 0.630
	import	2.154 ± 0.469
	export	2.283 ± 0.510
	dissipation	1.415 ± 0.306
Development capacity (DC)	total	19.539 ± 3.993
	internal	6.868 ± 1.868
	import	5.280 ± 1.078
	export	7.391 ± 1.348
	dissipation	5.017 ± 0.743
Overhead (ϕ)	total	13.792 ± 3.027
	internal	5.559 ± 1.282
	import	3.125 ± 0.957
	export	5.107 ± 0.923
	dissipation	3.602 ± 0.574
Extent of development (AC)	total	0.295 ± 0.028
	internal	0.181 ± 0.043
	import	0.416 ± 0.091
	export	0.307 ± 0.032
	dissipation	0.281 ± 0.045

TABLE E.10: Indices of system growth and development.

F

Complementary material – Chapter 6

F.1 Dynamic simulation for 20 years

Figures F.1 and F.2 show the dynamic simulation performed for 20 years, changing only the fishing effort on red shrimp: 1) when the fishing effort is higher than the actual, 2, 5 and 20 times (F.1); 2) when the fishing effort is lower with an order of 2, 5 and 20 (F.2). Figures F.3 and F.4 show the dynamic behaviour of components when both fishing and by-catch change simultaneously with the same intensities (that is both red shrimp and all other megafauna): 3) when the effort is 2, 5 and 20 time higher than the actual and 4) when it is lower F.4. If we would show all simulations we should make other 428 graphics like these.

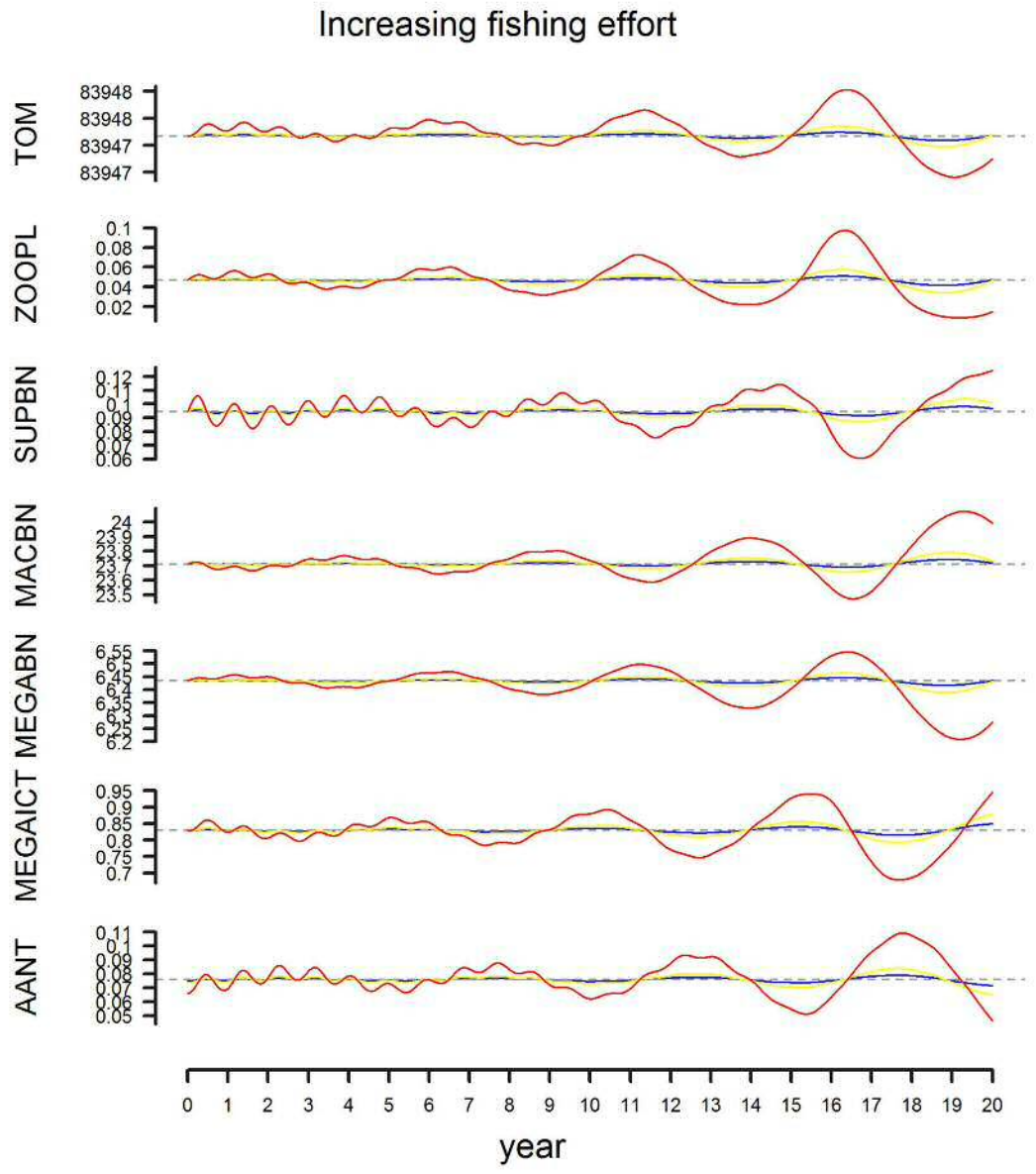

FIGURE F.1: Dynamic output when perturbing red shrimp biomass with increasing fishing effort. Blue line = 2 times the actual fishing flow; yellow line = 5 times the actual fishing flow; and red line = 20 times the actual fishing flow.

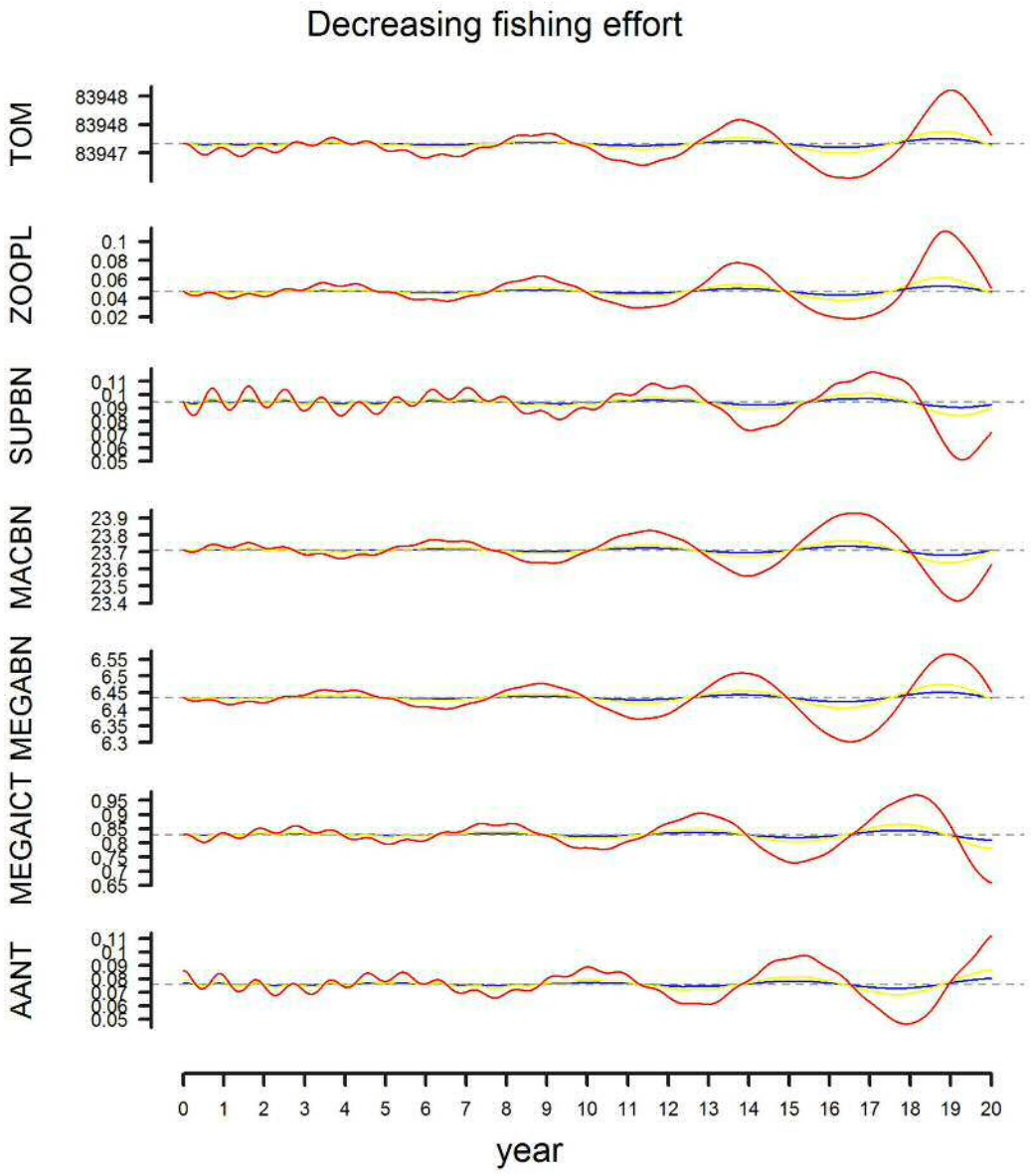

FIGURE F.2: Dynamic output when perturbing red shrimp biomass with decreasing fishing effort. Blue line = 2 times less the actual fishing flow; yellow line = 5 times less the actual fishing flow; and red line = 20 times less the actual fishing flow.

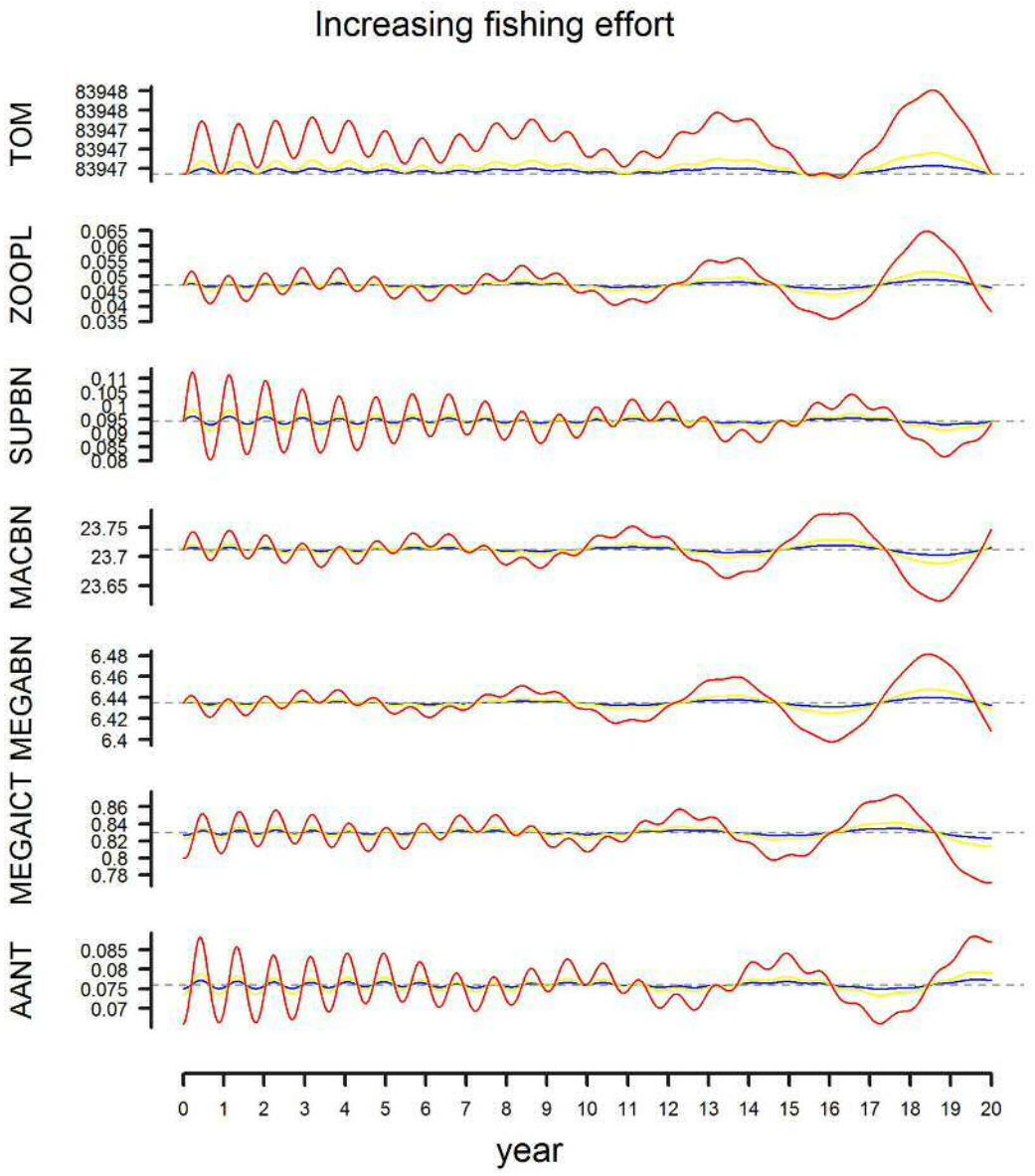

FIGURE F.3: Dynamic output when perturbing all megafauna biomasses with increasing fishing effort. Blue line = 2 times the actual fishing flow; yellow line = 5 times the actual fishing flow; and red line = 20 times the actual fishing flow.

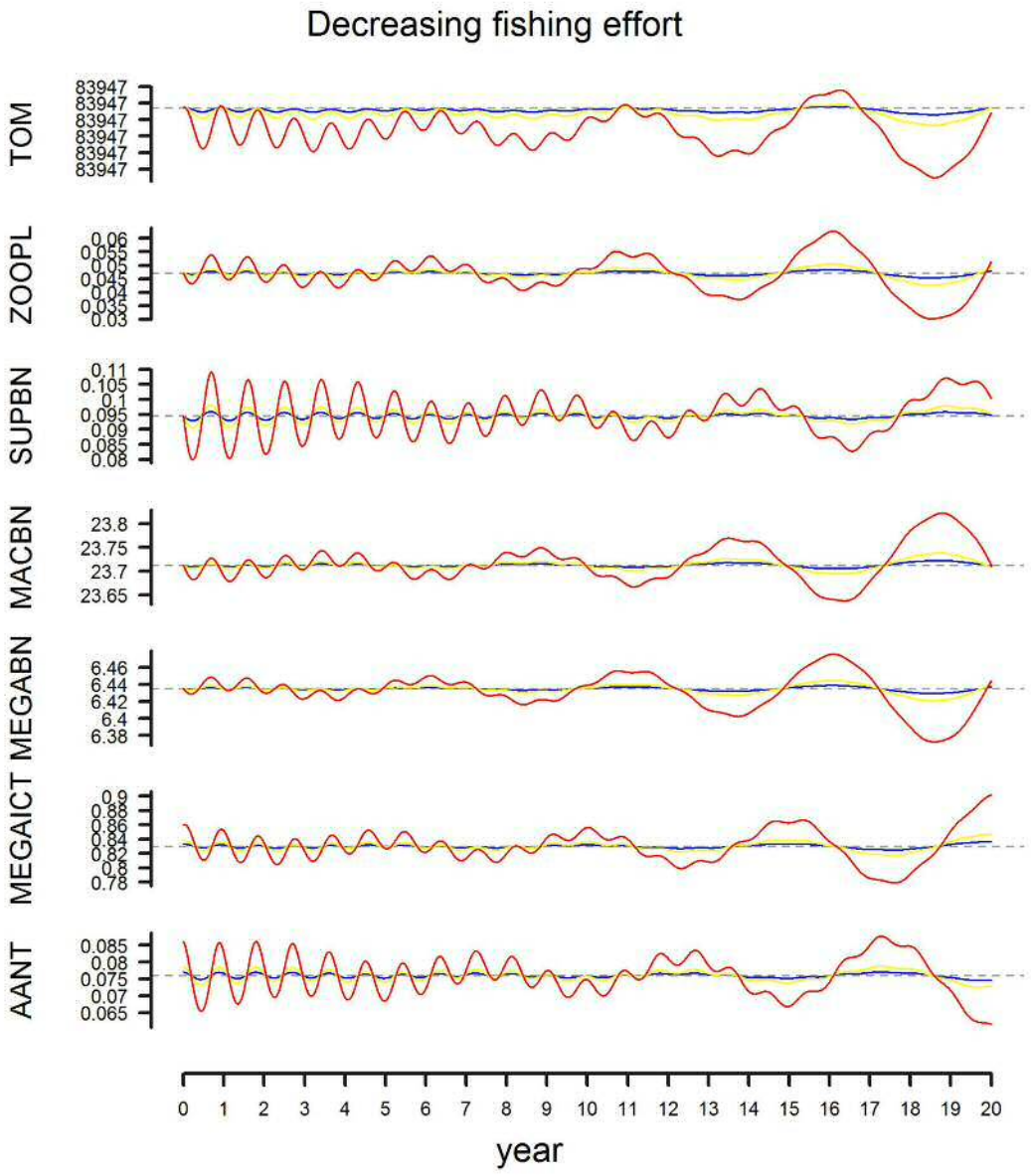

FIGURE F.4: Dynamic output when perturbing all megafauna biomasses with decreasing fishing effort. Blue line = 2 times less the actual fishing flow; yellow line = 5 times less the actual fishing flow; and red line = 20 times less the actual fishing flow.

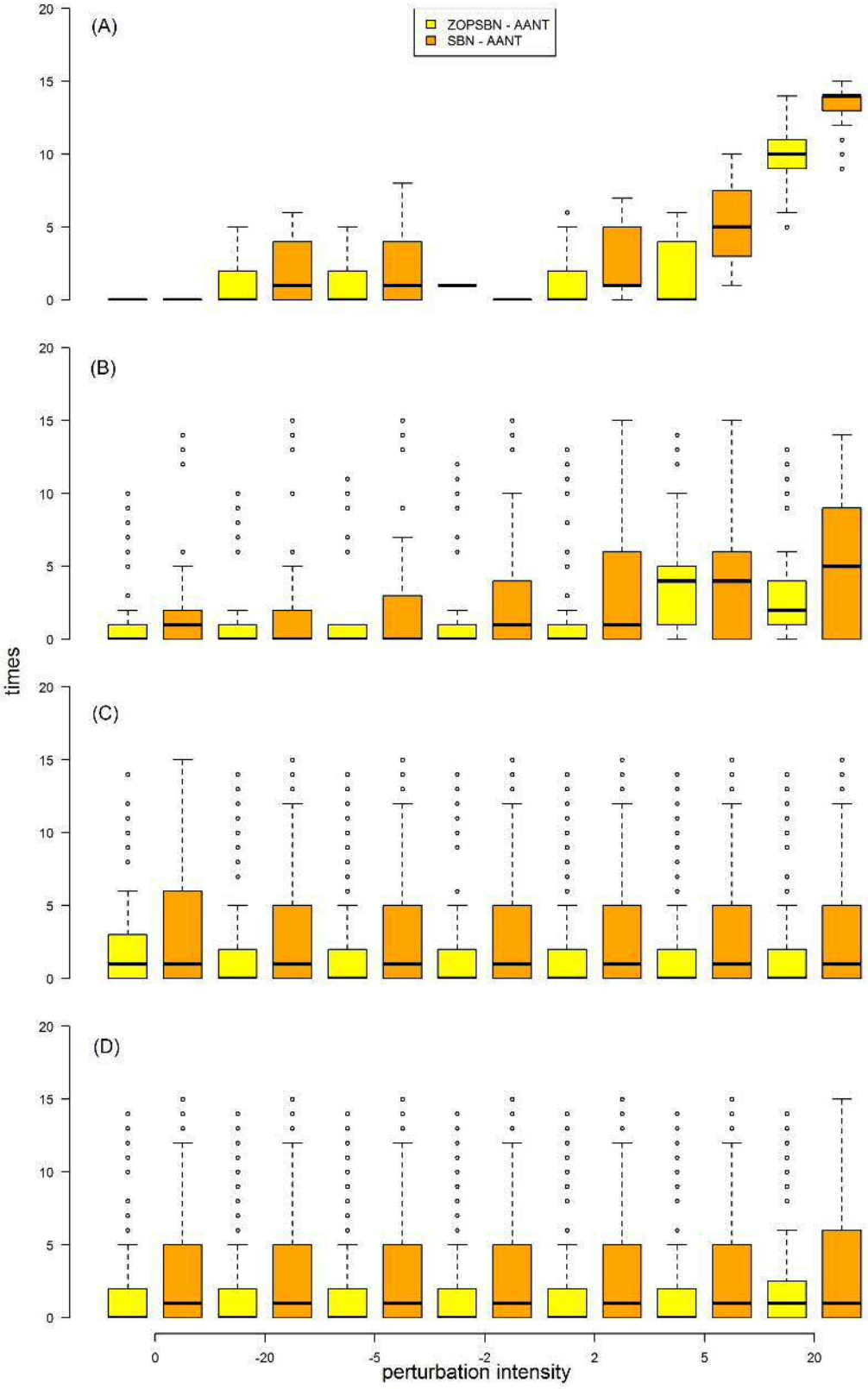
(A)
ZOPSBN - AANT
SBN - AANT
(B)
(C)
(D)
times
perturbation intensity
0
-20
-5
-2
2
5
20

FIGURE F.5

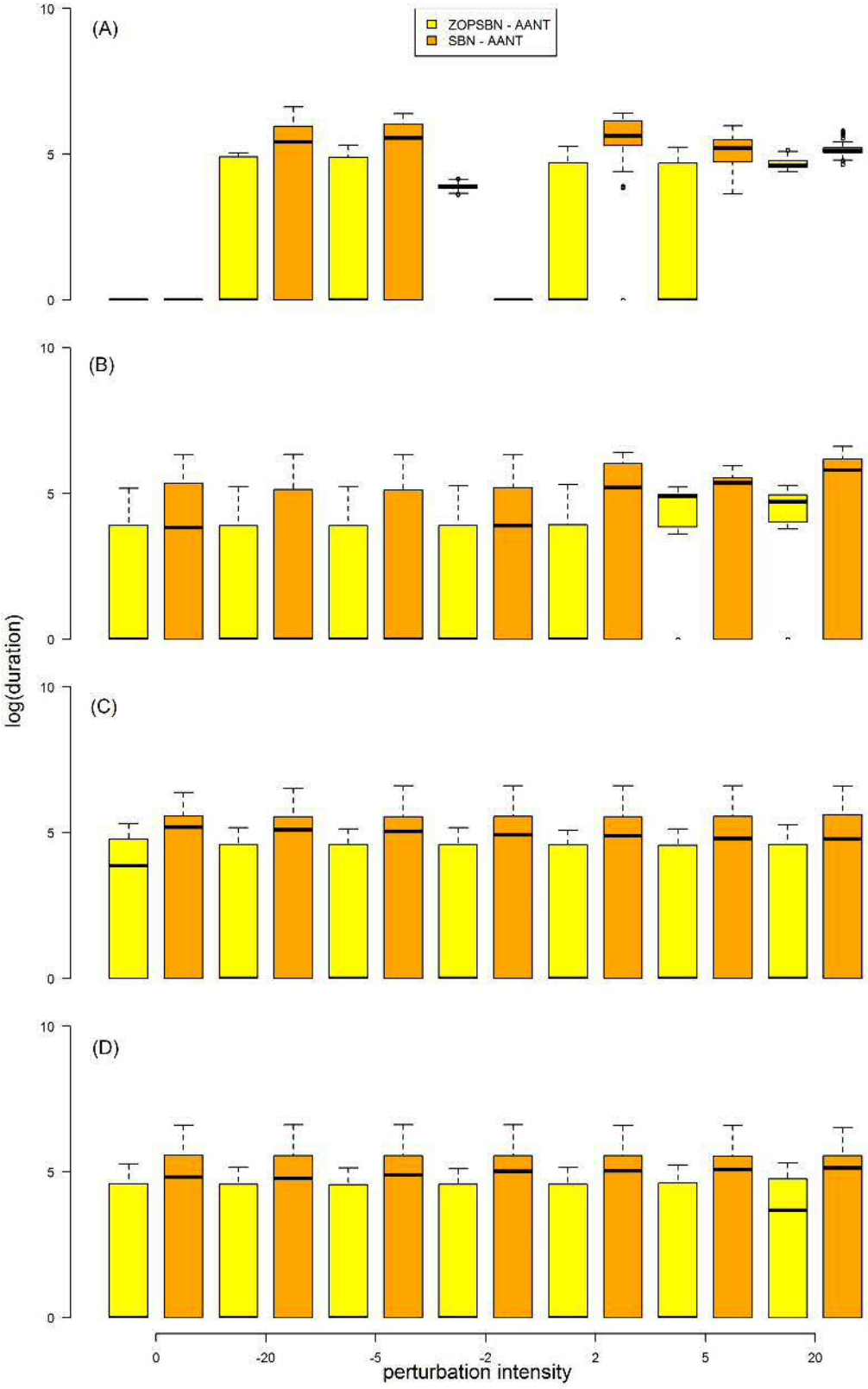
(A)
ZOPSBN - AANT
SBN - AANT
(B)
(C)
(D)
log(duration)
10
5
0
0
-20
-5
-2
2
5
20
perturbation intensity

FIGURE F.6

G
Offprint

G.1 Publications

Deep-Sea Research I 58 (2011) 323–337

Contents lists available at ScienceDirect

Deep-Sea Research I

journal homepage: www.elsevier.com/locate/dsri

A temporal analysis on the dynamics of deep-sea macrofauna: Influence of environmental variability off Catalonia coasts (western Mediterranean)

V. Mamouridis [a,*], J.E. Cartes [a], S. Parra [b], E. Fanelli [a], J.I. Saiz Salinas [c]

[a] Institut de Ciències del Mar, Passeig Marítim de la Barceloneta 37–49, 08003 Barcelona, Spain
[b] Instituto Español de Oceanografía, P.O. Box 130, 15080 La Coruña, Spain
[c] Dpto de Biología Animal y Genética, Fac. de Ciencias, Universidad del País Vasco, E-48080 Bilbao, Vizcaya, Spain

ARTICLE INFO

Article history:
Received 17 May 2010
Received in revised form
10 January 2011
Accepted 18 January 2011
Available online 23 February 2011

Keywords:
Macrofauna
Canyon
Food availability
Seasonal dynamics

ABSTRACT

A seasonal analysis of deep-sea infauna (macrobenthos) based on quantitative sampling was conducted over the Catalan Sea slope, within the Besòs canyon (at ~550–600 m) and on its adjacent slope (at 800 m). Both sites were sampled in February, April, June–July and October 2007. Environmental variables influencing faunal distribution were also recorded in the sediment and sediment/water interface. Dynamics of macrobenthos at the two stations showed differences in biomass/abundance patterns and trophic structures. Biomass was higher inside the Besòs canyon than on the adjacent slope. The community was mostly dominated by surface-deposit feeding polychaetes (Ampharetidae, Paraonidae, Flabelligeridae) and crustaceans (amphipods such as *Carangoliopsis spinulosa* and *Harpinia* spp.) inside the canyon, while subsurface deposit feeders (mainly the sipunculan *Onchnesoma steenstrupii*) were dominant over the adjacent slope. The taxonomic composition in the suprabenthic assemblages of polychaetes, collected on the adjacent slope by a suprabenthic sledge, was clearly different from that collected by the box-corer. The suprabenthic assemblage was dominated by carnivorous forms (mainly *Harmothoe* sp. and *Nephtys* spp.) and linked to higher near-bottom turbidity. Inside Besòs a clear temporal succession of species was related to both food availability and quality and the proliferation of opportunistic species was consistent with higher variability in food sources (TOC, C/N, $\delta^{13}C$) in comparison to adjacent slope. This was likely caused by a greater influence of terrigenous inputs from river discharges. Inside the canyon, Capitellidae, Spionidae and Flabelligeridae, in general considered as deposit feeders, were more abundant in June–July coinciding with a clear signal of terrigenous carbon (depleted $\delta^{13}C$, high C/N) in the sediments. By contrast, during October and under conditions of high water turbidity and increases of TOM, carnivorous polychaetes (Glyceridae, Onuphidae) increased. Total macrobenthos biomass found over Catalonian slopes were higher than that found in the neighboring Toulon canyon, probably because the two canyons are influenced by different river inputs, connected with distinct terrigenous sources.

1. Introduction

The deep sea, the largest habitat on the Earth, is composed of a variety of ecosystems distributed over hard and soft bottoms, hence, is not as homogeneous as once believed. Continental slopes alone, mainly covered by soft sediments (Pérès, 1985; Thistle, 2003), constitute a variety of habitats. Submarine canyons crossing the slopes comprise a mosaic of habitat patches and faunal assemblages (Reyss, 1971; Macquart-Moulin and Patriti, 1996; Vetter and Dayton, 1999; Stora et al., 1999; Curdia et al., 2004). Continental slopes and especially canyons crossing them, represent zones of matter and energy transfer between the continental shelf and the abyssal domain (Griggs et al., 1969; Gardner, 1989) often providing focused sources of high quality food (Rowe et al., 1982; Josselyn et al., 1983; Epping et al., 2002). Inside canyons the main energy flow depends on advective fluxes (Féral et al., 1990) and terrestrial inputs may be important in the ecodynamics of submarine canyons (de Stigter et al., 2007). Organic matter is often channeled along canyons, enhancing food supply to depocenters on adjacent slope areas where we can find hotspots of benthos production (Vetter and Dayton, 1999). This channeling can change seasonally, establishing varying seasonal environmental dynamics at the sea floor in and close to canyons, mostly driven by changes in food availability (Vetter, 1998). This may influence assemblage composition, life cycles of benthos and trophic relationships, including the roles of particular benthic taxa (Fanelli et al., 2011), prey for deep-sea shrimps (Cartes, 1994) and fishes (Madurell and Cartes, 2005; Fanelli and Cartes, 2010) on continental margins.

* Corresponding author.
E-mail address: mamouridis@icm.csic.es (V. Mamouridis).

0967-0637/$ - see front matter © 2011 Elsevier Ltd. All rights reserved.
doi:10.1016/j.dsr.2011.01.005

The distribution and diversity of deep macrobenthos have mainly been related with depth gradients at several spatial scales, and with sediment size (Tselepides and Eleftheriou, 1992; Stora et al., 1999). Small-scale changes in the sediment structure and in the distribution of food over sedimentary bottoms are associated with adaptation of fauna and with its high diversification in the deep sea (Sanders et al., 1965; Gage and Tyler, 1991). In the western Mediterranean many canyons traverse the continental slope close to mainland areas. The Balearic Basin in some way resembles a large submarine canyon, represented by the Valencia Trough, that separates the mainland and insular slopes (the latter belonging to the Balearic Islands). The mainland slope extending along the Catalonian coast is crossed by a system of tributary canyons (from N to S: Palamós, Blanes, Arenys/Besòs, Berenguera and Foix).

Quantitative data on benthic deep-sea macrofauna are still too scarce to describe the dynamics of margin systems. Studies on infaunal macrobenthic assemblages in the Mediterranean Deep Sea have been performed mainly by dredging, which permits only qualitative descriptions (Pérès and Picard, 1964; Carpine, 1970; Reyss, 1971; Vamvakas, 1970), and rarely by sediment cores (Tchukhtchin, 1964; Gerino et al., 1994; Stora et al., 1999) that allow quantitative analyses. Quantitative studies, both in the deep Mediterranean and elsewhere, have lacked until now a temporal/seasonal approach, that surprisingly reveals the crucial role of infauna in food webs around submarine canyons (Cartes, 1994; Cartes et al., 2002, 2009). Studies of ecosystem function on the Catalan slope have focused on megafauna, fishes and decapods crustaceans, collected by OTSB-14 and similar trawls (e.g. Cartes et al., 1994, 2009) and on suprabenthic macrofauna collected with MACER-GIROQ sledges (Cartes, 1998). There has also been a study of the distribution of megafaunal invertebrates, both epifauna and infauna (Cartes et al., 2009). The multidisciplinary project BIOMARE, focused on the natural variability of, and human impact on, marginal ecosystems off the Catalan coasts, included studies of the temporal dynamics of all macrofaunal compartments (the infauna for the first time) in deep environments and of the possible environmental factors influencing their distributions and biomass. The difficulty in collecting environmental and biological samples simultaneously is probably the reason for the lack of information regarding environmental coupling (as noted by Stora et al., 1999).

In this paper we present the first temporal study of deep-sea infauna (macrobenthos) based on a quantitative approach, a study conducted simultaneously in two characteristic environments of the Catalan slope. The seasonal dynamics of deep-sea macrobenthos (between 600 and 800 m) have been analyzed in the Mediterranean for the first time. Though our aims have been necessarily descriptive, our approach also includes an analysis of environmental variables influencing benthos communities. Our objectives were: (i) to describe seasonal changes of infaunal macrobenthos in two characteristic environments of the Catalan Slope, inside the *Besòs* canyon and on its adjacent slope at 800 m depth; (ii) to identify the main variables both in the sediment and close to the sediment–water interface (the Benthic Boundary Layer) that explain trends observed in the taxonomic composition and biomass of the infaunal macrobenthos.

2. Material and methods

2.1. Study area and sampling design

The sampling was performed along the mid-slope (Fig. 1) off the Catalonian coast (Balearic Basin: between 40°48′9N and 41°09′3N, and 2°04′0E and 2°35′4E) near Barcelona within the project BIOMARE (ref. CTM2006-13508-C02-02/MAR). Samples

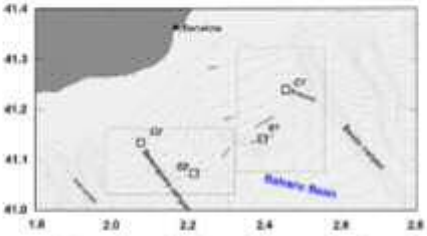

Fig. 1. Map of the study area off the Catalonian coast, showing positions of sampling stations in *Besòs* (*C1*) and *Berenguera* (*C2*) canyons and on adjacent slopes (*S1*, *S2*) inside the Valencia Trough. The symbol (::::::) indicates locations of Macer-GIROQ sledges.

were collected at four stations situated within two canyons and on their adjacent slopes. At two of these stations (the *Buscarró* canyon, *C1*, a tributary of the larger *Besòs* canyon and on its adjacent slope, *S1*), four cruises were performed seasonally (B1 cruise February 2007; B2 April 2007; B3 June–July 2007; B4 October 2007). In the *Berenguera* canyon station (*C2*), and the adjacent slope station (*S2*), sampling was carried out only in June–July 2007. The *Besòs* (*C1*) and *Berenguera* (*C2*) canyons stations were located at depths of ~550–600 m near the southern walls of the canyons, close to the canyon heads. The adjacent slope stations were located at ~800 m depth in two fishing grounds known by local fishermen as Serola (*S1*) and Abissinia (*S2*), close to *Besòs* and *Berenguera* canyons, respectively. Both canyons are also fishing grounds, though there was hardly any fishing activity at *C1* in the last 5 years. The seasonal analyses (e.g. PCAs, CCAs, see below) were based only on *C1* and *S1* samples.

A total of 34 box-cores were collected. The replicates (cores taken very close to the same positions, i.e. <200 m between replicates) were distributed as follows: cruise B1 (3 at *C1* and 3 at *S1*), cruise B2 (4 at *C1* and 4 at *S1*), cruise B3 (4 at *C1* and 3 at *C2*; 4 at *S1* and 1 at *S2*) and cruise B4 (4 at *C1* and 4 at *S1*). The box-corer used was a Reineck model, with 21 × 31 cm box sides, sampling a surface area of 0.065 m^2. The uppermost 20 cm of sediments were sieved through a 0.5 mm mesh size to retain macrofauna, as in other similar studies performed in the deep Mediterranean (see Stora et al., 1999). Infauna was sorted, classified to the lowest possible taxonomic level, counted and weighed (wet weight, WW).

Additional data on benthos (only polychaetes) were collected with a Macer-GIROQ sledge (Dauvin and Lorgeré, 1989), a sampling system used in earlier suprabenthos studies (Cartes et al., 2002). Mobile epibenthic macrofauna were collected at ~0 and 1.5 m above the seafloor. This sledge has 40 × 80 cm rectangular mouth apertures situated between 10–50, 55–95 and 100–140 cm from the bottom. The mesh size was of 500 μm. The volume of water filtered was estimated by means of a 2030R standard flowmeter (General Oceanics, Inc.) positioned within the aperture of nets. This measurement also allowed calculation of the volume filtered (between 339 and 475 m^3) by estimation of the area covered by each haul. SCANMAR sensors attached to the sledge gave the times of arrival/departure of the sledge at/from the bottom. During each cruise two stations at 650 and 800 m on the adjacent slope were sampled with the Macer-GIROQ sledge (see Fig. 1). The 800 m station coincided with the *S1* box-corer station.

2.2. Environmental data collection

Biological data were analyzed together with a number of environmental variables defining both the characteristics of the sediments and the near-bottom water column. During each

cruise, one CTD per station was performed in parallel to the biological sampling using Seabird-25 profilers furnished with pressure, temperature, salinity, fluorescence and turbidity sensors (obtaining 24 data sets s^{-1}). The CTD recorded data from the surface to 5 m above the bottom. Sediments were collected with a multi-corer at the same stations where box-cores were taken (three samples per multi-corer) and the first 5 cm were used for environmental analyses.

The CDT measured the following variables:

- Temperature and salinity 5 m above the sea bottom ($T_{5\ mab}$, $S_{5\ mab}$).
- Fluorescence ($f_{0\text{–}200\ m}$) as the sum of fluorometer readings each 1 m in vertical bins from surface to 200 m depth; values were proportional to Chl *a* and indicative of surface phytoplankton standing stock.
- Turbidity at 5 mab ($Turb_{5\ mab}$).

Multi-corer samples were used to measure the following parameters:

- Percentage of total sedimentary organic matter (TOM), calculated as the difference between dry weight (DW: 60 °C for 24 h until constant weight reached) and ash weight (500 °C in a furnace for 2 h).
- Percentage of total organic carbon (TOC), carbon–nitrogen ratios (C/N) and the stable isotope ratio ($\delta^{13}C$) in sediments (C13) (for details of sample treatment and isotope analysis see Fanelli and Cartes, 2008; Fanelli et al., 2009). $\delta^{13}C$ indicates the origin of food sources (terrigenous or pelagic) arriving on the seafloor. Detailed sediment C/N and $\delta^{13}C$ data will be published separately (Authors' unpubl. data).

REDX (Eh) was measured directly in box-corer sediments using a ThermoOrion 250A sensor. Voltage was read at the sediment surface and at 5 cm depth in the sediment.

Mean monthly flow estimates (m^3/s) for the main rivers discharging off the central Catalonian coasts (Llobregat, see Fig. 1) were obtained from the website http://aca-web.gencat.cat/aca/appmanager/aca/aca/. Phytoplankton pigment concentration (ppc, mgChl a/m^3) were obtained from http://reason.gsfc.nasa.gov/Giovanni. Values of ppc were used as indicators of the surface primary production in the area. A monthly average reading of ppc of the positions of stations was used.

2.3. Diversity and biomass trends by season

All infaunal taxa were classified to the lowest possible taxonomic level. Within BIOMARE, we attempted to analyze the stable isotopic composition of macrofauna. We therefore undertook an initial sorting of fauna on board the ship, and then froze specimens, remaining bulk samples and sediment at −20 °C for later analysis. In the laboratory, the macrofaunal sorting was completed and the animals classified into groups in order to obtain the required minimum masses for isotope analysis. This treatment partially damaged polychaetes. As a result, some specimens could only be determined to genus or family level.

Taxa were counted and weighted individually in order to obtain the wet weight (WW, grams, after eliminating water by blotting). Taxa/species abundance and biomass were standardized to individuals and weight/m^2, both per station (600 and 800 m) and cruise. For comparisons with data from other benthic studies, we transformed WW to dry weight (DW) using the factor 0.2 (source: EMPRELAT data base, Alfred Wegener Institute).

2.4. Statistical analysis

An analysis of all the box-core data was first conducted using nMDS, PERMANOVA and SIMPER. A seasonal analysis (PCA, CCA, biomass and diversity trends, etc.) was then carried out based on data from stations C1 and S1, where 3–4 replicate samples were available from all cruises.

All multivariate analyses were performed on individual box-core replicates. The non-parametric Multidimensional Scaling procedure (nMDS; Clarke and Warwick, 1994) was performed using Spearman's Rank Correlation as a distance measure. The matrix of all taxa identified was used (removing taxa appearing less than twice). Principal factors in the hauls ordination were: "habitat" (2 levels: canyon, CAN, vs adjacent slope, SLO), and "water condition" (=water column temperature conditions, with 2 levels: homogeneous, HOM, during February and April, and stratified, STR, during June–July and October).

Distance-based permutational multivariate analysis of variance (PERMANOVA, Anderson, 2001) was used in a 2 factors complete model design, testing the null hypothesis H_0 of no significant main effects and interaction. The factors included in the model, considered as fixed and crossed, were "habitat" and "water condition". The same matrix and distance measure were used as in the nMDSs and we applied a permutation of residuals under a reduced model (maximum number of permutations=9999) (Anderson and Legendre, 1999; Anderson and ter Braak, 2003). For each *pseudo-F* test, Monte Carlo and post-hoc tests were also obtained.

One-way SIMPER analysis (Clarke, 1993) was performed on the taxon matrix using Bray–Curtis distances in order to identify contributions of taxa to assemblages at the two habitats: inside the canyon and on the adjacent slope.

Principal components analysis (PCA) was performed on a correlation matrix of the environmental data, and a bi-plot was used to describe the resulting ordination patterns of samples. Canonical correspondence analysis (CCA) (ter Braak, 1986) was applied to study the association of environmental variables with taxon/species abundances. Three CCAs were constructed. The first used the broad matrix of taxa, the other two used separate species data matrices for the canyon and the adjacent slope sites. A permutation test with 500 random permutations was used to test the null hypothesis of no linear relationship between abundances and environmental variables, with $p < 0.05$ taken as significant.

Generalized additive models (GAMs) (Hastie and Tibshirani, 1986, 1990) using penalized cubic regression splines (Wood, 2006) were implemented to point out relationships between taxon biomasses and environmental/trophic variables. Independent models were initially constructed to identify variables with best explanatory values. Also interactions between variables were tested. The final models, selected according to both the Akaike information criterion (AIC: Akaike, 1970) and the percentage of deviance explained (%DE), had the following structure:

$$g(\mu) = \beta_0 + f(x,z)$$

where $\mu = E(Y)$ is the expected value of the response Y; $g(\cdot)$ is the link function, while β_0 is the intercept. The function $f(x, z)$ is an arbitrary smooth function representing the effect of the interaction between the two covariates, x and z, on the response.

The studied response variables were biomass of (1) total fauna, (2) polychaetes, (3) crustaceans and (4) molluscs. It was assumed that the underlying probability distribution of the response (biomass) belonged to the Gamma family (biomass being a continuous variable) and the appropriate link function was the natural logarithm. All predictors were continuous. Generalized Cross Validation criterion (GCV: Craven and Wahba, 1979; Gu et al., 1979) was used to select automatically smoothing parameters. Also taxon abundances were examined. Since models

Table 1
Species composition. Mean density of taxa — *N* (ind/m²) collected from stations at 600 m inside canyons (C1 and C2) and on the adjacent slope (S1 and S2).

Taxa	Canyon (600 m)	Adjacent slope (800 m)	Taxa	Canyon (600 m)	Adjacent slope (800 m)
Cnidaria			**Cumacea**		
Stephanoscyphus spp. Allman, 1874	0.0	2.0	*Diastyloides serrata* (G.O. Sars, 1865)	0.0	0.5
Archianellida			*Eplenaon ensis* (Bishop, 1981)	1.9	0.0
Archianellida unid	0.0	1.0	*Eudorella truncatula* (Bate, 1856)	7.7	0.5
Polychaeta			*Leucon longirostris* Sars, 1871	15.7	6.9
Ampharete sp. Malmgren, 1866	0.9	0.0	*Leucon macrochirus* (Fage, 1951)	1.9	2.1
Ampharetidae Malmgren, 1867	34.5	1.9	*Leucon siphonatus* Calman, 1905	5.8	0.0
Arabellidae Hartman, 1944	0.5	0.5	*Makrokylindrus gibraltarensis* (Bacescu, 1961)	0.0	3.8
Aricidea spp. Webster, 1879	7.6	6.4	*Makrokylindrus insignis* (G.O. Sars, 1871)	0.0	1.0
Capitellidae Grube, 1862	6.6	1.5	*Makrokylindrus longipes* (G.O. Sars, 1871)	0.9	0.0
Diplocirrus sp. Hasse, 1915	5.5	1.9	**Isopoda**		
Ilunicidae Berthold, 18	4.1	0.0	*Pleurantheus frevi* (Wägele, 1980)	5.0	4.0
Flabelligeridae Joseph Saint, 1894	0.9	0.5	*Chelator chelatus* (Stephensen, 1915)	7.5	6.9
Galathowenia sp. Kirkegaard, 1959	0.5	0.0	*Desmosoma lineatis* (Linnaeus, 1767)	0.9	0.5
Glycera sp. Savigny, 1818	0.9	0.5	*Eugerda* sp. Meinert, 1890.	1.9	0.0
Glyceridae Grube, 1850	3.2	2.9	*Gnathia* spp.[1] Leach, 1814	0.5	0.0
Levinsenia gracilis (Tauber, 1879)	2.8	2.9	*Ilyarachna longicornis* (G.O. Sars, 1864)	1.9	0.0
Levinsenia spp. Mesnil, 1897	3.6	1.5	**Tanaidacea**		
Lumbrineridae Schmarda, 1861	1.4	1.0	*Apseudes spinosus* (M. Sars, 1858)	0.5	0.0
Lumbrineris sp. Blainville, 1828	0.9	0.5	Tanaidacea unid	5.8	0.5
Maldanidae Malmgren, 1867	3.6	3.5	**Ostracoda**		
Marphysa bellii (Audouin & Milne Edwards, 1833)	4.8	0.5	Cypridinidae	3.8	0.0
Mediomastus sp. Hartman, 1944	0.0	0.5	Ostracoda unid	0.0	4.0
Melinna sp. Grube, 1869	10.9	0.5	**Pycnogonida**		
Nephtyidae sp. A Grube, 1850	2.4	0.5	Pycnogonida unid	1.9	0.0
Nephtys sp. Grube, 1850	0.9	0.0	Crustacea unid [L]	0.0	0.5
Notomastus sp. Sars, 1851 *(latericeus)*	0.5	0.5	**Caudofoveata**		
Opheliidae Malmgren, 1867	3.7	0.0	*Falcidens strigisquamatus* Salvini-Plawen, 1977	4.3	9.2
Orbiniidae Hartman, 1942	1.4	0.5	*Falcidens aequabilis* Salvini-Plawen, 1972	1.8	1.5
Paradiopatra cuadricuspis (M. Sars, 1872)	6.9	7.8	*Falcidens guttuosus* (Kowalesky, 1901)	6.2	0.0
Paradoneis lyra (Southern, 1914)	0.5	0.0	*Prochaetoderma allesi* (Scheltema & Ivanov, 2000)	0.5	0.5
Paraonidae Cerruti, 1909	3.6	2.9	*Prochaetoderma boucheti* Scheltema & Ivanov, 2000	8.1	0.0
Pilargidae St. Joseph, 1899	0.9	0.0	*Prochaetoderma* spp. Thiele, 1902	5.0	11.4
Pista sp. Malmgren, 1866	0.9	0.0	*Scutopus ventrolineatus* Salvini-Plawen, 1968	1.9	0.0
Prionospio sp. Malmgren, 1867	0.0	0.5	**Scaphopoda**		
Sabellidae Malmgren, 1867	0.5	0.0	Scaphopoda unid	3.8	0.0
Spionidae Grube, 1850	6.9	2.9	**Gastropoda**		
Syllidae Grube, 1850	0.5	0.0	*Eulimella nonlaevata* (Gaglini, 1992)	0.5	0.5
Terebellidae Grube, 1851	0.0	0.5	*Europa fusca* (Blainville, 1825)	1.9	0.0
Polychaeta unid [D]	1.4	0.5	**Bivalvia**		
Decapoda			*Abra longicallus* (Scacchi, 1894)	8.9	9.9
Calocaris macandreae (Bell, 1846)	2.1	1.5	*Axinulus croulinensis* (Jeffreys, 1847)	1.4	0.5
Ebalia cranchii (Leach, 1817)	0.5	0.0	*Cochlodesma tenerum* (Fischer, 1882)	0.5	0.0
Monodaeus couchi (Couch, 1851)	1.4	0.5	*Ennucula aegeensis* (Forbes,1844)	4.5	14.9
Copepoda			*Kelliella miliaris* (Philippi, 1844)	36.0	2.1
Calanoidea	0.9	9.2	*Lrdella cEmarinastri* La Perna 2004	1.8	1.5
Amphipoda			*Limatula hoecta* Allen, 2004	0.0	0.5
Carangolopsis spinulosa Ledoyer, 1970	82.9	12.8	*Mendicula ferruginosa* (Forbes, 1844)	0.5	0.5
Eriopisa elongata (Bruzelius, 1859)	0.9	0.5	*Yoldiella messanensis* (Jeffreys, 187)	0.5	4.9
Idunella nana (Schiecke, 1973)	0.0	0.5	**Sipuncula**		
Harpinia crenulata (Boeck, 1871)	12.8	0.0	*Aspidosiphon muelleri* Diesing, 1851	1.9	1.0
Harpinia dellewalleri Chevreux, 1910	5.4	3.5	*Nephasoma* cf. *abyssorum* (Koren & Danielssen)	0.0	1.9
Harpinia spp. Boeck, 1876	9.5	2.1	*Nephasoma* cf. *diaphanes* (Gerould, 1913)	0.0	1.9
Lilljeborgia psaltrica Krapp-Schickel, 1975	0.9	0.0	*Onchnesoma steenstrupii* Koren & Danielssen 1875	4.5	19.0
Maera schmidtii Stephensen, 1915	3.2	0.5	**Echiurida**		
Metaphoxus simplex (Bate, 1857)	3.7	4.0	*Echiurus abyssalis* Skorikov, 1906	0.0	0.5
Monoculodes sp. Stimpson, 1853	1.9	0.0	**Echinodermata**		
Orchomenella nana (Krøyer, 1846)	0.0	1.9	*Amphipholis squamata* (Delle Chiaje, 1828)	1.9	3.6
Paraphoxus oculatus (G.O. Sars, 1879)	6.4	0.5	*Amphiura chiajei* (Forbes, 1843)	18.6	0.0
Pardaliscidae Boeck, 1871	0.0	1.9	*Amphiura filiformis* (Müller, 1776)	0.9	0.0
Phoxocephalidae[D] G.O. Sars, 1891	0.0	0.5	*Amphiura* cf. *grandisquama* Lyman, 1869	1.9	0.0
Psammogammarus sp. A.S. Karaman, 1955	0.0	1.9	Ophiuroidea unid [1]	1.9	1.9
Sophrosyne hispana Chevreux, 1887	1.4	0.5	*Brissopsis lyrifera* (Forbes, 1841)	0.5	0.5
Urothoe corsica (Bellan-Santini, 1965)	1.4	6.4	**Nematoda**		
			Nematoda unid	0.9	4.4

for abundances yielded fairly similar patterns in regression analysis, only biomass results are reported.

Also the cumulative number of species (S) and the Shannon's index (H') were calculated considering all replicate by season.

All statistical analyses were performed using PRIMER6 and PERMANOVA+ (Clarke and Gorley, 2006), XLSTAT (Addinsoft TM) for CCAs and R2.9.0 (www.r-project.org) for general analyses, GAMs (mgcv-package) and PCA analyses.

3. Results

3.1. Taxonomic composition

A total of 106 taxa (ranging from species to families) was identified, belonging to 19 higher groups from Order to Class (Table 1). Although not identified to the lowest taxonomic level, polychaetes included the largest number of taxa (34). Among the groups identified to species, gammaridean amphipods were the most specious (at least 15 species), followed by cumaceans and bivalves (both with 9 species).

3.2. Diversity and biomass trends by habitat/season

The cumulative number of species showed some stabilization after the analysis of 3–4 cores at 800 m. However, at the shallowest station in Besòs canyon (Station C1, 600 m) we did not find any asymptotic stabilization of the cumulative number of species after analysis of 6 cores.

The number of species (S) increased from February to October both inside the canyon and at the adjacent slope (from 39 to 44 inside the canyon; from 32 to 48 at the adjacent slope: Fig. 2). S was higher inside the canyon, except in October 2007. Diversity measured as Shannon's index, H', increased from February to April both inside the canyon and on the adjacent slope, decreasing in June–July (especially inside the canyon) and increasing later (Fig. 2). Maximum H' was found in April inside the canyon, $H'=3.53$, and in October on the adjacent slope, $H'=3.56$.

Total biomass of infauna increased within Besòs canyon (C1) from February–April to June/July 2007 (Fig. 3a), while at the adjacent slope (S1) peaks of biomass were also found in February and again in June/July. Among individual taxa, polychaetes showed maximum biomass in June/July and October inside the canyon and in June/July at the adjacent slope. Crustaceans (mainly peracarids) showed maximum biomass in April inside the canyon and in February on the adjacent slope (one-way ANOVA at the adjacent slope: $F_{1,13}=16.000$, $p=0.002$; significant paired Tukey's comparisons: February > April, $p=0.004$; June/July > October, $p=0.005$). The remaining, rather secondary, taxa showed some irregular variations, perhaps influenced by the limited number of replicates. However, peaks of biomass were found regularly in February (for echinoderms inside the canyon and for bivalves at the adjacent slope) and in June/July (molluscs inside the canyon and sipunculans at the adjacent slope). Variance of data was high, and most temporal trends were not significant, except that of echinoderms in February (one-way ANOVA at adjacent slope: $F_{1,13}=9.152$, $p=0.011$, paired Tukey's significant comparisons: February > April, $p=0.001$; June–July > October, $p=0.003$). Total biomass and biomasses of crustaceans and echinoderms were higher inside the canyon than at the adjacent slope (t-test: total biomass, $p=0.074$; crustaceans, $p=0.006$; echinoderms, $p=0.002$).

All taxa (total infauna, polychaetes, peracarids (see Fig. 3b) sipunculans and echinoderms) showed the highest N (ind/m^2) in February 2007 inside the canyon. Bivalves represented an exception with peaks in April and June/July. Echinoderms also showed maximum N in June/July. These differences, however, were not significant. Only on the adjacent slope did we find significant seasonal changes in infauna abundance. This was true for total infauna N ($F_{1,13}=14.22$, $p=0.001$, higher in February than in October: Tukey's test, $p=0.021$, Fig. 3b), for crustaceans ($F_{1,13}=20.08$, $p=6\times10^{-4}$, higher N in February than in October: Tukey's test, $p=0.009$, Fig. 3b) and for echinoderms ($F_{1,13}=17.16$; $p=0.001$, higher N in February than in the other seasons: Tukey's tests, $p=0.001$). Total N was significantly higher inside the canyon

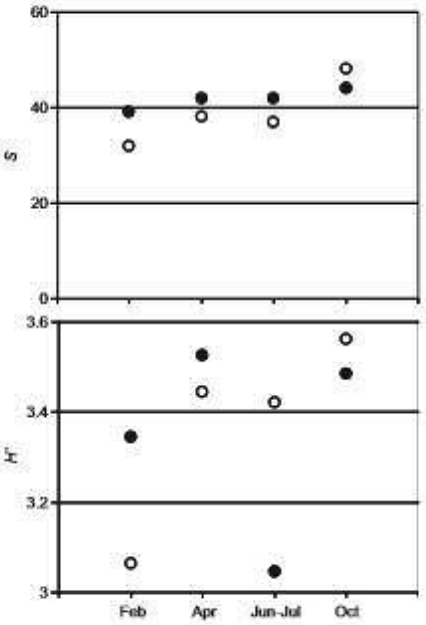

Fig. 2. Diversity expressed by the cumulative number of species (S) and Shannon's index (H') within the four surveys performed at C1 and at S1. Symbols indicate: ● = inside canyon, C1; ○ = at the adjacent slope, S1.

(338.2 ± 107.1) than at the adjacent slope (240.2 ± 71.4; t-tests; $p=0.004$).

Mean weight (Fig. 3c) showed the lowest values in February 2007 for polychaetes both inside the canyon and on the adjacent slope sites (one-way ANOVA at the adjacent slope: $F_{1,13}=5.16$, $p=0.016$; inside the canyon: $F_{1,13}=2.11$ $p=0.075$). Crustacean mean weight was low in October inside the canyon and on the adjacent slope (one-way ANOVA at adjacent slope: $F_{1,13}=4.24$, $p=0.057$). Inside the canyon, the mean weight for all dominant taxa (polychaetes, crustaceans and molluscs) increased in April, a tendency that was still evident in June/July for polychaetes and molluscs. This same tendency was observed at the adjacent slope, excluding molluscs, which had higher mean weight in February.

3.3. Assemblage structure: composition by habitat (canyon and adjacent slope)

The nMDS plot shows the hauls grouped according to both habitat (canyon or adjacent slope) and water column condition (stratified or homogenized) (Fig. 4a). Samples from the canyon are grouped in the left part of the graphic, while samples from the adjacent slope are grouped in the right part. In contrast samples collected during stratified water column condition occupy mainly the top, while samples collected during homogenized conditions occupy the bottom of the graphic.

The two-way PERMANOVA (Table 2) showed statistically significant main effects, i.e. effect of both habitat ($p=3\times10^{-4}$) and water column condition ($p=0.031$). The test did not showed a significant effect of the interaction between the two factors. Pairwise tests indicated higher abundance inside the canyon than

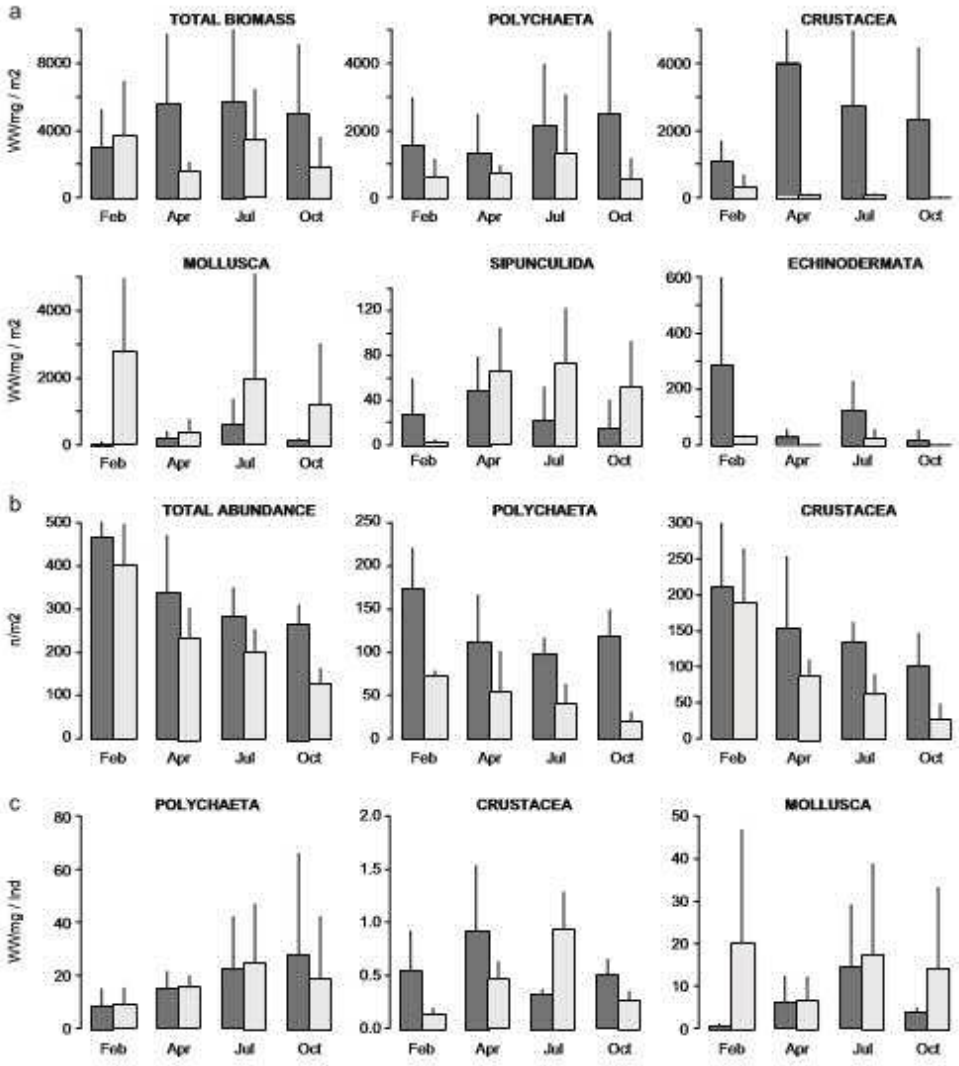

Fig. 3. (a) Annual mean biomass (WW mg/m^2) profiles of total infauna and major taxa; (b) Annual mean density (ind/m^2) profiles of total infauna, polychaetes and crustaceans; (c) Individual mean weight (WW mg/ind) of polychaetes, crustaceans and molluscs. All profiles regard to C1 and S1 samples. Bar color indicates habitat (black—canyon, gray—adjacent slope).

at the adjacent slope, especially under stratified water column conditions.

SIMPER analyses of abundances (Table 3) showed that the amphipod *Carangoliopsis spinulosa*, ampharetid polychaetes and amphipods of the genus *Harpinia* were the most abundant taxa at the canyon site, representing >50% of total abundance. At the adjacent slope site the sipunculan *Onchnesoma steenstrupii* dominated in the assemblage, followed by the bivalve *Ennucula aegeensis* and *C. spinulosa*. These three species together represented the 54.6% of the total abundance.

Polychaetes collected with the suprabenthic sledge were clearly different from species collected with the box-corer, as shown by the MDS analyses (Fig. 4b). This "suprabenthic" assemblage mainly comprised the genera *Harmothoe* (45.6% of abundance) and *Nephthys* (24.5%) and the family Spionidae (8.9%).

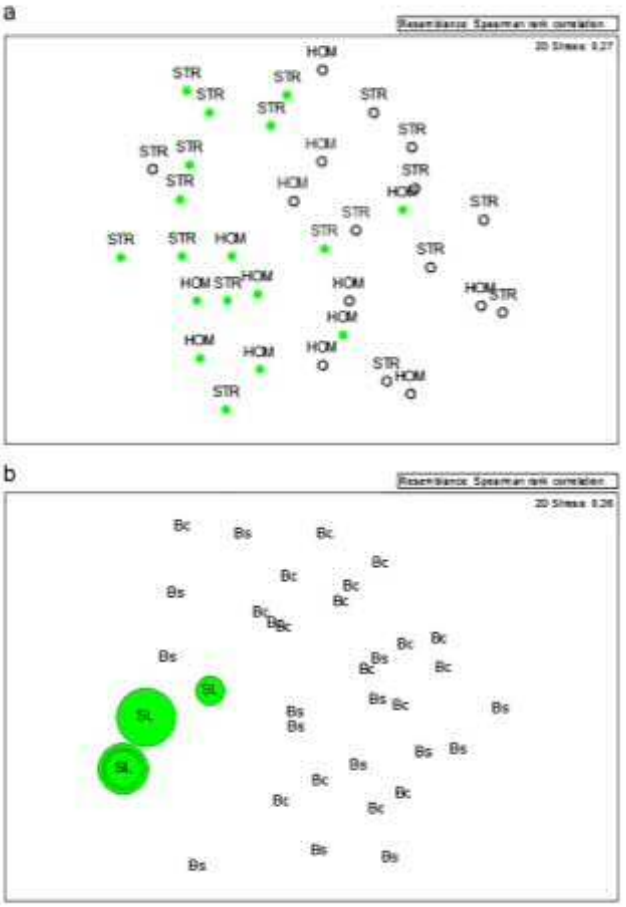

Fig. 4. (a) nMDS ordination of the matrix of taxa densities of box-core samples from all surveys and stations (C1, C2, S1 and S2). Labels indicated: HOM—water column homogenization and STR—water column stratification. Symbols indicate "habitat" (●—canyon; ○—adjacent slope). (b) nMDS ordination of polychaete densities, comparing infaunal vs suprabenthic assemblage: Bc—inside canyon box-core samples, Bs—adjacent slope box-core samples and SL—sledge samples. Bubbles indicate the density of dominant polychaete (the Polinoid *Harmothoe* sp.) in the suprabenthic assemblage.

Table 2
(a) Permanova based on Spearman rank correlation distance matrix of whole dataset (C1, C2, S1 and S2) and (b) pairwise tests (only significant tests are reported). Factors: habitat (levels: canyon, CAN; adjacent slope, SLO) and water condition (levels: homogenized, HOM, and stratified, STR).

Source	*df*	*MS*	*Pseudo-F*	*P-value*
(a) Main test				
Habitat	1	1.578	4654	3×10^{-4}
Water condition	1	0.766	2258	0.011
Habitat × water condition	1	0.335	0.988	0.448
Res	30	0.339		
Total	33			
(b) Pairwise tests				
CAN > SLO		HOM > STR		
CAN > SLO (within "STR" water cond)				

3.4. *Environmental variables*

Temperature ($T_{5\ mab}$) varied within a narrow range through the year both inside the canyon and especially at the adjacent slope (Fig. 5). Anyhow $T_{5\ mab}$ was always lower at the adjacent slope rather than at the canyon station. Inside the canyon site, $T_{5\ mab}$ increased between June/July and October. At the adjacent slope site $T_{5\ mab}$ was quite constant all year round except for a slight rise in April. There was a period of water column homogeneity in February and April and of stratification in June–October. Salinity 5 m above the bottom ($S_{5\ mab}$) ranged between 38.43 and 38.56 (Fig. 5). $S_{5\ mab}$ showed higher values at the canyon station, where it increased from April to October. This pattern was not observed at the adjacent slope where $S_{5\ mab}$ showed the same pattern found for $T_{5\ mab}$.

Table 3
One-way SIMPER analysis (factor: habitat) based on Bray–Curtis similarity (cut-off: 80%) using the whole dataset (C1, C2, S1 and S2). Percentage contribution and cumulative percentage of taxa are reported for each level of the factor, as well as the acronyms of taxa used in CCAs. Code refers to a 2 letters code indicating the Class or Order, which taxa belong to (AM—amphipods, PO—polychaetes, IS—isopods, SI: sipuncolans, EC—echinoderms, BI—bivalvia, CA—caudofoveats, CU—cumaceans).

Canyon *Average similarity: 28.29*					*Adjacent slope* *Average similarity: 22.09*				
Code	**Acronym**	**Taxon**	**Contrib%**	**Cum.%**	**Code**	**Acronym**	**Taxon**	**Contrib%**	**Cum.%**
AM	Cspi	*Carangoliopsis spinulosa*	20.14	20.14	SI	Oste	*Onchnesoma steenstrupii*	33.93	33.93
PO	Amph	Ampharetidae	15.99	36.12	BI	Emucu	*Emuscula aegeensis*	13.15	47.07
AM	Harp	*Harpinia* spp.	14.97	51.09	AM	Cspi	*Carangoliopsis spinulosa*	7.52	54.6
PO	Para	Paraonidae	5.06	56.15	CA	Pruc	*Prochaetoderma* spp.	6.53	61.13
AM	Poca	*Paraphoxus oculatus*	3.65	59.8	BI	Alon	*Abra longicallus*	5.55	66.68
PO	Flab	Flabelligeridae	3.31	63.12	PO	Para	Paraonidae	5.26	71.94
IS	Pfre	*Piksanthura fresli*	2.99	66.11	CA	Falc	*Falcidens* spp.	4.63	76.57
PO	Glyc	Glyceridae	2.98	69.09	CU	Llon	*Leucon longirostris*	2.52	79.1
SI	Oste	*Onchnesoma steenstrupii*	2.87	71.96	IS	Pfre	*Piksanthura fresli*	2.38	81.47
EC	Achi	*Amphiura chiajei*	2.76	74.71					
PO	Spio	Spionidae	2.18	76.9					
PO	Onup	Onuphidae	1.88	78.77					
PO	Capi	Capitellidae	1.74	80.52					

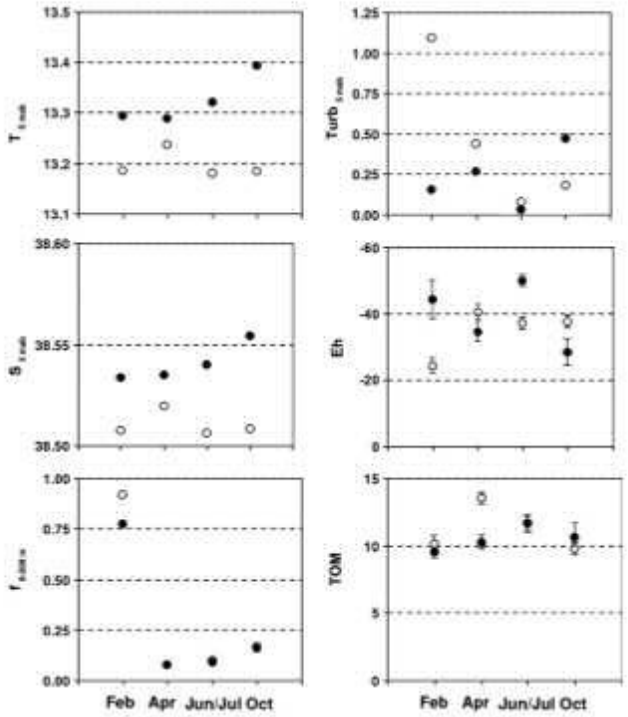

Fig. 5. Environmental variables as a function of season. Temperature 5 m above the bottom ($T_{5\ mab}$); salinity 5 m above the bottom ($S_{5\ mab}$); fluorescence ($f_{0-200\ m}$); water turbidity 5 m above the bottom ($Turb_{5\ mab}$); potential redox of sediments (Eh); and total organic matter (TOM) in sediments. Symbols: ● = canyon, 600 m station; ○ = 800 m station in the adjacent slope. Also standard error bars are reported for repeated measurements of Eh and TOM.

Fluorescence ($f_{0-200\ m}$) followed the same temporal pattern at both the canyon and the slope stations. As regularly happens in the study area with surface Chl *a* (satellite imagery, see below), maximum $f_{0-200\ m}$ was found in January–February (winter) and minimum $f_{0-200\ m}$ was observed in July–August (summer) (Fig. 5).

Water turbidity at 5 m above the seafloor ($Turb_{5\ mab}$) reached maximum values in February at the adjacent slope and in April

inside the canyon (Fig. 5). At both stations $Turb_{5\ mab}$ decreased in June/July, when minimum values were observed, increasing again in October.

REDOX Potential (Eh: Fig. 5) showed different trends at the canyon and the slope stations. Inside the canyon sediments were least reduced in February (−24.4 mV) with an abrupt drop in Eh in April–June/July–October (between −40.4 and −37.7 mV). At the adjacent slope Eh was on average a little more reduced than at the canyon station, with lower Eh in June/July than October. Inside the canyon the total organic matter (TOM) in sediments increased from February to June/July then decreased (Fig. 5). At the adjacent slope TOM increased from February to April and decreased in June/July and October. TOM was, on average, higher in samples taken at slope than inside the canyon, the difference being significant in April.

Flow volume of the most important rivers in the area was maximal in April–May (15.5–4.5 m^3/s) and minimal in June–July (2.5 m^3/s), followed by some increase in August–October (Fig. 6). Chl *a* at the surface, obtained by satellite imagery, decreased sharply from a maximum value in April to an annual minimum in July–August (Fig. 6).

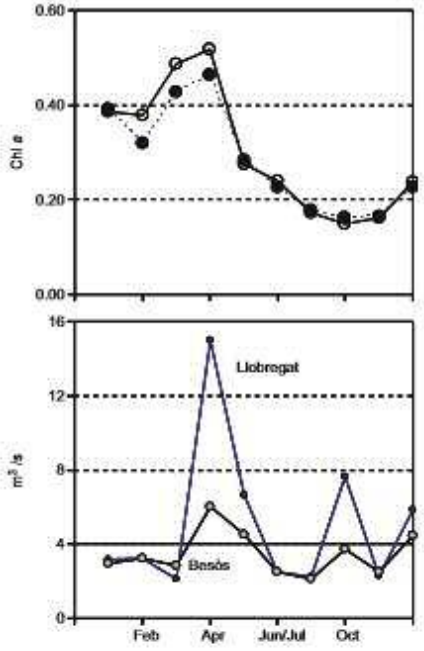

Fig. 6. Environmental variables: (a) Chl *a* in surface by satellite imagery (●: canyon, 600 m station; ○: 800 m station in the adjacent slope) and (b) river flow (m^3/s) of the two most important rivers in central Catalonian coasts.

3.5. *Influence of environmental variables*

The first two principal components in the PCA of *C1* stations (Fig. 7a) explained 46% and 32% of the total variance. A strong seasonality was evident in the ordination of samples, with habitat variables often associated with specific sample stations. Thus, fluorescence was associated with February (B1), river discharge, TOC and $\delta^{13}C$ with April (B2), C/N with July (B3) while $T_{5\ mab}$, $S_{5\ mab}$, $Turb_{5\ mab}$ and less reduced sediments (Eh) were associated with October (B4).

The first two principal components in the PCA for *S1* (adjacent slope: Fig. 7b) explained 44% and 36% of the total variance. Those samples also showed a seasonal relationship in the ordination, but it was less evident than that inside canyon. Moreover, the strength of the association with habitat variables varied across the canyon samples: February (B1) was coupled with fluorescence, but also with less reduced sediment (Eh) and turbidity; April (B2) was associated with river discharge, but also with $T_{5\ mab}$, $S_{5\ mab}$ and TOM; July–October (B3 and B4) were related to gradients of TOC (positively) and to $\delta^{13}C$ in the sediment (negatively).

Canonical correspondence analyses (CCAs; Fig. 8) produced an ordination of the most abundant taxa and their relationship with environmental variables, as a function of both habitat and temporality. CCA of the joint data set from *C1* and *S1* (Fig. 8) explained 89.8% of the total variance. The permutational test revealed a significant linear relationship between taxa abundances and environmental variables (*pseudo-F*=0.580; $p=0.009$).

Clear segregation between canyon station and adjacent slope samples was observed, with an evident association between canyon samples and the abundance of polychaetes and also of

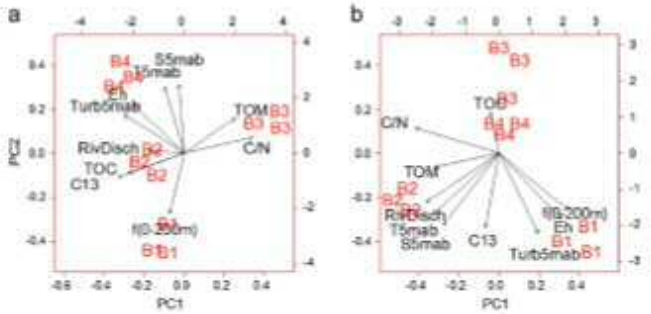

Fig. 7. PCAs of environmental variables collected inside Besòs canyon, *C1* (a) and its adjacent slope, *S1* (b). Labels: B1=February, B2=April, B3=June/July, B4=October; S5mab=salinity, T5mab=temperature, Turb5mab=turbidity, RivDisch=river discharge, TOC=percentage of total organic carbon, TOM=percentage of total organic matter, C/N=carbon-nitrogen ratio, C13=$\delta^{13}C$ in sediment, *f*(0–200 m)=fluorescence (0–200 m).

crustaceans. This segregation was mainly linked to higher salinity ($S_{5\ mab}$) and temperature ($T_{5\ mab}$) inside the canyon. Canyon samples were also linked to higher TOC, indicating a response to the amount of available food, and with C/N, i.e. organic matter quality. To a lesser extent canyon station samples were associated with higher river discharge, more reduced sediments and more depleted $\delta^{13}C$. Canyon samples were grouped in one subset. Seasonality is masked by stronger difference between habitats (Canyon vs adjacent slope), although to some extent that was related to the seasonal condition (e.g. *homogeneity* in B2, B1) of the water column. Adjacent slope samples showed some seasonal segregation, with different dominant taxa in each season. Caudofoveata and Echinoderms were related to Chl *a* and $Turb_{5\ mab}$ in February (B1) and to greater reduction of the sediments. Sipuncula and to a lesser extent Bivalvia were related to TOM and to enriched $\delta^{13}C$ values in July–October (B3–B4).

The two CCAs performed on dominant species (except polychaetes distinguished only to Family level) showed some ordination of species both at canyon station and on the adjacent slope (Figs. 9a and b). The CCA for station *C1* explained 75.1% of the total variance (Permutational test: *pseudo-F*=0.301, p=0.058). Sample ordination showed some seasonal pattern. B1 and B2 from February to April (obtained under *homogenized* water mass conditions) were located together in the left-upper part of the bi-plot, while samples collected under *stratified* conditions (B3 and B4 from July to October) were in the opposite corner. B1 and B2 were mainly associated with Paraonidae, *Harpinia* spp. and *O. steenstrupii*, which were positively related to Chl *a*, TOC, enriched $\delta^{13}C$ and high river discharge. B4 (July) cores were associated with Onuphidae and Glyceridae, both opportunistic carnivorous polychaetes, and with reduced Eh in sediments. Ampharetidae and the ophiuroid *Amphiura chiajei* were related more to high $T_{5\ mab}$ and $S_{5\ mab}$. A number of surface and sub-surface-deposit feeding polychaetes (Capitellidae, Spionidae, Flabelligeridae) were more abundant in B3 (July) cores and associated with high C/N. C/N is indicative of fresh OM, probably lipids, in sediments.

On the adjacent slope (*S1*) CCA explained 70.9% of the total variance and the permutational test was significant (*pseudo-F*=0.507, p=0.021). Samples showed some seasonal grouping (less clear than in the *Besòs* canyon CCA): B1 was associated with Caudofoveata (*Falcidens* spp., *Prochaetoderma* spp.), Paraonidae and with the amphipod *Carangoliopsis spinulosa*. These were positively correlated in turn with $Turb_{5\ mab}$, fluorescence and reduced Eh in sediments. Caudofoveats are surface-deposit feeders preying on foraminiferans (meiofauna) and Paraonidae, and they can also feed selectively on small diatoms. The bivalve *Abra longicallus* and the isopod *Paranthura fresii* seemed mainly associated with B2 in April and with a high number of variables; among the most important were TOC, TOM, enriched $\delta^{13}C$ in sediments and river discharge. *Onchnesoma steenstrupii* and the bivalve *Ennucula aegensis* were more abundant in July (B3) and October (B4) under conditions of low $Turb_{5\ mab}$ and high C/N in sediments.

3.5.1. Regression (generalized additive) models

Models with higher explanatory deviance are reported in Table 4. Total biomass, and the biomass of principal taxa, are functions of interactions among several environmental variables, including *T* (or *S*, strongly correlated with *T*) and trophic variables, especially TOC in the sediment, and to a lesser extent with river discharge, Chl a, C/N, $\delta^{13}C$ and turbidity.

Total biomass, as well as polychaete and crustacean biomasses, showed higher values when high TOC and low *T* were combined (figures not reported), while total biomass was positively related to C/N (fresh organic matter) and to *T*. Crustaceans and molluscs showed a strong positive relationship with changes in river discharges, as did molluscs with Chl *a* at medium values of *T*.

4. Discussion

This is the first temporal quantitative study performed on deep-sea macrobenthos in the Mediterranean Sea. Previous studies analyzed patterns of biomass and assemblage distribution as a function of depth (e.g. Tselepides and Eleftheriou, 1992; Stora et al., 1999) with no temporal element. In addition, most previous studies on Mediterranean benthos have been non-quantitative (e.g. Reyss, 1971), or they have been performed on large epifauna–infauna (i.e., megafauna) (Pérès and Picard, 1964; Pérès, 1985; Cartes et al., 2009). As benthos is the dominant trophic resource for fish and large crustaceans inside Catalonian canyons (e.g. Macpherson, 1981; Cartes, 1994; Cartes and Maynou, 1998; Carrassón and Cartes, 2002), quantitative studies on macrofauna are required to establish, for instance, mass-balance models. Environmental analyses of deep-sea macrofauna distributions have examined effects of depth (Pérès, 1985) and of a group of factors related with sediment characteristics (Reyss, 1971), especially grain size (Stora et al., 1999) and organic matter content

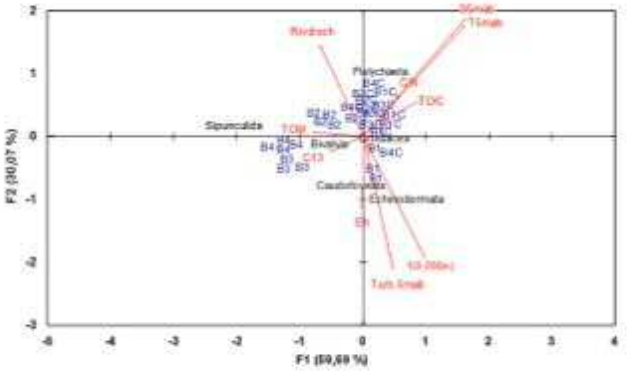

Fig. 8. CCA of major taxa, considering jointly Besòs canyon and its adjacent slope samples (C1 and S1 stations), with environmental variables. Label as in Fig. 7. The C's in labels identify canyon samples.

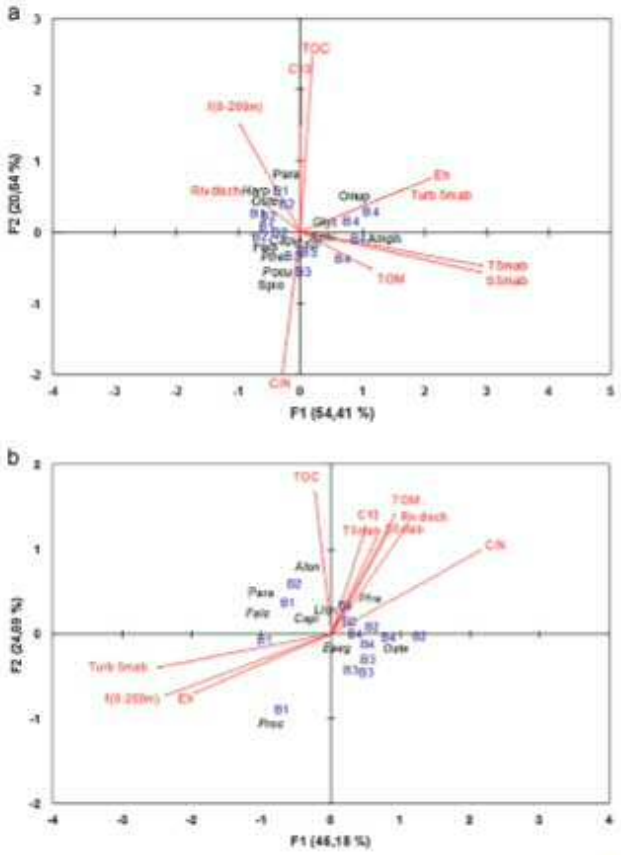

Fig. 9. CCA of dominant species inside Besòs canyon (a) and on the adjacent slope (b) with selected environmental variables. Labels as in Fig. 7. See acronym references of taxa in Table 3.

Table 4
Biomass GAMs for the macrofauna assemblage (C1 and S1 data only). For each response, explanatory covariates, significance of smoothing terms/parametric coefficients (p-value), GCV, AIC, adjusted *r*-squared (R^2) and deviance explained percentage (DE%) are reported.

	Model	*p*-value	GCV	AIC	R^2(adj)	DE (%)
Total biomass	$\sim f(T_{5\ multi}, TOC)$	0.006	1.071	281	0.236	75.3
	$\sim f(T_{5\ multi}, C/N)$	0.013	1.251	335	0.156	29.0
Polychaetes	$\sim f(S_{0\ multi}, TOC)$	0.014	1.194	235	0.430	72.8
Crustaceans	$\sim f(T_{5\ multi}, TOC)$	0.006	5.680	183	0.434	76.5
	$\sim f(T_{5\ multi}, RivDisch)$	0.013	4.956	230	0.228	46.8
Molluscs	$\sim f(T_{5\ multi}, RivDisch)$	0.031	4.989	190	0.089	39.1
	$\sim f(T_{5\ multi}, I_{0-200\ m})$	0.039	5.502	192	0.046	38.8

(Tselepides and Eleftheriou, 1992). These explanatory variables for macrobenthos variability have been evaluated along wide depth ranges over the continental slope (200–1000/2000 m). Macrofauna around Besòs canyon appears to be related mainly to the TOC in sediments, e.g. with the quantity of food. This relation has also been found deeper in both the Atlantic Ocean (Sibuet et al.,1989) and the Angola Basin (Kröncke and Türkay, 2003). As supported by a variety of statistical analyses, changes in macrofauna assemblages and trends in biomass are related with variables associated with sediment characteristics, particularly nutritional value (TOC, C/N, $\delta^{13}C$), but also with characteristics of near-bottom water masses (*T*, *S*), that is with the overall status of the benthic boundary layer (BBL: Gage and Tyler, 1991). Fresh organic matter inside the Besòs canyon in June–July has a terrigenous origin, as shown by the increase of C/N and depletion of $\delta^{13}C$ (Authors' unpubl. data). Apart from the highly depleted $\delta^{13}C$, the C/N ratio was very high in June–July, as expected from terrestrial POM (Thornton and McManus, 1994). Thus, inside the canyon the dominant energy flux was advective, two months delayed after the main peak of river discharges (April–May) in the area (Authors' unpubl. data). On the adjacent slope (at 800 m), C/N has lower values, and the food input seems less dependent

upon advective flux. Regarding water-mass dynamics, higher infaunal abundances was found inside *Besòs* when *T* and *S* were higher. This coincided with the arrival of the Levantine intermediate water (LIW) in the Balearic Basin, once the flow of winter intermediate water is interrupted in the area (López-Jurado et al., 2008). Changes in deep-water masses can influence the resuspension of particles and inputs of POM from other areas, in our case from the most productive region of the Ligurian Sea, situated to the east of the Balearic Basin.

We assumed in our study design that our sample replication would be enough to characterize infaunal communities, although species accumulation curves did not reach an asymptotic shape after analyzing 3 or 4 replicates per station at the *Besòs* canyon site. Stora et al. (1999) tested sample replicability in muddy bottoms of the neighboring Toulon canyon using the same 0.06 m^2 box-corer used here. Except for the shallowest stations (at 250 m), they concluded that "*3 replicates would have been enough to assess assemblage variation at depths between 500–2000 m*". The station *C1* was inside a submarine canyon, close to its head, where the temporal pattern of food supply was similar to that on the continental shelf at 60 m (e.g. $\delta^{13}C$: Authors' unpubl. data). This higher variability probably requires more replicates to fully capture the diversity of canyon fauna. However, our replicates, by contrast, showed higher *within cruise* affinity than *between cruise* affinity, as demonstrated in PCAs–CCAs where replicates belonging to the same cruise were grouped together and linked to the same specific environmental conditions.

4.1. Comparison with other quantitative studies

There are only a few quantitative studies on benthos in the deep Mediterranean (Tselepides and Eleftheriou, 1992; Stora et al., 1999). Off the deep Catalan slope mean annual biomass ranges between 3.1 g WW/m^2 at 800 m and 4.8 g WW/m^2 inside *Besòs* canyon (ca. 0.62–0.96 g DW/m^2, respectively). Biomass was approximately two-times higher than levels recorded in or close to Toulon canyon at comparable depths (500 m: 0.32–0.54 g DW/m^2: Stora et al., 1999). This could be related, among other things (e.g. seasonal variation), to the existence of a small river (mean annual flow 3.4 m^3/s in 2007) debouching to the north of Barcelona, of which the *Besòs* canyon is the natural extension, while the Toulon canyon is not an extension of any existing river on the continent (Stora et al., 1999) The higher diversity (*S*) (despite not including foraminiferans or classifying polychaetes to species level) and total abundance (338.2 ind/m^2) found within *Besòs* in comparison to the Toulon canyon channel station (*S*=36; *N*=176 ind/m^2: Stora et al., 1999) confirms that food availability is higher in our small canyon. As expected, our biomass data were clearly higher than values in the South Cretan Sea (Tselepides and Eleftheriou, 1992), where biomass (0.05–0.09 g DW/ m^2) was an order of magnitude lower than at comparable depths on Catalan slopes. This is explained by the increasing oligotrophy from west to east in the Mediterranean (Azov, 1991; Salihoglu et al., 1991) and by the particularly low food resources in the southern Aegean Sea (Tchukhtchin, 1964; Tselepides and Eleftheriou, 1992). On the Catalonian slope, sediment redox potential (Eh) was clearly lower (on average −40.7 mV) than in the South Aegean Sea (Tselepides and Eleftheriou, 1992), indicating higher POM availability for benthos.

The taxonomic composition of infauna varied between stations at different depths on the Catalonian slope. Inside the *Besòs* canyon polychaetes (Ampharetidae, Paraonidae, Flabelligeridae), amphipods (*Carangoliopsis spinulosa*, *Harpinia* spp., *Paraphoxus oculatus*) and the echinoderm *Amphiura chiajei* dominated. On the adjacent slope the sipunculan *Onchnesoma steenstrupii* and bivalves (*Ennucula aegeensis*, *Abra longicallus*) were more important, together with several caudofoveats (*Folcidens* spp., *Prochaetoderma* spp.). From a *trophic* perspective, surface deposit feeders (e.g. Ampharetidae among polychates and the echinoderm *A. chiajei*) dominated in *Besòs* canyon, replaced by subsurface deposit feeders (e.g. sipunculans) on the adjacent slope. This is consistent with existing literature on deep-sea macrobenthos food webs (Flach and Heip, 1996; Kröncke et al., 2003): species feeding mainly at the sediment surface are linked to fresh organic matter, whereas subsurface deposit feeders and predators are found in sediments with more refractory material. The same replacement of trophic guilds with depth was observed in the abyssal Indian Sea (Pavithran et al., 2009). Stora et al. (1999) found a similar increase of subsurface deposit feeders at 1000–1500 m in Toulon canyon. At our slope station, adjacent to *Besòs* canyon, we attributed the shift to higher habitat stability on deeper bottoms: temporal fluctuations of food sources (TOC, C/N, $\delta^{13}C$) are less evident on the adjacent slope than inside *Besòs* (Authors' unpubl. data). That reasonably explains why the *Besòs* canyon assemblage was dominated by surface deposit feeders throughout the year and seasonally by opportunistic trophic groups (Capitellidae, Flabelligeridae, Glyceridae), better able to adapt to rapid temporal changes in food inputs.

4.2. Dynamics of infauna assemblages

Continental shelf infaunal assemblages often show intra-annual variability, with shifting peaks of biomass and diversity during short lag times after triggering events (Grémare et al., 1997; de Juan and Cartes, unpublished). This is probably a consequence of both spatial heterogeneity and coupling with a diversified food source. Off Banyuls (western Mediterranean) both the highest growth rates of the deposit-feeding bivalve *Abra ovata* and peaks of meiofauna were found in spring, coupled with maximal pigment concentrations at the surface of the sediment (Grémare et al., 1997). Close to river mouths, the distribution of species is also related to fluctuations in hydrodynamic regime that influence substrate characteristics and particle resuspension. Sediment discharges of rivers can change species composition close to delta fronts (Akoumianaki and Nicolaidou, 2007; Cartes et al., 2007). Such information is not generally available for deep-sea systems.

The two stations we sampled on the Catalonian slopes showed of course differences in the amount of biomass (higher in the *Besòs* canyon), but also some important differences in dynamics Biomass in the canyon increased progressively from February to June–July, while at adjacent slope it remained low, increasing moderately in February and/or July. Also assemblage diversity inside canyon and on adjacent slope showed different patterns through the year. While station *C1* showed higher diversity during the period of water column homogeneity (February and April) with a minimum in June–July, the adjacent slope site showed higher diversity during the period of water column stratification with a minimum in February. This is probably linked to higher organic matter quantity (TOC) and quality of sedimentary food (higher C/N) inside *Besòs* canyon (Authors' unpubl. data) supplied by river discharges. At *Besòs* canyon we found depleted $\delta^{13}C$ values closer to those found at 60 m at a shelf station (Authors' unpubl. data). Depleted $\delta^{13}C$ indicates terrigenous origin of organic matter by river flows.

The quality of POM deposited at the seafloor determines changes in the composition and biomass of macrofauna communities (e.g. off Banyuls: Grémare et al., 1997, in the North Sea: Dauwe et al., 1998; Wieking, 2002). These changes correspond to the feeding types of the constituent taxa/species,

matches being established between the available food and the feeding modes of the dominant consumers. Highly mobile predators can proliferate, consuming new production derived from abundance peaks of species belonging to lower trophic levels. We found quite different polychaete assemblages inhabiting the sediment–water interface (sampled with suprabenthic sledges) and the sediment collected with the box-corer. Polynoidae (*Harmothoe* sp.) and Nephthydae (*Nephthys* sp.), large species feeding at a high trophic level (based on $\delta^{15}N$: Fanelli et al., in revision), dominated this mobile epibenthic assemblage. These predators showed a quite different dynamic from that of *infaunal* polychaetes. Higher biomasses of Polynoidae and Nephthydae were found in April decreasing in June–July on the adjacent slope (Fig. 10) following the same pattern as near-bottom turbidity (e.g. higher $Turb_{5\ mab}$ is associated with higher biomass of epibenthic-mobile polychaetes).

Among infauna, we found consistent relationships between feeding types and the quantity and quality of POM arriving on Catalonian slopes. At the level of broad taxa, polychaetes were more abundant under canyon environmental conditions that include: (i) high TOC and high C/N, which are indicative of high fresh food availability because C/N is often correlated with lipid contents (Bodin et al., 2007), an important source of fresh food for benthos (Grémare et al., 1997; Cartes et al., 2002); (ii) high river discharge, with a delay of ~2 months, which suggests an important food source of terrigenous origin for benthos; and (iii) increase of *T* and *S* indicating changes in water masses (LIW) in the study area (Hopkins, 1978). By contrast outside the canyon, caudofoveats and echinoderms (mainly small surface feeding ophiurids) were linked to high near-bottom turbidity and pigment fluorescence in the water column, conditions found in February. This suggests stronger coupling with peaks of primary production at surface. Caudofoveats (e.g. *Falcidens* spp.) are surface deposit feeders preying on foraminiferans (meiofauna) (Salvini-Plawen, 1981, 1988). Amphipholidae are surface deposit feeders (Buchanan, 1964), which probably benefit from turbidity increases (more suspended particles) close to the bottom. On the other hand, sipunculans are sub-surface deposit feeders (Romero-Wetzel, 1987) that were more abundant on the slope in October, when more recycled POM (enriched in $\delta^{13}C$) and rather more TOM (~10%) were found in sediments. In general, such ecological relationships are subject to strong spatio-temporal variations, with seasonal shifts in the species occupying the dominant trophic guilds. Sipunculans, for instance, can save up fresh labile material below the sediment–water interface (Galeron et al., 2009), hence becoming surface deposit feeders. Such relationships were more difficult to establish at species level, due to the lack of detailed information on species diets. In general, dominant species in the canyon during February and April (Paraonidae and *Harpinia* spp.) were more clearly related with variables indicating inputs of pigments in the water column, probably derived from the peak of surface primary production. Paraonidae are partially surface feeders (Fauchauld and Jumars, 1979) consuming diatoms, and foraminiferans, though only a single species has been studied (Röder, 1971). However, *Harpinia* spp. gave an isotopic signal corresponding to omnivory (Fanelli et al., 2009), and they may also prey on meiofauna. Most polychaetes (Capitellidae, Spionidae, Flabelligeridae) were more abundant in June–July in *Besòs* canyon coinciding with a decrease of TOC in sediments, but also with a clear signal of terrigenous carbon (depleted $\delta^{13}C$, high C/N: Cartes et al., 2010; Authors' unpubl. data). These polychaetes are considered to be opportunistic and non-selective in food-particle selection (Fauchauld and Jumars, 1979). Spionidae are potentially mobile and can behave as suspension-feeders (Pardo and Amaral, 2004), while Flabelligeridae are typically tubiculous. Inside *Besòs* canyon other surface deposit feeders were found in this period (e.g. the ampharetid *Melinna* sp.: Gaston, 1987, and *A. chiajei*: Buchanan, 1964). Surface deposit feeders also dominate (representing between 36% and 73% of abundance) in Toulon canyon assemblages (Stora et al., 1999) in samples mainly taken in the period May–July. By contrast over Catalan slopes, during October and under conditions of maximum water turbidity and increases of TOM and TOC, carnivorous polychaetes (Glyceridae, Onuphidae: Fauchauld and Jumars, 1979) were dominant, together with Ampharetidae, considered as surface deposit feeders. Carnivorous polychaetes were also more abundant at the two shallowest stations at Toulon canyon (Stora et al., 1999). This trophic group is more characteristic of disturbed areas (i.e. with high hydrodynamism) exposed to strong organic inputs (Pearson and Rosenberg, 1978). These conditions were likely found at the sediment–water interface rather than deeper in the sediment. This explains why carnivorous polychaetes (*Harmothoe* sp., *Nephthys* spp.) collected with the suprabenthic sledge dominated this "*suprabenthic*" habitat, showing their maximum abundance under higher $Turb_{5\ mab}$.

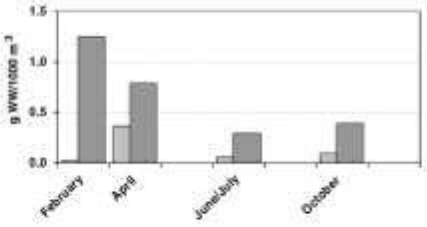

Fig. 10. Dynamics of suprabenthic polychaetes over the slopes during 2007 at 650 m (pale-gray bars) and 800 m (dark-gray bars). Both stations were on the adjacent slope (see Fig. 1).

At the slope site temporal relationships between species and environmental variables were less marked than in the *Besòs* canyon, as indicated by PCA and CCA results. This tendency is in agreement with higher fluctuations of food sources (TOC, C/N, $\delta^{13}C$) at the *Besòs* canyon (see above); conditions were more stable at the adjacent slope stations. The only consistent relationships at the adjacent slope were caudofoveats (*Falcidens* spp., *Prochaetoderma* spp.) and Paraonidae with $Turb_{5\ mab}$ and fluorescence, likely because these taxa are surface deposit feeders that can eat diatoms and foraminiferans (meiofauna) (Fauchald and Jumars, 1979; Jones and Baxter, 1987). As foraminiferans respond rapidly to inputs of fresh organic matter (Gooday, 1988), it is possible that they already reach high densities in February because the maximum of primary production at the surface begins in November–December off Catalan coasts (from http://reason.gsfc.nasa.gov/Giovanni).

In conclusion, the dynamics of macrobenthos at the two stations sampled over Catalonian slopes showed differences in biomass and abundance patterns and in their trophic structure. Biomass was higher inside the *Besòs* canyon than on the adjacent slope. Communities inside the canyon are mostly dominated by surface detritus polychaetes and crustaceans and on the adjacent slope by subsurface deposit feeders (mainly sipunculans). Also epibenthic-mobile assemblages of polychaetes were clearly different in composition from those of infauna, being composed of carnivorous forms associated with higher near-bottom turbidity. The proliferation of opportunistic species inside the *Besòs* canyon and a stronger temporal succession there of species in relation of food availability and quality were consistent with greater variability in food sources (TOC, C/N, $\delta^{13}C$) (Authors' unpubl. data) and with greater influence of terrigenous inputs by river discharges.

Total macrobenthos biomass found over Catalonian slopes was higher than that found in the neighboring Toulon canyon (Stora et al., 1999), probably because the canyons are differently conditioned by their relationships with rivers and river flows.

Acknowledgments

The authors thank all the participants of the BIOMARE (ref. CTM2006-13508-CO2-02/MAR) surveys, especially Vanesa Papiol and the crew of the F/V *García del Cid* for their inestimable help. A number of taxonomists helped us in the determination of different taxa. Our acknowledgements to Drs. C. Salas and S. Gofas (University of Málaga) for their help determining some bivalves and gastropods, and to Dr. L. Salvini-Plawen (University of Vienna) for caudofoveats. Finally we want to acknowledge reviewers for their useful hints to improve the manuscript. This study was designed within and financed by the project ANTROMARE(CTM2009-12214-CO2-01-MAR).

References

Akaike, H., 1970. Statistical predictor identification. Ann. Inst. Stat. Math. 22, 203–217.

Akoumianaki, I., Nicolaidou, A., 2007. Spatial variability and dynamics of macrobenthos in a Mediterranean delta front area: the role of physical processes. J. Sea Res. 57, 47–64.

Anderson, M.J., 2001. A new method for non-parametric multivariate analysis of variance. Austr. Ecol. 26, 32–46.

Anderson, M.J., Legendre, P., 1999. An empirical comparison of permutation methods for tests of partial regression coefficients in a linear model. J. Stat. Comput. Simul. 62, 271–303.

Anderson, M.J., ter Braak, C.J.F., 2003. Permutation tests for multi-factorial analysis of variance. J. Stat. Comput. Simul. 73, 85–113.

Azov, Y., 1991. Eastern Mediterranean—a marine desert? Mar. Pollut. Bull. 23, 225–232.

Bodin, N., Le Loch, F., Hily, C., 2007. Effect of lipid removal on carbon and nitrogen stable isotope ratios in crustacean tissues. J. Exp. Mar. Biol. Ecol. 341 (2), 168–175.

Buchanan, J.B., 1964. A comparative study of some of the features of the biology of *Amphiura filiformis* and *Amphiura chiajei* (Ophiuroidea) considered in relation to their distribution. J. Mar. Biol. Assoc. UK 44, 565–576.

Carpine, C., 1970. Ecologie de l'étage bathyal dans la Méditérranée occidentale. Mém. Inst. Océanogr. Monaco 62, 1–146.

Carrassón, M., Cartes, J.E., 2002. Trophic relationships in a Mediterranean deep-sea fish community: partition of food resources, dietary overlap and connections with the Benthic Boundary Layer. Mar. Ecol. Prog. Ser. 241, 41–55.

Cartes, J.E., 1994. Influence of depth and season on the diet of the deep-water aristeid *Aristeus antennatus* along the continental slope (between 400 to 2300 m) in the Catalan Sea (western Mediterranean). Mar. Biol. 120, 639–648.

Cartes, J.E., 1998. Dynamics of the bathyal benthic boundary layer in the northwestern Mediterranean: depth and temporal variations and their possible connections within deep-sea trophic webs. Prog. Oceanogr. 41, 111–139.

Cartes, J.E., Maynou, F., 1998. Daily ration estimates and comparative study of food consumption in nine species of deepwater decapod crustaceans of the NW Mediterranean. Mar. Ecol. Prog. Ser. 171, 221–231.

Cartes, J.E., Grémare, A., Maynou, F., Villora-Moreno, S., Dinet, A., 2002. Benthic boundary layer response to fluxes of labile particulate organic matter in the bathyal environment of the Catalan Sea (northwestern Mediterranean). Prog. Oceanogr. 53, 29–56.

Cartes, J.E., Papiol, V., Palanques, A., Guillén, J., Demestre, M., 2007. Dynamics of suprabenthos off the Ebro Delta (Catalan Sea, Western Mediterranean): spatial and temporal patterns and relationships with environmental factors. Estuarine Coastal Shelf Sci. 75, 501–515.

Cartes, J.E., Maynou, F., Fanelli, E., Romano, C., Mamouridis, V., Papiol, V., 2009. The distribution of megabenthic invertebrate epifauna in the Balearic Basin (western Mediterranean) between 400 and 2300 m. Environmental gradients influencing assemblages composition and biomass trends. J. Sea Res. 61, 244–257.

Cartes, J.E., Fanelli, E., Papiol, V., Maynou, F., 2010. Trophic relationships at intrannual spatial and temporal scales of macro and megafauna around a submarine canyon off the Catalonian coast (western Mediterranean). J. Sea Res. 63, 180–190.

Clarke, K.R., 1993. Non-parametric multivariate analyses of changes in community structure. Austr. J. Ecol. 18, 117–143.

Clarke, K.R., Warwick, M., 1994. Change in Marine Communities: An Approach to Statistical Analysis and Interpretation. Natural Environmental Research Council, UK.

Clarke, K.R., Gorley, R.N., 2006. PRIMER v6: User Manual/Tutorial. PRIMER-E, Plymouth.

Craven, P., Wahba, G., 1979. Smoothing noisy data with spline functions estimating the correct degree of smoothing by the methos of generalized cross-validation. Numer. Math. 31, 377–403.

Cunha, J., Carvalho, S., Ravara, A., Gaye, J.D., Rodrigues, A.M., Quintino, V., 2004. Deep macrobenthic communities from Nazaré Submarine Canyon (NW Portugal). Sci. Mar. 68, 171–180.

de Juan, S., Cartes, J.E. Influence of environmental factors on the dynamics of macrobenthic crustaceans in soft-bottoms from the Ebro Delta continental shelf (North-western Mediterranean). Unpublished.

de Stigter, Boer, H.W., de Jesús Mendes, P.A., Jesús, C.C., Thomsen, L., van den Berg, G.D., van Weering, T.C.E., 2007. Recent sediment transport and deposition in Nazaré Canyon, Portuguese continental margin. Mar. Geol. 246, 144–164.

Dauwe, B., Herman, P.M.J., Heip, C.H.R., 1998. Community structure and bioturbation potential of macrofauna at four North Sea stations with contrasting food supply. Mar. Ecol. Prog. Ser. 173, 67–83.

Dauvin, J.C., Lucgenê, J.C., 1989. Modification du traîneau Macer-GIROQ pour l'amélioration de l'échantillonnage quantitatif étagé de la faune suprabenthique. J. Rech. Océanogr. 14, 65–67.

Epping, E., van der Zee, C., Soetaert, K., Helder, W., 2002. On the oxidation and burial of organic carbon in sediments of the Iberian margin and Nazaré Canyon (NE Atlantic). Prog. Oceanogr. 52, 399–431.

Fanelli, E., Cartes, J.E., 2008. Spatio-temporal changes in gut contents and stable isotopes in two deep Mediterranean pandalids: influence on the reproductive cycle. Mar. Ecol. Prog. Ser. 355, 219–233.

Fanelli, E., Cartes, J.E., 2010. Temporal variations in the feeding habits and trophic levels of three deep-sea demersal fishes from the western Mediterranean Sea, based on stomach contents and stable isotope analyses. Mar. Ecol. Prog. Ser. 402, 213–232.

Fanelli, E., Cartes, J.E., Rumolo, P., Sprovieri, M., 2009. Food-web structure and trophodynamics of mesopelagic–suprabenthic bathyal macrofauna of the Algerian Basin based on stable isotopes of carbon and nitrogen. Deep-Sea Res. I 56, 1504–1520.

Fanelli, E., Papiol, V., Cartes, J.E., Rumolo, P., Brunet, C., Sprovieri, M., 2011. Food web structure of the epibenthic and infaunal invertebrates on the Catalan slope (NW Mediterranean): Evidence from d13C and d15N analysis. Deep-Sea Res. I 58, 98–109.

Fauchald, K., Jumars, P.A., 1979. The diet of worms: a study of polychaete feeding guilds. Oceanogr. Mar. Biol. Annu. Rev. 17, 193–284.

Féral, J.P., Ferrand, J.G., Guille, A., 1990. Macrobenthic physiological response to environmental fluctuations: the reproductive cycle and enzymatic polymorphism of a eurybathic seaurchin on the northwestern Mediterranean continental shelf and slope. Cont. Shelf. Res. 10, 1147–1155.

Flach, E., Heip, C.H.R., 1996. Vertical distribution of macrozoobenthos within the sediment on the continental slope of the Goban Spur area (NE Atlantic). Mar. Ecol. Progr. Ser. 141, 55–66.

Gage, D.J., Tyler, P.A., 1991. Deep-sea Biology: A Natural History of Organisms at the Deep-sea Floor. Cambridge University Press, Cambridge, UK.

Galeron, J., Menot, L., Renaud, N., Crassous, P., Khripounoff, A., Tréguier, C., Sibuet, M., 2009. Spatial and temporal patterns of benthic macrofaunal communities on the deep continental margin in the Gulf of Guinea. Deep-Sea Res. II, 56, 2299–2312.

Galub, G.H., Heath, M., Wahba, G., 1979. Generalized cross validation as a method for choosing a good ridge parameter. Technometrics 21, 215–223.

Gardner, W.B., 1989. Baltimore Canyonas a modern conduit of the sediment to the deep sea. Deep-Sea Res. 36(A), 323–358.

Gaston, G.R., 1987. Benthic Polychaeta of the Middle Atlantic Bight: feeding and distribution. Mar. Ecol. Progr. Ser. 36, 251–262.

Gerino, M., Stora, G., Durbec, J.P., 1994. Quantitative estimation of biodiffusive and bioadvective sediment mixing-in situ experimental approach. Oceanol. Acta 17, 547–554.

Gooday, A.J., 1988. A response by benthic Foraminifera to the deposition of phytodetritus in the deep-sea. Nature 332, 70–73.

Grémare, A., Amouroux, J.M., Charles, F., Dinet, A., Riaux-Gobin, C., Baudart, J., Medernach, L., Bodiou, J.Y., Vétion, G., Colomines, J.C., Albert, P., 1997. Temporal changes in the biochemical composition and nutritional value of the particulate organic matter available to surface deposit-feeders: a two year study. Mar. Ecol. Progr. Ser. 150, 195–206.

Griggs, G.B., Carey, A.G., Kulm, L.D., 1969. Deep-sea sedimentation and sediment fauna interaction in Cascadia Channel and on Cascadia Abyssal Plain. Deep-Sea Res. 16, 157–170.

Hastie, T., Tibshirani, R., 1986. Generalized additive models. Stat. sci. 1 (3), 297–318.

Hastie, T., Tibshirani, R., 1990. Generalized Additive Models. Monographs on Statistics and Applied Probability 43. CHAPMAN&HALL/CRC.

Hopkins, T., 1978. Physical Processes of the Western Mediterranean Sea. Estuarine Transport Processes. In: Kjerfve, B. (Ed.), Univ. South Carolina Press, pp. 269–309.

Jones, A., Baxter, J., 1987. Molluscs: Caudofoveata, Solenogastres, Polyplacophora and Scaphopoda. London: E. J. Brill/Dr. W.. Backhuys.

Josselyn, M.N., Cailliet, G., Niesen, T., Cowen, R., Hurley, A., Conner, J., Hawes, S., 1983. Composition, export and faunal utilization of drift vegetation in the salt river submarine canyon. Estuarine Coastal Shelf Sci. 17, 447–465.

Kröncke, I., Türkay, M., 2003. Structural and functional aspects of the benthic communities in the deep Angola Basin. Mar. Ecol. Prog. Ser. 260, 43–53.

Kröncke, I., Türkay, M., Fiege, D., 2003. Macrofauna communities in the eastern Mediterranean deep-sea. Mar. Ecol. 24 (3), 193–216.
López-Jurado, J., Monserrat, S., Marcos, M., 2008. Hydrodinamic conditions at the Balearic Islands during 2003–2004. J. Mar. Syst. 71 (3–4), 303–315.
Macpherson, E., 1981. Resource partitioning in a Mediterranean demersal fish community. Mar. Ecol. Progr. Ser. 4, 183–193.
Macquart-Moulin, C., Patriti, G., 1996. Accumulation of migratory micronekton crustaceans over the upper slope and submarine canyons of the northwestern Mediterranean. Deep-Sea Res. I 43 (5), 579–601.
Madurell, T., Cartes, J.E., 2005. Trophodynamics of a deep-sea demersal fish assemblage from the bathyal eastern Ionian Sea (Mediterranean Sea). Deep-Sea Res. I: Oceanogr. Res. Pap. 52 (11), 2049–2064.
Paxdo, E.V., Amaral, A.C.Z., 2004. Feeding behavior of *Scalelepis* sp. (Polychaeta: Spionidae). Braz. J. Oceanogr. 52, 75–79.
Pavithran, S., Ingole, B.S., Nanajkar, M., Raghukumar, C., Nath, B.N., Valsangkar, A.B., 2009. Composition of macrobenthos from the Central Indian Ocean Basin. J. Earth Syst. Sci. 118 (6), 689–700.
Pearson, T.H., Rosenberg, R., 1978. Macrobenthic succession in relation to organic enrichment and pollution of the marine environment. Oceanogr. Mar. Biol. Ann. Rev. 16, 229–311.
Pérès, J.M., 1985. History of the mediterranean biota and the colonization of the depths. In: Margalef, R. (Ed.), Western Mediterranean. Pergamon Press, pp. 198–232.
Pérès, J.M., Picard, J., 1964. Nouveau manuel de bionomie benthique de la mer Méditerranée. Re. Trav. Sta. Mar. d'Endoume 31, 5–137.
Reyss, D., 1971. Les canyons sous-marins de la mer catalane, le Rech du Cap et le Rech Lacaze Duthiers. 111. Les peuplements de la macrofaune benthique. Vie Milieu 22 (3), 529–613.
Röder, H., 1971. Gangsysteme von Paraonis fulgens Levinsen, 1883 (Polychaeta) in oekologischer, ethologischer und aktuopalaeontologischer Sicht. Senckenber. Marit. 3, 3–51.
Romero-Wetzel, M.B., 1987. Sipunculans as inhabitants of very deep, narrow burrows in deep-sea sediments. Mar. Biol. 96 (1), 87–91.
Rowe, G.T., Pulloni, P.T., Haedrich, R.L., 1982. The deep-sea macrobenthos on the continental margin of the northwest Atlantic Ocean. Deep-Sea Res. 29 (2A), 257–278.
Salihoglu, I., Saydam, C., Bastürk, O., Yilmaz, K., Go, D., Hatipoglu, E., Yilmaz, A., 1991. Transport of nutrients and chlorophyll-a by mesoscale eddies in the northeastern Mediterranean. Mar. Chem. 29, 375–390.
Salvini-Plawen, L.v., 1981. The molluscan digestive system in evolution. Malacologia 21, 371–401.
Salvini-Plawen, L.v., 1988. The structure and function of molluscan digestive systems. In: Trueman, E.R., Clarke, M.R. (Eds.), The Mollusca, vol. 11. Academic Press, San Diego, CA, pp. 301–380.
Sanders, H.L., Hessler, R.R., Hampson, G.r., 1965. An introduction to the study of deep-sea benthic faunal assemblages along the Gay Head-Bermuda transect. Deep-Sea Res 12, 845–867.
Sibuet, M., Lambert, C.E., Chesselet, R., Laubier, L., 1989. Density of the major size groups of benthic fauna and trophic input in deep basins of the Atlantic Ocean. J. Mar. Res. 47, 851–867.
Stora, G., Bourcier, M., Arnoux, A., Gerino, M., Campion, J., Gilbert, F., Durbec, J.P., 1999. The deep-sea macrobenthos on the continental slope of the north-western Mediterranean Sea: a quantitative approach. Deep-Sea Res. 46, 1339–1368.
Tchukhtchin, V.D., 1964. Quantitative data on benthos of the Tyrrhenean Sea. Trudy Sevast. Biol. St. 17, 48–50.
ter Braak, C.J.F., 1986. Canonical correspondence analysis: a new eigenvector technique for multivariate direct gradient analysis. Ecology 67, 1167–1179.
Thistle, D., 2003. On the utility of metazoan meiofauna for studying the soft-bottom deep sea. Vie Milieu 53, 97–101.
Thornton, S.F., McManus, J., 1994. Application of organic carbon and nitrogen stable isotope and C/N ratios as source indicators of organic matter provenance in estuarine systems: evidence from the Tay Estuary. Scotl. Estuarine Coastal Shelf Sci. 38, 219–233.
Tselepides, A., Eleftheriou, A., 1992. South Aegean (Eastern Mediterranean) continental slope benthos: macro-infaunal-environmental relationships. NATO Advanced Research Workshop, College Station, TX, USA. In: Rowe, G.T., Pariente, V. (Eds.), Deep Sea Food Chains and the Global Carbon Cycle. Kluwer Academic Publishers, Dordrecht, pp. 139–156.
Vamvakas, C., 1970. Peuplements benthiques des substrats meubles du sud de la mer Egée. Téthys 2, 89–130.
Vetter, E.W., 1998. Population dynamics of a dense assemblage of marine detritivores. J. Exp. Mar. Biol. Ecol. 226, 131–161.
Vetter, E.W., Dayton, P.K., 1999. Organic enrichment by macrophyte detritus, and abundance patterns of megafaunal populations in submarine canyons. Mar. Ecol. Progr. Ser. 186, 137–148.
Wieking, G., 2002. The macrofauna at the Dogger bank: food supply in relation to hydroclimate, Ph.D. thesis, University of Oldenburg, Germany.
Wood, S.N., 2006. Generalized Additive Models: An Introduction with R. CRC press, Boca Raton, FL.

Journal of Sea Research 65 (2011) 340–354

Contents lists available at ScienceDirect

Journal of Sea Research

journal homepage: www.elsevier.com/locate/seares

Deep-sea suprabenthos assemblages (Crustacea) off the Balearic Islands (western Mediterranean): Mesoscale variability in diversity and production

J.E. Cartes *, V. Mamouridis, E. Fanelli

Institut de Ciencies del Mar, CSIC, P.g Maritim de la Barceloneta, 37-49 08003 Barcelona, Spain

ARTICLE INFO

Article history:
Received 3 September 2010
Received in revised form 20 January 2011
Accepted 3 February 2011
Available online 18 February 2011

Keywords:
Suprabenthos
Western Mediterranean
Diversity
Production

ABSTRACT

The composition of suprabenthic crustacean assemblages, their diversity, production (P) and production/biomass (P/B) ratios, were analyzed at species level along two transects situated to the north (N) and south (S) of Mallorca (Balearic Islands, western Mediterranean) at depths between 134 m and 760 m, based on a ca. bi-monthly sampling performed between August 2003 and June 2004. Differences with depth and season in assemblage composition and diversity were analyzed as a function of the contrasting environmental features (e.g. water mass dynamics) of the two areas. We identified 187 species (18 decapods, 5 euphausiids, 16 mysids, 76 gammaridean amphipods, 13 hyperiids, 1 caprellid, 21 isopods and 37 cumaceans). Substantial mesoscale variability in the deep-sea suprabenthic assemblages coupled with diversity trends between the N and S transects were found. Seasonality was the most important gradient influencing the dynamics of suprabenthos over the upper (350 m) and middle (650–750 m) slope in the N area. Conversely, the S area appeared to be more stable temporally with depth as the main gradient inducing assemblage differences. Different depth-related patterns were observed both for diversity and P/B. To the north diversity was very low at the shelf-break, increasing on the upper-slope ($H' > 3.00$) and then decreasing again on the middle-slope. To the south diversity increased smoothly downward, reaching the highest values on the middle-slope. Regarding productivity, P/B was highest at intermediate depths to the north (over ca. 450–500 m), while to the south highest P/Bs were found deeper (over ca. 600–650 m). The higher P/B at intermediate depths found along N are likely due to higher % of organic matter (OM) in sediments, a product of oceanographic frontal systems. In particular, P/B was higher along N among omnivores and detritus feeders (e.g. *Andaniexis mimonectes*, *Lepechinella manco* and combined cumaceans), coupled to enriched OM in sediments, while along S mesoplanktonic carnivores (*Rhachotropis* spp.) had higher P/Bs. We conclude that on the north slope the influence of frontal systems and more active flow dynamics of different water masses (WIW and LIW) increases natural disturbance in the area, increasing productivity and diversity of suprabenthic peracarids in the Benthic Boundary Layer. Also, species showed a displacement of their average distributions (their Centres of Gravity, CoG) to shallower depths along N, which is another indicator of more favorable habitat conditions for suprabenthos in the 400–500 m range at N.

1. Introduction

The Benthic Boundary Layer (BBL) is a transitional zone (ecotone or ecocline) between pelagic and benthic domains (Dauvin and Vallet, 2006) occupied by a diverse community composed of vagile megafauna (e.g. fishes and large decapod crustaceans) and small swimming macrofauna (mainly peracarid crustaceans, copepods, eucarids and gelatinous taxa). The swimming macrofauna constitute the suprabenthos (= hyperbenthos) (Brunel et al., 1978). While the megafauna have a wider distribution both in the water column and in benthic domains, the deep-sea suprabenthos is highly diversified within the BBL (especially peracarids), and it must be adapted to live in that interface (ca. between 0 and 2 m above the bottom).

Suprabenthos has an important trophic role in deep-sea ecosystems as prey of important megafaunal species, (e.g. target species of fisheries, such as *M. merluccius* and *Aristeus antennatus*) (Cartes et al., 2001). Suprabenthic crustaceans (e.g. amphipods and cumaceans), occupy 2–3 trophic levels with some species exploiting detritus and others being carnivores on meiofauna and small zooplankton (Madurell et al., 2008; Fanelli et al., 2009a,b). Therefore, its exploitation of particulate organic matter (POM) and its role as prey make it a non-trivial compartment in the function of deep-sea trophic webs (Cartes et al., 2001). Suprabenthos are especially important in the diet of juvenile fish and decapods (Cartes et al., 2008a) and of fish in the Mediterranean below 1000 m (Carrassón and Cartes, 2002).

Seafloor dynamics have repeatedly been suggested to be affected by cyclic food availability, particularly periodic phytodetritus deposition

* Corresponding author. Tel.: +34 932309500; fax: +34 932309555.
E-mail address: jcartes@icm.csic.es (J.E. Cartes).

1385-1101/$ – see front matter
doi:10.1016/j.seares.2011.02.002

(vertical flux: Billett et al., 2001) and by advective fluxes in areas with mainland influence (e.g. via submarine canyons: Cartes et al., 2009a). Depth, seasonality and latitude are often the main gradients determining spatial and temporal changes in marine communities (Corliss et al., 2009; Rombouts et al., 2009), with the spatial (e.g. regional and global) and temporal scales adopted in such analyses being crucial (Watts et al., 1992; Crame, 2000). Latitudinal gradients, for instance, are important determinants of species richness in terrestrial ecology. By contrast the influence of latitude on diversity seems to be less consistent in marine environments (Rex et al., 2000), especially for some benthic taxa forming regional hotspots of diversity (Crame, 2000; Rombouts et al., 2009). Gradients such as depth or latitude are associated with an array of different environmental variables (e.g. water temperature |T|; salinity |S|; proportion of organic matter |OM| – see Cartes et al., 2008b; sediment grain size; and dissolved oxygen – see Dickinson, 1978) that act directly on organisms, influencing the distribution and diversity of species (e.g. in the case of planktonic copepods: Rombouts et al., 2009). Diversity patterns of benthos also can be related with latitudinal gradients at large spatial scales (Rex et al., 1997). At more local scales, spatial and temporal changes in biomass peaks of benthic species living at great depths have been related with highly productive zones and episodes (Billett et al., 2001 and Ruhl and Smith, 2004 in the abyss; Cartes et al., 2009a on the slope). Hypotheses have been proposed to explain trends in deep-sea species diversity. They relate to the stability of environments, to production rates and to predation pressure by the highest trophic levels (Gage and Tyler, 1991; Rex and Etter, 2010). However, exactly how diversity relates to environmental conditions or to local productivity is unknown for the deep sea, because of the lack of appropriate data sets (Corliss et al., 2009).

Suprabenthos are a vagile part of benthos, not quantitatively sampled with box-corers. However, these organisms are subject to gradients similar to those affecting benthos. Assemblage composition of deep-sea suprabenthos has mainly been related to depth (e.g. Western Mediterranean: Bellan-Santini, 1990; Cartes and Sorbe, 1993, 1997, 1999a; Cartes et al., 2003; Atlantic: Marques and Bellan-Santini, 1987; Brandt, 1995; Dauvin and Sorbe, 1995; Sorbe, 1999). Environmental coupling is well documented for shallow water species and communities, even at shelf-slope breaks (Joselson and Conley, 1997; Richoux et al., 2004). By contrast, the interaction between chemical and physical variables and assemblage dynamics of deep-sea suprabenthos has scarcely been studied (Elizalde et al., 1999; Cartes et al., 2008b), particularly at species level. Small-scale spatial variations among suprabenthic assemblages are poorly known, although some differences in the composition of species and trophic guilds between mainland and insular areas have been described (Cartes et al., 2009b). Even in stable environments such as deep-sea areas, spatial differences (*e.g.* in terms of biomass) among benthos can reach more than an order of magnitude between neighboring areas, which is often discussed in terms of differences in food supply (Dickinson and Carey, 1978; Lampitt et al., 1986). The biological cycles of deep-sea invertebrates have repeatedly been linked with cyclic food availability, often associated with periodic phytodetritus deposition (vertical flux: Richoux et al., 2004), less often to advective-terrigenous fluxes in areas with mainland influence (e.g. via submarine canyons: Buscail et al., 1990; Cartes et al., 2009b). Populations of marine species can occupy patches of high quality habitat, and they can exist as a number of metapopulations that may have limited exchange of individuals among them (Jacob and Sale, 2006), hence the importance of comparative studies at short and mesoscale levels. In shallow waters, local changes in environmental quality (e.g. food supply) may affect secondary production of species at short spatial scales (Cartes et al., 2009c).

In this study, the dynamics of suprabenthos have been simultaneously analyzed at a mesoscale in two areas around the Balearic Islands (in the North-West and South of Mallorca) in relation to environmental dynamics (see Cartes et al., 2008b). The two areas have different oceanographic conditions related with dynamics of water masses (López-Jurado et al., 2008) and primary production (Cartes et al., 2008b). In the Balearic Basin, the mainland slope off the Catalonian coast, could be defined as a hotspot of diversity with a substantial set of peracarid crustaceans newly described since the 1990 s (Cartes and Sorbe, 1997, 1999a; Jaume et al., 2002; Ruffo et al., 1999; San Vicente and Cartes, 2011). The Balearic Basin has the structure of a large submarine canyon, with differences between the mainland and insular slopes. For example, there are substantial variations in megafaunal depth distributions and assemblages (Cartes et al. 2009b). Differences in the current regime, in river discharges and in advective downward transport of POM may contribute to these faunal distinctions. In contrast, the ecology of suprabenthos on the insular slope has not been studied in detail (Cartes et al., 2003). While most current deep-sea research remains descriptive with exploratory objectives, and focuses at large geographic scales in search of hotspots of diversity, the aim of this study is to examine relationships among suprabenthic peracarid diversity and dynamics of environmental variables at a mesoscale level. We have compared two adjacent areas with different environmental conditions. Our specific objectives are: 1) to describe the main gradients responsible for spatio-temporal changes in suprabenthos assemblages distributed in adjacent areas, examining mesoscale differences between assemblages; 2) to compare trends in the distribution of diversity between the slopes to the northwest and to the south of Mallorca; and 3) to compare patterns of production (P and P/B ratios) between species inhabiting these two contrasting areas and explore whether the observed production differences are a function of environmental variability (water mass dynamics and local sea-surface productivity).

2. Materials and methods

2.1. Study area

The study was carried out in two areas (sampling transects) around Mallorca (Balearic Islands: western Mediterranean). Sampling was an aspect of the IDEA project (Fig. 1). One area was located on to the north (indicated as N: 38°98′ N–2°57′ E; 39°14′ N–2°76′ E), and the other to the south of the island of Mallorca (indicated as S: 39°68′ N–2°18′ E; 39°81′ N–2°37′ E) with a *ca.* 600 m minimum depth separating both areas in the Mallorca channel, between the islands of Mallorca and Eivissa (Cartes et al., 2008b).

The N area is close to the harbor of Sóller, adjacent to the Balearic sub-basin (between the northeast coast of the Iberian Peninsula and the Balearic Islands). This area is characterized by a narrow shelf and a slope that descends sharply, when compared to the S site. In general, we found higher water column variability at the north transect (López-Jurado et al., 2008). The differences in environmental conditions between N and S Mallorca are related with mesoscale hydrographic features: at N the occurrence of the Western Mediterranean Intermediate Water (WIW) and strong winds generate high variability of environmental factors such as salinity and temperature (López-Jurado et al., 2008). The S area is close to the Cabrera Archipelago and included in the Algerian sub-basin. There the shelf is flat and the slope descends gently; oceanographic variability at S is governed by eddies detaching from the Algerian current.

2.2. Sampling design and data collection

2.2.1. Biological data

Suprabenthos were sampled at four different depths (approximately over 150 m, 350 m, 650 m and 750 m) on both transects, a range including the shelf-break and the upper and middle slope. A total of 46 suprabenthos sledge hauls were performed during six cruises. All samples were taken during daytime on 3–7 August 2003,

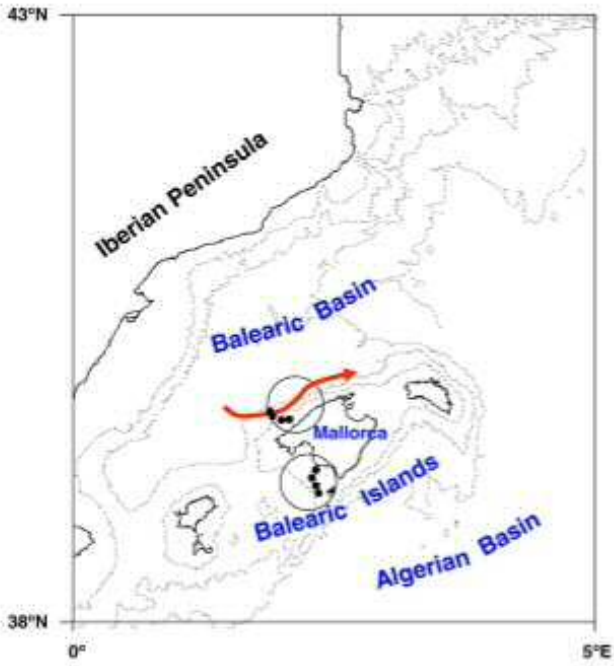

Fig. 1. Map of the two study areas (circles) around the Island of Mallorca, with stations (•) situated over 150, 350, 650 and 750 m. Arrow indicates the position of the front generated by the Balearic current flowing along the northwestern slope of the Island (from López-Jurado et al., 2008).

25 September–1 October 2003, 13–21 November 2003, 14–20 February 2004, 7–13 April 2004 and 23–28 June 2004. In two cruises, two stations situated off Sóller (IDEA1103: 750 m; IDEA0204: 150 m), could not be sampled due to bad weather conditions.

Suprabenthos were sampled with a Macer-GIROQ sledge, equipped with two superimposed nets with mouth openings between 10–40 cm and 50–90 cm above the bottom. Only the lower net samples, in which the largest amounts of fauna were found, were processed (see Cartes et al., 2008b for further details on the methodology). One haul was taken at each station because previous studies using sledges had shown that one haul was enough to characterize the community of suprabenthos for a particular area/time (Brattegard and Fossa, 1991). The sledge nets have 500 μm mesh openings and were trawled at *ca.* 1.5 knots. The durations of sledge hauls over the bottom were ca. 10 min. Both vessel speed times haul duration and flowmeter readings (attached to net mouths) were used to estimate the area of samples for standardizing abundances (individuals/100 m^2). Specimens were immediately sorted with the help of forceps and frozen on board at −20 °C (for later stable isotope analyses). Sorting was completed in a laboratory (sometimes of aliquots ranging from 1/2 to 1/8 of samples for the abundant smaller organisms, primarily copepods and ostracods). Animals were identified to the lowest possible taxonomic level under a stereomicroscope (at ×10–×40), with peracarids and eucarids identified to species and counted for statistical analyses.

2.2.2. Environmental data

Environmental data were collected for all stations and surveys. CTD transects (SBE911 and SBE25 profilers, and SB37-SM mounted on the mouth of a bottom trawl) were performed simultaneously with hauls collecting megafaunal fish and invertebrates at the same stations (see López-Jurado et al., 2008; Moranta et al., 1998, for details). Temperature at the surface (T_{sur}) and temperature and salinity at 5 m above the bottom (T_{5mab}; S_{5mab}) were measured. Sediment for granulometric and organic analyses were collected using a Shipeck grab. Sediment variables considered were the mean grain size (phi, in micrometers) and percentage of mud (see Cartes et al., 2008b, for more details). Total organic matter content (%TOM) of collected sediment was calculated as the difference between dry weight (DW: 80 °C during 24 h until reaching constant weight) and ash weight (500 °C in a furnace during 2 h). Phytoplankton pigment concentrations (ppc, in terms of mg Chl *a* m^{-2}) were obtained from http://reason.gsfc.nasa.gov/Giovanni, and used as indicators of the availability of food resources at the lowest levels of the trophic chain. Monthly average ppc values were used for the positions where the sledges/plankton net samples were taken. Data were from different periods: simultaneously, 1 and 2 months before samplings (indicated in the text as $Chla_{sim}$, $Chla_{1mo}$ and $Chla_{2mo}$). Among selected variables, those recorded at the surface and not depth-dependent (T_{sur}, Chl *a*) can be considered as seasonally dependent variables. Depth-dependent variables (the rest) were taken on or over the bottom at sampling stations ranging between 150 and 750 m depths.

2.3. Data analyses

Analyses were focused on suprabenthic species of peracarid and eucarid crustaceans excluding all non-swimming species/taxa (see Annex 1). Thus epibenthic and infaunal species (e.g. *Munida tenuimana* within Decapods, Tanaidacea, and Pycnogonida) and taxa

that are not peracarids or eucarids were not included in the multivariate analysis. Species/taxa appearing less than twice in hauls were removed from the data matrix, as were data from station IDEA0604 off Soller at 150 m depth that lacked any peracarids and eucarids.

Nonparametric Multidimensional Scaling (nMDS; Clarke et al., 1993) was performed, using the Spearman Rank Correlation as a distance measure, to visualize multivariate abundance patterns. Principal factors to bear in mind to explain the ordination of hauls were depth, area and season. seasonality was expressed either as Factor Season (Winter — November and February, Spring — April, Summer — June and August and Autumn — September) or as months for statistical analyses; in a second step we contrasted periods of water column homogenization (November, February and April) vs stratification (June, August and September).

Distance-based permutational multivariate analysis of variance (PERMANOVA, Anderson et al., 2008) was used to test three null hypotheses of no differences among the suprabenthic assemblages: i) between the two areas (N vs S), ii) among the four depths within each area and iii) among the four sampling seasons. The experimental design has three factors: area (with two levels), depth (with four levels, nested in area) and season (with four levels and crossed with area and depth). All factors were fixed. The same distance matrix was used as implemented in the nMDS. Permutation of residuals under a reduced model was used as the permutation method (maximum number of permutations = 9999), because of its good empirical results in giving the maximum discriminant power (Anderson and Legendre, 1999; Anderson and ter Braak, 2003). For each Pseudo-F test, and post-hoc tests for significant effects are also reported.

Two-way SIMPER analyses (Clarke, 1993) were performed on the Bray–Curtis distance of standardized data (N individuals/100 m^2) in order to identify species contributions in terms of abundance. Factors compared were depths (grouping the hauls at 650 and 750 m) and areas.

Species diversity (H', Shannon–Wiener index using $\log_e$) and number of species (S) were also calculated for each depth stratum, and depth-related trends were analyzed for N and S Mallorca areas.

Principal components analysis (PCA, based on Euclidean distances) was used for N and S separately, producing ordinations of stations (all depths and months) in a space with axes deduced by the reduction of the information given by environmental variables to two principal components explaining the variance of the system. These first components are typically correlated with some of the observed variables. The relationships between species assemblage structure and existing environmental gradients were tested by means of nonparametric Spearman rank correlations between nMDS dimensions of species abundance data and environmental variables simultaneously recorded.

Centres of Gravity (*CoG*, Stefanescu et al., 1992) indicating the optimal habitat of species, which are often located where the species also reach their maximum density, were calculated for abundances of the identified peracarids (see Cartes et al., 2009a). Calculations were done separately for N and S transects off Mallorca. Tests were performed comparing the two areas. We performed the analysis on suprabenthic peracarid species, which are well sampled with the sledge, excluding pelagic taxa (decapods, euphausiids and hyperiids).

All statistical analyses were performed by using PRIMER6 and PERMANOVA+ (Anderson et al., 2008; Clarke et al., 1993) and STATISTICA 7.0.

2.4. Secondary production estimates

For dominant species found in the study areas, seasonal trends in abundance were analyzed to establish their basic life cycles and determine cohort production intervals for P and P/B calculations by the Hynes–Hamilton or size–frequency method (Hynes and Coleman, 1968; Menzies, 1980). The calculations provided estimates of annual secondary production for peracarid species. Demographic categories of eucarids with planktotrophic larvae were not fully sampled with the suprabenthic sledge and were not considered for P and P/B calculations. Estimation of P (and P/B) involves calculation of an annual average length-frequency distribution (the mean annual cohort) from quantitative samples taken at evenly spaced intervals throughout the year. Production is then estimated as the sum of the losses of individuals from one size class to the next plus the biomass loss, compensated by the increase in mean individual weight with increasing age (Cartes and Sorbe, 1999b, Mees and Jones, 1997). The method is applied when it is not possible to identify and follow the growth/mortality of single cohorts through time, and it assumes linear growth patterns. Therefore, this method is suitable for short-lived and fast-growing species, such as those characteristic of suprabenthos.

The following formula was used (Hynes and Coleman, 1968):

$$P = \left[i \cdot \sum_{j=1}^{i-1} \left(d_j - d_{j+1} \right) \cdot \sqrt{b_j \cdot b_{j+1}} \right] \cdot \frac{12}{CPI}$$

where i is the number of size classes represented in the average length-frequency distribution, d_j and b_j are the density (ind m^{-2}) and the biomass (g WW m^{-2}), respectively, of the jth size class in the average length-frequency distribution and CPI is the cohort production interval (months) (Cartes and Sorbe, 1999b, Mees and Jones, 1997). Specimens belonging to dominant species at N and S transects off Mallorca were measured under a stereomicroscope (at ×10–×40 depending on the species) with the help of an ocular micrometer.

Mean annual biomass (B) of each species was calculated as the sum of the biomass of all size classes (b_j) in the average length-frequency distribution (Cartes and Sorbe, 1999b). For each species production/biomass ratio (P/B, productivity) was calculated as a standardized measure allowing comparisons among species having different individual biomass (Plante and Downing, 1989).

Determining the cohort production interval requires a basic knowledge of species life histories. In our study, CPI was taken when possible from data on the abundance of oostegal females and peaks of abundance of juveniles in the investigated areas, or from existing literature (e.g. Cartes and Sorbe, 1999b). Nevertheless, P/B can vary depending on latitude and geographic area. In any case, because our objective was a comparison of P and P/B between two nearby areas, rather than accurate estimation of secondary production, we consider the adopted/assumed estimates of CPI to be sufficiently valid.

Differences in secondary production (P) and P/B between the two areas at N and S of Mallorca were analyzed. The relative differences in production (R index) were calculated according to the following formula (Collie et al., 2000):

$$\%Diff = \left[\frac{(P_N - P_S)}{P_S} \right] \cdot 100$$

where P_N and P_S are the secondary production at the N and S of Mallorca, respectively. Differences in P/B ratio between N and S ($P/B_N - P/B_S$) were estimated as well.

Wilcoxon Sign Rank Test was performed between N and S values of P and P/B considering all taxa together and species grouped by taxon (mysids, amphipods and cumaceans). Tests on isopods were not performed because there were only a few species.

P and P/B of peracarid species were plotted against their optimal depth distributions (*CoG*) for the N and S transects, in order to compare depth-related trends between the areas.

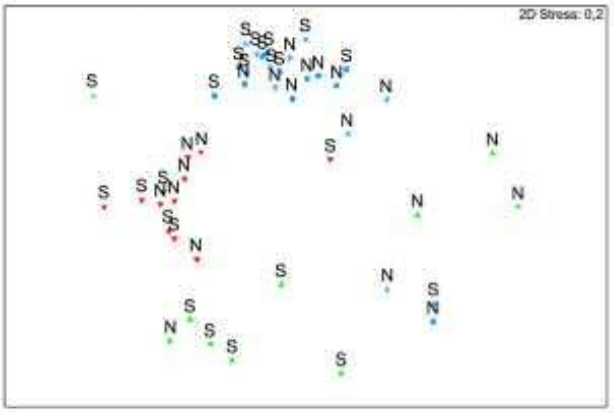

Fig. 2. MDS ordination for all samples. Labels indicate the sampling area (N: Northwest and S: South) around Mallorca. Symbols indicate the mean depth of each sledge haul (Δ = 150 m; ∇ = 350 m; □ = 650 m; and * = 750 m).

3. Results

3.1. Species composition

A total of 18540 peracarid and 323 eucarid specimens were identified in our sampling. The complete list with depth range inhabited by species/taxon to the N and S of Mallorca and with average abundances within the depth range is in Annex 1. Specimens identified belong to 187 species/taxa: 18 species of Decapoda, 5 of Euphausiacea, 16 of Mysidacea, 76 of Amphipoda Gammaridea, 13 of Hyperiidea, 1 Caprellidea, 21 of Isopoda and 37 of Cumacea. The centres of Gravity (*CoG*) of peracarid species were calculated and plotted against P and P/B (see Section 3.7). The Wilcoxon test showed evidence of significantly deeper values of *CoG* in the S than in the N ($V = 5$, $p < 0.001$).

3.2. Assemblage structure

An overall nMDS showed three well-defined assemblages, separated by depth ranges: samples taken at 150 m, 350 m and 650–750 m were clearly segregated from each other (Fig. 2). An nMDS performed separately for each bathymetric range (Fig. 3a–c) indicated a grouping or separation of samples from 350 m and 650–750 m by the condition of the water column (homogeneized in February, April and November vs stratified in June, August and September). In the deepest range, hauls were separated under the criterion of homogenized vs stratified only on the N transect (Fig. 3d).

PERMANOVA were statistically significant for all factors analyzed (Table 1a). Hauls (species composition or assemblages) at each depth range differed from those at the other depths, except those at 650 and 750 m that were statistically similar. Species composition differed by

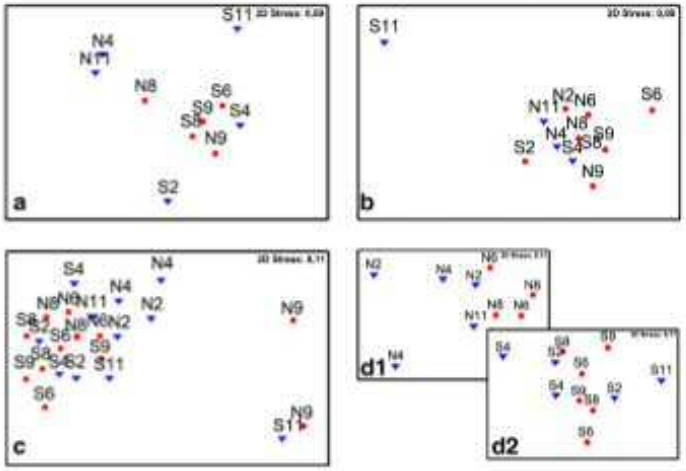

Fig. 3. MDS ordinations of samples from a) Shelf-break (150 m); b) Upper-slope (340 m); c) Middle-slope (650–750 m); d1) Middle-slope of N and d2) Middle-slope of S. Labels indicate Area (N = Northwest and S = South) and month (2 = February; 4 = April; 6 = June; 8 = August; 9 = September; and 11 = November); ∇ = homogeneity and ○ = stratification of the water column.

Table 1
PERMANOVA based on Spearman's rank correlation distance matrix of a) the whole dataset, b) hauls on S transect and c) hauls on N transect. Tests were done by pairwise comparisons only between contiguous periods (only significant tests reported).

Source	df	MS	Pseudo-F	Pairwise
a) Total				
Area	1	566720	8.68***	N ≠ S
Depth(area)	6	568920	8.73***	150 ≠ 350 ≠ 650 = 750; 650–750 N ≠ 650–750 S
Season	3	310170	4.75**	Spr = Sum ≠ Aut = Win = Spr
Res	34	65288		
Total	44			
b) South				
Depth	3	46856	7.13***	150 ≠ 350 ≠ 650 = 750
Season	4	9363	1.39 ns	
Res	16	6574		
Total	23			
c) North				
Depth	3	25406	10.28***	150 ≠ 350 ≠ 650 = 750
Season	4	9194	3.72*	Spr = Sum ≠ Aut ≠ Win = Spr
Res	13	2470		
Total	20			

ns: not significant.
*** $p<0.001$.
** $p<0.01$.
* $p<0.05$.

season only between those hauls collected in summer and autumn. Pairwise tests performed among depth strata (150, 350 and 650–750 m) showed significant differences for species composition at both N and S transects.

PERMANOVAs computed for each area showed significant differences among depths in both areas; however, there was a significant effect of season only along the N transect: summer, autumn and winter assemblages there were all distinctive (Table 1b–c).

As confirmed by SIMPER analyses, different species typified each bathymetric assemblage (Table 2a) and typified the N and S areas (Table 2b). Diversity was low at the shelf-break stations on both transects, which were inhabited by a few mysid and amphipod species. The upper and middle slope assemblages were less strongly dominated, with contributions to similarity among samples more evenly distributed among species. On the upper slope the most abundant species were *Hemilamprops normani*, *Boreomysis megalops* and *Rhachotropis integricauda*. *Munnopsurus atlanticus* and *Boreomysis arctica* were the dominants on the middle slope.

The N and S areas differed mainly in the increasing contribution of *M. atlanticus* in the S and the high abundance of *Nematoscelis megalops* in the N. A few species were observed almost exclusively in the N, such as *Primno macropa* and some other hyperiids.

3.3. Diversity patterns

Two different diversity patterns were observed in relation to depth (Table 3). In both areas the lowest value of H' was observed at the shelf-break, and it was greater on the slope. However, diversity at N was very low at the shelf-break, increasing on the upper-slope ($H'>3.00$) and then decreasing again on the middle-slope. At the S transect diversity increased smoothly, reaching the highest values on the middle-slope. One-way ANOVA showed significant differences in diversity both at the North transect (for H': $F_{3,21}=19.62$; $p=3\cdot10^{-5}$; for S: $F_{3,21}=11.58$; $p=3\cdot10^{-4}$), and at the south transect (for H': $F_{3,24}=3.58$; $p=0.04$; for S: $F_{3,24}=5.69$; $p=0.01$) areas. Paired comparisons (Tukey tests) between depth strata showed significant differences at North among all depth strata, both for H' (shelf-break vs upper slope: $p=10^{-5}$; upper slope vs middle slope: $p=0.01$) and for S (shelf-break vs upper slope: $p=4\cdot10^{-4}$; upper slope vs middle slope: $p=0.01$). By contrast, along the South transect Tukey tests were not significant when H' and S were compared between contiguous depth strata.

Table 2
Results of two-factor SIMPER analysis based on Bray–Curtis similarity (cut-off at 80%).

a) Factor depth		b) Factor area	
Species	Contrib %	Species	Contrib %
Shelf break (av. Sim.: 11.66)		North (av. Sim.: 24.76)	
Leptomysis gracilis	13.27	*Boreomysis arctica*	13.77
Primno macropa	13.07	*Munnopsurus atlanticus*	10.22
Anchialina agilis	11.36	*Nematoscelis megalops*	8.04
Westwoodilla rectirostris	11.04	*Rhachotropis caeca*	7.09
Hyperia schizogeneios	10.76	*Gnathia* sp.I.	5.14
Campylaspis glabra	7.24	*Brazelia typica*	4.96
Phronima sedentaria	4.90	*Hemilamprops normani*	4.88
Gnathia sp. I.	4.82	*Rhachotropis grimaldii*	2.86
Disconectes furcatum	4.77	*Campylaspis glabra*	2.83
Upper slope (av. Sim.: 27.80)		*Campylaspis sulcata*	2.70
Hemilamprops normani	11.88	*Tryphosites allenі*	2.27
Boreomysis megalops	11.81	*Rhachotropis rostrata*	2.10
Rhachotropis integricauda	9.32	*Syrrhoe affinis*	1.99
Campylaspis sulcata	7.09	*Ryarachna longicornis*	1.93
Gnathia sp. I.	5.25	*Stegocephaloides christianensis*	1.89
Campylaspis glabra	5.24	*Primno macropa*	1.73
Procampylaspis armata	4.24	*Hyperia schizogeneios*	1.62
Lepechinella manco	2.79	*Procampylaspis armata*	1.51
Anchialina agilis	2.78	*Gennadas elegans*	1.43
Scopelocheirus hopei	2.64	*Scopelocheirus hopei*	1.41
Ryarachna longicornis	2.25	*Bathymedon longirostris*	1.40
Monoculodes packardi	2.08	South (av. Sim.: 30.29)	
Bathymedon longirostris	1.98	*Munnopsurus atlanticus*	22.72
Westwoodilla rectirostris	1.88	*Boreomysis arctica*	13.01
Iphimedia thergetes	1.83	*Rhachotropis caeca*	7.64
Disconectes furcatum	1.81	*Tryphosites longipes*	4.07
Munnopsurus atlanticus	1.71	*Brazelia typica*	3.20
Lophogaster typicus	1.61	*Boreomysis megalops*	2.99
Rhachotropis grimaldii	1.55	*Rhachotropis rostrata*	2.99
Rhachotropis caeca	1.42	*Ryarachna longicornis*	2.90
Middle slope (av. Sim.: 30.66)		*Gnathia* sp. I.	2.83
Munnopsurus atlanticus	22.60	*Syrrhoe affinis*	2.72
Boreomysis arctica	17.17	*Rhachotropis integricauda*	2.50
Rhachotropis caeca	9.27	*Andaniexis mimonectes*	2.39
Brazelia typica	4.99	*Procampylaspis armata*	1.58
Nematoscelis megalops	4.37	*Belonectes parvus*	1.45
Rhachotropis rostrata	3.37	*Paramblyops rostrata*	1.38
Gnathia sp. I.	3.32	*Campylaspis glabra*	1.35
Tryphosites longipes	3.17	*Westwoodilla rectirostris*	1.34
Syrrhoe affinis	3.14	*Bathymedon longirostris*	1.28
Ryarachna longicornis	2.58	*Platysympus typicus*	1.16
Andaniexis mimonectes	1.99	*Leptomysis gracilis*	1.16
Rhachotropis grimaldii	1.82	*Campylaspis verrucosa*	1.13
Nicippe tumida	1.40		
Tryphosites allenі	1.35		

No significant differences were found comparing mean H' values of north with south samples from any depth range (Table 3). Also, the number of species showed the same trend as described for H' (Table 3).

3.4. Seasonal trends in species abundance

Abundance of dominant species showed similar seasonal trends in each bathymetric assemblage (Fig. 4). The distribution of species abundances did not differ statistically (Kolmogorov–Smirnov test; $p>0.1$) comparing N and S areas, so species abundances for N and S were plotted together.

At the shelf-break, all dominant (in abundance) species presented a single peak in abundance in summer (June–August). On the upper-slope, most species showed two evident peaks, in spring (April) and late summer (August). This was observed in two amphipods (*Rhachotropis integricauda* and *Lepechinella manco*), in the isopod *Disconectes furcatum* and in *Hemilamprops normani*, *Campylaspis sulcata* and *Campylaspis glabra*, the last being especially abundant in August. Two mysids showed a similar pattern, with the higher peak of

Table 1
PERMANOVA based on Spearman's rank correlation distance matrix of a) the whole dataset, b) hauls on S transect and c) hauls on N transect. Tests were done by pairwise comparisons only between contiguous periods (only significant tests reported).

Source	df	MS	Pseudo-F	Pairwise
a) Total				
Area	1	566720	8.68***	N ≠ S
Depth(area)	6	569920	8.73***	150 ≠ 350 ≠ 650 = 750; 650–750 N ≠ 650–750 S
Season	3	310170	4.75**	Spr = Sum ≠ Aut = Win = Spr
Res	34	65288		
Total	44			
b) South				
Depth	3	46856	7.13***	150 ≠ 350 ≠ 650 = 750
Season	4	9163	1.39 ns	
Res	16	6574		
Total	23			
c) North				
Depth	3	25406	10.28***	150 ≠ 350 ≠ 650 = 750
Season	4	9194	3.72*	Spr = Sum ≠ Aut ≠ Win = Spr
Res	13	2470		
Total	20			

ns: not significant.
*** p<0.001.
** p<0.01.
* p<0.05.

season only between those hauls collected in summer and autumn. Pairwise tests performed among depth strata (150, 350 and 650–750 m) showed significant differences for species composition at both N and S transects.

PERMANOVAs computed for each area showed significant differences among depths in both areas; however, there was a significant effect of season only along the N transect: summer, autumn and winter assemblages there were all distinctive (Table 1b–c).

As confirmed by SIMPER analyses, different species typified each bathymetric assemblage (Table 2a) and typified the N and S areas (Table 2b). Diversity was low at the shelf-break stations on both transects, which were inhabited by a few mysid and amphipod species. The upper and middle slope assemblages were less strongly dominated, with contributions to similarity among samples more evenly distributed among species. On the upper slope the most abundant species were *Hemilamprops normani*, *Boreomysis megalops* and *Rhachotropis integricauda*. *Munnopsurus atlanticus* and *Boreomysis arctica* were the dominants on the middle slope.

The N and S areas differed mainly in the increasing contribution of *M. atlanticus* in the S and the high abundance of *Nematoscelis megalops* in the N. A few species were observed almost exclusively in the N, such as *Primno macropa* and some other hyperiids.

3.3. Diversity patterns

Two different diversity patterns were observed in relation to depth (Table 3). In both areas the lowest value of *H'* was observed at the shelf-break, and it was greater on the slope. However, diversity at N was very low at the shelf-break, increasing on the upper-slope (*H'*>3.00) and then decreasing again on the middle-slope. At the S transect diversity increased smoothly, reaching the highest values on the middle-slope. One-way ANOVA showed significant differences in diversity both at the North transect (for *H'*: $F_{3,21}=19.62$; $p=3\cdot10^{-5}$; for *S'*: $F_{3,21}=11.58$; $p=3\cdot10^{-4}$), and at the south transect (for *H'*: $F_{3,24}=3.58$; $p=0.04$; for *S*: $F_{3,24}=5.69$; $p=0.01$) areas. Paired comparisons (Tukey tests) between depth strata showed significant differences at North among all depth strata, both for *H'* (shelf-break vs upper slope: $p=10^{-5}$; upper slope vs middle slope: $p=0.01$) and for *S* (shelf-break vs upper slope: $p=4\cdot10^{-4}$; upper slope vs middle slope: $p=0.01$). By contrast, along the South transect Tukey tests were not significant when *H'* and *S* were compared between contiguous depth strata.

Table 2
Results of two-factor SIMPER analysis based on Bray–Curtis similarity (cut-off at 80%).

a) Factor depth		b) Factor area	
Species	Contrib %	Species	Contrib %
Shelf break (av. Sim.: 11.66)		North (av. Sim.: 24.76)	
Leptomysis gracilis	13.27	*Boreomysis arctica*	13.77
Primno macropa	13.07	*Munnopsurus atlanticus*	10.22
Anchialina agilis	11.36	*Nematoscelis megalops*	8.04
Westwoodilla rectirostris	11.04	*Rhachotropis caeca*	7.09
Hyperia schizogeneios	10.76	*Gnathia sp.I.*	5.14
Campylaspis glabra	7.24	*Bruzelia typica*	4.96
Pleusimma solenaria	4.90	*Hemilamprops normani*	4.88
Gnathia sp. I.	4.82	*Rhachotropis grimaldii*	2.86
Disconectes furcatum	4.77	*Campylaspis glabra*	2.83
Upper slope (av. Sim.: 27.80)		*Campylaspis sulcata*	2.70
Hemilamprops normani	11.88	*Tryphosites alleni*	2.27
Boreomysis megalops	11.81	*Rhachotropis rostrata*	2.10
Rhachotropis integricauda	9.32	*Syrrhoe affinis*	1.99
Campylaspis sulcata	7.09	*Ryarachna longicornis*	1.93
Gnathia sp. I.	5.25	*Stegocephaloides christianensis*	1.89
Campylaspis glabra	5.24	*Primno macropa*	1.73
Procampylaspis armata	4.24	*Hyperia schizogeneios*	1.62
Lepechinella manco	2.79	*Procampylaspis armata*	1.51
Anchialina agilis	2.78	*Gennadas elegans*	1.43
Scopelocheirus hopei	2.64	*Scopelocheirus hopei*	1.41
Ryarachna longicornis	2.25	*Bathymedon longirostris*	1.40
Monoculodes packardi	2.08	South (av. Sim.: 30.29)	
Bathymedon longirostris	1.98	*Munnopsurus atlanticus*	22.72
Westwoodilla rectirostris	1.88	*Boreomysis arctica*	13.01
Nematoscelis megalops	1.83	*Rhachotropis caeca*	7.64
Disconectes furcatum	1.81	*Tryphosites longipes*	4.07
Munnopsurus atlanticus	1.71	*Bruzelia typica*	3.20
Lophogaster typicus	1.61	*Boreomysis megalops*	2.99
Rhachotropis grimaldii	1.55	*Rhachotropis rostrata*	2.99
Rhachotropis caeca	1.42	*Ryarachna longicornis*	2.90
Middle slope (av. Sim.: 30.66)		*Gnathia sp. I.*	2.83
Munnopsurus atlanticus	22.60	*Syrrhoe affinis*	2.72
Boreomysis arctica	17.17	*Rhachotropis integricauda*	2.50
Rhachotropis caeca	9.27	*Andaniexis mimonectes*	2.39
Bruzelia typica	4.99	*Procampylaspis armata*	1.58
Nematoscelis megalops	4.37	*Belonectes parvus*	1.45
Rhachotropis rostrata	3.37	*Paramblyops rostrata*	1.38
Gnathia sp. I.	3.32	*Campylaspis glabra*	1.35
Tryphosites longipes	3.17	*Westwoodilla rectirostris*	1.34
Syrrhoe affinis	3.14	*Bathymedon longirostris*	1.28
Ryarachna longicornis	2.58	*Platysympus typicus*	1.16
Andaniexis mimonectes	1.99	*Leptomysis gracilis*	1.16
Rhachotropis grimaldii	1.82	*Campylaspis verrucosa*	1.13
Nicippe tumida	1.40		
Tryphosites alleni	1.35		

No significant differences were found comparing mean *H'* values of north with south samples from any depth range (Table 3). Also, the number of species showed the same trend as described for *H'* (Table 3).

3.4. Seasonal trends in species abundance

Abundance of dominant species showed similar seasonal trends in each bathymetric assemblage (Fig. 4). The distribution of species abundances did not differ statistically (Kolmogorov–Smirnov test: p>0.1) comparing N and S areas, so species abundances for N and S were plotted together.

At the shelf-break, all dominant (in abundance) species presented a single peak in abundance in summer (June–August). On the upper-slope, most species showed two evident peaks, in spring (April) and late summer (August). This was observed in two amphipods (*Rhachotropis integricauda* and *Lepechinella manco*), in the isopod *Disconectes furcatum* and in *Hemilamprops normani*, *Campylaspis sulcata* and *Campylaspis glabra*, the last being especially abundant in August. Two mysids showed a similar pattern, with the higher peak of

Table 3
Trends of diversity. *H'* (Shannon–Wiener index), *S* (number of species), expressed as mean ± CL (95%) with number of hauls (n) for each bathymetric assemblage and total values, respectively in the north (N) and south (S) areas.

	H'	*S*	n
N			
Shelf-break	1.55 ± 0.29	8.00 ± 3.58	4
Upper-slope	3.23 ± 0.14	57.83 ± 8.96	6
Middle-slope	2.54 ± 0.28	31.54 ± 11.18	11
Total	2.55 ± 0.30	34.57 ± 9.96	21
S			
Shelf-break	2.23 ± 0.17	16.67 ± 4.66	6
Upper-slope	2.42 ± 0.4	39.5 ± 16.86	6
Middle-slope	2.81 ± 0.26	46.75 ± 10.07	12
Total	2.57 ± 0.2	37.42 ± 8.46	24

abundance in August (*Boreomysis megalops* and *Lophogaster typicus*), while one species of amphipod (*Schopelocheirus hopei*) showed a more unimodal pattern, being especially abundant in April.

On the middle-slope, species showed weaker fluctuations through the year in comparison to the shallower depths. The highest abundances of several species were observed in summer (June–August), and the more dominant species also peaked in abundance during winter (February), e.g. *Boreomysis arctica* and *Munnopsurus atlanticus*.

3.5. Environmental conditions of N and S

In PCA biplots for both N and S we can identify depth and seasonal gradients linked to some groups of hauls (Fig. 5). At N the first two principal components of the PCA explained 43.7% and 27.8% of the total variance, respectively. The main variables correlated with the first component were Chlorophyll *a* ($Chla_{Max}$, $Chla_{1mo}$ and $Chla_{2mo}$) and in the opposite direction T_{sur}, both of which are season-related variables (and not depth-dependent because they are recorded always at surface). The second component was linked to S_{mud} and % mud and in opposite direction median *phi*. April and February samples grouped together in the biplot, mainly related to Chl *a* readings, while August and September hauls grouped together related with (higher) T_{sur}.

At S the first two principal components explained 38.3% and 30.0% of the total variance. The first component depended more on median *phi* and $Chla_{1mo}$ and in the opposite direction on S_{mud} and T_{sur}. The second component depends more on % mud and $Chla_{Max}$. In contrast

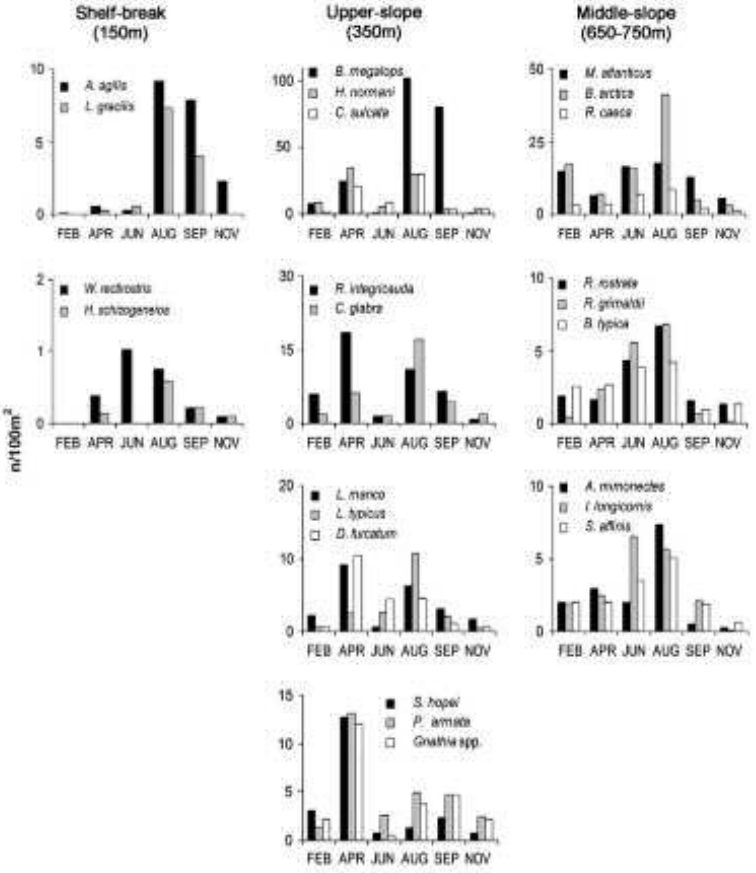

Fig. 4. Mean abundances (ind/100 m²) of the most abundant species during the sampling period.

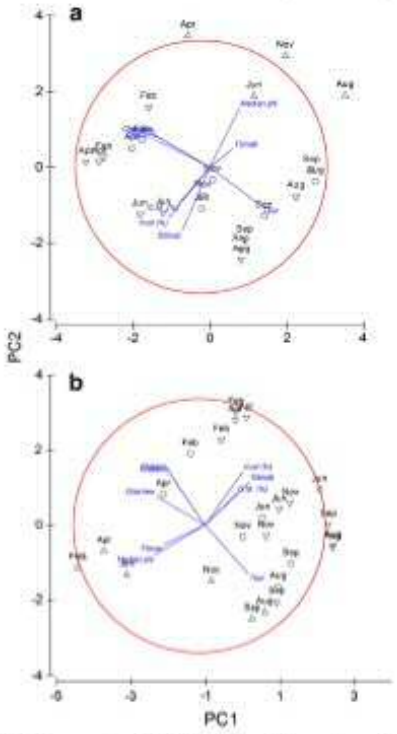

Fig. 5. Principal component analysis (PCA) ordination for the environmental variables recorded on a) N of Mallorca and b) S of Mallorca. Labels indicate month (Feb = February; Apr = April; Jun = June; Aug = August; Sep = September; and Nov = November). Symbols indicate depth range (Δ = Shelf-break; ○ = Upper-slope; and ∇ = Middle-slope).

to N, the environmental conditions were linked both to depth and seasonal gradients.

3.6. Correlations between MDS dimensions and environmental variables

Dimensions of the nMDS were significantly correlated with a number of the environmental variables explored (Table 4). Dimension-1, including all hauls from the two areas, was correlated with depth and chemical–physical variables of both water and sediment (e.g. S_{Smab} and OM%) and Dimension-2 correlated with T_{Smab}.

Different patterns were found in each depth assemblage (Table 4). At the shelf-break no significant correlations were found; on the upper-slope Dimension-1 was correlated with T_{Sup}, $Chla_{Sup}$ and %OM. On the middle-slope Dimension-1 was correlated with S_{Smab} and median *phi*. At N Dimension-1 was correlated with different water column variables (T_{Smab} and S_{Smab} and T_{Sup}). At S Dimension-1 was correlated with sediment-related variables such as %mud and median *phi*.

3.7. Secondary production

A total of 18,380 individuals were measured to estimate production and *P/B* for 30 target species in the two studied areas, together with *W* (mean individual weight, *Biomass*/Density) and *CPI* (Table 5). *CPI* was assumed to be the same in both N and S populations given the relative proximity of the two areas. Production varied between $1 \cdot 10^{-5}$ mgWW m^{-2} $year^{-1}$ for *Desconectes furcatum* and $10.5 \cdot 10^{-2}$ mgWW m^{-2} $year^{-1}$ for *Boreomysis arctica* (both at N). The P/B ratios were between 3.3 for *Lophogaster typicus* and 12.1 for *Andaniexis mimonectes* (the first in S, the second in N). Out of 30 species considered, 18 showed higher production estimates at S rather than at N (Fig. 6). Among amphipods 11 had higher values at S and only 3 at N. All isopods had higher values at S, while among mysids there was no evident trend. Among cumaceans, the trend was 4 higher values at N and 2 at S.

An opposite trend was observed in P/B values (Fig. 6): 18 species showed higher P/B values at N and 12 species at S. Many mysid and isopod species showed higher values at N as well as all cumaceans. On the contrary, among amphipods a majority of species showed higher values at S (9 species) than at N (5 species; Fig. 6).

The Wilcoxon Signed Rank Tests performed to compare P and P/B values between the two areas were not significant (P: V = 141, p = 0.924; P/B: V = 309, p = 0.059) considering all taxa. Testing each taxon separately showed significant p-values between N and S production for amphipods (P_S greater than P_N: V = 19, p-value = 0.018) and P/B values for cumaceans (P/B_N greater than P/B_S : V = 21, p-value = 0.016). No significant p-values were found for mysids.

Regarding depth-related trends of suprabenthos production (Fig. 7), *P* decreased progressively downward in the S area for species with deeper Centres of Gravity (*CoG*), while at N the distribution pattern of *P* was not clearly related to depth. In other words, we found the higher values of *P* at S distributed deeper than at N, though this trend was not significant (Mann–Witney test comparing N vs S *P* values). P/B followed two different patterns, with highest values at intermediate depths along N (over *ca.* 450–500 m), while at S the highest P/B was found

Table 4
Spearman's rank correlations between nMDS dimensions and environmental variables. N: Number of valid cases and r: Spearman's rank correlation. Only significant correlations are reported.

	Total		Upper-slope		Middle-slope		N Middle-slope		S Middle-slope	
	N	r	N	r	N	r	N	r	N	r
Dim1										
T_{Smab}	45	−0.446**	12	–	23	–	9	−0.733*	11	–
T_{Sup}	45	–	12	−0.226*	23	–	9	−0.783*	11	–
S_{Smab}	45	0.477***	12	−0.115	23	–	8	−0.867**	11	–
O. M. (%)	40	0.457**	10	−0.717*	20	–	7	–	10	–
Mud (%)	39	0.594***	10	–	19	–	7	–	10	−0.636*
Median phi	40	−0.623***	10	–	20	0.599**	7	–	10	0.758*
$Chla_{Sup}$	45	–	12	–	22	–	8	–	11	–
$Chla_{Sm}$	45	–	12	0.638*	22	–	8	–	11	–
Dim2										
T_{Smab}	45	0.476***	12	–	23	–	11	–	11	–

* p<0.05.
** p<0.01.
*** p<0.001.

deeper (over *ca.* 600–650 m) than at N. The mean CoG (± C.I. 95%) at N was 497 ± 30 m and 541 m ± 33 m. Applying a Mann–Witney test comparing P/B at N and S, we obtained significant ($p = 0.04$) differences. Also, 1-way ANOVA showed a significant difference at N, comparing the P/B of species for which *CoG* was <400 m, was between 400 and 500 m and was >500 m ($F_{2,30} = 6.7\%$; $p = 0.004$), with significantly higher P/B at 400–500 m (post-hoc Tukey results: <400 m vs 400–500 m: $p = 0.004$; 400–500 m vs >500 m: $p = 0.04$). No significant differences were found comparing P/B for the same depth groups ($F_{2,33} = 0.91$; $p = 0.41$).

Highest P/B were found at intermediate depths at N coincided with the highest diversity (both in terms of *S* and *H'*) found over the same depth strata (see above). At S we did not find such relationship.

4. Discussion

The biological diversity of the deep-sea still remains far from reasonably well known (Rex and Etter, 2010; Rex et al., 2000), despite the increasing effort devoted to the study of deep-sea fauna. Suprabenthos in the deep western Mediterranean (Balearic Basin and around the Balearic Islands) constitutes a good example of this. Since the end of the 1980s, when quantitative studies on deep-sea suprabenthos began in the Balearic Basin (Cartes and Sorbe, 1993, 1997; Cartes et al., 2001, 2003), most of the new species described (Jaume et al., 2000; Ruffo et al., 1999; San Vicente and Cartes, 2011) have proved to be relatively abundant and widely distributed in both the western and eastern basins (e.g. *Bathymedon longirostris*: Madurell and Cartes, 2003; *Dactylamblyops corberai*: San Vicente and Cartes, 2011). These findings were possible thanks to the use of the Macer-GIROQ suprabenthic sledge (Dauvin and Lorgeré, 1989) for exploring the deep sediment-water interface (Cartes et al., 1994). The use of suprabenthic sledges has shown that the distribution of deep-sea diversity depends not only upon the sampling area covered (Gage and Tyler, 1991) but upon the 3-dimensional distribution of the fauna in the water column, with peracarid crustaceans mainly distributed in the near bottom (0–1.5 m above the sea bed) habitat. Most of these animals escape box-corer sampling (see Cartes et al., 2009c), especially mysids with the highest swimming capacity among deep-sea peracarids.

We have found mesoscale variability between deep-sea suprabenthic assemblages and diversity trends in two neighboring zones to the north and south of the Balearic Islands. Seasonality was the most important factor influencing the dynamics of suprabenthos over the upper (350 m) and middle (650–750 m) slope, especially along the N transect. Conversely, the southern area appeared to be more temporally stable (see below) with depth being the main gradient influencing assemblage composition. Temporal dynamics of macrofauna (e.g. suprabenthos) have rarely been studied in the deep-sea environment (Cartes et al. 2003, 2008b; Sorbe, 1999), where studies are rather descriptive and focused on scanning wide areas in search of hotspots of diversity. Other studies have not been focused on mesoscale variability but on the depth and large-scale latitudinal gradients in the distribution of diversity (references in Gage and Tyler, 1991; Rex and Etter, 2010). Seasonality near Mallorca at N is confirmed by: i) our evaluation by PERMANOVA of seasonal MDS groups that proved to be significant along the entire slope sampled there; ii) our PCA results showing a better temporal segregation of samples at N, with a greater proportion of variance explained (43.7% for the first axis); and iii) stronger relationships at N with season-related variables such as Chl *a* and T_{sur}.

The N and S transects near Mallorca Island exhibit different levels of faunal variability related to the circulation of water masses (López-

Table 5
Production (*P*) and *P/B* estimates of the 32 target species. N, number of specimens measured; CPI: cohort production interval; *W*: mean individual weight. North and South correspond to Northwest and South of Mallorca.

Species	n	CPI	North P (mg WW/m² year)	P/B	W (mgWW/ind)	South P (mg WW/m²/year)	P/B	W (mg WW/ind)
Mysidacea								
Anchialina agilis	372	12	0.00023	4.07	0.00119	0.00012	3.59	0.00178
Boreomysis arctica	1949	6.5	0.01517	6.27	0.01448	0.01360	7.11	0.01040
Boreomysis megalops	2146	12	0.00858	4.83	0.00405	0.00825	4.78	0.00453
Erythrops neapolitana	226	12	0.00008	4.90	0.00073	0.00008	4.59	0.00082
Leptomysis gracilis	95	7	0.00052	6.59	0.02192	0.00162	6.00	0.02538
Lophogaster typicus	173	12	0.00070	5.37	0.00617	0.00115	3.32	0.02693
Mysideis parva	186	8	0.00022	4.65	0.00410	0.00021	4.85	0.00375
Amphipoda								
Andaniexisninonectes	512	4.5	0.00010	12.11	0.00028	0.00017	9.80	0.00052
Bathymedon longirostris	315	6.5	0.00040	7.91	0.00416	0.00070	8.44	0.00313
Bruzelia typica	352	6.5	0.00015	6.67	0.00118	0.00016	7.19	0.00098
Iberaustroe ilergetes	275	6.5	0.00002	8.25	0.00018	0.00004	0.49	0.00026
Lepechinella manco	377	5.9	0.00014	7.2	0.00037	0.00006	6.60	0.00033
Nicippe tumida	225	7	0.00037	6.79	0.00512	0.00064	6.48	0.00578
Rhachotropis caeca	815	6.5	0.00070	8.15	0.00183	0.00139	8.36	0.00173
Rhachotropis grimaldii	581	6	0.00079	8.7	0.00194	0.00036	8.98	0.00184
Rhachotropis integricauda	406	7	0.00011	10.39	0.00113	0.00061	10.80	0.00090
Rhachotropis rostrata	427	6.5	0.00078	6.26	0.0057	0.00094	6.46	0.00516
Stegocephaloides christianensis	213	6	0.00015	0.76	0.00137	0.00014	7.21	0.00160
Syrrhoe affinis	302	6.2	0.00031	6.47	0.00295	0.00068	6.52	0.00284
Syrrhoites gusilla	132	6.5	0.00028	7.72	0.00175	0.00034	8.11	0.00104
Westwoodilla rectirostris	176	7	0.00074	7.52	0.00821	0.00086	8.36	0.00443
Isopoda								
Discomeces furcatus	314	12	0.00001	4.31	0.00022	0.00001	4.98	0.00016
Eurycopa longicornis	642	12	0.00005	4.09	0.00036	0.00006	4.05	0.00037
Munneurus atlanticus	1876	8	0.00071	6.81	0.00186	0.00195	6.71	0.00178
Cumacea								
Campylaspis glabra	482	7.5	0.00005	5.47	0.00027	0.00004	5.01	0.00034
Campylaspis sulcata	947	7.3	0.00030	0.58	0.00014	0.00010	7.23	0.00018
Campylaspis verrucosa	245	7.5	0.00001	8.02	0.00034	0.00007	6.74	0.00050
Diastylioides serrata	177	5.8	0.00003	9.86	0.00020	0.00001	9.18	0.00027
Hemilamprops normani	869	4.7	0.00037	8.71	0.00046	0.00010	7.23	0.00021
Procampylaspis armata	449	6.5	0.00004	6.83	0.0004035	0.00014	6.17	0.00057

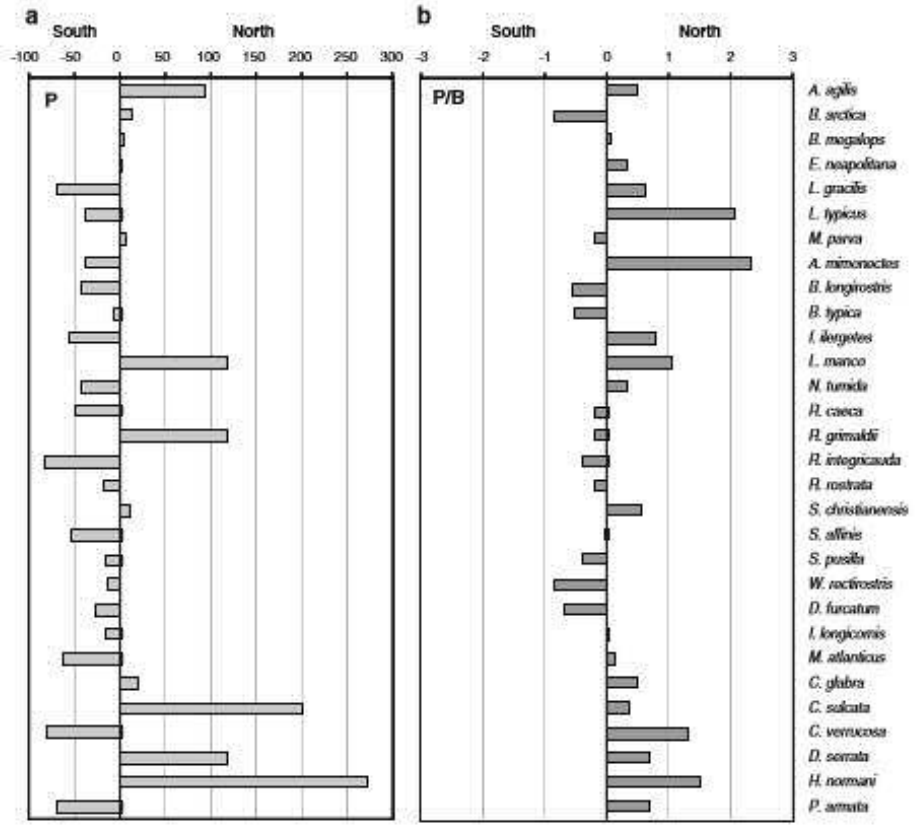

Fig. 6. Differences of secondary production (P, R index) (a) and P/B (b) of target species between the study areas to the south and northwest of Mallorca.

Jurado et al., 2008; Millot, 1999), which may have an effect on local food supply (Fernández de Puelles et al., 2004; Cartes et al., 2008b). This explains both the higher food consumption, energy content of diets and fecundity of top predators inhabiting the N area (i.e. *Merluccius merluccius*: Cartes et al., 2008c; Hidalgo et al., 2008; *Aristeus antennatus*: Cartes et al., 2009a; Guijarro et al., 2008;). The N area is subject to high productivity events (Estrada, 1996; Bosc et al., 2004), induced by the occurrence of stronger frontal systems linked to Northern and Balearic currents flowing along the slope (see Fig. 1 in López-Jurado et al., 2008), which in turn may contribute to increased zooplankton biomass (Cartes et al., 2008b). Frontal systems are especially strong in the Balearic sub-basin during winter, due to the intensity of winter winds (López-Jurado et al., 2008), decreasing in spring. By contrast, the Algerian basin is subject to more unpredictable events such as eddies generated by entry of Atlantic waters through the Straits of Gibraltar (López-Jurado et al., 2008). The occurrence/persistence of frontal systems at N may also explain: i) the highest diversity being found there at *ca.* 400 m, and ii) the shape of its P/B vs depth relation, with highest P/B values at *ca.* 400–500 m (Fig. 7). According to Font (1987) frontal thermohaline systems impinge on the slope in the Balearic Basin at *ca.* 400 m depth. Differences in the oceanographic regimes of the two areas could further explain the greater influence of seasonality along the N transect. The N area was influenced by a stronger "succession" in the temporal arrival of different water masses. The Winter and Levantine Intermediate waters (WIW, LIW mainly distributed between 150–300 m and 350–550 m respectively) arrived at N during April (WIW) and June (LIW), respectively (López-Jurado et al., 2008). WIW is characterized by minimum temperatures, while LIW has the region's maximum values of salinity and temperature for mid-slope waters (*ca.* over 300–500 m bottoms). The Western Mediterranean Deep Waters (WMDW), flowing below LIW, may interrupt the constant northward flow of LIW, especially during winter (López-Jurado et al., 2008). In summary, WIW, LIW and WMDW flow seasonally, arriving sequentially at the N transect, making oceanographic conditions more variable throughout the year than at S. The S area, lacking strong oceanographic frontal systems, constitutes a more uniform, stable, environment (López-Jurado et al., 2008). As a consequence no marked seasonal patterns in suprabenthos were found at S, and its faunal variation was mainly related to depth, particularly related to changes of T and S in the near-bottom water column. Both variables are more dependent upon depth at S (Cartes et al., 2008b).

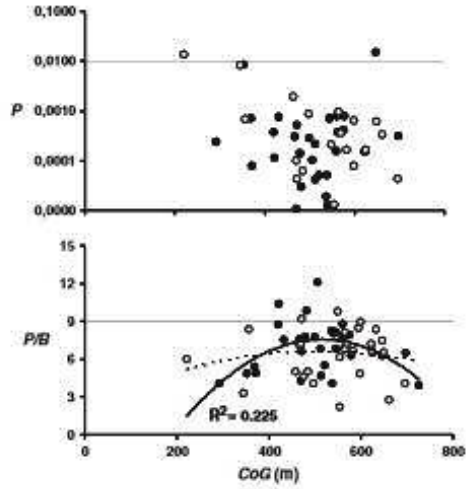

Fig. 7. Distribution of secondary production (P) and P/B of target species vs their centre of gravity (CoG) in the two areas at S (empty dots) and N (black dots) of Mallorca.

The possible influence of primary production on the diversity and productivity of the near-bottom suprabenthic community may consist of a local enrichment of sediments below the oceanographic front over the slope. This is apparent when comparing the available environmental information from our transects north and south of Mallorca:

i) There is a substantial increase, *ca.* 3-fold, in %TOM (total organic matter) in sediments during April–June at N, coinciding with a parallel increase of suprabenthos biomass (Cartes et al., 2008b). Although %TOM does not specifically indicate fresh input of organic matter and annual average TOM values are only slightly higher at N (4.9%) than at S (4.0%), the spring increase would indicate new OM inputs.
ii) REDOX potential is reduced in sediments at N in April–June (*ca.* −10 mV) compared with values at S, also suggesting a high input of fresh OM (Cartes et al., 2008b).
iii) The C/N of suprabenthos species analyzed in both areas indicated higher C/N and thus greater lipid content and better nutrition in the fauna at N (C/N ranging from 4.6 to 5.2 at N compared to 3.5 to 4.5 at S) (data in Fanelli et al. 2009a; Madurell et al. 2008). This may indicate higher C/N ratios in sediments (fresh OM, because C/N is an indirect measure of lipid content), considering the low trophic level (on average) of suprabenthos. This is further consistent with tendencies discussed above for top predators (*Merluccius merluccius*: Cartes et al., 2008c; Hidalgo et al., 2008; *Aristeus antennatus*: Cartes et al., 2009a; Guijarro et al., 2008).
iv) The stable isotope analysis (SIA) results performed at N (Madurell et al. 2008) and S (Fanelli et al. 2009a) suggest greater input of fresh OM at N. Higher $\delta^{13}C$ vs $\delta^{15}N$ correlations found at N after the peak of surface primary production are evidence for that (Fanelli et al. 2009a).

So, there is a general tendency at N for larger stocks and production affecting all the levels of the trophic web from macrofaunal detritus feeders to fish and large crustaceans. As Chl *a* in surface waters estimated from satellite imagery showed similar values and temporal tendencies in both areas (only some longer durations of Chl *a* peaks were evident at N: Cartes et al., 2008b), we hypothesize that the N transect must be more productive of suprabenthos through the influence of advective inputs of water masses, e.g. the WIW arriving from neighboring, highly productive, areas (e.g. the Gulf of Lyons).

4.1. Depth-related and spatial mesoscale trends in suprabenthos production and diversity

Secondary production showed a depth related trend. At the shelf-slope break were species with low P/B ratios (Fig. 7). Most of those had a univoltine life-cycle, particularly *Anchiolina agilis* with a single peak of abundance in August–September. It was also univoltine on the Bay of Biscay shelf (Sorbe, unp. data), showed a single peak of abundance in December off Ebro Delta at 50–60 m (Cartes et al., 2007) and in winter on the Adriatic Sea shelf (Ligas et al. 2009). Oostegal females were found in August off NW Mallorca and in December in shelf populations close to Ebro Delta (Cartes et al., 2007), so perhaps the unimodal pattern found here was biased by a seasonal offshore/inshore migratory movement or by incomplete sampling of the depth range occupied by shelf-break species. Bimodal patterns in abundance were prevalent among species living deeper on the slope.

Around Mallorca we found differences in production comparing the N and S transects, with a decrease of production with depth at S and higher P/B at intermediate depths at N. Cartes et al. (2009c) found short-scale (*ca.* 5 km) variations in P/B found off the Ebro River (linked to differences in temperature and organic matter (food supply) between stations. The slightly higher T (<0.05 °C) found to the south of Mallorca is not likely to have had a significant influence on either the degree of degradation of fresh POM arriving at the bottom or the P/B values of resident species. So, the higher P/B at intermediate depths at N was more likely due to greater %OM in sediments generated by the influence of overlying frontal systems. As a consequence, P/B was greater at N among omnivore-detritus feeders (e.g. *Andaniexis nimonectes*, *Lepechinella manco*, all cumaceans), coupled to enriched OM in sediments, while at S carnivores on mesoplankton (all *Rhachotropis* spp.) had the higher P/B (Fig. 6). Suprabenthos have a wide range of feeding strategies, from deposit and filter-feeders to carnivores, shown by the wide range of $\delta^{15}N$ signals (Madurell et al., 2008; Fanelli et al., 2009a), and species can occupy different habitats in relation to the available food.

According to the intermediate disturbance ecological hypothesis [adopted to Deep Sea Biology by Gage and Tyler (1991) from trends found in the diversity of trees in tropical rain forests and corals on tropical reefs (Connell, 1978)], the highest diversity is generally achieved in a non-equilibrium state that, if is not disturbed further, will progress toward low-diversity. A combination of physical (e.g. turbidity, bottom currents…) and biological factors (dispersal capability of species, trophic factors) disturb deep ecosystems controlling their diversity. Thus, diversity patterns vary according to environmental stability. Around Mallorca stability was higher deeper on the slope in terms of water masses present and also greater to the south of the island due to seasonally more uniform hydrographic conditions (López-Jurado et al., 2008). Trophic factors can influence diversity, growth rates and P/B ratios of the lowest trophic levels. Predation pressure (Dayton and Hessler, 1972) can maintain different levels of biodiversity at distinct, local or regional, spatial scales. Finding the lowest diversity at the shelf break around Mallorca, compared to deeper slopes, might be a consequence of strong hydrodynamism. The increase of diversity with depth of suprabenthos was parallel to an increase of TOM down the slope (Cartes et al., 2008b), which is indicative of higher deposition rates and of a greater environmental stability deeper. This general depth-related pattern was, however, locally broken by the high diversity linked to the highest P/B of species at *ca.* 400–500 m along the N transect.

In conclusion, on the upper slope at N the influence of frontal systems and the higher flow of different water masses (WIW and LIW) increased natural disturbance in the area, increasing P/B and diversity of suprabenthic peracarids at the BBL. The *average*

distribution of species, their mean CoG, was shallower at N compared to S, which is an indicator of more favorable habitat conditions for suprabenthos at N in the range from 400 to 500 m. This could be because P/B increases in populations submitted to some degree of disturbance (e.g. by human activities such as trawling: Jennings et al., 2001). Regarding diversity trends there are few empirical studies relating diversity and production in the deep sea. Diversity among planktonic copepods is higher in oligotrophic regions, and lower in upwelling areas (Rombouts et al., 2009). Benthic taxa exhibit the same general latitudinal gradients as zooplankton at a global scale, though some taxa (i.e. molluscs) can achieve high diversity (hotspots) also at a regional scale (Crame, 2000). This is somewhat similar to the trend found around Mallorca for peracarids at a mesoscale, with diversity at N being linked to hotspots of better productivity (higher disturbance) at intermediate depths. By contrast, in other benthic taxa (e.g. foraminiferans) higher diversity is found in areas with rather low productivity better production, used in a wide sense, decreasing for example in the North Atlantic basin where there is an abundant deposition of food (phytodetritus: Corliss et al., 2009). This suggests that the relationships between diversity and production may depend, further than the scale adopted, on the trophic levels under analysis, in other words on the proximity of target taxa to the primary food sources that they exploit.

Acknowledgments

The authors thank to all participants in the project IDEA (ref. REN2002-04535-C02-02/MAR) especially to participants on board the F/V *Moruti Nou* crews (Dr. J. L. López Jurado and Mr. M. Serra from the *Centre Oceanogràfic de Balears*, I.E.O.). We also thank the technical assistance in the sorting of Dr. T. Madurell and V. Papiol (I.C.M. Barcelona) on board and at laboratory. In its final stage objectives of this study were designed within and financed by the project ANTROMARE (CTM2009-12214-C02-01-MAR). We thank Dr. J. Junoy (Universidad de Alcalá de Henares) for his help in the identification of Aega incisa.

Appendix 1 Depth range and mean abundances of suprabenthos at N (a) and S (b) of Mallorca

Taxa	Bathymetric distribution	Abundance		Taxa	Bathymetric distribution	Abundance	
		N	S			N	S
Decapoda				*Rhachotropis* cf. *gracilis* Bonnier, 1896	696	–	0.035
Aristeus antennatus (Risso, 1816)	692	–	0.009	*Rhachotropis grimaldii* (Chevreux, 1888)	153–760	3.495	1.434
Nauchalia woodwardi Johnson, 1867	670	–	0.012	*Rhachotropis integricauda* Carausu, 1948	155–747	0.506	3.215
Gennadas elegans (Smith, 1882)	666–760	0.101	0.131	*Rhachotropis rostrata* Bonnier, 1896	335–752	1.533	1.756
Hippolyte cf. *huntii* (Gosse, 1877)	150	0.023	–	*Rhachotropis* spp. [B] Smith, 1883	356–682	0.028	0.011
Parapenaeus longirostris (Lucas, 1846)	335	–	0.007	*Scopelocheirus hopei* (A. Costa, 1851)	150–749	1.010	1.018
Pasiphaea multidentata Esmark, 1866	727	0.007	–	*Sophrosyne bispasa* (Chevreux, 1888)	155	–	0.009
Philocheras bispinosus (Hailstone, 1835)	155	–	0.002	*Stegocephaloides christianensis* (Boeck, 1871)	156–749	1.002	0.691
Philocheras echinulatus (M. Sars, 1861)	161–376	0.032	0.018	*Syncheilidum maculatum* Stebbing, 1906	347–747	0.669	0.128
Plesionika acanthonotus (S. I. Smith, 1882)	356–749	–	0.050	*Syrrhoe anguliper* Ledoyer, 1977	363	–	0.011
Plesionika gigliolii (Senna, 1903)	347–692	–	0.267	*Syrrhoe affinis* Chevreux, 1908	347–752	0.866	1.684
Plesionika martia (A. Milne-Edwards, 1883)	356–748	–	0.053	*Syrrhoe* sp. Goes, 1866	752	–	0.020
Polycheles typhlops Heller, 1862	611–692	0.018	0.009	*Syrrhoidae* G.O. Sars,1895.	365	0.011	–
Pontocaris lacazei (Gourret, 1887)	155–760	0.034	0.098	*Syrrhoites* cf. *bernardi* Karaman, 1986	363–365	0.021	0.054
Pontophilus norvegicus (Sars, 1861)	682	0.009	–	*Syrrhoites pusilla* Ledoyer, 1949	328–752	0.560	0.737
Pontophilus spinosus (Leach, 1815)	376	0.011	–	*Tmetonyx similis* (G. O. Sars, 1891)	347–682	0.008	0.009
Processa nouveli Al-Adhub & Williamson, 1975	150–692	0.178	0.177	*Tryphosella* cf. *longidactyla* Ruffo, 1985	695	0.031	–
Sergestes arcticus Krøyer, 1855	666–670	–	0.054	*Tryphosella* sp. Bonnier, 1893	670	–	0.012
Sergia robusta (Smith, 1882)	749	–	0.009	*Tryphosites alleni* Sexton, 1911	134–752	0.745	0.418
Euphausiacea				*Tryphosites longipes* (Bate & Westwood, 1861)	153–752	0.106	1.728
Euphausia krohni (Brandt, 1851)	150–753	0.122	0.285	*Urothoe corsica* Bellan-Santini, 1965	347–752	0.372	0.158
Meganyctiphanes norvegica (M. Sars, 1857)	363–760	0.054	0.111	*Urothoe elegans* (Bate, 1856)	749	–	0.009
Nematoscelis megalops G. O. Sars, 1883	156–760	0.541	0.375	*Westwoodilla caecula* (Bate, 1857)	352–611	–	0.031
Stylocheiron sp. G.O. Sars, 1883	156	–	0.011	*Westwoodilla rectirostris* (Della Vale, 1893)	148–747	0.630	1.047
Thysanopoda aequalis Hansen, 1905	611–753	0.015	0.018	Amphipoda Hyperiidea			
Euphausiacea unid. [D]	156–727	0.309	0.011	*Anchylomera blossevillei* Milne-Edwards, 1830	670	0.020	–
Mysidacea				*Hyperia latissima* Bovallius, 1887	370–734	0.060	–
Anchialina agilis (G.O. Sars, 1877)	134–376	2.633	1.035	*Hyperia schizogeneios* Stebbing, 1888	134–760	0.138	0.075
Boreomysis arctica Krøyer, 1861	335–760	6.249	9.676	Hyperiidea unid.	155–605	0.008	0.009
Boreomysis megalops G. O. Sars, 1872	155–376	9.775	10.743	*Hyperoche krøyeri* Bovall, 1887	148–753	0.009	0.062
Calyptomma puritani W. Tattersall, 1909	363–748	0.017	0.080	Lycaeidae Claus, 1879	150	0.012	–
Dactylamblyops sp. Holt and W. M. Tattersall, 1906	363–727	0.025	0.385	*Phronima sedentaria* (Forskal, 1775)	150–729	0.086	0.009
Erythrops neapolitana Colosi, 1929	153–749	0.538	0.935	*Phronima semifunata* Risso, 1822	148–760	0.068	0.019
Eucopia hansenii Nouvel, 1942	675–760	0.059	0.009	*Primno macropa* Guérin-Méneville, 1836	150–734	0.106	0.007
Haplostylus sp. [I] Kreumann, 1880	161–670	0.322	0.042	*Pseudolycaea pachypoda* (Claus, 1887)	171–675	0.010	0.011
Lepidomysis gracilis (G.O. Sars, 1864)	153–687	0.213	1.186	*Scina borealis* (G. O. Sars, 1895)	670–709	0.007	0.005
Lophogaster typicus M. Sars, 1857	155–692	1.113	0.688	*Scina crassicornis* (Fabricius, 1775)	148–760	0.039	0.029
Mysidetes parva Zimmer, 1915	347–752	1.018	0.590	*Vibilia armata* Bovallius, 1887	356–753	0.101	0.158
Parerythrops rostrata Holt & Tattersall, 1905	347–760	0.369	1.377	*Vibilia cultripes* Vosseler, 1901	747	–	0.010
Parapseudomma calloplura (Holt & Tattersall, 1905)	134–749	0.106	0.345	Amphipoda Caprellidea			
Parerythrops lobiancoi W. Tattersall, 1909	363–749	0.135	0.973	*Parvipalpus major* Carausu, 1941	161–363	0.036	0.018
Pseudomma sp. [J] G.O. Sars, 1870	347–363	–	0.051	Isopoda			
Siriella norvegica (G.O. Sars, 1869)	161–670	0.043	0.270	*Aega incisa* Schioedte and Meinert, 1879	148–752	–	0.087
Amphipoda Gammaridea				Anthuridae Leach, 1814	365–749	0.056	0.018
Ampelisca dalmatina G. Karaman, 1975	155–363	–	0.100	*Belonectes parvus* (Bonnier, 1896)	156–749	0.297	1.514
Ampelisca sp. Krøyer, 1842	150–363	0.030	0.120	*Natatolana borealis* (Lilljeborg 1851)	134–748	0.109	0.239

(continued on next page)

Appendix 1 (continued)

Taxa	Bathymetric distribution	Abundance		Taxa	Bathymetric distribution	Abundance	
		N	S			N	S
Amphilochoides serratipes (Norman, 1869)	362–373	0.080	0.065	*Notatolana* cf. *borealis*	650–752	0.010	0.021
Amphilochus brunneus Della Valle, 1893	155–747	0.024	0.195	Cymothoidae Leach, 1814	161–696	–	0.027
Andaniexis mimonectes Ruffo, 1975	150–752	2.393	1.942	*Chelator chelatus* Stephensen, 1915	347–760	0.236	0.294
Aoridae Poche, 1908	376–670	0.011	0.012	*Desmosoma lineare* (G. O. Sars, 1899)	376–749	0.056	0.049
Arcaijia longo mediterranea G. Karaman, 1986	363–670	–	0.045	*Disconectes* cf. *phallangium* (G. O. Sars, 1864)	365–747	0.981	0.073
Arrhis mediterraneus (Ledoyer, 1983)	328–749	1.038	0.302	*Disconectes furcatum* (GO Sars, 1870)	150–749	0.975	1.686
Atylus sp. Leach, 1815	161	–	0.009	*Disconectes* spp Wilson & Hessler, 1981	156–749	0.705	0.764
Bathymedon acutifrons Bonnier, 1896	362–749	0.199	0.145	*Eugerda filipes* (Hult, 1936)	365–760	0.143	0.007
Bathymedon bonnyhensis Ledoyer, 1983	356–752	0.111	0.167	*Eurycope* sp. G. O. Sars, 1864	365	0.149	–
Bathymedon longirostris Jaume, Cartes and Sorbe, 1998	335–760	0.821	1.912	Eurycopidae sp. 1 Hansen, 1916	153–749	0.725	0.378
Bathymedon massaloidiformis Ledoyer, 1983	356–749	0.036	0.167	*Eurydice* cf. *grimaldii* Dollfus, 1888	155–749	0.232	0.106
Bathymedon sp.[B] Sars, 1892	692	–	0.009	*Gnathia maxillaris* (Montagu, 1804)	161	–	0.009
Brucelia typica Boeck, 1871	156–760	1.413	1.476	*Gnathia* sp.[L] Leach, 1814	134–760	1.906	2.346
Coraphium spp. Latreille, 1806	363–749	–	0.084	*Hyperachna longicornis* (G. O. Sars, 1864)	153–752	2.316	2.701
Epimeria parasitica G. O. Sars, 1858	134–752	0.063	0.440	*Ischnomesus bispinosus* G.O. Sars, 1885	376–747	0.011	0.070
Eusiras leptocarpus G. O. Sars, 1895	365–752	0.048	0.160	*Munnopsis beddardi* (Tattersall, 1905)	150–682	0.020	–
Eusiras longipes Boeck, 1861	347–749	0.166	0.133	*Munnopsurus atlanticus* (Bonnier, 1896)	150–760	4.324	9.223
Gammaridae Latreille, 1802	153	–	0.011	*Syscenus infelix* Harger, 1880	362–370	0.017	–
Gammaridea unid.[D]	134–155	0.023	0.018	*Isopode* unid.[D]	696–749	–	0.023
Halice abyssi Boeck, 1871	363–749	0.084	0.092	Cumacea	–		
Halice walkeri (Ledoyer, 1973)	370–748	0.052	0.097	*Bathycuma brevirostris* (Norman, 1879)	747–749	–	0.028
Haliceroion angusicornis (Norman, 1869)	363–747	–	0.041	*Bodotria scorpioides* (Montagu, 1804)	134–370	0.034	0.018
Harpinopsis nirae Kaim-Malka 1976	134	0.023	–	*Campylaspis* cf. *Macrophthalma* G. O. Sars, 1879	347–747	–	0.019
Harpinia cf. *crenulata* (Boeck, 1871)	365	0.011	–	*Campylaspis glabra* G. O. Sars, 1878	150–752	2.926	1.378
Harpinia truncata G. O. Sars, 1891	376	0.033	–	*Campylaspis horridoides* Stephensen, 1915	362–749	0.064	0.059
Harpinia spp. Boeck, 1876	155–747	0.060	0.158	*Campylaspis rostrata* Calman, 1905	692	–	0.009
Idunella pinata Krapp-Schickel, 1975	365–747	0.054	0.010	*Campylaspis* sp. G. O. Sars, 1865	153–670	0.084	0.061
Iphinoestroe iliergetes (J. L. Barnard, 1964)	335–752	0.966	1.132	*Campylaspis squamifera* Fage, 1929	682	0.008	
Lembos sp.[J] Bate, 1857	363–365	0.019	–	*Campylaspis sulcata* G. O. Sars, 1870	148–752	6.520	1.547
Leptochiella manco J.L. Barnard, 1973	328–749	1.808	1.088	*Campylaspis vitrea* Calman, 1906	670–749	–	0.021
Lepidepecreum subchyseatum Ruffo & Schiecke, 1977	347–752	0.325	0.704	*Campylaspis verrucosa* G. O. Sars, 1866	171–752	0.287	1.403
Leucothoe liljeborgi Boeck, 1861	155–749	0.038	0.075	*Cumella spinoculeata* G.O. Sars, 1865	365–747	0.032	0.010
Lysianassa plumosa Boeck, 1871	670–752	–	0.070	*Cumellopsis puritani* Calman, 1905	347–376	0.044	0.076
Lysianassidae[E] (LeCroy, 2007)	155–749	0.068	0.073	*Cyclaspis longicaudata* G. O. Sars, 1865	171–752	–	0.497
Maera schmidti Stephensen, 1915	650–696	–	0.015	*Diastylis dorsiphora* Fage, 1940	749	–	0.053
Megamphopus sp. Norman, 1869	150–365	0.022	–	*Diastylis tumida* (Liljeborg, 1855)	328–734	0.047	0.064
Melitidae Bousfield, 1977	189	0.035	–	*Diastyloides hansoni* Fage, 1940	362–376	0.041	0.032
Melphidippella macra Norman, 1869	150–376	0.023	0.028	*Diastylis* sp. Say, 1818	362	0.008	–
Metaphoxus simplex (Bate, 1857)	356–749	0.033	0.069	*Diastyloides serrata* (G. O. Sars, 1865)	156–752	1.301	0.401
Monoculodes packardi Boeck, 1871	155–749	0.355	0.363	Diastylidae Bate, 1856	356–363	0.008	0.011
Monoculodes acutipes Ledoyer, 1983	352–749	0.160	0.321	*Epilenecon ennis* Bishop, 1983	376–692	0.011	0.009
Monoculodes griseus (Della Valle, 1893)	161–189	0.012	0.009	*Eudorella truncatula* (Bate, 1856)	365	0.021	–
Monoculodes sp.[H] Stimpson, 1853	155–747	0.051	0.052	*Hemilamprops normani* Bonnier, 1896	328–734	5.199	2.858
Micippe tumida Bruzelius, 1859	335–752	0.772	1.049	*Leptostylis macrura* G. O. Sars, 1870	150–749	0.726	0.336
Normanion ruffoi Diviacco & Vader, 1988	363	–	0.022	*Leptostylis* sp.[D] G. O. Sars, 1869	747	–	0.010
Oedicerotidae Lilljeborg, 1865	363–749	0.011	0.059	*Leucon affinis* (Fage, 1951)	171–752	0.270	0.177
Oedicerotopsis brevicornis Lilljeborg, 1865	328–760	0.164	0.188	*Leucon longirostris* (Calman, 1906)	161–752	0.048	0.229
Oedicerotidae Lilljeborg, 1865	152–747	0.042	0.072	*Leucon siphonatus* (Calman, 1906)	363–734	0.167	0.167
Orchomene humilis (A. Costa, 1853)	363–696	0.075	0.021	*Makrokylindrus anomalus* (Bonnier, 1896)	153	–	0.011
Orchomene grimaldii Chevreux, 1890	376–734	0.051	0.056	*Makrokylindrus gibraltarensis* (Barnard, 1961)	171–752	0.227	0.085
Orchomenella nana (Krøyer, 1846)	328–752	1.125	0.702	*Makrokylindrus insignis* (G. O. Sars, 1871)	156–376	0.011	0.022
Paracentromedon crenulatum (Chevreux, 1900)	696	–	0.007	*Makrokylindrus longipes* (G. O. Sars, 1871)	148–376	0.296	0.093
Paraphoxus oculatus (G. O. Sars, 1879)	370–734	0.095	0.007	*Makrokylindrus strebbingi* Stephensen, 1915	347–670	–	0.105
Parkfiraca mediterranea Bellan-Santini, 1985	611–752	0.094	0.108	*Makrokylindrus* sp. Stebbing, 1912	376	0.011	–
Pardaliscidae Boeck, 1871	363	–	0.011	Nannastacidae (Cumelle sp.)	363	–	0.022
Perioculodes longimanus (Bate and Westwood, 1868)	153–670	0.011	0.176	*Nannastacus unguiculatus* (Bate, 1859)	150–692	0.836	0.359
Phoxocephalidae sp. 1 G.O. Sars, 1891	347	–	0.009	*Platysympus typicus* (G. O. Sars, 1869)	171–752	0.049	1.014
Pleusymtes sp. J. L. Barnard, 1969	155	–	0.009	*Procampylaspis armata* Bonnier, 1896	153–760	1.047	2.732
Podoprion bolivari Chevreux, 1891	732–747	0.029	0.011	*Procampylaspis bonnieri* Calman, 1906	347–747	0.085	0.116
Pseudotiron bouvieri Chevreux, 1895	335–752	0.548	0.338	*Procampylaspis mediterranea* Ledoyer, 1987	376	0.011	–
Rhachotopsis caeca Ledoyer, 1977	134–760	2.416	4.301	*Procampylaspis* sp. Bonnier, 1896	347–747	0.054	0.085
Rhachotopsis glabra G. O. Sars, 1878	666–692	–	0.016	*Vemukylindrus hastatus* (Hansen, 1920)	365–376	0.032	–

References

Anderson, M.J., Legendre, P., 1999. An empirical comparison of permutation methods for tests of partial regression coefficients in a linear model. J. Stat. Comput. Simul. 62 (3), 271–303.

Anderson, M.J., ter Braak, C.J.F., 2003. Permutation tests for multifactorial analysis of variance. J. Stat. Comput. Simul. 73, 85–113.

Anderson, M.J., Gorley, R.N., Clarke, K.R., 2008. PERMANOVA + for PRIMER: Guide to Software and Statistical Methods. PRIMER-E, Plymouth, UK. 214 pp.

Bellan-Santini, D., 1990. Mediterranean deep-sea Amphipoda: composition, structure and affinities of the fauna. Prog. Ocean. 24, 275–387.

Billett, D.S.M., Bett, B.J., Rice, A.L., Thurston, M.H., Galéron, J., Sibuet, M., Wolff, G.A., 2001. Long-term change in the megabenthos of the Porcupine Abyssal Plain (NE Atlantic). Progress in Oceanography 50, 325–348.

Bosc, E., Bricaud, A., Antoine, D., 2004. Seasonal and interannual variability in algal biomass and primary production in the Mediterranean Sea, as derived from 4 years of SeaWiFS observations. Global Biogeochem. Cycles 18, 1–17.

Brandt, A., 1995. Peracarid fauna (Crustacea, Malacostraca) of the Northeast Water Polynya off Greenland: documenting close benthic-pelagic coupling in the Westwind Trough. Mar. Ecol. Prog. Ser. 121, 39–51.

Brattegard, T., Fossa, J.H., 1991. Replicability of an epibenthic sampler. J. Mar. Biol. Assoc. U. K. 71, 153–166.

Brunel, P.M., Besner, D., Messier, L., Poirier, D., Granger, D., Weinstein, M., 1978. Le traîneau Macer-GIROQ: appareil amélioré pour l'échantillonnage quantitatif de la petite faune nageuse au voisinage du fond. Int. Rev. Gesamten Hydrobiol. 63, 815–829.

Buscail, R., Pocklington, R., Daumas, R., Guidi, L., 1990. Fluxes and budget of organic matter in the benthic Boundary Layer over the northwestern Mediterranean. Cont. Shelf Res. 10, 1089–1122.

Carrassón, M., Cartes, J.E., 2002. Trophic relationships in a Mediterranean deep-sea fish community: partition of food resources, dietary overlap and connections within the Benthic Boundary Layer. Mar. Ecol. Prog. Ser. 241, 41–55.

Cartes, J.E., Sorbe, J.C., 1993. Les communautés suprabenthiques de la Mer Catalane (Méditerranée occidentale): données préliminaires sur la repartition bathymetrique et l'abondance des crustacés péracarides. Crustaceana 64, 155–171.

Cartes, J.E., Sorbe, J.C., 1997. Bathyal Cumaceans of the Catalan Sea (north-western Mediterranean): faunistic composition, diversity and near bottom distribution along the slope (between 389–1859 m). J. Nat. Hist. 31, 1041–1054.

Cartes, J.E., Sorbe, J.C., 1999a. Deep-water amphipods from the Catalan Sea slope (western Mediterranean): bathymetric distribution, assemblage composition and biological characteristics. J. Nat. Hist. 33 (8), 1133–1158.

Cartes, J.E., Sorbe, J.C., 1999b. Estimating secondary production in bathyal suprabenthic peracarid crustaceans from the Catalan Sea slope (western Mediterranean; 391–1255 m). J. Exp. Mar. Biol. Ecol. 239, 195–210.

Cartes, J.E., Sorbe, J.C., Sardà, F., 1994. Spatial distribution of deep-sea decapods and euphausiids near the bottom in the Northwestern Mediterranean. J. Exp. Mar. Biol. Ecol. 179, 131–144.

Cartes, J.E., Elizalde, M., Sorbe, J.C., 2001. Contrasting life-histories, secondary production, and trophic structure of peracarid assemblages of the bathyal suprabenthos from the Bay of Biscay (NE Atlantic) and the Catalan Sea (N Mediterranean) areas. Deep Sea Res. I 48, 2209–2232.

Cartes, J.E., Jaume, D., Madurell, T., 2003. Local changes in the composition and community structure of suprabenthic peracarid crustaceans on the bathyal Mediterranean: influence of environmental factors. Mar. Biol. 143 (4), 745–758.

Cartes, J.E., Papiol, V., Palanques, A., Guillén, J., Demestre, M., 2007. Dynamics of suprabenthos off the Ebro Delta (Catalan Sea, Western Mediterranean): spatial and temporal patterns and relationships with environmental factors. Estuar. Coast. Shelf Sci 75, 501–515.

Cartes, J.E., Papiol, V., Guijarro, B., 2008a. The feeding and diet of the deep-sea shrimp *Aristeus antennatus* off the Balearic Islands (Western Mediterranean): influence of environmental factors and relationships with biological cycle. Prog. Oceanogr. 79, 37–54.

Cartes, J.E., Madurell, T., Fanelli, E., López-Jurado, J.L., 2008b. Dynamics of suprabenthos-zooplankton communities around the Balearic Islands (western Mediterranean): Influence of environmental variables and effects on the biological cycle of *Aristeus antennatus*. J. Mar. Syst. 71 (3–4), 316–335.

Cartes, J.E., Hidalgo, M., Papiol, V., Massutí, E., Moranta, J., 2008c. Changes in the diet and feeding of the hake *Merluccius merluccius* in the shelf-break of Balearic islands (Western Mediterranean): influence of the mesopelagic–boundary community. Deep Sea Res. I 56, 344–365.

Cartes, J.E., Maynou, F., Fanelli, E., Papiol, V., Lloris, D., 2009a. Long-term changes in the composition and diversity of deep-slope megabenthos and trophic webs off Catalonia (Western Mediterranean): are trends related to climatic oscillations. Prog. Oceanogr. 82, 32–46.

Cartes, J.E., Maynou, F., Fanelli, E., Romano, C., Mamouridis, V., Papiol, V., 2009b. The distribution of megabenthic, invertebrate epifauna in the Balearic Basin (Western Mediterranean) between 400 and 2300 m: environmental gradients influencing assemblages composition and biomass trends. J. Sea Res. 61 (4), 244–257.

Cartes, J.E., Ligas, A., De Biasi, A.M., Pacciardi, L., Sartor, P., 2009c. Small-spatial scale changes in productivity of suprabenthic and infaunal crustaceans at the continental shelf of Ebro Delta (western Mediterranean). J. Exp. Mar. Biol. Ecol. 378, 40–49.

Clarke, K.R., 1993. Non-parametric multivariate analyses of changes in community structure. Aust. J. Ecol. 18, 117–143.

Clarke, K.R., Warwick, R.M., Brown, B.E., 1993. An index showing breakdown of seriation, related to disturbance, in a coral-reef assemblage. Mar. Ecol. Prog. Ser. 102, 153–160.

Collie, J.S., Hall, S.J., Kaiser, M.J., Poiner, I.R., 2000. A quantitative analysis of fishing impacts on shelf-sea benthos. J. Anim. Ecol. 69, 785–798.

Connell, J.H., 1978. Diversity in tropical rain forests and coral reefs. Science 199, 1302–1309.

Corliss, B.H., Brown, C.W., Sun, X., Showers, W.J., 2009. Deep-sea benthic diversity linked to seasonality of pelagic productivity. Deep Sea Res. I 56, 835–841.

Crame, J.A., 2000. Evolution and taxonomic diversity gradients in the marine realm: evidence from the composition of recent bivalve faunas. Paleobiology 26 (2), 188–214.

Dauvin, J.C., Lorgeré, J.C., 1989. Modification du traîneau Macer-GIROQ pour l'amélioration de l'échantillonnage quantitatif étagé de la faune suprabenthique. J. Rech. Océanogr. 14, 65–67.

Dauvin, J.C., Sorbe, J.C., 1995. Suprabenthic amphipods from the southern margin of the Cap Ferret Canyon (Bay of Biscay, north-eastern Atlantic Ocean): abundance and bathymetric distribution. Pol. Arch. Hydrobiol. 42, 441–460.

Dauvin, J.C., Vallet, C., 2006. The near bottom layer as an ecological boundary in marine ecosystems: diversity, taxonomic composition and community definitions. Hydrobiology 555, 49–58.

Dayton, P.K., Hessler, R.R., 1972. Role of biological disturbance in maintaining diversity in the deep sea. Deep Sea Res. 19, 199–208.

Dickinson, J.J., 1978. Faunal comparison of the Gammarid Amphipoda (Crustacea) in two bathyal basins of the California continental borderland. Mar. Biol. 48, 367–372.

Dickinson, J.J., Carey Jr., A.G., 1978. Distribution of gammarid Amphipoda (Crustacea) on Cascadia Abyssal Plain (Oregon). Deep Sea Res. 25, 97–106.

Elizalde, M., Weber, O., Pascual, A., Sorbe, J.C., Etcheber, H., 1999. Benthic response of *Munnopsurus atlanticus* (Crustacea, Isopoda) to the carbon content of the near-bottom sedimentary environment on the southern margin of Cap-Ferret Canyon (Bay of Biscay, northeastern Atlantic Ocean). Deep Sea Res. II 46, 2331–2344.

Estrada, M., 1996. Primary Production in the Northwestern Mediterranean. Sci. Mar. 60, 55–64.

Fanelli, E., Cartes, J.E., Rumolo, P., Sprovieri, M., 2009a. Food web structure and trophodynamics of mesopelagic–suprabenthic deep sea macrofauna of the Algerian basin (Western Mediterranean) based on stable isotopes of carbon and nitrogen. Deep Sea Res. I 56 (9), 1504–1520.

Fanelli, E., Cartes, J.E., Badalamenti, F., Rumolo, P., Sprovieri, M., 2009b. Trophodynamics of suprabenthic fauna on coastal muddy bottoms of the southern Tyrrhenian Sea (western Mediterranean). J. Sea Res. 61, 174–187.

Fernández de Puelles, M.L., Valencia, J., Vicente, L., 2004. Zooplankton variability and climatic anomalies from 1994 to 2001 in the Balearic Sea (Western Mediterranean) ICES. J. Mar. Sci. 61 (4), 492–500.

Font, J., 1987. The path of the Levantine intermediate water to the Alboran sea. Deep Sea Res. A 34, 1745–1755.

Gage, J.D., Tyler, P.A., 1991. Deep Sea Biology: a Natural History of Organisms at the Deep-Sea Floor. Cambridge University Press, Cambridge.

Guijarro, B., Massutí, E., Moranta, J., 2008. Population dynamics of the red-shrimp *Aristeus antennatus* in the Balearic Islands (Western Mediterranean): spatial–temporal differences and influence of environmental factors. J. Mar. Syst. 71, 385–402.

Hidalgo, M., Massutí, E., Moranta, J., Cartes, J.E., Lloret, J., Oliver, P., Morales-Nin, B., 2008. Seasonal and short spatial patterns in European hake (*Merluccius merluccius* L.) recruitment process at the Balearic Islands (western Mediterranean): the role of environment on distribution and condition. J. Mar. Syst. 71, 367–384.

Hynes, H.B.N., Coleman, M.J., 1968. A simple method of assessing the annual production of stream benthos. Limnol. Oceanogr. 13 (4), 569–573.

Jacob, P.K., Sale, P.F., 2006. Marine Metapopulations. Academic Press, San Diego, New York. 576 pp.

Jaume, D., Cartes, J.E., Boxhall, G.A., 2000. Shallow-water and not deep-sea as most plausible origin for cave-dwelling Paramisophria species (Copepoda: Calanoida: Arietellidae), with description of three new species from Mediterranean bathyal hyperbenthos and littoral caves. Cont. Zool. 68, 205–244.

Jennings, S., Dinmore, T.A., Duplisea, D.D., Warr, K.J., Lancaster, J.E., 2001. Trawling disturbance can modify benthic production processes. J. Anim. Ecol. 70, 459–475.

Josefson, A.B., Conley, D.J., 1997. Benthic response to a pelagic front. Mar. Ecol. Prog. Ser. 147, 47–62.

Lampitt, R.S., Billet, D.S.M., Rice, A.L., 1986. Biomass of the invertebrate megabenthos from 500 to 4100 m in the northeast Atlantic Ocean. Mar. Biol. 93 (1), 69–81.

Ligas, A., De Biasi, A.M., Demestre, M., Pacciardi, L., Sartor, P., Cartes, J.E., 2009. Effects of chronic trawling disturbance on the secondary production of suprabenthic and infaunal crustacean communities in the Adriatic Sea (NW Mediterranean). Cienc. Mar. 35 (2), 195–207.

López-Jurado, J.L., Marcos, M., Monserrat, S., 2008. Hydrographic conditions during the IDEA project (2003–2004). J. Mar. Syst. 71, 303–315.

Madurell, T., Cartes, J.E., 2003. The suprabenthic peracarid fauna collected at bathyal depths in the Ionian Sea (eastern Mediterranean). Crustaceana 76 (5), 611–624.

Madurell, T., Fanelli, E., Cartes, J.E., 2008. Isotopic composition of carbon and nitrogen of suprabenthos fauna in the NW Balearic Islands (Western Mediterranean). J. Mar. Syst. 71, 336–345.

Marques, J.C., Bellan-Santini, D., 1987. Amphipod crustaceans of the Portuguese coasts: fauna of the Mira Estuary (Alentejo, South-West coast). Cah. Biol. Markers 28 (3), 465–480.

Mees, J., Jones, M.B., 1997. The hyperbenthos. Oceanol. Mar. Biol. Ann. Rev. 35, 221–255.

Menzies, C.A., 1980. A note on the Hynes method of estimating secondary production. Limnol. Oceanogr. 25, 770–773.

Millot, C., 1999. Circulation in the Western Mediterranean Sea. J. Mar. Syst. 20, 423–442.

Moranta, J., Stefanescu, C., Massutí, E., Morales-Nin, B., Lloris, D., 1998. Fish community structure and depth-related trends on the continental slopes of the Balearic Islands (Algerian basin, western Mediterranean). Mar. Ecol. Prog. Ser. 171, 247–259.

Plante, C., Downing, J.A., 1989. Production of freshwater invertebrate populations in lakes. Can. J. Fish. Aquat. Sci. 46, 1489–1498.

Rex, M., Etter, R., 2010. Deep-Sea Diversity: Pattern and Scale. Harvard University Press. 368 pp.

Rex, M.A., Etter, R.J., Stuart, C.T., 1997. Large-Scale Patterns of Species Diversity in the deep-Sea Benthos. In: Ormond, R., Gage, J.D. (Eds.), Marine Biodiversity: Causes and Consequences. Cambridge University Press, pp. 94–121.

Rex, M.A., Stuart, C.T., Coyne, G., 2000. Latitudinal gradients of species richness in the deep-sea benthos of the North Atlantic. Proc. Nat. Acad. Sci. U.S.A. 97, 4082–4085.

Richoux, N.B., Thompson, R.J., Deibel, D., 2004. Population biology of hyperbenthic crustaceans in a cold water environment (Conception Bay, Newfoundland). 2. *Acanthostepheia malmgreni* (Amphipoda). Mar. Biol. 144 (5), 895–904.

Rombouts, I., Beaugrand, G., Ibáñez, F., Gasparini, S., Chiba, S., Legendre, L., 2009. Global latitudinal variation in marine copepod diversity and environmental factors. Proc. R. Soc. London, Ser. B 276, 3053–3062.

Ruffo, S., Cartes, J.E., Sorbe, J.C., 1999. A new bathyal species of the genus *Autonoe* from the Catalan Sea (NW Mediterranean. (Crustacea Amphipoda: Aoridae) Boll. I Mus. Civico di St. Nat. Verona. 22, 21–30.

Ruhl, H.A., Smith Jr., K.L., 2004. Shifts in deep-sea community structure linked to climate and food supply. Science 305, 513–515.
San Vicente, C., Cartes, J.E., 2011. *Dactylamblyops corbeni* n. sp., a new mysid (Crustacea: Mysida) from the deep Mediterranean Sea. Sci. Mar. 75 (3).
Snelbe, J.C., 1999. Deep-sea macrofaunal assemblages within the Benthic Boundary Layer of the Cap-Ferret Canyon (Bay of Biscay, northeastern Atlantic). Deep Sea Res. I 46, 2309–2330.
Stefanescu, C., Lloris, D., Rucabado, J., 1992. Deep-living demersal fishes in the Catalan Sea (western Mediterranean) below a depth of 1000 m. J. Nat. Hist. 26, 197–213.
Watts, M.C., Etter, R.J., Rex, M.A., 1992. Effects of Spatial and Temporal Scale on the Relationship of Surface Pigment Biomass to Community Structure in the Deep-Sea Benthos. In: Rowe, G.T., Pariente, V. (Eds.), Deep-Sea Food Chains and the Global Carbon Cycling. Kluwer, Dordrecht, pp. 245–254.

UNIVERSIDADE DE SANTIAGO DE COMPOSTELA
DEPARTAMENTO DE ESTATÍSTICA E INVESTIGACIÓN OPERATIVA

Extended Additive Regression for Analysing LPUE Indices in Fishery Research

V. Mamouridis, N. Klein, T. Kneib, C. Cadarso Suárez, F. Maynou

Report 13-01

Reports in Statistics and Operations Research

Extended Additive Regression for Analysing LPUE Indices in Fishery Research

Valeria Mamouridis*[1], Nadja Klein[2], Thomas Kneib[2], Carmen M. Cadarso Suárez[3] and Francesc Maynou[1]

[1] Institut de Ciències del Mar (CSIC), Passeig Marítim de la Barceloneta 37-49, 08003 Barcelona, Spain
[2]Georg-August University, Wilhelmsplatz 1, 37073 Gttingen, Germany
[3]Unidade de Bioestadística, Facultade de Medicina e Odontoloxía, USC, Rúa de San Francisco, s/n, 15782 Santiago de Compostela, Spein

29/10/2013

Abstract

We analysed the landings per unit effort (LPUE) from the Barcelona trawl fleet (NW Mediterranean) of the red shrimp (*Aristeus antennatus*) using the novel bayesian approach of additive extended regression or distributional regression, that comprises a generic framework providing various response distributions, such as the log-normal and the gamma and allows estimations for location and scale or shape (as the frequentist counterpart GAMLSS). The dataset covers a span of 17 years (1992-2008) during which the whole fleet has been monitored and consists of a broad spectrum of predictors: fleet-dependent (e.g. number of trips performed by vessels and their technical characteristics, such as the gross registered tonnage), temporal (inter- and intra-annual variability) and environmental (NAO index) variables. This dataset offers a unique opportunity to compare different assumptions and model specifications. So that we compared 1) log-normal versus gamma distribution assumption, 2) modelling only the expected LPUE versus modelling both expectation and scale (or shape) of LPUE, and finally 3) fixed versus random specifications for the catching unit effects (boats). Our preliminary results favour the gamma over the log-normal and modelling of both location and shape (in the case of the gamma) rather than only the location, while not noticeable differences occur in estimation when considering catching units as fixed or random.

Citation: Mamouridis, V., Klein, N., Kneib T., Cadarso Suárez, C.M., Maynou, F. 2013. Extended Additive Regression for Analysing LPUE Indices in Fishery Research. Reports in Statistics and Operations Research. Universidade de Santiago de Compostela. Departamento de Estatística e Investigación Operativa. Vol. 29/10/2013 (2013-01). available at: http://eio.usc.es/index.php/es/reports-.

*mamouridis@icm.csic.es

1 Introduction

In fishery research, the LPUE (Landings Per Unit Effort) is an index widely used in stock assessment to estimate the relative abundance of an exploited species (Mendelssohn and Cury, 1989; Marchal et al., 2002). It constitutes one of the most common pieces of information used in assessing the status of fish stocks and is reckoned in different ways depending on data availability. The "landings" portion of the measure is the quantity of the stock brought to the port by each vessel and is usually expressed as number of individuals or weight of the whole stock, while the "unit effort" portion refers to the unit of time spent by a unit of the gear used to catch (e.g. vessel or square meters of a net). Therefore, LPUE is a relative index, which use is based on the assumption that it is proportional to the natural quantity of the species, despite their proportionality has been debated in the past (e.g. Gulland, 1964; Bannerot and Austin, 1983).

The most commonly applied analyses on LPUE is its standardisation to remove the bias induced by influential factors that do not reflect the natural variability (Maunder et al., 2006). In fact, many factors can affect the index (e.g. time, seasonality, fishing area and fleet characteristics, among others), some of which (i.e. fishery related variables) if not considered can lead to biased interpretations of stock states. Here we model the LPUE using all available explanatory variables. For some of the influential variables, a simple linear impact on LPUE as often assumed in standard statistical models may not be flexible enough and alternative, semiparametric modelling approaches may be required. Moreover, in most cases LPUE data are collected repeatedly for the same catching units over time leading to the necessity to account for unobserved characteristics of these units to avoid correlations in the repeated measurements.

The most common class of regression models to determine the impact of covariates $x_1, \ldots, x_p$ on the expectation of the LPUE are generalized linear models (GLM, McCullagh and Nelder, 1989) and generalized additive models (GAM, Hastie and Tibshirani, 1986). In GLM the expectation of LPUE is related to a linear combination of the covariate effects, i.e.

$$E(\text{LPUE}_i) = h(\beta_0 + \beta_1 x_{i1} + \ldots + \beta_p x_{ip}), \qquad i = 1, \ldots, n$$

with a suitable transformation function h that ensures positivity of the expected LPUE and regression coefficients $\beta_0, \beta_1, \ldots, \beta_p$ (for GLM applications in LPUE analyses see (see Gotti et al., 1999; Maynou et al., 2003). Popular special cases for modelling LPUE include the gamma distribution or the normal distribution applied to log-transformed LPUE values (which is equivalent to assume a log-normal distribution). To overcome the limitation of GLMs to purely linear effects of covariates, generalized additive models, GAM have been introduced (see Damalas et al., 2007; Denis, 2002) where now the expectation is specified as

$$E(\text{LPUE}_i) = h(\beta_0 + f_1(x_{i1}) + \ldots + f_p(x_{ip})).$$

The nonlinear functions $f_1, \ldots, f_p$ remain unspecified and should be estimated flexibly from the data, for example using penalized spline approaches (see Wood, 2006; Ruppert et al., 2003).

Another direction for extending the GLM approach is the inclusion of catching unit-specific effects to acknowledge the effect that usually multiple observations are

collected and that unobserved heterogeneity remains even when accounting for some covariate effects. If the individual catching units are indexed as $i = 1,\ldots,n$ and the repeated measurement for one catching unit are indexed as $j = 1,\ldots,n_i$, the resulting model can be written as

$$E(\text{LPUE}_{ij}) = h(\beta_0 + \beta_1 x_{ij1} + \ldots + \beta_p x_{ijp} + \alpha_i), \qquad i = 1,\ldots,n,\ j = 1,\ldots,n_i.$$

The additional parameter α_i is introduced to stand for any effect specific to the catching unit that is not represented in the effects of covariates $x_1,\ldots,x_p$. Of course, similar extensions can be defined for generalized additive models. In the statistical community, the most common assumption for α_i would be the specification as a random effect, i.e. α_i i.i.d. $N(0,\tau^2)$, to acknowledge the fact that the catching units represent a sample from the population of catching units. This leads to the class of generalized linear mixed models (GLMMs, Pinheiro and Bates, 2000) or generalized additive mixed models (GAMMs, Wood, 2006). An alternative specification is to treat the α_i as usual, fixed parameters that result from dummy coding of the catching units. This may be considered more appropriated if, for example, the complete fleet of catching units for a specific area has been observed. We will return to this debate later when discussing the methods in more detail, see also Bishop et al. (2004), Cooper et al. (2004) or Helser et al. (2004) for the use of mixed models in this field.

Another important aspect when modelling LPUE is the choice of the response distribution. In most cases, skewed distributions have been considered, including in particular the gamma distribution (Maynou et al., 2003; Stefánsson, 1996), the log-normal distribution (Brynjarsdóttir and Stefánsson, 2004; Myers and Pepin, 1990) and the delta distribution (Gavaris, 1980; Pennington, 1983). The latter provides a form of zero-adjustment where zero catches are modelled separately from the nonnegative catches via a Bernoulli distribution. As a possibility to differentiate between gamma and log-normal distribution, the Kolmogorov-Smirnov test has been applied to fitted values from corresponding GLMs. Then, the distribution leading to a lower value for the test statistic can be considered to be closer to the distribution of the data (Brynjarsdóttir and Stefánsson, 2004; Stefánsson and Palsson, 1998).

In this paper, structured additive distributional regression models (Klein et al., 2013b) has been considered as a comprehensive, flexible class of models that encompasses all special cases discussed so far and a number of further extensions. More specifically, this class of models allows to deal with the following problems:

- Selection of the response distribution: Additive distributional regression comprises a generic framework providing various response distributions and in particular the log-normal and the gamma distributions. Extensions including zero-adjustment to account for an inflation of observations with zero catch would also be possible but not required in the data set considered later. Tools for effectively deciding between competing modelling alternatives will also be considered.
- Linear versus nonlinear effects: Effects of continuous covariates can be estimated nonparametrically based on penalized splines approximations that allow for a data-driven amount of smoothness and therefore deviation from the linearity assumption.

- Fixed versus random effects: Both fixed and random specifications for the catching unit-specific effects are supported and can be compared in terms of their ability to fit the data.
- Models for location, scale and shape: Instead of restricting attention to only modelling the expected LPUE, distributional regression allow to specify a further parameter of the distribution that correspond to scale or shape. This both enables for additional flexibility and a better understanding of how different covariates affect the distribution of LPUE.
- Mode of inference: Distributional regression can be formulated both from a frequentist and a Bayesian perspective and corresponding estimation schemes either rely on penalized maximum likelihood or Markov chain Monte Carlo simulations. This paper is focused on the Bayesian inference.

Structured additive distributional regression is in fact an extension of structured additive regression (STAR, Brezger and Lang, 2006; Fahrmeir et al., 2004) in the framework of generalized additive models for location, scale and shape (GAMLSS, Rigby and Stasinopoulos, 2005). The parameter specifications rely very much on STAR, a comprehensive class of regression models for the expectation of the response that comprises geoadditive models (Kammann and Wand, 2003), generalized additive models (Hastie and Tibshirani, 1986) and generalized additive mixed models (Lin and Zhang, 1999) as special cases.

Our analysts deals with the red shrimp (*Aristeus antennatus*) LPUE. The red shrimp is the target species for the deep-water trawl fishery in the Western Mediterranean (Bas et al., 2003), where catches have reached more than 1000 t/yr (FAO/FISHSTAT, 2011). This fishery is developed in deep-waters - 450 – 900 m - on the continental slope and near submarine canyons (Sardà et al., 1997; Tudela et al., 1998). *A. antennatus* LPUE has already been studied: its fluctuations have been related to changes in oceanographic conditions, e.g. at least partially triggered by changes in the North Atlantic Oscillation (Maynou, 2008) or explained by changes in the seasonal availability of the resource, linked to its life-cycle (Carbonell et al., 1999) and source demand (Sardà et al., 1997).

The main objective of this study is to demonstrate the usefulness of structured additive distributional regression in modelling and predict shrimp LPUE and to provide guidance for model choice and variable selection, questions that arise in the process of developing an appropriate model for a given data set. Therefore, we will discuss tools such as quantile residuals, information criteria and predictive mean squared errors to evaluate the ability of models to describe and predict LPUE adequately.

The rest of the paper is structured as follows: In Section 2 a description of the data set is given to illustrate the application of structured additive distributional regression. Section 3 provides an overview of the methods dealing with the real data set, including the choice of an appropriate response distribution and variable selection. In Section 4, we perform an extensive analysis of the red shrimp data, comparing different response distributions, regression specifications and random versus fixed effects for the repeated observations. The final Section 5 concludes and comments on main results and directions of future research.

2 Data description

Data proceed from the daily sale slips of the Barcelona trawling fleet, granted by the Barcelona Fishers' Association. This data set comprises the information for 21 trawlers, with their total monthly landings (*landings*, kg), their monthly number of trips performed (*trips*) and the Gross Registered Tonnage (*grt*, GRT). Furthermore, the monthly average value of the North Atlantic Oscillation index (NAO) was obtained from the web site of the Climatic Research Unit of the University of East Anglia (Norwich, UK): `http://www.met.rdg.ac.uk/cag/NAO/slpdata.html`. Then we computed the year average of NAO, whose relationship with landings of three years later has been detected through cross-correlation analysis in previous studies by Maynou (2008).

The total number of observations, N, amounts to $N = 2314$ using the whole fleet (21 trawlers) having practised deep-fishing in the period from January 1992 to December 2008 (17 complete years). Landings of the whole fleet were monitored over time, so, data depict the entire population of the fleet in the studied area and period. Red shrimp fishery is a specific fishery, thus, all the product caught on board appears in landings, due to its high commercial value, while, when landings are not reported for a given boat is due to its inactivity, rather than to zero catches of the source.

The landings and number of trips were used to estimate the "nominal" LPUE index,

$$lpue_{ij} = \frac{landings_{ij}}{trips_{ij}}, \tag{1}$$

where i and j refer to the observation i of the vessel j. The adjective "nominal" refers to the variable not standardized. Table 1 and the introductory part of this Section provide information on the variables in Equation 1. Trips are always performed in one day, hence, the *lpue* represents the daily biomass average caught by a boat during one day (kg d^{-1}) with a monthly resolution.

As in previous regression analysis (see)mamouridis2014 months associated to not significant parameters of the categorical variable *months* with categories $month_k$, $k = 1,\ldots,12$ were backward assembled into two categories of a new variable *period* (period of the year): *period*1 defines all months excluding June and November and *period*2 refers to June and November. All variables are summarised in Table 1.

3 Methodology

It has become quite popular to model the expected LPUE as a function of linear covariate effects. The results obtained from linear mean regression are easy to interpret but depreciated by possible misspecification due to a more complex underlying covariate structure, violation of homoscedastic errors or correlations caused by clustered data. To deal with these problems we apply Bayesian distributional structured additive regression models (Klein et al., 2013b) a model class originally proposed by Rigby and Stasinopoulos (2005) in a frequentist setting. The idea is to assume a parametric distribution for the conditional behaviour of the response and to describe each parameter

Table 1: List of variables.

Variable	Description
landings	the total catches landed at port by each boat in one month
lpue	the daily LPUE index for each boat calculated as in Eq. 1
code	a categorical variable assigned to each boat, $c = 1, \ldots, 21$
time	a total of 204 months from January 1992 to December 2008 coded with a letter and two digits, e.g. J92 is January 1992
trips	the number of trips performed by each vessel during one month
grt	Gross Registered Tonnage of each boat
nao_3	mean annual NAO index of 3 years before the year of estimated *lpue*
month	categorical variable with $m = 1, \ldots, 12$ from January to December
period	binary variable with grouped months holding the same effect *period*1 = all month excluding June and November *period*2 = June and November

of this distribution as a function of explanatory variables. In the following, only log-normal and gamma distribution are considered for LPUE, although also an extension to mixture distributions with point masses in zero would be possible as in Heller et al. (2006) or Klein et al. (2013a). Here they are not necessary since the response in this study is always greater than zero.

We consider the log-normal distribution with parameters μ_{ij} and σ_{ij}^2 such that

$$E(lpue_{ij}) = \exp\left(\mu_{ij} + \frac{\sigma_{ij}^2}{2}\right)$$

$$Var(lpue_{ij}) = \left(\exp\left(\sigma_{ij}^2\right) - 1\right) \exp\left(2\mu_{ij} + \sigma_{ij}^2\right).$$

Accordingly, $\log\left(lpue_{ij}\right)$ is normal distributed with $E(\log(lpue_{ij})) = \mu_{ij}$ and $Var(\log(lpue_{ij})) = \sigma_{ij}^2$. As an alternative, we assume a gamma distribution with parameters $\mu_{ij} > 0$, $\sigma_{ij} > 0$ and density

$$f(lpue_{ij}|\mu_{ij}, \sigma_{ij}) = \left(\frac{\sigma_{ij}}{\mu_{ij}}\right)^{\sigma_{ij}} \frac{lpue_{ij}^{\sigma_{ij}-1}}{\Gamma(\sigma_{ij})} \exp\left(-\frac{\sigma_{ij}}{\mu_{ij}} lpue_{ij}\right).$$

Then, the expectation and variance are given by

$$E(lpue_{ij}) = \mu_{ij}$$

and

$$Var(lpue_{ij}) = \frac{\mu_{ij}^2}{\sigma_{ij}}$$

such that μ_{ij} is the location parameter and the parameter σ_{ij} is inverse proportional to the variance.

All parameters involved are linked to structured additive predictors, yielding

$$\eta_{ij,\mu} = \mu_{ij} \qquad \eta_{ij,\sigma^2} = \log\left(\sigma_{ij}^2\right)$$

for the log-normal distribution where the log-link is used to ensure positivity of the σ_{ij}^2. For the gamma distribution, both parameters are restricted to be positive so that we obtain

$$\eta_{ij,\mu} = \log\left(\mu_{ij}\right) \qquad \eta_{ij,\sigma} = \log\left(\sigma_{ij}\right).$$

Dropping the parameter index, a generic structured additive predictor is of the form

$$\eta_{ij} = z_{ij}'\gamma + \sum_{p=1}^{P} f_p(x_{ijp}) + \alpha_i.$$

Here, z_{ij} is a vector containing binary, categorical or continuous linearly related variables and $f_1, \ldots, f_P$ are smooth functions of continuous variables $x_{ij1}, \ldots, x_{ijP}$ modelled by Bayesian P(enalized) splines (Lang and Brezger, 2004). The basic assumption is that the unknown functions f_p can be approximated by a linear combination of B-spline basis functions (Eilers and Marx, 1996). Hence, f_p can in matrix notation be written as $Z_p\beta_p$, where Z_p is the design matrix with B-spline basis functions evaluated at the observations and β_p is the vector of regression coefficients to be estimated. To enforce smoothness of the function estimates we use second order random walk priors for the regression coefficients such that

$$p(\beta_p|\tau_p^2) \propto \left(\tau_p^2\right)^{-0.5\text{rank}(K)} \exp\left(-\frac{1}{\tau_p^2}\beta_p' K \beta_p\right)$$

where $K = D'D$ for a second order difference matrix D and τ_p^2 are the smoothing variances with inverse gamma hyperpriors.

The additional, boat-specific effect α_i is introduced to represent any effect specific to the catching unit that is not represented in the covariate effects of $z_{ij}, x_{ij1}, \ldots, x_{ijP}$. A standard assumption for this effect would be α_i i.i.d. $N(0, \tau^2)$, to acknowledge the fact that the catching units represent a sample from the population of catching units. Alternatively, α_i can be treated as a fixed effect resulting from dummy coding of the different catching units. There has been considerable debate in the past (Bishop et al., 2004; Cooper et al., 2004; Helser et al., 2004; Venables and Dichmont, 2004) about whether it is more appropriate to specify α_i as random or fixed effects from a methodological perspective, but then random effects have been rarely considered (e.g. Marchal et al., 2007). One differentiation goes along the lines discussed above, i.e. differentiating between situations where the catching units in the data set define a (random) subsample of the population of the catching unit (which would favour the specification as random effects) and situations where (almost) the complete fleet has been observed (which would favour the specification as fixed effects). From the Bayesian perspective, this differentiation provides an incomplete picture since the differentiation between random and fixed parameters only corresponds to a difference in prior specifications. From a practical point of view the random effects assumption can also be seen as a possibility to regularise estimation in case of large numbers of catching units and/or

small individual time series where estimation of fixed effects may easily become unstable. Note also that in case of a fixed effects specification, no other time-constant covariates z_i characterising the catching units can be included since they can not be separated from the fixed effects. In our data set, this applies for the gross register tonnage which may be expected to provide important information on LPUE but which can not be included in a fixed effects analysis. This problem can be avoided for example by clustering catching units but with a probable loss of information (as the solution used in Mamouridis et al., 2014). In the next section, we compare the performance of random and fixed effects specifications based on model fit criteria to decide which model has a better explanatory ability.

Our inferences is based on efficient Markov chain Monte Carlo (MCMC) simulation techniques (for more details on distributional regression see (Klein et al., 2013b)). In principle, the approach in all models could also be performed in a frequentist setting (Stasinopoulos and Rigby, 2007) via direct optimization of the resulting penalized likelihood which is often achieved by Newton-type iterations with numerical differentiation. However, many models turned out to be numerically unstable leading to no estimation results or warnings concerning convergence. Therefore the study is restricted to the Bayesian analysis. The Bayesian approach with MCMC also reveals several additional advantages, e.g. simultaneous selection of the smoothing parameters due to the modularity of the algorithm, credibility intervals which are directly obtained as quantiles from the samples and the possibility to extend the model for instances with spatial variations. All models have been estimated in the free open source software BayesX (Belitz et al., 2012).

The performance of models is compared in terms of the Deviance Information Criterion, DIC (Spiegelhalter et al., 2002). The DIC is similar to the frequentist Akaike Information Criterion, compromising between the fit to the data and the complexity of the model. Furthermore it can easily be computed from a sample $\theta^1, \ldots, \theta^M$ of the posterior distribution $p(y|\theta)$,

$$\text{DIC} = 2\overline{D(\theta)} - D(\overline{\theta}),$$

with deviance $D(\theta) = -2\log\left(p(y|\theta)\right)$ and $\overline{D(\theta)} = \frac{1}{M}\sum_{m=1}^{M} D(\theta^m)$, $\overline{\theta} = \frac{1}{M}\sum_{m=1}^{M}\theta^m$ respectively. We also use the DIC to determine important variables and optimal predictors $\eta_{i,\mu}$ and η_{i,σ^2} or $\eta_{i,\sigma}$.

To validate the distribution assumption we used normalized quantile residuals. That allowed to decide between equivalent models under different response assumptions. Normalized quantile residuals are defined as $r_i = \Phi^{-1}(u_i)$. Here, Φ^{-1} is the inverse cumulative distribution function of a standard normal distribution and u_i is the cumulative distribution function of the estimated model and with plugged in estimated parameters. For consistent estimates, the residuals r_i, $i = 1, \ldots, n$ follow approximately a standard normal distribution if the estimated distribution is the true distribution. Therefore, models can be compared graphically in terms of quantile-quantile-plots.

Finally, to assess the predictive accuracy of the models we performed a k-fold Cross Validation using the mean squared error of prediction (MSEP)

$$\text{MSEP}_k = \frac{\sum_{i=1}^{N}\left[lpue_{i,k} - \hat{E}(lpue_{i,k})\right]^2}{N}.$$

Here $lpue_{i,k}$ is the observation i of subset k, $\hat{E}(lpue_{i,k})$ is the expectation of the prediction in the validation set, given parameters estimated on the k-th training set and N refers to the number of observations of the corresponding test set. We performed a 10 fold stratified (within each catching unit) random partition of the whole dataset to ensure a minimum number of observations for each boat in both the training and the validation sets. Taking the 10% of the data to built the latter, we ensure at least 10 observations per unit in the validation set. If at least one catching unit is not represented in one of the partitions, the prediction for the missing catching unit in fixed effects models could not be computed. This clarifies the usefulness in using mixed effects specification when interested on predictions for unobserved catching units.

4 Data analysis

4.1 Model diagnostics and comparison

During model building variables were selected using a stepwise forward procedure according to the DIC scores and the significance of their effect. Single models have been built first for each variable, to assess its explanatory potential. For each distribution the predictor for location has been modelled, adding one variable at a time till finding the best predictor. Then, using this "best" predictor for location, also the predictor for the second parameter, the scale or shape for log-normal or gamma respectively, has been modelled using the same procedure.

For both distributions, all models with single explanatory variable returned significant effects, except some categories of *code* and *month*. So that, we decide to model *month* effect as binary (*period*), after grouping categories (see Methodology Section and Mamouridis et al. (2014)). Conversely, *code* variable has not been merged, to allow the comparison between fixed and mixed effects models.

Assuming log-normal distribution and according to the ascending DIC, variables are ordered from *code* (DIC=17059.4 as random and DIC=17060.0 as fixed effect), then *trips*, *time*, *grt*, nao_3, to *period* (DIC=17735.7). The same ordination has been found assuming the gamma distribution with DIC scores ranged between DIC=16763.0 for *code* and DIC=17290.0 for *period*. Variables have been added in this order till the saturated model. Variables nao_3 and *grt* do not strongly improve model in terms of DIC scores (less then 20 units for each variable). However parameters are significantly different from zero and their incorporation effective to be discussed. We used the same procedure for the second predictor. According to the DIC, variables are ordered as follows: *code*, *trips*, *time*, *grt*, nao_3 and *period*. The effects of variables nao_3 *period* and *grt* for the second parameter were not significant.

According to the DIC scores, for log-normal assumption, the appropriate predictor structures for location η_μ and scale η_{σ^2}, are

$$\begin{aligned} \eta_\mu &= \beta_{0,\mu} + \beta_{1,\mu} period_2 + f_{1,\mu}(trips) + f_{2,\mu}(time) + f_{3,\mu}(nao_3) + \sum_i \alpha_{i,\mu} \\ \eta_{\sigma^2} &= \beta_{0,\sigma^2} + f_{1,\sigma^2}(trips) + f_{2,\sigma^2}(time) + \sum_i \alpha_{i,\sigma^2} \end{aligned} \tag{2}$$

for both fixed and mixed effects specification. Here the β_{k_j} are parameters associated to the intercept and linear fixed effects of the variable *period*. The α_{i_j} are parameters associated to the effects of *code*, specified as fixed in fixed effects models and as random in mixed effects models. Instead, f_{l_j} are smooth functions associated to nonlinear effects of the variables *trips*, *time* and nao_3. The second sub-index in all parameters, μ or σ^2, identifies which predictor the parameter or function belongs, η_μ or η_{σ^2} respectively.

Using fixed effects specification for *code* the inclusion of variable *grt* leads to instability, due to the reasons mentioned in Section 3, so then, the model with *grt* cannot be estimated in these cases. On the contrary, in mixed effects specification *grt* could be estimated but it leads to equal or lightly higher values of DIC score. Thus it has been backward eliminated, however the associated parameter was significantly different from zero and positive.

Under the gamma distribution assumption, the log-link function has been chosen, since the support of both parameters is the positive real domain and the final predictor structures for location and shape are

$$\begin{aligned} \eta_\mu &= \beta_{0,\mu} + \beta_{1,\mu} period_2 + f_{1,\mu}(trips) + f_{2,\mu}(time) + f_{3,\mu}(nao_3) + \sum_i \alpha_{i,\mu} \\ \eta_\sigma &= \beta_{0,\sigma} + f_{1,\sigma}(trips) + f_{2,\sigma}(time) + \sum_i \alpha_{i,\sigma} \end{aligned} \tag{3}$$

for both fixed and mixed effects specification. The notation here is the same specified for the log-normal models however here the second parameter, the shape, is denoted σ.

Table 2: Global scores of selected models. Columns indicate: M, refers to model coding (see specifications in the text); DEV, the residual deviance; EP: Effective total number of Parameters, DIC: Deviance Information Criterion, MSEP, mean and sd of the mean square error of predictions calculated through 10-fold validation.

M	DEV	EP	DIC	MSEP
M1	16163.9	47.1	16258.0	98.3 ± 12.3
M2	16164.2	46.8	16257.7	96.9 ± 12.4
M3	15138.4	91.2	15320.8	436.2 ± 434.9
M4	15142.7	87.2	15317.2	315.0 ± 307.4
M5	16095.7	45.6	16187.0	77.8 ± 11.5
M6	16096.8	43.9	16184.7	77.3 ± 11.7
M7	15027.1	90.9	15208.9	71.5 ± 9.2
M8	15032.4	86.9	15206.1	71.7 ± 9.4

The Table 2 provides a selection of models that we used for comparison purposes and their corresponding global parameters: the deviance, the effective number of parameters and the DIC, estimated on the whole dataset, and the MSEP calculated by predictions on the validation subsets as described in the methodology.

The eight models in table 2 present a combination between alternatives of the following assumptions:

(A) The log-normal (LN) or gamma (GA) as the underlying distribution assumption;

(B) Only location (LO) or both location and scale/shape (LS) parameters explicitly modelled using one or more explanatory variables;

(C) Effects of *code* as fixed or random leading to a fixed effects model (FI) or mixed effects model (MI) respectively;

So, model M1 is specified by A=LN, B=LO and C=FI; M2 by A=LN, B=LO and C=MI; M3 by A=LN, B=LS and C=FI; M4 by A=LN, B=LS and C=MI; M5 by A=GA, B=LO and C=FI; M6 by A=GA, B=LO and C=MI; M7 by A=GA, B=LS and C=FI; and M8 by A=GA, B=LS and C=MI. The predictors for location in models denoted as M1, M2, M5 and M6 (with B=LO) have the same structure of $\eta_{\mu_{ijk}}$ in Equations 2 and 3, while the corresponding predictor for scale/shape is simply the constant. Both predictors in models M3, M4, M7 and M8 correspond to Equations 2 and 3.

Concerning to (A), model specifications widely favour the gamma over the log-normal distribution. In fact DIC scores are lower under the gamma assumption, with approximately 100 scores of difference between analogous models (i.e. same variables specified in the predictors). The benefit in assuming the gamma distribution is also evident comparing MSEP scores (lower scores for better predictions). Nevertheless, results of log-normal models' MSEP is not entirely satisfactory, because when accounting for both predictors MSEP should behave as in the gamma models, i.e. lower scores than accounting only for the predictor η_μ. Regarding to the estimation of both predictors for first and second parameters (B), models under the gamma assumption show an improvement when explicitly modelling the dependence of second parameter σ from explanatory variables in both DIC and MSEP scores (both decrease). Contrariwise, under the log-normal assumption, however the DIC decreases, the MSEP increases and presents higher variance, suggesting worse predictions, when the second parameter is explicitly modelled. But as discussed few lines above, that is not realistic and follows a strange behaviour of η_{σ^2}, thus, we still working on this point. Finally no notable leaps have been observed between fixed and random effects models (C). Whereby the best DIC and MSEP scores and QQplots lead to the final model with predictors given in (3).

According to the DIC (Table 2) the model that better fits the data is the gamma model M8 whose predictors are given in Equation 3 specifying catching units as random effects.

The boxplots of MSEPs also favour the gamma assumption (see Figure 1 and values in Table 2). The minor MSEP better the prediction, MSEP results divide models into three distinguishable groups from highest to lowest mean MSEP: 1) log-normal models considering heteroscedasticity, 2) log-normal models considering constant variance (compare M1-M2 with M3-M4), and 3) all gamma models (compare M1-M4 with M5-M8). Within this group, modelling the shape in dependence to some variables, consistently decreases MSEP estimates, in terms of average and variance (compare M5-M6 with M7-M8).

In order to validate the distribution assumptions, QQplots for residuals are reported in Figure 2, from which it follows that:

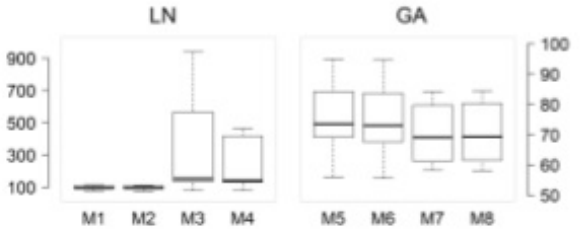

Figure 1: Boxplots for MSEP calculated for all models. See Table 2 and Equations in the text for model specifications.

- the residuals in gamma models almost follow the straight line (M5-M8 in the Figure), while in the log-normal they show upward-humped curves (M1-M4), suggesting a definitively "better approximation" of models to the gamma distribution.
- Modelling the second parameter in gamma models improves QQplot outputs, while the opposite happens for log-normal models. Focusing only in gamma models, the outlier is "absorbed" into the straight line in the right part validating the improvement in estimations (compare M5-M6 and M7-M8 in Figure 2).

We finally assess the normality for random effects for the model M8 corresponding to Equation 3. Figure 4.1 provides the QQplots of the random effects for both predictors. The majority of sample quantiles approximatively follow the normal quantiles, however they depart from it at the extremes, especially evident in the lower tails and for α_{pc} (on the left).

4.2 Description of partial effects

Estimations of linear fixed effects for A) μ and B) σ predictors of final model (3), to which we referred in the text as M8, are reported in table 3.

Table 3: Estimations of linear fixed effects for the final model, Eq. (3) associated to A) μ and B) σ respectively.

A)			B)	
	mean	sd	mean	sd
const	2.891	0.058	-1.551	0.099
$period_2$	-0.153	0.024		

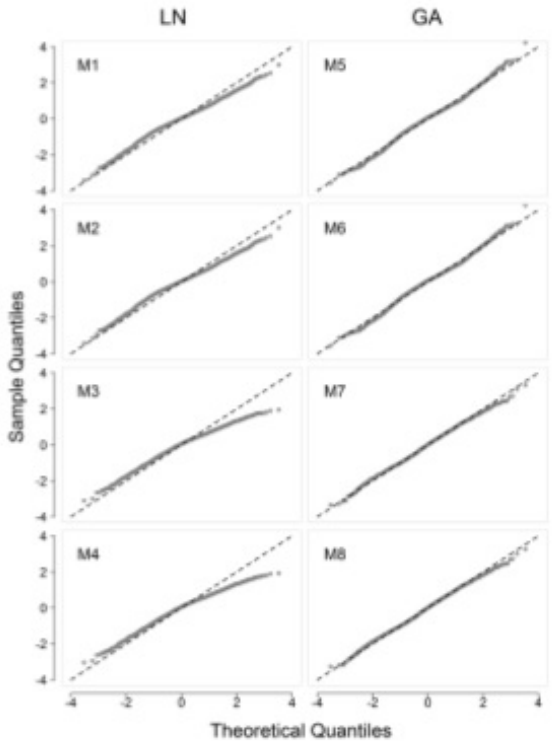

Figure 2: QQplots of residuals for selected log-normal and gamma models.

The categorical variable *period* describes the intra-annual variability and shows a negative effect during $period_2$, corresponding to June and November in comparison to the rest of the year. That should be related to a lower demand of this source during these months, as suggested by Sardà et al. (1997).

The variable *grt*, referring to the gross registered tonnage of boats, (not incorporated into the model because did not improve the DIC score) bears a significantly positive slope parameter (0.009 ± 0.003 when included), causes a linear increment on the predictor for location. We consider important to quantify its effect in order to compare

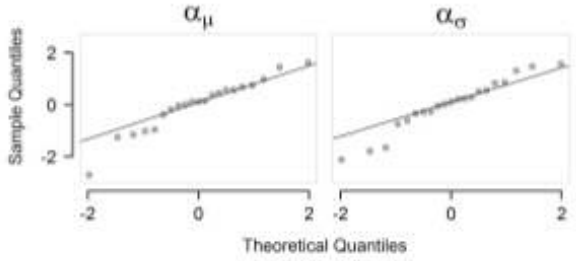

Figure 3: QQplots for normality of catching units as random effects in the mixed model M8. α_μ refer to random effects in the predictor for location, while α_σ refers to the predictor for the shape.

it with other fisheries, where, contrariwise, it could have a major effect. *grt* is not the only variable characterising a fleet, nevertheless is the only reliable for this fishery.

The second variable we can consider as fishery-related variable is represented by the catching units. Variable *code* captures all abilities of fishermen and technical characteristics of the fleet, appropriate technologies and strategies, e.g. the power and type of the engine, the net shape and the skipper's expertise and ability. Results (Figure ??) show that many trawlers have similar effects, while few of them hold or positive either negative effects. The former are very specialised and powerful boats that capture large amounts of the resource so then that leads to higher values of LPUE while the latter are not specialised trawlers that accordingly capture lower amounts, leading to lower LPUE (see the partial effects on μ). At the same time catching units associated to higher effects on the predictor of μ also present higher effects on the predictor for σ, while boats associated to lower effects on μ also hold lower effects on σ. In other words, more specialised catching units are able to capture more quantities of the recourse, and they also present less variability. Contrariwise landings of not specialised trawlers present more variability. This fraction of the fleet more likely is represented by boats that fish usually on the continental shelf and occasionally displace towards deeper waters going in search of the red shrimp, representing one of the most lucrative resources for the NW Mediterranean fisheries. It is likely to think that these boats have less knowledge of red shrimp fishing grounds (Maynou et al., 2003) and catch less.

Concerning to nonparametric effects (Figure 4.2), *trips* and *time* influence both η_μ and η_σ, while *nacr*$_3$ slightly affects only η_μ.

trips shows a negative effect on the predictor for μ when $trips \leq 8$, while positive otherwise. The rate of the effect decreases moving through the covariate interval till rising a plateau beginning around $trips = 17$. For extreme high values this covariate has

an uncertain effect. It is plausible that increasing the number of trips per month, more likely increase the ability to find high-concentration shoals inside the fishing grounds in a process of trial and error (as suggested by Sardà and Maynou 1998).

The effect of *time* on the predictor for μ is the most difficult to interpret, showing high inter-annual variability, certainly caused from unobservable multiple factors. Between 1992-1996, the function decreases while increases in next three years. We could not find a reasonable explanation to this trend. Afterwards, between 1999-2000, it drops till a minimum low followed by a rapid increase up to a pick in 2004. We believe that the minimum is related to both negative NAO observed in previous years and to the rising of fuel price started in 2000, that in turn is related to a lower number of trips performed by trawlers (see comments below and the discussion in Mamouridis et al., 2014). Then, for five years it presents a slightly oscillatory trend till the last year characterized by another positive pick probably related to the rise of the economic value of the resource, that offsets the increase in the fuel price.

Finally, the nao_3 has a moderate effect?? for this deep-sea species, being notoriously evident only when reaches anomalous values. Numerous studies on this and other fish stocks (e.g. Maynou, 2008; Báez et al., 2011) demonstrated that the NAO can have important effects when it reaches extreme values??, whether they are positive or negative. Our results show that nao_3 has a moderate effect?? for this deep-sea species, however they suggest that it can lead to the reduction of its biomass when reaches very negative values. Combining results of *time* and nao_3 effects and comparing data series

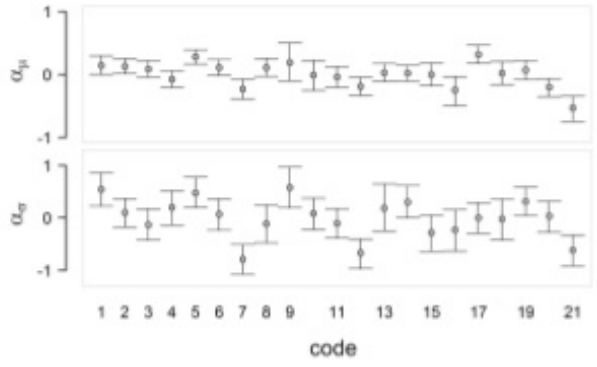

Figure 4: Interval plots of estimated random effects in the predictor for location (α_μ) and shape (α_σ) of model M8 on the upper and lower plots respectively. Bars indicates 95% CI.

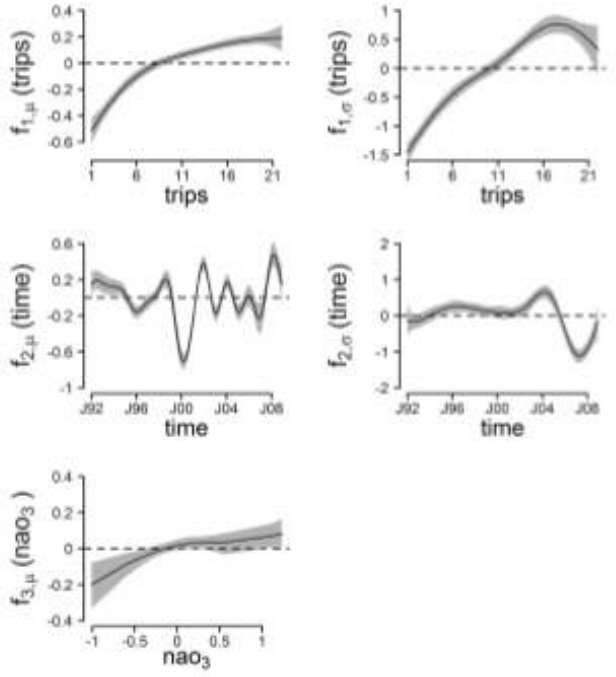

Figure 5: Nonparametric effects for the GA mixed effect of the selected gamma model (M8). Effects on predictor for μ (left side) and for σ (right side). Grey shapes represent 95% credible intervals.

of both the raw (or nominal) LPUE and the NAO, we believe that the LPUE low starting at the end of 1999 can be related to consecutive negative NAO during the previous four years, especially during 1996, corresponding to three years before the beginning of the decline of LPUE ??see][]mamouridis2014analisys. NAO leads to paucity of resources when it is low, while enhances productivity when it is high. Between $nao_3 = 0.50$ and $nao_3 = 1$ the effect increases however without significant evidences. In the middle region of the observed variable span, NAO shows any effect, that could represents a "buffering region" related to "normal" weather conditions for the stock.

All partial effects are linked to the expectation, E(LPUE), through the exponential of η_μ, such that, when partial effects of *trips*, *time* and nao_3 hire positive values, E(LPUE) is positive while negative otherwise. Regarding to the variance of LPUE, it is affected by both predictors being directly proportional to μ and inverse proportional to σ.

The effect of *trips* is negative for low values of the covariate ($trips \leq 10$) and positive for higher values. It also shows a high increment till a maximum corresponding to $trips = 17$, while decreasing again for higher values, although always positive. The effect of *time* is slightly negative before 1995 and slightly positive between 1995 and 2000. Then for two years has no effect and, in 2002, it switches clearly positive again till 2006, showing a high pick in 2004 and finally negative in the last years during 2006-2008, reaching an abrupt drop in late 2007.

Thus, regarding to the Var(LPUE), results show that values of covariates associated to positive effects in η_μ and negative effects in η_σ, in turn affect positively (increase) to the variance. We can also deduce that *time* and *trips* are drivers in causing the heteroscedasticity in LPUE, *times* mainly in last years when its effect on η_μ is positive and its effect on η_σ is strongly negative. This high variability could be related to different factors, probably of economic origin, such as the fuel and ex-vessel shrimp prises.

5 Conclusions

In this study distributional structured additive models have been proposed for the first time to model the LPUE, index widely used in fisheries research. Data deal with the LPUE of red shrimp (*A. antennatus*) from the Barcelona's fleet during years 1992 - 2008.

Our aims were: 1) find the best distribution in relation to the response variable, comparing gamma and log-normal distributions, 2) improve estimations modelling both predictors for first and second parameter 3) compare parameter specification for catching units, fixed versus mixed effects models, and finally 4) achieve new insights in the understanding of the effect that the explanatory variables considered have on the LPUE of red shrimp.

On a methodological viewpoint, distributional structured additive models, DSTAR, as the frequentist counterpart GAMLSS, permit the estimation of both first and second order moments of the LPUE, allowing more accurate estimations and the analysis of both the expectation and the variance of the response. Results indicate that explicitly modelling the second moment in dependence to appropriate explanatory variables can lead to better estimations and predictions. We also rose a more detailed understanding of the LPUE, that bears some amount of heteroscedasticity in the time span studied. This heteroscedasticity had been observed but could not be described in previous analysis (Mamouridis et al., 2014). In fact the analysis performed on almost the same data set, a frequentist approach using GAM accounting only for the location, could not avoid the heteroscedasticity in the residuals (see Figure 4 within). Here, the modelling of the shape, in the case of the gamma assumption, permitted to infer about the variance of he

response. Here we demonstrated that both the number of trips and the time influence the second parameter leading to changes in the variance.

Concerning to fixed versus mixed specification, in our study the fixed effects can be considered appropriate representing sampling units the whole population of the studied fleet, however mixed models permit more flexibility, such as the estimation of GRT effect. Consider that mixed models also allow to get prediction for unobserved catching units and in turn to generalise predictions outside the observed fishing population.

Acknowledgements

Authors would like to thank the Fisheries Directorate of Catalonia's Autonomous Government to facilitate access to the sales data of the Barcelona Fishers' Association, as well as fishers of Barcelona. This study was financed by the Spanish National Council of Research (CSIC) through the JAE-predoc grant program. Financial support from the German Research Foundation (DFG) grant KN 922/4-1 is gratefully acknowledged.

References

J.C. Báez, J.M. Ortiz de Urbina, R. Real, and D. Macías. Cumulative effect of the north atlantic oscillation on age-class abundance of albacore (thunnus alalunga). *Journal of Applied Ichthyology*, 27(6):1356–1359, 2011.

S. P. Bannerot and C. B. Austin. Using frequency distributions of catch per unit effort to measure fish-stock abundance. *Transactions of the American Fisheries Society*, 112:608–617, 1983.

C. Bas, F. Maynou, F. Sardà, and J. Lleonart. *Variacions demogràfiques a les poblacions d'espes demersals explotades: els darrers quaranta anys a Blanes i Barcelona*. Inst. Est. Catalans. Arxiu de la Sec. Cies, Barcelona, 2003.

C. Belitz, A. Brezger, T. Kneib, S. Lang, and N. Umlauf. Bayesx, 2012. - software for bayesian inference in structured additive regression models. version 2.1. available from http://www.bayesx.org. 2012.

J. Bishop, W.N. Venables, and Y.-G. Wang. Analysing commercial catch and effort data from a penaeid trawl fishery: A comparison of linear models, mixed models, and generalised estimating equations approaches. *Fisheries Research*, 70(23):179 – 193, 2004. ISSN 0165-7836. doi: http://dx.doi.org/10.1016/j.fishres.2004.08.003. URL http://www.sciencedirect.com/science/article/pii/S0165783604001651. <ce:title>Models in Fisheries Research: GLMs, {GAMS} and GLMMs</ce:title>.

A. Brezger and S. Lang. Generalized structured additive regression based on bayesian p-splines. *Computational Statistics & Data Analysis*, 50(4):967 – 991, 2006.

J. Brynjarsdóttir and G. Stefánsson. Analysis of cod catch data from icelandic groundfish surveys using generalized linear models. *Fisheries Research*, 70(23):195 – 208, 2004. ISSN 0165-7836. doi: http://dx.doi.org/10.1016/j.fishres.2004.08.004. URL http://www.sciencedirect.com/science/article/pii/S0165783604001663.

A. Carbonell, M. Carbonell, M. Demestre, A. Grau, and S. Monserrat. The red shrimp *Aristeus antennatus* (risso, 1816) fishery and biology in the balearic islands, western mediterranean. *Fisheries Research*, 44(1):1–13, 1999.

A. B. Cooper, A. Rosenberg, G. Stefansson, and M. Mangel. Examining the importance of consistency in multi-vessel trawl survey design based on the U.S. west coast groundfish bottom trawl survey. *Fisheries Research*, 70(2-3):239–250, December 2004. ISSN 01657836. doi: 10.1016/j.fishres.2004.08.006. URL http://linkinghub.elsevier.com/retrieve/pii/S0165783604001699.

D. Damalas, P. Megalofonou, and M. Apostolopoulou. Environmental, spatial, temporal and operational effects on swordfish (*Xiphias gladius*) catch rates of eastern Mediterranean Sea longline fisheries. *Fisheries Research*, 84(2):233–246, April 2007. ISSN 01657836. doi: 10.1016/j.fishres.2006.11.001. URL http://linkinghub.elsevier.com/retrieve/pii/S0165783606003845.

V. Denis. Spatio-temporal analysis of commercial trawler data using General Additive models: patterns of Loliginid squid abundance in the north-east Atlantic. *ICES Journal of Marine Science*, 59(3):633–648, June 2002. ISSN 10543139. doi: 10.1006/jmsc.2001.1178. URL http://icesjms.oxfordjournals.org/cgi/doi/10.1006/jmsc.2001.1178.

P. H. C. Eilers and B. D. Marx. Flexible smoothing with *b*-splines and penalties. *Statistical Science*, 11(2):89–102, 1996.

L. Fahrmeir, T. Kneib, and S. Lang. Penalized structured additive regression for space-time data: a bayesian perspective. *Statistica Sinica*, 14(3):731–762, 2004.

FAO/FISHSTAT. Fao fisheries department, fishery information, data and statistics unit. fishstatj, a tool fot fishery statistical analysis, release 2.0.0, 2011.

S. Gavaris. Use of a multiplicative model to estimate catch rate and effort from commercial data. *Canadian Journal of Fisheries and Aquatic Sciences*, 37(12):2272–2275, 1980. doi: 10.1139/f80-273. URL http://www.nrcresearchpress.com/doi/abs/10.1139/f80-273.

R. Gotti, F. Alvarez, and S. Adlerstein. Application of generalized linear modeling to catch rate analysis of western mediterranean fisheries: the castellon trawl fleet as a case study. *Fisheries Research*, 42(3):291 – 302, 1999. ISSN 0165-7836. doi: http://dx.doi.org/10.1016/S0165-7836(99)00039-9. URL http://www.sciencedirect.com/science/article/pii/S0165783699000399.

J. A. Gulland. Catch per unit effort as a measure of abundance. *Rapp. P.-V. Reun., Comm. Int. Explor. Mer Mediter*, 155:8 – 14, 1964.

T. Hastie and R. Tibshirani. Generalized additive models. *Statistical science*, pages 297–310, 1986.

G. Heller, Stasinopoulos D. M., and Rigby R. A. The zero-adjusted inverse Gaussian distribution as a model for insurance data. In J.Newell J. Hinde, J.Einbeck, editor, *Proceedings of the 21th International Workshop on Statistical Modelling*, 2006.

T. E. Helser, A. E. Punt, and R. D. Methot. A generalized linear mixed model analysis of a multi-vessel fishery resource survey. *Fisheries Research*, 70(23):251 – 264, 2004. ISSN 0165-7836. doi: http://dx.doi.org/10.1016/j.fishres.2004.08.007. URL http://www.sciencedirect.com/science/article/pii/S0165783604001705.

E. E. Kammann and M. P. Wand. Geoadditive models. *Journal of the Royal Statistical Society: Series C (Applied Statistics)*, 52(1):1–18, 2003.

N. Klein, M. Denuit, T. Kneib, and S. Lang. Nonlife ratemaking and risk management with bayesian additive model for location scale and shape. Technical report, 2013a. URL http://eeecon.uibk.ac.at/wopec2/repec/inn/wpaper/2013-24.pdf.

N. Klein, T. Kneib, and S. Lang. Bayesian structured additive distributional regression. Technical report, 2013b. URL http://eeecon.uibk.ac.at/wopec2/repec/inn/wpaper/2013-23.pdf.

S. Lang and A. Brezger. Bayesian p-splines. *Journal of Computational and Graphical Statistics*, 13(1):183–212, 2004.

X. Lin and D. Zhang. Inference in generalized additive mixed modelsby using smoothing splines. *Journal of the Royal Statistical Society: Series B (Statistical Methodology)*, 61(2):381–400, 1999. ISSN 1467-9868. doi: 10.1111/1467-9868.00183. URL http://dx.doi.org/10.1111/1467-9868.00183.

V. Mamouridis, F. Maynou, and G. Aneiros Pérez. Analysis and standardization of landings per unit effort of red shrimp *Aristeus antennatus* from the trawl fleet of barcelona (nw mediterranean). *Scientia Marina*, 78:INSERT, 2014. doi: 10.3989/scimar.03926.14A.

P. Marchal, C. Ulrich, K. Korsbrekke, M. Pastoors, and B. Rackham. A comparison of three indices of fishing power on some demersal fisheries of the north sea. *ICES Journal of Marine Science: Journal du Conseil*, 59(3):604–623, 2002. doi: 10.1006/jmsc.2002.1215. URL http://icesjms.oxfordjournals.org/content/59/3/604.abstract.

P. Marchal, Bo A., B. Caillart, O. Elgaard, O. Guyader, H. Hovgaard, A. Iriondo, F. Le Fur, J. Sacchi, and M. Santurtún. Impact of technological creep on fishing effort and fishing mortality, for a selection of european fleets. *ICES Journal of Marine Science: Journal du Conseil*, 64(1):192–209, 2007.

M. N. Maunder, J. R. Sibert, A. Fonteneau, J. Hampton, P. Kleiber, and S. J. Harley. Interpreting catch per unit effort data to assess the status of individual stocks and communities. *ICES Journal of Marine Science: Journal du Conseil*, 63(8):1373–1385, 2006. doi: 10.1016/j.icesjms.2006.05.008. URL http://icesjms.oxfordjournals.org/content/63/8/1373.abstract.

F. Maynou. Environmental causes of the fluctuations of red shrimp (Aristeus antennatus) landings in the Catalan Sea. *Journal of Marine Systems*, 71(3-4):294–302, June 2008. ISSN 09247963. doi: 10.1016/j.jmarsys.2006.09.008. URL http://linkinghub.elsevier.com/retrieve/pii/S0924796307001935.

F. Maynou, M. Demestre, and P. Sanchez. Analysis of catch per unit effort by multivariate analysis and generalised linear models for deep-water crustacean fisheries off barcelona (nw mediterranean). *Fisheries Research*, 65(1-3):257–269, December 2003. ISSN 01657836. doi: 10.1016/j.fishres.2003.09.018. URL http://linkinghub.elsevier.com/retrieve/pii/S0165783603002479.

P. McCullagh and J.A. Nelder. *Generalized Linear Models*. Chapman & Hall, London, 1989.

R. Mendelssohn and P. Cury. Temporal and spatial dynamics of a coastal pelagic species, sardinella maderensis off the ivory coast. *Canadian Journal of Fisheries and Aquatic Sciences*, 46(10):1686–1697, 1989. doi: 10.1139/f89-214. URL http://www.nrcresearchpress.com/doi/abs/10.1139/f89-214.

R. A. Myers and P. Pepin. The robustness of lognormal-based estimators of abundance. *Biometrics*, pages 1185–1192, 1990.

M. Pennington. Efficient estimators of abundance, for fish and plankton surveys. *Biometrics*, 39(1):281–286, 1983.

J. C. Pinheiro and D. M. Bates. *Mixed.Effects Models in S and S-PLUS*. 2000.

R. A. Rigby and D. M. Stasinopoulos. Generalized additive models for location, scale and shape. *Journal of the Royal Statistical Society: Series C (Applied Statistics)*, 54(3):507–554, 2005. ISSN 1467-9876. doi: 10.1111/j.1467-9876.2005.00510.x. URL http://dx.doi.org/10.1111/j.1467-9876.2005.00510.x.

D. Ruppert, M. P. Wand, and Ra. J. Carroll. *Semiparametric regression Vol. 12*. Cambridge University Press, 2003.

F. Sardà and F. Maynou. Assessing perceptions: do catalan fishermen catch more shrimp on fridays? *Fisheries Research*, 36:149157, 1998.

F. Sardà, F. Maynou, and L. Talló. Seasonal and spatial mobility patterns of rose shrimps *Aristeus antennatus* in the western mediterranean: results of a long-term study. *Marine Ecology Progress Series*, 159:133141, 1997.

D. J. Spiegelhalter, N. G. Best, B. P. Carlin, and A. van der Linde. Bayesian measures of model complexity and fit. *Journal of the Royal Statistical Society. Series B (Statistical Methodology)*, 64(4):583–639, 2002.

D. M. Stasinopoulos and R. A. Rigby. Generalized additive models for location scale and shape (gamlss) in r. *Journal of Statistical Software*, 23(7):1–46, 2007.

G. Stefánsson. Analysis of groundfish survey abundance data: combining the glm and delta approaches. *ICES Journal of Marine Science: Journal du Conseil*, 53(3):577–588, 1996. doi: 10.1006/jmsc.1996.0079. URL http://icesjms.oxfordjournals.org/content/53/3/577.abstract.

G. Stefánsson and O. K. Palsson. Points of view: A framework for multispecies modelling of arcto-boreal systems. *Reviews in Fish Biology and Fisheries*, 8:101–104, 1998.

S. Tudela, F. Maynou, and M. Demestre. Influence of submarine canyons on the distribution of the deep-water shrimp, aristeus antennatus (risso, 1816) in the nw mediterranean. *Crustaceana*, 7(2):217225, 1998.

W. N. Venables and C. M. Dichmont. Glms, gams and glmms: an overview of theory for applications in fisheries research. *Fisheries research*, 70(2):319–337, 2004.

S. Wood. *Generalized Additive Models: an introduction with R*. CRC Press, 2006.

Deep-Sea Research I 76 (2013) 52–65

Contents lists available at SciVerse ScienceDirect

Deep-Sea Research I

journal homepage: www.elsevier.com/locate/dsri

Geomorphological, trophic and human influences on the bamboo coral *Isidella elongata* assemblages in the deep Mediterranean: To what extent does Isidella form habitat for fish and invertebrates?

J.E. Cartes [a,*], C. Lolacono [a,c], V. Mamouridis [a], C. López-Pérez [a], P. Rodríguez [b]

[a] Institut de Ciències del Mar, C.I.S.C., Passeig Marítim de La Barceloneta, 37–49, 08003 Barcelona, Spain
[b] Unitat de Tecnologia Marina, C.I.S.C., Passeig Marítim de La Barceloneta, 37–49, 08003 Barcelona, Spain
[c] National Oceanographic Centre (NOC), European Way, Southampton SO14 3ZH, United Kingdom

ARTICLE INFO

Article history:
Received 17 August 2012
Received in revised form
11 January 2013
Accepted 20 January 2013
Available online 9 February 2013

Keywords:
Bamboo coral
Isidella elongata
Deep Mediterranean
Canyons
Forming habitat
Fish
Invertebrates
Trophic relationships
Stable isotopy

ABSTRACT

We analyzed what are the best ecological conditions for megafauna associated with the bamboo coral *Isidella elongata* based on the geomorphological, physical and trophic information taken in 3 stations (St1, St2, St3) off the southern Catalonian coasts at 620 m depth in June 2011. Results were compared with assemblage compositions recorded in past cruises (May 1992, 1994) at the same 3 stations. St1 was in a fishing ground exploited since the 1940s over a relatively wide slope at ca. 22 km from the nearest canyon head; St2 and St3 were on a narrower slope closer to canyon heads and to the Ebro river mouth than St1. *I. elongata* had formed (to May 1994, at least) a dense coral *forest* at St2–St3 (to ca. 255 colonies/ha at St3), and some isolated colonies (to ca. 0.9 colonies/ha) were still collected in 2011. Fish and invertebrate communities significantly differed between St1 and St2/St3, with two macrourid fishes (*Trachyrhynchus trachyrhynchus* and *Nezumia aequalis*) and two decapods (*Plesionika martia* and *Plesionika acanthonotus*) more abundant at St2/St3. The following ecological indicators imply better food conditions for megafauna at St2–St3 and for *I. elongata* itself: (i) greater density of zooplankton (copepods, euphausiids, and others) as potential prey for planktivores (including *I. elongata*); (ii) greater biomass and mean weight of epifaunal and infaunal deposit feeders; (iii) higher feeding intensity, *F*, at St3 for benthos feeders (*Phycis blennoides*, *N. aequalis* and *Aristeus antennatus*). Also, at St2–St3 we found higher near-bottom turbidity (indicating particle resuspension: food for suspension feeders) and finer and more reduced (E_h) sediments. The results let us suggest that corals and accompanying fauna preferently found optimal ecological conditions in the same habitat, while habitat-forming capacity by *I. elongata* seemed weak to generate these conditions. Coral *forests* may enhance detritus accumulations around them, improving habitat conditions for benthos feeders (e.g. macrourid fish). At St3 our side-scan sonar recorded three types of tracks produced by trawler doors, which match with three identified vessels occasionally operating in the area. After this low fishing activity off the Ebro Delta since the mid-1990s, almost all colonies of *I. elongata* has been removed. However, this impact has hardly altered fish and invertebrate composition without any significant loss of diversity, pointing also toward a rather low capacity of *I. elongata* facies in forming habitat for megafauna on muddy bottoms of the Mediterranean slope.

1. Introduction

One of the most important factors generating heterogeneity in the seafloor landscape over muddy bottoms of continental margins is the occurrence of fields (or meadows) of sessile colonial organisms such as cnidarians, Hexactinellid sponges and deep-water gorgonian corals. Within a relatively homogeneous environment such as the deep sea, gorgonian fields are important because they may increase habitat complexity, enhance marine community diversity at meso-spatial scales and increase ecological niche dimensions (Gage and Tyler, 1991).

Bamboo corals (Fam. Isididae) are gorgoniaceans distributed worldwide in deep waters (mainly between 200 and 1500 m depth, but also to abyssal depths, Etnoyer and Morgan, 2005; Maynou and Cartes, 2012) with 138 known species. Most species form single-species fields on soft-bottom sediments. As colonial corals have a ramified tree form, the association of colonies more or less spaced over the seafloor is known under different names deriving from terrestrial landscapes (*meadows*, *fields*, even *forests*: e.g. Krieger and Wing, 2002, Etnoyer and Morgan, 2005).

* Corresponding author. Tel.: +34 93 230 95 00; fax: +34 93 230 95 55.
E-mail address: jcartes@icm.csic.es (J.E. Cartes).

0967-0637/$ – see front matter © 2013 Elsevier Ltd. All rights reserved.
http://dx.doi.org/10.1016/j.dsr.2013.01.006

Some species have colonies reaching to 3 m height (Krieger and Wind, 2002) that are long lived (Andrews et al., 2002). Ages based on ^{14}C data suggest longevities for isidids from the Gulf of Alaska of 75–126 years (Roark et al., 2005) and radial growth rates of ~110 μm/yr for *Isidella* sp. off Tasmania. Ages and growth rates vary widely among genera, even those inhabiting the same depth and area (Sherwood et al., 2009). In comparison to deep-water corals in the subclasses Hexacorallia, gorgoniaceans are poorly known, especially in their ability to form essential habitat for other organisms (Fossa et al., 2002; Krieger and Wind, 2002; Etnoyer and Morgan, 2005; Metaxas and Davis, 2005), their influence on trophic relationships and their role as refuge areas for large fauna (fish, decapod crustaceans: Krieger and Wing, 2002). Indications of higher abundance and larger size of some commercial fish in *Lophelia pertusa* reefs compared with surrounding areas may be related with higher food availability in the reefs (Husebø et al., 2002), and this possible role for *Isidella elongata* in the western Mediterranean has been discussed recently (Maynou and Cartes, 2012; Cartes et al., 2009a).

Little has been published about communities associated with *I. elongata* facies since the basic distribution, depth and slope preferences of this soft coral were established (Dieuzeide, 1960; Pérès, 1985). One of the few exceptions is the recent compilation by Maynou and Cartes (2012) of all information originated by trawl surveys in the Balearic Basin in the last three decades. *Isidella elongata* (with colonies to 70 cm height) is almost exclusively restricted to the Mediterranean Sea, but extending by transport of larvae in the westward outflow to the adjacent Gulf of Cadiz and North Morocco (Grasshoff, 1988; 1989). It inhabits compact slope muds between 500 and 1200 m depth on slopes not exceeding a 5% gradient (Pérès, 1967; Bellan-Santini, 1985; Oceana, 2011). Other and special adaptations are known for bamboo corals; for example, they can reach high densities in oxygen minimum zones throughout the deep Northeast Pacific (Baco, 2007). Some fish and decapod crustaceans reach maximum densities in bottoms inhabited by *I. elongata*, which is the case of the deep-water shrimps *A. antennatus* and *P. martia*, both of high commercial interest (Maynou and Cartes, 2012). However, as depth is the main factor affecting the distribution and density of marine species (Gage and Tyler, 1991; Cartes et al., 2009a), it is unknown whether these species are really associated with the habitat that *Isidella* may generate or they share a preference for a common bathymetric range with concrete physical and trophic characteristics. Analyses of assemblages associated with *I. elongata* incorporating simultaneous environmental data have never been performed.

In addition to natural variability, human impacts altered not only shelf (Watling, 2005) but also deep-sea ecosystems, e.g. in the NE Atlantic in the last 20 yrs (Hall-Spencer et al., 2007). The most evident human effect on *Isidella* fields has been from trawling activity (Maynou and Cartes, 2012), though likely that was not the only impact. Some authors (Pérès, 1985) have suggested indirect effects on soft-bottom communities from the historic deforestation done in Mediterranean countries with consequent increases in sediment runoff by rivers. This may in turn increase turbidity close to the bottom in *Isidella* habitats, enhancing clogging in polyps and altering their function as active filter feeders (Rogers, 1999). This is feasible in the case of *I. elongata*, considering that isidid polyps are non-retractile. In any case, trawling activity removes colonies of this rigid gorgonian, cutting the calcareous bases of the colony near the sea floor. The stumps can remain in the mud for a long time (Maynou and Cartes, 2012). In addition, the effects that bottom-trawling (e.g. tracks of doors trawlers) has on soft-bottoms, the biological diversity and production, are well known, although information is almost restricted to highly impacted areas of the continental shelf (Jennings et al., 2001; Gray et al., 2006). The occurrence and persistence of tracks and their biological effects on deep-sea ecosystems is almost unknown (but see for hard-cold *L. pertusa* reefs: Fossa et al., 2002; Mortensen et al., 2008).

In addition to an initial study by Maynou and Cartes (2012), we report here a mesoscale study on three slope stations, analyzing possible geomorphological, physical and trophic differences among them in order to define the optimal habitat characteristics of *I. elongata* and slope communities associated with this gorgonian. In 1994, we found pristine *forests* of *I. elongata* off Catalonian coasts near the Ebro River (north-western Mediterranean), where trawling activity began 2 years later. This gave us the opportunity to compare the current state of *I. elongata* communities through the design of the experimental survey ANTROMARE0611. The objectives of this study are: (i) to characterize and compare fish and invertebrate assemblages co-existing with different *I. elongata* fields; (ii) to analyse the effect of bottom-trawling on the diversity and composition of these communities; and (iii) to investigate physical environmental factors (geomorphological, geophysical and climatic) that may explain mesoscale spatial variability of *I. elongata* communities.

2. Methods

2.1. Study area

The study area corresponds to the upper slope (300–1000 m depth) of the continental margin, off the Ebro delta (Fig. 1). The area alternates between smooth open slope regions, 2°–4° gradient, and steep areas associated with steep tributary canyons 1 km wide on average, converging to the Valencia Channel (Figs. 1 and 2). Three stations, from N to S, St1 (40°54N–1°35 E), St2 (40°41N–01°26 E) and St3 (40°34N–01°26E) were sampled over the slope of S Catalonian coasts between the Cape of Salou and the Ebro River Delta (Fig. 1) at depths between 615 and 648 m. Samples were collected on board the R/V *Sarmiento de Gamboa* during the cruise ANTR0611 (18–25 June 2011, project ANTROMARE, CTM2009-12214-C02-01). St2 and St3 were located at depths inhabited by the *facies* of the gorgoniacean *I. elongata* (as recorded in the cruise GeoDelta1 in May 1994) while St1 was in front of the port of Tarragona, an area historically (since the 1940s) submitted to substantial trawling in search of the red shrimp *A. antennatus*.

2.2. Geomorphological data

Geomorphological information was recorded using the deep-sea multibeam echosounder Atlas Hydrosweep DS, emitting 184 beams at a frequency of 14.5–16 kHz, the deep-towed large-scale Sidescan Sonar system Edge-Tech 2400-DSS/DT-1, emitting a frequency of 120 kHz and covering 1 km^2 areas, and dotted with 400 kHz sub-bottom profiles (only at S3). Post-processing of multibeam data was performed with the CARIS-HIPS software system. After correcting the soundings for water column sound velocity variations and cleaning them with a ping graphical editor, gridding of the filtered data was carried out to obtain the final digital terrain model. Footprint resolution was 20 m for the insonified areas. Side Scan Sonar (SSS) records were visualized and compiled into a high-resolution mosaic image (1 m) using SonarWiz software from Cheasepeake Technology. Side Scan Sonar (SSS) hauls (on St3) were performed previously to trawling in that area.

2.3. Fauna data

The biomass and structure of megafauna (fish, decapod crustaceans, and epibenthic invertebrates) assemblages and of infauna/zooplankton were analysed among stations. Megafauna was

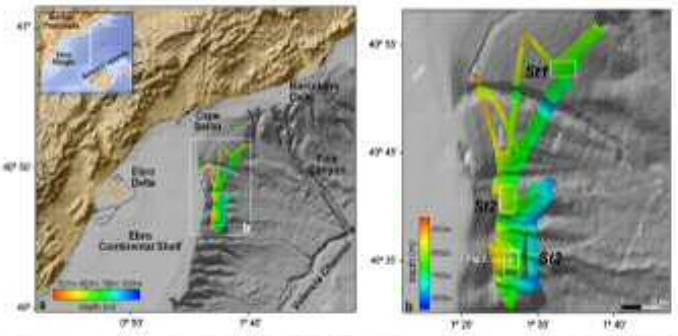

Fig. 1. (a) Topographic and bathymetric map of the southern Catalan Margin (Ebro Margin). Topographic data comes from the SRTM-3 grid. Bathymetry integrates low resolution data from the Spanish Oceanographic Institute (IEO, 2001) (grey) with high resolution data (coloured) acquired during ANTR0611 cruise. (b) study area, covered by the high-resolution multibeam data in ANTR0611. St1, St2 and St3 correspond to the sampling stations. The inset in St3 indicates the area swept within ANTR0611 cruise by the side scan sonar (Fig. 2).

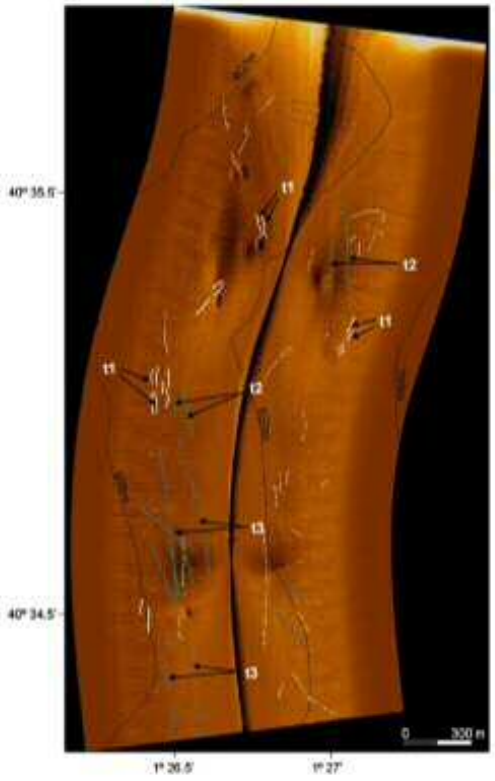

Fig. 2. Side scan sonar image collected over the St3 (corresponding to the area with the highest density of *Isidella elongata* according to the data from 1994). Dotted lines represent the marks from the doors of the trawling fishing boats operating in the area. The distance between the door tracks has been used to distinguish three main types of fishing trawlers with average distance of 30 m (t1), 60 m (t2), and 120 m (t3).

sampled using a single-warp trawl, the OTSB-14, a standard sampler for study of deep-sea megafauna (Merrett et al., 1991) and used by the I.C.M. deep-sea ecology group since the 1980s (Cartes et al., 2009b). Three replicate, tows at the same soundings, were performed at each station. A total of nine hauls with an effective towing time of 20 min were carried out. Infauna was sampled at St1, St2 and St3 with a Reyneck box-corer (21 × 31 cm box sides). Four replicate samples were collected per station.

A 1-warp trawl MTS-25, with some different characteristics (vertical height: 2 m; codend mesh size: 10 mm) than the OTSB-14 (1.2 m height; 6 mm at codend) (see Cartes et al., 2009b) was used to compare ANTR0611 hauls and cruises performed in 1995 in the same area (see data treatment).

On board and in the laboratory megafauna was identified at species level, counted, weighed and measured for length (fish, TL, mm; crustaceans, CL, mm) for each species. Taxonomic identification of species was done by members of the I.C.M. deep-sea ecology group, with wide experience in the identification of deep fauna. Infauna was sieved through 0.5 mm mesh on board, fixed in buffered formaldehyde and sorted in the laboratory. Animals were assigned to higher taxa (e.g. polychaetes, crustaceans, and others), counted and weighed. Abundance and biomass (individuals or grams per ha for megafauna; g/m^2 for infauna) were obtained.

Zooplankton was sampled at St1, St2 and St3 by means of a 1-m^2 WP2 plankton net equipped with an opening–closing mechanism; 1000DT General Oceanics Ltd. The distance to the bottom of hauls was recorded by a SCANMAR sensor attached to the WP2 net. Distance of the net from the bottom was between ca. 4 and 43 m at soundings between 611 and 650 m. The WP2 was equipped with 500 μm mesh and trawled at a speed of ca. 1.5 knots. The durations of tows were 10 min. Standard 2030 flowmeters (General Oceanics Inc.) were attached to the mouths of nets to measure the amount of water filtered and/or the distance covered in each haul. Volumes of filtered water were 1574.8 m^3 (St1), 1264.9 m^3 (St2) and 423.6 m^3 (St3). All sampling was performed during daytime.

In May 1992 (ZONAP1) and May 1994 (GeoDelta 1), two cruises were performed to the south of the Catalonian coast with hauls at the locations of St1, St2 and St3 of ANTROMARED611. Hauls were performed with an OTSB-14 during ZONAP1 and with a MTS-25 in GeoDelta 1. The composition (fish and crustaceans) of two hauls from ZONAP1 (Z1, Z19) at St1, and three from GeoDelta 1 (GD1-44, 45 and 48) at St2/St3 were selected for a comparative

analysis between the two periods sampled (the 1990s and 2011). Data on epibenthic invertebrates – determined by the same authors – were available only for ZONAP1.

2.4. Environmental data

Environmental data were recorded in order to interpret mesoscale variability among stations. We recorded physico-chemical data both on near-bottom water column (T, S, O_2, turbidity and fluorescence) and on sediment (potential REDOX, E_h, and the total organic matter, %TOM).

Environmental variables were recorded by CTD casts taken prior to the fauna samplings with a SBE25 profiler equipped with Niskin bottles and sensors for the variables *P* (pressure), *T* (temperature in °C), *S* (salinity in pss), O_2 (oxygen concentration in ml/l), turbidity and fluorescence (the last two in voltage units). One CTD profile was performed at each station to ca. 5 m above the seafloor. For each variable the averages at 5 m above the bottom (e.g. $T_{5\ mab}$; $S_{5\ mab}$) were calculated at the depths where OTSB-14 hauls were performed.

A total of 12 box-cores were performed, with four replicates (core taken over ca. the same position, i.e. < 30 m of distance between replicates) at each station (St1, St2, St3). The box corer used sampled a surface of 0.065 m^2. Once on board some environmental records were obtained from undisturbed sediment: (i) REDOX from sediments in each core using a ThermoOrion 250A sensor. Voltage was read at 1 cm and at 5 cm in the mud; and (ii) the total organic matter (%TOM) content of sediments calculated as difference between dry weight (DW: 60 °C until constant weight) and ash weight (500 °C for 2 h) based on three replicates per core.

2.5. Trophic variables

Trophic variables were also analysed at the three stations. The availability of main prey for megafauna was sampled for infauna and zooplankton. Assimilated food in tissues by means of stable isotope analyses ($\delta^{13}C$ and $\delta^{15}N$) and gut fullness were performed for eight dominant species in slope assemblages.

The first uppermost 20 cm of sediments taken with box-corers were sieved through a 0.5 mm mesh to retain macrofauna. Three zooplankton samples (one per station) were also performed. Fauna was immediately fixed in buffered formaldehyde on board. Total biomass (wet weight after eliminating blotting water, g) of macroinfauna were measured (wet weight) and mean biomass per station based on four replicates was calculated. In the case of zooplankton, in addition of total biomass, copepods and broad large taxa were counted and weighed. Some characteristic species (jellies such as *Salpa fusiformis*, *Abylopsis tetragona* and *Solmissus* spp., fish – *Cyclothone braueri* – and euphausiids – *Nematoscelis megalops* were identified. Biomass was standardized (to 1000 m^3) for the three hauls for taxa/species. One haul is sufficient to represent the faunistic composition of zooplankton in a given depth/period. In fact, in all zooplankton studies in open waters (e.g. Scotto di Carlo et al., 1984) no replicates are performed (1 station= 1 haul/depth sampled).

The *trophic condition* of the three areas sampled was compared between St1, St2 and St3 based on two approaches:

1) The assimilated food by means of stable isotope analyses (SIA), i.e. $\delta^{13}C$ and $\delta^{15}N$, of tissues of eight dominant species. Target species included a deposit feeder (*Calocaris macandreae*), a filter feeder/carnivore (the mysid *Boreomysis arctica*) and six top predators (three decapods: *A. antennatus*, *P. martia* and *Polycheles typhlops*; three fishes: *P. blennoides*, *N. aequalis* and *Notacanthus bonapartei*). Three specimens per species of comparable sizes – whenever possible – were collected at each station and submitted to a standard protocol for SIA analyses (Fanelli et al., 2011a, 2011b).
2) The gut fullness (*F*=stomach content weight/body weight, in gWW) of species as an estimation of food consumed Average *F* values were calculated per station based on ten specimens per species for the six predatory species, some of them potential scavengers, listed above; and
3) the study of the diet of the red shrimp *A. antennatus*. All methods on fullness and diet of deep-water shrimps are explained in detail elsewhere (Cartes, 1994; Cartes et al., 2008).

2.6. Long-term data

Historical data were also obtained to characterize basic environmental conditions in the 1990s and 2011 for a comparative analysis of assemblages: (i) *T* and *S* in the Balearic basin of the water mass at the depth of 600 m (close to depths sampled in GD1, May 1994) were downloaded from MEDATLAS database; (ii) Climatic data (the NAO_{winter} and the NAO_{spring} calculated from the three monthly records simultaneous with and previous to our samples (NAO_{sm} and $NAO_{1\ month}$ and $NAO_{2\ months}$). NAO indices were downloaded from the Climatic Research Unit of East Anglia University (*http://www.cru.uea.ac.uk*); and (iii) Ebro River monthly flow data (m^3/s) were compiled from data provided by the *Confederación Hidrográfica del Ebro* (*http://www.chebro.es/*) for years (months) when we sampled.

Both Catch Per Unit effort (CPUE, mainly kg/day of *A. antennatus*) and mean number of trawlers/day (capturing *A. antennatus*) for the two ports nearest to St1 (Tarragona) and St2/St3 (Sant Carles de La Rápita) were downloaded from the database of the Catalonia local government *http://captures/depRecursos/WEB_Pesca/diariaCatalunya.html*. Both CPUE and number of trawlers were taken as a proxy of the fishing effort performed in the area on *L. elongata* habitats.

2.7. Fauna data treatment

Data on faunal composition (abundance, ind./ha) were analyzed by n-MDS techniques in search of affinities between hauls composition. Multi-dimensional scaling (MDS) was applied to the similarity matrix generated for clustering, after removing from matrices species appearing less than twice in all hauls. We performed analyses at three levels:

1) for all species of fish and decapods;
2) for fish and decapods, but only considering benthopelagic species, that is, after excluding small mesopelagic species from data matrices; and
3) on epibenthic invertebrates (mesopelagic species also excluded).

Second approach was done to remove small swimming fauna in order to correct the use of two different trawl types (the OTSB-14 and the MTS-25: see Cartes et al., 2009b). MTS-25 has a higher vertical height (2 m) and larger mesh size at codend (10 mm) than the OTSB-14 (1.2 m height; 6 mm). Removing small swimming fauna (e.g. sergestid shrimps or myctophids and gonadostomatids) allows a proper comparison of communities between 2011 and the GD1 cruise in 1994.

The similarity measure used in MDS was the Bray–Curtis index (after log-transformation of data). The non-parametric, rank-order Spearman's correlation was used for 2011 vs. 1990s

comparisons, also to correct the use of the OTSB-14 and the MTS-25. SIMPER analyses (Clarke and Ainsworth, 1993) were performed with Bray–Curtis distances for standardized number to identify: (i) the main species contributing to each assemblage, and (ii) the dissimilarity of assemblages between the stations and the main species contributing to this dissimilarity. 1 and 2-way PERMANOVA analyses (on different data matrices) were performed to test spatio-temporal significance in species composition. Factors tested were latitude (LAT), parallel to stations distribution from noth (St1) to south (St3), with three levels (St1, St2, St3) and period (with two levels: 2011, 1990s). The software used was PRIMER 6.0+PERMANOVA (Clarke and Warwick, 1995; Anderson et al., 2008).

Diversity (species richness, S and eveness, J) of megafauna was calculated by station (St1, St2, St3) and period (2011 and the 1990s). Diversity indices comparisons were performed using (i) all fish and decapods species; (ii) these taxa excluding mesopelagic species and (iii) epibenthic invertebrates (excluding GD1 in where epibenthic invertebrates were not identified). Comparison of fish and decapods was based only on large benthopelagic species, due to the higher codend mesh size of trawls used in GD1. The total biomass (g/ha) and the mean size (mean weight, g/ind.) of fish, decapods and the rest of invertebrates were also calculated and compared among stations.

2.8. Analysis of environmental factors

Possible relationships between megafaunal composition (based on benthopelagic species, after excluding small mesopelagic species) and environmental variables were explored by Canonical Correspondence Analysis (CCA: Ter Braak, 1986) based on two approaches: (i) comparison within ANTR0611 hauls; and (ii) comparing the composition and environmental conditions in 1994 and 2011, taking account only of hauls in the St2 and St3 areas (with *Isidella* colonies) to remove the spatial variability evident in the data of 2011. CCA is a multivariate technique for extracting synthetic environmental gradients from ecological data (Ter Braak and Verdonschot, 1995). Data were log-transformed for CCAs.

3. Results

3.1. Geomorphological data

The three sampling areas (St1, St2, St3) were located in the slope region at very similar depths (ca. 600 m) (Fig. 1b). St1, isolated from St2 to St3, corresponds to a fishing ground located on an open slope area ca. 22 km from the nearest canyon head (to the SW) (Fig. 1b). St2 and St3 are both in open slope interfluve areas adjacent to canyons but in smaller grounds compared to St1 and closer to canyon heads (at ca. 6.2–9 km, Fig. 1b). Furthermore, St2 and St3 are closer to the mouth of the Ebro River (ca. 50 km) than St1 (Fig. 1a), hence probably more affected by the sedimentary inputs of the Ebro plume and by POM advection via submarine canyons associated to the runoff of this large river. Slope gradients were calculated between 600 and 650 m depth following the main direction of the trawling activities and resulted higher at St3 (0.95–6°) than at St1 and St2 (0.15–0.83°).

Side scan sonar data collected in the St3 revealed some fishing activity, with 28 tracks mapped in a relatively small area, 11 of them reflecting parallel tracks of the doors (Fig. 2). The distance between the door tracks, grouped in three main categories (25–30 m (t1), 100–120 m (t2) and a single pair of ca. 60 m (t3) (Fig. 2), suggest at least three different fishing trawlers operating in the area, probably corresponding to different engine power and length/size. Tracks were mostly parallel to isobaths (Fig. 2) in agreement with fishing strategy of trawlers in the area.

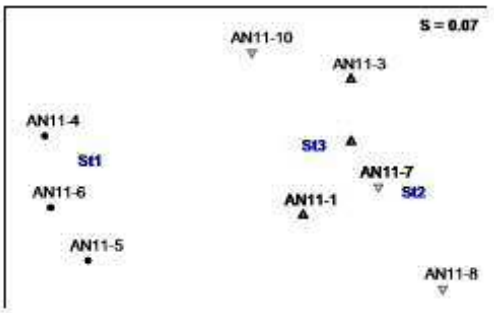

Fig. 3. n-MDS for megafauna abundance composition in June 2011. Data from hauls collected by OTSB-14 hauls performed during ANTR0611. (● St1: hauls 4, 5, 6; ▽ St2: hauls 7, 8, 10; ▲ St3: hauls 1, 2, 3).

3.2. Analysis on fauna composition and biomass

n-MDS on the composition (megafauna abundance, ind./ha) of OTSB-14 hauls performed during ANTR0611 showed a significant segregation between hauls performed on St1 and St2/St3 (Fig. 3; PERMANOVA: PseudoF=2.56, p =0.02; post-hoc t> 2.5, p < 0.05 for St1 vs St2/St3) but no significant differences between the compositions at St2 and St3 (t=0.8; p=0.71). St2 and St3 are dominated by the same five species in the same rank order (Table 1): (1) *Sergestes arcticus*; (2) *A. antennatus*; (3) *C. braueri*; (4) *P. blennoides* and (5) *Polycheles typholps*, accumulating 62.7 and 63.5% of abundance estimates. At St1 *P. blennoides* and adult *Lampanyctus crocodilus* were dominant among fish, while among decapods both *A. antennatus* and *P. typhlops* were significantly less abundant that at St2/St3 (Table 1). MDS gave similarly significant results when comparing the three stations after removing mesopelagic species (see also Table 1). Among fish, ranking after *P. blennoides* at St2 were *L. crocodilus* (adults) and *N. bonapartei* with the same species and *T. trachyrhynchus* at St3. In general percentage of dissimilarity between stations (for the whole assemblage) was similar, higher between St1 and St3 (51.2) than between St1 and St2 (35.2), and between St2 and St3 (47.7). Dominant species (*S. arcticus*, *A. antennatus* and *P. blennoides*) accumulated the higher dissimilarity among stations. Among less dominant species was remarkable that at St1 neither *N. bonapartei* nor *T. trachyrhynchus* were among dominant fish. Another rattail, *N. aequalis*, was also much less abundant at St1. Among benthopelagic decapods *Plesionika* spp. were more abundant both at St2 and St3 than at St1.

n-MDS based on the composition of megafauna comparing the period 1992–1994 and the hauls of 2011 (Spearman's rank correlation) showed significant differences (2-way PERMANOVA test) as a function of the two factors analyzed: (i) factor LAT (df=2; pseudo$F$=6.05; p=0.0002); (ii) factor period (df=1; pseudo$F$=8.74; p=0.0001), with the LAT × period interaction being non-significant (Fig. 4a). Segregation between hauls taken at St1 (both Z1-7/Z1-19 from 1992 and hauls from 2011) and St2/St3 (both GD hauls from 1994 to 2011 hauls) were as evident or even clearer in plots (Fig. 4a) than segregation between the two periods (1992–1994 vs 2011). Post-hoc comparisons between stations in June 2011 gave significant differences (1-way PERMANOVA) in fish and decapod composition between St1 and St2; (t=3.78; p=0.0004) and St1 and St3 (t=2.63; p=0.0005). n-MDS

Table 1
SIMPER for OTSB-14 hauls performed during ANTR611.

St1		
Average similarity: 67.68		
Species	**Av. Abund**	**Contrib%**
Phycis blennoides	27.97	17.8
Lamprogrus crocodilus	24.84	13.5
*Cyclothone braueri	19.61	10.79
*Sergestes arcticus	18	10.79
Aristeus antennatus	11.96	6.39
Calocaris macandreae	11.64	5.87
*Benthocuma glaciale	7.44	4.56
*Argyropelecus hemigymnus	7.31	4.42
*Gennadas elegans	5.63	3.29
Munida tenuimana	5.61	3.19
*Paraphaeo sivado	3.76	2.51
Paraphaeo multidentata	4.04	2
*Sergia robusta	3.18	1.8
*Pandalina profunda	4.64	1.71
*Myctophum punctatum	2.29	1.42
St2		
Average similarity: 57.15		
Species	**Av. Abund**	**Contrib%**
*Sergestes arcticus	60.88	33.46
Aristeus antennatus	48.05	10.74
*Cyclothone braueri	20.82	8.26
Phycis blennoides	10.6	5.56
Polycheles typhlops	7.48	4.72
Plesionika acanthonotus	5.83	3.78
Lamprogrus crocodilus	9.35	3.7
Notacanthus bonapartei	7.53	3.24
*Argyropelecus hemigymnus	5.74	3.09
*Gennadas elegans	16.73	2.8
Pagurus alatus	6.39	2.72
Calocaris macandreae	5.36	2.47
Plesionika martia	5.2	2.36
*Benthocuma glaciale	3.63	1.89
*Myctophum punctatum	2.5	1.52
St3		
Average similarity: 67.23		
Species	**Av.Abund**	**Contrib%**
*Sergestes arcticus	56.78	29.22
Aristeus antennatus	24.02	12.6
*Cyclothone braueri	23.86	8.79
Phycis blennoides	11.57	7.48
Polycheles typhlops	11.58	5.38
Plesionika martia	9.69	4.72
Calocaris macandreae	8.45	4.56
*Argyropelecus hemigymnus	7.31	3.32
*Gennadas elegans	5.79	2.26
Plesionika acanthonotus	4.73	2.2
Trachyrhynchus scabrus	3.7	1.96
*Sergia robusta	3.05	1.84
*Paraphaeo sivado	4.61	1.39
*Benthocuma glaciale	4.07	1.32

* Indicates mesopelagic fish and decapods.

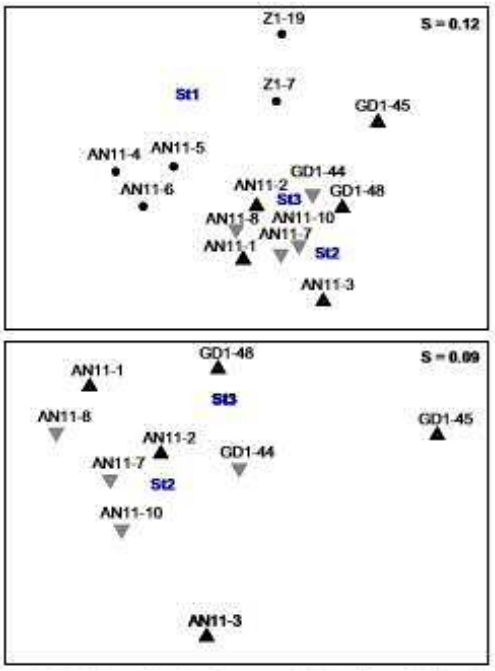

Fig. 4. n-MDS for megafauna abundance composition (small mesopelagic species excluded) in 2011 and in the 1990s. Hauls were performed in June 2011 (ANTR0611) and cruises in 1992 (Zoniap, Z) and 1995 (GeoDelta, GD1). (a) All hauls; (b) hauls taken at St2 and St3. ● St1: hauls 4, 5, 6 and Z1; ▼ St2: hauls 7, 8, 10 and GD1-44; ▲ St3: hauls 1, 2, 3 and GD1-41, 45.

based only on St2, St3 (Fig. 4b) stations (those with *I. elongata* occurring in one or both of the two periods studied) showed similar distribution of hauls above explained (Fig. 4a) with a Stress = 0.09. The *t*-test was significant ($t = 1.68$; $p = 0.02$) when the two periods (1992–1994 vs 2011) were compared.

SIMPER on stations (LAT) composition evidenced the dominance of *A. antennatus* at St2 and St3 (Table 2). This species accumulated, together with other important species (*P. blennoides*, *P. martia*, *P. acanthonotus* and *P. typholps*) ca. 65% of total abundance in both stations. *A. antennatus* was less abundant at St1, and species different from those at St2/St3, such as *Munida tenuimana* and *L. crocodilus*, appeared among the top five dominant species. When the 1990s and 2011 assemblages were compared the same five species appeared at St2/St3 in 2011. Dissimilarity between 1994 and 2011 was 52.9. The most dominant species (*A. antennatus*, *P. martia* and *P. blennoides*) accumulated the highest dissimilarities between 1994 and 2011 with *A. antennatus* being less abundant in 1994. Among the less dominant species two macrourids (*N. aequalis* and especially *T. trachyrhynchus*) were more abundant in 1994 (Table 2).

n-MDS on the composition of invertebrates (abundance, ind./ha, Table 3) of OTSB-14 evidenced a significant segregation between hauls performed on St1 and St2/St3 (Fig. 5; PERMANOVA: Pseudo$F = 2.61$, $p = 0.02$; post-hoc $t > 1.84$, $p < 0.05$ for St1 vs St2/St3) but no significant differences between the compositions at St2 and St3 ($t = 1.17$; $p = 0.27$). Dissimilarity between stations was higher between St1 and St2/St3 (51.8, 49.9, respectively) than between St2 and St3 (43.3). The highest dissimilarities between St1 and St2/St3 were accumulated (to 37–56% of dissimilarity) by peracarid crustaceans (the mysid *B. arctica* and the isopod *Natatolana borealis*), for the holothuroid *Molpadia musculus*, the gastropods *Aporrhais serresianus* and *Euspira fusca* and the bivalve *Abra longicallus*. *N. borealis* and *E. fusca* were more abundant on St1 (Table 3). Among low dominant species *I. elongata* represented by a few colonies at St2/st3 accumulated 5.7–6.3% of dissimilarity. Trophic guild to each species was given based on the information on diets and stable isotopes published by Fanelli et al. (2011a) in the same area. The clearest trend (Table 3) was the increase of detritus feeders (DF) at St2/St3 (e.g. the echinoderms *M. musculus* and *Mesothuria intestinalis*; the two sipunculans), together with active suspension feeders (ASF; the two bivalves) and the filter feeder (FF) *B. arctica*. Comparison of invertebrate composition between 1992 and 2011 over St1

Table 2
SIMPER for OTSB-14 hauls performed during ANTR611 and cruises in the 1990s (Zimap, Z; GeoDelta, GD1). Small mesopelagic fish and decapods were removed from data matrix.

1990s		
Average similarity: 40.36		
Species	**Av.Abund**	**Contrib%**
Plesionika martia	19.33	13.62
Trachyrhynchus scabrus	8.67	13.52
Plesionika acanthonotus	11	13.52
Phycis blennoides	6.67	12.01
Aristeus antennatus	16	7.75
Pagurus alatus	4	6.74
Polycheles typhlops	7.67	6.74
Pontocaris lacazei	2.67	5.87
Nezumia aequalis	4	5.27
Munida tenuimana	5.33	3.58
Symphurus ligulatus	3	3.37
2011		
Average similarity: 58.77		
Species	**Av.Abund**	**Contrib%**
Aristeus antennatus	45.5	25.37
Phycis blennoides	12.83	15.64
Polycheles typhlops	11	11.42
Plesionika martia	8.67	8.34
Plesionika acanthonotus	6.17	6.84
Lampanyctus crocodilus	9.33	5.3
Notacanthus bonaparte	7.33	4.07
Sergia robusta	3.5	3.21
Trachyrhynchus scabrus	3.83	3.1
Pagurus alatus	5.5	2.93
Munida tenuimana	2.17	2.17
Polycheles muticlentata	2.83	2.08

evidenced an increase of scavengers (*N. borealis* and *E. fusca*) and a decrease of the deposit feeder *Brissopsis lyrifera* from 1992 to 2011 (Table 3).

Diversity (*S* and *J*) indices for megafauna (fish and decapods) were calculated by station (Table 4). Mean *S* was higher at St2 and St3 (34 species) than at St1 (30.7), while *J* was higher at St1, and this tendency was the same both for all species and when only considering large benthopelagic species. Comparing the diversity at St2, St3 (only large benthopelagic species) between 1990s and 2011, we did not find any significant loss of diversity or any other significant trend. Twenty-three species of epibenthic invertebrates were identified during ANTR0611 hauls. For epibenthic invertebrates, *S* was higher, though not significantly, at St2 than at St3, with lower *J* to the south. When *S* was compared between St1 vs St2/St3, the *t* test gave significant results ($p < 0.05$).

Biomass increased from St1 to southern stations (St2, St3) both for fish (non-significant *t* test) and decapod crustaceans ($t=2.55$, $p=0.03$), while the biomass of the other invertebrates (mainly cephalopods by weight) was higher at St1 ($t=3.12$, $p=0.02$; Fig. 6). The increase of size (mean weight) was progressive from north (St1) to south (St2, St3) for fishes and decapod crustaceans, although non-significant comparing St1 vs St2/St3 (*t* test), while the mean weight of other invertebrates was higher at St1 ($t=2.61$, $p=0.03$).

3.3. Environmental data from ANTR0611 cruise

Characteristics of water masses at the three stations were similar or identical regarding *S* and *T* close to the sea bottom and flourometry at the sea surface (Table 5). $O_{2\ 5\ mab}$ was slightly higher (5.97 mg/l) at St3 in comparison to St2 and St1. By contrast turbidity increased significantly (1-way ANOVA, $F=47.1$, $p < 0.001$) from north (St1) to south (St3) as can also be observed in the turbidity profile ca. 50 m above the bottom

Table 3
List of invertebrates (except decapods) collected in ANTR611, indicating their feeding guilds. ASF: Active suspension feeders; PSF: passive suspension feeders; FF: filter feeders.C: carnivores; Sc: scavengers; DF: deposit feeders.

	Density (ind/ha)				Feeding Guild
	St1 40°54 N	St2 40°41 N	St3 40°32 N	St1 21	
Cnidaria					
Isidella elongata	0	0.52	0.86	0	PSF
Anthipatharia	0	0	0.33	0	PSF
Polychaeta					
Nephtys hombergi	0	0	0	0.16	C
Chirimia biceps (Maldanidae)	0.30	0.27	0	0	DF
Crustacea					
Brazelia typica	0	0	0.23	0	C
Cirolana borealis	9.17	3.39	2.58	1.66	C-Sc
Bathymysis arctica	9.57	7.84	24.66	5.12	FF-C
Eucopia hanseni	0.27	0.25	0	0.16	C
Lophogaster typicus	0	0.85	0	0	C
Lepas anatifera	0	0	1.82	0	ASF
Bivalvia					
Abra longicallus	0	3.05	0.98	0.90	ASF
Limatula gwyni	0	0	0.30	0	ASF
Cephalopoda					
Bathypolipus sponsalis	0.31	0	0.23	0	C
Histioteuthis reversa	0.61	0	0.33	0	C
Neorossia caroli	0	0	0	0.15	C
Heteroteuthis dispar	0	0	0	0.48	C
Gastropoda					
Aporrhais serresianus	0.30	5.70	1.42	0.15	C
Eunpira fusca	2.42	0.80	0.23	0.60	C
Buccinoides cinnabarina	0	0	0.77	0.48	C
Scaphopoda					
Dentalium agilis	0	0.25	0	0	DF
Sipunculida					
Phascolosoma granulatum	0	0.25	0.33	0	DF
Sipunculus norvegicus	0	0.25	0.30	0.65	DF
Enteropneusta					
Glandiceps talaboti	0	0.25	0	0	DF
Echinodermata					
Brissopsis lyrifera	1.15	1.37	0.30	12.11	DF
Mesothuria intestinalis	0	0.25	0.70	0	DF
Molpadia musculus	1.12	5.12	3.70	1.61	DF

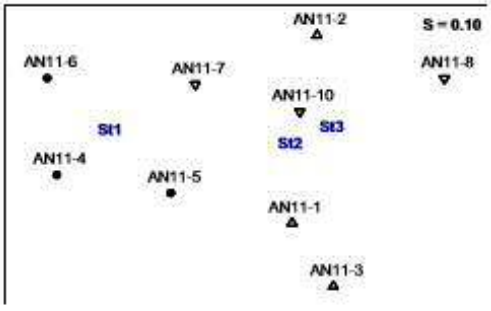

Fig. 5. n-MDS for invertebrates abundance composition in June 2011. Data from hauls collected by OTSB-14 (● St1: hauls 4, 5, 6; V St2: hauls 7, 8, 10; Δ St3: hauls 1, 2, 3).

(Fig. 7, St3 profile not included due to continuous malfunction of the turbidimeter).

Sediment variables showed an increase in total organic matter (TOM) at St2 (7.98%) compared to St1 and St3, but the clearest

Table 4
Diversity (S, 1/*l* and J) of the fish, decapods and epibenthic invertebrates (decapods excluded) of hauls performed during ANT/XXIV/1 and cruises in the 1990s (Zimap, Z; Geodelta, GD1). Results are given by station (St1, St2, St3) for all taxa and excluding small mesopelagics for 1990s vs 2011 comparisons.

All species					
	S	***J***		***S***	***J***
2010			1990s		
St1	30.7	2.84	**St1**	32.0	2.67
St2	34.0	2.63			
St3	34.0	2.77			
Excluded mesopelagics					
	S	***J***		***S***	***J***
2010			1990s		
St1	18.3	2.19	**St1**	22.5	2.53
St2	20.7	2.30			
St3	21.7	2.52	**St2/3**	19.0	2.45
Epibenthic invertebrates					
	S	***J***		***S***	***J***
2010			1990s		
St1	7.0	1.39	**St1**	7.5	1.40
St2	10.0	1.51			
St3	10.0	1.95			

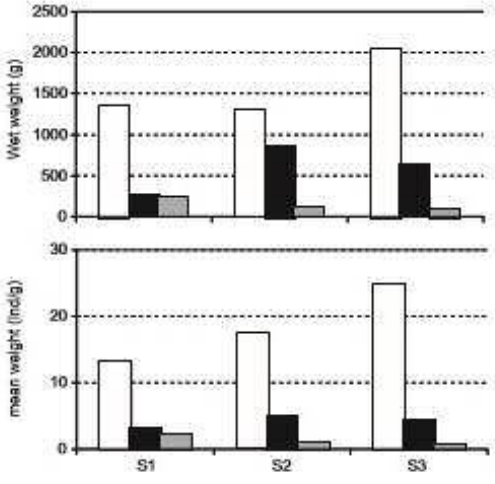

Fig. 6. Biomass (wet weight/ha) and mean weight (gWW/individual) of megafauna in ANT/XXIV/1. ▭ fishes; ■ decapods; ▭ other invertebrates). St1, St2, St3 are the three stations sampled.

trend (not significant due to low *n*) was found in E_h, with more reduced REDOX values at St2 and St3 and less reduced at St1 (1-way ANOVA $F=4.1$, $p>0.1$). Greater accumulation of sediments and higher %TOM coincided with intermediate values of turbidity near the bottom.

3.4. Trophic data

The stations varied regarding infauna (benthic macrofauna) density (Fig. 8). Polychaetes, crustaceans (mainly amphipods and cumaceans) and sipunculans were more abundant at St3. However, the clearest tendencies were the larger mean size of polychaetes and sipunculans (main detritus feeding taxa) at St3

Table 5
Characteristics of the water column and %TOM of sediments at the three stations (St1, St2, St3) sampled in ANT/XXIV/1 over 620–670 m.

	St1	**St2**	**St3**	**1-way ANOVA**
	40°54N	**40°41N**	**40°32N**	
T_{South}	13.12	13.16	13.12	ns
S_{South}	38.50	38.50	38.50	ns
O_{South}	5.91	5.89	5.97	$p<0.05$
$Turb_{South}$	0.239	0.326	0.420*	$p<0.001$
Fluor	0.014	0.014	0.014	ns
TOM(%)	7.80	7.98	7.66	ns
mV (1 cm)	−57.75	−73.57	−62.70	ns
mV (5 cm)	−53.90	−60.37	−61.23	$p<0.1$

S3 turbidity (*t*) was calculated for the 50 highest records of *t* at the closest 50 mab because of continuous malfunction of the turbidimeter at that station.

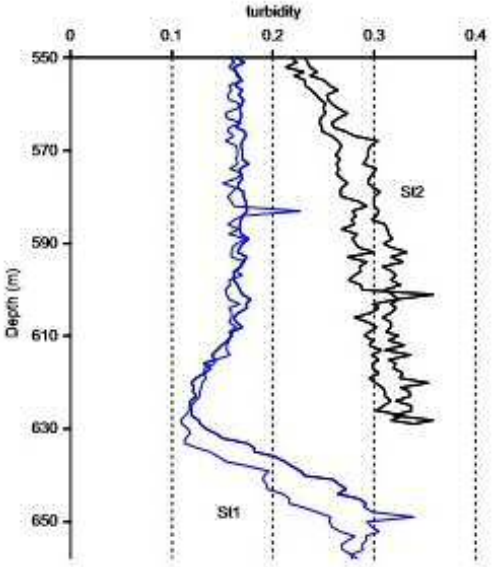

Fig. 7. Profiles of turbidity (voltage) near the bottom at St1 and St2 obtained in CTD casts in June 2011. St3 profile was not included because of malfunction of the turbidimeter.

and the increasing size of polychaetes from north (St1) to south (St2/St3).

Zooplankton biomass increased from north to south (Table 6), with higher biomass at St2 and especially over St3 (21.1 gWW/1000 m^3) than at St1. Gelatinous plankton dominated in volume (mainly *S. fusiformis*, *A. tetragona*, *Chelophyes appendiculata* and *Solmissius* spp.) at all stations with a similar increase of biomass from St1 to St2/St3. Crustaceans of different sizes (and trophic level) such as euphausiids (*N. megalops*), decapods (*S. arcticus*) and copepods all increased their biomass at St2 and St3, in parallel to the tendency found for total zooplankton biomass (Table 6). The teleost *C. braueri* also followed the same tendency.

The amounts of food in stomachs of fish and decapod species were significantly different between stations only for two fish (*P. blennoides* and *N. aequalis*) both showing increasing *F* from north (St1) to south (St3)(Table 7). All macrophagous species

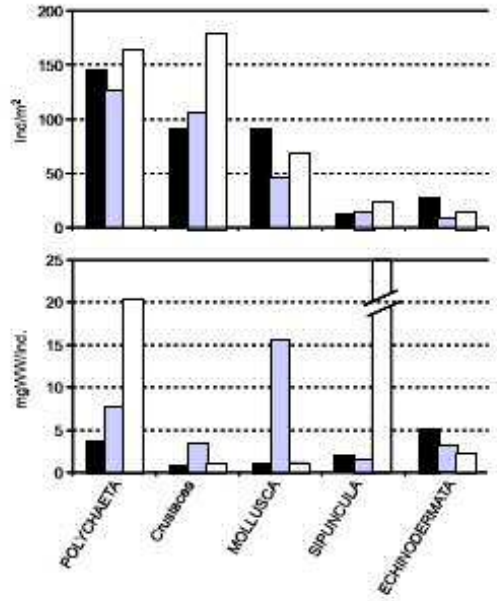

Fig. 8. Abundance (individuals/m²) and mean weight (mg WW/individual) of main taxa of infauna in June 2011. Three stations were sampled: St1; St2; St3) mean weight for sipunculans at St3 was 152.2 mgWW/ind.

Table 6
Main zooplankton taxa and species identified from the three stations (St1, St2, St3) sampled in ANT80611.

ZOOPLANKTON	St1	St2	St3
	40°54N	40°41N	40°32N
g WW/1000m3			
Total	4.140	5.472	21.138
Mesopelagic Crustacea			
Gennadas elegans	0.031	0	0
Sergestes arcticus	0	0.277	0.595
Nematoscelis megalops	0.054	0.062	0.415
Calanoidea	1.184	1.980	5.813
Gelatinous plankton			
Abylopsis tetragona	0	0.621	4.795
Chelophyes appendiculata	0	0	0.271
Lensia spp.	0.620	0.188	0.097
Solmissus spp.	1.848	0.188	2.174
Periphilla periphilla	0	0.043	0
Salpa fusiformis	0.001	1.104	2.557
Fish			
Cyclothone braueri	0.159	0.313	2.528
Notolepis rissoi	0	0.028	0

preying mainly on benthos (the cited *P. blennoides* and *N. aequalis* together with *A. antennatus*) showed higher *F* at St3 (Table 7). Exceptions were: (i) the lobster *P. typhlops*, with scavenging habits that showed higher *F* at St1; (ii) *B. arctica*, a filter feeder and (iii) the deposit feeder *C. macandreae*.

The diet of *A. antennatus* did not change significantly among the three stations sampled (n-MDS, Bray–Curtis distance; PERMANOVA ($df=2$; pseudoF=0.97; $p=0.52$) with no significant post-hoc comparison among stations (MDS not included).

Stable isotope content did not vary significantly among the three stations, although this could be in part due to the low number of replicates (Table 7). Both $\delta^{15}N$ and $\delta^{13}C$ reflect assimilated food in tissues, rather than ingested food deduced from diets or fullness. No significant relationships were found regarding food sources ($\delta^{13}C$) exploited by species, though more $\delta^{13}C$ enrichment was found from north (St1) to south (St3) in *C. macandreae*, the only territorial (sedentary) species analyzed, and in the benthos-feeding fishes *P. blennoides* and *N. aequalis*. The significant differences found in $\delta^{15}N$ results in the case of *P. martia* and *N. bonapartei* are attributable to the slightly greater sizes of specimens at St2 and St1 compared to St3.

3.5. Long-term environmental data

T and *S* in the Balearic basin of the water mass at the depth of 600 m (close to depths sampled in GD1, May 1994) were 13.13 °C and 38.49 pss. As climatic data we used the NAO_{winter} data in 1994 (3.03) and in 2011 (−1.57) and the NAO_{spring}, respectively 1.78 in 1994 and 0.83 in 2011.

Another factor considered was the biomass (g/ha) of *L. elongata* in each haul. Biomass ranged (over St2, St3) from 18.1 to 255.9 g/ha in 1994 to 0 (no live colonies)—1.5 g/ha in 2011.

Both CPUE (kg of *A. antennatus*/day) and mean number of trawlers/day indicated the sharply different trawling activity in the two ports nearest to St1 (Tarragona) and St2/St3 (Sant Carles de La Rápita) between 2000 and 2010. We consider both CPUE and number of trawlers as indicators of fishing effort on *Isidella* habitats. Trawling began at St2/St3 areas in 1996. There was relatively low fishing effort on fishing grounds close to St3, with means of only 0.9 vessels operating per day and mean *A. antennatus* catches of 9.7 kg/day with long periods without any vessel operating there (68% of weeks without trawling activity). By contrast the number of vessels operating per day at St1 was 6.8, with mean catches of 189.5 kg/day of *gamba* (mainly *A. antennatus*) and 97% of weeks with trawling activity.

CPUE and vessels/day taken 3 months after ANTROMARE0611 cruise (since 1st April 2011) showed catches of 12.6 kg/day and 0.5 (range between 0 and 2) vessels/day in the surrounding area to St2/St3 with an accumulative number of vessels operating=4. These are comparative data, and the fishing effort was in part done on areas the same as or close to ANTROMARE0611 sampling stations, although it is impossible to know the precise effort on St1, St2 or St3.

3.6. Environmental analyses on assemblages

The CCA performed on the hauls taken over the three stations sampled in June 2011 related St2/St3 hauls with different physical conditions in the water column and sediments than those found significant at St1 (Fig. 9a). At St3 we found, together with isolated colonies of *L. elongata*, more reduced sediments (the most negative E_h) and the highest values of turbidy close to the bottom. At St2, where calcareous bases of *L. elongata* were still collected, were found the highest levels of %TOM, with high *T* and *S* in the near-bottom water column (albeit small increases). The species more closely related with St3 conditions were the two rattails (*N. aequalis* and *T. trachyrhynchus*), the two species of *Plesionika* (*P. martia* and *P. acanthonotus*) and *P. typhlops*. *A. antennatus* and *N. bonapartei* were more related with hauls taken, and conditions found, at St2. By contrast, the species more abundant on the highly impacted fishing ground of St1 (AN11-4, 5, 6) were the teleosteans *P. blennoides* and *L. crocodilus*, the shark *Galeus melastomus* and the decapods *M. tenuimana* and *Monodaeus*

Table 7
Comparison (by stations, St1, St2, St3) of some trophic variables (stable isotopes of $\delta^{13}C$ and $\delta^{15}N$ and stomach fullness, *F*) in some selected dominant species of fish and decapods at slope communities belonging to different trophic levels and strategies.

	$\delta^{15}N$				$\delta^{13}C$				*F*			
	St1	St2	St3	1-way ANOVA	St1	St2	St3	1-way ANOVA	St1	St2	St3	1-way ANOVA
B. arctica	5.03	5.03	5.89	ns	−17.48	−17.95	−17.72	ns				
C. macandreae	5.25	5.04	5.51	ns	−16.92	−16.70	−16.82	ns				
P. typilops		8.59	8.44	ns		−15.70	−15.54	ns	0.0042	0.0015	0.0014	ns
P. murtia	7.13	7.46	6.68	6.79 ($p=0.03$)	−16.20	−16.02	−16.51	ns	0.0142	0.0090	0.0053	ns
A. antennatus	8.83	8.65	8.75	ns	−15.55	−15.91	−15.37	ns	0.0066	0.0050	0.0073	ns
P. blennoides	8.42	8.65	8.63	ns	−18.09	−17.96	−17.82	ns	0.0026	0.0033	0.0048	5.99 ($p=0.04$)
N. aequalis	9.82	11.5	10.5	4.74 ($p=0.06$)	−16.67	−15.74	−16.13	ns	0.0008	0.0009	0.0026	6.79 ($p=0.03$)
N. bonapartei	10.5	9.07	8.81	5.99 ($p=0.04$)	−15.37	−15.69	−16.08	ns	0.0026	0.0012	0.0017	ns

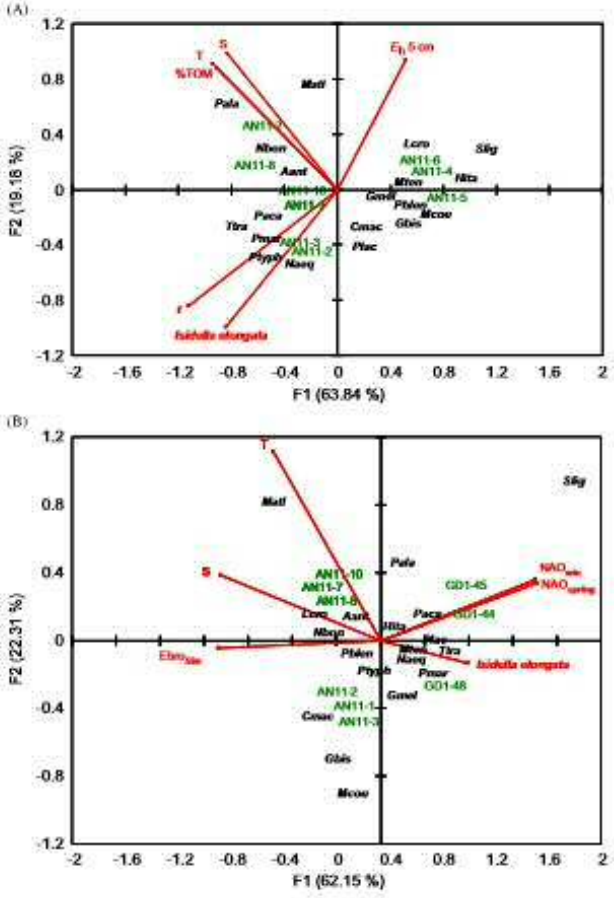

Fig. 9. Canonical correspondence analyses (CCA) performed on 1994 and 2011 hauls and environmental information. (A) CCA on data from the three stations, St1, St2 and St3 sampled in June 2011; (B) CCA performed on the composition and environmental conditions of St2 and St3 areas (with *Isidella* colonies) between 1994 and 2011. *T*: temperature; *S*: Salinity; *t*: turbidity; E_h: Redox potential; NAO_{winter}: winter NAO; $Ebro_{Mar}$: Ebro river discharge (m^3/s) at the same month (records of the last 30 days) of samplings.

couchi. Sediments were less reduced and %TOM was lower at St1 than at St2, while the near-bottom water column showed lower turbidity at St1 than at St2/St3, probably due to its geomorphology.

Comparing assemblages between 1994 and 2011 (at St2/St3, exclusively) and including climatic variables, CCA showed essentially the same group of species, linked as above with reduced sediment E_b and high turbidity close to the bottom. The two rattails, *N. aequalis* and *T. trachyrhynchus*, and shrimp *P. martia* were linked to highest densities of *L. elongata* in hauls in the pristine conditions found in 1994 (Fig. 9b). Climatic conditions in that period were characterized by higher (positive) values of NAO index. By contrast, hauls taken in the same area in 2011 were characterized by lower NAO (even negative in the case of NAO_{winter}) and higher T and S in overlying water masses. *A. antennatus* and *N. bonapartei* appeared more linked to these hydrographic conditions, rather than to low values of NAO.

4. Discussion

The preferred habitat conditions for deep-sea, soft-bottom-living bamboo (Isididae) corals are not fully known, both regarding the corals' own preferences and the conditions that corals may create (Krieger and Wing, 2002; Metaxas and Davis, 2005). Metabolism of corals is dependent on temperature, measured for example by proxy Mg/Ca ratios in skeletons at different time-scales (Thresher et al. 2010). However, this variable may have insignificant effects on *L. elongata* over deep-Mediterranean margins due to the high habitat stability (below 200 m) in T and S conditions. At central Catalan coasts over 650 m (the same depth of ANTR0611 sampling) we found very small seasonal variations in T_{Strath} (13.29–13.39 °C) and S_{Strath} (38.53–38.55 pss)(Papiol et al., 2012). Thus, the habitat preference of *L. elongata* in the deep Mediterranean may depend on other factors (e.g. geomorphology, trophic factors) than those significant in other areas (e.g. Nova Scotia: Metaxas and Davis, 2005) with stronger gradients of T and substrate type. We attempt to analyse this for the slope off the Ebro delta, in the context of the still poor knowledge of natural variability of bathyal muddy bottoms. The three stations sampled in ANTR0611 scarcely differed, as expected, in the water column characteristics, but we found differences in the geomorphology and sediment characteristics, probably as a function of the proximity to canyon heads and of distance to the nearest river mouth (as discussed by Cartes et al., 2009a; Mamouridis et al., 2011). The trends for %TOM and E_b among the three stations were identical to those found in May 1994 at the same three locations (Maynou and Sardá, 1997). Higher %TOM at St2 and more reduced values of E_b at St2 and St3 were then associated with pristine *L. elongata* grounds. Finer sediments were also found at St2–St3 compared to St1, with IGSD sorting coefficient of 1.661–1.683 at St2–St3 and of 1.847 at St1 (F. Maynou, unpublished data). We found in 2011 that St2–St3 had (and likely did have in 1994) better food conditions for species co-existing with *L. elongata* grounds, for both benthos and zooplankton feeders. Benthos feeders found higher biomass and mean size of benthic (macrofauna) prey. Also, stronger aggregation of near-bottom macroplankton was found as food source for zooplankton feeders (including *L. elongata* itself). This higher zooplankton aggregation co-occurred with higher near-bottom turbidity at St2–St3.

Like other gorgonians, bamboo corals are passive suspension feeders, with prey consisting mainly of small copepods (as observed for shallow-water species: Orejas et al., 2001). This is consistent with low $\delta^{15}N$ levels of *L. elongata* (7.58‰) found in the area (authors, unp. data; see also Fanelli et al., 2011a, 2011b). Regarding species associated with *L. elongata*, ROV observations over coral grounds have only confirmed the preferred depth range of *L. elongata* (e.g. 680–750 m in the Ionian Sea: Mytilineou et al., 2009), without precise observations of associated fish or invertebrates. That is mainly because some species avoid ROVs. Our analysis suggests two contrasting categories of fish and decapods co-existing with *L. elongata* fields (mainly at St3, an area which had dense coral formations to around 255 colonies/ha): (i) the rattails *N. aequalis* and *T. trachyrhynchus*, preferentially preying on benthos (e.g. *C. macandreae*, polychaetes, ophiuroids: Carrassón and Cartes, 2002) and (ii) two pandalid shrimps (*P. martia* and *P. acanthonotus*), both non-migrating plankton feeders (Cartes, 1993). Some pandalids (*Pandalus propinquus*), it has been suggested, find refuge in *Primnoa* fields (Buhl-Mortensen and Mortensen, 2004), while *P. martia* was found to be linked to *L. elongata* fields by Maynou and Cartes (2012). However, it has been uncertain whether the species are really associated to the habitat generated by *Isidella* colonies, or whether fish, pandalids and corals share a preference for common trophic conditions. The highest densities of *P. martia* and *P. acanthonotus* over St2/St3 were coupled with higher densities of jellyfish and mesopelagic crustaceans, main prey of both shrimps (Cartes, 1993, Fanelli and Cartes, 2008), and with calanoid copepods, whose nauplii may be captured by corals. As zooplankton tends to accumulate over slope features such as steep walls (at seamounts or shelf-breaks: Vereshchaka, 1995; Genin, 2004) or canyon heads (Macquart Moulin and Patriti, 1996), it seems likely that *L. elongata* and *Plesionika* spp. found common preferred habitats where zooplankton tends to aggregate. These aggregations probably relate to the high (between 0.95 and 6°) inclinations and near-bottom turbidity (reflecting higher POM or high zooplankton availability) found on the slope at St3. *P. martia* is one of the most abundant species over other Mediterranean slope areas (Cartes et al., 1994; Maynou and Cartes, 2000) not necessarily inhabited by *L. elongata*. Trophic factors may also influence benthos feeders, which showed higher food consumption (gut fullness) due to higher density and bigger prey at St2/St3. The proximity of canyons at St2/St3 may favour higher food availability for benthos-feeding fish. Also, coral forests, thanks to the fan-structure of colonies, may favour detritus accumulations around them, improving habitat conditions for deposit feeders of benthos and for benthos feeders. So benthos-feeding rattails would be the species most related with the capacity of *L. elongata* to regulate habitat conditions. By contrast, species such as *A. antennatus* were more related in our analyses with changes in physical condition of the water column and with climatic oscillations. Maynou (2008) and Cartes et al. (2011) reported the long-term relationships between *A. antennatus* catches and NAO oscillations. Under positive NAO zooplankton increases in the northwestern Mediterranean (Cartes et al., 2009c), which may favour the increase of *Plesionika* spp. (as evidenced in CCAs) and of plankton feeders in general. Stable isotopes also pointed to a similar origin of food exploited by large predators in areas with (St2–St3) and without (St1) *Isidella*, probably due to the swimming mobility of fish and crustaceans among stations. Only the burrowing shrimp *C. macandreae*, due to its territorial behaviour and detritus feeding habits, showed a trend of enriched $\delta^{13}C$ at St2 and St3. That matches the expected trend of enriched $\delta^{13}C$ in food webs more dependent on sedimented and recycled POM (Fanelli et al., 2011a).

4.1. Impact on *Isidella elongata* communities

The only species disappearing from St2/St3 since 1994 after *L. elongata* was (almost) removed by trawling was the majid crab *Rochinia (Anamathia) rissoana*, associated with deep corals (including *L. elongata*: Dieuzeide, 1960; *L. pertusa*: Carlier et al., 2009) in the Mediterranean. As probably happens with relict hard corals in the western Mediterranean (e.g. in Santa Maria de Leuca: Carlier et al., 2009), *L. elongata* forms rather sparse colonies

separated by ca. 4–5 m (as deduced from densities at St3 of ca. 255 colonies/ha and ROV images in Oceana, 2008). This sharply contrasts with: (i) the highly diverse decapod fauna associated with cold-water corals forming reefs on the Galicia Bank (e.g. six galatheid and chyrostylid crabs *Munidopsis* spp., *Uroptychus* spp., Cartes et al., 2012), and (ii) the higher megafaunal diversity on the Mid-Atlantic Ridge in *L. pertusa* reefs compared with no reef bottoms (Mortensen et al., 2008). The increase of decapod biomass over the *I. elongata* ground and the loss of invertebrate diversity found by Maynou and Cartes (2012) seems generally confirmed in our study. However, we found none of the groups that live associated by direct/indirect trophic relationships with other deep gorgonians (*Primnoa* sp., Krieger and Wing, 2002), such as sea stars or nudibranchs. The nudibranch *Bathydoris cinnabarina* was uncommon and, although collected at St3, was also found at St1 in the absence of *Isidella*. *Primnoa* spp. also generates habitat for small macrofauna (mainly amphipods; Buhl Mortensen and Mortensen, 2004). The quite different morphology of *Primnoa* and the Mediterranean *I. elongata* may generate different habitat conditions for small macrofauna (e.g. amphipods); *Primnoa* has a dense bush shape and can reach 2 m height (Krieger and Wing, 2002), while *I. elongata* has thin branches and is smaller. This suggests that, as found for *Primnoa-Paragorgia* forests Off Nova Scotia (Metaxas and Davis, 2005), the occurrence of deep-water corals may not always result in increasing diversity of megafauna. Generation of habitat for megafauna by corals may also be influenced by its morphology and density. In the case of *Isidella* in the Mediterranean, we should also consider the low diversity of deep Mediterranean ecosystems, considered as impoverished Atlantic fauna by the particular paleoecology of this Sea (Pérès, 1985). Fields of *I. elongata* may enhance trophic conditions for some species (as discussed above), but their occurrence did not significantly alter the species composition of mobile megafauna. Another aspect often attributable to bamboo coral facies, their effect as nursery areas, cannot be evaluated in this study due to the lack of a temporal sampling. The expected loss of diversity by trawling effect on bamboo coral *facies* was confirmed in our analysis only for benthic invertebrates associated with *Isidella* grounds, with higher diversity at St2/St3 in comparison to the fishing ground at St1. However, this tendency could also be attributable (in part) to higher POM available for deposit and active suspension feeders at St2/St3, where most species in these guilds (sipunculans, holothurians such as *M. musculus* and *A. longicallus*) increased in comparison to St1.

In 1994, we found after a monitoring cruise a pristine seafloor (at St2 and St3), with dense *I. elongata* fields (to 255 colonies/ha, at St3), which may represent a landscape similar to that seen in recent images (2010) taken on *Ses Olives* mount in the deep Mediterranean. Densities of *I. elongata* were the highest (Maynou and Cartes, 2012) found by trawling in the western Mediterranean. The area in St2/St3 likely remained protected from trawling activity simply because it was unknown by fishermen and far from nearest fishery ports (at 81 km, ca. 4 h 30 min from Sant Carles). Meanwhile, trawlers in Catalonia continue increasing their engine power and displacement to go farther away in search of new fishing grounds, and fisheries in the area surrounding St2/St3 began in 1996. At St3 the side-scan sonar recorded to three types of tracks produced by trawler doors with different separations (of ca. 30, 70 and 100–120 m between doors), suggesting that low fishing activity (with the action of only three vessels (mean/day=0.47, deduced from Sant Carles landing data for *A. antennatus*) was enough to remove almost all colonies of *I. elongata* from the Ebro slope in the last 15 yrs. The largest trawlers fishing on *A. antennatus* off Catalonian coasts may reach spacing between doors of 100–120 m (J.A. Caparrós, pers. comm.), as confirmed at St3 by side-scan images. In shallow water, Tuck et al. (1998) found that otter-trawl trails remain visible for over 18 months after the end of trawling on muddy bottoms (at 35 m) in a semi-enclosed fjord. Palanques et al. (2001) observed tracks at least 1 year old on muddy bottoms of the outer shelf off the Llobregat River, ca. 90 km north of St1. Moderate sedimentation rates recorded around canyon systems in the Gulf of Lions (e.g. 0.09–0.18 cm/yr: Miralles et al., 2005), an area subject to discharge from the Rhone of similar magnitude that of the Ebro (runoff to 1344 m^3/s, daily; monthly average of 520 m^3/s in 2011), suggest persistence of tracks in bathyal muds for long periods. However, the persistence of tracks observed on the Ebro slope could be of lower duration, because we found 3 months before SSS hauls tracks from three to four vessels coinciding with maximum of four boats landing *A. antennatus* in Sant Carles port. If we assume that tracks observed correspond to 3 vessels from Sant Carles operating in search of *A. antennatus* (with low catches between 2008 and 2010), effort on St3 would be rather low. On intense exploited grounds as at St1 (and similar grounds off Barcelona) it was impossible to find any live colonies of *I. elongata* as we did at St3/St2; there were not even calcareous coral bases remaining in the mud (Maynou and Cartes, 2012). The low activity at St3 was enough to remove *I. elongata* from the pristine grounds observed 17 years before, reducing densities to isolated colonies (0.9 colonies/ha). This impact, however, hardly altered fish and invertebrate composition.

5. Conclusions

It is assumed that meadow-forming corals on both hard and soft bottoms (e.g. Isididae) have the capacity to generate special habitats for fish and invertebrates that *Isidella* bottoms (Pérès, 1985) sustain diversity and increase both biomass (Maynou and Cartes, 2012) and species recruitment. After an analysis incorporating environmental information, we suggest that this habitat-forming- capacity was rather low for bamboo corals on soft sediment (at least for conditions in St3). This conclusion agrees of that of Metaxas and Davis (2005). The removal of *I. elongata* from soft bottoms caused small loss of diversity. Any impact would likely have been by reduction of POM accumulation and some loss of habitat quality for benthos and some benthos-feeding fishes. Good habitat conditions (in terms of food availability) found in areas with the highest densities of bamboo corals on the Ebro slope may be attributable to geomorphological features, local enrichment by river discharge and the occurrence of submarine canyons. These factors combined may enhance both food quality of sediment for benthos and zooplankton aggregations. *I. elongata* found its optimal ecological conditions in the same areas as some macrourid fish and pandalid shrimps. *I. elongata* has intensively, and it may still being, removed from pristine areas by trawlers searching new fishing grounds. A future measure intended to protect habitats generated by this gorgonian could be to create closed areas where *I. elongata* formed important fields, expecting natural regeneration. This should be preferently done in areas where the species find their optimal ecological conditions. These conditions were found (and above defined) in our study over St3, in where even some living colonies still remained. Although preservation of natural habitats, under increasing threats from human overpopulation, is a priority and an urgent task, we also need to correctly evaluate the natural variability and the ecological conditions affecting marine species, most of which remain unknown.

Acknowledgements

This research was performed and financed within the framework of the MICYT project ANTROMARE (CTM2009-12214-C02-01-MAR). We thank especially to crew members of, and to all participants in,

the cruise ANTR0611 on board O/V *Sarmiento de Gamboa*, especially to A. Castellón and the rest of the U.T.M. members. Also to Dr. M. Vargas-Yáñez, I.E.O. Málaga, Spain, who downloaded MEDATLAS data used in our analyses and to Dr. F. Maynou (ICM Barcelona) by the critical reading of our article. Stable isotope analyses were supervised by Dr. P. Rumolo in the *Istituto per l'Ambiente Marino Costero* of Naples (C.N.R., Italy), which collaboration was deeply appreciated.

References

Anderson, M.J., Gorley, R.N., Clarke, K.R., 2008. PERMANOVA+ for PRIMER: Guide to Software and Statistical Methods. PRIMER-E, Plymouth, UK.

Andrews, A.H., Cordes, E.E., Mahoney, M.M., Munk, K., Coale, K.H., Cailliet, G.M., Heiletz, J., 2002. Age, growth and radiometric age validation of a deep-sea, habitat-forming gorgonian (*Primnoa resedaeformis*) from the Gulf of Alaska. Hydrobiologia 471, 101–110.

Baco, A.R., 2007. Exploration for deep-sea corals on North Pacific seamounts and islands. Oceanography 20 (4), 108–117.

Bellan-Santini, D., 1985. The Mediterranean benthos: reflections and problems raised by a classification of the benthic assemblages. In: Moraitou-Apostolopoulou, M., Kiortsis, V. (Eds.), Mediterranean Marine Ecosystems. Plenum Press, New York, pp. 1019–1048.

Buhl Mortensen, L., Mortensen, P.B., 2004. Crustaceans associated with the deep-water gorgonian corals *Paragorgia arborea* (L., 1758) and *Primnoa resedaeformis* (Gunn., 1763). J. Nat. Hist. 38, 1233–1247.

Carlier, A., Le Guilloux, E., Olu, K., Sarrazin, J., Mastrototaro, F., Taviani, M., Clavier, J., 2009. Trophic relationships in a deep Mediterranean cold-water coral bank (Santa Maria di Leuca, Ionian Sea). Mar. Ecol. Prog. Ser. 397, 125–137.

Carrassón, M., Cartes, J.E., 2002. Trophic relationships in a Mediterranean deep-sea fish community: partition of food resources, dietary overlap and connections within the Benthic Boundary Layer. Mar. Ecol. Prog. Ser. 241, 41–55.

Cartes, J.E., 1993. Diets of deep-water pandalid shrimps on the western Mediterranean slope. Mar. Ecol. Prog. Ser. 96, 49–61.

Cartes, J.E., 1994. Influence of depth and season on the diet of the deep-water aristeid *Aristeus antennatus* along the continental slope (400 to 2300 m) in the Catalan Sea. Mar. Biol. 120, 639–648.

Cartes, J.E., Company, J.B., Maynou, F., 1994. Deep-water decapod crustacean communities in the northwestern Mediterranean: influence of submarine canyons and season. Mar. Biol. 120, 221–230.

Cartes, J.E., Papiol, V., Guijarro, B., 2008. The feeding and diet of the deep-sea shrimp Aristeus antennatus off the Balearic Islands (western Mediterranean): influence of environmental factors and relationships with biological cycle. Prog. Oceanogr. 79, 37–54.

Cartes, J.E., Maynou, F., Fanelli, E., Romano, C., Mamouridis, V., Papiol, V., 2009a. The distribution of megabenthic, invertebrate epifauna in the Balearic Basin (western Mediterranean) between 400 and 2300 m: environmental gradients influencing assemblages composition and biomass trends. J. Sea Res. 66, 244–257.

Cartes, J.E., Maynou, F., Lloris, D., Gil de Sola, L., García, M., 2009b. Influence of trawl type on the composition, abundance and diversity estimated for deep benthopelagic fish and decapod assemblages off the Catalan coasts (western Mediterranean). Sci. Mar. 73 (4), 725–737.

Cartes, J.E., Maynou, F., Fanelli, E., Papiol, V., Lloris, D., 2009c. Long-term changes in the composition and diversity of deep-slope megabenthos and trophic webs off Catalonia (western Mediterranean): are trends related to climatic oscillations? Prog. Oceanogr. 82, 32–46.

Cartes, J.E., Maynou, F., Fanelli, E., 2011. Nile damming as plausible cause of extinction and drop in abundance of deep-sea shrimp in the western Mediterranean over broad spatial scales. Prog. Oceanogr. 91 (3), 286–294.

Cartes, J.E., Papiol, V., Valeiras, X., Frutos, I., Macpherson, E., Punzón, A., Serrano, A., 2012. Distribution and biogeographic trends of decapod assemblages from Galicia Bank (NE Atlantic) with connexions with different water masses. In: Thirteenth International Symposium on Oceanography of the Bay of Biscay, ISOBAY13, 11–13 April 2012, Santander, Spain. pp. 106.

Clarke, K.R., Ainsworth, M., 1993. A method of linking multivariate community structure to environmental variables. Mar. Ecol. Prog. Ser. 92, 205–219.

Clarke, K.R., Warwick, R.M., 1995. Changes in Marine Communities: An Approach to Statistical Analysis and Interpretation. Natural Environment Research Council, United Kigdom.

Dieuzeide, R., 1960. Les fonds chalutables a 600 m. par le travers de Castiglione. Recherchers sur la faces a *Isidella elongata* Esper. Bull. Sta. Acquic. Pêches Castiglione 2, 9–86.

Etnoyer, P., Morgan, L.E., 2005. Habitat forming deep-sea corals in the northeast Pacific Ocean. In: Freiwald, A., Roberts, J.M. (Eds.), Cold-Water Corals and Ecosystems. Springer-Verlag, Heidelberg, pp. 331–343.

Fanelli, E., Cartes, J.E., 2008. Spatio-temporal variability in the diet of two pandalid shrimps in the western Mediterranean evidenced by gut-contents and stable isotope analysis: influence on the reproductive cycle. Mar. Ecol. Prog. Ser. 92 (355), 219–233.

Fanelli, E., Papiol, V., Cartes, J.E., Rumolo, P., Brunet, C., Sprovieri, M., 2011a. Food web structure of the epibenthic and infaunal invertebrates on the Catalan slope (NW Mediterranean): evidence from $\delta^{13}C$ and $\delta^{15}N$ analysis. Deep-Sea Res. I 58 (1), 98–109.

Fanelli, E., Papiol, V., Cartes, J.E., 2011b. Food web structure of deep-sea macrozooplankton and micronekton off the Catalan slope: insight from stable isotopes. J. Mar. Syst. 87 (1), 79–89.

Fossà, J.H., Mortensen, P.B., Furevik, D.M., 2002. The deep-water coral *Lophelia pertusa* in Norwegian waters: distribution and fishery impacts. Hydrobiologia 471, 1–12.

Gage, J.D., Tyler, P.A., 1991. Deep Sea Biology: A Natural History of Organisms at the Deep-Sea Floor. Cambridge University Press, Cambridge.

Genin, A., 2004. Bio-physical coupling in the formation of zooplankton and fish aggregations over abrupt topographies. J. Mar. Syst. 50, 3–20.

Grasshoff, M., 1988. Die Gorgonaria der Expeditionen von Travailleur 1880–1882 und Talisman 1883 (Cnidaria, Anthozoa). Zoosystema 8 (1), 9–38.

Grasshoff, M., 1989. The straits of Gibraltar as a faunistic barrier: the gorgonaceans, pennatulaceans, and antipatharians of the BALGIM cruise (Cnidaria: Anthozoa). Senckenb. Marit. 20 (5–6), 201–223.

Gray, J.S., Dayton, P., Thrush, S., Kaiser, M.J., 2006. On effects of trawling, benthos and sampling design. Mar. Poll. Bull. 52 (8), 840–843.

Hall-Spencer, J., Rogers, A., Davies, J., Foggo, A., 2007. Deep-sea coral distribution on seamounts, oceanic islands, and continental slopes in the northeast Atlantic. In: George, R.Y., Cairns, S.D. (Eds.), Conservation and Adaptive Management of Seamount and Deep-Sea Coral Ecosystems. Rosenstiel School of Marine and Atmospheric Science of the University of Miami, pp. 135–146.

Husebø, A., Nøttestad, L., Fossà, J.H., Furevik, D.M., Jørgensen, S.B., 2002. Distribution and abundance of fish in deep-sea coral habitats. Hydrobiologia 471, 101–110.

Jennings, S., Dinsone, T.A., Duplisea, D.D., Warr, K.J., Lancaster, J.E., 2001. Trawling disturbance can modify benthic production processes. J. Anim. Ecol. 70, 459–475.

Krieger, K.J., Wing, B.L., 2002. Megafauna associations with deep-water corals (*Primnoa* spp.) in the Gulf of Alaska. Hydrobiologia 471, 83–90.

Macquart Moulin, C., Patriti, G., 1996. Accumulation of migratory micronekton crustaceans over the upper slope and submarine canyons of the northwestern Mediterranean. Deep-Sea Res. 43 (5), 579–601.

Mamouridis, V., Cartes, J.E., Parra, S., Fanelli, E., Saiz Salinas, J.I., 2011. A temporal analysis on the dynamics of deep-sea macrofauna: influence of environmental variability off Catalonia coasts (western Mediterranean). Deep-Sea Res. I 58, 323–337.

Maynou, F., 2008. Influence of the north Atlantic Oscillation on Mediterranean deep-sea shrimp landings. Clim. Res. 36, 253–257.

Maynou, F., Cartes, J.E., 2000. Community structure of bathyal decapod crustaceans off south-west Balearic Islands (western Mediterranean): seasonality and regional patterns in zonation. J. Mar. Biol. Assoc. U. K. 80, 789–798.

Maynou, F., Cartes, J.E., 2012. Effects of trawling on fishes and invertebrates from deep-sea coral facies of *Isidella elongata* in the western Mediterranean. J. Mar. Biol. Assoc. U. K. 92 (7), 1501–1507.

Maynou, F., Sardá, F., 1997. *Nephrops norvegicus* population and morphometrical characteristics in relation to substrate heterogeneity. Fish. Res. 30 (1–2), 139–149.

Merrett, N.R., Gordon, J.D.M., Stehman, M., Headrich, R.L., 1991. Deep demersal fish assemblage structure in the Porcupine Seabight (eastern north Atlantic): slope sampling by three different trawls compared. J. Mar. Biol. Assoc. U. K. 71, 329–358.

Metaxas, A., Davis, J.E., 2005. Megafauna associated with assemblages of deep-water corals on the Scotian slope. J. Mar. Biol. Assoc. U. K. 85, 1381–1390.

Mytilineou, C., Smith, J.C., Politou, C., Kallergis, M., Manoussakis, I., Papathanassiou, E., 2009. Demersal deep-water species observations during remote operated vehicle surveys. In: Hellenic Symposium on Oceanography and Fisheries, 13–16 May 2009, Patra, Greece.

Miralles, J., Radakovitch, O., Aloisi, J.C., 2005. 210Pb sedimentation rates from the northwestern Mediterranean margin. Mar. Geol. 216, 155–167.

Mortensen, P.B., Buhl-Mortensen, L., Gebruk, A.V., Krylova, E.M., 2008. Occurrence of deep-water corals on the mid-Atlantic ridge based on MAR-ECO data. Deep-Sea Res. II 55, 142–152.

Orejas, C., Gili, J., López-González, P., Arntz, W., 2001. Feeding strategies and diet composition of four Antarctic cnidarian species. Polar Biol. 24, 620–627.

Palanques, A., Guillén, J., Puig, P., 2001. Impact of bottom trawling on water turbidity and muddy sediment of an unfished continental shelf. Limnol. Oceanogr. 46 (5), 1100–1110.

Papiol, V., Cartes, J.E., Fanelli, E., Maynou, F., 2012. Intramnual changes in benthopelagic assemblages over the middle slope in the Balearic Basin (NW Mediterranean Sea): influence of environmental variables. Deep Sea Res. I. 61, 84–99.

Pérès, J.M., 1967. The Mediterranean benthos. Ocean Mar. Biol. Ann. Rev. 5, 449–533.

Pérès, J.M., 1985. History of the Mediterranean biota and the colonization of depths. In: Margalef, R. (Ed.), Key Environments: Western Mediterranean. Pergamon Press Ltd, Oxford.

Oceana, 2011. Montañas submarinas de las Islas Baleares: Canal de Mallorca 2011 Propuesta de protección para Ausias March, Emile Baudot y Ses Olives. Oceana Report, Fundación Biodiversidad. 61 pp.

Roark, E.B., Guilderson, T.P., Flood-Page, S., Dunbar, R.B., Ingram, B.L., Fallon, S.J., McCulloch, M., 2005. Radiocarbon-based ages and growth rates of bamboo corals from the Gulf of Alaska. Geophys. Res. Lett. 32, L04606, http://dx.doi.org/10.1029/2004GL021919.

Rogers, A.D., 1999. The biology of *Lophelia pertusa* and other deep-water reef forming corals and impacts from human activities. Int. Rev. Hydrobiol. 84, 315–406.

Scotto di Carlo, E., Iamora, A., Presi, E., Hure, J., 1984. Vertical zonation patterns for Mediterranean copepods from the surface to 3000 m at a fixed station in the Tyrrhenian Sea. J. Plankton Res. 6, 1031–1056.
Sherwood, O.A., Thresher, R.E., Fallon, S.J., Davies, D.M., Trull, T.W., 2009. Multi-century time-series of 15N and 14C in bamboo corals from deep Tasmanian seamounts: evidence for stable oceanographic conditions. Mar. Ecol. Prog. Ser. 397, 209–218.
Thresher, R.E., Wilson, N.C., MacRae, C.M., Neil, H., 2010. Temperature effects on the calcite skeletal composition of deep-water gorgonians (Isididae). Geochim. Cosmochim. Acta 74 (16), 4655–4670, http://dx.doi.org/10.1016/j.gca.2010.05.024.
Ter Braak, C.J.F., 1986. Canonical correspondence analysis: a new eigenvector technique for multivariate direct gradient analysis. Ecology 67 (5), 1167–1179.
Ter Braak, C.J.F., Verdonschot, P.F.M., 1995. Canonical correspondence analysis and related multivariate methods in aquatic ecology. Aquat. Sci. 57, 255–289.
Tuck, I.D., Hall, S.J., Robertson, M.J., Armstrong, E., Basford, D.J., 1998. Effects of physical trawling disturbance in a previously unfished sheltered Scottish sea loch. Mar. Ecol. Prog. Ser. 162, 227–242.
Vereshchaka, A.L., 1995. Macroplankton in the near-bottom layer of continental slopes and seamounts. Deep-Sea Res. I 42, 1639–1668.
Watling, L., 2005. The global destruction of bottom habitats by mobile fishing gear. In: Crowder, L., Norse, E.A. (Eds.), Marine Conservation Biology. Island Press.

SCIENTIA MARINA 78(1)
March 2014, 000-000, Barcelona (Spain)
ISSN-L: 0214-8358
doi: http://dx.doi.org/10.3989/scimar.03926.14A

Analysis and standardization of landings per unit effort of red shrimp *Aristeus antennatus* from the trawl fleet of Barcelona (NW Mediterranean)

Valeria Mamouridis [1], Francesc Maynou [1], Germán Aneiros Pérez [2]

[1] Institut de Ciències del Mar, CSIC, Pg. Marítim de la Barceloneta 37-49, 08003 Barcelona, Spain.
E-mail: mamouridis@icm.csic.es
[2] Facultade de Informática, Campus de Elviña s/n, Universidade da Coruña, 15071 A Coruña, Spain.

Summary: Monthly landings and effort data from the Barcelona trawl fleet (NW Mediterranean) were selected to analyse and standardize the landings per unit effort (LPUE) of the red shrimp (*Aristeus antennatus*) using generalized additive models. The dataset covers a span of 15 years (1994-2008) and consists of a broad spectrum of predictors: fleet-dependent (e.g. number of trips performed by vessels and their technical characteristics, such as the gross registered tonnage), temporal (inter- and intra-annual variability), environmental (North Atlantic Oscillation [NAO] index) and economic (red shrimp and fuel prices) variables. All predictors individually have an impact on LPUE, though some of them lose their predictive power when considered jointly. That is the case of the NAO index. Our results show that six variables from the whole set can be incorporated into a global model with a total explained deviance (ED) of 43%. We found that the most important variables were effort-related predictors (trips, tonnage, and groups) with a total ED of 20.58%, followed by temporal variables, with an ED of 13.12%, and finally the red shrimp price as an economic predictor with an ED of 9.30%. Taken individually, the main contributing variable was the inter-annual variability (ED=12.40%). This high ED value suggests that many factors correlated with inter-annual variability, such as environmental factors (the NAO in specific years) and fuel price, could in turn affect LPUE variability. The standardized LPUE index with the effort variability removed was found to be similar to the fishery-independent abundance index derived from the MEDITS programme.

Keywords: LPUE; standardized LPUE; *Aristeus antennatus*; generalized additive models; NW Mediterranean; deep-water fisheries.

Análisis y estandarización de los desembarcos por unidad de esfuerzo de la gamba roja *Aristeus antennatus* por la flota de arrastre de Barcelona (Mediterráneo noroccidental)

Resumen: Se llevó a cabo un análisis del volumen de desembarcos por unidad de esfuerzo (LPUE) de la gamba roja (*Aristeus antennatus*) de la flota de arrastre en el puerto de Barcelona (Mediterráneo noroccidental) mediante modelos aditivos generalizados (GAM). El conjunto de datos cubre un periodo de 15 años (1994-2008) y consiste en un amplio espectro de predictores: variables dependientes de la flota (el número de mareas efectuadas por cada embarcación y las características técnicas de estas, como el tonelaje bruto), temporales (variabilidad inter- e intra-anual), ambientales (índice de Ocilación del Atlántico Norte [NAO]) y económicas (precio de la gamba roja y precio del combustible). Todos los predictores a nivel individual tienen impacto sobre LPUE, pero algunos de ellos pierden su poder explicativo cuando se consideran conjuntamente con otros, como en el caso del índice NAO. Nuestros resultados muestran que seis variables del conjunto pueden incorporarse en un modelo global con una desvianza total explicada ED=43%. Las variables más importantes fueron aquellas relacionadas con el esfuerzo (número de mareas, tonelaje y grupos), con desviana ED=20.58%, después las variables temporales, las cuales presentaron ED=13.12%, y finalmentelos predictores económicos representados por el precio de la gamba con ED=9.30%. A nivel individual, la variable con mayor contribución es la variabilidad inter-anual (ED=12.40%). Este elevado valor de desviana sugiere que muchos factores correlacionados con el tiempo pueden afectar la variabilidad de LPUE, como los factores ambientales (NAO en años particulares) y económicos, como el precio del combustible. La estandarización de LPUE con respecto al esfuerzo proporciona un índice de abundancia de la gamba roja muy parecido al índice de abundancia independiente de la pesquería obtenido mediante el programa de campañas experimentales MEDITS.

Palabras clave: LPUE; LPUE estandardizada; *Aristeus antennatus*; modelos aditivos generalizados; Mediterráneo noroccidental; pesquerías de profundidad.

Citation/Como citar este artículo: Mamouridis V., Maynou F., Aneiros Pérez G. 2014. Analysis and standardization of landings per unit effort of red shrimp *Aristeus antennatus* from the trawl fleet of Barcelona (NW Mediterranean). Sci. Mar. 78(1): 000-000. doi: http://dx.doi.org/10.3989/scimar.03926.14A

Editor: C. Froglia.

Received: July 23, 2013. **Accepted**: December 10, 2013. **Published**: March 7, 2014.

INTRODUCTION

Deep-water red shrimp is one of the main resources in Mediterranean fisheries in terms of landings and economic value (Bas et al. 2003), primarily in Spain and Algeria, where catches reach more than 1000 t year^{-1} (FAO-FISHSTAT 2011). In the Mediterranean Sea, two red shrimp species, *Aristeus antennatus* and *Aristaeomorpha foliacea*, are caught by specialized trawl fleets operating on the upper and middle continental slope. The distribution of these two species varies geographically and in the NW Mediterranean catches are composed exclusively of *A. antennatus* (Bas et al. 2003).

The deep-water distribution of stocks extends to below 2000 m depth (Cartes and Sardà 1992) but commercial trawlers fish from 400 to 900 m depth. The red shrimp life-cycle includes seasonal, bathymetric and spatial migrations of different fractions of the population with great size and sex segregation: juveniles and small-sized males are more abundant in autumn and early winter in submarine canyons, while reproductive females concentrate on the open slope fishing grounds in late winter and spring (Sardà et al. 1997). This complex life cycle, coupled with a relatively long life span (more than 10 years according to Orsi Relini 2013) differentiates this species from tropical coastal shrimp resources elsewhere (Neal and Maris 1985).

The catches of *A. antennatus* show inter-annual fluctuations that have been related to environmental factors determining strong recruitment (Carbonell et al. 1999, Maynou 2008). Maynou (2008) suggested that winter NAO (North Atlantic Oscillation) is positively correlated with landings of *A. antennatus* two to three years later and that enhanced trophic resources for maturing females in winter and early spring result in stronger recruitments. The NAO has been demonstrated to be a pervasive environmental driver in other marine stocks elsewhere in the Mediterranean and Atlantic (e.g. Brodziak and O'Brien 2005, Dennard et al. 2010). However, the effect of technical and economic variables has received less attention. For instance, in the red shrimp fishery of the NW Mediterranean, Maynou et al. (2003) showed the importance of individual fisher behaviour in determining catch rates, and Sardà and Maynou (1998) discuss the effect of prices on changes of daily fishing effort targeting this species. Intra-annual variability in landings has been linked to market-driven variations in prices, which may result in changes in the fishing effort applied to the stocks, as the trawl fleet moves to alternative resources (Sardà et al. 1997).

Despite the commercial importance of *A. antennatus* in the Mediterranean (Sardà et al. 1997), deriving standardized catches or landings per unit effort (CPUE or LPUE) is not straightforward because of the lack of reliable time series at regional or sub-regional level (Lleonart and Maynou 2003). In fact, determining the abundance of marine stocks is notoriously a widespread problem (Hilborn and Walters 1992). Methodologies basically rely on two different data sources: fisheries-dependent or fisheries-independent data. Fisheries-dependent data tend to be the preferred source to assess the status of marine stocks (Lassen and Medley 2000) but since the applicability of these traditional assessment methods is limited when it comes to crustaceans, fisheries-independent methods are usually preferred. However, fisheries-independent experimental trawl surveys in the western Mediterranean (Mediterranean International Trawl Surveys: MEDITS, Bertrand et al. 2002) are also problematic because they only partially cover the distribution depth range of *A. antennatus*. Thus, fisheries-dependent data are indeed used but methods that require age data are avoided and instead only regression style methods are used. For instance, in the Spanish Mediterranean sub-area 6 (ca. 1000 km long) just 4 to 12 trawl hauls are carried out annually in the 500-800 m depth stratum and none any deeper (Cardinale et al. 2012). Additionally, obtaining reliable landings including age information is problematic owing to difficulties in determining age in crustaceans (Orsi Relini et al. 2013). In these cases the information collected by a fishery is the main source of abundance data available (Maunder et al. 2006) and, when appropriately standardized, can be used to produce series of population abundance that should help fishery managers to promote the sustainable production of marine stocks.

Here, we evaluate the landings per unit effort from the daily sale slips provided by the Barcelona Fishers' Association from 1994 to 2008, corresponding to all the commercial transactions involving *A. antennatus* by a total of 21 trawlers operating on continental slope fishing grounds. The landings of *A. antennatus* have varied by almost an order of magnitude in this area in the last ten years, from a historical low of 13 t year^{-1} in 2006 to 96 t year^{-1} in 2012. Considering that the average ex-vessel price of the species in this period was 36 € kg^{-1} (among the highest seafood prices in Europe), these inter-annual fluctuations in landings have important economic consequences. Fisheries in Spanish Mediterranean waters are allowed between 50 and 1000 m depth for a maximum of 12 hours per day during daytime, except weekends. Hence, trawl skippers must decide which fishing grounds to visit taking into account that on the continental shelf they can be reached in a shorter time but will produce relatively cheap finfish, whereas deep-water fishing produces more valuable red shrimp but entails high economic costs and the risk of losing or damaging fishing gear.

The main objective of this study was to establish the factors influencing the LPUE (see e.g. Denis et al. 2002 for terminology) of *A. antennatus* in order to evaluate their relative importance (fishery-related, economic and environmental), which can be considered to manage effort constraints and to obtain a standardized series of LPUE as a reliable relative abundance index to assess natural abundance. We used generalized additive models (GAMs: Hastie and Tibshirani 1990) to capture the possible nonlinear dependence of LPUE on explanatory variables (Su et al. 2008, among others).

MATERIALS AND METHODS

Data source

Trawlers from the Barcelona port operate on the continental shelf and slope fishing grounds (50-1000 m depth) located between 1°50' and 2°50' longitude east and 40°50' and 41°30' latitude north (Sardà et al. 1997). The fleet operates on a daily basis (with mandatory exit from port after 6 am and return to port before 6 pm) and a limited license system whereby total effort in the area has been frozen since 1986. New boats are only permitted if an existing boat is decommissioned. In addition to effort control, the only other measure of control is limiting mesh sizes (minimum 40 mm cod-end stretch mesh size) and neither in the study area nor in any other Mediterranean areas is there output control. Fish is auctioned daily at the premises of the port fish market and all transactions are recorded electronically for statistical purposes by the Barcelona Fishers' Association.

We used the daily sale slips containing all transactions of red shrimp (*A. antennatus*) over the period 1994-2008 to calculate the total monthly landings (kg month^{-1}, *lands*), the effort measured as total number of trips performed monthly by each vessel (number of trips per month, *trips*), and the monthly average ex-vessel shrimp price (€ kg^{-1}, *shprice*). The same data set contained information on the engine power (horse power, *hp*) and gross registered tonnage (tons, *grt*), which we used as boat capacity indicators. As an indicator of fishing costs we used the average monthly fuel price (10^{-3} € L^{-1}, *fprice*) from the EUROSTAT website: http://ec.europa.eu/energy/observatory/oil/bulletin_en.htm . As the environmental driver we used the NAO index, taken from the website of the Climate Analysis Group of the University of Exeter (UK): http://www1.secam.ex.ac.uk/cat/NAO. We considered: *nao*1, *nao*2 and *nao*3, corresponding to one, two and three years before the year of observed landings, using the significant time lags reported in Maynou (2008).

The response variable, *lpue*, was estimated as

$$lpue = \frac{lands}{trips} \qquad (1)$$

hence, *lpue* is the monthly average landings of one vessel in each trip, corresponding to one fishing day (kg boat^{-1} day^{-1}), which will form the basis for providing a standardized abundance index.

To assess the individual effect of each vessel, a numeric variable *code* was assigned to each of the 21 vessels in the fleet. Each observation was attributed to a sequential *time* variable from January 1994 to December 2008 (180 months) and a *month* variable describing the month of the year. Two more variables were derived a posteriori from *code* and *month*, after checking for statistical differences among their categories in the model, and then by performing the Tukey Honest Significant Differences test (TukeyHSD). We thus derived the new variables, *group* and *period*, for *code* and *month*, respectively. The *group* variable combines the 21 trawlers into three groups of increasing *lpue* and *period* is a binary variable which classifies the months in "high effect" (*period1*: all months excluding June and November) and "low effect" (*period2*: June and November). All variables are shown in Table 1.

Model construction

We used generalized additive models, GAM, as described by Hastie and Tibshirani (1990)

$$G(y) = x\beta + \Sigma\, s_j(x_j) + \varepsilon$$

where $G(\cdot)$ is the link function, y is the response variable, x is the vector of linear predictors (explanatory variables), β is the corresponding vector of parameters, x_j are scalar predictors with unknown nonlinear effects represented by the functions $s_j(\cdot)$, and ε is the random error.

The model building process consists of the following steps: 1) selection of the underlying distribution of the response (see Section 2.2.2 for more details); 2) selection of predictors building independent models for each covariant deleting insignificant effects in the final model; 3) selection between correlated predictors through the Pearson correlation coefficient (threshold value: ρ=|0.6|) to avoid problems of collinearity (Brauner and Shacham 1998) using the covariant with the most explanatory potential; and 4) analysis of residuals diagnostics.

Table 1. – List of variables.

Variable	description (units)
lpue	landings per unit effort derived from *lands* and *trips* (kg boat^{-1} day^{-1})
lands	total monthly landings per vessel (kg month^{-1})
time	time index of months, t=1, ..., 180, from Jan 1994 to Dec 2008
trips	number of trips performed by each vessel during the time t
hp	engine power of vessels
grt	gross registered tonnage of vessels
shprice	red shrimp ex-vessel price (€ kg^{-1})
fprice	fuel price one month before the observed lands (10^{-3} € L^{-1})
nao_k	mean annual NAO index, k=1, ..., 3 years before the year of observed lands
*month**	12 categories corresponding to months
period	2 categories: *period1*, all months excluding June and Nov; *period2*, June and Nov
*code***	21categories corresponding to a code assigned to each vessel
group	3 categories corresponding to groups of vessel

* Differences between pairs of categories of the variable *month* were checked through Tukey HSD test. Non-significantly different categories were grouped to create the new variable *period*, to which the same test was applied.
** The same procedure was applied for the variable *code*, to create the variable *group* (all significant tests with p<0.001).

All analyses were performed in R3.0.1 (mgcv-Rpackage: Wood 2006). The generalized cross validation (GCV: Craven and Wahba 1979) and the outer Newton iteration procedure were used to estimate model parameters. GCV is preferable to the UBRE/AIC method in the case of unknown smoothing parameters λ (Wood 2006). Second order *P*-spline as defined by Marx and Eilers (1998) was used as a smoother for nonlinear functions.

Theoretical response probability function

Landings per unit effort are usually modelled following Gaussian or gamma distribution functions, often without formal justifications (Stefánsson 1996). Here, we assigned a theoretical probability function to the *lpue*, using nonparametric techniques described by Wassermann (2005). The density function, $f(y_a)$, was estimated using a histogram and the Gaussian kernel, where the *nrd* described by Scott 1992 was the rule-of-thumb used to select the bandwidth.

The empirical cumulative distribution function, $F(y_a)$, and the 95% lower, $L(y_a)$ and upper, $U(y_a)$, confidence intervals were calculated as follows:

$$F(y_a) = [rank(y_a) - 0.5] / N$$

$$L(y_a) = max\{F(y_a) - \varepsilon_a, 0\}$$

$$U(y_a) = min\{F(y_a) + \varepsilon_a, 1\},$$

where $rank(y_a)$ is the ranked vector of observations and ε_a is the associated vector of errors resulting from the DKW (Dvoretzky-Kiefer-Wolfowitz) inequality

$$\varepsilon_a = \sqrt{\tfrac{1}{2n}\log_e\left(\tfrac{2}{\alpha}\right)}$$

The hypothesis tested is H_0: $F(y_a)=F_0(y_a)$ versus the alternative hypothesis H_1: $F(y_a)\neq F_0(y_a)$, where $F_0(y_a)$ is a theoretical function belonging to the exponential family, especially $F_0(y_a)=Ga(a,b)$, the gamma distribution, whose density function is

$$p(y) \propto y^{(a-1)} e^{(-by)}$$

for $y>0$. Parameters a and b are derived from the estimated expectation, $E(y)=a/b$, and variance $Var(y)=a/b^2$. Then the resulting distribution functions were graphically compared.

Selection criteria and explained deviance

Both AIC (Akaike 1973) and percentage of explained deviance (ED) were used as selection criteria: the selected model presented both the lowest AIC and the highest ED and all term parameters significantly different from zero.

The ED for each variable was also calculated in order to determine their relative importance in the final model. The residual deviance of the full model and the deviances of reduced models (i.e. the model excluding variable x_i) were calculated to derive the proportion explained by variable x_i:

$$DE{:}x_i = [D(\text{reduced model}) - D(\text{full model})]/D(\text{null model})$$

where $D(\cdot)$ is the deviance for a given model and in the reduced model variable x_i is omitted.

LPUE standardization

The model used for standardization was built in order to avoid dependency on fleet variables, maintaining environmental variables, which are expected to be related to the natural abundance of the species. The standardized LPUE is then

$$lpue_a = E(lpue) + (lpue - E(lpue|_{\theta=\hat{\theta},\,\lambda=\hat{\lambda}})) \quad (2)$$

where *lpue* is the "nominal" or "raw" LPUE defined in Equation 1, $E(lpue)$ is the unconditional expectation of the LPUE and $E(lpue|_{\theta=\hat{\theta},\,\lambda=\hat{\lambda}})$ is the conditional expectation of the LPUE given the vectors of parameters θ and λ estimated using the appropriate standardization model.

Finally we compared our standardized LPUE with an alternative abundance index derived from fisheries-independent data, available in the technical report SGMED-12-11 (Cardinale et al. 2012, pp. 136-150) after normalization of both variables.

RESULTS

Overview of data and response distribution

Figure 1 provides the raw *lpue* time series as reckoned in Equation 1 with its spline estimation (upper plot) and annual average of the NAO index (lower plot). The *lpue* series, initially constant, started to decline at the end of 1998 with a sharp maximum low in the period 1999-2000. Then the trend changed to inter-annual variation. Conversely, the NAO index shows the lowest records in the period 1995-1996. The *lpue* begins to decrease after three years from the first year of negative NAO. In Figure 2 the time series of the fuel price shows an increasing trend during the observed period (upper panel). The total number of trips per month performed by the whole fleet declines during the same period (middle panel), but it declines only at the beginning of the fuel price rise, then remaining almost constant (lower panel). Low *lpue* in the period 2000-2001 is also related to the peak of *fprice* in the same period (compare upper panels of Figs 1 and 2).

Characteristics of *lpue* are plotted in Figure 3. The probability density function (*pdf*) is positively skewed (upper panels). Data hold atypical values in the right tail (see the box-plot, left middle panel) and the distribution function of the gamma distribution lies approximately inside the 95% confidence intervals of the empirical cumulative distribution function (*ecdf*) of *lpue* (right middle panel). Finally, the QQ-plots for the gamma and the Gaussian distributions provide evidence of a better fit of data to the gamma rather than the Gaussian distribution (on the left and the right lower panels respectively).

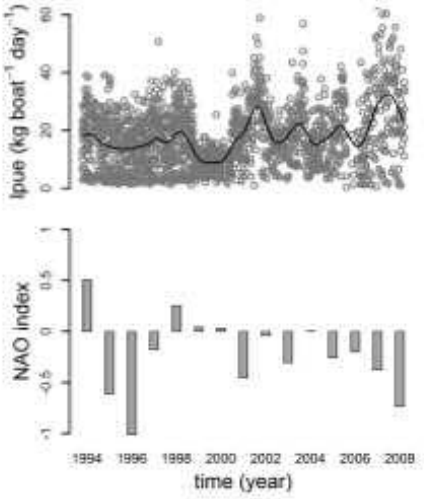

Fig. 1. – Time series from 1994 to 2008 of LPUE data and spline estimation (upper panel) and mean annual North Atlantic Oscillation (NAO) (lower panel).

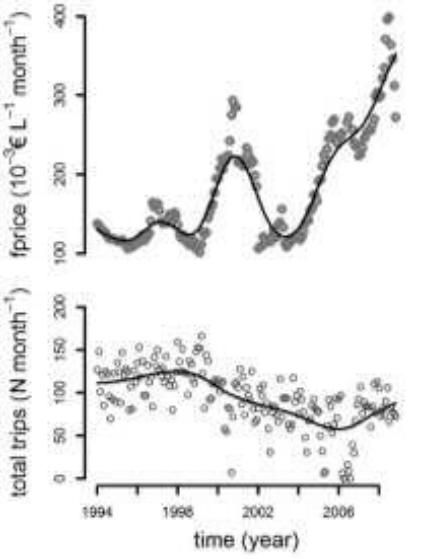

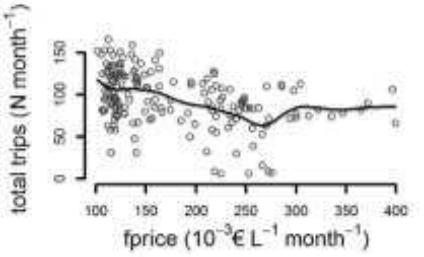

Fig. 2. – From top to bottom: spline estimation of the fuel price, monthly total number of trips performed by the fleet from year 1996 to 2008, and relationship between the fuel price and the total monthly number of trips.

Model building and comparison

The model building process is summarized in Table 2. All linear terms are reported before all smooth functions. Models are sorted in ascending order of total ED, with the exception of models 11 and 12, corresponding to the GLM version of the final model 7 and the standardization model respectively. In comparison with the GLM (model 11), GAM's AIC decreases and the ED increases substantially (1.56 times), though the number of degrees of freedom increases considerably (df_{GAM}=27.7 versus df_{GLM}=9). Variables *grt* and *time* were selected as better predictors than *hp* and *fprice*, respectively, according to the Pearson correlation coefficients (*grt*-*hp* was ρ=0.61; *time*-*fprice* ρ=0.69) and larger ED of former variables. All other correlations were ρ<|0.6|.

Table 2 incorporates the NAO terms, though their explanatory potential in the full model is too weak to be significant. Adding NAO terms to model 7 (Table 2: models 8, 9, 10) did not improve model fit in terms of ED and AIC. Nevertheless, we found significant NAO effect in less complex models.

The descriptive model

The final model for *A. antennatus* LPUE is

$$\log_e(lpue) = \theta + \alpha\, grt + \beta\, period2 + \Sigma_{k=2,3}(\gamma_k\, group_j) + s_1(trips) + s_2(time) + s_3(shprice) + \varepsilon \quad (3)$$

where $lpue \sim Ga(a,b)$, $\log_e$ is the link function, θ is the intercept, α is the parameter associated with the linear effect of *grt*, and β and γ_k are the effects associated with the categorical variables *period* and *group*. $s_j(\cdot)$ are the smooth functions associated with *trips*, *time* and *shprice*, while ε represents the random errors of the model.

Figure 4 shows the diagnostic plots for the selected model. These plots show the results for the best model (corresponding to Equation 3 in the text and model 7 in Table 2). Residual quantiles lie on the straight line of the theoretical quantiles, although slightly heavy-tailed; in the histogram, residuals are consistent with normality and the relationship between response and fitted values is linear and positive. Residuals versus the linear predictor (that is, the sum of all partial effects) show a faint heteroscedasticity.

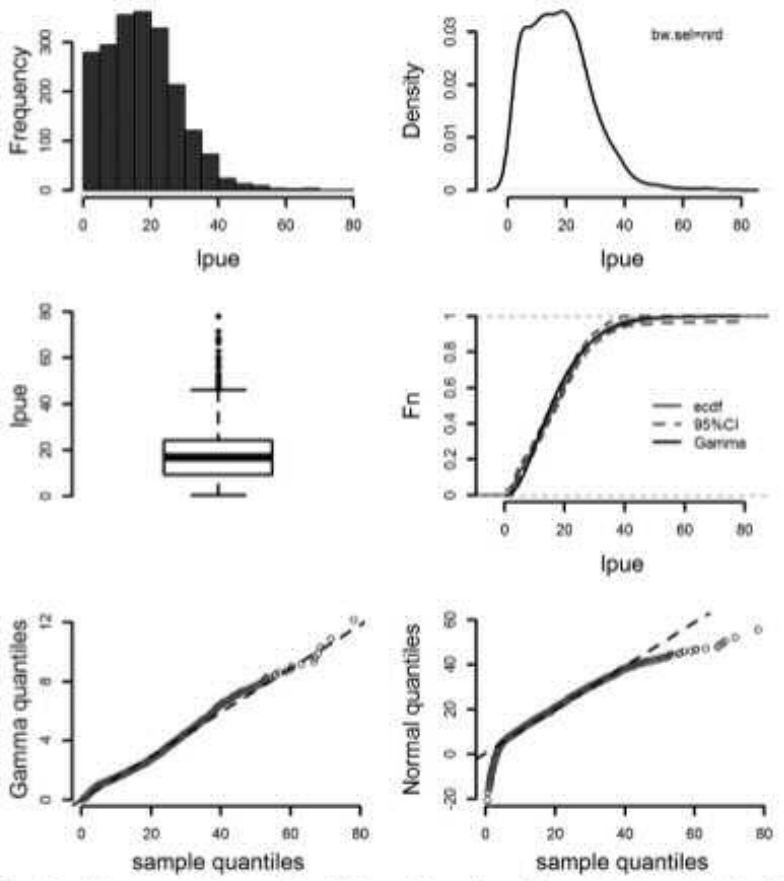

Fig. 3. – From left to right, upper panels, histogram and kernel density estimations of *lpue*; middle panels, box-plot and cumulative distribution function of data and of the gamma distribution; lower panels, QQ-plots of sample quantiles versus gamma and normal distribution quantiles.

Table 2. – Model construction. *N*, number associated with each model; model, model's right part of the formula; *df*, model's degree of freedom; RD, residual deviance, ED, percentage of deviance explained by each model; AIC, Akaike Information Criterion; term$^{(ns)}$, insignificant terms in a model; term$^{(*)}$, terms not incorporated in next steps (i.e. models with the incorporation of *hp* or *fprice* gave a lower ED than the incorporation of *grt* and *time*, respectively). Model 12 is the model used for standardization.

N	*model*	*df*	RD	ED (%)	AIC
1	*Int*	2	863.8	0	13544
2	*Int+hp*$^{(*)}$	3	844.4	2.2	13501
2.1	*Int+grt*	3	815.3	5.6	13432
3	*Int+grt+group*	5	741.0	14.2	13250
4	*Int+grt+group+period*	6	734.7	15	13235
5	*Int+grt+group+period+s(trips)*	8.9	627.8	27.3	12936
6	*Int+grt+group+period+s(trips)+s(fprice)*$^{(*)}$	12.4	614.0	28.9	12900
6.1	*Int+grt+group+period+s(trips)+s(time)*	24.8	527.0	39	12632
7	*Int+grt+group+period+s(trips)+s(time)+s(shprice)*	27.7	493.5	43.0	12512
8	*Int+grt+group+period+s(trips)+s(time)+s(shprice)+s(nao1)*$^{(ns)}$	28.7	493.3	43.0	12513
9	*Int+grt+group+period+s(trips)+s(time)+s(shprice)+s(nao2)*$^{(ns)}$	28.7	493.5	43.0	12514
10	*Int+grt+group+period+s(trips)+s(time)+s(shprice)+s(nao3)*$^{(ns)}$	28.7	493.4	43.0	12513
11	*Int+grt+group+period+trips+time+shprice*	9	626.4	27.5	12932
12	*Int+grt+code+s(trips)*	24.75	608.7	29.5	12910

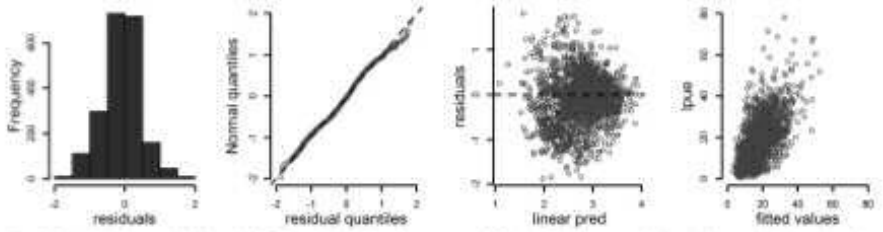

Fig. 4. – Residual diagnostics for model 7. From left to right: histogram and QQ-plot of deviance residuals; deviance residuals against linear predictor; response against fitted values.

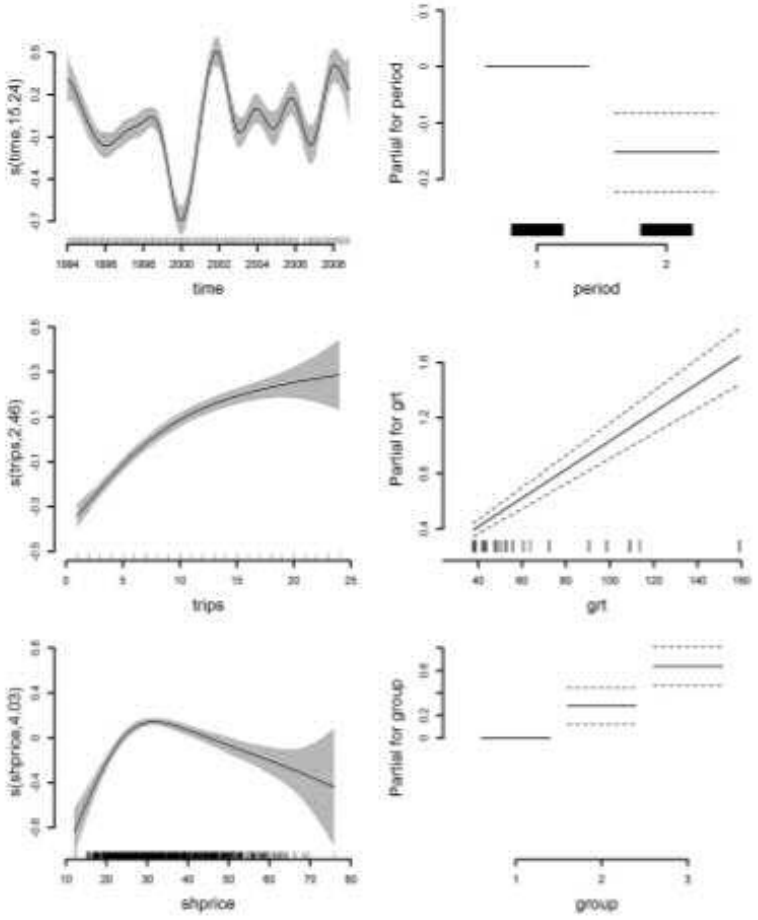

Fig. 5. – Partial effects of model 7. Bayesian credible intervals (95%).

Table 3. – Results of the final model (Eq. 3). Results associated with (a) linear terms, (b) smooth terms and (c) global estimations. Mean, estimation of the mean; std, standard deviation; *t*, value of *t*-statistic; *F*, the *F* statistic value; *p*, p-value to the *t* or the *F* statistic; ED, percentage of deviance explained by each term; *edf*, effective degrees of freedom; λ, estimated smoothing parameter; *df*, total degree of freedom; *sc*, the scale parameter of the regression; R^2(adj), adjusted R-squared; AIC, Akaike Information Criterion; GCV, generalized cross validation; ED tot (%), percentage of total deviance explained by the model.

(a) Linear terms	mean	std	*t*	*p*	ED (%)
intercept	1.746	0.103	16.980	<2e-16	0
period2	-0.152	0.035	-4.383	1.24e-05	0.72
group2	0.281	0.081	3.449	5.75e-04	3.58
group3	0.637	0.086	7.404	2.02e-13	
grt	0.010	0.001	16.205	<2e-16	5.62
(b) Smooth terms	*edf*	λ	*F*	*p*	ED (%)
s(time)	15.239	0.011	24.82	<2e-16	12.40
s(trips)	2.457	30.007	71.01	<2e-16	11.38
s(shprice)	4.026	0.059	26.36	<2e-16	9.30
(c) Global					
df	*sc*	R^2(adj)	AIC	GCV	ED tot (%)
27.722	0.274	0.488	12512	0.282	43.00

Table 3 shows results related to (a) the linear part, (b) the smooth functions and (c) the global parameters of the final model (Eq. 3), with a total explained deviance of 43.00%. The predictor with the highest explanatory potential was *time* (ED=12.40%), which captured the intra-annual fluctuations in red shrimp, *lpue*. The second predictor in terms of explained deviance was *trips* (ED=11.38%). Red shrimp price was the third most important predictor (ED=9.30%). Other variables such as *grt*, *group* and *period* had less impact. The model returned all significant parameters ($p<<0.001$). All partial effects are reported in Figure 5. The partial effect for *time* shows a substantial difference before and after the period 1999-2000, when a clear drop is exhibited in the shape. Before this threshold the shape is almost constant, whereas after the abrupt decay increasing variation is observed over recent years. Predictor *trips* represents a positive and monotonic relationship, reaching a plateau for *trips*>15; *shprice* reached its maximum value around 30 € kg^{-1}; *lpue* was significantly lower for *period2*, representing June and November, than for the rest of the year (*period1*). There were significant differences between the three groups of vessels. Variable *grt* showed a positive linear effect, meaning that larger vessels had higher *lpue*.

LPUE standardization

The model used to standardize *A. antennatus* LPUE is

$$\log_e(lpue) = \theta + \alpha\, grt + \Sigma_{j=1,21}(\gamma_j\, code_j) + s(trips) + \varepsilon \quad (4)$$

where *lpue*~*Ga* (*a*,*b*), θ is the intercept, α the parameter for *grt* and γ_j the effects associated with *code*. *s*(*trips*) is the smooth function for *trips* and ε the random errors. With the aim of standardizing, this model comprises all fleet-dependent variables, whose effect must be removed from the nominal value. The diagnostic plots show reasonably good outputs (not shown).

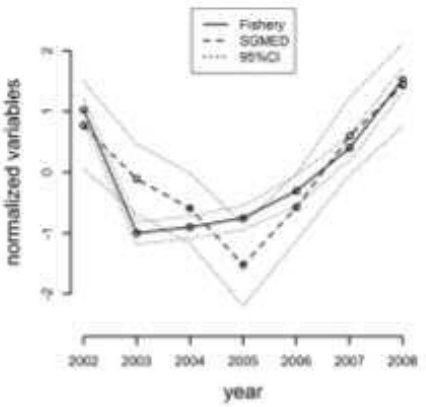

Fig. 6. – Comparison between the fishery-derived index (standardized LPUE) and the SGMED index. Variables have been normalized for comparison.

Finally, LPUE index and the SGMED in 2002-2008 with their confidence intervals after normalization of variables are plotted in Figure 6. The normalized Barcelona fishery's LPUE, calculated using Equations 4 and 2, has narrower confidence intervals than the normalized SGMED index. Only in 2004 were the two indices statistically different and in 2005 index estimates were at the limit of the other CI. Thus, five out of seven estimates can be considered equivalent.

DISCUSSION

This study presents models for relative abundance of *A. antennatus* harvested by one important Catalan fleet in the NW Mediterranean from 1994 to 2008. To our knowledge it is the first combined use of commercial fisheries data from Spain analysing environmental and economic variables with GAM techniques. Our objectives were: 1) to define the relative importance of predictors (model 7, Tables 2 and 3) and 2) to construct a standardized fishery-dependent index to compare with fishery-independent indices (Fig. 6). The results contribute to the identification of simple roles in red shrimp fishery management.

The role of explanatory variables

We incorporated effort, temporal, economic and environmental variables into a global regression model to evaluate their relative importance. Model 7 captures LPUE variability with a total deviance of 43% explained by six predictors. In order to quantify the different sources of LPUE variability, we found that the set of fishery-related variables (*trips*, *grt* and *groups*) was the most important source, with an ED of 20.58%, followed by temporal (*time* and *period*, ED=13.12%) and finally economic variables (*shprice*, ED=9.30%). Among the variables taken from fishery

data, *trips* has provided the greatest impact to date. A low number of trips per month could be associated with generalist trawlers operating usually on the continental shelf and with less knowledge about red shrimp fishing grounds than trawlers specialized in this fishery (Maynou et al. 2003), suggesting that the higher activity of non-specialized trawlers in deep-water harbours yields lower LPUE values (see Fig. 5: partial effect for *trips*). Conversely, boats performing a higher number of trips per month are expert in deep-water fishing grounds and their skippers are more likely to find high-concentration shoals through a process of trial and error (as hypothesized by Sardà and Maynou 1998). Boat characteristics (*grt*) also influence LPUE, as was to be expected. The greater the gross registered tonnage, the higher the LPUE that is observed. The variable *group* captures other capabilities of fishermen and technical characteristics of vessels, such as the type of engine, net shape and skipper's expertise, which have been shown to positively bias the LPUE (Maynou et al. 2003, Marriott et al. 2011) and are expected to be important in many fisheries (Maunder and Punt 2004). The importance of these predictors implies that their influence should be eliminated during standardization.

Inter-annual variable (*time*) is much more important than intra-annual variable (*period*) (Table 3). The former is more strongly determined by a range of sources, such as environmental and economic drivers, than the latter. The same order of importance was found by Maynou et al. (2003). The LPUE was almost constant before 1999–2000, when a sharp decline was observed. We hypothesized a relationship with low NAO in the previous three years (see Fig. 1 and the introduction) that confirms the findings of Maynou (2008) and a possible relationship with the increase in fuel prices beginning in 2000. The following years were characterized by high inter-annual variability, when the price of fuel increased and showed greater variations. We believe that the trend could be explained by economic factors (Fig. 2), especially since very high fuel-related costs are incurred in the fishing of red shrimp as a result of it being performed in deep-water (Sardà et al. 1997).

The partial effect of ex-vessel prices, *shprice*, shows a parabolic-like shape and significant explanatory potential (ED=9.30%). Low selling prices do not induce fishermen to practice this deep-water fishery, because they could not offset the high associated costs, and trawlers would rather switch to continental shelf fisheries, with lower costs and lower risk. When there are profits to be made, probably owing to the low availability of the product, fishermen practice this deep-water fishery more intensely and landings per unit effort also increase. At the higher sales price bracket (i.e. more than about 30 € kg^{-1}) decreasing landing rates mean higher sale prices. Here, an alternation of cause and effect between the two variables probably comes into play. As mentioned, *fprice* is also an important explanatory variable, although it was not inserted in the final model because of its correlation with *time*. Fuel price has a significant effect on LPUE and can reach approximately 1.6% of explained deviance (as can be deduced from the model building process in Table 2).

Implications for management

Obtaining information on deep-sea species population dynamics is notoriously difficult, but our analysis suggests that the peculiarity of red shrimp fishery makes it possible to use fishery-dependent data to accurately describe the relative abundance of this resource. There are no discards for this fishery and the by-catch fraction, represented for example by *Merluccius merluccius* and *Micromesistius poutassou*, is small. These characteristics enable landings to be considered equivalent to catches and interchange LPUE and CPUE as indices (Hilborn and Walters 1992, Denis et al. 2002).

In turn, the definition of the relative importance of explanatory variables enables their impact on LPUE to be understood and makes intervention on the relevant variables possible from a management perspective. Fishery-related variables tend to have a significant effect on LPUE (ED=21% in our case), and management measures aiming to reduce fishing mortality in this heavily harvested stock (Cardinale et al. 2012) could be based on limiting the size of the trawlers. Furthermore, the number of trips permitted in deep-water fishing grounds in this fishery could be limited, for example, by defining a threshold when the number of trips does not significantly increase the partial effect for LPUE (see Fig. 5).

In addition, to evaluate the impact of predictors on the LPUE, the regression analysis could be the basis to provide a standardized index for assessing species stocks. Standardization of landings data allows an index of the real species abundance to be developed, assuming that the explanatory variables available remove (or explain) most of the variation in the data that is not attributable to natural changes (Maunder and Punt 2004). We advocate the selection of effort predictors for standardization.

Trends in CPUE (and LPUE) are usually assumed to reflect changes in the abundance of marine stocks (Maunder and Punt 2004), but the raw index is often not proportional to abundance (Maunder et al. 2006). The raw LPUE is in fact dependent on many human factors that could be avoided. Time variables have a strong relationship with the abundance and environmental factors, which in turn are related to abundance, so they cannot be used in the model during standardization (e.g. see Maunder and Punt 2004). The economic source of variability should be considered, but shrimp price and LPUE realistically have a cause-effect relationship, so they could be not properly used. Conversely, fishery-related variables seem to be the most reliable for this purpose.

During the study period, the fleet was practically constant, making monthly trips a good indicator of fishing effort and landing ability, and remained almost constant despite potential technological creep (Marriott et al. 2011) because no significant changes in fishing technology have occurred in the area in the last 20 years.

Studies of deep-water systems, where harsh conditions limit methods for evaluating fisheries, often suffer from a lack of data in order to assess stock status.

Although the goal of fisheries managers is to promote sustainable production of fish stocks through formal stock assessment, it is often impractical to collect fishery-independent data in isolated or harsh environments. In these cases the information collected by a fishery is the main (or only) source of abundance data available (Maunder et al. 2006).

ACKNOWLEDGEMENTS

The authors would like to express their sincere thanks to the Fisheries Directorate of the Government of Catalonia for giving access to the sales data of the Barcelona Fishers' Association, as well as to fishers of Barcelona. The first author is also very grateful to A. Rodríguez Casal and C. Cadarso Suárez for transmitting their knowledge in nonparametric statistics, to A. Gallen for revising the English and to M. Reyes for his suggestions on the manuscript. G. Aneiros is partly supported by Grant number MTM2011-22392 from the Ministerio de Ciencia e Innovación (Spain). Finally, this study was financed by the Spanish National Research Council (CSIC) through the JAE-predoc grant programme.

REFERENCES

Akaike H. 1973. Information theory as an extension of the maximum likelihood principle. In: Petrov B.N., Csáki F. (eds), Proc. 2nd Int. Symp. Information Theory, Akadémiai Kiadó, Budapest, pp. 267-281.

Ras C., Maynou F., Sardà F., Lleonart J. 2003. Variacions demogràfiques a les poblacions d'espècies demersals explotades: els darrers quaranta anys a Blanes i Barcelona. Inst. Est. Catalans. Arxiu de la Sec. Ciències, Barcelona.

Bertrand J.A., de Sola L.G., Papaconstantinou C., Relini G., Souplet A. 2002. The general specifications of the MEDITS surveys. Sci. Mar. 66: 9-17.

Brauner N., Shacham M. 1998. Role of range and precision of the independent variable in regression of data. Am. Inst. Chem. Eng. J. 44: 603-611. http://dx.doi.org/10.1002/aic.690440311

Brodziak J., O'Brien L. 2005. Do environmental factors affect recruits per spawner anomalies of New England groundfish? ICES J. Mar. Sci. 62: 1394-1407. http://dx.doi.org/10.1016/j.icesjms.2005.04.019

Carbonell A., Carbonell M.S., Demestre M., Grau A., Monserrat S. 1999. The red shrimp *Aristeus antennatus* (Risso, 1816) fishery and biology in the Balearic Islands, western Mediterranean. Fish. Res. 44: 1-13. http://dx.doi.org/10.1016/S0165-7836(99)00079-X

Cardinale M., Osio G.C., Charef A. (eds). 2012. Report of the Scientific, Technical and Economic Committee for Fisheries on Assessment of Mediterranean Sea stocks – part 1. JRC Scientific and Policy Reports. European Commission.

Cartes J.E., Sardà F. 1992. Abundance and diversity of decapod crustaceans in the deep-Catalan sea (western Mediterranean). J. Nat. Hist. 26: 1305-1323. http://dx.doi.org/10.1080/00222939200770741

Craven P., Wahba G. 1979. Smoothing noisy data with spline functions: estimating the correct degree of smoothing by the method of generalized cross-validation. Numer. Mat. 31: 377-403. http://dx.doi.org/10.1007/BF01404567

Denis V., Lejeune J., Robin J.P. 2002. Spatio-temporal analysis of commercial trawler data using General Additive models: patterns of Loliginid squid abundance in the north-east Atlantic. ICES J. Mar. Sci. 59: 633-648. http://dx.doi.org/10.1006/jmsc.2001.1178

Dennard S.T., MacNeil M.A., Treble M.A., Campana S., Fisk A.T. 2010. Hierarchical analysis of a remote, Arctic, artisanal longline fishery. ICES J. Mar. Sci. 67: 41-51. http://dx.doi.org/10.1093/icesjms/fsp220

FAO-FISHSTAT. 2011. FAO Fisheries Department, Fishery information, Data and Statistics Unit. FishstatJ, a tool for fishery statistical analysis, release 2.0.0. FAO, Rome.

Hastie T., Tibshirani R. 1990. Generalized additive models. Chapman Hall, London.

Hilborn R., Walters C.J. 1992. Quantitative Fisheries Stock Assessment. Chapman & Hall, New York. http://dx.doi.org/10.1007/978-1-4615-3598-0

Lassen H., Medley P. 2000. Virtual population analysis. A practical manual for stock assessment. FAO Fisheries Technical Paper. No. 400. FAO, Rome. 129 p.

Lleonart J., Maynou F. 2003. Fish stock assessments in the Mediterranean: state of the art. Sci. Mar. 67: 37-49.

Marriott R.J., Wise B., St John J. 2011. Historical changes in fishing efficiency in the west coast demersal scalefish fishery, Western Australia: implications for assessment and management. ICES J. Mar. Sci. 68: 76-86. http://dx.doi.org/10.1093/icesjms/fsq157

Marx B.D., Eilers P.H.C. 1998. Direct generalized additive modelling with penalized likelihood. Comput. Statist. Data Anal. 28: 193-209. http://dx.doi.org/10.1016/S0167-9473(98)00033-4

Maunder M. N., Punt A. E. 2004. Standardizing catch and effort data: a review of recent approaches. Fish. Res. 70: 141-159. http://dx.doi.org/10.1016/j.fishres.2004.08.002

Maunder M. N., Sibert J. R., Fonteneau A., Hampton J., Kleiber P., Harley S.J. 2006. Interpreting catch per unit effort data to assess the status of individual stocks and communities. ICES J. Mar. Sci. 63: 1373-1385. http://dx.doi.org/10.1016/j.icesjms.2006.05.008

Maynou F. 2008. Environmental causes of the fluctuations of red shrimp (*Aristeus antennatus*) landings in the Catalan Sea. J. Mar. Sys. 71: 294-302. http://dx.doi.org/10.1016/j.jmarsys.2006.09.008

Maynou F., Demestre M., Sánchez P. 2003. Analysis of catch per unit effort by multivariate analysis and generalized linear models for deepwater crustacean fisheries off Barcelona (NW Mediterranean). Fish. Res. 64: 257-269. http://dx.doi.org/10.1016/j.fishres.2003.09.018

Neal R.A., Maris R.C. 1985. Fishing biology of shrimps and shrimplike animals. In: Provenzano A.J. (ed.) The Biology of Crustacea Vol 10: Economic aspects: fisheries and culture. Academic Press Inc.

Orsi Relini L., Mannini A., Relini G. 2013. Updating knowledge on growth, population dynamics, and ecology of the blue and red shrimp, *Aristeus antennatus* (Risso, 1816), on the basis of the study of its statars. Mar. Ecol. 34: 90-102. http://dx.doi.org/10.1111/j.1439-0485.2012.00528.x

Sardà F., Maynou F. 1998. Assessing perceptions: do Catalan fishermen catch more shrimp on Fridays? Fish. Res. 36: 149-157. http://dx.doi.org/10.1016/S0165-7836(98)00102-7

Sardà F., Maynou F., Talló L. 1997. Seasonal and spatial mobility patterns of rose shrimps *Aristeus antennatus* in the Western Mediterranean: results of a long-term study. Mar. Ecol. Prog. Ser. 159: 133-141. http://dx.doi.org/10.3354/meps159133

Scott D.W. 1992. Multivariate Density Estimation: Theory, Practice, and Visualization. Wiley, New York. http://dx.doi.org/10.1002/9780470316849

Stefánsson G. 1996. Analysis of groundfish survey abundance data: combining the GLM and delta approaches. ICES J. Mar. Sci. 53: 577-588. http://dx.doi.org/10.1006/jmsc.1996.0079

Su N.J., Yeh S.Z., Sun C.L., Punt A.E., Chen Y., Wang S.P. 2008. Standardizing catch and effort data of the Taiwanese distant-water longline fishery in the western and central Pacific Ocean for bigeye tuna, *Thunnus obesus*. Fish. Res. 90: 235-246. http://dx.doi.org/10.1016/j.fishres.2007.10.024

Wasserman L. 2005. All of Nonparametric Statistics. Springer, New York.

Wood S. N. 2006. Generalized Additive Models: An Introduction with R. CRC/Chapman Hall, Boca Raton, Florida.

Marine Biodiversity Records, page 1 of 5. © Marine Biological Association of the United Kingdom, 2014
doi:10.1017/S1755267214000153; Vol. 7; e16; 2014 Published online

New records of *Phascolosoma turnerae* (Sipuncula: Phascolosomatidae) from the Balearic Basin, Mediterranean Sea

J.I. SAIZ[1], J.E. CARTES[2], V. MAMOURIDIS[2], A. MECHO[2] AND M.A. PANCUCCI-PAPADOPOULOU[3]

[1]Department of Zoology and Cell Biology, UPV/EHU, PO Box 644, 48080 Bilbao, Spain, [2]Institut de Ciències del Mar (CSIC), Passeig Marítim de la Barceloneta 37-49, 08003 Barcelona, Spain, [3]Hellenic Centre for Marine Research, PO Box 712, 19013 Anavissos, Greece

Specimens of the deep-water sipunculan worm Phascolosoma (Phascolosoma) turnerae *were recently collected from the western part of the Mediterranean Sea. This species is characterized by hooks showing a peculiar anterior stout and long projection at their base. A key to all the* Phascolosoma *species found in the Mediterranean Sea is included.*

Keywords: *Phascolosoma turnerae*, new records, western Mediterranean, sipunculan worm

Submitted 6 August 2013; accepted 24 January 2014

INTRODUCTION

The genus *Phascolosoma* Leuckart, 1828, is one of the most species-rich genera within the phylum Sipuncula (Murina, 1984; Gibbs & Cutler, 1987; Cutler, 1994), with the majority of its species showing a preference for the warmer shallow waters of the world's oceans (Murina, 1975). However, a few phascolosomatid species are rare in their geographical distribution (Cutler, 1994), since they show preferences for deep cold waters instead.

Deep-sea communities in the Mediterranean are poorly known (Bazairi *et al.*, 2010). Recent studies conducted over the slope of the Balearic Basin (western Mediterranean) revealed the presence of deep-sea phascolosomatids (Cartes *et al.*, 2009). They were identified as *Phascolosoma turnerae* Rice, 1985 in a taxonomic checklist of the sipunculan fauna for the Mediterranean Sea (Coll *et al.*, 2010). The new phascolosomatids inhabited muddy bottoms in the Balearic Basin. From this area, a total of 7 other species of sipunculans have been collected (Cartes *et al.*, 2009; Mamouridis *et al.*, 2011; Tecchio *et al.*, 2013) by using different bottom trawls and box-corers at depths between 427 and 2265 m. This relatively high diversity of sipunculans was related to their ability in exploiting particulate organic matter of different quality (more or less degraded), arriving at bathyal depths, as inferred by the quite different stable isotope $\delta^{15}N$ found in *Aspidosiphon muelleri* Diesing, 1851 and *Sipunculus norvegicus* Danielssen, 1869 (respectively 5.39‰ and 9.57‰, Fanelli *et al.*, 2011), two dominant sipunculan species inhabiting the investigated area (Cartes *et al.*, 2009).

After a detailed anatomical study of the phascolosomatid specimens collected, we observed anatomical features unknown to any previously recorded Mediterranean species (Pancucci-Papadopoulou *et al.*, 1999) of the genus *Phascolosoma* Leuckart, 1828. Thus, the aims of the present study are: (1) to report this new faunistic finding for the Mediterranean Sea; and (2) to select reliable characters for the distinction of closely related species. The ecological information of those collected specimens is also discussed.

Corresponding author:
J.I. Saiz
Email: ji.saiz@ehu.es

MATERIALS AND METHODS

Specimens of deep-sea phascolosomatids were collected during trawling operations of the RV 'García del Cid' in the north-western part of the Mediterranean Sea. Station names, coordinates, depths, sampling dates and number of specimens are listed as follows:

—Station BIOM3-OTSB4; 41°07.130′–41°07.841′N 2°22.497′–2°27.977′E; 1039–1103 m; 01/07/2007; 2 specimens.
—Station PROMETEO3 M-28; 41°07′60″N 02°52′16″E; 1500 m; 13 May 2009; 1 specimen.

Immediately after sampling, all samples were preserved in 4% borax-buffered formaldehyde, prepared using seawater. Once in the laboratory, the material was studied using standard dissecting techniques and both binocular and compound microscopes. The species identification was based mainly on the works of Cutler (1994) and Pancucci-Papadopoulou *et al.* (1999). Voucher material was deposited at the Institut de Ciències del Mar (CSIC).

RESULTS

SYSTEMATICS

Phascolosoma (Phascolosoma) turnerae Rice, 1985
(Figure 1A–F)

Trunk 23–44 mm long and 9–12 mm wide, light brown in colour (Figure 1A). Skin opaque to translucent. Papillae

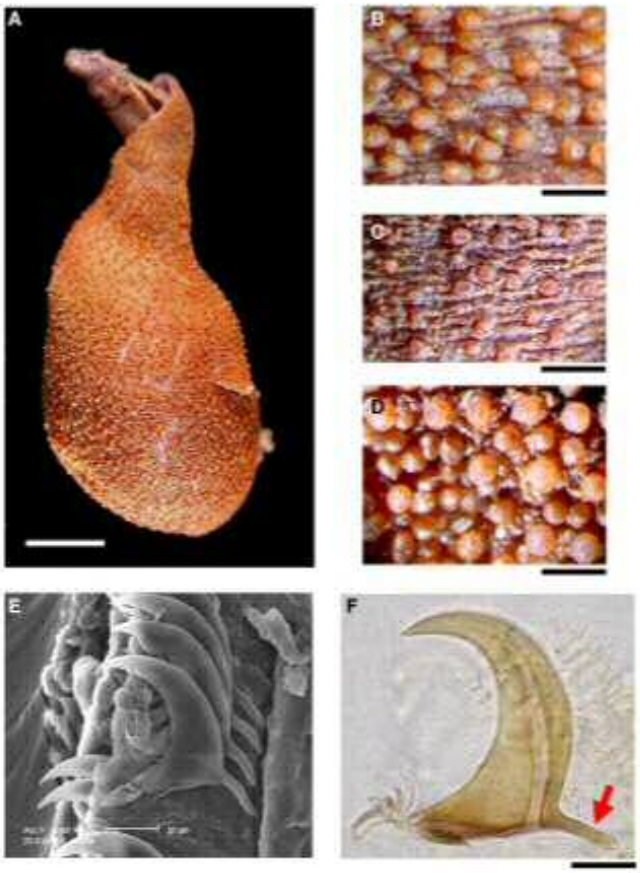

Fig. 1. *Phascolosoma (Phascolosoma) turnerae*: (A) external view; (B) papillae in the anterior part of the trunk; (C) papillae in the middle part of the trunk; (D) papillae at the trunk end; (E) scanning electron micrograph of a hook ring; (F) detail of a hook under the light microscope. Red arrow indicates the characteristic long basilateral extension of the hook. Scale bars: A, 5 mm; B and D, 0.5 mm; C, 0.3 mm; F, 20 μm.

distributed over the entire trunk, larger and more densely packed at both ends (Figure 1B, D). Introvert 25–42 mm long with some pigmented bands. About 28 digitiform tentacles unpigmented. About 90 hook rings, many incomplete. Under the microscope hooks appear slightly curved without a secondary tooth (Figure 1E). Height 50–75 μm. At the posterior base of the hooks there are long toes and a basal wart. A long clear streak with some expansion is noted. No triangles, but with a characteristic long basilateral extension (Figure 1F). Tubuliform papillae about 10 μm high are placed between the hook rings. Internally, the longitudinal musculature has about 30–34 anastomosing bands. Circular musculature also split in fine bands. Four retractors the ventral arising from 6–8 bands, whereas the dorsal arise from 7–8 bands. The distance from the ventral insertions to the trunk end is 5–10 mm. Gut organized in about 15 spirals. Spindle muscle present and attached posteriorly. Two nephridia, 11 mm long with the posterior 2 mm free. Nephridiopores open a little anterior to the anus. Gonads observed at the base of the ventral retractors.

DISCUSSION

A total of 5 species of *Phascolosoma* have been reported from the Mediterranean Sea at coastal waters varying from 0 to 230 m deep (Pancucci-Papadopoulou *et al.*, 1999). The collection of deep-water phascolosomatids in the mainland slope of the Balearic Basin was remarkable, since we were unable to relate them to any representative of the genus *Phascolosoma* for the Mediterranean Sea. According to Cutler (1994), the nature of the hooks appears to be species-specific within this sipunculan genus and a global key for the identification of all valid species was constructed by using basically the detailed study of the hooks under the light microscope. In this way, the

presence of characteristic hooks with anterior prong-like extensions related our specimens to only the two species exhibiting this character: *Phascolosoma turnerae* Rice, 1985; and *P. saprophagicum* Gibbs, 1987. Gibbs (1987) differentiated the two species by: (i) the height of the hooks (> 45–80 µm in *P. turnerae* vs 20–25 µm in *P. saprophagicum*); and (ii) the external shape of the hooks (sharply-pointed in *P. turnerae* vs bluntly-rounded in *P. saprophagicum*). Since our specimens showed sharply bent hooks, 50–75 µm tall, we have identified them with *P. turnerae*.

The faunistic finding is also interesting from an ecological approach. The species was described originally by Rice (1985) inhabiting submerged wood at bathyal depths in the Strait of Florida and the Gulf of Mexico. The large abundance of sipunculans boring the wood persuaded this author to note a biological association between this sipunculan species and the wood. Similarly, our BIOM3-OTSB4 specimens were collected (after 4.5 ha of trawling) together with a large piece (~25 kg) of a tree trunk, some tree leaves (from purple beech, *Fagus sylvatica*) and *Posidonia oceanica* remains, suggesting this ground located near Besós Canyon could be a depocentre area for terrestrial-shelf material. These terrestrial inputs are patchily distributed over the slope (authors, unpublished data), although they are more frequent in the mainland than in the insular slope of the Balearic Basin, with higher levels of total organic matter at 1000–1100 m (Fanelli *et al.*, 2013). $\delta^{13}C$ stable isotope signals on sediments close to the BIOM3-OTSB4 haul (between −23.6‰/−24.8‰ Fanelli *et al.*, 2013) also suggests an enrichment of terrigenous sediments there.

Almost simultaneously Edmonds (1985) described a new species, *Phascolosoma kapalum*, from deep bottoms off Australia. In this paper, there was no indication of wood occupation by the sipunculans. Later on, Edmonds (1992) compared specimens of *P. kapalum* with *P. turnerae* and decided that the two taxa were conspecific, the first name being a junior synonym of the last one. The finding of an extra specimen from a piece of rotting wood off the Great Barrier Reef (Australia) confirmed the character of a deep-sea wood dweller. However, in the review of the subgenus *Phascolosoma* achieved by Cutler & Cutler (1990), they identified further specimens from bathyal depths in the Gulf of Mexico, but this time the association was noted with tubeworm aggregations near a cold water seep. Other more ecological papers (Olu *et al.*, 1996, 2010; MacAvoy *et al.* 2005; Cordes *et al.*, 2006, 2007) reported the species also in mussel beds and sediments at the base of the tubeworm aggregations from different cold seep sites around the Gulf of Mexico, but also offshore the Orinoco River delta in South America (at 1950–2080 m deep in sediment samples).

Another rare phascolosomatid, *P. saprophagicum* Gibbs, 1987, was collected from bathyal depths close to Chatham Island (New Zealand). Several specimens were obtained from the crevices and between the attached mussels on a large piece of decaying bone corresponding to a whale skull. Both *P. saprophagicum* and *P. turnerae* are the only representatives of the genus colonizing bizarre ephemeral habitats in deeper waters. Moreover, both species share this unique basal projection at the anterior base of the hook. Whereas we can suspect the existence of some genetic affinity between the two species, only DNA has been sequenced by now from *P. turnerae* (Kawauchi *et al.*, 2012). Consequently, *P. turnerae* and *P. saprophagicum*, remain separate valid entities, as was proposed in the last monograph about the phylum (Cutler, 1994).

Recently, a comprehensive and detailed study on the reproductive biology and life-history of *P. turnerae* was published (Rice *et al.*, 2012), since the authors were able to maintain several specimens in captivity for long periods of time. Interestingly, other kinds of habitats were reported for the species, such as authigenic carbonate rocks and bundles of plant fibres, which inspired the authors to design artificial collectors of deep-sea phascolosomatids. The species was additionally found in bathyal depths close to the Bahamas and Barbados, showing by now a disjunct geographical distribution of two remote areas: the western Atlantic and south-western Pacific Oceans. To explain this gap, Rice *et al.* (2012) suggested the possibility of a wider distribution than currently known for *P. turnerae*. This hypothesis is today more plausible, with the discovery of *P. turnerae* in bathyal depths of the Mediterranean Sea (Bienhold *et al.*, 2013; our findings). In this way, these locations within the Mediterranean Sea represent an intermediate spot between the two remote areas where the species was previously collected. The presence of *P. turnerae* in the Mediterranean Sea has also implications in a potential connection of disjunct metapopulations of *P. turnerae* from both sides of the Atlantic Ocean. Dispersal trajectories of planktonic larvae were simulated in a recent study of this wood-dwelling species (Young *et al.*, 2012). Its larvae were capable of reaching the mid-Atlantic off Newfoundland, a distance of more than 3000 km, during a long drifting period. Consequently, the possibility of a genetic exchange from west to east in the North Atlantic Drift current is even more probable, specimens of *P. turnerae* having been collected in the Mediterranean Sea.

Finally, we were unable to note a direct association of *P. turnerae* with sunken wood in the western part of the Mediterranean Sea. However, Bienhold *et al.* (2013) did recently by deploying wood colonization experiments offshore the River Nile delta at a depth of 1690 m (eastern Mediterranean Sea). In our case, *P. turnerae* was the only sipunculan species collected in both hauls, while other sipunculans are relatively abundant from other sampling sites (Cartes *et al.*, 2009; Mamouridis *et al.*, 2011; Tecchio *et al.*, 2013) over the investigated slope. In general, surface deposit-feeder invertebrates were poorly represented in the first reported haul (only 1 holothurian, *Mesothuria intestinalis*), while the rest of invertebrates were—based on stable isotope analyses in the same area (Fanelli *et al.*, 2011, in 2013)—both filter feeders (1 bivalve *Abra longicallus*; 1 holothurian *Ypsilothuria bitentaculata*) and carnivores (1 seastar *Ceramaster grenadensis*). This suggests that inputs of fresh organic matter, as found deeper (e.g. over 1600 m, Cartes *et al.*, 2009), are low within the trawled area, indirectly reinforcing the idea that *P. turnerae* would have as food source ephemeral material derived from terrestrial inputs, such as remains of wood.

KEY TO THE GENUS *PHASCOLOSOMA* LEUCKART 1828, FROM THE MEDITERRANEAN SEA (MODIFIED FROM PANCUCCI-PAPADOPOULOU *ET AL.* (1999) TO ACCOMMODATE THE NEW RECORD)

1a. Hooks under the light microscope exhibiting an anterior stout and long projection at the base of their convex side ..... *P. turnerae*

1b. Hooks without an anterior projection at the base of their convex side 2
2a. More than 50 complete and incomplete rings of hooks over the full everted introvert 3
2b. Less than 50 complete and incomplete rings of hooks ..4
3a. Hooks with a posterior crescent area, many >75 µm tall; preanal papillae are smooth cones; pigment bands on introvert ..... *P. stephensoni*
3b. Hooks with a granular triangle at their anterior base, but without crescents, most <75 µm tall; no pigment bands on introvert ..... *P. granulatum*
4a. Large rounded hump on concave side of the hook; preanal papillae smooth, posteriorly directed, cone shaped ..... *P. perlucens*
4b. Concave side of hook smooth or with small tooth 5
5a. Hooks with distinct triangle; narrow band of red cone-shaped preanal papillae ..... *P. scolops*
5b. Hook triangle indistinct or absent; preanal papillae not distinct from dome-shaped trunk papillae *P. agassizii agassizii.*

ACKNOWLEDGEMENTS

This study was funded by the Spanish Ministry of Science projects ANTROMARE (J.E.C. and V.M. ref. CTM2009-12214-C02-01/MAR) and PROMETEO (A.M. ref. CTM2007-66316-C02/MAR). The authors thank all the participants of both scientific cruises. Special thanks to Dr Th. Kanellopoulos for scanning electronic microscope shooting at the HCMR premises in Anavyssos.

REFERENCES

Bazairi H., Ben Haj S., Boero F., Cebrian D., De Juan S., Limam A., Lleonart J., Torchia G. and Rais C. (2010) *The Mediterranean Sea biodiversity: state of the ecosystems, pressures, impacts and future priorities.* Tunis: UNEP-MAP RAC/SPA, 100 pp.

Bienhold C., Pop Ristova P., Wenzhöfer F., Dittmar T. and Boetius A. (2013) How deep-sea wood falls sustain chemosynthetic life. *PLoS ONE* 8, e53590. doi:10.1371/journal.pone.0053590.

Cartes J., Maynou F., Fanelli E., Romano C., Mamouridis V. and Papiol V. (2009) The distribution of megabenthic, invertebrate epifauna in the Balearic Basin (western Mediterranean) between 400 and 2300 m: environmental gradients influencing assemblages composition and biomass trends. *Journal of Sea Research* 61, 244–257.

Coll M., Piroddi C., Steenbeek J., Kaschner K., Lasram F.B.R., Aguzzi J., Ballesteros E., Bianchi C.N., Corbera J., Dailianis T., Danovaro R., Estrada M., Froglia C., Galil B.S., Gasol J.M., Gertwagen R., Gil J., Guilhaumon F., Kesner-Reyes K., Kitsos M.-S., Koukouras A., Lampadariou N., Laxamana E., Lotze H.K., Martin D., Mouillot D., Oro D., Raicevich S., Rius-Barile J., Saiz-Salinas J.I., San Vicente C., Somot S., Templado J., Turon X., Vafidis D., Villanueva R. and Voultsiadou E. (2010) The biodiversity of the Mediterranean Sea: estimates, patterns, and threats. *PLoS ONE* 5, e11842. doi:10.1371/journal.pone.0011842.

Cordes E.E., Bergquist D.C., Predmore B.L., Jones C., Deines P., Telesnicki G. and Fisher C.R. (2006) Alternate unstable states: convergent paths of succession in hydrocarbon-seep tubeworm-associated communities. *Journal of Experimental Marine Biology and Ecology* 339, 159–176.

Cordes E.E., Carney S.L., Hourdez S., Carney R.S., Brooks J.M. and Fisher C.R. (2007) Cold seeps of the deep Gulf of Mexico: community structure and biogeographic comparisons to Atlantic equatorial belt seep communities. *Deep-Sea Research I* 54, 637–653.

Cutler N.J. and Cutler E.B. (1990) A revision of the subgenus *Phascolosoma* (Sipuncula: *Phascolosoma*). *Proceedings of the Biological Society of Washington* 103, 691–730.

Cutler E.B. (1994) *The Sipuncula: their systematics, biology, and evolution.* Ithaca, NY: Cornell University Press, 453 pp.

Edmonds S.J. (1985) A new species of *Phascolosoma* (Sipuncula) from Australia. *Transactions of the Royal Society of South Australia* 109, 43–44.

Edmonds S.J. (1992) A note on *Phascolosoma turnerae* (Sipuncula). *Transactions of the Royal Society of South Australia* 116, 151.

Fanelli E., Papiol V., Cartes J.E., Rumolo P., Brunet C. and Sprovieri M. (2011) Food web structure of the megabenthic, invertebrate epifauna on the Catalan slope (NW Mediterranean): evidence from $\delta^{13}C$ and $\delta^{15}N$ analysis. *Deep-Sea Research I* 58, 98–109.

Fanelli E., Papiol V., Cartes J.E., Rumolo P. and López-Pérez C. (2013) Trophic webs of deep-sea megafauna on mainland and insular slopes of the NW Mediterranean: a comparison by stable isotope analysis. *Marine Ecology Progress Series* 490, 199–221.

Gibbs P.E. (1987) A new species of *Phascolosoma* (Sipuncula) associated with a decaying whale's skull trawled at 880 m depth in the south-west Pacific. *New Zealand Journal of Zoology* 14, 135–137.

Gibbs P.E. and Cutler E.B. (1987) A classification of the phylum Sipuncula. *Bulletin of the British Museum of Natural History, Zoology* 52, 43–58.

Kawauchi G.Y., Sharma P.P. and Giribet G. (2012) Sipuncular phylogeny based on six genes, with a new classification and the descriptions of two new families. *Zoologica Scripta* 41, 186–210.

MacAvoy S.E., Fisher C.R., Carney R.S. and Macko S.A. (2005) Nutritional associations among fauna at hydrocarbon seep communities in the Gulf of Mexico. *Marine Ecology Progress Series* 292, 51–60.

Mamouridis V., Cartes J.E., Parra S., Fanelli E. and Saiz Salinas J.I. (2011) A first temporal analysis on the dynamics of deep-sea macrofauna: influence of environmental variability off Catalonia coasts (western Mediterranean). *Deep-Sea Research I* 58, 323–337.

Murina V.V. (1975) The geographical distribution of marine worms of the phylum Sipuncula of the World Ocean. In Rice M.E. and Todorović M. (eds) *Proceedings of the International Symposium on the Biology of Sipuncula and Echiura Volume 1.* Belgrade, Serbia: Naučno Delo, pp. 3–18.

Murina G.-V.V. (1984) Ecology of Sipuncula. *Marine Ecology Progress Series* 17, 1–7.

Olu K., Sibuet M., Harmegnies F., Foucher J.-P. and Fiala-Medioni A. (1996) Spatial distribution of diverse cold seep communities living on various diapiric structures of the southern Barbados prism. *Progress in Oceanography* 38, 347–376.

Olu K., Cordes E.E., Fisher C.R., Brooks J.M., Sibuet M. and Desbruyères D. (2010) Biogeography and potential exchanges among the Atlantic Equatorial Belt cold-seep faunas. *PLoS ONE* 5, e11967. doi: 10.1371/journal.pone.0011967.

Pancucci-Papadopoulou M.A., Murina G.V.V. and Zenetos A. (1999) *The phylum Sipuncula in the Mediterranean Sea. Monographs on Marine Sciences.* Athens: National Center for Marine Research, 109 pp.

Rice M.E. (1985) Description of a wood dwelling sipunculan, *Phascolosoma turnerae*, new species. *Proceedings of the Biological Society of Washington* 98, 54–60.

Rice M.E., Reichardt H.G., Piraino J. and Young C.M. (2012) Reproduction, development, growth, and the length of larval life of *Phascolosoma turnerae*, a wood-dwelling deep-sea sipunculan. *Invertebrate Biology* 131, 204–215.

Tecchio S., Ramirez-Llodra E., Aguzzi J., Sanchez-Vidal A., Flexas M., Sardà F. and Company J.B. (2013) Seasonal fluctuations of deep megabenthos: finding evidence of standing stock accumulation in a flux-rich continental slope. *Progress in Oceanography* 118, 188–198.

and

Young C.M., He R., Emlet R.B., Li Y., Qian H., Arellano S.M., Van Gaest A., Bennett K.C., Wolf M., Smart T.I. and Rice M.E. (2012) Dispersal of deep-sea larvae from the Intra-American Seas: simulations of trajectories using ocean models. *Integrative and Comparative Biology* 52, 483–496.

Correspondence should be addressed to:
J.I. Saiz
Department of Zoology and Cell Biology
University of the Basque Country/EHU
PO Box 644, 48080 Bilbao, Spain
email: ji.saiz@ehu.es

G.2 Congress presentations

G.2.1 A temporal analysis on the dynamics of deep-sea macrofauna: influence of environmental variability off Catalonia coasts (Western Mediterranean)

Authors: Mamouridis V, Cartes JE, Parra S, Fanelli E, Saiz Salinas JI

Location: 12th Deep Sea Biology Symposium, 7-10 June 2010, Reykjavik, Iceland.

Abstract: A seasonal analysis of deep-sea infauna (macrobenthos) based on quantitative sampling was conducted over the Catalan Sea slope, within Besòs canyon (at ca. 550 m) and on its adjacent slope (at 800 m). Both sites were sampled in February, April, June-July and October 2007. Environmental factors influencing faunal distribution were also recorded in the sediment and sediment/water interface. Dynamics of macrobenthos at the two stations showed differences in biomass/abundance patterns and in their trophic structure. Biomass was higher inside Besòs canyon than on the adjacent slope at 800 m. The community is mostly dominated by opportunistic surface-deposit feeding polychaetes (such as Ampharetidae) and crustaceans (such as *Carangoliopsis spinulosa*) inside Besòs canyon, while subsurface deposit feeders (mainly the sipunculan *Onchnesoma steenstrupii*) were dominant over the adjacent slope. A clearly different taxonomic composition was found on adjacent slope between infaunal and suprabenthic assemblages of polychaetes, the latter collected by a suprabenthic sledge. It was dominated by carnivorous forms (mainly *Harmothoe* sp.) and linked to higher near-bottom turbidity. Inside canyon a clear temporal succession of species in relation to food availability and quality and the proliferation of opportunistic species was consistent with higher variability in food sources (%TOC, C/N, C13) there compared to adjacent slope. This was caused by the influence of terrigenous inputs of river discharges. Spionidae and Flabelligeridae, in general considered as suspension-feeders, were more abundant in June-July coinciding with a clear signal of terrigenous C (depleted C13, high C/N) in sediments. By contrast, during October and under conditions of high water turbidity and increases of %TOM, opportunistic carnivorous polychaetes (Glyceridae, Onuphidae) increased. Total macrobenthos biomass found over Catalonian slopes, were higher than that found in the neighbouring Toulon canyon, probably because the two canyons are conditioned by different terrigenous sources, as the distinct connexion with river flows.

G.2.2 Additive Mixed Models applied to the study of red shrimp CPUE: comparison between frequentist and Bayesian perspectives

Authors: Valeria Mamouridis, Germń Aneiros Pérez2, Carmen Cadarso Suárez, Francesc Maynou

Location: AMEMR, 27-30 June, Plymouth, UK

Type of communication: Poster

Abstract: We explore the formulation of operational predictive models of fisheries resources based on an example dealing with red shrimp (Aristeus antennatus) CPUE in the Catalonian port of Barcelona. We follow a regression analysis framework, using environmental and fleet variables as predictors. Generalized additive mixed models (GAMMs) are proposed as flexible alternatives to the parametric modelling approaches traditionally applied in fishery research (mainly GLMs). Two different approaches are considered and compared: (a) the frequentist approach, using restricted likelihood (REML), and implemented in the R-package mgcv, and (b) Bayesian approach based on two different methods (i) the Markov Chain Monte Carlo simulation (full Bayesian) and (ii) the empirical Bayesian REML, both implemented in the BayesX software. The two main purposes of the study are (1) to highlight the importance of using mixed effects in such models, and (2) to compare the three methods (frequentist REML, empirical Bayesian REML and full Bayesian) for fitting variance components, fixed and mixed effects in selected models.

Frequentist or Bayesian Additive Mixed Models? A comparison of perspectives to provide better estimates of CPUE

Valeria Mamouridis*[1], Germán Aneiros Pérez[2], Carmen Cadarso Suarez[3], Francesc Maynou[1]

Purposes

The CPUE (Catch per Unit Effort) is an index of relative species abundance used in fisheries research.

1. Improve red shrimp (*Aristeus antennatus*) CPUE modelling [1], by the incorporation in a joint model of: (a) additional (environmental and effort) predictors, (b) **random effects** for fishing vessels [2], (c) smooth functions.

2. Compare available methods to achieve aim 1: (a) Frequentist REstricted Maximum Likelihood, REML (**FR**), (b) Empirical Bayesian version of REML (**EB**), (c) Full Bayesian Markov Chain Monte Carlo, MCMC, simulation (**FB**).

The model

The final model, whose three estimations were compared, belongs to the class of GAMMs, Generalized Additive Mixed Models, and is

$$ln(cpue) = \alpha + \beta grt + f(time) + g(trips) + h(nao3) + \gamma p2 + \sum_{j=1}^{J} b_j vessel + \epsilon \quad (1)$$

where $cpue \in Gamma(a, b)$, α, β and γ are the linear fixed parameters, $f(\cdot)$, $g(\cdot)$ and $h(\cdot)$ represent the smooth functions, b_j's are random effects of vessels and ϵ the regression residuals.

Partial effects - EB method

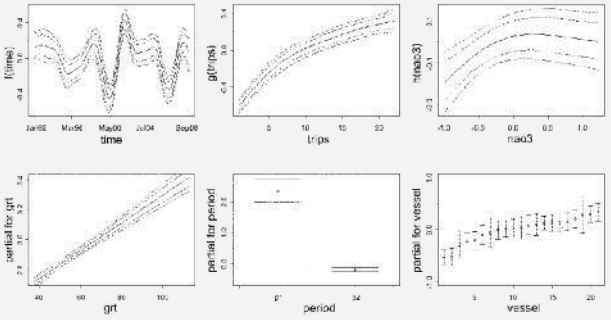

Percentage of Deviance Explained (DE%) by fixed effects.

	$g(trips)$	grt	$period$	$f(time)$	$h(nao3)$	*model* (1)	*linear model*
DE%	14.73	4.73	3.67	2.92	2.54	28.60	18.42

Comparing methods by MSEP

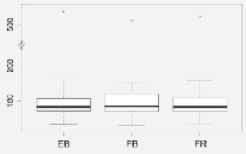

Percentage of the lowest MSEP between FR, EB and FB for the J subsets:

$$\{EB_j < FB_j\} \bigcap \{EB_j < FR_j\} = 48\%$$
$$\{FR_j < FB_j\} \bigcap \{FR_j < EB_j\} = 28\%$$
$$\{FB_j < EB_j\} \bigcap \{FB_j < FR_j\} = 24\%$$

Contacts

* E-mail: mamouridis@icm.csic.es.
1 Institut de Ciències del Mar, CSIC, Psg Marítim de la Barceloneta 37-49, 08003 Barcelona, Spain, 2 Facultade de Informática, Campus de Elviña s/n, 15071, A Coruña, Spain, 3 Facultade de Medicina e Odontoloxía, R/ de San Francisco, s/n, 15782 Santiago de Compostela, Spain.

Goals

1. What is new in red shrimp CPUE model: $(a.i)$ Effort predictor ($trips$) is the most important sources of variability. $(a.ii)$ The NAO (North Atlantic Oscillation) index is to date the only environmental predictor available for deep sea fisheries. (b) Random effects allow to predict for unknown vessels. (c) Smooth functions increase the explanatory power of the model.

2. There is no difference in predictions between methods, however the EB gives lowest MSEP in almost the 50% of subsets.

Variables

Response

$cpue$	monthly CPUE for each vessel, $= landing/\#trips\ (kg\ day^{-1})$ [a], $i = 1, \ldots, 2314$

Predictors

$time$	months from 01-1992 to 12-2008 $t = 1, \ldots, 204$
$vessel$	a numeric code assigned to each vessel, $j = 1, \ldots, 21$
$trips$	number of trips performed by vessel j during month t
grt	Gross Registered Tonnage of vessels
$nao3$	mean annual NAO index of 3 years before the year of observed $landing$
$period$	categorical with 2 levels, $p2$: June and November; $p1$: otherwise

[a] Catches are landed daily and $1\ day = 1\ trip$

Methodology

The frequentist REML was used to obtain the final model (1) with the highest deviance explained, after checking model assumptions (the R-package mgcv [3] was implemented). Predictors were selected by a stepwise forward procedure and 2-nd order P-spline was used as smoother.
Afterwards, model (1) was fitted through the two Bayesian inferences using *BayesX* software [4]. $J = 21$ subsets, excluding $vessel\ j$, were used to estimate model (1) by each method. The mean square error of predictions, MSEP, was calculated on predictions from subset $-j$ on subset j and used as comparative criterion.

References

[1] Maynou, F., Demestre, M., Sánchez, P., 2004. *Fish. Res. 65: 257-269.*
[2] Cooper, A.B., Rosenberg, A.A., Stefánsson, G., Mangel, M., 2004. *Fish. Res. 70: 239-250.*
[3] Wood, S.N., 2011 *J. Roy. Stat. Soc. B , 73: 1, 3-36.*
[4] Brezger, A., Kneib, T., Lang, S., 2005. *J. Stat. Software, 14 (11): 1-22.*

Acknowledgments

Authors thank Dr. T. Kneib for his hints on BayesX usage.

G.2.3 ANALYZING CPUE INDICES IN FISHERY RESEARCH THROUGH STRUCTURED ADDITIVE REGRESSION MODELS

Authors: Mamouridis V, Kneib T, Cadarso Suárez C, Maynou F.

Location: World Fisheries Congress, 7-11 May 2012, Edinburgh, Scotland.

Type of communication: E- poster

Abstract: We explore the formulation of operational predictive models of fisheries resources based on an example dealing with red shrimp (*Aristeus antennatus*) CPUE from the port of Barcelona (NW Mediterranean) between years 1992 and 2008. We follow a regression analysis framework, using temporal, environmental and fleet variables as predictors. At date, the models most commonly used to analyze such index are the Generalized Linear Models (GLM) and more recently Generalized Additive Models (GAM), both by means of the frequentist inference. In the present study we propose an innovative Bayesian approach: the STructured Additive Regression (STAR) models. Inference for STARs can be performed either with a full Bayes (FB) or an empirical Bayes (EB) inference. They comprise a broad class of models, including Generalized Additive Models (GAM) and Generalized Additive Mixed Models (GAMM) which are here presented and compared, using both EB and FB inferences. Still few studies have been related the use of fixed and mixed effects models to fisheries research, comparing GLMs with Generalized Linear Mixed Models (GLMM). A mixed effects model consists of both fixed and random effects. Fixed effects are parameters associated with certain repeatable levels of a factor or with the entire population, while random effects are associated with unrepeatable levels drawn at random from the population. Depending on researcher's purposes, an effect can be considered either fixed or random. According to this definition, in the majority of fishery context, the effect of the fishing vessel must be considered as random. In the present work we discuss both alternatives. The main purposes of this study are: 1. Propose for the first time STAR models for analyzing abundance indices, providing a guide in the construction of models; Highlight the validity of both fixed and mixed effects models depending on studies purposes.

G.2.4 Frequentist or Bayesian Mixed Models? A comparison to provide better estimates of CPUE

Authors: Mamouridis V, Cadarso Suárez C, Aneiros Pérez G, Maynou F. *Location*: BAS2012, Barcelona, Spain

Frequentist or Bayesian Mixed Models? A comparison to provide better estimates of CPUE
Student oral presentation

Valeria Mamouridis[1], Carmen Cadarso Suarez[2], Germán Aneiros Pérez[3], Francesc Maynou[1]

[1] Institut de Ciències del Mar, CSIC, Psg Marítim de la Barceloneta 37–49, 08003 Barcelona, Spain. E-mail: mamouridis@icm.csic.es
[2] Facultade de Medicina e Odontoloxía, R/ de San Francisco, s/n, 15782 Santiago de Compostela, Spain.
[3] Facultade de Informática, Campus de Elviña s/n, 15071, A Coruña, Spain.

Abstract: Generalizad Additive Mixed Models were used to make up a regression analysis applied to red shrimp CPUE. Mixed Models are required when units are not repeatable, such as the case of fishing boats. We also compared the methodologies actually in use: the frequentist REML, the full Bayesian by MCMC tecniques and the empirical Bayesian methods.

Keywords: GAMM; Fisheries; CPUE; REML; MCMC.

1 Introduction

In fisheries research, regression models are often used to analyze CPUE (Catch per Unit Effort), an index of relative abundance of an exploited species. To date CPUE has been mainly analyzed through Generalized Linear Models (GLM), e.g. Goñi et al. (1999), and rarely Generalized Additive Models (GAM) e.g. Damalas et al. (2007). Instead, fishery data usually hold a random nature, being associated to fishing vessels, that are in fact unrepeatable units. That is not conteplated in such kind of models. In very few occasions random effects has been considered, e.g. using Generalizad Linear Mixed Models (GLMM), e.g. Cooper et al. (2004).
On the other side, recent advancements in regression methodologies provide many estimators of random effects in a Generalized Additive Mixed model (GAMM) framework using frequentist (Lin and Zhang, 1999) or Bayesian (Fahrmeir and Lang, 2001) inference.
In this work we present a regression analysis of red shrimp (*Aristeus antennatus*) CPUE from the port of Barcelona (Spain). The last update of red shrimp CPUE modeling in the NW Mediterranean Sea was through GLM (Maynou et al, 2003).

2 Methodology

WE can devide the methodology in two steps:

1. The frequentist REML was used, implementing the R-package mgcv (Wood, 2006), to obtain the final model, that is, after checking assumptions, the one with the highest deviance explained (DE%). Predictors were selected by a stepwise forward procedure and 2-nd order P-spline was used as smoother.
2. Afterwards, the final model was fitted using the two Bayesian inferences as well, with the implementation of *BayesX* software (Brezger et al., 2005). $J = 21$ subsets, excluding *vessel* j, were used to estimate the model by each method. Then they were compared using the mean square error of predictions, MSEP, calculated on predictions from subset $\{J - j\}$ on subset $\{j\}$.

Variables implemented in the model are reported in Table 1.

TABLE 1. Variables used in the study.

Name	Description
y	monthly CPUE for each vessel, $i = 1, \ldots, 2314$
time	months from 01-1992 to 12-2008, $t = 1, \ldots, 204$
ves	a numeric code assigned to each vessel, $j = 1, \ldots, 21$
trips	number of trips performed monthly by each vessel, j during month t
grt	Gross Registered Tonnage of vessels
nao3	NAO index of 3 years before the observed *cpue*
period	season variable with 2 levels, *p2*: Jun and Nov; *p1*: otherwise

3 Results

The selected final model belongs to the class of GAMMs:

$$ln(y) = \alpha \beta \ \ grt + f(time) + g(trips) + h(nao3) + \gamma p2 + \sum_{j=1}^{J} b_j ves + \epsilon \quad (1)$$

where $\epsilon \in Gamma(a, b)$.
The partial effects of model 1 are visualized in Figure 1. Effort predictor (*trips*) is the most important sources of variability. The NAO (North Atlantic Oscillation) index is to date the only environmental predictor available for deep sea fisheries. Random effects allow to predict for unknown boat effects. Smooth functions increase the explanatory power of the model.

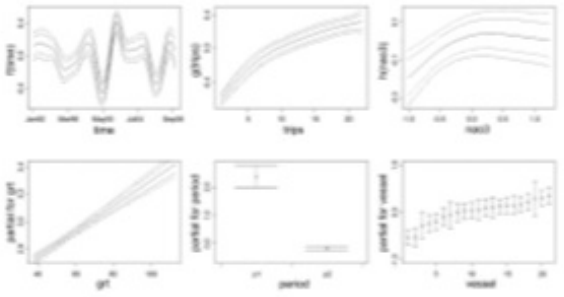

FIGURE 1. Partial effects of model 1 estimated through EB method.

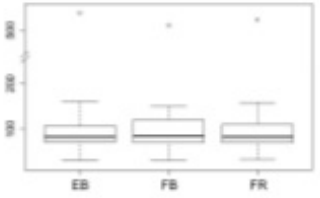

FIGURE 2. Box plot of MSEP estimated for the different methods.

Figure 2 shows that there is no difference in predictions between methods, however the EB gives lowest MSEP in almost the 50% of subsets.

4 Conclusion

That study updates the red shrimp CPUE modeling through the implementation of effort and environmental predictors, of smooth functions and random effects. It also demonstrate that there is no difference in predictions between methods. The use of mixed models permits to infer on the entire population however when units, boats in this case, are not repeatable.

Acknowledgments: Authors thank Dr. T. Kneib for his hints on BayesX usage.

References

Brezger, A., Kneib, T., Lang, S. (2005). BayesX : Analyzing Bayesian Structured Additive Regression Models. *Journal of Statistical Software*, **14** (11), 1-22.

Cooper, A.B., Rosenberg, A.A., Stefánsson, G., Mangel, M. (2004). Examining the importance of consistency in multi-vessel trawl survey design based on the U.S. west coast groundfish bottom trawl survey. *Fisheries Research*, **70**: 239-250.

Damalas, D., Megalofonou, P. and Apostolopoulou, M. (2007). Environmental, spatial, temporal and operational effects on swordfish (*Xiphias gladius*) catch rates of eastern Mediterranean Sea longline fisheries. *Fisheries Research*, **84**, 233-246.

Fahrmeir, L. and Lang, S. (2001). Bayesian inference for generalized additive mixed models based on Markov random field priors. *Journal of the Royal Statistical Society C*, **50**, 201-220.

Goñi, R., Alvarez, F. and Adlerstein, S. (1999). Application of generalized linear modeling to catch rate analysis of Western Mediterranean fisheries: the Castellón trawl fleet as a case study. *Fisheries Research*, **42**, 291-302.

Lin, X. and Zhang, D. (1999). Inference in generalized additive mixed models using smoothing splines. *Journal of the Royal Statistical Society, Series B*, **61**, 381-400.

Maynou, F., Demestre, M. and Sánchez, P. (2004). Analysis of catch per unit effort by multivariate analysis and generalised linear models for deep-water crustacean fisheries off Barcelona (NW Mediterranean). *Fisheries Research*, **65**, 257-269.

Wood, S.N. (2006). *Generalized Additive Models: An Introduction with R*. CRC Chapman & Hall, Boca Raton, Florida.

G.2.5 Dynamic simulations of food webs with R

Authors: Valeria Mamouridis, Laurine Burdorf, Karline Soetaert *Location*: BAS2012, Barcelona, Spain

Dynamic simulations of food webs with R
Student oral presentation

Valeria Mamouridis[1], Laurine Burdorf[2], Karline Soetaert[2]

[1] Institut de Ciències del Mar, CSIC, Psg Marítim de la Barceloneta 37-49, 08003 Barcelona, Spain.E-mail: mamouridis@icm.csic.es
[2] NIOZ (Royal Netherlands Institute for Sea Research) Yerseke, Korringaweg 7, P.O. Box 140, 4400 AC Yerseke, The Netherlands.

Abstract: We present a methodology to create and dynamically simulate food webs in the open source software R. This is done in three steps. First a plausible binary food web is generated with a preset number of species (S) and links (L). Then a quantified steady-state foodweb is generated using linear inverse modeling (LIM) techniques. Thirdly, the food web flows are converted into dynamic formulations. The flexibility of this methodology allows to study the stability of these webs and how they react when perturbed.

Keywords: food webs; linear inverse models; dynamic models.

1 Introduction

Food webs describe who eats whom in an ecosystem. For a given number of species S, and links L, a food web can be represented by an $S \times S$ matrix **S**, where if the species i is a prey of species j then element $s_{i,j} = 1$ while $s_{i,j} = 0$ otherwise. This is a "binary food web". However, species interactions are only feasible if enough energy is transferred to the predator. To assess the energetic feasibility, a foodweb needs to be quantified. This generates a $S \times S$ flow matrix **X**, whose elements x are estimates of the magnitude of each feeding flow. This is a "quantified food web".
Theoretical ecologists have suggested simple models to generate binary food webs, based on the assumption that $L \in U(0,1)$ (i.e. random and cascade models: Cohen and Newman, 1985) or $L \in B(\alpha\beta\ )$, (i.e. niche model: Williams and Martinez, 2000; and nested-hierarchy model: Cattin et al. 2004). The two latter models describe more realistic food webs.
On the other hand, applied ecologists have used Linear Inverse Modeling (LIM) to quantify the flows of real food webs (see van Oevelen et al., 2010), given an incomplete data set. The LIM methodology consists in solving the following linear problem for the unknown flows x:

$$\mathbf{Ex} = \mathbf{F} \quad (1)$$
$$\mathbf{Ax} \approx \mathbf{B} \quad (2)$$

$$\mathbf{Gx} > \mathbf{H} \tag{3}$$

Here the first and/or second set of equations typically contain the component's mass balance equations and observed data, while the third set of equations holds physiological information and positivity constraints (i.e. the flows have a direction).
A LIM returns a "steady-state" snapshot of a food web, although the behavior of food webs under changing conditions is often of interest. This implies that the food web should be written as a dynamic model and solved by numerical integration.
Recently the R software has been made suitable for solving LIMs and for dynamic simulation thanks to two add-on packages (the R-package limSolve (Soetaert et al., 2009), and deSolve (Soetaert et al., 2010).

2 Methodology

We present how these three approaches can be combined in R:

1. We first generate binary food webs according to a theoretical model. Three functions generate the random, the cascade and the niche binary webs.

2. We then check the (energetic) feasibility, using the LIM methodology and quantify the flows. To do this, we convert the binary matrices into a LIM (1) assuming a minimal "growth efficiency" when consuming a species. If the LIM can be solved, then the problem is feasible and allows to estimate the flows.

3. The stability and long-term behavior of the quantified food web is then studied in dynamic simulations. To generate the dynamic system the species biomasses are needed, to convert the total ingestion and respiration rates into mass-specific rates and second order rates. We assumed allometric scaling of rates according to the trophic level of each species. The Jacobian matrix of the dynamic system allows to check the model's stability properties.

3 Examples

Figure 1 gives an illustration of the three types of simulated food webs. The random model was not feasible and could not be solved given the energetic constraints, so its flows are not represented. The cascade and niche model were feasible and the flows could be quantified. Figure 2 represents the the dynamic simulation made for the niche food web. The output represents a stable unperturbated foodweb (black line), and an increasingly instable foodweb when perturbed (the red and green lines).

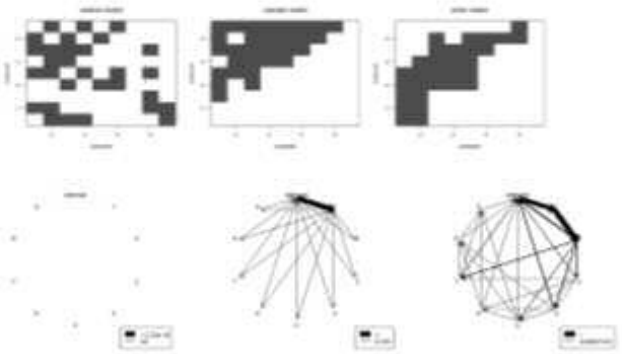

FIGURE 1. The binary food web and the quantitative food web for the three theoretical models.

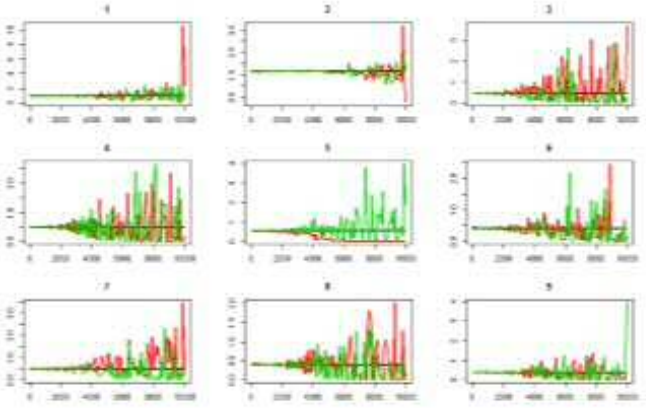

FIGURE 2. Output of the dynamic simulation for a niche food web.

4 Conclusion

The functions implemented in the open source framework R will allow to study the effect of human and environmental perturbations on artificially

generated food webs.

Acknowledgments: The first author thanks to the CSIC grant program JAE-predoc, that made possible this study.

References

Cattin, M-F., Bersier, L-F., Banasek-Richter, C. et al. (2004). Phylogenetic constraints and adaptation explain food-web structure. *Nature*, **427**, 835-837.

Cohen, J.E. and Newman, C. M. (1985) A stochastic theory of community food webs I. Models and aggregated data. *Proceeding of the Royal Society of London, B*, **224**, 449461.

Soetaert, K., Van den Meersche, K., van Oevelen, D. (2009) limSolve: Solving Linear Inverse Models. R-package version 1.5.1.

Soetaert, K., Petzoldt, T. and Setzer R.W. (2010). Solving Differential Equations in R: Package deSolve. *Journal of Statistical Software*, **33** (9), 1-25.

van Oevelen, D., Van den Meersche, K., Meysman, F.J.R., et al. (2010). Quantifying Food Web Flows Using Linear Inverse Models. *Ecosystems*, **13**, 32-45.

Williams, R.J. and Martinez, N.D. (2000). Simple rules yield complex food webs. *Nature*, **404**, 180183.

G.2.6 Structured Additive Distributional Regression in Fishery Research

Author: Valeria Mamouridis

Location: 29/10/2013, Aula Departamento de Análise, Facultad de Matemáticas, USC, Santiago de Compostela, Spain

Type of communication: conference

Structured Additive Distributional Regression in Fishery Research

Valeria Mamouridis
Institut de Ciències del Mar (ICM-CSIC)
mamouridis@icm.csic.es

The quantification of abundance or biomass of an exploited species is extremely important in fishery research, so that indices of relative abundance are widely used to assess the status of the stock and manage the fishing activity. Indices of relative abundance are widely used for these purposes. They are influenced by many factors, some of which if not considered could lead to biased interpretations of stock states. Those indices are influenced by many factors, some of which, if not considered, could lead to biased interpretations of stock states. Regression analysis has become common in this field in order to define the different sources of variability (e.g. time, seasonality and fleet characteristics, among others) and eliminate those that deviate the index from the natural abundance of the species in a process named standardization (Maunder and Punt, 2004). In standard statistical models, it is often assumed that some of the influential variables have a simple linear impact, which may be not flexible enough. An alternative could be the use of semi-parametric models. Another important aspect is the choice of the response distribution. In most cases skewed distributions have been considered, including the gamma, the log-normal and delta distributions (e.g. Maynou et al., 2003; Brynjarsdóttir and Stefánsson, 2004; Gavaris, 1980). Furthermore, data are collected for a limited ensemble of catching units, e.g. the trawling boats. This implies to acknowledge the fact that the catching units represent a sample from the population and leads to the use of random effects. Finally, explanatory variables could influence the expectation but also higher moments of the response distribution, such as scale or shape.

The complexity of data in fishery research can be captured only partially by classical models such as generalised additive models (GAM, Hastie and Tibshirani, 1986) or the more recent generalised additive mixed models (GAMMs, Wood, 2006). A wider approach is given by the class of generalised additive models for location, scale and shape (GAMLSS, Rigby and Stasinopoulos, 2005), which Bayesian equivalent is represented by structured additive distributional regression (DSTAR: Klein et al., 2013). DSTAR models provide efficient approximations using Markov Chain Monte Carlo inference to deal with a variety of aims related to this applied field: 1) the possibility to estimate both linear and smooth effects, 2) the selection within different distribution function, 3) the incorporation of fixed and random effects and 4) the estimation of further parameters of the distribution than the location.

The talk aims to demonstrate the flexibility of DSTAR in modelling abundance indices and to provide a guidance for the model choice and variable selection, questions that arise in the process of developing an appropriate model for a given data set.

References

Brynjarsdóttir, J., Stefánsson, G., 2004. Analysis of cod catch data from Icelandic groundfish surveys using generalized linear models. Fisheries Research 70.2: 195-208.

Hastie, T. J., Tibshirani, R. J., 1990. Generalized Adolitive Models. No. 43. CRC Press.

Gavaris, S., 1980. Use of a multiplicative model to estimate catch rate and effort from commercial data. Canadian Journal of Fisheries and Aquatic Sciences 37.12: 2272-2275.

Klein, N., Kneib, T., Lang, S., 2013. Bayesian Generalized Additive Models for Location, Scale and Shape for Zero-Inated and Overdispersed Count Data. Technical Report.

Maunder, M. N., Punt, A. E., 2004. Standardizing catch and effort data: a review of recent approaches. Fisheries Research 70.2: 141-159.

Maynou, F., Demestre, M., Sánchez, P., 2003. Analysis of catch per unit effort by multivariate analysis and generalised linear models for deep-water crustacean fisheries off Barcelona (NW Mediterranean). Fisheries Research 65.1: 257-269.

Rigby, R. A., Stasinopoulos, D. M., 2005. Generalized additive models for location, scale and shape. Journal of the Royal Statistical Society: Series C (Applied Statistics) 54.3: 507-554.

Wood, S., 2006. Generalized additive models: an introduction with R. CRC Press.

G.2.7 Multivariate techniques in ecology: The infauna associated to a CWC habitat (facies of *Isidella elongata*), influences of fishing activity and natural variability. Oral presentation.

Authors: Valeria Mamouridis

Location: 11th of June, 2014 Faculty of Medicine, University of Santiago de Compostela, Spain

Abstract: Deep-sea communities associated to the so-called cold water corals (CWC), show unique complexity and species diversity, because corals act as potential areas of foraging, refuge and breeding for many deep-sea species, enhancing their ecological dimensions. In early 90, the coral *Isidella elongata* formed pristine forests on soft sediments in the north-western Mediterranean but from 1996 the habitat has been subjected to fishing activity. During the present study we found pour density colonies of the coral (decreased from 255 colonies/ha to 0.9 colonies/ha). We analysed infauna samples from two different habitats, mud and coral mud habitats, through multivariate analysis. We also investigated possible mesoscale gradients related to environmental variability. Despite the start of the fishing, we found that samples were segregated mainly according to the habitat, but also high variability within the same habitat has been observed. The coral mud habitat showed higher heterogeneity of species composition and biomasses and was dominated by detritivores (mainly crustaceans), while in mud habitat we found higher importance of carnivorous than in coral mud habitat. The higher quality of organic source in coral mud habitat and other favorable environmental variables with respect to the mud habitat permit to identify different infaunal assemblages.

G.2.8 EFFECTS OF DEEP-SEA FISHERIES ON THE DYNAMICS OF BATHYAL FOOD WEBS (NW MEDITERRANEAN). Oral presentation.

Authors: Valeria Mamouridis

Location: 11th of June, 2014 Faculty of Medicine, University of Santiago de Compostela, Spain

Abstract: We explored the dynamics of a food web (who eats whom) in the bathyal ecosystem of the NW Mediterranean at 600-650m depth using real data from 8 cruises performed during years 2007 and 2011. This ecosystem is historically subjected to the fishery of red shrimp. We considered two inputs of carbon: the organic matter from the vertical fall through the water column and from the advective transport through the slope, and four outputs (loss of carbon): the burial process in sediments, the dissipation through respiration, and the loss due to the fishing activity on target (red shrimp) and on no- target species (fish and few invertebrates, called by-catch). Internal components of the food web are: the total organic matter in sediment, the macrobenthos, the zooplankton- micronekton and the suprabenthos, that rely directly on the organic matter in sediments and inputs, and the megafauna components (megabenthos, megaichthyofauna and the red shrimp), that prey on previous compartments. The most of the carbon flows through the macrobenthos, that play a key structural role in the community. The actual fishing effort and its low changes makes components to oscillate around their mean values, while its removal affects substantially the megabenthos (big invertebrates), that shows an initial decrement of its biomass and a recovery after long term (20 years). Changes in fishing activity also produce alternations of top predators' biomass as a result of competition.

The macrofauna associated to the deep-sea coral *Isidella elongata*: human impact and natural variability

V Mamouridis[1]*, JE Cartes[1] & E Fanelli[2]

1. Institut de Ciències del Mar (CSIC), Passeig Marítim de la Barceloneta 37-49, 08003 Barcelona, Spain.
2. Marine Environment Research Center - ENEA Santa Teresa, Pozzuolo di Lerici 19032 (SP) Italy.

⋆ mamouridis@icm.csic.es

Introduction

Deep-sea habitats associated to cold water corals (CWC) show unique complexity and species diversity, acting as potential areas of foraging, refuge and breeding for many deep-sea species enhancing their ecological niche dimensions. An example is the bamboo coral *Isidella elongata* that formed pristine forests on soft sediments off the Ebro river mouth (NW Mediterranean) till 1996, when *Isidella* habitat began to be subjected to fishing activity [1].

Main Objectives

1. Analyse the infauna associated to two different habitats: (a) mud habitat, and (b) mud coral habitat.
2. Define the differences in biomass, abundance and taxonomic diversity between both habitats.
3. Investigate possible mesoscale gradients related to environmental variability.

Materials and Methods

Figure 1: The study area.

The study area is located on the slope of the Catalan Sea, NW Mediterranean (Figure 1): we sampled three stations at 613-619 m depth in June 2011. St1 (a) is in a mud habitat without the *Isidella elongata* and a fishing ground since 50's; St2 and St3 (b) are mud coral habitat, subjected to rather low fishing activity since mid 90's, with 2-3 boats sporadically operating in the area [2]. Here coral density has reduced from 255 to 0.9 colonies/ha [2].

We collected (macro)infauna using a Reyneck box-corer, with a surface of 0.065 m^2 cm and then sieved samples through 0.5 mm mesh size (4 replicates per station, N=12). We collected also environmental variables: temperature (T5mab), salinity (S5mab), turbidity (Turb5mab) and oxygen concentration (O5mab) in the near-bottom water and total organic matter (tom) and redox potential in sediments at 1 and 5 cm from surface (mv1cm, mv5cm). All statistical analysis were performed using the R-package Vegan v2.0-10.

Results

A total of 81 taxa has been identified. For the five major groups were counted in ascending order 35 taxa of polychaets, 25 crustaceans, 8 mollusca, 5 sipunculans and 2 echinoderms. The overall abundance and biomass were 392.30±138.30 n/m^2 and 3.42±4.68 g/m^2 respectively and specifically, in mud habitat were 407.69±164.98 n/m^2 and 0.97±0.98 g/m^2 and in mud coral habitat 384.61±134.87 n/m^2 and 4.64±5.38 g/m^2.

factor	R	F	δ
habitat	0.11^{ns}	1.73**	0.90**
station	0.25*	1.53**	0.91*

Table 1: ANOSIM (R), PERMANOVA (F) and MRPP (δ) tests. Response: biomass, explanatory factors: habitat and station.

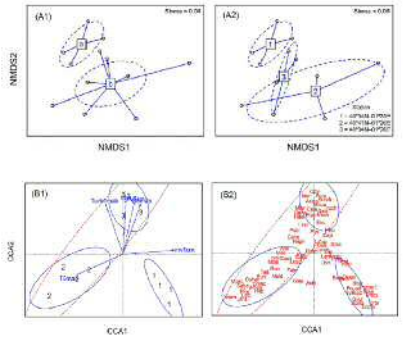

Figure 2: (A) nMDS on biomass matrix. Points represent boxcorers. In (A1) ellipses define 95% confidence areas from centroids according the habitat, (a = mud, b = mud coral) and in (A2) according to stations (St1, St2, St3). Replicates of same levels are combined with the corresponding centroid. (B) CCA constrained with factors habitat and position (coordinates) on biomass matrix: (B1) the sites ordination (numbers) with environmental variables (vectors), that all returned significant relationship with two first dimensions ($\leq$0.005), (B2) the corresponding species ordination. Ellipses depict 0.95 confidence regions of factor station (continuous lines) and habitat (dashed line).

	Taxa	ab	rel	cum		Taxa	ab	rel	cum
(a)	*Prochaetoderma* spp.	50.00	11.81	11.81	(b)	*Leucon longirostris*	26.92	6.54	6.54
	Leucon longirostris	34.61	8.18	20.00		*Chelator chelatus*	17.30	4.20	10.74
	Ennucula aegeensis	30.76	7.27	27.27		*Prochaetoderma* spp.	17.30	4.20	14.95
	Amphipholis squamata	30.76	7.27	34.54		*Kelliella miliaris*	15.38	3.73	18.69
	Carangoliopsis spinulosa	26.92	6.36	40.90		*Aricidea* sp.	13.46	3.27	21.96
	Prionospio spp.	15.38	3.63	44.54		Maldanidae	13.46	3.27	25.23
	Scololepis sp.	15.38	3.63	48.18		*Harpinia dellavallei*	13.46	3.27	28.50
	Oweniidae	11.53	2.72	50.90		*Harpinia truncata*	13.46	3.27	31.77
						Nematoda	13.46	3.27	35.04
						Carangoliopsis spinulosa	11.53	2.80	37.85
						Levinsenia gracilis	9.61	2.33	40.18
						Prionospio sp.	9.61	2.33	42.52
						Syllidae sp.	9.61	2.33	44.85
						Pseudogerda filipes	9.61	2.33	47.19
						Ostracoda	9.61	2.33	49.53
						Amphipholis squamata	9.61	2.33	51.86

Table 2: Mean taxa abundance (ab, n/m^2) calculated for (a) mud and (b) mud coral habitats. rel: relative, and cum: cumulative percentages up to 50% of the total.

Conclusions

- Habitat (nMDS A1) and stations (nMDS A2) were the main factors in sample segregation when considering biomasses, that are significantly higher in mud coral habitat (b), while abundances are higher in mud habitat (a).
- Mud coral habitat showed also high variability and heterogeneity in biomasses with respect to mud habitat (ANOSIM).
- Also species composition was heterogeneous in mud coral habitat with the coexistence of different types of detritivorous species, while mud habitat was co-dominated by both detritivores and carnivores (mainly the caudofoveats *Prochaetoderma* spp.).
- The community structure was also related to environmental conditions (CCA): the wider spectrum of different detritivores in mud coral habitat could be a consequence of the higher availability (higher tom) and variability in source quality (labile and refractory detritus, higher turbidity, lower mv1cm, higher oxygen concentration) and other favourable conditions, such that different types of basal consumers were observed, on the contrary in mud habitat where the source is limited and less heterogeneous the community is composed by less number of species and carnivores (on meiofauna) show higher relative abundance.
- Some similar findings concerning the abundances and the different trophic organizations of infaunal communities have been also observed comparing other deep-sea habitats, e.g. canyons [3, 4] and in the same mud coral habitat for the megafaua [2].
- The lower functional diversity in the mud habitat can also be related with the higher trawling activity compared to mud coral stations.

References

[1] Maynou, F and Cartes, JE, 2012. Effects of trawling on fish and invertebrates from deep-sea coral facies of *Isidella elongata* in the western Mediterranean. *Journal of the Marine Biological Association of the United Kingdom. 92(7): 1501–1507.*

[2] Cartes, JE and Lolacono, C and Mamouridis, V and López-Pérez, C and Rodríguez, P, 2013. Geomorphological, trophic and human influences on the bamboo coral *Isidella elongata* assemblages in the deep Mediterranean: To what extent does *Isidella* form habitat for fish and invertebrates? *Deep Sea Research Part I: Oceanographic Research Papers, 76: 52–65.*

[3] Mamouridis, V and Cartes, JE and Parra, S and Fanelli, E and Saiz Salinas, JI, 2011. A temporal analysis on the dynamics of deep-sea macrofauna: influence of environmental variability off Catalonia coasts (western Mediterranean). *Deep Sea Research Part I: Oceanographic Research Papers, 58(4): 323–337.*

[4] Stora, G and Bourcier, M and Arnoux, A and Gerino, M and Campion, J Le and Gilbert, F and Durbec, JP, 1999. The deep-sea macrobenthos on the continental slope of the northwestern Mediterranean Sea: a quantitative approach. *Deep Sea Research Part I: Oceanographic Research Papers, 46(8): 1339–1368.*

Acknowledgements

Authors thank all participants to the project ANTROMARE (CTM2009-12214-C02-01).

Figure 3: (A) *Isidella elongata* (Esper, 1788), ROV image from the CORALIG survey, (B) *Leucon longirostris* Sars, 1871, (C) Caudofoveata.

G.2.9 Poster

Location: 11/2014, 2nd International Ocean Research Conference, Barcelona

Trophodynamics in a bathyal food web (NW Mediterranean) controlled by food limitations and fishing activity

V Mamouridis[1]*, D van Oevelen[2], K Soetaert[2], F Maynou[1], E Fanelli[3], JE Cartes[1]

1. Institut de Ciències del Mar (CSIC), Passeig Marítim de la Barceloneta 37-49, 08003 Barcelona, Spain.
2. NIOZ, Korringaweg 7, 4401 NT Yerseke, Netherlands
3. Marine Environment Research Center - ENEA Santa Teresa, Pozzuolo di Lerici 19032 (SP) Italy.

* mamouridis@icm.csic.es

Introduction

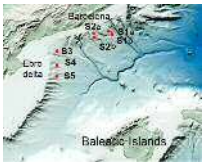

Figure 1: The study area.

We present a dynamic simulation of a bathyal food web quantified using site-specific data from the continental slope (600-800 m depth, years 2007 and 2011), Catalan Sea (Figure 1).

Many works have been performed assessing the importance of resource limitation (bottom-up control) or predation (top-down control) in regulating and structuring ecosystems, e.g. [1, 2, 3].

The continental slope is dominated by detritivores feeding on different types of detritus but also by species with benthic or bentho-pelagic behaviours and a wider range of their trophic niche feeding partially on detritus and on other metazoa (see e.g. [4]).

Aims

1. Investigate the response of the bathyal food web under two types of perturbation: bottom-up (induced by resource limitation) and top-down (induced by fishing activity).
2. Detect the existence of trophic cascades including the humans as top predator, that fish the red shrimp (*Aristeus antennatus*), or competition for food.

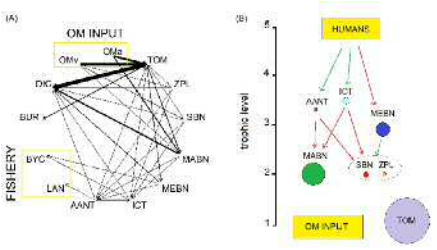

Figure 2: (A) Food web net flows and (B) trophic position of components with examples of possible hypotheses of trophic cascades. Arrows colours indicate positive effect of upper on lower levels (green) and negative effect (red). Colours associated to compartments: orange = zooplankton (ZPL); red = suprabenthos (SBN); green = macrobenthos (MABN); blue = invertebrates from megafauna (MEBN); light blue = fish from megafauna (ICT); violet = red shrimp *Aristeus antennatus* (AANT).

The simulation

After quantifying the food web in steady-state using linear inverse modelling (LIM, citevanoevelen2010), we run it dynamically through 5 years under perturbations induced by resource limitation and by fishing activity, both for three cases:

1. unchanged biomass (base), used to estimate all original flows,
2. add to the biomass the value corresponding to p times the original flow, input of organic carbon or output due to fishery (more), and
3. decreasing the biomass to the value corresponding to p times the original flow (less).

We repeated the simulations for different magnitudes of p, $p = 5, 10, 20$, returning a total of 25 different scenarios. The dynamic model is basically

$$\frac{dx}{dt} = \sum f(x, p^1, t) - \sum f(y, p^2, t) \quad (1)$$

where the flows are functions $f(\cdot)$ of e.g. the state variable (x), parameters (p^1) and time (t).

We then calculated relative biomasses of faunal components for each time and the presence/absence of change in relative biomasses between each possible interaction ($I = 15$).

We also imposed a trade-off of 2 for both the proportion between the original biomass of each component (used to estimate the flows) and its biomass at time $t \neq t_0$ and the proportion between biomasses of couples of components to ensure that at least one biomass is doubled with respect to the other to give evidence of a significant change.

We used the R-packages LIM [5] and deSolve [6].

Results

We found shift of relative biomasses for some components as shown in Table 1 and the most representative outputs among all scenarios are shown in Figure 3.

	(A) $p = 5$			(B) $p = 10$			(C) $p = 20$		
	base	more	less	base	more	less	base	more	less
base									
more	ZA	ZA	ZA	ZA SA SZ	ZA SA SZ	ZA SA SZ	ZA SA SZ	ZA SA SZ	ZA SA SZ
less	ZA ZMa ZMe ZI	ZA ZMa ZMe ZI	ZA ZMa ZMe ZI						

Table 1: Affected relationships for each scenario. ZA=ZPL-AANT, SA=SBN-AANT, SZ=SBN-ZPL, ZMa=ZPL-MABN, ZMe=ZPL-MEBN, ZI=ZPL-ICT. In rows are the levels of OM INPUT while in columns are the levels of FISHING EFFORT.

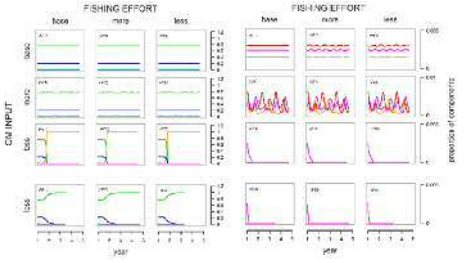

Figure 3: On the left: simulation output for all components; on the right: simulation output showing only less abundant components.

Conclusions

- There is no impact due to fishery neither evidences of any top-down mechanism, i.e. trophic cascades for all scenarios. On the contrary bottom-up controls can occur especially when resources are limited. In fact modifying the fishing effort maintaining the input constant the proportions of components do not change in time. On the contrary the proportion changes when the resource is modified.
- When the resource input is higher there are alternative states of no-dominant components (zooplankton, suprabenthos and the red shrimp), but their proportion remains low during the simulated period.
- When the resource is limited but still high the unique component that grows is the zooplankton, that feeds directly on allochthonous resource and does not depend on the organic matter in sediments. When the resource is strongly limited all components show changes in their relative biomass but any shift occurs and the (macro)infauna is the component that predominates in the food web.
- The continental slope ecosystem is based on detritus derived from the aboveground photic systems. We thus suggest that a detritus food web is affected by the dynamics of the source and not by the consumer, a control type called "donor control" [7].

References

[1] Worm, B and Myers, RA, 2003. Meta-analysis of cod-shrimp interactions reveals top-down control in oceanic food webs. *Ecology, 84(1): 162–173.*

[2] Sala, E and Boudouresque, CF and Harmelin-Vivien, M, 1998. Fishing, trophic cascades, and the structure of algal assemblages: evaluation of an old but untested paradigm. *Oikos: 425–439.*

[3] Hunter, MD and Price, PW, 1992. Playing chutes and ladders: heterogeneity and the relative roles of bottom-up and top-down forces in natural communities. *Ecology, 73(3): 723–732.*

[4] Papiol, V and Cartes, JE and Fanelli, E and Rumolo, P, 2013. Food web structure and seasonality of slope megafauna in the NW Mediterranean elucidated by stable isotopes: Relationship with available food sources. *Journal of Sea Research, 77: 53–69.*

[5] van Oevelen, D and Van den Meersche, K and Meysman, FJR and Soetaert, K and Middelburg, JJ and Vézina, AF, 2010. Quantifying food web flows using linear inverse models. *Ecosystems, 13(1): 32–45.*

[6] Soetaert, K and Petzoldt, T and Setzer, RW, 2010. Solving differential equations in R: Package deSolve. *Journal of Statistical Software, 33(9): 1–25.*

[7] DeAngelis, DL, 1980. Energy flow, nutrient cycling, and ecosystem resilience. *Ecology: 764–771.*

Acknowledgements

Authors thank all participants of the projects BIOMARE (CTM2006-13508-CO2-02/MAR) and ANTROMARE (CTM2009-12214-C02-01).

G.2.10 Poster

Location: 11/2014, 2nd International Ocean Research Conference, Barcelona

References

Abelló, P and FJ Valladares (1988), 'Bathyal decapod crustaceans of the Catalan Sea (northwestern Mediterranean)', *Mésogée* **48**, 97–102.

Akaike, H (1973), Information theory and an extension of the maximum likelihood principle, *in* C. F.Petrov BN, ed., 'Second international symposium on information theory', Akademinai Kiado, Budapest, pp. 267–281.

Akoumianaki, I and A Nicolaidou (2007), 'Spatial variability and dynamics of macrobenthos in a Mediterranean delta front area: the role of physical processes', *Journal of Sea Research* **57**(1), 47–64.

Aldebert, Y and L Recasens (1996), 'Comparison of methods for stock assessment of European hake *Merluccius merluccius* in the Gulf of Lions (Northwestern Mediterranean)', *Aquatic Living Resources* **9**(01), 13–22.

Alldredge, AL and MW Silver (1988), 'Characteristics, dynamics and significance of marine snow', *Progress in oceanography* **20**(1), 41–82.

Allesina, S and RE Ulanowicz (2004), 'Cycling in ecological networks: Finn's index revisited', *Computational biology and chemistry* **28**(3), 227–233.

Alonzo, SH, PV Switzer and M Mangel (2003), 'An ecosystem-based approach to management: using individual behaviour to predict the indirect effects of Antarctic krill fisheries on penguin foraging', *Journal of Applied Ecology* **40**(4), 692–702.

Anderson, J, N Carvalho, F Contini and J Virtanen (2012), 'The 2012 Annual Economic Report on the EU Fishing Fleet (STECF-12-10)', *Technical report. Scientific, Technical and Economic Committee for Fisheries European Commissions. Luksemburg* .

Anderson, MJ (2001), 'A new method for non-parametric multivariate analysis of variance', *Austral Ecology* **26**(1), 32–46.

Anderson, MJ and C Ter Braak (2003), 'Permutation tests for multi-factorial analysis of variance', *Journal of Statistical Computation and Simulation* **73**(2), 85–113.

Anderson, MJ and P Legendre (1999), 'An empirical comparison of permutation methods for tests of partial regression coefficients in a linear model', *Journal of Statistical Computation and Simulation* **62**(3), 271–303.

Andersson, JH, JWM Wijsman, PMJ Herman, JJ Middelburg, K Soetaert and C Heip (2004), 'Respiration patterns in the deep ocean', *Geophysical Research Letters* **31**(3).

Angelini, R and AA Agostinho (2005), 'Parameter estimates for fishes of the upper Paraná River floodplain and Itaipu reservoir (Brazil)', *Naga, Worldfish Center Quarterly* **28**(1–2), 53–57.

Arntz, WE, VA Gallardo, D Gutiérrez, E Isla, LA Levin, J Mendo, C Neira, GT Rowe, J Tarazona and M Wolff (2006), 'El Niño and similar perturbation effects on the benthos of the Humboldt, California, and Benguela Current upwelling ecosystems', *Advances in Geosciences* **6**, 243–265.

Aronson, RB (1989), 'Brittlestar beds: low-predation anachronisms in the British Isles', *Ecology* **70**(4), 856–865.

Aronson, RB (1990), 'Onshore-offshore patterns of human fishing activity', *Palaios* **5**(1), 88–93.

Aronson, RB (1992), 'Biology of a scale-independent predator-prey interaction', *Marine Ecology Progress Series* **89**(1), 1–13.

Ascher, UM and LR Petzold (1998), *Computer methods for ordinary differential equations and differential-algebraic equations*, Vol. 61, Society for Industrial and Applied Mathematics, Philadelphia.

Azov, Y (1991), 'Eastern Mediterranean - a marine desert?', *Marine Pollution Bulletin* **23**, 225–232.

Báez, JC, JM Ortiz de Urbina, R Real and D Macías (2011), 'Cumulative effect of the North Atlantic Oscillation on age-class abundance of albacore (*Thunnus alalunga*)', *Journal of Applied Ichthyology* **27**(6), 1356–1359.

Baldwin, RJ, RC Glatts and KL Smith Jr (1998), 'Particulate matter fluxes into the benthic boundary layer at a long time-series station in the abyssal NE Pacific:: composition and fluxes', *Deep Sea Research Part II: Topical Studies in Oceanography* **45**(4–5), 643–665.

Banašek-Richter, C, M-F Cattin and L-F Bersier (2004), 'Sampling effects and the robustness of quantitative and qualitative food-web descriptors', *Journal of Theoretical Biology* **226**(1), 23–32.

Bannerot, SP and CB Austin (1983), 'Using Frequency Distributions of Catch per Unit Effort to Measure Fish-Stock Abundance', *Transactions of the American Fisheries Society* **112**, 608–617.

Baretta-Bekker, JG, JW Baretta and W Ebenhöh (1997), 'Microbial dynamics in the marine ecosystem model ERSEM II with decoupled carbon assimilation and nutrient uptake', *Journal of Sea Research* **38**(3), 195–211.

Bas, C, F Maynou, F Sardà and J Lleonart (2003), *Variacions demogràfiques a les poblacions d'espècies demersals explotades: els darrers quaranta anys a Blanes i Barcelona*, Vol. 135, Institut d'Estudis Catalans. Arxiu de la Secció de Ciències, Barcelona.

Bax, NJ (1985), 'Application of multi- and univariate techniques of sensitivity analysis to SKEBUB, a biomass-based fisheries ecosystem model, parameterized to Georges Bank', *Ecological Modelling* **29**(1), 353–382.

Begley, J and D Howell (2004), 'An overview of Gadget, the Globally applicable Area-Disaggregated General Ecosystem Toolbox ICES CM 2004/FF: 13'.
URL: *http://www. hafro. is/gadget*

Belitz, C, A Brezger, T Kneib, S Lang and N Umlauf (2012), 'Bayesx, 2012. - Software for Bayesian inference in structured additive regression models. Version 2.1'.
URL: *http://www.bayesx.org*

Bell, JD (1983), 'Effects of depth and marine reserve fishing restrictions on the structure of a rocky reef fish assemblage in the north-western Mediterranean Sea', *Journal of Applied Ecology* pp. 357–369.

Bellan-Santini, D (1990), 'Mediterranean deep-sea amphipods: composition, structure and affinities of the fauna', *Progress in Oceanography* **24**(1), 275–287.

Berlow, EL, AM Neutel, JE Cohen, PC De Ruiter, BO Ebenman, M Emmerson, JW Fox, VAA Jansen, J Iwan Jones and GD Kokkoris (2004), 'Interaction strengths in food webs: issues and opportunities', *Journal of Animal Ecology* **73**(3), 585–598.

Bersier, LF, C Banasek-Richter and MF Cattin (2002), 'Quantitative descriptors of food-web matrices', *Ecology* **83**(9), 2394–2407.

Bertignac, M, P Lehodey and J Hampton (1998), 'A spatial population dynamics simulation model of tropical tunas using a habitat index based on environmental parameters', *Fisheries Oceanography* **7**(3–4), 326–334.

Bertrand, JA, LG de Sola, C Papaconstantinou, G Relini and A Souplet (2002), 'The general specifications of the MEDITS surveys', *Scientia Marina* **66**, 9 – 17.

Beverton, RJH and SJ Holt (1957), *On the dynamics of exploited fish populations*, Chapman & Hall, London.

Bianchini, ML and S Ragonese (1994), Life cycles and fisheries of the deep-water red shrimps *Aristaeomorpha foliacea* and *Aristeus antennatus*, *in* 'Proceedings of the International workshop held in the Istituto di Tecnologia della Pesca e del Pescato, Mazara del Vallo. NTR-ITPP Special Publication', Vol. 3, pp. 1–87.

Billett, DSM, RS Lampitt, AL Rice and RFC Mantoura (1983), 'Seasonal sedimentation of phytoplankton to the deep-sea benthos', *Nature* **302**(5908), 520 – 522.

Bishop, J, WN Venables and Y-G Wang (2004), 'Analysing commercial catch and effort data from a Penaeid trawl fishery: A comparison of linear models, mixed models, and generalised estimating equations approaches', *Fisheries Research* **70**(2–3), 179 – 193.

Bodin, N, F Le Loc'h and C Hily (2007), 'Effect of lipid removal on carbon and nitrogen stable isotope ratios in crustacean tissues', *Journal of Experimental Marine Biology and Ecology* **341**(2), 168–175.

Bogstad, B, KH Hauge and Ø Ulltang (1997), 'MULTSPEC–a multi-species model for fish and marine mammals in the Barents Sea', *Journal of Northwest Atlantic Fishery Science* **22**, 317–341.

Botsford, LW, JC Castilla and CH Peterson (1997), 'The management of fisheries and marine ecosystems', *Science* **277**(5325), 509–515.

Brander, KM (2005), 'Cod recruitment is strongly affected by climate when stock biomass is low', *ICES Journal of Marine Science* **62**(3), 339–343.

Brauner, N and M Shacham (1998), 'Role of range and precision of the independent variable in regression of data', *AIChE journal* **44**(3), 603–611.

Brey, T (2001), 'Population dynamics in benthic invertebrates. A virtual handbook. Version 01.2.'.
URL: *http://www.thomas-brey.de/science/virtualhandbook/navlog/index.html*

Brezger, A and S Lang (2006), 'Generalized structured additive regression based on Bayesian P-splines', *Computational Statistics & Data Analysis* **50**(4), 967 – 991.

Brodziak, J and L O'Brien (2005), 'Do environmental factors affect recruits per spawner anomalies of New England groundfish?', *ICES Journal of Marine Science: Journal du Conseil* **62**(7), 1394–1407.

Broecker, WS (1991), 'The great ocean conveyor', *Oceanography* **4**(2), 79–89.

Brown, JH and JF Gillooly (2003), 'Ecological food webs: high-quality data facilitate theoretical unification', *Proceedings of the National Academy of Sciences* **100**(4), 1467–1468.

Brynjarsdóttir, J and G Stefánsson (2004), 'Analysis of cod catch data from Icelandic groundfish surveys using generalized linear models', *Fisheries Research* **70**(2–3), 195 – 208.

Buchanan, JB (1964), 'A comparative study of some features of the biology of Amphiura filiformis and Amphiura chiajei (Ophiuroidea) considered in relation to their distribution', *Journal of the Marine Biological Association of the UK* **44**, 565–576.

Buesseler, KO, CH Lamborg, PW Boyd, PJ Lam, TW Trull, RR Bidigare, JKB Bishop, KL Casciotti, F Dehairs, M Elskens, M Honda, DM Karl, DA Siegel, MW Silver, DK Steinberg, J Valdes, B Van Mooy and S Wilson (2007), 'Revisiting carbon flux through the ocean's twilight zone', *Science* **316**(5824), 567–570.

Buhl-Mortensen, L, A Vanreusel, AJ Gooday, LA Levin, IG Priede, P Buhl-Mortensen, H Gheerardyn, NJ King and M Raes (2010), 'Biological structures as a source of habitat heterogeneity and biodiversity on the deep ocean margins', *Marine Ecology* **31**(1), 21–50.

Burd, AB, DA Hansell, DK Steinberg, TR Anderson, J Arístegui, F Baltar, SR Beaupre, KO Buesseler, F DeHairs, GA Jackson, DC Kadko, R Koppelmann, Lampitt RS, T Nagata, T Reinthaler, C Robinson, BC Robison, C Tamburini and T Tanaka (2010), 'Assessing the apparent imbalance between geochemical and biochemical indicators of meso-and bathypelagic biological activity: What the $#! is wrong with present calculations of carbon budgets?', *Deep Sea Research Part II: Topical Studies in Oceanography* **57**(16), 1557–1571.

Burdige, DJ, WM Berelson, KH Coale, J McManus and KS Johnson (1999), 'Fluxes of dissolved organic carbon from California continental margin sediments', *Geochimica et Cosmochimica Acta* **63**(10), 1507–1515.

Buscail, R, R Pocklington and C Germain (1995), 'Seasonal variability of the organic matter in a sedimentary coastal environment: sources, degradation and accumulation (continental shelf of the Gulf of Lionsnorthwestern Mediterranean Sea)', *Continental Shelf Research* **15**(7), 843–869.

Buscail, R, R Pocklington, R Daumas and L Guidi (1990), 'Fluxes and budget of organic matter in the benthic boundary layer over the northwestern Mediterranean margin', *Continental Shelf Research* **10**(9), 1089–1122.

Butterworth, DS and RB Thomson (1995), 'Possible effects of different levels of krill fishing on predators–some initial modelling attempts', *Commission for the Conservation of Antarctic Marine Living Resources Science* **2**, 79–97.

Caddy, JF (1983), 'The cephalopods: factors relevant to their population dynamics and to the assessment and management of stocks', *Advances in assessment of world cephalopod resources. FAO Fisheries Technical Paper* **231**, 416–449.

Canals, M, R Danovaro, S Heussner, V Lykousis, P Puig, F Trincardi, A Calafat, X Durrieu de Madron, A Palanques and A Sànchez-Vidal (2009), 'Cascades in Mediterranean submarine grand canyons', *Oceanography* **22**(1), 26–43.

Carbonell, A, J Lloret and M Demestre (2008), 'Relationship between condition and recruitment success of red shrimp (*Aristeus antennatus*) in the Balearic Sea (Northwestern Mediterranean)', *Journal of Marine Systems* **71**(3), 403–412.

Carbonell, A, M Carbonell, M Demestre, A Grau and S Monserrat (1999), 'The red shrimp *Aristeus antennatus* (Risso, 1816) fishery and biology in the Balearic Islands, Western Mediterranean', *Fisheries Research* **44**(1), 1–13.

Cardinale, M, GC Osio and A (eds) Charef (2012), 'Report of the Scientific, Technical and Economic Committee for Fisheries on Assessment of Mediterranean Sea stocks part 1.', *JRC Scientific and Policy Reports. European Commission* .

Cardona, L, M Sales and D López (2007), 'Changes in fish abundance do not cascade to sea urchins and erect algae in one of the most oligotrophic parts of the Mediterranean', *Estuarine Coastal and Shelf Science* **72**(1), 273–282.

Carpenter, JH (1965), 'The Chesapeake Bay Institute technique for the Winkler dissolved oxygen method', *Limnology and Oceanography* **10**(1), 141–143.

Carpenter, SR and JF Kitchell (1988), 'Consumer control of lake productivity', *BioScience* pp. 764–769.

Carpenter, SR, JF Kitchell and JR Hodgson (1985), 'Cascading trophic interactions and lake productivity', *BioScience* **35**(10), 634–639.

Carpenter, SR, JJ Cole, JR Hodgson, JF Kitchell, ML Pace, D Bade, KL Cottingham, TE Essington, JN Houser and DE Schindler (2001), 'Trophic cascades, nutrients, and lake productivity: whole-lake experiments', *Ecological Monographs* **71**(2), 163–186.

Carpine, C (1970), 'Ecologie de l'étage bathyal dans la Méditerranée occidentale', *Mémoires de lInstitut Océanographique de Monaco* **2**, 1–146.

Carrassón, M and JE Cartes (2002), 'Trophic relationships in a Mediterranean deep-sea fish community: partition of food resources, dietary overlap and connections within the benthic boundary layer', *Marine Ecology Progress Series* **241**, 41–55.

Cartes, JE (1994), 'Influence of depth and season on the diet of the deep-water aristeid *Aristeus antennatus* along the continental slope (400 to 2300 m) in the Catalan Sea (western Mediterranean)', *Marine Biology* **120**(4), 639–648.

Cartes, JE (1998), 'Dynamics of the bathyal Benthic Boundary Layer in the northwestern Mediterranean: depth and temporal variations in macrofaunal–megafaunal communities and their possible connections within deep-sea trophic webs', *Progress in Oceanography* **41**(1), 111–139.

Cartes, JE, A Grémare, F Maynou, S Villora-Moreno and A Dinet (2002), 'Bathymetric changes in the distributions of particulate organic matter and associated fauna along a deep-sea transect down the Catalan sea slope (Northwestern Mediterranean)', *Progress in Oceanography* **53**(1), 29–56.

Cartes, JE, C LoIacono, V Mamouridis, C López-Pérez and P Rodríguez (2013), 'Geomorphological, trophic and human influences on the bamboo coral *Isidella elongata* assemblages in the deep Mediterranean: To what extent does *Isidella* form habitat for fish and invertebrates?', *Deep Sea Research Part I: Oceanographic Research Papers* **76**, 52–65.

Cartes, JE, D Jaume and T Madurell (2003), 'Local changes in the composition and community structure of suprabenthic peracarid crustaceans on the bathyal Mediterranean: influence of environmental factors', *Marine Biology* **143**(4), 745–758.

Cartes, JE, E Fanelli, D Lloris and J Matallanas (2013), 'Effect of environmental variations on sharks and other top predators in the deep Mediterranean Sea over the last 60 years', *Climate Research* **55**(3), 239–251.

Cartes, JE, E Fanelli, V Papiol and F Maynou (2010), 'Trophic relationships at intrannual spatial and temporal scales of macro and megafauna around a submarine canyon off the Catalonian coast (western Mediterranean)', *Journal of Sea Research* **63**(3), 180–190.

Cartes, JE and F Maynou (1998), 'Food consumption by bathyal decapod crustacean assemblages in the western Mediterranean: predatory impact of megafauna and the food consumption-food supply balance in a deep-water food web', *Marine Ecology Progress Series* **171**, 233–246.

Cartes, JE, F Maynou and E Fanelli (2011), 'Nile damming as plausible cause of extinction and drop in abundance of deep-sea shrimp in the western Mediterranean over broad spatial scales', *Progress in Oceanography* **91**(3), 286–294.

Cartes, JE, F Maynou, E Fanelli, C Romano, V Mamouridis and V Papiol (2009), 'The distribution of megabenthic, invertebrate epifauna in the Balearic Basin (western Mediterranean) between 400 and 2300 m: Environmental gradients influencing assemblages composition and biomass trends', *Journal of Sea Research* **61**(4), 244–257.

Cartes, JE, F Maynou, F Sardà, JB Company, D. Lloris and S Tudela (2004), *The Mediterranean deep-sea ecosystems: an overview of their diversity, structure, functioning and anthropogenic impacts, with a proposal for conservation*, Málaga, IUCN and Rome, WWF, chapter Part I. The Mediterranean deep-sea ecosystems: an overview of their diversity, structure, functioning and anthropogenic impacts, pp. 9–38.

Cartes, JE, F Maynou, P Abelló, M Emelianov, LG de Sola and M Solé (2011), 'Long-term changes in the abundance and deepening of the deep-sea shrimp *Aristaeomorpha foliacea* in the Balearic Basin: Relationships with hydrographic changes at the Levantine Intermediate Water', *Journal of Marine Systems* **88**(4), 516–525.

Cartes, JE and F Sardà (1992), 'Abundance and diversity of decapod crustaceans in the deep-Catalan sea (western Mediterranean)', *Journal of Natural History* **26**, 1305–1323.

Cartes, JE and F Sardà (1993), 'Zonation of deep-sea decapod fauna in the Catalan Sea (Western Mediterranean)', *Marine Ecology Progress Series* **94**, 27–27.

Cartes, JE and JC Sorbe (1996), 'Temporal population structure of deep-water cumaceans from the western Mediterranean slope', *Deep Sea Research Part I: Oceanographic Research Papers* **43**(9), 1423–1438.

Cartes, JE and JC Sorbe (1999), 'Deep-water amphipods from the Catalan Sea slope (western Mediterranean): Bathymetric distribution, assemblage composition and biological characteristics', *Journal of Natural History* **33**(8), 1133–1158.

Cartes, JE, T Brey, JC Sorbe and F Maynou (2002), 'Comparing production biomass ratios of benthos and suprabenthos in macrofaunal marine crustaceans', *Canadian journal of fisheries and aquatic sciences* **59**(10), 1616–1625.

Cartes, JE, T Madurell, E Fanelli and JL López-Jurado (2008), 'Dynamics of suprabenthos-zooplankton communities around the Balearic Islands (western Mediterranean): Influence of

environmental variables and effects on the biological cycle of *Aristeus antennatus*', *Journal of Marine Systems* **71**(3), 316–335.

Cartes, JE, V Mamouridis and E Fanelli (2011), 'Deep-sea suprabenthos assemblages (Crustacea) off the Balearic Islands (western Mediterranean): Mesoscale variability in diversity and production', *Journal of Sea Research* **65**(3), 340–354.

Cartes, JE, V Papiol, A Palanques, J Guillén and M Demestre (2007), 'Dynamics of suprabenthos off the Ebro Delta (Catalan Sea: western Mediterranean): Spatial and temporal patterns and relationships with environmental factors', *Estuarine, Coastal and Shelf Science* **75**(4), 501–515.

Cartes, JE, V Papiol and B Guijarro (2008), 'The feeding and diet of the deep-sea shrimp *Aristeus antennatus* off the Balearic Islands (Western Mediterranean): Influence of environmental factors and relationship with the biological cycle', *Progress in Oceanography* **79**(1), 37–54.

Casini, M, J Lövgren, J Hjelm, M Cardinale, J-C Molinero and G Kornilovs (2008), 'Multi-level trophic cascades in a heavily exploited open marine ecosystem', *Proceedings of the Royal Society B: Biological Sciences* **275**(1644), 1793–1801.

Cattin, MF, LF Bersier, C Banašek-Richter, R Baltensperger and JP Gabriel (2004), 'Phylogenetic constraints and adaptation explain food-web structure', *Nature* **427**(6977), 835–839.

Christensen, V (1996), 'Managing fisheries involving predator and prey species', *Reviews in Fish Biology and Fisheries* **6**(4), 417–442.

Christensen, V (1998), 'Fishery-induced changes in a marine ecosystem: insight from models of the Gulf of Thailand', *Journal of Fish Biology* **53**(sA), 128–142.

Christensen, V and CJ Walters (2004), 'Ecopath with Ecosim: methods, capabilities and limitations', *Ecological modelling* **172**(2), 109–139.

Christensen, V and D Pauly (1992), 'ECOPATH IIa software for balancing steady-state ecosystem models and calculating network characteristics', *Ecological Modelling* **61**(3), 169–185.

Christensen, V, S Guenette, JJ Heymans, CJ Walters, R Watson, D Zeller and D Pauly (2003), 'Hundred-year decline of North Atlantic predatory fishes', *Fish and Fisheries* **4**(1), 1–24.

Clarke, KR (1993), 'Non-parametric multivariate analyses of changes in community structure', *Australian Journal of Ecology* **18**(1), 117–143.

Clarke, KR and RM Warwick (1994), *Change in marine communities: an approach to statistical analysis and interpretation*, Natural Environment Research Council Plymouth.

Clarke, KR and RN Gorley (2006), 'PRIMER V6: user manual/tutorial', *Primer-E Ltd. Plymouth* .

Coelho, R and K Erzini (2008), 'Life history of a wide-ranging deepwater lantern shark in the north-east Atlantic, *Etmopterus spinax* (Chondrichthyes: Etmopteridae), with implications for conservation', *Journal of Fish Biology* **73**(6), 1419–1443.

Cohen, JE and CM Newman (1985), 'A stochastic theory of community food webs: I. Models and aggregated data', *Proceedings of the Royal society of London. Series B. Biological sciences* **224**(1237), 421–448.

Coll, M, A Santojanni, I Palomera, S Tudela and E Arneri (2007), 'An ecological model of the Northern and Central Adriatic Sea: analysis of ecosystem structure and fishing impacts', *Journal of Marine Systems* **67**(1), 119–154.

Coll, M, H K Lotze and TN Romanuk (2008), 'Structural degradation in Mediterranean Sea food webs: testing ecological hypotheses using stochastic and mass-balance modelling', *Ecosystems* **11**(6), 939–960.

Coll, M, I Palomera, S Tudela and F Sardà (2006), 'Trophic flows, ecosystem structure and fishing impacts in the South Catalan Sea, Northwestern Mediterranean', *Journal of Marine Systems* **59**(1), 63–96.

Coll, M and S Libralato (2012), 'Contributions of food web modelling to the ecosystem approach to marine resource management in the Mediterranean Sea', *Fish and Fisheries* **13**(1), 60–88.

Coll, M, S Libralato, S Tudela, I Palomera and F Pranovi (2008), 'Ecosystem overfishing in the ocean', *PLoS one* **3**(12), e3881.

Colloca, F, M Cardinale, A Belluscio and G Ardizzone (2003), 'Pattern of distribution and diversity of demersal assemblages in the central Mediterranean sea', *Estuarine, Coastal and Shelf Science* **56**(3), 469–480.

Colomb, A, J Le Fur and D Gascuel (2004), MOOVES: an individual-based model to study the functioning of a tropical ecosystem and its reaction to fishing pressure, *in* 'The Fourth European Conference on Ecological Modelling ECEM 2004', pp. 37–38.

Company, JB and F Sardà (1998), 'Metabolic rates and energy content of deep-sea benthic decapod crustaceans in the western Mediterranean Sea', *Deep-Sea Research Part I* **45**(11), 1861–1880.

Constable, AJ (2006), Using the EPOC modelling framework to assess management procedures for Antarctic krill in Statistical Area 48: evaluating spatial differences in productivity of Antarctic krill, *in* 'Workshop document presented to WG-EMM subgroup of CCAMLR. Commission for the Conservation of Antarctic Marine Living Resources. WG-EMM-06/38'.

Cooper, AB, A Rosenberg, G Stefansson and M Mangel (2004), 'Examining the importance of consistency in multi-vessel trawl survey design based on the U.S. west coast groundfish bottom trawl survey', *Fisheries Research* **70**(2-3), 239–250.

Corliss, BH (1979), 'Size variation in the deep-sea benthonic foraminifer Globocassidulina subglobosa (Brady) in the southeast Indian Ocean', *The Journal of Foraminiferal Research* **9**(1), 50–60.

Craven, P and G Wahba (1979), 'Smoothing noisy data with spline functions: estimating the correct degree of smoothing by the method of generalised cross-validation', *Numerische Mathematik* **31**(4), 377–403.

Curdia, J, S Carvalho, A Ravara, JD Gage, AM Rodrigues and V Quintino (2004), 'Deep macrobenthic communities from Nazaré submarine canyon (NW Portugal)', *Scientia Marina* **68**(1), 171–180.

Cury, P, A Bakun, RJM Crawford, A Jarre, RA Quiñones, LJ Shannon and HM Verheye (2000), 'Small pelagics in upwelling systems: patterns of interaction and structural changes in "wasp-waist" ecosystems', *ICES Journal of Marine Science: Journal du Conseil* **57**(3), 603–618.

Cury, P and L Shannon (2004), 'Regime shifts in upwelling ecosystems: observed changes and possible mechanisms in the northern and southern Benguela', *Progress in Oceanography* **60**(2), 223–243.

Cury, P, L Shannon and YJ Shin (2003), *Responsible fisheries in the marine ecosystem*, CABI, chapter The Functioning of Marine Ecosystems: a Fisheries Perspective, pp. 103–123.

Damalas, D, P Megalofonou and M Apostolopoulou (2007), 'Environmental, spatial, temporal and operational effects on swordfish (*Xiphias gladius*) catch rates of eastern Mediterranean Sea longline fisheries', *Fisheries Research* **84**(2), 233–246.

Danovaro, R, A Dinet, G Duineveld and A Tselepides (1999), 'Benthic response to particulate fluxes in different trophic environments: a comparison between the Gulf of Lions–Catalan Sea (western-Mediterranean) and the Cretan Sea (eastern-Mediterranean)', *Progress in Oceanography* **44**(1), 287–312.

Danovaro, R and M Serresi (2000), 'Viral density and virus-to-bacterium ratio in deep-sea sediments of the Eastern Mediterranean', *Applied and environmental microbiology* **66**(5), 1857–1861.

Danovaro, R, N Della Croce, A Eleftheriou, M Fabiano, N Papadopoulou, C Smith and A Tselepides (1995), 'Meiofauna of the deep Eastern Mediterranean Sea: distribution and abundance in relation to bacterial biomass, organic matter composition and other environmental factors', *Progress in oceanography* **36**(4), 329–341.

Daskalov, Georgi M, Alexander N Grishin, Sergei Rodionov and Vesselina Mihneva (2007), 'Trophic cascades triggered by overfishing reveal possible mechanisms of ecosystem regime shifts', *Proceedings of the National Academy of Sciences* **104**(25), 10518–10523.

Dauwe, B, PMJ Herman, CHR Heip et al. (1998), 'Community structure and bioturbation potential of macrofauna at four North Sea stations with contrasting food supply', *Marine Ecology Progress Series* **173**, 67–83.

Day, JH (1967), *A monograph on the Polychaeta of southern Africa*, British Museum (Natural History), London.

de Forges, BR, JA Koslow and GCB Poore (2000), 'Diversity and endemism of the benthic seamount fauna in the southwest Pacific', *Nature* **405**(6789), 944–947.

de Juan, S and JE Cartes (2011), 'Influence of environmental factors on the dynamics of macrobenthic crustaceans on soft-bottoms of the Ebro Delta continental shelf (northwestern Mediterranean)'.

De Ruiter, PC, AM Neutel and JC Moore (1995), 'Energetics, patterns of interaction strengths, and stability in real ecosystems', *Science* pp. 1257–1257.

de Ruiter, PC, V Wolters and JC Moore (2005), *Dynamic food webs: multispecies assemblages, ecosystem development and environmental change*, Vol. 3, Academic Press.

DeAngelis, DL (1980), 'Energy flow, nutrient cycling, and ecosystem resilience', *Ecology* pp. 764–771.

DeAngelis, DL and LJ Gross (1992), *Individual-based models and approaches in ecology: populations, communities and ecosystems.*, Chapman & Hall.

Demestre, M (1995), '*Aristeus antennatus* (Decapoda: Dendrobranchiata)', *Marine Ecology Progress Series* **127**, 57–64.

Demestre, M and J Lleonart (1993), 'Population dynamics of *Aristeus antennatus* (Decapoda: Dendrobranchiata) in the northwestern Mediterranean', *Scientia Marina* **57**(2–3), 183–189.

Demestre, M and JM Fortuño (2013), 'Reproduction of the deepwater shrimp *Aristeus antennatus* (Decapoda: Dendrobranchiata)', *Marine Ecology Progress Series* **84**, 41–51.

Demirov, E and N Pinardi (2002), 'Simulation of the Mediterranean Sea circulation from 1979 to 1993: Part I. The interannual variability', *Journal of Marine Systems* **33**, 23–50.

Denis, V (2002), 'Spatio-temporal analysis of commercial trawler data using General Additive models: patterns of Loliginid squid abundance in the north-east Atlantic', *ICES Journal of Marine Science* **59**(3), 633–648.

Dennard, ST, MA MacNeil, MA Treble, S Campana and AT Fisk (2010), 'Hierarchical analysis of a remote, Arctic, artisanal longline fishery', *ICES Journal of Marine Science: Journal du Conseil* **67**(1), 41–51.

Deuser, WG, EH Ross and RF Anderson (1981), 'Seasonality in the supply of sediment to the deep Sargasso Sea and implications for the rapid transfer of matter to the deep ocean', *Deep Sea Research Part A. Oceanographic Research Papers* **28**(5), 495–505.

Devine, JA, KD Baker and RL Haedrich (2006), 'Fisheries: deep-sea fishes qualify as endangered', *Nature* **439**(7072), 29–29.

Diffendorfer, JE, PM Richards, GH Dalrymple and DL DeAngelis (2001), 'Applying Linear Programming to estimate fluxes in ecosystems or food webs: an example from the herpetological assemblage of the freshwater Everglades', *Ecological Modelling* **144**(2), 99–120.

D'Onghia, G, P Maiorano, L Sion, A Giove, F Capezzuto, R Carlucci and A Tursi (2010), 'Effects of deep-water coral banks on the abundance and size structure of the megafauna in the Mediterranean Sea', *Deep Sea Research Part II: Topical Studies in Oceanography* **57**(5), 397–411.

D'ortenzio, F and M Ribera d'Alcalà (2009), 'On the trophic regimes of the Mediterranean Sea: a satellite analysis', *Biogeosciences* **6**(2), 139–148.

Duda, AM and K Sherman (2002), 'A new imperative for improving management of large marine ecosystems', *Ocean & Coastal Management* **45**(11), 797–833.

Duffy, JE (2003), 'Biodiversity loss, trophic skew and ecosystem functioning', *Ecology Letters* **6**(8), 680–687.

Dulvy, NK, Y Sadovy and JD Reynolds (2003), 'Extinction vulnerability in marine populations', *Fish and Fisheries* **4**(1), 25–64.

Durrieu De Madron, X, A Abassi, S Heussner, A Monaco, JC Aloisi, O Radakovitch, P Giresse, R Buscail and P Kerherve (2000), 'Particulate matter and organic carbon budgets for the Gulf of Lions (NW Mediterranean)', *Oceanologica Acta* **23**(6), 717–730.

Eilers, PHC and BD Marx (1996), 'Flexible Smoothing with B-splines and Penalties', *Statistical Science* **11**(2), 89–102.

Elner, RW and RL Vadas Sr (1990), 'Inference in ecology: the sea urchin phenomenon in the northwestern Atlantic', *American Naturalist* pp. 108–125.

Epping, E, C van der Zee, K Soetaert and W Helder (2002), 'On the oxidation and burial of organic carbon in sediments of the Iberian margin and Nazaré Canyon (NE Atlantic)', *Progress in Oceanography* **52**(2), 399–431.

Estes, JA, J Terborgh, JS Brashares, ME Power, J Berger, WJ Bond, SR Carpenter, TE Essington, RD Holt and JBC Jackson (2011), 'Trophic downgrading of planet earth', *Science* **333**(6040), 301–306.

Estes, JA and JF Palmisano (1974), 'Sea otters: their role in structuring nearshore communities', *Science* **185**(4156), 1058–1060.

Estes, JA, MT Tinker, TM Williams and DF Doak (1998), 'Killer whale predation on sea otters linking oceanic and nearshore ecosystems', *Science* **282**(5388), 473–476.

Estrada, M (1996), 'Primary production in the northwestern Mediterranean', *Scientia Marina* **60**, 55–64.

Estrada, M and R Margalef (1988), 'Supply of nutrients to the Mediterranean photic zone along a persistent front', *Oceanologica Acta* **9**, 133–142.

Fahrmeir, L, T Kneib and S Lang (2004), 'Penalized structured additive regression for space-time data: a Bayesian perspective', *Statistica Sinica* **14**(3), 731–762.

Fanelli, E and JE Cartes (2008), 'Spatio-temporal changes in gut contents and stable isotopes in two deep Mediterranean pandalids: influence on the reproductive cycle', *Marine Ecology Progress Series* **355**, 219–233.

Fanelli, E and JE Cartes (2010), 'Temporal variations in the feeding habits and trophic levels of three deep-sea demersal fishes from the western Mediterranean Sea, based on stomach contents and stable isotope analyses', *Marine Ecology Progress Series* **402**, 213–232.

Fanelli, E, JE Cartes, P Rumolo and M Sprovieri (2009), 'Food-web structure and trophodynamics of mesopelagic–suprabenthic bathyal macrofauna of the Algerian Basin based on stable isotopes of carbon and nitrogen', *Deep Sea Research Part I: Oceanographic Research Papers* **56**(9), 1504–1520.

Fanelli, E, JE Cartes and V Papiol (2011), 'Food web structure of deep-sea macrozooplankton and micronekton off the Catalan slope: insight from stable isotopes', *Journal of Marine Systems* **87**(1), 79–89.

Fanelli, E, V Papiol, JE Cartes, P Rumolo, C Brunet and M Sprovieri (2011), 'Food web structure of the epibenthic and infaunal invertebrates on the Catalan slope (NW Mediterranean): Evidence from δ^{13}C and δ^{15}N analysis', *Deep Sea Research Part I: Oceanographic Research Papers* **58**(1), 98–109.

FAO (2003), *Fisheries management 2: The ecosystem approach to fisheries. FAO Technical Guidelines for Responsible Fisheries*, Vol. 4, FAO, Rome, Italy.

FAO (2009), *Rapport de la trente-troisième session de la Commission gènérale des pêches pour la Méditerranée (CGPM)*, FAO, Rome, Italy.

FAO/FISHSTAT (2011), 'FAO Fisheries Department, Fishery information, Data and Statistics Unit. FishstatJ, a tool fot fishery statistical analysis, release 2.0.0'.

Fath, BD and BC Patten (1999), 'Review of the foundations of network environ analysis', *Ecosystems* **2**(2), 167–179.

Fauchald, K and PA Jumars (1979), *The diet of worms: a study of polychaete feeding guilds*, Aberdeen University Press, Aberdeen.

Felleman, FL, JR Heimlich-Boran and RW Osborne (1991), 'The feeding ecology of killer whales (*Orcinus orca*) in the Pacific Northwest', *Dolphin societies: discoveries and puzzles* pp. 113–147.

Féral, J-P, J-G Ferrand and A Guille (1990), 'Macrobenthic physiological responses to environmental fluctuations: the reproductive cycle and enzymatic polymorphism of a eurybathic sea-urchin on the northwestern Mediterranean continental shelf and slope', *Continental Shelf Research* **10**(9), 1147–1155.

Fernandez-Arcaya, U, E Ramirez-Llodra, G Rotllant, L Recasens, H Murua, I Quaggio-Grassiotto and JB Company (2013), 'Reproductive biology of two macrourid fish, *Nezumia aequalis* and *Coelorinchus mediterraneus*, inhabiting the NW Mediterranean continental margin (400–2000m)', *Deep Sea Research Part II: Topical Studies in Oceanography* **92**, 63–72.

Ferretti, F, RA Myers, F Serena and HK Lotze (2008), 'Loss of large predatory sharks from the Mediterranean Sea', *Conservation Biology* **22**(4), 952–964.

Finn, JT (1976), 'Measures of ecosystem structure and function derived from analysis of flows', *Journal of theoretical Biology* **56**(2), 363–380.

Finn, JT (1980), 'Flow analysis of models of the Hubbard Brook ecosystem', *Ecology* **61**(3), 562–571.

Finnoff, D and J Tschirhart (2003), 'Protecting an endangered species while harvesting its prey in a general equilibrium ecosystem model', *Land Economics* **79**(2), 160–180.

Finnoff, D and J Tschirhart (2008), 'Linking dynamic economic and ecological general equilibrium models', *Resource and Energy Economics* **30**(2), 91–114.

Fiorentino, F (2009), 'La situazione delle risorse ittiche nelle aree di pesca siciliane ed il contributo delle scienze della pesca per un nuovo sviluppo sostenibile. Rapporto Annuale sulla Pesca e sullAcquacoltura in Sicilia 2009', *Osservatorio della Pesca del Mediterraneo* pp. 77–109.

Flach, E and C Heip (1996), 'Vertical distribution of macrozoobenthos within the sediment on the continental slope of the Goban Spur area (NE Atlantic)', *Marine Ecology Progress Series* **141**(1), 55–66.

Frank, KT, B Petrie, JS Choi and WC Leggett (2005), 'Trophic cascades in a formerly cod-dominated ecosystem', *Science* **308**(5728), 1621–1623.

Frank, KT, B Petrie and NL Shackell (2007), 'The ups and downs of trophic control in continental shelf ecosystems', *Trends in Ecology & Evolution* **22**(5), 236–242.

Frank, KT, B Petrie, NL Shackell and JS Choi (2006), 'Reconciling differences in trophic control in mid-latitude marine ecosystems', *Ecology Letters* **9**(10), 1096–1105.

Fredj, G and L Laubier (1985), *Mediterranean Marine Ecosystems*, Plenum Press, New York and London, chapter The deep Mediterranean benthos, pp. 109–146.

Fretwell, SD (1987), 'Food chain dynamics: the central theory of ecology?', *Oikos* pp. 291–301.

Fromentin, JM and B Planque (1996), '*Calanus* and environment in the eastern North Atlantic. 2. Role of the North Atlantic Oscillation on *Calanus finmarchicus* and *C. helgolandicus*', *Marine Ecology Progress Series* **134**, 11–118.

Fulton, EA, ADM Smith and AE Punt (2005), 'Which ecological indicators can robustly detect effects of fishing?', *ICES Journal of Marine Science: Journal du Conseil* **62**(3), 540–551.

Fulton, EA, ADM Smith and CR Johnson (2004), 'Biogeochemical marine ecosystem models I: IGBEM-a model of marine bay ecosystems', *Ecological Modelling* **174**(3), 267–307.

Fulton, EA, JS Parslow, ADM Smith and CR Johnson (2004), 'Biogeochemical marine ecosystem models II: the effect of physiological detail on model performance', *Ecological Modelling* **173**(4), 371–406.

Gage, JD and PA Tyler (1991), *Deep-sea biology: a natural history of organisms at the deep-sea floor*, Cambridge University Press.

Galeron, J, L Menot, N Renaud, P Crassous, A Khripounoff, C Treignier and M Sibuet (2009), 'Spatial and temporal patterns of benthic macrofaunal communities on the deep continental margin in the Gulf of Guinea', *Deep Sea Research Part II: Topical Studies in Oceanography* **56**(23), 2299–2312.

Garcia-Ladona, E, A Castellon, J Font and J Tintore (1996), 'The Balearic current and volume transports in the Balearic basin', *Oceanologica Acta* **19**(5), 489–497.

García Rodríguez, M and A Esteban (1999), 'On the biology and fishery of *Aristeus antennatus* (Risso, 1816),(Decapoda, Dendrobranchiata) in the Ibiza channel (Balearic Islands, Spain)', *Scientia Marina* **63**(1), 27–37.

García Rodríguez, M, JL Pérez Gil, A Esteban, N Carrasco and A Carbonell (2007), Stock assessment of red shrimp (*Aristeus antennatus*) exploited by the Spanish trawl fishery (1996–2006) in the Geographical Sub-Area 06 (Northern Spain), *in* 'Scientific Advisory Committe of the GFCM 9th Meeting of the Sub-Committee on Stock Assessment (SCSA) Working Group on Demersals Document n° 2', 10-12 September, Athens Greece.

Garcia, S (1986), 'Seasonal trawling bans can be very successful in heavily overfished areas: the "cyprus effect"', *The WorldFish Center Working Papers* .

Gardner, WD (1989), 'Baltimore Canyon as a modern conduit of sediment to the deep sea', *Deep Sea Research Part A. Oceanographic Research Papers* **36**(3), 323–358.

Garrison, LP, JS Link, DP Kilduff, MD Cieri, B Muffley, DS Vaughan, A Sharov, B Mahmoudi and RJ Latour (2010), 'An expansion of the MSVPA approach for quantifying predator–prey interactions in exploited fish communities', *ICES Journal of Marine Science: Journal du Conseil* **67**(5), 856–870.

Garstang, W (1900), 'The impoverishment of the sea. A critical summary of the experimental and statistical evidence bearing upon the alleged depletion of the trawling grounds', *Journal of the Marine Biological Association of the United Kingdom (New Series)* **6**(01), 1–69.

Gaston, GR (1987), 'Benthic polychaeta of the Middle Atlantic Bight: feeding and distribution', *Marine Ecology Progress Series* **36**(3), 251–262.

Gavaris, S (1980), 'Use of a Multiplicative Model to Estimate Catch Rate and Effort from Commercial Data', *Canadian Journal of Fisheries and Aquatic Sciences* **37**(12), 2272–2275.

Gerino, M, G Stora and JP Durbec (1994), 'Quantitative estimation of biodiffusive and bioadvective sediment mixing-in-situ experimental approach', *Oceanologica acta* **17**(5), 547–554.

Gili, JM, F Pages, J Bouillon, A Palanques, P Puig, S Heussner, A Calafat, M Canals and A Monaco (2000), 'A multidisciplinary approach to the understanding of hydromedusan populations inbiting Mediterranean submarine canyons', *Deep Sea Research Part I: Oceanographic Research Papers* **47**(8), 1513–1533.

Gili, JM, J Bouillon, A Palanques and P Puig (1999), 'Submarine canyons as habitats of prolific plankton populations: three new deep-sea Hydroidomedusae in the western Mediterranean', *Zoological Journal of the Linnean Society* **125**(3), 313–329.

Glover, AG and CR Smith (2003), 'The deep-sea floor ecosystem: current status and prospects of anthropogenic change by the year 2025', *Environmental Conservation* **30**(3), 219–241.

Glud, RN (2008), 'Oxygen dynamics of marine sediments', *Marine Biology Research* **4**(4), 243–289.

Golub, GH, M Heath and G Wahba (1979), 'Generalized cross-validation as a method for choosing a good ridge parameter', *Technometrics* **21**(2), 215–223.

Goñi, R, F Alvarez and S Adlerstein (1999), 'Application of generalized linear modeling to catch rate analysis of Western Mediterranean fisheries: the Castellón trawl fleet as a case study', *Fisheries Research* **42**(3), 291 – 302.

Gontikaki, E, D van Oevelen, K Soetaert and U Witte (2011), 'Food web flows through a subarctic deep-sea benthic community', *Progress in Oceanography* **91**(3), 245–259.

Gooday, AJ (1988), 'A response by benthic Foraminifera to the deposition of phytodetritus in the deep sea', *Nature* **332**(6159), 70 – 73.

Gooday, AJ, CM Turley and JA Allen (1990), 'Responses by Benthic Organisms to Inputs of Organic Material to the Ocean Floor: A Review', *Philosophical Transactions of the Royal Society of London. Series A, Mathematical and Physical Sciences* **331**(1616), 119–138.

Gordon, JDM (2001), 'Deep-water fisheries at the Atlantic Frontier', *Continental Shelf Research* **21**(8), 987–1003.

Gori, A, C Orejas, T Madurell, L Bramanti, M Martins, E Quintanilla, P Marti-Puig, C Lo Iacono, P Puig and S Requena (2013), 'Bathymetrical distribution and size structure of cold-water coral populations in the Cap de Creus and Lacaze-Duthiers canyons (northwestern Mediterranean)', *Biogeosciences* **10**(3).

Goutx, M, SG Wakeham, C Lee, M Duflos, C Guigue, Z Liu, B Moriceau, R Sempéré, M Tedetti and J Xue (2007), 'Composition and degradation of marine pArticles with different settling velocities in the northwestern Mediterranean Sea', *Limnology and oceanography* **52**(4), 1645.

Grassle, FJ and HL Sanders (1973), 'Life histories and the role of disturbance', *Deep Sea Research and Oceanographic Abstracts* **20**(7), 643–659.

Gremare, A, JM Amouroux and F Charles (1997), 'Temporal changes in the biochemical composition and nutritional value of the particulate organic matter available to surface deposit-feeders: a two year study', *Oceanographic Literature Review* **44**(9), 934–935.

Griggs, GB, AG Carey Jr and LD Kulm (1969), 'Deep-sea sedimentation and sediment-fauna interaction in Cascadia Channel and on Cascadia Abyssal Plain', *Deep Sea Research and Oceanographic Abstracts* **16**(2), 157–170.

Guidetti, P and E Sala (2007), 'Community-wide effects of marine reserves in the Mediterranean Sea', *Marine Ecology Progress Series* **335**, 43–56.

Gulland, JA (1964), Catch per unit effort as a measure of abundance, *in* 'Rapport et PV de la Commission international pour l'Exploration Scientifique de la Mer Méditerranéer', Vol. 155, pp. 8–14.

Haedrich, RL, NR Merrett and NR O'Dea (2001), 'Can ecological knowledge catch up with deep-water fishing? A North Atlantic perspective', *Fisheries Research* **51**(2), 113–122.

Hairer, E, SP Nørsett and G Wanner (2008), *Solving ordinary differential equations I: nonstiff problems*, Vol. 1, Springer Science & Business.

Hairston, N, F Smith and L Slobodkin (1960), 'Community structure, population control and competition', *American Naturalist* **94**, 421–425.

Hall Jr, RO and JL Meyer (1998), 'The trophic significance of bacteria in a detritus-based stream food web', *Ecology* **79**(6), 1995–2012.

Hamre, J and E Hatlebakk (1998), System model (systmod) for the norwegian sea and the barents sea, *in* 'Models for multispecies management', Springer, pp. 93–115.

Harris, PT and T Whiteway (2011), 'Global distribution of large submarine canyons: Geomorphic differences between active and passive continental margins', *Marine Geology* **285**(1), 69–86.

Hastie, Trevor J and Robert J Tibshirani (1990), *Generalized additive models*, Vol. 43, CRC Press.

Hecker, B (1990), 'Photographic evidence for the rapid flux of pArticles to the sea floor and their transport down the continental slope', *Deep Sea Research Part A. Oceanographic Research Papers* **37**(12), 1773–1782.

Heleno, R, C Garcia, P Jordano, A Traveset, JM Gómez, N Blüthgen, J Memmott, M Moora, J Cerdeira, S Rodríguez-Echeverría, H Freitas and JM Olesen (2014), 'Ecological networks: delving into the architecture of biodiversity', *Biology letters* **10**(1), 20131000.

Helser, TE, AE Punt and RD Methot (2004), 'A generalized linear mixed model analysis of a multi-vessel fishery resource survey', *Fisheries Research* **70**(2–3), 251 – 264.

Herbland, A and B Voituriez (1979), 'Hydrological structure analysis for estimating the primary production in the tropical Atlantic Ocean', *Journal of Marine Research* **37**(1), 87–101.

Hilborn, R and CJ Walters (1992), *Quantitative Fisheries Stock Assessment*, Chapman & Hall.

Hirata, H and RE Ulanowicz (1984), 'Information theoretical analysis of ecological networks', *International journal of systems science* **15**(3), 261–270.

Hollowed, AB, N Bax, R Beamish, J Collie, M Fogarty, P Livingston, J Pope and JC Rice (2000), 'Are multispecies models an improvement on single-species models for measuring fishing impacts on marine ecosystems?', *ICES Journal of Marine Science: Journal du Conseil* **57**(3), 707–719.

Holme, NA (1984), 'Fluctuations of *Ophiothrix fragilis* in the western English Channel', *Journal of the Marine Biological Association of the United Kingdom* **64**(02), 351–378.

Hopkins, TS (1978), 'Physical processes in the Mediterranean basins', *Estuarine transport processes* pp. 269–310.

Hughes, TP (1994), 'Catastrophes, phase shifts, and large-scale degradation of a Caribbean coral reef', *SCIENCE-NEW YORK THEN WASHINGTON-* pp. 1547–1547.

Hunter, MD and PW Price (1992), 'Playing chutes and ladders: heterogeneity and the relative roles of bottom-up and top-down forces in natural communities.', *Ecology* **73**(3), 723–732.

Huvenne, VAI, PA Tyler, DG Masson, EH Fisher, C Hauton, V Hühnerbach, TP Le Bas and GA Wolff (2011), 'A picture on the wall: innovative mapping reveals cold-water coral refuge in submarine canyon', *PloS one* **6**(12), e28755.

Huxel, GR and K McCann (1998), 'Food web stability: the influence of trophic flows across habitats.', *American Naturalist* **152**, 460–469.

Jackson, JBC, MX Kirby, WH Berger, KA Bjorndal, LW Botsford, BJ Bourque, RH Bradbury, R Cooke, J Erlandson, JA Estes, TP Hughes, S Kidwell, CB Lange, HS Lenihan, JM Pandolfi, CH Peterson, RS Steneck, MJ Tegner and RR Warner (2001), 'Historical overfishing and the recent collapse of coastal ecosystems', *Science* **293**(5530), 629–637.

Jennings, S and MJ Kaiser (1998), 'The effects of fishing on marine ecosystems', *Advances in marine biology* **34**, 201–352.

Johannes, RE (1998), 'The case for data-less marine resource management: examples from tropical nearshore finfisheries', *Trends in Ecology & Evolution* **13**(6), 243 – 246.

Jones, AM and JM Baxter (1987), *Molluscs: Caudofoveata, Solenogastres, Polyplacophora and Scaphopoda: Keyes and Notes for the Identification of Species*, number 37, Brill Archive.

Jordi, A and S Hameed (2009), 'Influence of the Icelandic low on the variability of surface air temperature in the Gulf of Lion: implications for intermediate water formation', *Journal of Physical Oceanography* **39**(12), 3228–3232.

Josselyn, MN, GM Cailliet, TM Niesen, R Cowen, AC Hurley, J Connor and S Hawes (1983), 'Composition, export and faunal utilization of drift vegetation in the Salt River submarine canyon', *Estuarine Coastal and Shelf Science* **17**(4), 447–465.

Jurado-Molina, J, PA Livingston and JN Ianelli (2005), 'Incorporating predation interactions in a statistical catch-at-age model for a predator-prey system in the eastern Bering Sea', *Canadian Journal of Fisheries and Aquatic Sciences* **62**(8), 1865–1873.

Kaiser, MJ and BE Spencer (1996), 'The effects of beam-trawl disturbance on infaunal communities in different habitats', *Journal of Animal Ecology* pp. 348–358.

Kammann, EE and MP Wand (2003), 'Geoadditive models', *Journal of the Royal Statistical Society: Series C (Applied Statistics)* **52**(1), 1–18.

Kenyon, KW (1969), 'The sea otter in the eastern Pacific Ocean', *North American Fauna* pp. 1–352.

Kinder, TH and G Parrilla (1987), 'Yes, some of the Mediterranean outflow does come from great depth', *Journal of Geophysical Research* **92**(C3), 2901–2906.

Klein, N, T Kneib and S Lang (2013), Bayesian Structured Additive Distributional Regression, Technical report.
URL: *http://eeecon.uibk.ac.at/wopec2/repec/inn/wpaper/2013-23.pdf*

Klepper, O and JPG Van de Kamer (1987), 'The use of mass balances to test and improve the estimates of carbon fluxes in an ecosystem', *Mathematical Biosciences* **85**(1), 37–49.

Koen-Alonso, M and P Yodzis (2005), 'Multispecies modelling of some components of the marine community of northern and central Patagonia, Argentina', *Canadian Journal of Fisheries and Aquatic Sciences* **62**(7), 1490–1512.

Kones, JK, K Soetaert, D van Oevelen and JO Owino (2009), 'Are network indices robust indicators of food web functioning? a monte carlo approach', *Ecological Modelling* **220**(3), 370–382.

Kones, JK, K Soetaert, D van Oevelen, JO Owino and K Mavuti (2006), 'Gaining insight into food webs reconstructed by the inverse method', *Journal of Marine Systems* **60**(1), 153–166.

Koslow, JA, GW Boehlert, JDM Gordon, RL Haedrich, P Lorance and N Parin (2000), 'Continental slope and deep-sea fisheries: implications for a fragile ecosystem', *ICES Journal of Marine Science: Journal du Conseil* **57**(3), 548–557.

Kröncke, I and M Türkay (2003), 'Structural and functional aspects of the benthic communities in the deep Angola Basin', *Marine Ecology Progress Series* **260**, 43–53.

Kröncke, I, M Türkay and D Fiege (2003), 'Macrofauna communities in the Eastern Mediterranean deep sea', *Marine Ecology* **24**(3), 193–216.

Lang, S and A Brezger (2004), 'Bayesian P-Splines', *Journal of Computational and Graphical Statistics* **13**(1), 183–212.

Lassen, H and P Medley (2000), Virtual population analysis. A practical manual for stock assessment. FAO Fisheries, Technical Report No. 400, FAO, Rome.

Latham II, LG (2006), 'Network flow analysis algorithms', *Ecological Modelling* **192**(3), 586–600.

Latham II, LG and EP Scully (2002), 'Quantifying constraint to assess development in ecological networks', *Ecological Modelling* **154**(1), 25–44.

Lehodey, P, F Chai and J Hampton (2003), 'Modelling climate-related variability of tuna populations from a coupled ocean–biogeochemical-populations dynamics model', *Fisheries Oceanography* **12**(4–5), 483–494.

Lehodey, P, I Senina and R Murtugudde (2008), 'A spatial ecosystem and populations dynamics model (SEAPODYM)–Modeling of tuna and tuna-like populations', *Progress in Oceanography* **78**(4), 304–318.

Levin, LA and M Sibuet (2012), 'Understanding continental margin biodiversity: a new imperative', *Annual Review of Marine Science* **4**, 79–112.

Libralato, S, M Coll, M Tempesta, A Santojanni, M Spoto, I Palomera, E Arneri and C Solidoro (2010), 'Food-web traits of protected and exploited areas of the Adriatic Sea', *Biological Conservation* **143**(9), 2182–2194.

Lin, X and D Zhang (1999), 'Inference in generalized additive mixed models by using smoothing splines', *Journal of the Royal Statistical Society: Series B (Statistical Methodology)* **61**(2), 381–400.

Lindeman, RL (1942), 'The trophic-dynamic aspect of ecology', *Ecology* **23**(4), 399–417.

Livingston, PA and RD Methot (1998), 'Incorporation of predation into a population assessment model of eastern Bering Sea walleye pollock', *Fishery stock assessment models* pp. 663–678.

Lleonart, J and F Maynou (2003), 'Fish stock assessments in the Mediterranean: state of the art', *Scientia Marina* **67**, 37–49.

Lohrenz, SE, RA Arnone, DA Wiesenburg and IP DePalma (1988), Satellite detection of transient enhanced primary production in the western Mediterranean Sea, Technical report, DTIC Document.

López-Jurado, JL, M Marcos and S Monserrat (2008), 'Hydrographic conditions affecting two fishing grounds of Mallorca island (Western Mediterranean): during the IDEA Project (2003–2004)', *Journal of Marine Systems* **71**(3), 303–315.

MacArthur, R (1955), 'Fluctuations of animal populations and a measure of community stability', *ecology* **36**(3), 533–536.

Mackay, A (1981), 'The generalized inverse', *Practical Computing* **Sep.**, 108–110.

Macpherson, E (1981), 'Resource partitioning in a Mediterranean fish community', *Marine Ecology Progress Series* **4**, 183–193.

Macquart-Moulin, C and G Patriti (1996), 'Accumulation of migratory micronekton crustaceans over the upper slope and submarine canyons of the northwestern Mediterranean', *Deep Sea Research Part I: Oceanographic Research Papers* **43**(5), 579–601.

Madurell, T and JE Cartes (2005), 'Trophodynamics of a deep-sea demersal fish assemblage from the bathyal eastern Ionian Sea (Mediterranean Sea)', *Deep Sea Research Part I: Oceanographic Research Papers* **52**(11), 2049–2064.

Mahaut, ML, M Sibuet and Y Shirayama (1995), 'Weight-dependent respiration rates in deep-sea organisms', *Deep Sea Research Part I: Oceanographic Research Papers* **42**(9), 1575–1582.

Mamouridis, V, F Maynou and G Aneiros Pérez (2014), 'Analysis and standardization of landings per unit effort of red shrimp *Aristeus antennatus* from the trawl fleet of Barcelona (NW Mediterranean)', *Scientia Marina* **78**, 7–16.

Mamouridis, V, JE Cartes and E Fanelli (2014*a*), Multivariate techniques in ecology: The infauna associated to a CWC habitat (facies of *Isidella elongata*), influences of fishing activity and natural variability.

Mamouridis, V, JE Cartes and E Fanelli (2014*b*), The macrofauna associated to the deep-sea coral *Isidella elongata*: human impact and natural variability.

Mamouridis, V, JE Cartes, S Parra, E Fanelli and JI Saiz Salinas (2011), 'A temporal analysis on the dynamics of deep-sea macrofauna: influence of environmental variability off Catalonia coasts (western Mediterranean)', *Deep Sea Research Part I: Oceanographic Research Papers* **58**(4), 323–337.

Marchal, P, B Andersen, B Caillart, O Eigaard, O Guyader, H Hovgaard, A Iriondo, F Le Fur, J Sacchi and M Santurtún (2007), 'Impact of technological creep on fishing effort and fishing mortality, for a selection of European fleets', *ICES Journal of Marine Science: Journal du Conseil* **64**(1), 192–209.

Marchal, P, C Ulrich, K Korsbrekke, M Pastoors and B Rackham (2002), 'A comparison of three indices of fishing power on some demersal fisheries of the North Sea', *ICES Journal of Marine Science: Journal du Conseil* **59**(3), 604–623.

Margalef, R and J Castellví (1967), 'Fitoplancton y producción primaria de la costa catalana, de julio de 1966 a julio de 1967', *Investigación Pesquera* **31**(3), 491–502.

Marriott, RJ, B Wise and J St John (2011), 'Historical changes in fishing efficiency in the west coast demersal scalefish fishery, Western Australia: implications for assessment and management', *ICES Journal of Marine Science: Journal du Conseil* **68**(1), 76–86.

Martinez, ND (1992), 'Constant connectance in community food webs', *American Naturalist* pp. 1208–1218.

Marty, JC and J Chiavérini (2010), 'Hydrological changes in the Ligurian Sea (NW Mediterranean, DYFAMED site) during 1995–2007 and biogeochemical consequences', *Biogeosciences Discussions* **7**(1), 1377–1406.

Marty, JC, J Chiavérini, MD Pizay and B Avril (2002), 'Seasonal and interannual dynamics of nutrients and phytoplankton pigments in the western Mediterranean Sea at the DYFAMED time-series station (1991–1999)', *Deep Sea Research Part II: Topical Studies in Oceanography* **49**(11), 1965–1985.

Marx, BD and PHC Eilers (1998), 'Direct generalized additive modeling with penalized likelihood', *Computational Statistics & Data Analysis* **28**(2), 193–209.

Maunder, MN and AE Punt (2004), 'Standardizing catch and effort data: a review of recent approaches', *Fisheries Research* **70**(2), 141–159.

Maunder, MN, JR Sibert, A Fonteneau, J Hampton, P Kleiber and SJ Harley (2006), 'Interpreting catch per unit effort data to assess the status of individual stocks and communities', *ICES Journal of Marine Science: Journal du Conseil* **63**(8), 1373–1385.

May, RM (1972), 'Will a large complex system be stable?', *Nature* **238**, 413–414.

Maynou, F (2008), 'Environmental causes of the fluctuations of red shrimp (*Aristeus antennatus*) landings in the Catalan Sea', *Journal of Marine Systems* **71**(3–4), 294–302.

Maynou, F and JE Cartes (1998), 'Daily ration estimates and comparative study of food consumption in nine species of deep-water decapod crustaceans of the NW Mediterranean', *Marine Ecology Progress Series* **171**, 221–231.

Maynou, F, M Demestre and P Sanchez (2003), 'Analysis of catch per unit effort by multivariate analysis and generalised linear models for deep-water crustacean fisheries off Barcelona (NW Mediterranean)', *Fisheries Research* **65**(1–3), 257–269.

Maynou, F, M Sbrana, P Sartor, C Maravelias, S Kavadas, D Damalas, JE Cartes and G Osio (2011), 'Estimating trends of population decline in long-lived marine species in the Mediterranean Sea based on fishers' perceptions', *PloS one* **6**(7), e21818.

McCann, KS (2000), 'The diversity–stability debate', *Nature* **405**(6783), 228–233.

McClanahan, TR and E Sala (1997), 'A Mediterranean rocky-bottom ecosystem fisheries model', *Ecological Modelling* **104**(2), 145–164.

McClanahan, TR and SH Shafir (1990), 'Causes and consequences of sea urchin abundance and diversity in Kenyan coral reef lagoons', *Oecologia* **83**(3), 362–370.

McCullagh, P and JA Nelder (1989), *Generalized Linear Models*, Chapman & Hall, London.

McDonald, AD, E Fulton, LR Little, R Gray, KJ Sainsbury and VD Lyne (2006), *Complex Science for a Complex World: Exploring Human Ecosystems with Agents*, ANU E Press, chapter Multiple use management strategy evaluation for coastal marine ecosystems using InVitro, pp. 265–279.

Mendelssohn, R and P Cury (1989), 'Temporal and Spatial Dynamics of a Coastal Pelagic Species, Sardinella maderensis off the Ivory Coast', *Canadian Journal of Fisheries and Aquatic Sciences* **46**(10), 1686–1697.

Menge, BA (1995), 'Indirect effects in marine rocky intertidal interaction webs: patterns and importance', *Ecological monographs* **65**(1), 21–74.

Merino, G, C Karlou-Riga, I Anastopoulou, F Maynou and J Lleonart (2007), 'Bioeconomic simulation analysis of hake and red mullet fishery in the Gulf of Saronikos (Greece)', *Scientia Marina* **71**(3), 525–535.

Merrett, NR, RL Haedrich, JDM Gordon and M Stehmann (1991), 'Deep demersal fish assemblage structure in the Porcupine Seabight (eastern North Atlantic): results of single warp trawling at lower slope to abyssal soundings', *Journal of the Marine Biological Association of the United Kingdom* **71**(02), 359–373.

Millot, C, I Taupier-Letage and M Benzohra (1990), 'The Algerian eddies', *Earth-Science Reviews* **27**(3), 203–219.

Minas, HJ (1968), 'A propos d'une remontee d'eau "profonde" dans les parages du Golfe de Marseille (octobre 1964): Consequences biologiques', *Cahier Oceanographique* **20**, 641–674.

Minas, HJ, B Coste and M Minas (1984), 'Oceanographie du detroit de Gibraltar et des parages annexes', *Le Courrier du CNRS* **57**, 10–17.

Miquel, JC, SW Fowler, J La Rosa and P Buat-Menard (1994), 'Dynamics of the downward flux of pArticles and carbon in the open northwestern Mediterranean Sea', *Deep Sea Research Part I: Oceanographic Research Papers* **41**(2), 243–261.

Moksnes, PO, M Gullström, K Tryman and S Baden (2008), 'Trophic cascades in a temperate seagrass community', *Oikos* **117**(5), 763–777.

Möllmann, C, B Müller-Karulis, G Kornilovs and MA St John (2008), 'Effects of climate and overfishing on zooplankton dynamics and ecosystem structure: regime shifts, trophic cascade, and feedback loops in a simple ecosystem', *ICES Journal of Marine Science: Journal du Conseil* **65**(3), 302–310.

Möllmann, C, M Lindegren, T Blenckner, L Bergström, M Casini, R Diekmann, J Flinkman, B Müller-Karulis, S Neuenfeldt, JO Schmidt, M Tomczak, R. Voss and A Gårdmark (2013), 'Implementing ecosystem-based fisheries management: from single-species to integrated ecosystem assessment and advice for Baltic Sea fish stocks', *ICES Journal of Marine Science: Journal du Conseil* **71**(5), 1187–1197.

Moore, JC, EL Berlow, DC Coleman, PC de Ruiter, Q Dong, A Hastings, N Collins Johnson, KS McCann, K Melville, PJ Morin, K Nadelhoffer, AD Rosemond, DM Post, JL Sabo, KM Scow, MJ Vanni and DH Wall (2004), 'Detritus, trophic dynamics and biodiversity', *Ecology letters* **7**(7), 584–600.

Moore, JC and PC de Ruiter (2012), *Energetic food webs: an analysis of real and model ecosystems*, Oxford University Press, Oxford UK.

Moranta, J, C Stefanescu, E Massutí, B Morales-Nin and D Lloris (1998), 'Fish community structure and depth-related trends on the continental slope of the Balearic Islands (Algerian basin, western Mediterranean)', *Marine Ecology Progress Series* **171**, 247–259.

Moranta, J, E Massutí and B Morales-Nin (2000), 'Fish catch composition of the deep-sea decapod crustacean fisheries in the Balearic Islands (western Mediterranean)', *Fisheries Research* **45**(3), 253–264.

Morato, T, R Watson, TJ Pitcher and D Pauly (2006), 'Fishing down the deep', *Fish and Fisheries* **7**(1), 24–34.

Mori, M and DS Butterworth (2004), 'Consideration of multispecies interactions in the Antarctic: a preliminary model of the minke whale–blue whale–krill interaction', *African Journal of Marine Science* **26**(1), 245–259.

Mori, M and DS Butterworth (2005), 'Modelling the predator-prey interactions of krill, baleen whales and seals in the Antarctic', *IWC Scientific committee paper SC/57 O* **21**.

Mori, M and DS Butterworth (2006), 'A first step towards modelling the krill-predator dynamics of the Antarctic ecosystem', *CCAMLR Science* **13**, 217–277.

Myers, RA and B Worm (2005), 'Extinction, survival or recovery of large predatory fishes', *Philosophical Transactions of the Royal Society B: Biological Sciences* **360**(1453), 13–20.

Myers, RA and P Pepin (1990), 'The robustness of lognormal-based estimators of abundance', *Biometrics* **1**, 1185–1192.

Neal, RA and RC Maris (1985), *The Biology of Crustacea Vol 10: Economic aspects: fisheries and culture*, Academic Press Inc., chapter Fisheries biology of shrimps and shrimplike animals.

Nédélec, H (1982), Ethologie alimentaire de *Paracentrotus lividus* dans la baie Galeria (Corse) et son impact sur les peuplements phytobenthiques, PhD thesis, Université Pierre et Marie Curie and Université Aix-Marseille II, Marseille.

Neutel, AM, JAP Heesterbeek and PC de Ruiter (2002), 'Stability in real food webs: weak links in long loops', *Science* **296**(5570), 1120–1123.

Niquil, N, GA Jackson, L Legendre and B Delesalle (1998), 'Inverse model analysis of the planktonic food web of Takapoto Atoll (French Polynesia)', *Marine Ecology Progress Series* **165**, 17–29.

Nittrouer, CA and LD Wright (1994), 'Transport of particles across continental shelves', *Reviews of Geophysics* **32**(1), 85–113.

Odum, EP (1969), 'The strategy of ecosystem development', *Science* **164**, 262–270.

Odum, HT (1957), 'Trophic structure and productivity of Silver Springs, Florida', *Ecological Monographs* **27**(1), 55–112.

Oksanen, T (1990), 'Exploitation ecosystems in heterogeneous habitat complexes', *Evolutionary Ecology* **4**(3), 220–234.

Oliver, P (1993), 'Analysis of fluctuations observed in the trawl fleet landings of the Balearic Islands', *Scientia Marina* **57**, 219–227.

O'Neill, RV (1969), 'Indirect estimation of energy fluxes in animal food webs', *Journal of Theoretical Biology* **22**(2), 284–290.

Orsi Relini, L, A Mannini and G Relini (2013), 'Updating knowledge on growth, population dynamics, and ecology of the blue and red shrimp, *Aristeus antennatus* (Risso, 1816), on the basis of the study of its instars', *Marine Ecology* **34**, 90–102.

Paine, RT (1980), 'Food webs: linkage, interaction strength and community infrastructure', *Journal of Animal Ecology* **49**(3), 667–685.

Palanques, A, X Durrieu de Madron, P Puig, J Fabres, J Guillén, A Calafat, M Canals, S Heussner and J Bonnin (2006), 'Suspended sediment fluxes and transport processes in the Gulf of Lions submarine canyons. The role of storms and dense water cascading', *Marine Geology* **234**(1), 43–61.

Palkovacs, EP, MT Kinnison, C Correa, CM Dalton and AP Hendry (2012), 'Fates beyond traits: ecological consequences of human-induced trait change', *Evolutionary Applications* **5**(2), 183–191.

Paloheimo, JE and LM Dickie (1964), 'Abundance and fishing success', *Rapports et Proces-Verbaux des Réunions du Conseil International pour l'Exploration de la Mer* **155**.

Papaconstantinou, C and H Farrugio (2000), 'Fisheries in the Mediterranean', *Mediterranean Marine Science* **1**(1), 5–18.

Papiol, V, JE Cartes, E Fanelli and F Maynou (2012), 'Influence of environmental variables on the spatio-temporal dynamics of bentho-pelagic assemblages in the middle slope of the Balearic Basin (NW Mediterranean)', *Deep Sea Research Part I: Oceanographic Research Papers* **61**(0), 84–99.

Papiol, V, JE Cartes, E Fanelli and P Rumolo (2013), 'Food web structure and seasonality of slope megafauna in the NW Mediterranean elucidated by stable isotopes: Relationship with available food sources', *Journal of Sea Research* **77**(0), 53–69.

Parapar, J, C Alós, J Núñez, J Moreira, E López, F Aguirrezabalaga, C Besteiro and A Martínez (2012), *Fauna Iberica 36: Annelida Polychaeta III*, Museo Nacional de Ciencias Naturales, CSIC, Madrid.

Pardo, EV and AC Zacagnini Amaral (2004), 'Feeding behavior of *Scolelepis* sp.(Polychaeta: Spionidae)', *Brazilian Journal of Oceanography* **52**(1), 74–79.

Patten, BC (1995), 'Network integration of ecological extremal principles: exergy, emergy, power, ascendency, and indirect effects', *Ecological Modelling* **79**(1), 75–84.

Patten, BC and M Higashi (1984), 'Modified cycling index for ecological applications', *Ecological Modelling* **25**(1), 69–83.

Pauly, D (1982), 'A method to estimate the stock-recruitment relationship of shrimps', *Transactions of the American Fisheries Society* **111**(1), 13–20.

Pauly, D (1985), 'Population dynamics of short-lived species, with emphasis on squids', *NAFO Scientific Council Studies* **9**, 143–154.

Pauly, D (1996), 'One hundred million tonnes of fish, and fisheries research', *Fisheries Research* **25**(1), 25–38.

Pauly, D, V Christensen and C Walters (2000), 'Ecopath, Ecosim, and Ecospace as tools for evaluating ecosystem impact of fisheries', *ICES Journal of Marine Science: Journal du Conseil* **57**(3), 697–706.

Pauly, D, V Christensen, J Dalsgaard, R Froese and F Torres (1998), 'Fishing down marine food webs', *Science* **279**(5352), 860–863.

Pavithran, S, BS Ingole, M Nanajkar, C Raghukumar, BN Nath and AB Valsangkar (2009), 'Composition of macrobenthos from the central Indian Ocean Basin', *Journal of Earth System Science* **118**(6), 689–700.

Pearson, TH and R Rosenberg (1978), *Oceanography and marine biology: an annual review*, Vol. 16, CRC Press Taylor & Francis Group, chapter Macrobenthic succession in relation to organic enrichment and pollution of the marine environment.

Pennington, M (1983), 'Efficient Estimators of Abundance, for Fish and Plankton Surveys', *Biometrics* **39**(1), 281–286.

Pérès, JM (1985), *History of the Mediterranean biota and the colonization of the depths*, Vol. 7, Pergamon Press Oxford.

Pérès, JM and J Picard (1964), 'Nouveau manuel de bionomie benthique de la Mer Mediterranee', *Recueil des Travaux de la Station Marine d'Endoume* **31**(47), 1–137.

Pikitch, EK, C Santora, EA Babcock, A Bakun, R Bonfil, DO Conover, P Dayton, P Doukakis, D Fluharty, B Heneman, ED Houde, J Link, PA Livingston, M Mangel, MK McAllister, J Pope and KJ Sainsbury (2004), 'Ecosystem-Based Fishery Management', *Science* **305**(5682), 346–347.

Pimm, SL (1984), 'The complexity and stability of ecosystems', *Nature* **307**(5949), 321–326.

Pimm, SL (1991), 'Food web patterns and their consequences', *Nature* **350**, 669–674.

Pimm, SL and JH Lawton (1980), 'Are food webs divided into compartments?', *The Journal of Animal Ecology* pp. 879–898.

Pinheiro, JC and DM Bates (2000), *Mixed Effects Models in S and S-PLUS*, New York.

Pinnegar, JK, NVC Polunin, P Francour, F Badalamenti, R Chemello, ML Harmelin-Vivien, B Hereu, M Milazzo, M Zabala, G d'Anna and C Pipitone (2000), 'Trophic cascades in benthic marine ecosystems: lessons for fisheries and protected-area management', *Environmental Conservation* **27**(02), 179–200.

Pipitone, C, F Badalamenti, G D'Anna and B Patti (2000), 'Fish biomass increase after a four-year trawl ban in the Gulf of Castellammare (NW Sicily, Mediterranean Sea)', *Fisheries Research* **48**(1), 23–30.

Piroddi, C, G Bearzi and V Christensen (2010), 'Effects of local fisheries and ocean productivity on the northeastern Ionian Sea ecosystem', *Ecological Modelling* **221**(11), 1526–1544.

Plagányi, E (2007), *Models for an ecosystem approach to fisheries*, number 477, FAO, Rome.

Plagányi, E and D Butterworth (2006), A spatial multi-species operating model (SMOM) of krill–predator interactions in small-scale management units in the Scotia Sea, *in* 'Workshop document presented to WG–EMM subgroup of CCAMLR (Commission for the Conservation of Antarctic Marine Living Resources), WG–EMM–06/12', p. 28.

Polis, GA (1999), 'Why are parts of the world green? Multiple factors control productivity and the distribution of biomass', *Oikos* **86**, 3–15.

Polis, GA and DR Strong (1996), 'Food web complexity and community dynamics', *American Naturalist* **147**(5), 813–846.

Politou, C, S Kavadas, Ch Mytilineou, A Tursi, R Carlucci and G Lembo (2003), 'Fisheries resources in the deep waters of the Eastern Mediterranean (Greek Ionian Sea)', *Journal of Northwest Atlantic Fishery Science* **31**, 35.

Polovina, JJ (1984), 'Model of a coral reef ecosystem', *Coral reefs* **3**(1), 1–11.

Power, ME (1992), 'Top-down and bottom-up forces in food webs: do plants have primacy', *Ecology* **73**(3), 733–746.

Prena, J, P Schwinghamer, TW Rowell, DC Gordon, KD Gilkinson, WP Vass and DL McKeown (1999), 'Experimental otter trawling on a sandy bottom ecosystem of the Grand Banks of Newfoundland: analysis of trawl bycatch and effects on epifauna', *Marine Ecology Progress Series* **181**, 107–124.

Prieur, L and M Tiberti (1984), 'Identification et échelles des processus près du front de la mer Ligure', *Rapport Committee international Mer Méditerranée* **29**, 35–36.

Puig, P, A Palanques, DL Orange, G Lastras and M Canals (2008), 'Dense shelf water cascades and sedimentary furrow formation in the Cap de Creus Canyon, northwestern Mediterranean Sea', *Continental Shelf Research* **28**(15), 2017–2030.

Puig, P, AS Ogston, BL Mullenbach, CA Nittrouer and RW Sternberg (2003), 'Shelf-to-canyon sediment-transport processes on the Eel continental margin (northern California)', *Marine Geology* **193**(1), 129–149.

Punt, AE and DS Butterworth (1995), 'The effects of future consumption by the Cape fur seal on catches and catch rates of the Cape hakes. 4. Modelling the biological interaction between Cape fur seals *Arctocephalus pusillus pusillus* and the Cape hakes *Merluccius capensis* and *M. paradoxus*', *South African Journal of Marine Science* **16**(1), 255–285.

Purcell, SW and DS Kirby (2006), 'Restocking the sea cucumber *Holothuria scabra*: Sizing no-take zones through individual-based movement modelling', *Fisheries Research* **80**(1), 53–61.

Pusceddu, A, S Bianchelli, M Canals, A Sanchez-Vidal, X Durrieu De Madron, S Heussner, V Lykousis, H de Stigter, F Trincardi and R Danovaro (2010), 'Organic matter in sediments of canyons and open slopes of the Portuguese, Catalan, Southern Adriatic and Cretan Sea margins', *Deep Sea Research Part I: Oceanographic Research Papers* **57**(3), 441–457.

Ragonese, S and ML Bianchini (1996), 'Growth, mortality and yield-per-recruit of the deep-water shrimp Aristeus antennatus (Crustacea-Aristeidae) of the Strait of Sicily (Mediterranean Sea)', *Fisheries Research* **26**(1), 125–137.

Reid, K and JP Croxall (2001), 'Environmental response of upper trophic-level predators reveals a system change in an Antarctic marine ecosystem', *Proceedings of the Royal Society of London. Series B: Biological Sciences* **268**(1465), 377–384.

Reid, PC, EJV Battle, SD Batten and KM Brander (2000), 'Impacts of fisheries on plankton community structure', *ICES Journal of Marine Science: Journal du Conseil* **57**(3), 495–502.

Reyss, D (1971), 'Les canyons sous-marins de la mer Catalane: le rech du Cap et le rech Lacaze-Duthiers. III. Les peuplements de macrofaune benthique', *Vie Milieu* **22**(3B), 529–613.

Rigby, RA and DM Stasinopoulos (2005), 'Generalized additive models for location, scale and shape', *Journal of the Royal Statistical Society: Series C (Applied Statistics)* **54**(3), 507–554.

Righini, P and A Abella (1994), 'Life cycle of *Aristeus antennatus* and *Aristaeomorpha foliacea* in the Northern Tyrrhenian Sea', *NTRITPP Special Publication* **3**, 29–30.

Roberts, J Murray, Andrew J Wheeler and André Freiwald (2006), 'Reefs of the deep: the biology and geology of cold-water coral ecosystems', *Science* **312**(5773), 543–547.

Röder, H (1971), 'Gangsysteme von Paraonis fulgens Levinsen 1883 (Polychaeta) in ökologischer, ethologischer und aktuopaläontologischer Sicht', *Senckenbergiana maritima* **3**, 3–51.

Roff, JC, K Middlebrook and F Evans (1988), 'Long-term variability in North Sea zooplankton off the Northumberland coast: productivity of small copepods and analysis of trophic interactions', *Journal of the Marine Biological Association of the United Kingdom* **68**(01), 143–164.

Romero-Wetzel, MB (1987), 'Sipunculans as inhabitants of very deep, narrow burrows in deep-sea sediments', *Marine Biology* **96**(1), 87–91.

Rooney, Neil, Kevin McCann, Gabriel Gellner and John C Moore (2006), 'Structural asymmetry and the stability of diverse food webs', *Nature* **442**(7100), 265–269.

Ross, SW and AM Quattrini (2007), 'The fish fauna associated with deep coral banks off the southeastern United States', *Deep Sea Research Part I: Oceanographic Research Papers* **54**(6), 975–1007.

Rotterman, LM and TS Jackson (1988), *Sea otter, Enhydra lutris*, Marine Mammal Commission.

Rowe, GT, PT Polloni and RL Haedrich (1982), 'The deep-sea macrobenthos on the continental margin of the northwest Atlantic Ocean', *Deep Sea Research Part A. Oceanographic Research Papers* **29**(2), 257–278.

Rudstam, LG, G Aneer and M Hildén (1994), 'Top-down control in the pelagic Baltic ecosystem', *Dana* **10**, 105–129.

Ruhl, HA, JA Ellena and KL Smith (2008), 'Connections between climate, food limitation, and carbon cycling in abyssal sediment communities', *Proceedings of the National Academy of Sciences* **105**(44), 17006–17011.

Ruhl, HA and KL Smith (2004), 'Shifts in deep-sea community structure linked to climate and food supply', *Science* **305**(5683), 513–515.

Ruppert, D, MP Wand and RaJ Carroll (2003), *Semiparametric regression Vol. 12*, Cambridge University Press, Cambridge.

Sala, E (1997*a*), 'Fish predators and scavengers of the sea urchin Paracentrotus lividus in protected areas of the north-west Mediterranean Sea', *Marine Biology* **129**(3), 531–539.

Sala, E (1997*b*), 'The role of fishes in the organization of a Mediterranean sublittoral community: II: Epifaunal communities', *Journal of Experimental Marine Biology and Ecology* **212**(1), 45–60.

Sala, E, CF Boudouresque and M Harmelin-Vivien (1998), 'Fishing, trophic cascades, and the structure of algal assemblages: evaluation of an old but untested paradigm', *Oikos* **82**, 425–439.

Sala, E and M Zabala (1996), 'Fish predation and the structure of the sea urchin *Paracentrotus lividus* populations in the NW Mediterranean', *Marine Ecology Progress Series* **140**(1), 71–81.

Salat, J, MA Garcia, A Cruzado, A Palanques, L Arín, D Gomis, J Guillén, A de León, J Puigdefàbregas, J Sospedra and Z Velásquez (2002), 'Seasonal changes of water mass structure and shelf slope exchanges at the Ebro Shelf (NW Mediterranean)', *Continental Shelf Research* **22**(2), 327–348.

Salihoğlu, İ, C Saydam, Ö Başẗurk, K Yilmaz, D Göçmen, E Hatipo?lu and A Yilmaz (1990), 'Transport and distribution of nutrients and chlorophyll-*a* by mesoscale eddies in the north-eastern Mediterranean', *Marine chemistry* **29**, 375–390.

Salvini-Plawen, Lv (1981), 'The molluscan digestive system in evolution', *Malacologia* **21**(37), l–40.

Salvini-Plawen, Lv (1988), 'The structure and function of molluscan digestive systems', *The Mollusca* **11**, 301–379.

Salvini-Plawen, Lv (2009), 'Geographical notes on iberian caudofoveata (mollusca)', *Iberus* **27**, 107–112.

San Martín Peral, G (2004), *Fauna ibérica. Vol. 21. Annelida polychaeta II*, Museo Nacional de Ciencias Naturales, CSIC, Madrid.

Sanders, HL (1968), 'Marine benthic diversity: a comparative study', *American Naturalist* (925), 243–282.

Sanders, HL, RR Hessler and GR Hampson (1965), 'An introduction to the study of deep-sea benthic faunal assemblages along the Gay Head-Bermuda transect', *Deep Sea Research and Oceanographic Abstracts* **12**(6), 845–867.

Sardà, F (1998), 'Symptoms of overexploitation in the stock of the Norway lobster (*Nephrops norvegicus*) on the "Serola Bank" (western Mediterranean Sea off Barcelona)', *Scientia Marina* **62**(3), 295–299.

Sardà, F and F Maynou (1998), 'Assessing perceptions: do Catalan fishermen catch more shrimp on Fridays?', *Fisheries Research* **36**, 149–157.

Sardà, F, F Maynou and L Talló (1997), 'Seasonal and spatial mobility patterns of rose shrimps *Aristeus antennatus* in the Western Mediterranean: results of a long-term study', *Marine Ecology Progress Series* **159**, 133–141.

Sardà, F and JE Cartes (1993), 'Relationship between size and depth in decapod crustacean populations on the deep slope in the Western Mediterranean', *Deep Sea Research Part I: Oceanographic Research Papers* **40**(11), 2389–2400.

Sardà, F, JE Cartes and W Norbis (1994), 'Spatio-temporal structure of the deep-water shrimp *Aristeus antennatus* (Decapoda:Aristeidae) population in the western Mediterranean', *Fishery Bulletin (US)* **92**, 599–607.

Scheffer, M, S Carpenter, JA Foley, C Folke and B Walker (2001), 'Catastrophic shifts in ecosystems', *Nature* **413**(6856), 591–596.

Scheffer, M, SH Hosper, ML Meijer, B Moss and E Jeppesen (1993), 'Alternative equilibria in shallow lakes', *Trends in Ecology & Evolution* **8**(8), 275–279.

Schindler, DW (2006), 'Recent advances in the understanding and management of eutrophication', *Limnology and Oceanography* **51**(1), 356–363.

Scott, DW (2009), *Multivariate density estimation: theory, practice, and visualization*, Vol. 383, John Wiley & Sons Inc.

Sekine, M, H Nakanishi, M Ukita and S Murakami (1991), 'A shallow-sea ecological model using an object-oriented programming language', *Ecological modelling* **57**(3), 221–236.

Shackell, NL, KT Frank, JAD Fisher, B Petrie and WC Leggett (2010), 'Decline in top predator body size and changing climate alter trophic structure in an oceanic ecosystem', *Proceedings of the Royal Society B: Biological Sciences* **277**(1686), 1353–1360.

Shears, NT and RC Babcock (2002), 'Marine reserves demonstrate top-down control of community structure on temperate reefs', *Oecologia* **132**(1), 131–142.

Shin, Y-J and P Cury (2001), 'Exploring fish community dynamics through size-dependent trophic interactions using a spatialized individual-based model', *Aquatic Living Resources* **14**(2), 65–80.

Shin, Y-J and P Cury (2004), 'Using an individual-based model of fish assemblages to study the response of size spectra to changes in fishing', *Canadian Journal of Fisheries and Aquatic Sciences* **61**(3), 414–431.

Shiomoto, A, K Tadokoro, K Nagasawa and Y Ishida (1997), 'Trophic relations in the subarctic North Pacific ecosystem: possible feeding effect from pink salmon', *Marine Ecology Progress Series* **150**(1), 75–85.

Shurin, JB, ET Borer, EW Seabloom, K Anderson, CA Blanchette, B Broitman, SD Cooper and BS Halpern (2002), 'A cross-ecosystem comparison of the strength of trophic cascades', *Ecology letters* **5**(6), 785–791.

Shurin, JB, JL Clasen, HS Greig, P Kratina and PL Thompson (2012), 'Warming shifts top-down and bottom-up control of pond food web structure and function', *Philosophical Transactions of the Royal Society B: Biological Sciences* **367**(1605), 3008–3017.

Sibuet, M, CE Lambert, R Chesselet and L Laubier (1989), 'Density of the major size groups of benthic fauna and trophic input in deep basins of the Atlantic Ocean', *Journal of Marine Research* **47**(4), 851–867.

Smith, KL, HA Ruhl, BJ Bett, DSM Billett, RS Lampitt and RS Kaufmann (2009), 'Climate, carbon cycling, and deep-ocean ecosystems', *Proceedings of the National Academy of Sciences* **106**(46), 19211–19218.

Soetaert, K and D van Oevelen (2009*a*), 'LIM: Linear Inverse Model examples and solution methods', *R package version* **1**.

Soetaert, K and D van Oevelen (2009*b*), 'Modeling food web interactions in benthic deep-sea ecosystems. A practical guide', *Oceanography* **22**.

Soetaert, K and T Petzoldt (2010), 'Inverse modelling, sensitivity and monte carlo analysis in R using package FME', *Journal of Statistical Software* **33**(3), 1–28.

Soetaert, K, T Petzoldt and RW Setzer (2010*a*), 'Solving differential equations in R', *The R Journal* **2**.

Soetaert, K, T Petzoldt and RW Setzer (2010*b*), 'Solving differential equations in R: Package deSolve', *Journal of Statistical Software* **33**(9), 1–25.

Sparholt, H (1995), Using the MSVPA/MSFOR model to estimate the right-hand side of the Ricker curve for Baltic cod, *in* 'ICES Journal of Marine Science: Journal du Conseil', Vol. 52, Oxford University Press, pp. 819–826.

Sparre, P (1991), 'Introduction to multispecies virtual population analysis', *ICES Journal of Marine Science: Journal du Conseil* **193**, 12–21.

Spiegelhalter, DJ, NG Best, BP Carlin and A van der Linde (2002), 'Bayesian Measures of Model Complexity and Fit', *Journal of the Royal Statistical Society. Series B (Statistical Methodology)* **64**(4), 583–639.

Spiller, DA and TW Schoener (1994), 'Effects of top and intermediate predators in a terrestrial food web', *Ecology* **75**(1), 182–196.

Stasinopoulos, DM and RA Rigby (2007), 'Generalized Additive Models for Location Scale and Shape (GAMLSS) in R', *Journal of Statistical Software* **23**(7), 1–46.

Steele, JH (1998), 'Regime shifts in marine ecosystems', *Ecological Applications* **8**(sp1), S33–S36.

Stefanescu, C, B Morales-Nin and E Massutí (1994), 'Fish assemblages on the slope in the Catalan Sea (Western Mediterranean): influence of a submarine canyon', *JMBA-Journal of the Marine Biological Association of the United Kingdom* **74**(3), 499–512.

Stefánsson, G (1996), 'Analysis of groundfish survey abundance data: combining the GLM and delta approaches', *ICES Journal of Marine Science: Journal du Conseil* **53**(3), 577–588.

Stefánsson, G and OK Palsson (1998), 'Points of view: A framework for multispecies modelling of Arcto-boreal systems', *Reviews in Fish Biology and Fisheries* **8**, 101–104.

Steneck, RS, J Vavrinec and AV Leland (2004), 'Accelerating trophic-level dysfunction in kelp forest ecosystems of the western north atlantic', *Ecosystems* **7**(4), 323–332.

Stige, LC, G Ottersen, K Brander, K-S Chan and NC Stenseth (2006), 'Cod and climate: effect of the North Atlantic Oscillation on recruitment in the North Atlantic', *Marine Ecology Progress Series* **325**, 227–241.

Stora, G, M Bourcier, A Arnoux, M Gerino, J Le Campion, F Gilbert and JP Durbec (1999), 'The deep-sea macrobenthos on the continental slope of the northwestern Mediterranean Sea: a quantitative approach', *Deep Sea Research Part I: Oceanographic Research Papers* **46**(8), 1339–1368.

Strauss, SY (1991), 'Indirect effects in community ecology: their definition, study and importance', *Trends in Ecology & Evolution* **6**(7), 206–210.

Strong, DR (1992), 'Are trophic cascades all wet? Differentiation and donor-control in speciose ecosystems', *Ecology* **73**(3), 747–754.

Su, N-J, S-Z Yeh, C-L Sun, AE Punt, Y Chen and S-P Wang (2008), 'Standardizing catch and effort data of the Taiwanese distant-water longline fishery in the western and central Pacific Ocean for bigeye tuna, *Thunnus obesus*', *Fisheries Research* **90**(1), 235–246.

Taylor, L and G Stefánsson (2004), Gadget models of cod-capelin-shrimp interactions in Icelandic waters, Technical report, ICES Document CM.

Taylor, LA and D Taeknigardur (2011), Gadget models of cod–shrimp interactions in icelandic waters, Technical report, RH–03–2011. Science Institute, University of Iceland.

Tchukhtchin, VD (1964), 'Quantitative data on benthos of the Tyrrhenian Sea', *Trudy Sevastopol Biological Station* **17**, 48–50.

Tecchio, S, M Coll, V Christensen, JB Company, E Ramírez-Llodra and F Sarda (2013), 'Food web structure and vulnerability of a deep-sea ecosystem in the NW Mediterranean Sea', *Deep Sea Research Part I: Oceanographic Research Papers* **75**, 1–15.

Ter Braak, CJF (1986), 'Canonical correspondence analysis: a new eigenvector technique for multivariate direct gradient analysis', *Ecology* **67**(5), 1167–1179.

Thistle, D (2003), 'On the utility of metazoan meiofauna for studying the soft-bottom deep sea', *Vie et Milieu* **53**(2–3), 97–102.

Thomson, RB, DS Butterworth, IL Boyd and JP Croxall (2000), 'Modeling the consequences of Antarctic krill harvesting on Antarctic fur seals', *Ecological Applications* **10**(6), 1806–1819.

Thornton, SF and J McManus (1994), 'Application of organic carbon and nitrogen stable isotope and C/N ratios as source indicators of organic matter provenance in estuarine systems: evidence from the Tay Estuary, Scotland', *Estuarine, Coastal and Shelf Science* **38**(3), 219–233.

Thorson, JT and EJ Ward (2014), 'Accounting for vessel effects when standardizing catch rates from cooperative surveys', *Fisheries Research* **155**, 168–176.

Thorson, JT and J Berkson (2010), 'Evaluating single-and multi-species procedures to estimate time-varying catchability functional parameters', *Fisheries Research* **101**(1), 38–49.

Thurstan, RH, S Brockington and CM Roberts (2010), 'The effects of 118 years of industrial fishing on UK bottom trawl fisheries', *Nature Communications* **1**(15), 1–6.

Tjelmeland, S and B Bogstad (1998), 'MULTSPEC–a review of a multispecies modelling project for the Barents Sea', *Fisheries Research* **37**(1), 127–142.

Tjelmeland, S and U Lindstrøm (2005), 'An ecosystem element added to the assessment of Norwegian spring-spawning herring: implementing predation by minke whales', *ICES Journal of Marine Science: Journal du Conseil* **62**(2), 285–294.

Trenkel, VM, JK Pinnegar, JL Blanchard and AN Tidd (2004), Can multispecies models be expected to provide better assessments for Celtic Sea groundfish stocks, *in* 'ICES Annual Science Conference, Vigo, ICES CM'.

Tsagarakis, K, M Coll, M Giannoulaki, S Somarakis, Costas Papaconstantinou and A Machias (2010), 'Food-web traits of the North Aegean Sea ecosystem (Eastern Mediterranean) and comparison with other Mediterranean ecosystems', *Estuarine, Coastal and Shelf Science* **88**(2), 233–248.

Tselepides, A and A Eleftheriou (1992), South Aegean (Eastern Mediterranean) Continental Slope Benthos: Macroinfaunal-Environmental Relationships, *in* 'Deep-sea food chains and the global carbon cycle', Springer, pp. 139–156.

Tselepides, A, K-N Papadopoulou, D Podaras, W Plaiti and D Koutsoubas (2000), 'Macrobenthic community structure over the continental margin of Crete (South Aegean Sea, NE Mediterranean)', *Progress in Oceanography* **46**(2), 401–428.

Tudela, S, F Maynou and M Demestre (1998), 'Influence of Submarine Canyons on the Distribution of The Deep-Water Shrimp, *Aristeus antennatus* (risso, 1816) In The NW Mediterranean', *Crustaceana* **7**(2), 217–225.

Ulanowicz, RE (1986), *Growth and development: ecosystems phenomenology*, Springer-Verlag New York.

Ulanowicz, RE (2000), *Ecological integrity: Integrating Environment, Conservation, and Health. Island Press, Washington, DC*, chapter Toward the measurement of ecological integrity, pp. 99–113.

Ulanowicz, RE (2004), 'Quantitative methods for ecological network analysis', *Computational Biology and Chemistry* **28**(5), 321–339.

Ulanowicz, RE and JS Norden (1990), 'Symmetrical overhead in flow networks', *International Journal of Systems Science* **21**(2), 429–437.

Valiela, I (1995), *Marine ecological processes*, Springer.

Vamvakas, C (1970), 'Peuplements benthiques des substrats meubles du sud de la Mer Egée', *Tethys* **2**(1), 89–130.

Van den Meersche, K, K Soetaert and D Van Oevelen (2009), 'xsample (): An R function for sampling linear inverse problems', *Journal of Statistical Software* **30**(1), 1–15.

Van Dover, CL (1995), 'Ecology of mid-Atlantic ridge hydrothermal vents', *Geological Society, London, Special Publications* **87**(1), 257–294.

Van Dover, CL, CR German, KG Speer, LM Parson and RC Vrijenhoek (2002), 'Evolution and biogeography of deep-sea vent and seep invertebrates', *Science* **295**(5558), 1253–1257.

van Oevelen, D, G Duineveld, M Lavaleye, F Mienis, K Soetaert and CHR Heip (2009), 'The cold-water coral community as a hot spot for carbon cycling on continental margins: A food-web analysis from Rockall Bank (northeast Atlantic)', *Limnology and Oceanography* **54**(6), 1829.

van Oevelen, D, K Soetaert and C Heip (2012), 'Carbon flows in the benthic food web of the Porcupine Abyssal Plain: The (un) importance of labile detritus in supporting microbial and faunal carbon demands', *Limnology and Oceanography* **57**(2), 645–664.

van Oevelen, D, K Soetaert, JJ Middelburg, PMJ Herman, L Moodley, I Hamels, T Moens and CHR Heip (2006), 'Carbon flows through a benthic food web: Integrating biomass, isotope and tracer data', *Journal of Marine Research* **64**(3), 453–482.

van Oevelen, D, K Soetaert, R García, H C de Stigter, M R Cunha, A Pusceddu and R Danovaro (2011), 'Canyon conditions impact carbon flows in food webs of three sections of the Nazaré canyon', *Deep Sea Research Part II: Topical Studies in Oceanography* **58**(23), 2461–2476.

van Oevelen, D, K Van den Meersche, FJR Meysman, K Soetaert, JJ Middelburg and AF Vézina (2010), 'Quantifying food web flows using linear inverse models', *Ecosystems* **13**(1), 32–45.

van Oevelen, D, M Bergmann, K Soetaert, E Bauerfeind, C Hasemann, M Klages, I Schewe, T Soltwedel and NE Budaeva (2011), 'Carbon flows in the benthic food web at the deep-sea observatory HAUSGARTEN (Fram Strait)', *Deep Sea Research Part I: Oceanographic Research Papers* **58**(11), 1069–1083.

Venables, WN and CM Dichmont (2004), 'GLMs, GAMs and GLMMs: an overview of theory for applications in fisheries research', *Fisheries Research* **70**(2), 319–337.

Verity, PG, V Smetacek and TJ Smayda (2002), 'Status, trends and the future of the marine pelagic ecosystem', *Environmental Conservation* **29**(02), 207–237.

Vetter, EW (1998), 'Population dynamics of a dense assemblage of marine detritivores', *Journal of Experimental Marine Biology and Ecology* **226**(1), 131–161.

Vetter, EW and PK Dayton (1998), 'Macrofaunal communities within and adjacent to a detritus-rich submarine canyon system', *Deep-Sea Research Part II: Topical Studies in Oceanography* **45**(1–3), 25–54.

Vetter, EW and PK Dayton (1999), 'Organic enrichment by macrophyte detritus, and abundance patterns of megafaunal populations in submarine canyons', *Marine Ecology Progress Series* **186**, 137–148.

Vézina, AF and C Savenkoff (1999), 'Inverse modeling of carbon and nitrogen flows in the pelagic food web of the northeast subarctic Pacific', *Deep Sea Research Part II: Topical Studies in Oceanography* **46**(11), 2909–2939.

Vézina, AF and T Platt (1988), 'Food web dynamics in the ocean. 1. Best-estimates of flow networks using inverse methods', *Marine Ecology Progress Series* **42**(3), 269–287.

Vicente-Serrano, SM and RM Trigo (2011), *Hydrological, Socioeconomic and Ecological Impacts of the North Atlantic Oscillation in the Mediterranean Region*, Vol. 46, Springer, London and New York.

Viéitez Martín, JM, G San Martín Peral and C Alos Calvo (2004), *Fauna ibérica. Annelida polychaeta I*, Vol. 25, Museo Nacional de Ciencias Naturales, CSIC, Madrid.

Vinogradov, ME and VB Tseitlin (1983), *Deep-sea biology. The sea*, Vol. 8, chapter Deep-sea pelagic domain (aspects of bioenergetics), pp. 123–165.

Virnstein, RW (1977), 'The importance of predation by crabs and fishes on benthic infauna in Chesapeake Bay', *Ecology* **58**(6), 1200–1217.

Walsh, JJ (1991), 'Importance of continental margins in the marine biogeochemical cycling of carbon and nitrogen', *Nature* **350**(6313), 53–55.

Walters, C, D Pauly and V Christensen (1999), 'Ecospace: prediction of mesoscale spatial patterns in trophic relationships of exploited ecosystems, with emphasis on the impacts of marine protected areas', *Ecosystems* **2**(6), 539–554.

Walters, C, D Pauly, V Christensen and JF Kitchell (2000), 'Representing density dependent consequences of life history strategies in aquatic ecosystems: EcoSim II', *Ecosystems* **3**(1), 70–83.

Walters, C, V Christensen and D Pauly (1997), 'Structuring dynamic models of exploited ecosystems from trophic mass-balance assessments', *Reviews in fish biology and fisheries* **7**(2), 139–172.

Walters, CJ and SJD Martell (2004), *Fisheries ecology and management*, Princeton University Press.

Warren, PH (1994), 'Making connections in food webs', *Trends in Ecology & Evolution* **9**(4), 136–141.

Wasserman, L (2006), *All of nonparametric statistics*, Vol. 4, Springer New York.

Watters, GM, JT Hinke, K Reid and S Hill (2005), A krill–predator–fishery model for evaluating candidate management procedures, *in* 'Convention on the Conservation of Antarctic Marine Living Resources (CCAMLR) Working Group on Ecosystem Monitoring and Management Working Paper WG-EMM', Vol. 5, pp. 14–15.

Watters, GM, JT Hinke, K Reid and S Hill (2006), 'KPFM2, be careful what you ask for–you just might get it', *CCAMLR document WG-EMM-06/22* .

Wieking, G (2002), The macrofauna at the Dogger Bank: food supply in relation to hydroclimate, PhD thesis, University of Oldenburg.

Wieking, G and I Kröncke (2003), 'Macrofauna communities of the Dogger Bank (central North Sea) in the late 1990s: spatial distribution, species composition and trophic structure', *Helgoland Marine Research* **57**(1), 34–46.

Wilberg, MJ, JT Thorson, BC Linton and J Berkson (2009), 'Incorporating time-varying catchability into population dynamic stock assessment models', *Reviews in Fisheries Science* **18**(1), 7–24.

Williams, RJ and ND Martinez (2000), 'Simple rules yield complex food webs', *Nature* **404**(6774), 180–183.

Winberg, GG (1956), 'Rate of metabolism and food requirements of fishes', *Fisheries Research Board of Canada. Translation Series* **194**, 1–202.

Wood, S (2006), *Generalized Additive Models: an introduction with R*, CRC Press, London.

Woodward, G, DC Speirs and AG Hildrew (2005), 'Quantification and resolution of a complex, size-structured food web', *Advances in ecological research* **36**, 85–135.

Worm, B, EB Barbier, N Beaumont, JE Duffy, C Folke, BS Halpern, JBC Jackson, HK Lotze, F Micheli and SR Palumbi (2006), 'Impacts of biodiversity loss on ocean ecosystem services', *Science* **314**(5800), 787–790.

Worm, B, R Hilborn, JK Baum, TA Branch, JS Collie, C Costello, MJ Fogarty, EA Fulton, JA Hutchings, S Jennings, OP Jensen, HK Lotze, PM Mace, TR McClanahan, C Minto, SR Palumbi, AM Parma, D Ricard, AA Rosenberg, R Watson and D Zeller (2009), 'Rebuilding global fisheries', *Science* **325**(5940), 578–585.

Worm, B and RA Myers (2003), 'Meta-analysis of cod-shrimp interactions reveals top-down control in oceanic food webs', *Ecology* **84**(1), 162–173.

WWF/IUCN (2004), *The Mediterranean deep-sea ecosystems: an overview of their diversity, structure, functioning and anthropogenic impacts, with a proposal for conservation*, IUCN, Málaga and WWF, Rome.

Yodzis, P (1998), 'Local trophodynamics and the interaction of marine mammals and fisheries in the Benguela ecosystem', *Journal of Animal Ecology* **67**(4), 635–658.

Yodzis, P and S Innes (1992), 'Body size and consumer-resource dynamics', *American Naturalist* **139**(6), 1151–1175.

Zavatarelli, M and GL Mellor (1995), 'A numerical study of the Mediterranean Sea circulation', *Journal of Physical Oceanography* **25**(6), 1384–1414.

Zhou, S, ADM Smith, AE Punt, AJ Richardson, M Gibbs, EA Fulton, S Pascoe, C Bulman, P Bayliss and K Sainsbury (2010), 'Ecosystem-based fisheries management requires a change to the selective fishing philosophy', *Proceedings of the National Academy of Sciences* **107**(21), 9485–9489.

Zorach, AC and RE Ulanowicz (2003), 'Quantifying the complexity of flow networks: how many roles are there?', *Complexity* **8**(3), 68–76.